FRONTOTEMPORAL LOBAR DEGENERATION AND AMYOTROPHIC LATERAL SCLEROSIS: GENETICS, CLINICAL AND PATHOLOGICAL FEATURES, AND DISEASE MECHANISMS

EDITED BY: Annakaisa Haapasalo, Alberto Lleo and Anne Marja Remes
PUBLISHED IN: Frontiers in Neuroscience, Frontiers in Neurology and Frontiers in Genetics

frontiers Research Topics

frontiers

ISSN 1664-8714
ISBN 978-2-88971-777-4
DOI 10.3389/978-2-88971-777-4

About Frontiers

Frontiers is more than just an open-access publisher of scholarly articles: it is a pioneering approach to the world of academia, radically improving the way scholarly research is managed. The grand vision of Frontiers is a world where all people have an equal opportunity to seek, share and generate knowledge. Frontiers provides immediate and permanent online open access to all its publications, but this alone is not enough to realize our grand goals.

Frontiers Journal Series

The Frontiers Journal Series is a multi-tier and interdisciplinary set of open-access, online journals, promising a paradigm shift from the current review, selection and dissemination processes in academic publishing. All Frontiers journals are driven by researchers for researchers; therefore, they constitute a service to the scholarly community. At the same time, the Frontiers Journal Series operates on a revolutionary invention, the tiered publishing system, initially addressing specific communities of scholars, and gradually climbing up to broader public understanding, thus serving the interests of the lay society, too.

Dedication to Quality

Each Frontiers article is a landmark of the highest quality, thanks to genuinely collaborative interactions between authors and review editors, who include some of the world's best academicians. Research must be certified by peers before entering a stream of knowledge that may eventually reach the public - and shape society; therefore, Frontiers only applies the most rigorous and unbiased reviews.
Frontiers revolutionizes research publishing by freely delivering the most outstanding research, evaluated with no bias from both the academic and social point of view. By applying the most advanced information technologies, Frontiers is catapulting scholarly publishing into a new generation.

What are Frontiers Research Topics?

Frontiers Research Topics are very popular trademarks of the Frontiers Journals Series: they are collections of at least ten articles, all centered on a particular subject. With their unique mix of varied contributions from Original Research to Review Articles, Frontiers Research Topics unify the most influential researchers, the latest key findings and historical advances in a hot research area! Find out more on how to host your own Frontiers Research Topic or contribute to one as an author by contacting the Frontiers Editorial Office: frontiersin.org/about/contact

FRONTOTEMPORAL LOBAR DEGENERATION AND AMYOTROPHIC LATERAL SCLEROSIS: GENETICS, CLINICAL AND PATHOLOGICAL FEATURES, AND DISEASE MECHANISMS

Topic Editors:
Annakaisa Haapasalo, University of Eastern Finland, Finland
Alberto Lleo, Hospital de la Santa Creu i Sant Pau, Spain
Anne Marja Remes, University of Oulu, Finland

Citation: Haapasalo, A., Lleo, A., Remes, A. M., eds. (2021). Frontotemporal Lobar Degeneration and Amyotrophic Lateral Sclerosis: Genetics, Clinical and Pathological Features, and Disease Mechanisms. Lausanne: Frontiers Media SA. doi: 10.3389/978-2-88971-777-4

Table of Contents

frontiers in Neuroscience

REVIEW
published: 29 March 2019
doi: 10.3389/fnins.2019.00304

Toward a Glutamate Hypothesis of Frontotemporal Dementia

*Alberto Benussi[1], Antonella Alberici[1], Emanuele Buratti[2], Roberta Ghidoni[3], Fabrizio Gardoni[4], Monica Di Luca[4], Alessandro Padovani[1] and Barbara Borroni[1]**

[1] Neurology Unit, Department of Clinical and Experimental Sciences, University of Brescia, Brescia, Italy, [2] International Centre for Genetic Engineering and Biotechnology, ICGEB, Trieste, Italy, [3] IRCCS Istituto Centro San Giovanni di Dio Fatebenefratelli, Brescia, Italy, [4] Department of Pharmacological and Biomolecular Sciences, University of Milan, Milan, Italy

Frontotemporal dementia (FTD) is a heterogenous neurodegenerative disorder, characterized by diverse clinical presentations, neuropathological characteristics and underlying genetic causes. Emerging evidence has shown that FTD is characterized by a series of changes in several neurotransmitter systems, including serotonin, dopamine, GABA and, above all, glutamate. Indeed, several studies have now provided preclinical and clinical evidence that glutamate is key in the pathogenesis of FTD. Animal models of FTD have shown a selective hypofunction in *N*-methyl *D*-aspartate (NMDA) and α-amino-3-hydroxyl-5-methyl-4-isoxazolepropionic acid (AMPA) receptors, while in patients, glutamatergic pyramidal neurons are depleted in several areas, including the frontal and temporal cortices. Recently, a selective involvement of the AMPA GluA3 subunit has been observed in patients with autoimmune anti-GluA3 antibodies, which accounted for nearly 25% of FTD patients, leading to a decrease of the GluA3 subunit synaptic localization of the AMPA receptor and loss of dendritic spines. Other *in vivo* evidence of the involvement of the glutamatergic system in FTD derives from non-invasive brain stimulation studies using transcranial magnetic stimulation, in which specific stimulation protocols have indirectly identified a selective and prominent impairment in glutamatergic circuits in patients with both sporadic and genetic FTD. In view of limited disease modifying therapies to slow or revert disease progression in FTD, an important approach could consist in targeting the neurotransmitter deficits, similarly to what has been achieved in Parkinson's disease with dopaminergic therapy or Alzheimer's disease with cholinergic therapy. In this review, we summarize the current evidence concerning the involvement of the glutamatergic system in FTD, suggesting the development of new therapeutic strategies.

Keywords: frontotemporal dementia, frontotemporal lobar degeneration, glutamate, neurotransmitter, autoimmunity, transcranial magnetic stimulation

OPEN ACCESS

Edited by:
Annakaisa Haapasalo, University of Eastern Finland, Finland

Reviewed by:
Yannick Vermeiren, University of Antwerp, Belgium
Rafael Linden, Federal University of Rio de Janeiro, Brazil

****Correspondence:***
Barbara Borroni
barbara.borroni@unibs.it

Specialty section:
This article was submitted to Neurodegeneration, a section of the journal Frontiers in Neuroscience

Received: *04 February 2019*
Accepted: *18 March 2019*
Published: *29 March 2019*

Citation:
Benussi A, Alberici A, Buratti E, Ghidoni R, Gardoni F, Di Luca M, Padovani A and Borroni B (2019) Toward a Glutamate Hypothesis of Frontotemporal Dementia. Front. Neurosci. 13:304. doi: 10.3389/fnins.2019.00304

INTRODUCTION

Frontotemporal dementia (FTD) is one of the most common neurodegenerative conditions after Alzheimer's Disease (AD), characterized by behavioral abnormalities, language impairment, and deficits of executive functions (Bang et al., 2015). The different clinical features have been grouped in different variants, represented by the behavioral variant of FTD (bvFTD) (Rascovsky et al., 2011),

the agrammatic variant of Primary Progressive Aphasia (avPPA) and the semantic variant of PPA (svPPA) (Gorno-Tempini et al., 2011). Over the past ten years, for a common sharing of the same genetic and pathological determinants, atypical extrapyramidal conditions, including Corticobasal Syndrome (CBS) and Progressive Supranuclear Palsy (PSP), but also motor neuron disease (MND), were grouped under the same frontotemporal lobar degeneration (FTLD) disease spectrum (Litvan et al., 1996; Armstrong et al., 2013; Burrell et al., 2016). Concomitantly, the structural and functional brain correlates of each phenotype have been precisely reported (Rohrer et al., 2011). FTLD selectively affects the frontal and temporal regions, in which the main neuropathological hallmarks are constituted primarily by tau or TAR DNA-binding protein 43 (TDP-43) depositions (Spillantini and Goedert, 2013; Neumann and Mackenzie, 2019).

The identification of genetic mutations associated with FTLD helped to elucidate the underlying pathology, with mutations in *Microtubule Associated Protein Tau (MAPT)* causing tau accumulation, and *Granulin (GRN)* or the expansion on *chromosome 9 open reading frame 72 (C9orf72)* being associated with TDP-43 inclusions (Borroni and Padovani, 2013). Lastly, reappraisal of the pathological criteria for subtyping FTLD cases has benefited from some refinements, being updated with recent immunohistochemical, biochemical, and genetic advances (Cairns et al., 2007). In addition to FTLD-Tau or FTLD-TDP, several other neuropathological depositions have been defined, including FTLD-FET [with positivity for the FET family of DNA/RNA-binding proteins, comprising the fused in sarcoma (FUS), TATA-binding protein-associated factor 2N (TAF-15) and Ewing sarcoma protein (EWS)], FTLD-UPS (with inclusions of proteins of the ubiquitin-proteasome system) and FTLD-ni (with no inclusions observed) (Sieben et al., 2012; Van Mossevelde et al., 2018). Other uncommon genetic mutations have been described, including *valosin containing protein* (*VCP*) (Watts et al., 2004; van der Zee et al., 2009), *sequestosome 1* (*SQSTM1*) (Rubino et al., 2012; Le Ber et al., 2013; van der Zee et al., 2014; Kovacs et al., 2016), and *TANK-binding kinase 1* (*TBK1*) (Freischmidt et al., 2015; Gijselinck et al., 2015; Pottier et al., 2015), with an underlying TDP-43 pathology, *charged multivesicular body protein 2B* (*CHMP2B*) (Skibinski et al., 2005; Holm et al., 2009), associated with FTLD-UPS, and *FUS* mutations (Broustal et al., 2010; Van Langenhove et al., 2010) probably associated to FTLD-FET (no autopsy confirmation in patients with FTD to date but only in patients with amyotrophic lateral sclerosis) (Benussi et al., 2015a).

Despite the giant step forward in the knowledge of clinical, imaging, genetic and biological underpinnings of the disease, the absence of a reliable biomarker to predict the ongoing neuropathology represents a major limit to develop disease-modifying therapies that target tau or TDP-43 deposits, and that could be administered only to subjects with known pathogenetic mutations (Bang et al., 2015; Borroni et al., 2015). Moreover, it is still unknown whether tau and TDP-43 deposits represent the initial mechanism or simply the result of other trigger events.

Indeed, two different approaches might be pursued in the next future for treatment purposes: on one hand, there is urgent need to develop diagnostic markers able to identify the specific proteinopathies associated with FTLD, on the other, it might be possible to characterize neurotransmitter deficits shared by the entire FTLD spectrum (Rohrer et al., 2011).

Emerging evidence has now shown that FTD is characterized by a series of changes in several neurotransmitter systems, including serotonin, dopamine, GABA and, above all, glutamate (Murley and Rowe, 2018) (see **Table 1**).

The recent identification of anti-AMPA GluA3 antibodies in the serum and in the cerebrospinal fluid (CSF) from FTLD patients (Borroni et al., 2017) has suggested that the impairment of glutamate neurotransmission through an autoimmune mechanism might be considered as a possible target to slow or revert the disease. In this framework, we can hypothesize that a restoration of the appropriate glutamatergic stimulation could be reached by modulating (i) the immune system or (ii) the glutamatergic receptors, developing the latter approach in analogy to what has been demonstrated effective for Parkinson or Alzheimer disease, with dopaminergic and cholinergic therapies, respectively (Murley and Rowe, 2018).

In this review, we summarize the current evidence concerning the involvement of the glutamatergic system in FTD, suggesting the development of new therapeutic strategies.

MOLECULAR BIOLOGY

Glutamate, which represents the main excitatory neurotransmitter in the brain, largely contributes to memory and learning processes (Bliss and Collingridge, 1993), while being also involved in brain damage when abnormally activated in several conditions, including brain ischemia, epilepsy and neurodegeneration (Bowie, 2008). Glutamate exerts its functions at the synaptic level through both ionotropic (iGluR) and metabotropic glutamate receptors (mGluR).

iGluR are cation permeable tetramers, distinguished in *N*-methyl *D*-aspartate (NMDA), α-amino-3-hydroxyl-5-methyl-4-isoxazolepropionic acid (AMPA) and kainate (KA) on the basis of their affinity properties, the selectivity for different ions and the ability to generate rapid or slow electric kinetics. NMDA receptors (NMDAR) are known to mediate plasticity phenomena, as long-term potentiation (LTP) (Lescher et al., 2012), with a critical role of extra synaptic receptor subtype 2B (NR2B) subunit-containing ones (Paoletti et al., 2013). AMPA receptors are primarily involved in synaptic plasticity by modifications of subunits editing and composition, or interactions with different receptors and phosphorylation (Opazo et al., 2010; Huganir and Nicoll, 2013).

mGluR are a family of receptors coupled to G proteins, activating different transduction signals, mainly represented by phospholipase C and adenylate cyclase (Castillo et al., 2010). mGluRs contribute to neuronal plasticity and cognitive abilities, being able to mediate self-dependent forms of LTP and long-term depression (LTD) (Wang et al., 2015; Longhena et al., 2017).

Several evidences arise from both preclinical and clinical studies, showing the involvement of the glutamate

neurotransmitter receptors, both iGluR and mGluR in the pathogenesis of FTLD.

In murine cortical neurons, silencing the FTD-associated gene granulin (*GRN*) decreases the expression of extra synaptic NR2B-containing NMDAR (Longhena et al., 2017); on the other hand, hyper-phosphorylated tau enhances glutamate release and produces an overactivation of the same receptor ending with neuron death, that can eventually be reduced by stimulating its reuptake through the astrocytic glutamate transporter 1 (GLT1)/excitatory amino acid transporter 2 (EAAT2) (Decker et al., 2016). Furthermore, FTLD has been related to the dysfunction in RNA pathways (Sephton and Yu, 2015), as corroborated by evidence that *FUS* depletion downregulates the transcription of GluA1, an essential AMPA-subunit involved in LTP phenomena (Udagawa et al., 2015). In that regard, also *charged multivesicular body protein 2b (CHMP2B)* FTD-related mutation increases GluA2 expression by disrupting microRNA levels (Gascon et al., 2014).

Knock out of the *glutamate ionotropic receptor AMPA type subunit 3* gene *(GRIA3)* produces modifications in social behavior with an increase in aggressiveness (Adamczyk et al., 2012): in a recent study GluA3-containing AMPAR turned to be dormant receptors, triggered by a peculiar intracellular signaling pathway (Renner et al., 2017). Neuronal activity stimulated by AMPAR activation induces tau release from mature cortical neurons in a calcium-dependent way, suggesting the glutamatergic modulation as a further approach to prevent tau depositions (Pooler et al., 2013). Autoantibodies for the GluA3 subunit of AMPARs have been identified both in the serum and CSF of FTD patients (Borroni et al., 2017), characterized by a bvFTD phenotype with presenile onset, absence of an autosomal dominant pattern of inheritance, and greater bitemporal atrophy. These anti-GluA3 antibodies lead to a reduction of the synaptic levels of GluA3-containing AMPARs both in rat primary neurons and in human neurons differentiated from induced pluripotent stem cells (iPSCs). In addition, the presence of GluA3 antibodies in the CSF induced a loss of dendritic spine density, and increased levels of tau protein *in vitro* human neurons (Borroni et al., 2017).

Interestingly, Leuzy et al. (2016) reported a reduced availability of mGlur5 in bvFTD patients. Several observations argued for a link between autoimmunity and FTD (Alberici et al., 2018), and more recently, it was demonstrated a significant increase in frequency of anti-nuclear antibodies (ANA) observed in FTD patients, as compared to normal control subjects (Cavazzana et al., 2018). According to these findings, it might be hypothesized that an immune system dysregulation results into an abnormal production of autoantibodies directed against the GluA3 subunit, causing a deficit in glutamatergic transmission, eventually leading to FTLD.

The involvement of glutamatergic transmission has also been reported in amyotrophic lateral sclerosis (ALS), which is part of the FTLD-ALS spectrum disorder, in which a glutamate-induced excitotoxicity of motor neurons has been hypothesized (Blasco et al., 2014). Deficient editing of the GluR2 AMPA receptor subunit (Kawahara et al., 2004) and a diminished functional transport of glutamate and reduced EAAT2 immunoreactivity has been observed in motor neurons of patients with ALS (Rothstein et al., 1992, 1995). These findings further support the possible complex role of glutamatergic transmission abnormalities in the pathophysiology of FTD-ALS.

Other possible modulators of glutamatergic transmission which have been shown to be impaired in FTD are serotonin (5-HT) and GABA. 5-HT has been shown to differently modify glutamate mediated effects, acting on distinct 5-HT receptor subtypes both at the pre-synaptic and post-synaptic site and in different brain regions: in the frontal cortex glutamate release is inhibited by serotonin whereas in the prefrontal cortex serotonin enhances glutamatergic transmission (Dawson et al., 2001; Ciranna, 2006). In FTD, a dysfunction of the serotoninergic system has been frequently observed (Bowen et al., 2008; Vermeiren et al., 2016), possibly opening an avenue for glutamatergic modulation through serotonin regulation (Huey et al., 2006).

Furthermore, GABA, which is the predominant inhibitory neurotransmitter in the brain with different functions other that merely counteracting excitatory glutamatergic neurons, has been shown to be impaired in FTD patients. Initial studies have shown that a subgroup of GABAergic neurons that bind calbinidin-D28k are reduced in the upper neocortical layers of the frontal and temporal cortices in FTD (Ferrer, 1999), while gamma oscillations and coherence, which reflect GABA inhibition, are reduced between the frontal lobes of patients with behavioral variant FTD (Hughes et al., 2018). These findings are corroborated by reports of the toxic effects mediated by tau

TABLE 1 | Evidence for neurotransmitter deficits in frontotemporal dementia.

	Type of evidence			
Neurotransmitter	**Neurobiological**	**Neurophysiological**	**Neuroradiological**	**Pharmacological**
Glutamate	+	+	+	−
GABA	+	+	−	−
Serotonin	+	−	+	+
Dopamine	+	−	+	+
Acetylcholine	−	−	−	−
Noradrenaline	−	−	±	+

+: evidence of neurotransmitter deficit; −: no evidence of neurotransmitter deficit.

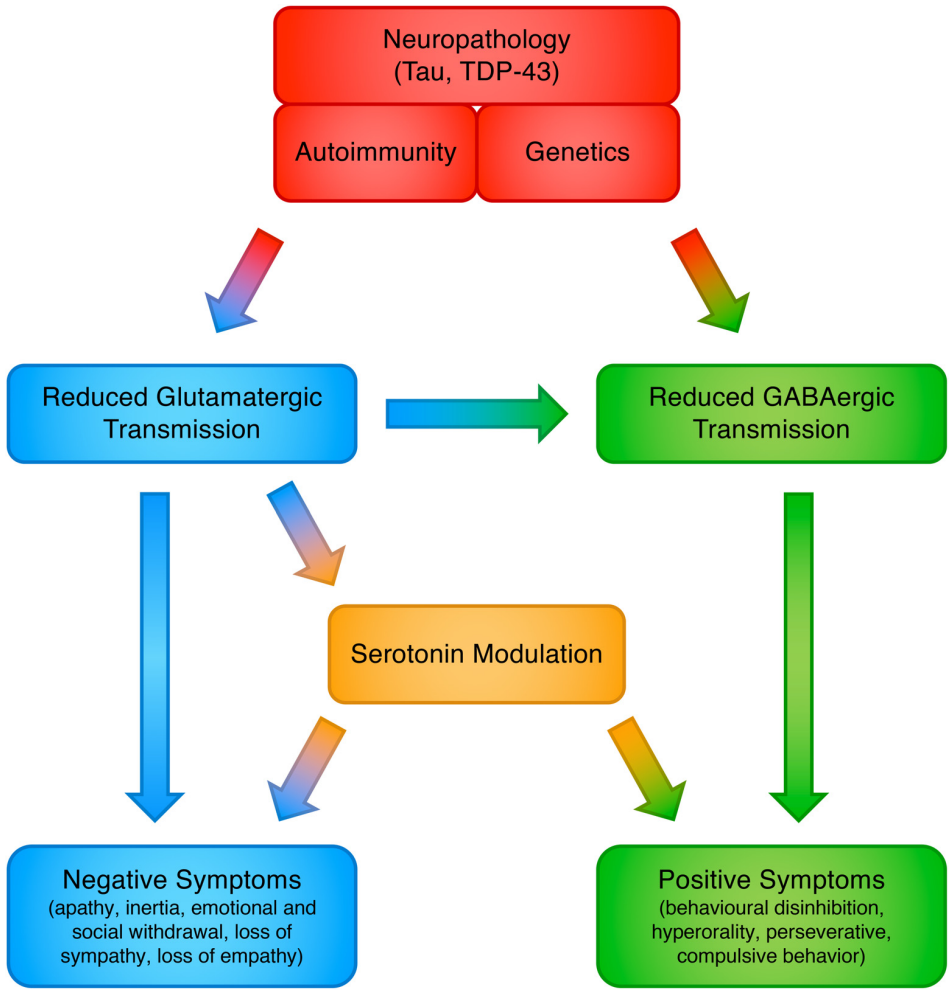

FIGURE 1 | Proposed model for the involvement of neurotransmitter systems in frontotemporal dementia.

and TDP-43 on GABAergic interneurons, leading to a loss of GABAergic function in animal models (Levenga et al., 2013; Yamashita and Kwak, 2014).

NEUROPHYSIOLOGY

Indirect evidence of the involvement of the glutamatergic system in FTD also comes from neurophysiological studies using both *in vitro* and *in vivo* techniques.

In vitro studies in transgenic mice expressing pathological human tau (V337M mutation), which is one of the main pathological hallmarks of FTD, have shown both AMPA and NMDA receptor hypofunction in the ventral striatum and insular cortex, which were reversible after the administration of cycloserine, an NMDA receptor co-agonist (Warmus et al., 2014). Further *in vitro* studies in transgenic mice carrying a *CHMP2B* mutation, which is another gene associated with FTD, have also shown altered AMPA receptor composition and function in the medial prefrontal cortex (Gascon et al., 2014).

In vivo neurophysiological evidence of the involvement of glutamatergic circuits in FTD mainly comes from non-invasive brain stimulation studies using transcranial magnetic stimulation (TMS) (Borroni et al., 2018). In this context, different paired-pulse TMS paradigms have been implemented to assess intracortical inhibitory and excitatory interneuronal circuits (Benussi et al., 2015b; Rossini et al., 2015). In particular, intracortical facilitation (ICF), which consists in a physiological facilitation elicited by applying a subthreshold conditioning magnetic stimulus followed by a suprathreshold test stimulus at an inter stimulus interval of 6–30 ms, has shown to depend mainly on glutamatergic circuits in the primary motor cortex (Ziemann et al., 2015), with NMDA receptor antagonists decreasing ICF (Ziemann et al., 1998; Schwenkreis et al., 1999).

Reduced ICF has been observed in patients with genetic FTD, carrying a *GRN* or *C9orf72* mutation, even in the presymptomatic phases of disease, compared to non-carrier first degree relatives (Benussi et al., 2016). These dysfunctions correlated with reduced cortical thickness and surface area of the right insula in presymptomatic *GRN* carriers, suggesting

that glutamatergic impairment in the presymptomatic phases of *GRN*-related FTD could reflect the beginning of insular dysfunction, even in absence of cognitive or behavioral abnormalities (Gazzina et al., 2018).

Recently, the reduction of ICF has been observed up to 30 years before expected symptom onset in a very large cohort of *GRN* and *C9orf72* mutation carriers compared to non-carriers, long before the onset of clinical and neuroimaging abnormalities (Benussi et al., 2019).

An impairment of ICF has also been observed in sporadic FTD (Burrell et al., 2011; Benussi et al., 2017), confirming how this biomarker may be useful not only to track disease progression, but also to distinguish FTD from other forms of dementias, even in the early disease stages (Benussi et al., 2018a; Padovani et al., 2018).

Regarding other syndromes in the FTLD spectrum, a reduced ICF has been also observed in patients with CBS and PSP, highlighting how this technique may also be used to distinguish other atypical parkinsonian disorders, including dementia with Lewy bodies (Benussi et al., 2018b).

Alterations in ICF have been observed also in patients with both sporadic and familial ALS; however, contrary to what has been observed in FTD, an increase in ICF seems to be predominant (Geevasinga et al., 2015; Van den Bos et al., 2018). It is still debated if cortical hyperexcitability might act as an adaptive process in response to peripheral neurodegeneration and could serve as a neuroprotective strategy, or if cortical hyperexcitability may serve as a final common pathway in ALS, mediating neuronal degeneration via a trans-synaptic glutamate process (Geevasinga et al., 2015).

TREATMENT APPROACHES: TARGETING GLUTAMATERGIC NEUROTRANSMISSION

Currently there are no approved treatments for FTD, and there are no therapies able to stop or alter the disease course. Pharmacological treatments to date have mostly concerned the off-label use of medications for symptomatic management. Recent advancements in understanding the molecular and genetic basis of FTD, and several clinical trials based on these insights are underway and have been reviewed elsewhere (Tsai and Boxer, 2016).

Glutamate neurotransmission has been considered a possible target for FTD symptomatic treatment. Memantine, a NMDA receptor antagonist with an indication for the treatment of moderate to severe AD (Tariot et al., 2004), was studied in two randomized, placebo-controlled trials over 52 and 26 weeks in FTD (Vercelletto et al., 2011; Boxer et al., 2013). Both studies failed to demonstrate significant benefits on behavioral disturbances or clinical global impression of change.

The recent observations of an effect exerted by the AMPARs activation on tau aggregation renewed the interest of glutamatergic modulation as a further approach to prevent tau depositions (Pooler et al., 2013; Borroni et al., 2017). Moreover, the identification of autoantibodies directed against GluA3 subunits provided evidence for an autoimmune dysregulation as a possible pathogenetic mechanism in FTD (Alberici et al., 2018). The link between autoimmune antibodies and neurodegeneration has been previously shown in the anti-IgLON5-related tauopathy, in which extensive neuropathological tau and TDP-43 inclusions have been observed (Sabater et al., 2014), placing these disorders at the convergence of neurodegenerative and autoimmune mechanisms. However, further research is necessary to validate these findings and elucidate the mechanisms by which these, or still other unidentified auto-antibodies, induce pathologic protein aggregates and neurodegeneration.

The feasibility of targeting an autoimmune response is an attractive potential therapeutic approach, suggesting immunomodulatory therapies as an evidence-based approach to treat FTLD. In the absence of prospective and randomized clinical trials for the treatment of autoimmune encephalitis, literature data are based on case reports with anti-NMDA, or more rarely, anti-AMPA receptor encephalitis (Dalmau and Graus, 2018). We can hypothesize that scavenging anti-GluA3 antibodies by using immunomodulation might restore glutamatergic transmission, thus slowing or reverting FTLD neurodegenerative process. Alternatively, in agreement with the glutamatergic hypothesis, and in analogy to what has been proposed for schizophrenia, positive allosteric modulators of AMPA receptors as well as orthosteric ligands and modulators of metabotropic glutamatergic receptors in particular ligands acting on mGlu receptors might be considered promising potential medications in FTLD (Menniti et al., 2013).

The modulation of glutamatergic transmission via 5-HT regulation may also be a promising approach to seek. Favorable evidence with selective serotonin reuptake inhibitors (SSRIs) has been observed in FTD patients, with several open label and placebo-controlled studies with SSRIs showing an improvement of several behavioral symptoms, as disinhibition, irritability and depression (Moretti et al., 2003; Lebert et al., 2004; Anneser et al., 2007; Herrmann et al., 2012; Hughes et al., 2015). However, it is still not known if this is a direct effect on serotoninergic transmission or possibly an indirect downstream effect on glutamatergic systems.

Regarding GABAergic therapies, evidence is currently lacking for a clinical efficacy in FTD patients.

CONCLUSION

We have observed how the involvement of the glutamatergic system may play a key role in the pathogenesis of FTD both from a biological and neurophysiological perspective. This implication may open several avenues regarding treatment options which will have to be verified experimentally, both from a symptomatic but also possibly disease modifying approach.

The involvement of glutamate in FTLD may answer some of the open issues in this field, yet we caution that FTD symptoms almost certainly do not flow from a single neurotransmitter abnormality. Indeed, this proposed model does not negate the involvement of other neurotransmitters,

which have already been observed in FTLD, including GABA, serotonin and dopamine, and all of these may be ultimately brought together in a unified and interconnected framework (Murley and Rowe, 2018) (see **Figure 1**). Restoring these deficits, individually or in combination, has the potential to improve cognitive, behavioral and motor symptoms. More realistically, in fact the ultimate phenotypic expression probably arises from combinations of neurotransmitter abnormalities, genetic mutations, and environmental factors; combinations that may vary considerably from patient to patient.

Another interesting avenue worth pursuing is the potential for this amino-acid to act as a biomarker, either in establishing the diagnosis or as a measure of disease progression. Direct measurements in the CSF have shown a negative correlation between glutamate levels with verbally agitated behavior in FTD patients (Vermeiren et al., 2013). On the other hand, indirect measurements come from magnetic resonance spectroscopy of FTD patients in which glutamate/glutamine levels have been found to be reduced in the frontal and temporal lobes (Ernst et al., 1997; Sarac et al., 2008) and from neurophysiological studies with TMS, showing in both sporadic and genetic FTD a reduced ICF, which is partially mediated by glutamatergic transmission. In future, glutamate levels could also be indirectly assessed with electroencephalography (EEG) (Lally et al., 2014) or by TMS-EEG evoked potentials (Cash et al., 2016). To define which direct or indirect biomarker of glutamatergic neurotransmission might be the most useful and informative has still to be elucidated, considering the lack of studies on the subject, with different biomarkers perhaps providing distinct information from both a physiopathological and topographical perspective.

In conclusion, it is therefore now clear that the role of glutamate in FTD can represent an interesting and innovative approach to better understand the underlying ongoing neurodegenerative process in this pathology, although further investigations will be needed in order to increase our biological understanding of the disease, which will probably be contingent to the development of appropriate models and biomarkers for glutamatergic drug development.

AUTHOR CONTRIBUTIONS

All authors gave their substantial contribution to conception and design of the manuscript and drafting the manuscript and revising it critically for important intellectual content, approved the manuscript in its present form for publication, and agreed to be accountable for all aspects of the work in ensuring that questions related to the accuracy or integrity of any part of the work are appropriately investigated and resolved.

FUNDING

This work was supported by the Italian Ministry of Health (Ricerca Corrente).

ACKNOWLEDGMENTS

We thank Marcello Giunta for his significant contributions to the manuscript.

REFERENCES

Adamczyk, A., Mejias, R., Takamiya, K., Yocum, J., Krasnova, I. N., Calderon, J., et al. (2012). GluA3-deficiency in mice is associated with increased social and aggressive behavior and elevated dopamine in striatum. *Behav. Brain Res.* 229, 265–272. doi: 10.1016/j.bbr.2012.01.007

Alberici, A., Cristillo, V., Gazzina, S., Benussi, A., Padovani, A., and Borroni, B. (2018). Autoimmunity and frontotemporal dementia. *Curr. Alzheimer Res.* 15, 602–609. doi: 10.2174/1567205015666180119104825

Anneser, J. M. H., Jox, R. J., and Borasio, G. D. (2007). Inappropriate sexual behaviour in a case of ALS and FTD: successful treatment with sertraline. *Amyotroph. Lateral Scler.* 8, 189–190. doi: 10.1080/17482960601073543

Armstrong, M. J., Litvan, I., Lang, A. E., Bak, T. H., Bhatia, K. P., Borroni, B., et al. (2013). Criteria for the diagnosis of corticobasal degeneration. *Neurology* 80, 496–503. doi: 10.1212/WNL.0b013e31827f0fd1

Bang, J., Spina, S., and Miller, B. L. (2015). Frontotemporal dementia. *Lancet* 386, 1672–1682. doi: 10.1016/S0140-6736(15)00461-4

Benussi, A., Alberici, A., Ferrari, C., Cantoni, V., Dell'Era, V., Turrone, R., et al. (2018a). The impact of transcranial magnetic stimulation on diagnostic confidence in patients with Alzheimer disease. *Alzheimers Res. Ther.* 10:94. doi: 10.1186/s13195-018-0423-6

Benussi, A., Dell'Era, V., Cantoni, V., Ferrari, C., Caratozzolo, S., Rozzini, L., et al. (2018b). Discrimination of atypical parkinsonisms with transcranial magnetic stimulation. *Brain Stimul.* 11, 366–373. doi: 10.1016/j.brs.2017.11.013

Benussi, A., Cosseddu, M., Filareto, I., Dell'Era, V., Archetti, S., Sofia Cotelli, M., et al. (2016). Impaired long-term potentiation-like cortical plasticity in presymptomatic genetic frontotemporal dementia. *Ann. Neurol.* 80, 472–476. doi: 10.1002/ana.24731

Benussi, A., Di Lorenzo, F., Dell'Era, V., Cosseddu, M., Alberici, A., Caratozzolo, S., et al. (2017). Transcranial magnetic stimulation distinguishes Alzheimer disease from frontotemporal dementia. *Neurology* 89, 665–672. doi: 10.1212/WNL.0000000000004232

Benussi, A., Gazzina, S., Premi, E., Cosseddu, M., Archetti, S., Dell'Era, V., et al. (2019). Clinical and biomarker changes in presymptomatic genetic frontotemporal dementia. *Neurobiol. Aging* 76, 133–140. doi: 10.1016/j.neurobiolaging.2018.12.018

Benussi, A., Padovani, A., and Borroni, B. (2015a). Phenotypic heterogeneity of monogenic frontotemporal dementia. *Front. Aging Neurosci.* 7:171. doi: 10.3389/fnagi.2015.00171

Benussi, A., Padovani, A., and Borroni, B. (2015b). Transcranial magnetic stimulation in Alzheimer's Disease and cortical dementias. *J. Alzheimers Dis. Parkinsonism* 5:197.

Blasco, H., Mavel, S., Corcia, P., and Gordon, P. H. (2014). The glutamate hypothesis in ALS: pathophysiology and drug development. *Curr. Med. Chem.* 21, 3551–3575. doi: 10.2174/0929867321666140916120118

Bliss, T. V., and Collingridge, G. L. (1993). A synaptic model of memory: long-term potentiation in the hippocampus. *Nature* 361, 31–39. doi: 10.1038/361031a0

Borroni, B., Benussi, A., Archetti, S., Galimberti, D., Parnetti, L., Nacmias, B., et al. (2015). Csf p-tau181/tau ratio as biomarker for TDP pathology in frontotemporal dementia. *Amyotroph. Lateral Scler. Front. Degener.* 16, 86–91. doi: 10.3109/21678421.2014.971812

Borroni, B., Benussi, A., Premi, E., Alberici, A., Marcello, E., Gardoni, F., et al. (2018). Biological, neuroimaging, and neurophysiological markers in frontotemporal dementia: three faces of the same coin. *J. Alzheimers Dis.* 62, 1113–1123. doi: 10.3233/JAD-170584

Borroni, B., and Padovani, A. (2013). Dementia: a new algorithm for molecular diagnostics in FTLD. *Nat. Rev. Neurol.* 9, 241–242. doi: 10.1038/nrneurol.2013.72

Borroni, B., Stanic, J., Verpelli, C., Mellone, M., Bonomi, E., Alberici, A., et al. (2017). Anti-AMPA GluA3 antibodies in frontotemporal dementia: a new molecular target. *Sci. Rep.* 7:1006. doi: 10.1038/s41598-017-06117-y

Bowen, D. M., Procter, A. W., Mann, D. M. A., Snowden, J. S., Esiri, M. M., Neary, D., et al. (2008). Imbalance of a serotonergic system in frontotemporal dementia: implication for pharmacotherapy. *Psychopharmacology* 196, 603–610. doi: 10.1007/s00213-007-0992-8

Bowie, D. (2008). Ionotropic glutamate receptors & CNS disorders. *CNS Neurol. Disord. Drug Targets* 7, 129–143. doi: 10.2174/187152708784083821

Boxer, A. L., Knopman, D. S., Kaufer, D. I., Grossman, M., Onyike, C., Graf-Radford, N., et al. (2013). Memantine in patients with frontotemporal lobar degeneration: a multicentre, randomised, double-blind, placebo-controlled trial. *Lancet Neurol.* 12, 149–156. doi: 10.1016/S1474-4422(12)70320-4

Broustal, O., Camuzat, A., Guillot-Noël, L., Guy, N., Millecamps, S., Deffond, D., et al. (2010). FUS mutations in frontotemporal lobar degeneration with amyotrophic lateral sclerosis. *J. Alzheimers. Dis.* 22, 765–769.

Burrell, J. R., Halliday, G. M., Kril, J. J., Ittner, L. M., Götz, J., Kiernan, M. C., et al. (2016). The frontotemporal dementia-motor neuron disease continuum. *Lancet* 388, 919–931. doi: 10.1016/S0140-6736(16)00737-6

Burrell, J. R., Kiernan, M. C., Vucic, S., and Hodges, J. R. (2011). Motor neuron dysfunction in frontotemporal dementia. *Brain* 134, 2582–2594. doi: 10.1093/brain/awr195

Cairns, N. J., Bigio, E. H., Mackenzie, I. R. A., Neumann, M., Lee, V. M. Y., Hatanpaa, K. J., et al. (2007). Neuropathologic diagnostic and nosologic criteria for frontotemporal lobar degeneration: consensus of the consortium for frontotemporal lobar degeneration. *Acta Neuropathol.* 114, 5–22. doi: 10.1007/s00401-007-0237-2

Cash, R. F. H., Noda, Y., Zomorrodi, R., Radhu, N., Farzan, F., Rajji, T. K., et al. (2016). Characterization of glutamatergic and GABAA-Mediated neurotransmission in motor and dorsolateral prefrontal cortex using paired-pulse TMS–EEG. *Neuropsychopharmacology* 42, 502–511. doi: 10.1038/npp.2016.133

Castillo, C. A., León, D. A., Ballesteros-Yáñez, I., Iglesias, I., Martín, M., and Albasanz, J. L. (2010). Glutamate differently modulates metabotropic glutamate receptors in neuronal and glial cells. *Neurochem. Res.* 35, 1050–1063. doi: 10.1007/s11064-010-0154-y

Cavazzana, I., Alberici, A., Bonomi, E., Ottaviani, R., Kumar, R., Archetti, S., et al. (2018). Antinuclear antibodies in Frontotemporal Dementia: the tip's of autoimmunity iceberg? *J. Neuroimmunol.* 325, 61–63. doi: 10.1016/j.jneuroim.2018.10.006

Ciranna, L. (2006). Serotonin as a modulator of glutamate- and GABA-mediated neurotransmission: implications in physiological functions and in pathology. *Curr. Neuropharmacol.* 4, 101–114. doi: 10.2174/157015906776359540

Dalmau, J., and Graus, F. (2018). Antibody-mediated encephalitis. *N. Engl. J. Med.* 378, 840–851. doi: 10.1056/NEJMra1708712

Dawson, L. A., Nguyen, H. Q., and Li, P. (2001). The 5-HT6 receptor antagonist SB-271046 selectively enhances excitatory neurotransmission in the rat frontal cortex and hippocampus. *Neuropsychopharmacology* 25, 662–668. doi: 10.1016/S0893-133X(01)00265-2

Decker, J. M., Krüger, L., Sydow, A., Dennissen, F. J., Siskova, Z., Mandelkow, E., et al. (2016). The Tau/A152T mutation, a risk factor for frontotemporal-spectrum disorders, leads to NR2B receptor-mediated excitotoxicity. *EMBO Rep.* 17, 552–569. doi: 10.15252/embr.201541439

Ernst, T., Chang, L., Melchor, R., and Mehringer, C. M. (1997). Frontotemporal dementia and early Alzheimer disease: differentiation with frontal lobe H-1 MR spectroscopy. *Radiology* 203, 829–836. doi: 10.1148/radiology.203.3.9169712

Ferrer, I. (1999). Neurons and their dendrites in frontotemporal dementia. *Dement. Geriatr. Cogn. Disord.* 10, 55–60. doi: 10.1159/000051214

Freischmidt, A., Wieland, T., Richter, B., Ruf, W., Schaeffer, V., Müller, K., et al. (2015). Haploinsufficiency of TBK1 causes familial ALS and fronto-temporal dementia. *Nat. Neurosci.* 18, 631–636. doi: 10.1038/nn.4000

Gascon, E., Lynch, K., Ruan, H., Almeida, S., Verheyden, J. M., Seeley, W. W., et al. (2014). Alterations in microRNA-124 and AMPA receptors contribute to social behavioral deficits in frontotemporal dementia. *Nat. Med.* 20, 1444–1451. doi: 10.1038/nm.3717

Gazzina, S., Benussi, A., Premi, E., Paternicò, D., Cristillo, V., Dell'Era, V., et al. (2018). Neuroanatomical correlates of transcranial magnetic stimulation in presymptomatic granulin mutation carriers. *Brain Topogr.* 31, 488–497. doi: 10.1007/s10548-017-0612-9

Geevasinga, N., Menon, P., Nicholson, G. A., Ng, K., Howells, J., Kril, J. J., et al. (2015). Cortical Function in asymptomatic carriers and patients with C9orf72Amyotrophic lateral sclerosis. *JAMA Neurol.* 72, 1268–1274. doi: 10.1001/jamaneurol.2015.1872

Gijselinck, I., Van Mossevelde, S., van der Zee, J., Sieben, A., Philtjens, S., Heeman, B., et al. (2015). Loss of TBK1 is a frequent cause of frontotemporal dementia in a Belgian cohort. *Neurology* 85, 2116–2125. doi: 10.1212/WNL.0000000000002220

Gorno-Tempini, M. L., Hillis, A. E., Weintraub, S., Kertesz, A., Mendez, M., Cappa, S. F., et al. (2011). Classification of primary progressive aphasia and its variants. *Neurology* 76, 1006–1014. doi: 10.1212/WNL.0b013e31821103e6

Herrmann, N., Black, S. E., Chow, T., Cappell, J., Tang-Wai, D. F., and Lanctôt, K. L. (2012). Serotonergic function and treatment of behavioral and psychological symptoms of frontotemporal dementia. *Am. J. Geriatr. Psychiatry* 20, 789–797. doi: 10.1097/JGP.0b013e31823033f3

Holm, I. E., Isaacs, A. M., and Mackenzie, I. R. A. (2009). Absence of FUS-immunoreactive pathology in frontotemporal dementia linked to chromosome 3 (FTD-3) caused by mutation in the CHMP2B gene. *Acta Neuropathol.* 118, 719–720. doi: 10.1007/s00401-009-0593-1

Huey, E. D., Putnam, K. T., and Grafman, J. (2006). A systematic review of neurotransmitter deficits and treatments in frontotemporal dementia. *Neurology* 66, 17–22. doi: 10.1212/01.wnl.0000191304.55196.4d

Huganir, R. L., and Nicoll, R. A. (2013). AMPARs and synaptic plasticity: the last 25 years. *Neuron* 80, 704–717. doi: 10.1016/j.neuron.2013.10.025

Hughes, L. E., Rittman, T., Regenthal, R., Robbins, T. W., and Rowe, J. B. (2015). Improving response inhibition systems in frontotemporal dementia with citalopram. *Brain* 138, 1961–1975. doi: 10.1093/brain/awv133

Hughes, L. E., Rittman, T., Robbins, T. W., and Rowe, J. B. (2018). Reorganization of cortical oscillatory dynamics underlying disinhibition in frontotemporal dementia. *Brain* 141, 2486–2499. doi: 10.1093/brain/awy176

Kawahara, Y., Ito, K., Sun, H., Ito, M., Kanazawa, I., and Kwak, S. (2004). GluR4c, an alternative splicing isoform of GluR4, is abundantly expressed in the adult human brain. *Brain Res. Mol. Brain Res.* 127, 150–155. doi: 10.1016/j.molbrainres.2004.05.020

Kovacs, G. G., van der Zee, J., Hort, J., Kristoferitsch, W., Leitha, T., Höftberger, R., et al. (2016). Clinicopathological description of two cases with SQSTM1 gene mutation associated with frontotemporal dementia. *Neuropathology* 36, 27–38. doi: 10.1111/neup.12233

Lally, N., Mullins, P. G., Roberts, M. V., Price, D., Gruber, T., and Haenschel, C. (2014). Glutamatergic correlates of gamma-band oscillatory activity during cognition: a concurrent ER-MRS and EEG study. *Neuroimage* 85(Pt 2), 823–833. doi: 10.1016/j.neuroimage.2013.07.049

Le Ber, I., Camuzat, A., Guerreiro, R., Bouya-Ahmed, K., Bras, J., Nicolas, G., et al. (2013). SQSTM1 mutations in french patients with frontotemporal dementia or frontotemporal dementia with amyotrophic lateral sclerosis. *JAMA Neurol.* 70, 1403–1410. doi: 10.1001/jamaneurol.2013.3849

Lebert, F., Stekke, W., Hasenbroekx, C., and Pasquier, F. (2004). Frontotemporal dementia: a randomised, controlled trial with trazodone. *Dement. Geriatr. Cogn. Disord.* 17, 355–359. doi: 10.1159/000077171

Lescher, J., Paap, F., Schultz, V., Redenbach, L., Scheidt, U., Rosewich, H., et al. (2012). MicroRNA regulation in experimental autoimmune encephalomyelitis in mice and marmosets resembles regulation in human multiple sclerosis lesions. *J. Neuroimmunol.* 246, 27–33. doi: 10.1016/j.jneuroim.2012.02.012

Leuzy, A., Zimmer, E. R., Dubois, J., Pruessner, J., Cooperman, C., Soucy, J.-P., et al. (2016). In vivo characterization of metabotropic glutamate receptor type 5 abnormalities in behavioral variant FTD. *Brain Struct. Funct.* 221, 1387–1402. doi: 10.1007/s00429-014-0978-3

Levenga, J., Krishnamurthy, P., Rajamohamedsait, H., Wong, H., Franke, T. F., Cain, P., et al. (2013). Tau pathology induces loss of GABAergic interneurons leading to altered synaptic plasticity and behavioral impairments. *Acta Neuropathol. Commun.* 1:34. doi: 10.1186/2051-5960-1-34

Litvan, I., Agid, Y., Calne, D., Campbell, G., Dubois, B., Duvoisin, R. C., et al. (1996). Clinical research criteria for the diagnosis of progressive supranuclear

palsy (Steele-Richardson-Olszewski syndrome): report of the NINDS-SPSP international workshop. *Neurology* 47, 1–9. doi: 10.1212/WNL.47.1.1

Longhena, F., Zaltieri, M., Grigoletto, J., Faustini, G., La Via, L., Ghidoni, R., et al. (2017). Depletion of progranulin reduces GluN2B-containing NMDA receptor density, tau phosphorylation and dendritic arborization in mouse primary cortical neurons. *J. Pharmacol. Exp. Ther.* 363, 164–175. doi: 10.1124/jpet.117.242164

Menniti, F. S., Lindsley, W. C., Conn, P. J., Pandit, J., Zagouras, P., and Volkmann, R. A. (2013). Allosteric modulators for the treatment of schizophrenia: targeting glutamatergic networks. *Curr. Top. Med. Chem.* 13, 26–54. doi: 10.2174/1568026611313010005

Moretti, R., Torre, P., Antonello, R. M., Cazzato, G., and Bava, A. (2003). Frontotemporal dementia: paroxetine as a possible treatment of behavior symptoms: a randomized, controlled, open 14-month study. *Eur. Neurol.* 49, 13–19. doi: 10.1159/000067021

Murley, A. G., and Rowe, J. B. (2018). Neurotransmitter deficits from frontotemporal lobar degeneration. *Brain* 141, 1263–1285. doi: 10.1093/brain/awx327

Neumann, M., and Mackenzie, I. R. A. (2019). Review: neuropathology of non-tau frontotemporal lobar degeneration. *Neuropathol. Appl. Neurobiol.* 45, 19–40. doi: 10.1111/nan.12526

Opazo, P., Labrecque, S., Tigaret, C. M., Frouin, A., Wiseman, P. W., De Koninck, P., et al. (2010). CaMKII triggers the diffusional trapping of surface AMPARs through phosphorylation of stargazin. *Neuron* 67, 239–252. doi: 10.1016/j.neuron.2010.06.007

Padovani, A., Benussi, A., Cantoni, V., Dell'Era, V., Cotelli, M. S., Caratozzolo, S., et al. (2018). Diagnosis of mild cognitive impairment due to Alzheimer's disease with transcranial magnetic stimulation. *J. Alzheimers Dis.* 65, 221–230. doi: 10.3233/JAD-180293

Paoletti, P., Bellone, C., and Zhou, Q. (2013). NMDA receptor subunit diversity: impact on receptor properties, synaptic plasticity and disease. *Nat. Rev. Neurosci.* 14, 383–400. doi: 10.1038/nrn3504

Pooler, A. M., Polydoro, M., Wegmann, S., Nicholls, S. B., Spires-Jones, T. L., and Hyman, B. T. (2013). Propagation of tau pathology in Alzheimer's disease: identification of novel therapeutic targets. *Alzheimers Res. Ther.* 5, 1–8. doi: 10.1186/alzrt214

Pottier, C., Bieniek, K. F., Finch, N., van de Vorst, M., Baker, M., Perkersen, R., et al. (2015). Whole-genome sequencing reveals important role for TBK1 and OPTN mutations in frontotemporal lobar degeneration without motor neuron disease. *Acta Neuropathol.* 130, 77–92. doi: 10.1007/s00401-015-1436-x

Rascovsky, K., Hodges, J. R., Knopman, D., Mendez, M. F., Kramer, J. H., Neuhaus, J., et al. (2011). Sensitivity of revised diagnostic criteria for the behavioural variant of frontotemporal dementia. *Brain* 134, 2456–2477. doi: 10.1093/Brain/Awr179

Renner, M. C., Albers, E. H., Gutierrez-Castellanos, N., Reinders, N. R., van Huijstee, A. N., Xiong, H., et al. (2017). Synaptic plasticity through activation of GluA3-containing AMPA-receptors. *eLife* 6:e25462. doi: 10.7554/eLife.25462

Rohrer, J. D., Lashley, T., Schott, J. M., Warren, J. E., Mead, S., Isaacs, A. M., et al. (2011). Clinical and neuroanatomical signatures of tissue pathology in frontotemporal lobar degeneration. *Brain* 134, 2565–2581. doi: 10.1093/brain/awr198

Rossini, P. M., Burke, D., Chen, R., Cohen, L. G., Daskalakis, Z., Di Iorio, R., et al. (2015). Non-invasive electrical and magnetic stimulation of the brain, spinal cord, roots and peripheral nerves: basic principles and procedures for routine clinical and research application. An updated report from an I.F.C.N. Committee. *Clin. Neurophysiol.* 126, 1071–1107. doi: 10.1016/j.clinph.2015.02.001

Rothstein, J. D., Martin, L. J., and Kuncl, R. W. (1992). Decreased glutamate transport by the brain and spinal cord in amyotrophic lateral sclerosis. *N. Engl. J. Med.* 326, 1464–1468. doi: 10.1056/NEJM199205283262204

Rothstein, J. D., Van Kammen, M., Levey, A. I., Martin, L. J., and Kuncl, R. W. (1995). Selective loss of glial glutamate transporter GLT-1 in amyotrophic lateral sclerosis. *Ann. Neurol.* 38, 73–84. doi: 10.1002/ana.410380114

Rubino, E., Rainero, I., Chio, A., Rogaeva, E., Galimberti, D., Fenoglio, P., et al. (2012). SQSTM1 mutations in frontotemporal lobar degeneration and amyotrophic lateral sclerosis. *Neurology* 79, 1556–1562. doi: 10.1212/WNL.0b013e31826e25df

Sabater, L., Gaig, C., Gelpi, E., Bataller, L., Lewerenz, J., Torres-Vega, E., et al. (2014). A novel non-rapid-eye movement and rapid-eye-movement parasomnia with sleep breathing disorder associated with antibodies to IgLON5: a case series, characterisation of the antigen, and post-mortem study. *Lancet Neurol.* 13, 575–586. doi: 10.1016/S1474-4422(14)70051-1

Sarac, H., Zagar, M., Vranjes, D., Henigsberg, N., Bilić, E., and Pavlisa, G. (2008). Magnetic resonance imaging and magnetic resonance spectroscopy in a patient with amyotrophic lateral sclerosis and frontotemporal dementia. *Coll. Antropol.* 32(Suppl. 1), 205–210.

Schwenkreis, P., Witscher, K., Janssen, F., Addo, A., Dertwinkel, R., Zenz, M., et al. (1999). Influence of the N-methyl-d-aspartate antagonist memantine on human motor cortex excitability. *Neurosci. Lett.* 270, 137–140. doi: 10.1016/S0304-3940(99)00492-9

Sephton, C. F., and Yu, G. (2015). The function of RNA-binding proteins at the synapse: implications for neurodegeneration. *Cell. Mol. Life Sci.* 72, 3621–3635. doi: 10.1007/s00018-015-1943-x

Sieben, A., Van Langenhove, T., Engelborghs, S., Martin, J.-J., Boon, P., Cras, P., et al. (2012). The genetics and neuropathology of frontotemporal lobar degeneration. *Acta Neuropathol.* 124, 353–372. doi: 10.1007/s00401-012-1029-x

Skibinski, G., Parkinson, N. J., Brown, J. M., Chakrabarti, L., Lloyd, S. L., Hummerich, H., et al. (2005). Mutations in the endosomal ESCRTIII-complex subunit CHMP2B in frontotemporal dementia. *Nat. Genet.* 37, 806–808. doi: 10.1038/ng1609

Spillantini, M. G., and Goedert, M. (2013). Tau pathology and neurodegeneration. *Lancet Neurol.* 12, 609–622. doi: 10.1016/S1474-4422(13)70090-5

Tariot, P. N., Farlow, M. R., Grossberg, G. T., Graham, S. M., McDonald, S., Gergel, I., et al. (2004). Memantine treatment in patients with moderate to severe Alzheimer disease already receiving donepezil: a randomized controlled trial. *JAMA* 291, 317–324. doi: 10.1001/jama.291.3.317

Tsai, R. M., and Boxer, A. L. (2016). Therapy and clinical trials in frontotemporal dementia: past, present, and future. *J. Neurochem.* 138(Suppl.), 211–221. doi: 10.1111/jnc.13640

Udagawa, T., Fujioka, Y., Tanaka, M., Honda, D., Yokoi, S., Riku, Y., et al. (2015). FUS regulates AMPA receptor function and FTLD/ALS-associated behaviour via GluA1 mRNA stabilization. *Nat. Commun.* 6:7098. doi: 10.1038/ncomms8098

Van den Bos, M. A. J., Higashihara, M., Geevasinga, N., Menon, P., Kiernan, M. C., and Vucic, S. (2018). Imbalance of cortical facilitatory and inhibitory circuits underlies hyperexcitability in ALS. *Neurology* 91, e1669–e1676. doi: 10.1212/WNL.0000000000006438

van der Zee, J., Pirici, D., Van Langenhove, T., Engelborghs, S., Vandenberghe, R., Hoffmann, M., et al. (2009). Clinical heterogeneity in 3 unrelated families linked to VCP p.Arg159His. *Neurology* 73, 626–632. doi: 10.1212/WNL.0b013e3181b389d9

van der Zee, J., Van Langenhove, T., Kovacs, G. G., Dillen, L., Deschamps, W., Engelborghs, S., et al. (2014). Rare mutations in SQSTM1 modify susceptibility to frontotemporal lobar degeneration. *Acta Neuropathol.* 128, 397–410. doi: 10.1007/s00401-014-1298-7

Van Langenhove, T., van der Zee, J., Sleegers, K., Engelborghs, S., Vandenberghe, R., Gijselinck, I., et al. (2010). Genetic contribution of FUS to frontotemporal lobar degeneration. *Neurology* 74, 366–371. doi: 10.1212/WNL.0b013e3181ccc732

Van Mossevelde, S., Engelborghs, S., van der Zee, J., and Van Broeckhoven, C. (2018). Genotype–phenotype links in frontotemporal lobar degeneration. *Nat. Rev. Neurol.* 14, 363–378. doi: 10.1038/s41582-018-0009-8

Vercelletto, M., Boutoleau-Bretonnière, C., Volteau, C., Puel, M., Auriacombe, S., Sarazin, M., et al. (2011). Memantine in behavioral variant frontotemporal dementia: negative results. *J. Alzheimers. Dis.* 23, 749–759. doi: 10.3233/JAD-2010-101632

Vermeiren, Y., Janssens, J., Aerts, T., Martin, J. J., Sieben, A., Van Dam, D., et al. (2016). Brain serotonergic and noradrenergic deficiencies in behavioral variant frontotemporal dementia compared to early-onset Alzheimer's Disease. *J. Alzheimers Dis.* 53, 1079–1096. doi: 10.3233/JAD-160320

Vermeiren, Y., Le Bastard, N., Van Hemelrijck, A., Drinkenburg, W. H., Engelborghs, S., and De Deyn, P. P. (2013). Behavioral correlates of cerebrospinal fluid amino acid and biogenic amine neurotransmitter alterations in dementia. *Alzheimers Dement.* 9, 488–498. doi: 10.1016/j.jalz.2012.06.010

Wang, Z., Neely, R., and Landisman, C. E. (2015). Activation of Group I and Group II metabotropic glutamate receptors causes LTD and LTP of electrical synapses in the rat thalamic reticular nucleus. *J. Neurosci.* 35, 7616–7625. doi: 10.1523/JNEUROSCI.3688-14.2015

Warmus, B. A., Sekar, D. R., McCutchen, E., Schellenberg, G. D., Roberts, R. C., McMahon, L. L., et al. (2014). Tau-mediated NMDA receptor impairment underlies dysfunction of a selectively vulnerable network in a mouse model of frontotemporal dementia. *J. Neurosci.* 34, 16482–16495. doi: 10.1523/JNEUROSCI.3418-14.2014

Watts, G. D. J., Wymer, J., Kovach, M. J., Mehta, S. G., Mumm, S., Darvish, D., et al. (2004). Inclusion body myopathy associated with Paget disease of bone and frontotemporal dementia is caused by mutant valosin-containing protein. *Nat. Genet.* 36, 377–381. doi: 10.1038/ng1332

Yamashita, T., and Kwak, S. (2014). The molecular link between inefficient GluA2 Q/R site-RNA editing and TDP-43 pathology in motor neurons of sporadic amyotrophic lateral sclerosis patients. *Brain Res.* 1584, 28–38. doi: 10.1016/j.brainres.2013.12.011

Ziemann, U., Chen, R., Cohen, L. G., and Hallett, M. (1998). Dextromethorphan decreases the excitability of the human motor cortex. *Neurology* 51, 1320–1324. doi: 10.1212/WNL.51.5.1320

Ziemann, U., Reis, J., Schwenkreis, P., Rosanova, M., Strafella, A., Badawy, R., et al. (2015). TMS and drugs revisited 2014. *Clin. Neurophysiol.* 126, 1847–1868. doi: 10.1016/j.clinph.2014.08.028

Conflict of Interest Statement: The authors declare that the research was conducted in the absence of any commercial or financial relationships that could be construed as a potential conflict of interest.

frontiers in Neuroscience

ORIGINAL RESEARCH
published: 04 April 2019
doi: 10.3389/fnins.2019.00298

Persistent and Progressive Outer Retina Thinning in Frontotemporal Degeneration

Benjamin J. Kim[1], Murray Grossman[2], Delu Song[1], Samantha Saludades[1], Wei Pan[1], Sophia Dominguez-Perez[2], Joshua L. Dunaief[1], Tomas S. Aleman[1], Gui-Shuang Ying[1] and David J. Irwin[2]*

[1] Department of Ophthalmology, Scheie Eye Institute, Perelman School of Medicine, University of Pennsylvania, Philadelphia, PA, United States, [2] Department of Neurology, Frontotemporal Lobar Degeneration Center, Perelman School of Medicine, University of Pennsylvania, Philadelphia, PA, United States

Objective: While Alzheimer's disease is associated with inner retina thinning measured by spectral-domain optical coherence tomography (SD-OCT), our previous cross-sectional study suggested outer retina thinning in frontotemporal degeneration (FTD) patients compared to controls without neurodegenerative disease; we sought to evaluate longitudinal changes of this potential biomarker.

Methods: SD-OCT retinal layer thicknesses were measured at baseline and after 1–2 years. Clinical criteria, genetic analysis, and a cerebrospinal fluid biomarker (total tau: β-amyloid) to exclude likely underlying Alzheimer's disease pathology were used to define a subgroup of predicted molecular pathology (i.e., tauopathy). Retinal layer thicknesses and rates of change in all FTD patients (n = 16 patients, 30 eyes) and the tauopathy subgroup (n = 9 patients,16 eyes) were compared to controls (n = 30 controls, 47 eyes) using a generalized linear model accounting for inter-eye correlation and adjusting for age, sex, and race. Correlations between retinal layer thicknesses and Mini-Mental State Examinations (MMSE) were assessed.

Results: Compared to controls, returning FTD patients (143 vs. 130 μm, p = 0.005) and the tauopathy subgroup (143 vs. 128 μm, p = 0.03) had thinner outer retinas but similar inner layer thicknesses. Compared to controls, the outer retina thinning rate was not significant for all FTD patients (p = 0.34), but was significant for the tauopathy subgroup (−3.9 vs. 0.4 μm/year, p = 0.03). Outer retina thickness change correlated with MMSE change in FTD patients (Spearman rho = 0.60, p = 0.02) and the tauopathy subgroup (rho = 0.73, p = 0.04).

Conclusion: Our finding of FTD outer retina thinning persists and longitudinally correlates with disease progression. These findings were especially seen in probable tauopathy patients, which showed progressive outer retina thinning.

Keywords: frontotemporal degeneration, optical coherence tomography, retina, tauopathy, progressive supranuclear palsy

OPEN ACCESS

Edited by:
Annakaisa Haapasalo, University of Eastern Finland, Finland

Reviewed by:
Michel Cayouette, Montreal Clinical Research Institute (IRCM), Canada
Ilaria Piano, University of Pisa, Italy

****Correspondence:***
Benjamin J. Kim
benjamin.kim@uphs.upenn.edu

Specialty section:
This article was submitted to Neurodegeneration, a section of the journal Frontiers in Neuroscience

Received: *27 December 2018*
Accepted: *15 March 2019*
Published: *04 April 2019*

Citation:
Kim BJ, Grossman M, Song D, Saludades S, Pan W, Dominguez-Perez S, Dunaief JL, Aleman TS, Ying G-S and Irwin DJ (2019) Persistent and Progressive Outer Retina Thinning in Frontotemporal Degeneration. Front. Neurosci. 13:298. doi: 10.3389/fnins.2019.00298

INTRODUCTION

Frontotemporal degeneration (FTD) syndromes can have clinical presentations that overlap with Alzheimer's Disease (AD) (Irwin et al., 2015). Up to 30% of clinically diagnosed FTD patients receive a primary neuropathologic diagnosis of AD (Kertesz et al., 2005; Knibb et al., 2006; Irwin et al., 2013). There are predominantly two pathologic FTD subtypes (i.e., frontotemporal lobar degeneration, FTLD): FTLD-Tau, which has inclusions of the microtubule-associated protein tau, and FTLD-TDP, which has TAR DNA-binding protein 43 (TDP-43) inclusions (Irwin et al., 2015). FTD clinical trials are challenged by an inability to determine the causative molecular pathology of patients until autopsy.

Spectral-domain optical coherence tomography (SD-OCT) provides highly reproducible retinal thickness measurements in cognitively impaired patients (Loh et al., 2017). We previously found photoreceptor thinning visualized by SD-OCT in mice with a mutation in *RP1*, a microtubule-associated protein (Song et al., 2014). Since tau is a microtubule-associated protein also expressed in the retina, we hypothesized that tauopathies may have photoreceptor abnormalities detectable by SD-OCT. In a cross-sectional study of FTD patients predominantly composed of probable tauopathy patients, we found that FTD is associated with outer retina (photoreceptor layer) thinning compared to normal controls (Kim et al., 2017). This contrasts with numerous reports of SD-OCT detected inner retina (nerve fiber and ganglion cell layer) thinning associated with AD and confirmed with histopathology (Hinton et al., 1986; Cheung et al., 2015; Coppola et al., 2015; Garcia-Martin et al., 2016; Chan et al., 2018). Furthermore, amyotrophic lateral sclerosis, which has clinical-pathological overlap with FTLD-TDP, is associated with inner retina thinning (Irwin et al., 2015; Volpe et al., 2015).

Longitudinal SD-OCT measurements can provide invaluable data that substantiates cross-sectional data, demonstrates temporal relationships between retinal layers and disease outcomes, and provides causal evidence for the hypothesis that outer retina thinning is associated with progressive tau pathology in FTD. Here, we report longitudinal data for our cohort of deeply phenotyped FTD patients and controls.

MATERIALS AND METHODS

Participants

The recruitment of patients and controls at baseline was described previously (Kim et al., 2017). Briefly, consecutive patients with FTD clinical syndromes [progressive supranuclear palsy (PSP), corticobasal syndrome (CBS), primary progressive aphasia (PPA), and behavioral variant of FTD (bvFTD)] were prospectively enrolled at the Penn Frontotemporal Degeneration Center of the University of Pennsylvania. These patients were all reviewed in a consensus conference and diagnosed according to published clinical criteria (Rascovsky et al., 2011; Irwin et al., 2015; Hoglinger et al., 2017). Neurologists masked to SD-OCT data performed a Mini-Mental State Examination (MMSE) within 12 months of enrollment. Twenty-seven patients were evaluated at baseline.

To determine subgroups, we used the same methodology as the one employed in our previous study (Kim et al., 2017). We used a combination of previously validated cerebrospinal fluid (CSF) (Irwin et al., 2012; Lleo et al., 2018), genetic (Irwin et al., 2015), and clinical criteria (Gorno-Tempini et al., 2011; Irwin et al., 2015; Hoglinger et al., 2017) predictive of underlying pathology to define subgroups (tauopathy, TDP-43, and unknown pathology) of highly predictive pathologic subtypes. First, patients with a total tau:Aβ ratio > 0.34 were considered to have presumed AD and excluded from analyses (Shaw et al., 2009; Irwin et al., 2012, 2013). Next, patients were genotyped according to risk of hereditary disease for pathogenic mutations based on structured pedigree analysis (Wood et al., 2013). This included *MAPT* (OMIM:157140), which is predictive of FTLD-Tau, and the following mutations predictive of FTLD-TDP: progranulin (*GRN*) (OMIM:138945), *C9orf72* (OMIM: 61426), and *TARDBP* p.I383V (OMIM: 605078; p.N39OS). Finally, patients meeting criteria for clinical phenotypes of PSP, non-fluent PPA, and CBS (along with non-AD CSF and absence of GRN mutation) were categorized as FTLD-Tau, as sporadic FTLD-TDP is rare in these clinical phenotypes. Those meeting criteria for the semantic variant of PPA were categorized as FTLD-TDP due to the rarity of sporadic FTLD-Tau with this phenotype (Litvan et al., 1996; Josephs et al., 2006; Irwin et al., 2013; Hoglinger et al., 2017; Spinelli et al., 2017).

At baseline, 44 consecutive healthy controls were prospectively recruited as previously described from the Scheie Eye Institute (Kim et al., 2017). These controls had no history of diabetes or neurodegenerative disease and were originally intended for several SD-OCT studies of different diseases.

From August 2015 to January 2018, we asked patients and controls to return for a single follow-up retinal imaging visit that was approximately 1–2 years after their baseline visit. At this follow-up visit, all participants had another comprehensive, dilated eye examination to diagnose any new ophthalmic disease. Patients also had another neurological exam including a MMSE within 4 months of their follow-up retinal imaging visit. No autopsy data became available for any patient with a follow-up visit.

The University of Pennsylvania Institutional Review Board approved this study, and all participants (or caregivers when appropriate) provided written informed consent in accordance with the Declaration of Helsinki.

SD-OCT Protocol and Image Analysis

At the follow-up visit, all participants completed an SD-OCT imaging protocol using the same methodology as the one employed in our baseline study (Kim et al., 2017). All participants underwent SD-OCT imaging with the Heidelberg Spectralis (Heidelberg Engineering, Carlsbad, CA, United States) with a standard macular volume scan protocol of 20° images, 25 high-resolution raster scans, and automated real time averaging of 25. Images met OSCAR-IB quality control criteria that relate to macular volume scans (Tewarie et al., 2012). An analyst masked to clinical information segmented individual retinal layers using

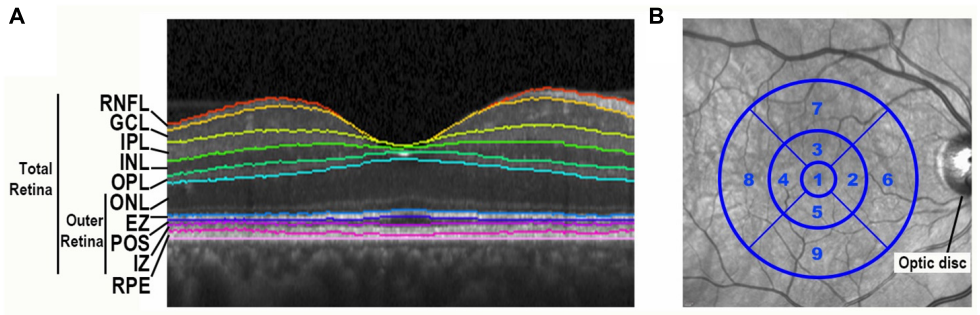

FIGURE 1 | Spectral-domain optical coherence tomography retinal image segmentation and ETDRS grid centered on the fovea. **(A)** Segmentation of a spectral-domain optical coherence tomography (SD-OCT) retina image by the Iowa Reference Algorithm. A portion of a SD-OCT image taken through the fovea is shown with retinal layers labeled. RNFL, retinal nerve fiber layer; GCL, ganglion cell layer; IPL, inner plexiform layer; INL, inner nuclear layer; OPL, outer plexiform layer; ONL, outer nuclear layer; EZ, ellipsoid zone; POS, photoreceptor outer segments; IZ, interdigitation zone; RPE, retinal pigment epithelium. **(B)** The standard Early Treatment Diabetic Retinopathy Study (ETDRS) grid is centered on the fovea of an infrared fundus image.

the well-validated Iowa Reference Algorithm (IRA) (v3.6), and algorithm segmentation errors were manually corrected (Li et al., 2006; Garvin et al., 2009; Abramoff et al., 2010). This algorithm segmented 11 optical interfaces (10 layers) and provided thickness readings for the 9 regions of the standard Early Treatment of Diabetic Retinopathy Study (ETDRS) grid centered at the fovea. Total retina thickness (neurosensory retina) was defined as the distance from the retinal nerve fiber layer's inner boundary, including the internal limiting membrane, to the interdigitation zone's outer boundary. To focus on photoreceptor layers, the outer retina thickness was defined as the distance from the outer nuclear layer's (ONL) inner boundary to the interdigitation zone's outer boundary (**Figure 1A**). With this definition, the outer retina thickness does not include the outer plexiform layer (OPL), as the OPL thickness is partially composed of horizontal and bipolar cell dendrites. Remaining consistent with our baseline study, analyses of retinal layers focused on the average of the central 5 regions of the fovea-centered ETDRS grid, which is an area with a 3 mm diameter (**Figure 1B**).

Statistical Analyses

As pre-specified, we excluded participants (or eyes) with eye diseases that may affect the retinal thickness including macular disease, retinal vascular disease, diabetic or hypertensive retinopathy, glaucoma or optic nerve disease, significant ocular media opacity, high refractive error (±6.00 diopters spherical equivalent), intraocular surgery within 90 days, or poor image quality (**Figure 2**).

We calculated the annual rate (microns per year) of retinal layer thickness change as: [(follow-up visit thickness − baseline thickness)/(months of follow-up)] × 12. We compared each of the retinal layer thicknesses measured at the follow-up time point and its annual rate of change from baseline between all patients versus controls and between each of the subgroups (tauopathy, TDP-43, unknown pathology) versus controls using generalized linear models (Liang and Zeger, 1986). These models were performed with and without adjustment for participant demographics, as age, sex, and race are known to affect retinal layer thicknesses in normal subjects (Kashani et al., 2010; Girkin et al., 2011; Demirkaya et al., 2013). The statistical adjustment for age, sex, and race is performed by including these items as covariates in the multivariable regression models for comparing retinal thickness between FTD and controls. For participants with two study eyes eligible for this study, inter-eye correlations were accounted for by using the generalized estimating equations (GEE) (Liang and Zeger, 1986). The GEE was initially developed to analyze correlated data from longitudinal repeated measures; it has been commonly applied to analyze correlated eye data, accounting for the inter-eye correlation when using the eye as the unit of analysis (Ying et al., 2017).

For all patients and the probable tauopathy subgroup, we calculated the Spearman correlation of MMSE with outer retina thickness, ONL, and ellipsoid zone (EZ) thickness. For the Spearman correlation, the average thickness of 2 eyes was used for participants with data from 2 study eyes. All statistical analyses were performed with SAS v9.4 (SAS Institute Inc., Cary, NC, United States). Two-sided $p < 0.05$ was considered statistically significant.

Data Availability

Anonymized data for this study will be shared by request from any qualified investigator.

RESULTS

Demographics

The study enrolled 27 FTD patients and 44 controls without neurodegenerative disease. After the baseline visit, two FTD patients expired and therefore were unavailable for a follow-up visit. Eighteen of the remaining 25 (72%) patients completed a follow-up visit at a mean of 15.6 months after the baseline visit (**Table 1**). Of 44 controls, 1 participant expired after baseline, and 32 of the remaining 43 (74%) controls completed a follow-up visit at a mean of 14.5 months after the baseline visit. **Figure 2** details the reasons for missed follow-up and

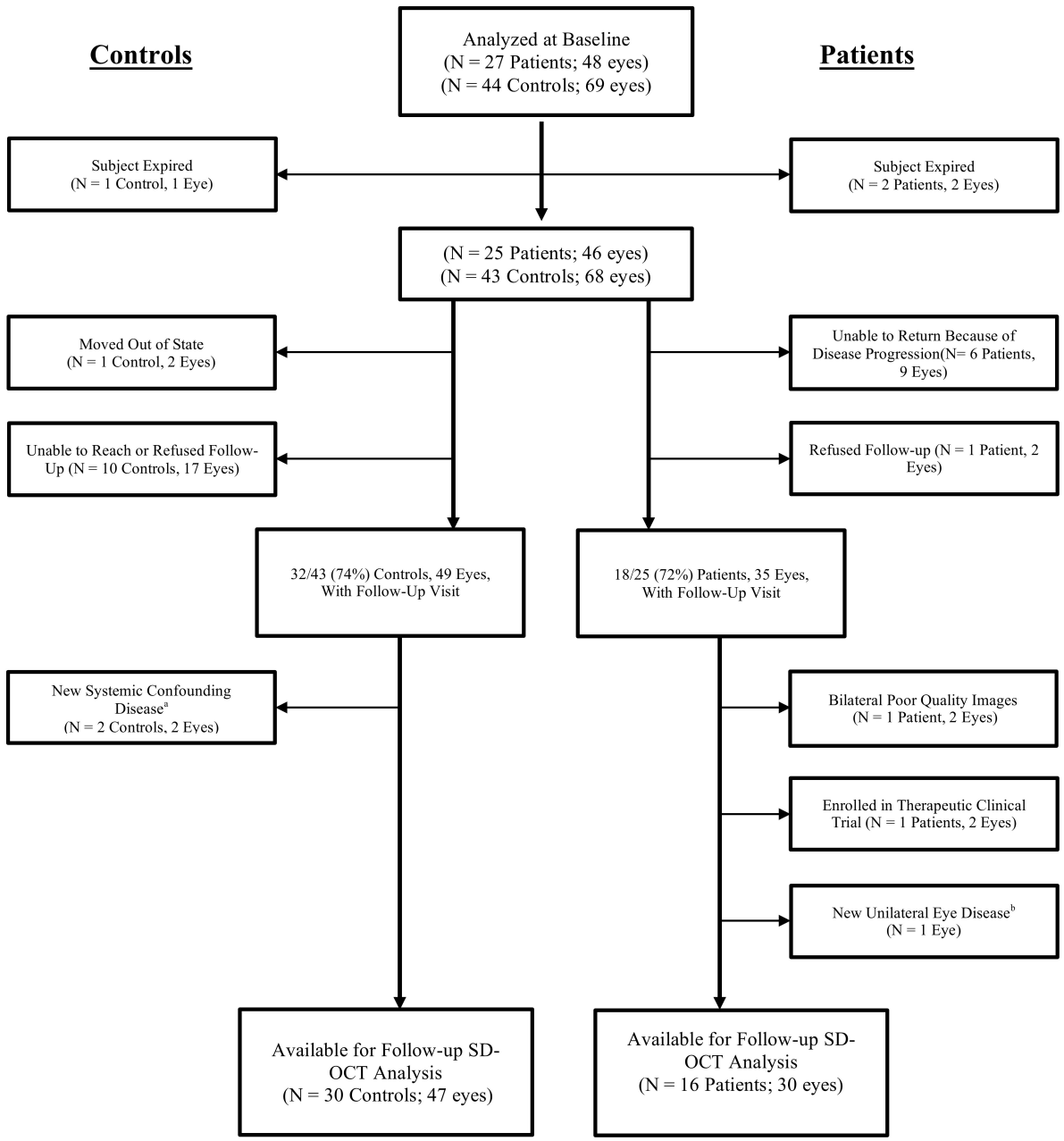

FIGURE 2 | Flow diagram of excluded subjects and eyes prior to analysis. Every patient was diagnosed with a frontotemporal degeneration clinical syndrome. SD-OCT, spectral domain optical coherence tomography. [a]One control received a new diagnosis of Parkinson's disease. One control developed severe systemic hypertension with evidence of new hypertensive retinopathy in the study eye. [b]One patient developed mild macroaneurysm of a retinal vessel at the macula in one eye.

exclusion from statistical analyses. Ultimately, 16 FTD patients (30 eyes) and 30 controls (47 eyes) were included in longitudinal data analyses. As expected from the baseline demographics, compared to controls, the FTD patients had a similar percentage of male participants but had a greater mean age and a higher percentage of Caucasian race (**Table 1**). All but one of the patients had CSF biomarker analysis to exclude AD. This patient met clinical criteria for PSP, which neuropathologically is highly specific for a tauopathy (Litvan et al., 1996; Josephs et al., 2006; Hoglinger et al., 2017).

Nine patients (16 eyes) met criteria for the probable tauopathy subgroup and their demographics are shown in **Table 1**. This subgroup included patients with the following clinical diagnoses: 4 PSP, 3 CBS, 1 non-fluent PPA, and one patient with behavioral variant of FTD with features of the semantic variant of PPA that had a *MAPT* E10+16 C > T mutation.

TABLE 1 | Demographic characteristics of FTD patients and controls.

		Controls (*N* = 30)	All FTD patients (*N* = 16)	*p*-value[a]	Probable tauopathy subgroup (*N* = 9)	*p*-value[b]
Months of follow-up						
	Mean (*SD*)	14.5 (3.2)	15.6 (4.4)	0.31	15.2 (4.2)	0.56
	Minimum, Maximum	12, 25	11, 24		11, 24	
Age at baseline (years)						
	Mean (*SD*)	53.1 (11.3)	65.6 (8.2)	<0.001	65.8 (6.7)	<0.001
	Minimum, Maximum	26, 77	53, 87		53, 76	
Sex, *n* (%)						
	Male	9 (30.0)	6 (37.5)	0.53	2 (22.2)	1.00
	Female	21 (70.0	10 (62.5)		7 (77.8)	
Race, *n* (%)						
	Caucasian	16 (53.3)	13 (81.3)	<0.001	7 (77.8)	0.01
	African–American	12 (40.0)	0 (0.0)		0 (0.0)	
	Other/unknown	2 (6.7)	3 (18.8)		2 (22.2)	

FTD, frontotemporal degeneration; SD, standard deviation. [a]p-value for comparison of controls and patients. [b]p-value for comparison of controls and probable tauopathy subgroup.

TABLE 2 | Comparisons of retinal layer thicknesses (microns) between all patients and normal controls at follow-up visit.

	Unadjusted analysis			Adjusted analysis[c]		
Retinal layer[a]	Controls (*N* = 30, 47 eyes) Mean (*SE*)	Patients (*N* = 16, 30 eyes) Mean (*SE*)	*p*-value[b]	Controls (*N* = 30, 47 eyes) Mean (*SE*)	Patients (*N* = 16, 30 eyes) Mean (*SE*)	*p*-value[b]
Total retina	304 (2.3)	301 (3.1)	0.47	306 (3.1)	299 (4.6)	0.27
Outer retina	142 (1.4)	133 (2.1)	**0.008**	143 (1.6)	130 (2.9)	**0.005**
RNFL	23.5 (0.4)	24.3 (0.6)	0.35	23.8 (0.5)	23.9 (0.8)	0.87
GCL	39.6 (1.1)	39.5 (1.1)	0.96	38.2 (1.6)	41.4 (1.7)	0.28
IPL	38.9 (0.9)	39.6 (1.1)	0.68	39.6 (1.3)	39.0 (1.4)	0.89
INL	35.7 (0.5)	35.4 (0.8)	0.78	36.1 (0.6)	35.0 (1.0)	0.47
OPL	24.5 (0.6)	29.2 (1.2)	**0.01**	24.7 (0.8)	28.7 (1.4)	0.053
ONL	96.1 (1.2)	90.1 (1.8)	**0.04**	98.6 (1.5)	86.3 (2.3)	**0.003**
EZ	15.1 (0.1)	14.2 (0.1)	**<0.001**	15.1 (0.2)	14.3 (0.2)	**0.007**
POS	11.8 (0.4)	10.7 (0.5)	0.22	11.4 (0.6)	11.4 (0.8)	0.99
IZ	18.9 (0.5)	17.6 (0.5)	0.17	18.3 (0.6)	18.5 (0.8)	0.88
RPE	18.2 (0.5)	19.0 (0.7)	0.43	18.7 (0.7)	18.2 (0.9)	0.70

SE, standard error; RNFL, retinal nerve fiber layer; GCL, ganglion cell layer; IPL, inner plexiform layer; INL, inner nuclear layer; OPL, outer plexiform layer; ONL, outer nuclear layer; EZ, ellipsoid zone; POS, photoreceptor outer segments; IZ, interdigitation zone; RPE, retinal pigment epithelium. [a]Spectral domain optical coherence tomography (SD-OCT) parameters (in microns) are the average of five central subfields (central and 4 parafoveal subfields) of the Early Treatment Diabetic Retinopathy Study (ETDRS) grid centered at the foveola. Total retina: distance from RNFL to IZ; Outer Retina: distance from ONL to IZ. [b]Inter-eye correlation of SD-OCT measurements was accounted for using generalized estimating equations (GEE); significant values ($p < 0.05$) in bold letters. [c]Adjusted for age, sex, and race.

Comparison of Retinal Thicknesses at Follow-Up Between Patients and Controls

First, we compared the retinal layer thicknesses between all FTD patients and controls cross-sectionally at the follow-up visit time-point only. For the outer retina thickness, we used our pre-specified definition (see section "Materials and Methods" and **Figure 1A**) which includes all retinal photoreceptor layers but does not include the outer plexiform layer (OPL) as the OPL thickness is composed, in part, of horizontal and bipolar cell dendrites. Compared to controls, FTD patients had a thinner ONL, EZ, and outer retina thickness in both univariate analysis and multivariate analysis adjusted for age, sex, and race (all $p < 0.05$, **Table 2**). Observed outer retina thickness values at baseline and follow-up for each eye are shown in **Table 3** for FTD patients and **Table 4** for controls. The OPL of FTD patients was thicker than that of controls in univariate analysis ($p = 0.01$), but this was not significant in multivariate analysis ($p = 0.053$, **Table 2**).

Next, we compared the retinal layer thicknesses at the follow-up visit between only the probable tauopathy subgroup and controls. The tauopathy subgroup had a significantly thinner EZ and outer retina thickness than controls, even after adjusting by age, sex, and race (all $p < 0.05$, **Table 5**). Tauopathy patients also

TABLE 3 | Outer retina thickness measurements (microns) at baseline and follow-up for frontotemporal degeneration patients (*N* = 16 patients, 30 eyes).

Subject number	Subgroup	Eye	Baseline outer retina thickness	Follow-up outer retina thickness	Change in outer retina thickness	Length of follow-up (months)
1	Probable tauopathy	OS	144.7	142.9	−1.8	12
2	Probable tauopathy	OD	108.8	109.4	0.6	11
		OS	120.8	118.0	−2.8	11
3	Probable tauopathy	OD	143.2	145.1	1.9	13
		OS	143.9	147.7	3.9	13
4	Probable tauopathy	OD	130.2	127.0	−3.2	19
		OS	132.9	123.8	−9.1	19
5	Probable tauopathy	OD	129.1	115.3	−13.7	18
		OS	130.5	127.2	−3.3	18
6	Probable tauopathy	OD	140.6	136.6	−4.0	14
		OS	143.7	142.5	−1.2	14
7	Probable tauopathy	OD	140.7	127.4	−13.3	12
		OS	124.1	125.3	1.2	12
8	Probable tauopathy	OS	150.5	151.7	1.2	12
9	Probable tauopathy	OD	141.8	122.0	−19.8	24
		OS	136.8	121.2	−15.6	24
10	Probable TDP	OD	123.4	146.5	23.1	12
		OS	117.1	124.3	7.2	12
11	Probable TDP	OD	124.5	136.6	12.1	24
		OS	142.1	140.5	−1.6	24
12	Unknown pathology	OD	151.2	152.6	1.4	12
		OS	137.0	149.4	12.4	12
13	Unknown pathology	OD	122.8	133.0	10.3	21
		OS	137.8	118.4	−19.4	21
14	Unknown pathology	OD	128.5	125.3	−3.2	13
		OS	142.5	130.2	−12.2	13
15	Unknown pathology	OD	137.8	130.1	−7.7	18
		OS	140.5	141.5	1.0	18
16	Unknown pathology	OD	133.4	130.7	−2.8	12
		OS	134.7	136.3	1.5	12

TDP, TAR DNA binding protein.

had a significantly thinner total retina thickness in the univariate analysis (p = 0.04), but this difference was not significant after adjusting for age, sex, and race (p = 0.07, **Table 5**). There was non-significant thinning of the ONL in the univariate analysis (p = 0.11) and this became significant (p = 0.02) in the multivariate analysis.

Comparisons of the Rate of Retinal Layer Thickness Change Between Patients and Controls

We compared the annual rate of change for the retinal layer thickness between all FTD patients and controls. The FTD patients did not show a significant difference in the rate of change of retinal layer thicknesses as compared to controls (**Table 6**). After adjusting for age, sex, and race, the FTD patients demonstrated an inner nuclear layer rate of thinning that was of borderline significance compared to controls (−0.5 vs. +0.2 μm/year, p = 0.046). There was no significant difference in the rate of outer retina change (p = 0.34, **Table 6**).

When evaluating only the probable tauopathy subgroup compared to controls, we found a significant rate of thinning of the outer retina (p = 0.04) and a significant rate of thickening of the OPL (p = 0.02) in univariate analysis (**Table 7**). After adjusting for age, sex, and race, the probable tauopathy subgroup showed a significant rate of thinning of the ONL (p = 0.04), inner nuclear layer (INL, p = 0.02), and outer retina (p = 0.03) compared to controls (**Table 7**). The rate of OPL thickening remained significant (p = 0.008). **Figure 3** shows representative images of progressive outer retina thinning in a probable tauopathy patient compared to a control of similar demographics.

Retinal Thickness Correlations With the Change in Disease Severity

Using the retinal layer thicknesses (ONL, EZ, and outer retina) that we found to be different from controls, we evaluated the correlation of these SD-OCT retinal thicknesses and MMSE. Among all FTD patients, the baseline measurements of outer retina, ONL, and EZ thicknesses were not significantly correlated

TABLE 4 | Outer retina thickness measurements (microns) at baseline and follow-up for normal controls (*N* = 30 subjects, 47 eyes).

Subject number	Eye	Baseline outer retina thickness	Follow-up outer retina thickness	Change in outer retina thickness	Length of follow-up (months)
1	OD	145.6	144.9	−0.7	13
	OS	144.5	146.0	1.6	13
2	OD	120.9	118.5	−2.3	13
	OS	121.8	120.0	−1.8	13
3	OS	149.9	149.6	−0.3	13
4	OD	137.8	138.9	1.1	24
	OS	145.5	147.3	1.8	24
5	OD	136.7	144.0	7.2	13
6	OS	139.2	139.3	0.1	13
7	OD	147.1	147.3	0.2	13
	OS	149.1	150.3	1.1	13
8	OD	143.5	139.8	−3.8	13
	OS	140.8	139.3	−1.4	13
9	OD	138.2	128.2	−10.0	12
	OS	135.0	138.9	4.0	12
10	OS	147.0	152.9	6.0	12
11	OS	139.0	136.2	−2.7	13
12	OD	150.5	156.2	5.7	13
	OS	157.3	161.0	3.7	13
13	OD	145.7	147.3	1.7	25
14	OD	151.6	149.0	−2.7	13
	OS	155.1	151.1	−4.0	13
15	OD	137.8	137.1	−0.7	13
	OS	135.6	133.6	−2.1	13
16	OS	130.4	140.3	9.9	13
17	OD	147.2	145.5	−1.7	13
	OS	135.9	133.6	−2.4	13
18	OD	152.0	151.2	−0.8	13
19	OD	135.6	141.4	5.8	13
	OS	132.0	128.8	−3.2	13
20	OS	176.8	166.7	−10.0	16
21	OD	145.4	141.2	−4.2	20
	OS	135.4	139.8	4.4	20
22	OD	138.5	134.7	−3.8	14
	OS	141.3	137.2	−4.1	14
23	OD	138.8	134.0	−4.8	17
	OS	140.2	144.1	3.8	17
24	OD	149.0	142.1	−6.9	18
	OS	142.2	140.3	−1.9	18
25	OD	122.2	124.2	1.9	12
26	OD	146.1	139.2	−7.0	13
27	OD	148.4	149.0	0.6	13
28	OD	132.2	140.2	8.0	14
	OS	138.6	138.0	−0.6	14
29	OD	142.6	144.9	2.3	14
	OS	145.7	144.3	−1.4	14
30	OS	132.3	154.6	22.3	17

with the change of MMSE (all $p \geq 0.60$, **Table 8**). However, the SD-OCT follow-up measurements of the ONL (rho = 0.54, $p = 0.04$) and outer retina (rho = 0.56, $p = 0.03$) were positively correlated with the follow-up MMSE. The change of thickness of the ONL (rho = 0.69, $p = 0.005$) and outer retina (rho = 0.79, $p < 0.001$) were also positively correlated with the follow-up MMSE. Additionally, the change of thickness of the outer retina were positively correlated with the change of MMSE (rho = 0.60, $p = 0.02$, **Table 8**).

Among only the probable tauopathy subgroup, the change of thickness of the outer retina was positively correlated with the follow-up MMSE (rho = 0.75, $p = 0.03$). Furthermore, the change of the outer retina thickness was positively correlated with the change of the MMSE (rho = 0.73, $p = 0.04$, **Table 8**).

Analysis of TDP-43 and Unknown Pathology Subgroups

There were two probable TDP-43 patients (four eyes), including one patient with a hexanucleotide expansion in *C9orf72*. Compared to controls, the probable TDP subgroup had no significant findings for the thickness of any of the retinal layers in unadjusted analysis and an adjusted analysis (data not shown). Similarly, compared to controls, the probable TDP subgroup had no significant findings for the rate of thickness change of any of the retinal layers in unadjusted and an adjusted analysis (data not shown).

Five behavioral variant of FTD patients (10 eyes) were categorized as unknown molecular pathology due to the poor predictive value for molecular pathology of this clinical FTD syndrome (Irwin et al., 2015). Compared to controls, the unknown pathology subgroup had no significant findings for the thickness of any of the retinal layers in unadjusted analysis and an adjusted analysis (data not shown). Similarly, compared to controls, the unknown pathology subgroup had no significant findings for the rate of thickness change of any of the retinal layers in unadjusted and an adjusted analysis (data not shown).

DISCUSSION

Spectral-domain optical coherence tomography imaging is increasingly investigated as a biomarker for neurodegenerative conditions. Before using this potential biomarker in clinical care or clinical trials, longitudinal data is critically important to understand the rate of retinal layer change and how retinal layer thicknesses temporally relate to disease subgroups and outcomes. Longitudinal SD-OCT studies in dementia patients are scarce with only a few reports (Shen et al., 2013; Choi et al., 2016; Mutlu et al., 2018) suggesting that inner retina layer thicknesses may be a marker for dementia progression (Choi et al., 2016) or development (Mutlu et al., 2018). There is no longitudinal SD-OCT data for FTD to our knowledge. With a group of deeply phenotyped FTD patients followed for about 16 months, our study demonstrates persistent outer retina thinning with no development of inner retina thinning compared to normal controls, and the thinning of the outer retina significantly correlated with the decline in MMSE. The results from this longitudinal study, along with our previously reported cross-sectional study in the same study cohort (Kim et al., 2017), support the outer retina thickness as a potential biomarker for FTD patients.

TABLE 5 | Comparisons of retinal layer thicknesses (microns) between probable tauopathy subgroup patients and normal controls at follow-up visit.

	Unadjusted analysis			Adjusted analysis[c]		
Retinal layer[a]	**Controls (*N* = 30, 47 eyes) Mean (*SE*)**	**Probable tauopathy patients (*N* = 9, 16 eyes) Mean (*SE*)**	***p*-value[b]**	**Controls (*N* = 30, 47 eyes) Mean (*SE*)**	**Probable tauopathy patients (*N* = 9, 16 eyes) Mean (*SE*)**	***p*-value[b]**
Total retina	304 (2.3)	292 (2.9)	**0.04**	305 (2.9)	291 (4.9)	0.07
Outer retina	142 (1.4)	130 (3.2)	**0.03**	143 (1.6)	128 (4.4)	**0.03**
RNFL	23.5 (0.4)	23.5 (0.9)	0.96	23.5 (0.5)	23.4 (1.3)	0.92
GCL	39.6 (1.1)	37.7 (1.1)	0.33	38.9 (1.4)	39.7 (2.1)	0.79
IPL	38.9 (0.9)	37.5 (1.4)	0.49	39.1 (1.1)	36.9 (1.9)	0.40
INL	35.7 (0.5)	34.0 (0.7)	0.14	35.8 (0.6)	33.8 (0.8)	0.11
OPL	24.5 (0.6)	29.5 (1.9)	0.07	24.9 (0.8)	28.4 (2.2)	0.19
ONL	96.1 (1.2)	89.1 (2.5)	0.11	97.6 (1.4)	85.2 (3.7)	**0.02**
EZ	15.1 (0.1)	14.0 (0.1)	**0.002**	15.0 (0.2)	14.3 (0.2)	**0.02**
POS	11.8 (0.4)	10.1 (0.5)	0.09	11.6 (0.6)	10.7 (1.0)	0.49
IZ	18.9 (0.5)	17.0 (0.7)	0.13	18.4 (0.6)	18.2 (1.1)	0.86
RPE	18.2 (0.5)	20.1 (0.8)	0.17	18.5 (0.6)	19.1 (1.1)	0.67

SE, standard error; RNFL, retinal nerve fiber layer; GCL, ganglion cell layer; IPL, inner plexiform layer; INL, inner nuclear layer; OPL, outer plexiform layer; ONL, outer nuclear layer; EZ, ellipsoid zone; POS, photoreceptor outer segments; IZ, interdigitation zone; RPE, retinal pigment epithelium. [a]Spectral domain optical coherence tomography (SD-OCT) parameters (in microns) are the average of five central subfields (central and 4 parafoveal subfields) of the Early Treatment Diabetic Retinopathy Study (ETDRS) grid centered at the foveola. Total retina: distance from RNFL to IZ; Outer Retina: distance from ONL to IZ. [b]Inter-eye correlation of SD-OCT measurements was accounted for using generalized estimating equations (GEE); significant values ($p < 0.05$) in bold letters. [c]Adjusted for age, sex, and race.

TABLE 6 | Comparisons of rate (microns per year) of retinal layer thickness change between all patients and controls.

	Unadjusted analysis			Adjusted analysis[c]		
Retinal layer[a]	**Controls (*N* = 30, 47 eyes) Mean (*SE*)**	**Patients (*N* = 16, 30 eyes) Mean (*SE*)**	***p*-value[b]**	**Controls (*N* = 30, 47 eyes) Mean (*SE*)**	**Patients (*N* = 16, 30 eyes) Mean (*SE*)**	***p*-value[b]**
Total retina	0.5 (0.6)	0.1 (0.9)	0.81	0.9 (0.8)	−0.2 (1.3)	0.60
Outer retina	0.1 (0.7)	−0.9 (1.3)	0.52	0.7 (0.8)	−1.5 (1.6)	0.34
RNFL	0.3 (0.3)	0.9 (0.4)	0.31	0.3 (0.4)	1.0 (0.6)	0.36
GCL	−1.0 (0.5)	−0.9 (1.1)	0.95	−1.3 (0.8)	−0.4 (1.3)	0.61
IPL	1.1 (0.5)	0.1 (1.0)	0.38	1.6 (0.8)	−0.4 (1.2)	0.26
INL	0.0 (0.2)	−0.2 (0.2)	0.42	0.2 (0.2)	−0.5 (0.2)	**0.046**
OPL	−0.2 (0.4)	1.1 (0.8)	0.22	−0.5 (0.5)	1.5 (0.9)	0.09
ONL	−0.1 (0.4)	−1.0 (0.9)	0.45	0.3 (0.6)	−1.5 (1.1)	0.23
EZ	−0.1 (0.1)	−0.3 (0.1)	0.11	−0.1 (0.1)	−0.3 (0.1)	0.23
POS	0.1 (0.1)	0.1 (0.2)	0.91	0.1 (0.2)	0.2 (0.3)	0.73
IZ	0.2 (0.3)	0.2 (0.4)	0.94	0.3 (0.3)	0.1 (0.4)	0.82
RPE	−0.1 (0.3)	−0.1 (0.5)	0.93	−0.3 (0.3)	0.1 (0.5)	0.69

SE, standard error; RNFL, retinal nerve fiber layer; GCL, ganglion cell layer; IPL, inner plexiform layer; INL, inner nuclear layer; OPL, outer plexiform layer; ONL, outer nuclear layer; EZ, ellipsoid zone; POS, photoreceptor outer segments; IZ, interdigitation zone; RPE, retinal pigment epithelium. [a]Spectral domain optical coherence tomography (SD-OCT) parameters (in microns) are the average of five central subfields (central and 4 parafoveal subfields) of the Early Treatment Diabetic Retinopathy Study (ETDRS) grid centered at the foveola. Total retina: distance from RNFL to IZ; Outer Retina: distance from ONL to IZ. [b]Inter-eye correlation of SD-OCT measurements was accounted for using generalized estimating equations (GEE); significant values ($p < 0.05$) in bold letters. [c]Adjusted for age, sex, and race.

Although there has been some mild inconsistency in OCT studies of AD patients, the large majority of OCT studies (Coppola et al., 2015; Garcia-Martin et al., 2016), as well as histopathologic data (Hinton et al., 1986; Koronyo et al., 2017), have shown that AD is associated with inner retina thinning (retinal nerve fiber layer and ganglion cell layer) without outer retina abnormalities (Uchida et al., 2018). The exact cause for the inner retina thinning is unclear, but it may be related to Aβ toxicity within the inner retina as opposed to being a reflection of generalized neuronal loss within the central nervous system (Koronyo et al., 2017). Importantly, our longitudinal data of FTD patients did not show any evidence of retinal

TABLE 7 | Comparisons of rate (microns per year) of retinal layer thickness change between probable tauopathy subgroup patients and controls.

	Unadjusted analysis			Adjusted analysis[c]		
Retinal layer[a]	Controls (*N* = 30, 47 eyes) Mean (*SE*)	Patients (*N* = 9, 16 eyes) Mean (*SE*)	*p*-value[b]	Controls (*N* = 30, 47 eyes) Mean (*SE*)	Patients (*N* = 9, 16 eyes) Mean (*SE*)	*p*-value[b]
Total retina	0.5 (0.6)	−0.8 (0.7)	0.29	0.8 (0.7)	−1.8 (1.0)	0.09
Outer retina	0.1 (0.7)	−3.2 (1.2)	**0.04**	0.4 (0.7)	−3.9 (1.3)	**0.03**
RNFL	0.3 (0.3)	0.8 (0.4)	0.32	0.3 (0.4)	0.8 (0.6)	0.52
GCL	−1.0 (0.5)	0.8 (1.1)	0.24	−1.2 (0.7)	1.4 (1.8)	0.24
IPL	1.1 (0.5)	−1.4 (1.0)	0.08	1.5 (0.7)	−2.5 (1.6)	0.06
INL	0.0 (0.2)	−0.5 (0.3)	0.11	0.2 (0.2)	−0.9 (0.3)	**0.02**
OPL	−0.2 (0.4)	2.7 (0.8)	**0.02**	−0.3 (0.4)	3.3 (0.9)	**0.008**
ONL	−0.1 (0.4)	−2.2 (0.8)	0.08	0.1 (0.5)	−2.9 (1.1)	**0.04**
EZ	−0.1 (0.1)	−0.4 (0.1)	0.09	−0.1 (0.1)	−0.4 (0.2)	0.22
POS	0.1 (0.1)	0.1 (0.3)	0.90	0.1 (0.2)	0.0 (0.3)	0.84
IZ	0.2 (0.3)	−0.6 (0.4)	0.11	0.2 (0.3)	−0.7 (0.5)	0.14
RPE	−0.1 (0.3)	0.9 (0.6)	0.12	−0.2 (0.3)	1.0 (0.7)	0.14

SE, standard error; RNFL, retinal nerve fiber layer; GCL, ganglion cell layer; IPL, inner plexiform layer; INL, inner nuclear layer; OPL, outer plexiform layer; ONL, outer nuclear layer; EZ, ellipsoid zone; POS, photoreceptor outer segments; IZ, interdigitation zone; RPE, retinal pigment epithelium. [a]Spectral domain optical coherence tomography (SD-OCT) parameters (in microns) are the average of five central subfields (central and 4 parafoveal subfields) of the Early Treatment Diabetic Retinopathy Study (ETDRS) grid centered at the foveola. Total retina: distance from RNFL to IZ; Outer Retina: distance from ONL to IZ. [b]Inter-eye correlation of SD-OCT measurements was accounted for using generalized estimating equations (GEE); significant values ($p < 0.05$) in bold letters. [c]Adjusted for age, sex, and race.

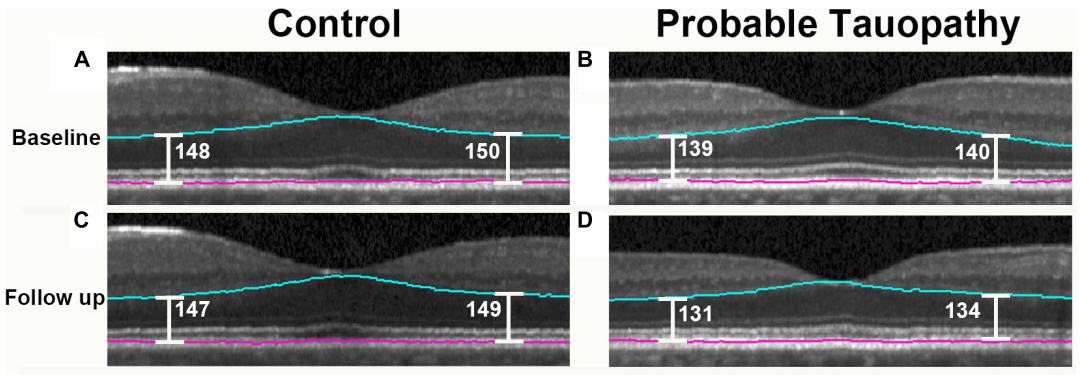

FIGURE 3 | Probable tauopathy patient with progressive outer retina thinning compared to a control. Representative spectral domain optical coherence tomography (SD-OCT) images centered on the fovea are shown. A 63 year-old Caucasian male control at baseline and 13 months later are shown in **(A,C)**. These images are compared with a 69 year-old Caucasian male probable tauopathy patient at baseline and 12 months later as shown in **(B,D)**. The Iowa Reference Algorithm segmentation lines outlining the outer retina are shown in blue and pink. To show outer retina thickness measurements in these images, point measurements were made nasal and temporal from the foveal center using the caliper function of the Heidelberg Spectralis (Heidelberg Engineering, Carlsbad, CA, United States) and labeled in white.

nerve fiber layer or ganglion cell layer thinning, and we used an image segmentation algorithm that revealed inner retina thinning in other dementia patients (Mutlu et al., 2018). This suggests that inner retina thinning is unlikely to be a late finding for our cohort of patients, and argues that the outer retina thinning we observed is unlikely to have resulted from non-specific neuronal loss. Thus, specific dementias may have specific retinal abnormalities, and our longitudinal data show that the inexpensive, safe, and quick retinal imaging of SD-OCT could help to distinguish FTD from AD.

We found significantly progressive outer retina thinning only in our tauopathy subgroup. This implicates tau pathology in FTD as a cause of the outer retina thinning, although our data does not enable us to comment on the exact mechanism by which a tauopathy affects photoreceptors. While AD also is a tauopathy, tau abnormalities in AD are composed of a mixture of 3R and 4R tau with paired, helical filaments (Irwin et al., 2015). This contrasts with the primarily 3R or 4R alone (not mixed) tauopathy with straight filaments of FTLD-Tau and, along with the Aβ toxicity of AD, may explain differences between retinas of AD and FTLD-Tau. SD-OCT may be most useful as a distinguishing biomarker for FTLD-Tau, and further investigation is needed.

TABLE 8 | Spearman correlation between retinal layers and Mini-Mental State Examination for all FTD patients and probable tauopathy subgroup.

	Baseline SD-OCT with change of MMSE		Follow-up SD-OCT with follow-up MMSE		Change of SD-OCT with follow-up MMSE		Change of SD-OCT with change of MMSE		
Retinal layer thickness[a]	**rho[b]**	***p*-value[c]**	**rho[d]**	***p*-value[c]**	**rho[d]**	***p*-value[c]**	**rho[d]**	***p*-value[c]**	**Patient group**
Outer retina	−0.12	0.65	0.56	**0.03**	0.79	**<0.001**	0.60	**0.02**	FTD patients
Outer nuclear layer	0.02	0.93	0.54	**0.04**	0.69	**0.005**	0.46	0.09	
EZ	0.14	0.60	0.19	0.49	0.13	0.65	0.19	0.49	
Outer retina	0.43	0.25	0.56	0.15	0.75	**0.03**	0.73	**0.04**	Probable tauopathy subgroup
Outer nuclear layer	0.49	0.18	0.51	0.19	0.51	0.19	0.55	0.16	
EZ	0.38	0.31	0.08	0.84	−0.14	0.73	−0.04	0.93	

Significant values ($p < 0.05$) in bold letters. SD-OCT, spectral domain optical coherence tomography; MMSE, mini-mental state examination; EZ, ellipsoid zone; FTD, frontotemporal degeneration. [a]Correlation was determined with the average of the 5 central subfields of the Early Treatment Diabetic Retinopathy Study grid. [b]For FTD patients: N = 16; median number of months between baseline and follow-up MMSE = 17 (interquartile range, 12–24 months); median baseline MMSE = 28 (interquartile range, 26–29); median follow-up MMSE = 26 (interquartile range, 23–28). For probable tauopathy subgroup: N = 9; median number of months between baseline and follow-up MMSE = 15 (interquartile range, 12–27 months); median baseline MMSE = 26 (interquartile range, 24–29); median follow-up MMSE = 25 (interquartile range, 20–28). [c]For subjects with 2 study eyes, the average of the 2 eyes was correlated. [d]For FTD patients: N = 15; median number of months between baseline and follow-up MMSE = 17 (interquartile range, 12–25 months); median baseline MMSE = 28 (interquartile range, 26–29); median follow-up MMSE = 26 (interquartile range, 24–28). For probable tauopathy subgroup: N = 8; median number of months between baseline and follow-up MMSE = 19 (interquartile range, 13–27 months); median baseline MMSE = 27 (interquartile range, 24–29); median follow-up MMSE = 26 (interquartile range, 22–28).

Interestingly, inner retina thinning has been reported in patients with a progranulin mutation and patients with amyotrophic lateral sclerosis, both of which are neurodegenerative diseases associated with a TDP-43 proteinopathy (Ward et al., 2014; Volpe et al., 2015). This also suggests that our finding of outer retina thinning seen in comparing all of our FTD patients to controls may be driven by our tauopathy patients. Further, it indicates that SD-OCT may have potential to distinguish FTLD-Tau from FTLD-TDP. While another report has seen inner retina thinning in a group of 17 FTD patients, patients in this study were not separated into probable tauopathy or TDP-43 subgroups (Ferrari et al., 2017). The inner retina thinning reported in this previous study may have been related to a high proportion of TDP-43 related pathology, but this is unclear without autopsy. Because of the disease heterogeneity of FTD, we believe that SD-OCT studies of these patients should use biomarkers and deep phenotyping whenever possible, as we have done in this study. Our findings remain to be confirmed at autopsy.

Depending on the disease, the inner or outer retina may become edematous (thicken) before later developing atrophic changes (thinning) (Sadigh et al., 2013; Rovere et al., 2015). Longitudinal data are therefore needed to determine if a potential retinal biomarker found in a cross-sectional study remains a significant finding over time. In this study, we found that thin layers did not become thickened or vice versa. Interestingly, we also found significant rates of change in retinal layers not involving photoreceptors. There was a significant rate of OPL thickening for the tauopathy subgroup, and this corresponds with non-significant OPL thickening seen in our cross-sectional data. In contrast to other retina layers, the OPL can be difficult to accurately segment (Oberwahrenbrock et al., 2015). However, two cross-sectional studies of PSP patients compared to normal controls have also shown non-significant thickening of the OPL and thinning of the ONL (Schneider et al., 2014), with significant thinning of the ONL seen in one of the studies (Albrecht et al., 2012). This is important because PSP patients are highly likely to have tau pathology (Litvan et al., 1996; Josephs et al., 2006; Hoglinger et al., 2017). The thickening of the OPL is potentially related to the sprouting of bipolar and horizontal cell dendrites from the OPL into the neighboring ONL as the ONL thins from photoreceptor atrophy (Fariss et al., 2000; Liets et al., 2006; Schneider et al., 2014). We also observed a significant rate of INL thinning compared to controls in both FTD patients and the probable tauopathy subgroup. The INL is the layer that contains the nuclei of bipolar, horizontal, and amacrine cells; it is not part of the inner retina thinning (composed of retinal nerve fiber layer and ganglion cell layer) typically associated with AD. These findings may be related to tau, which has been found within the INL and photoreceptors in the human retina (Leger et al., 2011; Schon et al., 2012).

In our baseline study, we found that the outer retina thickness correlates with the MMSE for FTD patients (Kim et al., 2017). Our longitudinal data shows outer retina thickness correlations with MMSE in several ways, confirming these data. While the baseline SD-OCT measurements did not predict a change of MMSE, there were especially robust findings for the correlation of the change of outer retina thickness with the follow-up MMSE in FTD patients ($p < 0.001$). This suggests that the baseline measurement of the outer retina thickness in these patients was too variable between patients to predict a change in MMSE, but the amount of change over time for this measurement (the rate of change) likely had less variability enabling its correlation with the change in MMSE. Additional studies of correlations with other severity measures specific to FTD are planned.

The strengths of our data are several-fold. Most current biomarker studies in FTD use clinically defined samples only, which limits meaningful interpretations in regards to underlying pathophysiology of this pathologically heterogeneous spectrum of neurodegenerative conditions. We employed rigorous methodology that includes deep endophenotyping of patients with autopsy-validated CSF biomarkers and genetic data to characterize our cohort. While not a complete substitute for autopsy data, AD CSF biomarkers appear to not only differentiate AD from controls, but also from forms of FTLD (Shaw et al., 2009; De Meyer et al., 2010; Irwin et al., 2012, 2013; Lleo et al., 2018). Thus, non-fluent PPA and CBS patients in our cohort are unlikely to have primary AD neuropathology, and the clinical diagnosis of PSP is highly specific for FTLD-Tau (Hoglinger et al., 2017). Further, while non-fluent PPA and CBS can also be associated with underlying FTLD-TDP pathology with *GRN* mutation, sporadic FTLD-TDP with these clinical features are rare (Grossman, 2012). Thus, our combination of CSF, genetic, and clinical criteria enable us to exclude AD and define a probable tauopathy subgroup with confidence. As additional study strengths, we performed eye exams to exclude confounding diseases and used a well-validated SD-OCT image segmentation algorithm. While follow-up studies of dementia patients have inherent challenges, we also had excellent retention for this study. It is unlikely that the missing data from subjects lost to follow-up would have altered our key results as the tauopathy patients that were unable to return because of disease progression probably would have had even more outer retina thinning.

The weaknesses of our study are primarily that the sample size of this longitudinal study is limited. Our findings should be replicated in a larger study. Without autopsy data, it is also possible that some patients in our cohort have mixed pathologies as opposed to "pure" FTLD (Kovacs, 2016; Lleo et al., 2018). Still, our multimodal biomarker approach to deeply phenotype our cohort is an excellent approach as autopsy-confirmed data in FTD is rare. Lastly, while our study subjects were consecutively recruited, the controls had different demographic features. Our data accounted for this by including statistical adjustment for age, sex, and race. Furthermore, our results are completely aligned with our baseline study and pre-specified hypothesis, suggesting the veracity of our findings. Larger studies would enable evaluation of the influence of demographic features such as sex on outer retina thickness measurements.

This is the first longitudinal report of SD-OCT retinal imaging in a group of deeply phenotyped FTD patients. Our findings of persistent outer retina thinning in FTD, and progressive outer retina thinning in the probable tauopathy subgroup implicates a potential tau-related mechanism for outer retina thinning. The correlations with disease severity again provide independent evidence of the significance of these findings. SD-OCT thus has potential as a biomarker for FTD. Future studies are aimed at directly comparing probable tauopathy patients to TDP-43 and AD patients across time, ultimately following patients to autopsy to confirm the molecular pathology.

AUTHOR CONTRIBUTIONS

BK, MG, JD, and DI contributed conception and design of the study. BK, MG, DS, SS, WP, SD-P, TA, G-SY, and DI performed acquisition and analysis of data. BK, MG, DS, JD, G-SY, and DI drafted the manuscript and figures.

FUNDING

This study was supported by NIH grants AG017586, NS053488, AG052943, 2-P30-EY01583-26, K23NS088341 (to DI), and KL2TR001879 (to DS). Funding was also provided by the Penn Institute on Aging and in the form of block grants for general research purposes to the Scheie Eye Institute by Research to Prevent Blindness (New York, NY, United States) and the Paul and Evanina Mackall Foundation Trust (Chicago, IL, United States).

ACKNOWLEDGMENTS

The authors thank Kyungmoo Lee (The University of Iowa) for assistance with the Iowa Reference Algorithm.

REFERENCES

Abramoff, M. D., Garvin, M. K., and Sonka, M. (2010). Retinal imaging and image analysis. *IEEE Rev. Biomed. Eng.* 3, 169–208. doi: 10.1109/RBME.2010.2084567

Albrecht, P., Muller, A. K., Sudmeyer, M., Ferrea, S., Ringelstein, M., Cohn, E., et al. (2012). Optical coherence tomography in parkinsonian syndromes. *PLoS One* 7:e34891. doi: 10.1371/journal.pone.0034891

Chan, V. T. T., Sun, Z., Tang, S., Chen, L. J., Wong, A., Tham, C. C., et al. (2018). Spectral domain-optical coherence tomography measurements in Alzheimer's disease: a systematic review and meta-analysis. *Ophthalmology* doi: 10.1016/j.ophtha.2018.08.009 [Epub ahead of print].

Cheung, C. Y., Ong, Y. T., Hilal, S., Ikram, M. K., Low, S., Ong, Y. L., et al. (2015). Retinal ganglion cell analysis using high-definition optical coherence tomography in patients with mild cognitive impairment and Alzheimer's disease. *J. Alzheimers Dis.* 45, 45–56. doi: 10.3233/JAD-141659

Choi, S. H., Park, S. J., and Kim, N. R. (2016). Macular ganglion cell -inner plexiform layer thickness is associated with clinical progression in mild cognitive impairment and Alzheimers disease. *PLoS One* 11:e0162202. doi: 10.1371/journal.pone.0162202

Coppola, G., Di Renzo, A., Ziccardi, L., Martelli, F., Fadda, A., Manni, G., et al. (2015). Optical coherence tomography in Alzheimer's disease: a meta-analysis. *PLoS One* 10:e0134750. doi: 10.1371/journal.pone.0134750

De Meyer, G., Shapiro, F., Vanderstichele, H., Vanmechelen, E., Engelborghs, S., De Deyn, P. P., et al. (2010). Diagnosis-independent Alzheimer disease biomarker signature in cognitively normal elderly people. *Arch. Neurol.* 67, 949–956. doi: 10.1001/archneurol.2010.179

Demirkaya, N., van Dijk, H. W., van Schuppen, S. M., Abramoff, M. D., Garvin, M. K., Sonka, M., et al. (2013). Effect of age on individual retinal layer thickness in normal eyes as measured with spectral-domain optical coherence tomography. *Invest. Ophthalmol. Vis. Sci.* 54, 4934–4940. doi: 10.1167/iovs.13-11913

Fariss, R. N., Li, Z. Y., and Milam, A. H. (2000). Abnormalities in rod photoreceptors, amacrine cells, and horizontal cells in human retinas with retinitis pigmentosa. *Am. J. Ophthalmol.* 129, 215–223. doi: 10.1016/S0002-9394(99)00401-8

Ferrari, L., Huang, S. C., Magnani, G., Ambrosi, A., Comi, G., and Leocani, L. (2017). Optical coherence tomography reveals retinal neuroaxonal thinning in frontotemporal dementia as in Alzheimer's disease. *J. Alzheimers Dis.* 56, 1101–1107. doi: 10.3233/JAD-160886

Garcia-Martin, E., Bambo, M. P., Marques, M. L., Satue, M., Otin, S., Larrosa, J. M., et al. (2016). Ganglion cell layer measurements correlate with disease severity in patients with Alzheimer's disease. *Acta Ophthalmol.* 94, e454–e459. doi: 10.1111/aos.12977

Garvin, M. K., Abramoff, M. D., Wu, X., Russell, S. R., Burns, T. L., and Sonka, M. (2009). Automated 3-D intraretinal layer segmentation of macular spectral-domain optical coherence tomography images. *IEEE Trans. Med. Imaging* 28, 1436–1447. doi: 10.1109/TMI.2009.2016958

Girkin, C. A., McGwin, G. Jr., Sinai, M. J., Sekhar, G. C., Fingeret, M., Wollstein, G., et al. (2011). Variation in optic nerve and macular structure with age and race with spectral-domain optical coherence tomography. *Ophthalmology* 118, 2403–2408. doi: 10.1016/j.ophtha.2011.06.013

Gorno-Tempini, M. L., Hillis, A. E., Weintraub, S., Kertesz, A., Mendez, M., Cappa, S. F., et al. (2011). Classification of primary progressive aphasia and its variants. *Neurology* 76, 1006–1014. doi: 10.1212/WNL.0b013e31821103e6

Grossman, M. (2012). The non-fluent/agrammatic variant of primary progressive aphasia. *Lancet Neurol.* 11, 545–555. doi: 10.1016/S1474-4422(12)70099-6

Hinton, D. R., Sadun, A. A., Blanks, J. C., and Miller, C. A. (1986). Optic-nerve degeneration in Alzheimer's disease. *N. Engl. J. Med.* 315, 485–487. doi: 10.1056/NEJM198608213150804

Hoglinger, G. U., Respondek, G., Stamelou, M., Kurz, C., Josephs, K. A., Lang, A. E., et al. (2017). Clinical diagnosis of progressive supranuclear palsy: the movement disorder society criteria. *Mov. Disord.* 32, 853–864. doi: 10.1002/mds.26987

Irwin, D. J., Cairns, N. J., Grossman, M., McMillan, C. T., Lee, E. B., Van, Deerlin VM, et al. (2015). Frontotemporal lobar degeneration: defining phenotypic diversity through personalized medicine. *Acta Neuropathol.* 129, 469–491. doi: 10.1007/s00401-014-1380-1

Irwin, D. J., McMillan, C. T., Toledo, J. B., Arnold, S. E., Shaw, L. M., Wang, L. S., et al. (2012). Comparison of cerebrospinal fluid levels of tau and Abeta 1-42 in Alzheimer disease and frontotemporal degeneration using 2 analytical platforms. *Arch. Neurol.* 69, 1018–1025. doi: 10.1001/archneurol.2012.26

Irwin, D. J., Trojanowski, J. Q., and Grossman, M. (2013). Cerebrospinal fluid biomarkers for differentiation of frontotemporal lobar degeneration from Alzheimer's disease. *Front. Aging Neurosci.* 5:6. doi: 10.3389/fnagi.2013.00006

Josephs, K. A., Petersen, R. C., Knopman, D. S., Boeve, B. F., Whitwell, J. L., Duffy, J. R., et al. (2006). Clinicopathologic analysis of frontotemporal and corticobasal degenerations and PSP. *Neurology* 66, 41–48. doi: 10.1212/01.wnl.0000191307.69661.c3

Kashani, A. H., Zimmer-Galler, I. E., Shah, S. M., Dustin, L., Do, D. V., Eliott, D., et al. (2010). Retinal thickness analysis by race, gender, and age using stratus OCT. *Am. J. Ophthalmol.* 149, 496–502e1. doi: 10.1016/j.ajo.2009.09.025

Kertesz, A., McMonagle, P., Blair, M., Davidson, W., and Munoz, D. G. (2005). The evolution and pathology of frontotemporal dementia. *Brain* 128(Pt 9), 1996–2005. doi: 10.1093/brain/awh598

Kim, B. J., Irwin, D. J., Song, D., Daniel, E., Leveque, J. D., Raquib, A. R., et al. (2017). Optical coherence tomography identifies outer retina thinning in frontotemporal degeneration. *Neurology* 89, 1604–1611. doi: 10.1212/WNL.0000000000004500

Knibb, J. A., Xuereb, J. H., Patterson, K., and Hodges, J. R. (2006). Clinical and pathological characterization of progressive aphasia. *Ann. Neurol.* 59, 156–165. doi: 10.1002/ana.20700

Koronyo, Y., Biggs, D., Barron, E., Boyer, D. S., Pearlman, J. A., Au, W. J., et al. (2017). Retinal amyloid pathology and proof-of-concept imaging trial in Alzheimer's disease. *JCI Insight* 2:93621. doi: 10.1172/jci.insight.93621

Kovacs, G. G. (2016). Molecular pathological classification of neurodegenerative diseases: turning towards precision medicine. *Int. J. Mol. Sci.* 17:E189. doi: 10.3390/ijms17020189

Leger, F., Fernagut, P. O., Canron, M. H., Leoni, S., Vital, C., Tison, F., et al. (2011). Protein aggregation in the aging retina. *J. Neuropathol. Exp. Neurol.* 70, 63–68. doi: 10.1097/NEN.0b013e31820376cc

Li, K., Wu, X., Chen, D. Z., and Sonka, M. (2006). Optimal surface segmentation in volumetric images–a graph-theoretic approach. *IEEE Trans Pattern Anal Mach Intell.* 28, 119–134. doi: 10.1109/TPAMI.2006.19

Liang, K., and Zeger, S. (1986). Longitudinal data analysis using generalized linear models. *Biometrika* 73, 13–22. doi: 10.1093/biomet/73.1.13

Liets, L. C., Eliasieh, K., van der List, D. A., and Chalupa, L. M. (2006). Dendrites of rod bipolar cells sprout in normal aging retina. *Proc. Natl. Acad. Sci. U.S.A.* 103, 12156–12160. doi: 10.1073/pnas.0605211103

Litvan, I., Agid, Y., Calne, D., Campbell, G., Dubois, B., Duvoisin, R. C., et al. (1996). Clinical research criteria for the diagnosis of progressive supranuclear palsy (Steele-Richardson-Olszewski syndrome): report of the NINDS-SPSP international workshop. *Neurology* 47, 1–9. doi: 10.1212/WNL.47.1.1

Lleo, A., Irwin, D. J., Illan-Gala, I., McMillan, C. T., Wolk, D. A., Lee, E. B., et al. (2018). A 2-Step cerebrospinal algorithm for the selection of frontotemporal lobar degeneration subtypes. *JAMA Neurol.* 75, 738–745. doi: 10.1001/jamaneurol.2018.0118

Loh, E. H., Ong, Y. T., Venketasubramanian, N., Hilal, S., Thet, N., Wong, T. Y., et al. (2017). Repeatability and reproducibility of retinal neuronal and axonal measures on spectral-domain optical coherence tomography in patients with cognitive impairment. *Front. Neurol.* 8:359. doi: 10.3389/fneur.2017.00359

Mutlu, U., Colijn, J. M., Ikram, M. A., Bonnemaijer, P. W. M., Licher, S., Wolters, F. J., et al. (2018). Association of retinal neurodegeneration on optical coherence tomography with dementia: a population-based study. *JAMA Neurol.* 75, 1256–1263. doi: 10.1001/jamaneurol.2018.1563

Oberwahrenbrock, T., Weinhold, M., Mikolajczak, J., Zimmermann, H., Paul, F., Beckers, I., et al. (2015). Reliability of intra-retinal layer thickness estimates. *PLoS One* 10:e0137316. doi: 10.1371/journal.pone.0137316

Rascovsky, K., Hodges, J. R., Knopman, D., Mendez, M. F., Kramer, J. H., Neuhaus, J., et al. (2011). Sensitivity of revised diagnostic criteria for the behavioural variant of frontotemporal dementia. *Brain* 134(Pt 9), 2456–2477. doi: 10.1093/brain/awr179

Rovere, G., Nadal-Nicolas, F. M., Agudo-Barriuso, M., Sobrado-Calvo, P., Nieto-Lopez, L., Nucci, C., et al. (2015). Comparison of retinal nerve fiber layer thinning and retinal ganglion cell loss after optic nerve transection in adult albino rats. *Invest. Ophthalmol. Vis. Sci.* 56, 4487–4498. doi: 10.1167/iovs.15-17145

Sadigh, S., Cideciyan, A. V., Sumaroka, A., Huang, W. C., Luo, X., Swider, M., et al. (2013). Abnormal thickening as well as thinning of the photoreceptor layer in intermediate age-related macular degeneration. *Invest. Ophthalmol. Vis. Sci.* 54, 1603–1612. doi: 10.1167/iovs.12-11286

Schneider, M., Muller, H. P., Lauda, F., Tumani, H., Ludolph, A. C., Kassubek, J., et al. (2014). Retinal single-layer analysis in Parkinsonian syndromes: an optical coherence tomography study. *J. Neural. Transm.* 121, 41–47. doi: 10.1007/s00702-013-1072-3

Schon, C., Hoffmann, N. A., Ochs, S. M., Burgold, S., Filser, S., Steinbach, S., et al. (2012). Long-term in vivo imaging of fibrillar tau in the retina of P301S transgenic mice. *PLoS One* 7:e53547. doi: 10.1371/journal.pone.0053547

Shaw, L. M., Vanderstichele, H., Knapik-Czajka, M., Clark, C. M., Aisen, P. S., Petersen, R. C., et al. (2009). Cerebrospinal fluid biomarker signature in Alzheimer's disease neuroimaging initiative subjects. *Ann. Neurol.* 65, 403–413. doi: 10.1002/ana.21610

Shen, Y., Shi, Z., Jia, R., Zhu, Y., Cheng, Y., Feng, W., et al. (2013). The attenuation of retinal nerve fiber layer thickness and cognitive deterioration. *Front. Cell Neurosci.* 7:142. doi: 10.3389/fncel.2013.00142

Song, D., Grieco, S., Li, Y., Hunter, A., Chu, S., Zhao, L., et al. (2014). A murine RP1 missense mutation causes protein mislocalization and slowly progressive photoreceptor degeneration. *Am. J. Pathol.* 184, 2721–2729. doi: 10.1016/j.ajpath.2014.06.010

Spinelli, E. G., Mandelli, M. L., Miller, Z. A., Santos-Santos, M. A., Wilson, S. M., Agosta, F., et al. (2017). Typical and atypical pathology in primary progressive aphasia variants. *Ann. Neurol.* 81, 430–443. doi: 10.1002/ana.24885

Tewarie, P., Balk, L., Costello, F., Green, A., Martin, R., Schippling, S., et al. (2012). The OSCAR-IB consensus criteria for retinal OCT quality assessment. *PLoS One* 7:e34823. doi: 10.1371/journal.pone.0034823

Uchida, A., Pillai, J. A., Bermel, R., Bonner-Jackson, A., Rae-Grant, A., Fernandez, H., et al. (2018). Outer retinal assessment using spectral-domain optical coherence tomography in patients with alzheimer's and parkinson's disease. *Invest. Ophthalmol. Vis. Sci.* 59, 2768–2777. doi: 10.1167/iovs.17-23240

Volpe, N. J., Simonett, J., Fawzi, A. A., and Siddique, T. (2015). Ophthalmic manifestations of amyotrophic lateral sclerosis (an american ophthalmological society thesis). *Trans. Am. Ophthalmol. Soc.* 113, T12.

Ward, M. E., Taubes, A., Chen, R., Miller, B. L., Sephton, C. F., Gelfand, J. M., et al. (2014). Early retinal neurodegeneration and impaired ran-mediated nuclear import of TDP-43 in progranulin-deficient FTLD. *J. Exp. Med.* 211, 1937–1945. doi: 10.1084/jem.20140214

Wood, E. M., Falcone, D., Suh, E., Irwin, D. J., Chen-Plotkin, A. S., Lee, E. B., et al. (2013). Development and validation of pedigree classification criteria for frontotemporal lobar degeneration. *JAMA Neurol.* 70, 1411–1417. doi: 10.1001/jamaneurol.2013.3956

Ying, G. S., Maguire, M. G., Glynn, R., and Rosner, B. (2017). Tutorial on biostatistics: linear regression analysis of continuous correlated eye data. *Ophthalmic Epidemiol.* 24, 130–140. doi: 10.1080/09286586.2016.1259636

Conflict of Interest Statement: The authors declare that the research was conducted in the absence of any commercial or financial relationships that could be construed as a potential conflict of interest.

frontiers in Neuroscience

REVIEW
published: 11 April 2019
doi: 10.3389/fnins.2019.00335

The Pathobiology of TDP-43 C-Terminal Fragments in ALS and FTLD

Britt A. Berning[1] *and Adam K. Walker*[1,2]*

[1] *Neurodegeneration Pathobiology Laboratory, Queensland Brain Institute, University of Queensland, Brisbane, QLD, Australia,* [2] *Centre for Motor Neuron Disease Research, Department of Biomedical Sciences, Faculty of Medicine and Health Sciences, Macquarie University, North Ryde, NSW, Australia*

During neurodegenerative disease, the multifunctional RNA-binding protein TDP-43 undergoes a vast array of post-translational modifications, including phosphorylation, acetylation, and cleavage. Many of these alterations may directly contribute to the pathogenesis of TDP-43 proteinopathies, which include most forms of amyotrophic lateral sclerosis (ALS) and approximately half of all frontotemporal dementia, pathologically identified as frontotemporal lobar degeneration (FTLD) with TDP-43 pathology. However, the relative contributions of the various TDP-43 post-translational modifications to disease remain unclear, and indeed some may be secondary epiphenomena rather than disease-causative. It is therefore critical to determine the involvement of each modification in disease processes to allow the design of targeted treatments. In particular, TDP-43 C-terminal fragments (CTFs) accumulate in the brains of people with ALS and FTLD and are therefore described as a neuropathological signature of these diseases. Remarkably, these TDP-43 CTFs are rarely observed in the spinal cord, even in ALS which involves dramatic degeneration of spinal motor neurons. Therefore, TDP-43 CTFs are not produced non-specifically in the course of all forms of TDP-43-related neurodegeneration, but rather variably arise due to additional factors influenced by regional heterogeneity in the central nervous system. In this review, we summarize how TDP-43 CTFs are generated and degraded by cells, and critique evidence from studies of TDP-43 CTF pathology in human disease tissues, as well as cell and animal models, to analyze the pathophysiological relevance of TDP-43 CTFs to ALS and FTLD. Numerous studies now indicate that, although TDP-43 CTFs are prevalent in ALS and FTLD brains, disease-related pathology is only variably reproduced in TDP-43 CTF cell culture models. Furthermore, TDP-43 CTF expression in both transgenic and viral-mediated *in vivo* models largely fails to induce motor or behavioral dysfunction reminiscent of human disease. We therefore conclude that although TDP-43 CTFs are a hallmark of TDP-43-related neurodegeneration in the brain, they are not a primary cause of ALS or FTLD.

Keywords: amyotrophic lateral sclerosis (ALS), motor neuron disease (MND), TDP-43, neurodegeneration, frontotemporal lobar degeneration (FTLD-TDP)

OPEN ACCESS

Edited by:
Annakaisa Haapasalo, University of Eastern Finland, Finland

Reviewed by:
Valentina Bonetto, Istituto Di Ricerche Farmacologiche Mario Negri, Italy
Dietmar R. Thal, KU Leuven, Belgium

***Correspondence:**
Adam K. Walker
adam.walker@uq.edu.au

Specialty section:
This article was submitted to Neurodegeneration, a section of the journal Frontiers in Neuroscience

Received: *25 January 2019*
Accepted: *22 March 2019*
Published: *11 April 2019*

Citation:
Berning BA and Walker AK (2019) The Pathobiology of TDP-43 C-Terminal Fragments in ALS and FTLD. Front. Neurosci. 13:335. doi: 10.3389/fnins.2019.00335

INTRODUCTION

Carboxyl-terminal fragments (CTFs) of *trans* active response DNA binding protein of 43 kDa (TDP-43) are frequently detected in the brains of people with amyotrophic lateral sclerosis (ALS) and frontotemporal lobar degeneration (FTLD) (Neumann et al., 2006). TDP-43 CTFs are therefore largely considered a hallmark of these diseases. However, TDP-43 CTFs are rarely detected in the characteristic pathological TDP-43 inclusions of motor neurons in the ALS spinal cord (Igaz et al., 2008), and exogenous expression of these fragments in cells and small animal models only variably recapitulates aspects of ALS and FTLD. In this review, we summarize how TDP-43 CTFs are formed and degraded and highlight how differences in the ability of distinct cell populations to generate or degrade TDP-43 CTFs may account for the regional variation in CTF levels in the brain and spinal cord in disease. We also critique evidence from human post-mortem tissue as well as cell culture and animal models of ALS and FTLD to conclude that, although TDP-43 CTFs are closely associated with disease pathology, they do not appear to play a causal role in disease onset or progression. The intention of this critique is to shift research attention toward molecular events that play a clear, causal role in the etiology of ALS and FTLD in order to improve the design of treatments targeted at disease-relevant dysfunctions related to TDP-43.

TDP-43 Biology

TDP-43 is a 414-amino acid protein encoded by the *TARDBP* gene. It is ubiquitously expressed and predominantly locates to the nucleus owing to a nuclear localization signal (NLS) (Winton et al., 2008). TDP-43 also contains a nuclear export sequence that facilitates cytoplasmic shuttling (Ayala et al., 2008), although more recent work suggests that TDP-43 may also passively diffuse between the nucleus and cytoplasm (Ederle et al., 2018; Pinarbasi et al., 2018). The domain architecture of TDP-43 is similar to that of other RNA binding proteins, including an N-terminal domain with two highly conserved RNA recognition motifs (RRM1 and RRM2), each approximately 60 residues long, that preferentially bind RNA with UG repeat sequences (Buratti and Baralle, 2001). TDP-43 targets a wide range of RNA transcripts, including pre-mRNA, microRNA, and long intronic sequences (Polymenidou et al., 2011; Tollervey et al., 2011; Xiao et al., 2011; Colombrita et al., 2012; Narayanan et al., 2013). This enables TDP-43 to critically regulate a multitude of RNA processing pathways, such as alternative splicing, transcriptional repression, RNA stability, and microRNA biogenesis (Mercado et al., 2005; Kawahara and Mieda-Sato, 2012). TDP-43 also tightly regulates its own transcription via a negative feedback loop that maintains consistent protein levels; by binding to the 3′ untranslated region (UTR) of its own messenger RNA (mRNA), TDP-43 promotes degradation of the *TARDBP* transcript (Ayala Y. M. et al., 2011). This exquisite transcriptional control is demonstrated by the finding that TDP-43 protein levels do not differ between heterozygous *Tardbp* knockout mice and wild-type controls (Sephton et al., 2010). This self-regulatory function is essential to cell survival as both depletion and overexpression of TDP-43 are toxic *in vivo* and in cultured cells (Johnson et al., 2008; Kraemer et al., 2010; Voigt et al., 2010; Wu et al., 2010).

In addition to the direct RNA-binding functions of TDP-43, the glycine-rich C-terminal domain of TDP-43 mediates protein-protein interactions (Buratti et al., 2005; Buratti and Baralle, 2008; Freibaum et al., 2010; Uversky, 2015; Santamaria et al., 2017), which likely play additional roles in TDP-43 biochemistry. *In silico* analysis predicts that the C-terminal tail is inherently disordered and of low complexity (Bryson et al., 2005). This region of the TDP-43 protein mediates liquid–liquid phase separation (Conicella et al., 2016; Li et al., 2018a,b), a necessary step in the formation of membraneless organelles such as stress granules (Liu-Yesucevitz et al., 2010; Molliex et al., 2015; Mackenzie et al., 2017; Santamaria et al., 2017; Uversky, 2017; Fang et al., 2018). TDP-43 also undergoes a myriad of post-translational modifications, including ubiquitination, phosphorylation, and acetylation, that alter its structure and biochemical function (for reviews, see Sambataro and Pennuto, 2017; Buratti, 2018).

ALS and FTLD Disease and TDP-43 Pathology

Amyotrophic lateral sclerosis is a fatal neurodegenerative disorder that is typically adult-onset, and is characterized by progressive loss of upper motor neurons in the motor cortex and corticospinal tract, and lower motor neurons in the spinal cord (Robberecht and Philips, 2013). This leads to denervation and rapid atrophy of specific muscle groups, which usually eventuates in death by respiratory failure (Neudert et al., 2001). Over 97% of ALS cases, both sporadic and familial, feature TDP-43-positive inclusions in the cytoplasm of affected neurons (Ling et al., 2013). In addition, TDP-43 inclusions in frontal and anterior temporal lobe regions are the hallmark of some forms of frontotemporal dementia (FTD). Rather than affecting the motor system, in FTD these inclusions are associated with the progressive development of deficits in behavior, affect and language processing with relative sparing of memory and visuo-spatial skills, at least early in disease (Kirshner, 2014; Bang et al., 2015). At post-mortem, this form of FTD is classified as FTLD with TDP-43 pathology (FTLD-TDP), and accounts for approximately half of FTD cases, distinguished from cases in which pathological tau, fused in sarcoma (FUS) or other proteins predominate (Ling et al., 2013).

In ALS and FTLD patients, surviving neurons with TDP-43 pathology typically show accumulation of TDP-43 in cytoplasmic inclusions, and clearance of nuclear TDP-43, suggesting that TDP-43 pathogenicity may proceed via both loss of normal function as well as toxic gains of function. In disease, TDP-43 inclusions have varying morphologies, ranging from neuronal cytoplasmic inclusions with compact rounded or skein-like appearance, to short or long dystrophic neurites, to rare intranuclear inclusions or glial (primarily oligodendrocytic) inclusions (Neumann et al., 2006, 2009). The presence of various forms of TDP-43 pathology in both ALS and FTLD suggests that these diseases may occur as manifestations of a spectrum of TDP-43-related disease (Geser et al., 2010; Ling et al., 2013). Furthermore, as disease advances, many people living with ALS develop impairments in letter fluency, executive function and

behavior that, to a degree, resemble behavioral-variant FTD (Crockford et al., 2018). However, recent neuropathological findings suggest that FTLD cases present with distinct forms of TDP-43 pathology in comparison with ALS and FTLD-ALS cases, indicating divergent mechanisms of disease pathogenesis that nonetheless involve the same protein, TDP-43 (Tan et al., 2017b). Further research is therefore required to understand how and why unique TDP-43 pathology develops in distinct diseases, as well as in different subtypes of one disease.

Based on the distribution and morphology of TDP-43 species, FTLD-TDP pathology can be stratified into at least four subtypes, which partially correlate with the underlying genetics and clinical presentation (Mackenzie et al., 2011; Van Mossevelde et al., 2018). In updated consensus nomenclature, the two most common subtypes are FTLD-TDP type A, which is defined by the presence of many neuronal cytoplasmic TDP-43 inclusions and short dystrophic neurites primarily in cortical layer 2, and FTLD-TDP type B, which is defined by many cytoplasmic TDP-43 inclusions that are distributed throughout all cortical layers, with few dystrophic neurites (Mackenzie et al., 2011; Tan et al., 2013). The rarer FTLD-TDP type C pathology presents with few cytoplasmic TDP-43 inclusions but abundant long dystrophic neurites primarily in cortical layer 2, and the very rare FTLD-TDP type D pathology, linked with mutations in the valosin-containing protein gene (*VCP*), has few cytoplasmic TDP-43 inclusions but many lentiform neuronal intranuclear inclusions throughout the cortical layers (Mackenzie et al., 2011; Tan et al., 2013). Additional subtypes of TDP-43 pathology have also been suggested, such as rapidly progressive FTD cases with widespread TDP-43 pathology and distinct patterns of TDP-43 CTFs (termed 'type E,' Lee E. B. et al., 2017), although the wider prevalence of this form of disease is unclear. Recent work has shown that FTLD-TDP subtypes may also be distinguished according to the classes of proteins that become insoluble in addition to TDP-43 (Laferriere et al., 2019).

Although underlying TDP-43 pathology does not always correlate with genetics or disease phenotype, mutations to the progranulin (*GRN*) gene are generally associated with type A TDP-43 pathology, whereas hexanucleotide repeat expansions in *C9orf72*, which is the most common genetic cause of ALS and FTLD-TDP, most frequently result in type B pathology (Mackenzie et al., 2011; Boeve et al., 2012). Patients who have developed both FTLD and ALS disease features also tend to exhibit type B TDP-43 pathology in the brain at autopsy (Mackenzie et al., 2011). Overall, the involvement of TDP-43 pathology in different forms of disease indicates the key role that TDP-43 plays in pathophysiology. The large variety of genetic factors, inclusion morphologies and clinical symptoms related to TDP-43 suggests that numerous contributing biochemical mechanisms likely converge on common pathogenic pathways in disease.

TDP-43 and Neurodegenerative Disorders

Pathological TDP-43 is also evident in approximately 30–70% of Alzheimer's disease patients, particularly those with fast progressing disease and advanced β-amyloid plaque and neurofibrillary tangle pathology (Josephs et al., 2016), and the presence of TDP-43 pathology is associated with mutation to the *APOE ε4* gene independent of β-amyloid pathology (Wennberg et al., 2018). TDP-43 pathology is observed in Parkinson's Disease (Nakashima-Yasuda et al., 2007) and Huntington's Disease (Schwab et al., 2008), and accumulates in astrocytes and white matter in the brains of patients with the rare neurodegenerative disorder Alexander disease (Walker et al., 2014). Phosphorylated TDP-43 was also associated with cognitive decline related to aging (Wilson et al., 2019). The presence of abnormal TDP-43 in numerous neurodegenerative disorders suggests that it may be a point of convergence in cellular dysfunction and death, despite diverse upstream disease mechanisms.

TDP-43 CTFs ARE CHARACTERISTIC OF DISEASE PATHOLOGY IN BRAIN BUT ARE RARELY DETECTED IN SPINAL CORD

Examination of post-mortem ALS and FTLD-TDP brain tissue reveals the presence of low molecular weight TDP-43 species in addition to the full-length protein in detergent-insoluble protein fractions, which contain aggregated proteins, regardless of whether the person had ALS or FTLD (Neumann et al., 2006; Igaz et al., 2008). Immunoblotting using antibodies targeting the TDP-43 C-terminal domain consistently detects one or multiple fragments from the C-terminal portion of TDP-43 of approximately 25 kDa in the frontal and temporal lobes of people with ALS and FTLD. Henceforth we refer to these TDP-43 CTFs as CTF-25 (see **Figure 1**). CTFs of approximately 15 and 35 kDa (CTF-35) have also been detected in ALS and FTLD nervous tissue (Tsuji et al., 2012b; Xiao et al., 2015), although much less frequently and with inconsistency between studies (Lee et al., 2011). Evidence for the presence of TDP-43 CTFs in ALS or FTLD post-mortem tissue is summarized in **Table 1**. For consistency, we have re-categorized the results from early FTLD studies that used alternative nomenclature relating to the previous conflicting FTLD-U nomenclature systems (Mackenzie et al., 2006; Sampathu et al., 2006) according to the more recent consensus FTLD-TDP subtyping (Mackenzie et al., 2011).

Immunoblotting using antibodies that specifically recognize phosphorylated epitopes (notably serines S403, S404, S409, S410) in the C-terminal domain of TDP-43 consistently detects CTF-25 in the brains of both FTLD-TDP and ALS patients (Hasegawa et al., 2008; Inukai et al., 2008; Neumann et al., 2009; Arai et al., 2010; Tsuji et al., 2012a,b, Kametani et al., 2016; Watanabe et al., 2018). Although these antibodies typically demonstrate a greater abundance of CTF-25 than full-length TDP-43 in the detergent-insoluble protein fraction (Tsuji et al., 2012a,b), the relative abundance of TDP-43 CTFs in relation to full-length TDP-43 varies according to the specific TDP-43 antibody used, with other studies reporting relatively low levels of CTF-25 (Arai et al., 2006; Neumann et al., 2006). Upon phosphatase treatment, the ∼25 kDa band detected by

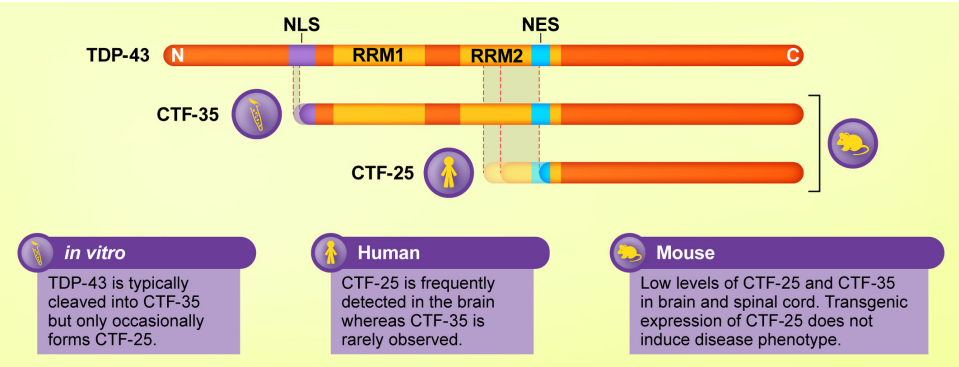

FIGURE 1 | Schematic diagram of major TDP-43 C-terminal fragments (CTFs) and their cleavage sites and functional domains, and the experimental models in which they are most commonly detected. Although CTF-35 is frequently formed in cellular and *in vitro* assays of TDP-43 proteinopathies, this fragment is rarely observed in ALS or FTLD brain tissue, where CTF-25 predominates. Mouse models of TDP-43 exhibit low levels of both fragments. Thus, cleavage of TDP-43 varies according to model and species.

TABLE 1 | Summary of studies examining the presence of TDP-43 CTF-25 in postmortem brain and spinal cord tissue from people with ALS and FTLD-TDP.

Disease		Tissue Type	Presence of CTFs	Major Findings
ALS		Brain	+	• Increased CTFs compared to healthy controls in frontal and temporal cortices (Hasegawa et al., 2008; Tsuji et al., 2012a; Tsuji et al., 2012b; Kwong et al., 2014; Smethurst et al., 2016), hippocampus, substantia nigra, striatum, medulla and pons (Tsuji et al., 2012a), and in studies where brain region was not specified (Inukai et al., 2008; Zhang et al., 2009; Kametani et al., 2016)
			−	• No CTFs in temporal cortex or cerebellum (Neumann et al., 2006; Tsuji et al., 2012a) • Low levels of CTFs in the frontal cortex of some patients (Neumann et al., 2006)
		Spinal Cord	?	• CTFs faintly detected in the lumbar spinal cord, less abundant than full-length TDP-43 (Tsuji et al., 2012a; Smethurst et al., 2016) • Low levels of CTFs in both ALS and healthy control tissue (Giordana et al., 2010) • CTFs observed in one patient with a *TARDBP* mutation (Q343R) but not in sporadic ALS patients (Yokoseki et al., 2008) • 35 kDa fragment was detected in the ALS spinal cord (Xiao et al., 2015)
			−	• No CTFs (immunoblotting) in lumbar spinal cord (Neumann et al., 2006, 2009; Igaz et al., 2008; Uchida et al., 2012) • No CTFs (immunohistochemistry) in spinal cord ventral horn (Igaz et al., 2008; Kwong et al., 2014)
FTLD-TDP	Type A	Brain	+	• CTFs detected in cortex (Neumann et al., 2006; Igaz et al., 2008; Arai et al., 2010; Tsuji et al., 2012a,b; Lee E. B. et al., 2017; Porta et al., 2018) and hippocampus (Neumann et al., 2006)
	Type B	Brain	+	• CTFs detected in cortex (Igaz et al., 2008; Arai et al., 2010; Tsuji et al., 2012a,b; Lee E. B. et al., 2017; Porta et al., 2018)
	Type C	Brain	+	• CTFs detected in cortex (Neumann et al., 2006, 2007; Igaz et al., 2008; Arai et al., 2010; Hasegawa et al., 2011; Tsuji et al., 2012a,b; Lee E. B. et al., 2017; Watanabe et al., 2018; Porta et al., 2018), hippocampus (Neumann et al., 2006; Tsuji et al., 2012a) and striatum (Tsuji et al., 2012a)
			−	• No CTFs in cerebellum, substantia nigra, pons, medulla or thalamus (Tsuji et al., 2012a)
	Type D	Brain	?	• Low levels of CTFs variably detected in frontal and temporal cortices (Neumann et al., 2007)
	Type E	Brain	+	• Multiple CTFs between 23 and 26 kDa detected in frontal cortex (Lee E. B. et al., 2017)

"+" indicates overt presence, "−" indicates no presence and "?' indicates very low level detection or unclear findings.

immunoblotting appears as multiple bands ranging from 18 to 27 kDa in size (Neumann et al., 2006). N-terminal sequencing of TDP-43 CTFs purified from FTLD-TDP brains has revealed a CTF-25 with a cleavage site at arginine residue 208 (Igaz et al., 2009) or asparagine residues 219 or 247 (Nonaka et al., 2009). A 32–35 kDa CTF has also been predicted to arise from cleavage at residue 89 (Zhang et al., 2007) and high throughput analysis of ALS brains indicates numerous other cleavage sites (Nonaka et al., 2009; Kametani et al., 2016).

The N-terminal portion resulting from TDP-43 cleavage has proven difficult to detect experimentally in human autopsy tissues (Igaz et al., 2008; Kwong et al., 2014), although other studies have suggested the presence of ∼32 kDa and ∼35 kDa truncated N-terminal TDP-43 proteins resulting from cleavage by

asparaginyl endopeptidase (Herskowitz et al., 2012) and calpains (Yamashita et al., 2012, 2016). However, it has been suggested that any resultant N-terminal fragment of TDP-43 is likely rapidly degraded following cleavage of the full-length protein (Pesiridis et al., 2011; Buratti, 2018).

Although fragments of the C-terminal portion of TDP-43 are often regarded as a molecular signature of TDP-43 proteinopathies, the presence of TDP-43 CTFs does not necessarily correlate with neurodegeneration. Despite the post-mortem evidence for the presence of TDP-43 CTFs in both the ALS and FTLD brain, structural magnetic resonance imaging as well as post-mortem analysis reveals widespread brain atrophy in FTLD (Broe et al., 2003; Consonni et al., 2018; Sellami et al., 2018), whereas patients with ALS exhibit milder, focal thinning of the primary motor and pre-motor cortices and damage to the corticospinal tract (Roccatagliata et al., 2009; Chen and Ma, 2010; Verstraete et al., 2012). Further to this, TDP-43 CTFs are typically not detected in the ALS spinal cord (Neumann et al., 2006; Igaz et al., 2008; Uchida et al., 2012; Kwong et al., 2014), despite the dramatic tissue loss associated with disease progression (Branco et al., 2014). Instead, immunohistochemical studies have reported co-labeling of lower motor neuron inclusion bodies with antibodies directed against both the N- and C-termini of TDP-43, suggesting the inclusions primarily comprise the full-length protein (Igaz et al., 2008). The studies that have detected TDP-43 CTFs in the ALS spinal cord show that they are much less abundant than full-length TDP-43 (Neumann et al., 2009; Giordana et al., 2010; Smethurst et al., 2016). This indicates that TDP-43 CTFs may not be a prerequisite for neurodegeneration (Lee et al., 2011). The possibility that CTFs promote more rapid neurodegeneration and therefore fail to be detected in the ALS spinal cord at post-mortem seems unlikely, given that the fragments continue to be observed in the cortex regardless of cell loss. Further examination is therefore necessary to establish whether these fragments play a causal role in disease.

Numerous studies have attempted to correlate the relative abundance of the several TDP-43 CTFs between 18 and 27 kDa detected by immunoblotting with FTLD-TDP subtype or diagnosis of ALS. Despite progress in this area, low sample sizes, poor resolution of the immunoblots and heterogeneity in the neuropathology of patients with TDP-43 proteinopathies have obscured distinction of a reliable immunoblot pattern of CTFs (Arai et al., 2006, 2010; Hasegawa et al., 2008; Inukai et al., 2008). To address this, a large-scale biochemical examination of FTLD brain tissue from 42 individuals was conducted (Neumann et al., 2009). Although some similarity with previously reported patterns was observed (Hasegawa et al., 2008; Inukai et al., 2008), the overall relative abundance of low molecular weight species of TDP-43 could not be mapped to genetic risk factor or clinico-pathological subtype. A recent study reported that the levels of a 26 kDa CTF were higher than those of other lower molecular weight CTFs in FTLD-TDP patients with type E pathology compared to patients with types A, B, or C pathology (Lee E. B. et al., 2017). More sensitive methods of detection and quantification of various CTFs are required to fully elucidate their relative abundance in disease tissues.

GENERATION OF TDP-43 CTFs

In addition to transcriptional autoregulation, TDP-43 may be cleaved into smaller fragments before being enzymatically degraded to maintain physiological levels (Ling et al., 2010; Huang et al., 2014). TDP-43 is processed by a range of cysteine proteases, including caspases and calpains. In TDP-43 proteinopathies, disease-related factors such as cell stress and genetic mutations may modulate the activity of these enzymes. Assays of TDP-43 fragmentation using both mammalian cell lines and primary neuronal cultures frequently demonstrate the presence of CTF-35. This fragment is rarely observed in human post-mortem tissue (Neumann et al., 2006, 2009; Hasegawa et al., 2008) although interestingly, it has been reported in lymphoblastoid cells derived from ALS patients (Kabashi et al., 2008; Rutherford et al., 2008). Conversely, CTF-25, a pathological signature of the ALS and FTLD brain, was often undetected in these cell experiments, or was only observed at low levels. This brings into question the extent to which cell assays of TDP-43 cleavage can be extrapolated to human disease. It also suggests that the mechanisms of TDP-43 fragmentation and potentially the biochemical effects of the TDP-43 fragments may vary according to experimental model and biological sample (highlighted in **Figure 1**). These observations illuminate the importance of interpreting data from cell culture studies within the context of findings from human and animal investigations.

Caspases

Prior to the discovery of TDP-43 as the primary component of insoluble inclusions in ALS and FTLD (Neumann et al., 2006), elevated caspase-3 activity had been noted in the anterior horn and motor cortex of ALS patients (Martin, 1999), as well as in degenerating astrocytes and neurons exhibiting DNA damage in the superior frontal gyrus and anterior pole of the temporal lobe of the FTLD brain (Su et al., 2000). Since then, numerous studies have confirmed TDP-43 as a caspase substrate (Thiede et al., 2005; Van Damme et al., 2005; Dix et al., 2008), with the TDP-43 amino acid sequence containing three putative caspase-3 consensus sites that correspond to CTFs of approximately 42, 35, and 25 kDa (Zhang et al., 2007). Experiments in human cell lines demonstrate cleavage of TDP-43 by a range of caspases including caspase-3, -4, and -7 (Rutherford et al., 2008; Cassel et al., 2012; De Marco et al., 2014; Li et al., 2015).

Cell Stress

Elevation of cleaved caspase-3 and -9 is associated with the generation of CTF-35 under conditions of cell stress. These include treatment with the classic apoptotic insult staurosporine (Dormann et al., 2009; Suzuki et al., 2011) or chemical inducers of endoplasmic reticulum (ER) stress such as thapsigargin, dithiothreitol, or tunicamycin (Suzuki et al., 2011), hyper-osmotic pressure induced by treatment with D-sorbitol (Dewey et al., 2011; Wobst et al., 2017), and chronic oxidative stress in the form of exposure to paraquat, an inhibitor of the mitochondrial electron transport chain (Meyerowitz et al., 2011). However, CTF-25 fragments were not observed in these studies (Meyerowitz et al., 2011; Wobst et al., 2017), or were only

faintly detected (Dormann et al., 2009; Suzuki et al., 2011). In a rat model of acute stroke, ischaemic neurons demonstrated elevated levels of soluble CTF-25 and activated caspase-3 (Kanazawa et al., 2011).

Although numerous other studies have substantiated the effect of cellular stress on TDP-43 cleavage, they did not examine whether this occurred via caspase activation. For instance, arsenite-induced oxidative stress generated CTF-35, an effect which was dependent on increased translation of the stress response gene *GADD34* (Goh et al., 2018). Inhibition of the ubiquitin-proteasome system by treatment with epoxomicin or MG132 was associated with cytoplasmic TDP-43 fragments of approximately 32–35 kDa, and relatively low levels of CTF-25, in both immortalized neuronal cell lines and primary hippocampal and cortical cultures (Ayala V. et al., 2011; van Eersel et al., 2011). Proteasome inhibition also exacerbated the aggregation of ectopically expressed CTFs (Walker et al., 2013; Ishii et al., 2017). Interestingly, while decreased proteasomal activity has been reported in cell culture models of mutant *VCP*, which accounts for a small proportion of people with FTLD (Gitcho et al., 2009b), TDP-43 CTF-25 is variably detected at low levels in the brains of people with *VCP*-linked FTLD (Neumann et al., 2007).

Progranulin Deficiency

Mutations to the *GRN* gene have also been proposed to mediate caspase-induced cleavage of TDP-43, although the initial evidence for this has since been largely invalidated. The majority of *GRN* mutations linked to FTLD are non-sense or frameshift mutations resulting in haploinsufficiency (Lopez de Munain et al., 2008) or missense mutations affecting *GRN* stability (van der Zee et al., 2007), all of which ultimately confer a loss of function of the progranulin protein. An early study posited *GRN* deficiency as the molecular mechanism underlying TDP-43 cleavage by caspase-3, showing activation of caspase-3 and the formation of TDP-43 CTF-25 and CTF-35 following knockdown of the *GRN* transcript by RNA interference in HeLa and H4 neuroglioma cells (Zhang et al., 2007). However, this finding was not supported by subsequent experiments in multiple cell models. *GRN* knockdown in HeLa and SH-SY5Y neuroblastoma cells did not trigger caspase-3 activation or TDP-43 cleavage (Dormann et al., 2009). In another study, equivalent levels of TDP-43 fragments of 36 kDa and smaller were detected in the nuclei of HeLa cells transfected with *GRN* siRNA, as well as in control mock-transfected cells (Shankaran et al., 2008). This suggests that not all breakdown products of TDP-43 are associated with disease, mirroring other studies in which low levels of TDP-43 CTFs were detected under baseline conditions (Dormann et al., 2009; Caragounis et al., 2010; Nishimoto et al., 2010; Meyerowitz et al., 2011).

Animal models of *GRN* deficiency similarly fail to support a critical role for *GRN* in TDP-43 fragmentation. Mutant $GRN^{-/-}$ mice do not exhibit TDP-43 truncation (Dormann et al., 2009) and display normal nuclear localization of TDP-43 and no difference in caspase-3 activation (Dormann et al., 2009; Ahmed et al., 2010). Caspase-3 activation and apoptosis were observed in mixed primary cortical cultures from $GRN^{-/-}$ mice, however, no proteolytic processing of TDP-43 occurred (Kleinberger et al., 2010). Similarly, downregulation of *GRN* in zebrafish does not cause TDP-43 truncation or mislocalization (Shankaran et al., 2008). Although wild-type mice exhibit increased cytosolic TDP-43 and decreased progranulin levels in denervated motor neurons following sciatic axotomy, there is no evidence of TDP-43 fragmentation (Moisse et al., 2009).

The Physiological Relevance of Caspase Cleavage of TDP-43

Studies examining caspase-mediated cleavage of TDP-43 have primarily used cellular assays that rely on the induction of apoptosis, or examination of post-mortem tissue from end-stage ALS and FTD patients. As an executioner caspase that is typically activated during programmed cell death, it is plausible that caspase-3 activation is a late-stage event that occurs at the onset of apoptosis rather than driving the initial cellular dysfunction in TDP-43 proteinopathies. To investigate this possibility, neuronal cell lines were exposed to sub-lethal doses of inducers of oxidative or ER stress (hydrogen peroxide and thapsigargin, respectively) (Ayala V. et al., 2011). Importantly, increased levels of cleaved caspase-3 were not observed, indicating that the activation of caspase-3 and subsequent cleavage of TDP-43 occurs after other pathological events that cause the onset of cell dysfunction, and may be a relatively late event in TDP-43 pathology.

Alternatively, caspase-cleavage of TDP-43 may play a physiological role in the maintenance of TDP-43 homeostasis. Examination of the time-course of fragmentation following overexpression of full-length TDP-43 identified ER membrane-bound caspase-4 as being responsible for initial cleavage at asparagine residue 174 to produce CTF-25 (Li et al., 2015). This subsequently activated caspase-3/7 to accelerate the generation of a 35 kDa fragment. It was concluded that caspase-4 monitors the amount of full-length TDP-43 accumulated in the ER and cleaves a small portion of the protein when optimal levels are exceeded (Li et al., 2015). Interestingly, this caspase was also elevated in the brains of rhesus macaques injected with TDP-43 M337V, where TDP-43 CTF pathology was also observed (Yin et al., 2019). In another study, a TDP-43 mutant resistant to caspase cleavage triggered cell death more rapidly than wild-type TDP-43 (Suzuki et al., 2011). Based on these findings, caspase-cleavage may be a protective cellular response triggered by other pathological factors, such as excessive levels of full-length TDP-43.

Calpains

The use of caspase inhibitors in studies of cell stress demonstrates that fragmentation of TDP-43 can occur via pathways that are independent of caspase processing (Meyerowitz et al., 2011; Nan et al., 2018). Calpains are a family of calcium-dependent, non-lysosomal cysteine proteases, the activation of which is modulated by the influx and efflux of Ca^{2+} into the cell (Baudry and Bi, 2016). Calpain activation may also contribute to TDP-43 truncation. This likely arises from dysregulation of Ca^{2+} and concomitant glutamate excitotoxicity, both of which have been broadly associated with pathological alterations in the brains of people with ALS and FTLD (Van Den Bosch et al., 2006;

Murley and Rowe, 2018). Calpain has been identified as the major protease responsible for the cleavage of TDP-43 into CTF-25 and CTF-35 in two mouse models of traumatic brain injury, as well as cellular models of neurotoxicity (Yang et al., 2014). Other studies also point to a relationship between excitotoxicity and cleavage of TDP-43 but these did not examine the role of calpains. For instance, induction of excitotoxicity via blockade of glutamine transport produced a 37 kDa TDP-43 fragment in rat spinal cord organotypic slice cultures (Ayala V. et al., 2011). Further, TDP-43 was cleaved into CTF-25 and CTF-35 under conditions of restricted intracellular Ca^{2+} (De Marco et al., 2014). Although this was attributed to the activity of caspases rather than calpains, it nonetheless implicates general dysregulation of Ca^{2+} homeostasis in the cleavage of TDP-43 into CTFs.

Evidence from cell and *in vitro* assays has also linked calpain activation with the generation of fragments from the N-terminal portion of TDP-43, with a range of cleavage sites between residues 229–346 in the C-terminal domain (Yamashita et al., 2012). Enzyme levels of both calpain-1 and calpain-2 were elevated in the spinal cord and primary motor cortex of patients with FTLD and motor neuron disease (MND) where 25 and 35 kDa N-terminal fragments were detected (Yamashita et al., 2012). However, 35 kDa TDP-43 fragments are infrequently detected in human neuropathology studies, and the presence of N-terminal TDP-43 fragments has not been previously reported, despite systematic examination of ALS and FTLD patient tissue (Igaz et al., 2008). Therefore, the pathophysiological relevance of the 35 kDa N-terminal fragment remains to be determined.

Alternatively Translated Isoforms

Several lines of evidence suggest that TDP-43 CTFs may also be produced via translation of an alternative transcript which is upregulated in disease. Site-specific mutagenesis and *in vitro* transcription/translation assays have identified two novel TDP-43 isoforms of 35 and 25 kDa which are generated under baseline conditions and in the absence of caspase activity (Nishimoto et al., 2010). The 35 kDa TDP-43 CTF may be accounted for by alternative in-frame translation from a downstream initiation codon of a specific splice variant which is upregulated in ALS spinal cords (Xiao et al., 2015). This variant has a 91 base pair splicing deletion at exon 2 and produces a gene product encoding a 35 kDa protein, proposed to be due to altered ribosomal scanning (Xiao et al., 2015). The presence of this protein was validated in ALS spinal cord tissue using an antibody directed against its predicted N-terminus, and when ectopically expressed in primary motor neurons it formed cytoplasmic aggregates and reduced cell viability (Xiao et al., 2015). In another study, analysis of alternatively spliced transcripts arising from the *TARDBP* locus in human cortex revealed three splice variants encoding a unique C-terminal sequence that directed localization of the expressed protein to the cytoplasm when transduced in human neuroglioma cells (D'Alton et al., 2015). However, the involvement of these proteins in human disease remains unclear, and there is as yet no evidence that the splice variants are expressed as proteins in the human brain. Nonetheless, although the generation of TDP-43 CTFs by post-translational modification to the TDP-43 protein is well established, it remains possible that CTFs may also arise from alterations at the transcriptional level.

Effect of Disease-Linked Genetic Mutations on TDP-43 CTF Generation

Genetic mutations linked with TDP-43 proteinopathies and ALS/FTD, including mutations to *TARDBP*, *C9orf72*, ataxin 2 (*ATXN2*) and superoxide dismutase 1 (*SOD1*), may confer vulnerability to caspase-cleavage of TDP-43. Numerous *TARDBP* mutations are linked to both familial and sporadic ALS or FTD (Gitcho et al., 2008, 2009a; Kabashi et al., 2008; Sreedharan et al., 2008). The majority of these mutations reside within the C-terminal domain and it is therefore plausible that they affect the biochemistry of the TDP-43 C-terminal region, including its susceptibility to proteolytic cleavage (Pesiridis et al., 2009). In line with this, studies using lymphoblastoid cells from patients harboring different *TARDBP* mutations indicate that specific mutations may predispose TDP-43 to fragmentation under baseline conditions (Corrado et al., 2009) or during proteasomal inhibition (Kabashi et al., 2008; Rutherford et al., 2008). Similarly, TDP-43 CTFs were detected in the spinal cord of a patient with a mutation causing a Q343R amino acid substitution, whereas no CTFs were detected in other sporadic ALS cases (Yokoseki et al., 2008). Furthermore, the A315T mutation has been shown to form persistent TDP-43 fragments that are resistant to further degradation by proteases (Guo et al., 2011). The disease-associated D169G mutation, which resides in the RRM1 region outside the C-terminal domain (Kabashi et al., 2008), is also associated with caspase-3 cleavage due to the enhanced stability and hydrophobic interactions of the RRM1 core afforded by a subtle local conformational change to the ß-turn region containing the mutation (Chiang et al., 2016).

Hexanucleotide expansions in the *C9orf72* gene account for the largest proportion of familial ALS and FTLD cases (DeJesus-Hernandez et al., 2011; Renton et al., 2011; McCann et al., 2017). However, whether repeat-associated non-AUG (RAN) translation of the intronic GGGGCC hexanucleotide repeat in *C9orf72*-linked ALS and FTLD promotes TDP-43 fragmentation via caspase-3 activation has not been directly addressed. Overexpression of the glycine-alanine dipeptide repeat protein (poly GA), which is produced by RAN-translation of the *C9orf72* hexanucleotide expansion, in cultured cells induces caspase-3 activation and ER stress (Zhang et al., 2014), and poly GA peptides have also been associated with production of a TDP-43 fragment of approximately 30 kDa (Lee Y. B. et al., 2017). Further experiments addressing the precise link between *C9orf72* mutation and TDP-43 pathology, including proteolytic cleavage, are therefore warranted.

Elevation of activated caspase-3 has been noted in the spinal motor neurons of ALS patients harboring intermediate length polyQ expansions (27–33 CAG repeats) in *ATXN2*, which confers increased risk of ALS (Elden et al., 2010; Hart and Gitler, 2012). Expression of ataxin 2 with intermediate length glutamine tracts (31Q) in neuronal and non-neuronal cell lines increased the levels of a 30 kDa TDP-43 CTF (Hart and Gitler, 2012). Importantly, these effects on TDP-43 CTF generation were not observed

when shorter (22Q, normal) or longer (39Q, spinocerebellar ataxia-associated) ataxin 2 proteins were expressed (Hart and Gitler, 2012). It is unclear whether *ATXN2* expansions are mechanistically linked to caspase activation and TDP-43 cleavage, although knockdown of endogenous ataxin 2 in transgenic TDP-43 mice ameliorates disease and may slightly decrease levels of insoluble TDP-43 CTF-35 (Becker et al., 2017).

Mutations to the SOD1 gene were the first reported cause of ALS (Rosen et al., 1993). Motor neuron-like NSC-34 cells form TDP-43 CTFs when incubated with aggregates of recombinant human SOD1 harboring the disease-causative G93A mutation (Zeineddine et al., 2017) or transfected with this particular mutant (Jeon et al., 2018). Some studies in SOD1 mutant mice (G85R and G93A substitutions) have also demonstrated the deposition of TDP-43 CTFs in the spinal cord, albeit at very low levels and late in disease (Cai et al., 2015; Jeon et al., 2018). However, another study found no evidence of TDP-43 fragmentation in SOD1 mice, and no mechanism underlying SOD1-mediated cleavage of TDP-43 has been proposed (Shan et al., 2009). Further to this, TDP-43 pathology is not found in neural tissue from people with ALS with SOD1 mutations (Mackenzie et al., 2007; Tan et al., 2007). It remains likely that any TDP-43 pathology associated with mutations to SOD1 is a minor player in disease and secondary to late-stage neurodegeneration.

DEGRADATION AND CELLULAR CLEARANCE OF TDP-43 CTFs

In an effort to develop treatments to effectively clear TDP-43 pathology, numerous molecules have been identified as capable of degrading both full-length and fragmented TDP-43, including ubiquilin-2 (UBQLN2) (Cassel and Reitz, 2013) and poly(A)-binding protein nuclear 1 (PABPN1) (Chou et al., 2015). However, there are various conditions under which CTFs may be subjected to different clearance mechanisms compared to full-length TDP-43, which may contribute to their differential accumulation.

Molecular chaperones such as heat shock proteins (HSPs) are central to maintaining cellular proteostasis, including protein degradation via chaperone-mediated autophagy, and are commonly dysregulated in neurodegenerative diseases (Yerbury et al., 2016). The degradation of TDP-43 CTFs may be regulated by heat shock transcriptional factor 1 (HSF1) (Lin et al., 2016), which can induce HSP70. In line with this, the level of endogenous CTF-35 was unchanged following proteasome inhibition in cells overexpressing HSF-1 (Lin et al., 2016), which may be attributed to decreased caspase cleavage of TDP-43, or enhanced chaperone-mediated clearance of CTF-35. HSP70 levels were increased following expression of TDP-43 CTFs of varying sizes in cultured cells but this did not occur following full-length TDP-43 expression (Zhang et al., 2010). HSPB8 is another small HSP that may contribute to cellular clearance of TDP-43 fragments. In NSC-34 cells, upregulation of HSPB8 was greater following expression of CTF-25 and CTF-35 compared to full-length TDP-43, and the levels of insoluble CTF-25 were dramatically decreased following HSPB8 overexpression, compared to mild decreases in insoluble CTF-35 and full-length TDP-43 (Crippa et al., 2016).

The ubiquitin-proteasome system may also contribute to cellular clearance of TDP-43 CTFs. In cultured cells, the E3 ligase cullin-2 RING complex has been shown to enhance the ubiquitination and degradation of CTF-35 but not full-length TDP-43 (Uchida et al., 2016). Although it has been reported that the adaptor protein sequestresome 1 (p62/SQSTM1), which transports ubiquitinated proteins for proteasomal degradation, decreases aggregation of full-length TDP-43 as well as 15 and 25 kDa fragments (Brady et al., 2011), another study found p62 overexpression specifically lowered levels of CTF-35 but not full-length TDP-43 (Tanji et al., 2012). The proteasome has been shown to degrade a broad range of TDP-43 variants, including the full-length protein, disease-linked mutants and CTFs (Scotter et al., 2014; Chou et al., 2015; Wang X. et al., 2015; Crippa et al., 2016; Cicardi et al., 2018). However, CTF-25 is more sensitive to degradation by autophagy than CTF-35 or full-length TDP-43, as demonstrated by pharmacological inhibition or activation of the autophagy pathway (Scotter et al., 2014; Wang X. et al., 2015; Crippa et al., 2016; Cicardi et al., 2018). VCP has been shown to be important for functional autophagy (Ju et al., 2009), and mutations to *VCP* cause rare cases of FTLD-TDP type D. This suggests a potential link between VCP and the clearance of TDP-43. Expression of FTLD-linked VCP mutant proteins in cell culture increases cytoplasmic TDP-43 but does not lead to production of TDP-43 CTFs (Gitcho et al., 2009b). However, FTLD-TDP type D with *VCP* mutation is characterized by accumulation of intranuclear, not cytoplasmic, TDP-43 pathology. The cause of nuclear TDP-43 pathology in FTLD-TDP type D remains unclear, although the relatively low abundance of TDP-43 CTFs in these cases (Neumann et al., 2007) highlights the importance of extra-nuclear accumulation of TDP-43 in the generation of CTFs.

The N-terminal region of each TDP-43 CTF may determine the specific pathway through which it is degraded (Kasu et al., 2018). Arginyltransferase (ATE), the enzyme responsible for post-translational arginylation, has been implicated in signaling processes required for the degradation of intracellular proteins by autophagy or UPS pathways. Numerous proteins associated with neurodegenerative diseases have been identified as substrates of ATE, including β-amyloid, α-synuclein and TDP-43 CTFs (Galiano et al., 2016). The Arg/N-end rule pathway targets proteins and peptide fragments with destabilizing, unacetylated N-terminal residues, such as TDP-43 fragments cleaved at Arg208, Asp219, and Asp247, for proteolytic degradation (Brower et al., 2013). When expressed in mouse fibroblasts deficient for ATE, TDP-43 CTFs aggregate, suggesting that they are selectively degraded by the Arg/N-end rule pathway as a protective response to failing proteostasis and neurodegeneration (Brower et al., 2013). More recent work has shown that, whereas TDP-43 fragments beginning at residue 247 are degraded primarily by the Arg/N-end rule pathway, degradation of fragments with an N-terminal at residue 219 can occur independently of ATE (Kasu et al., 2018). Further dissection of the precise mechanisms of degradation of the different TDP-43 CTFs and the role of ATE is therefore warranted.

There are several experimental caveats to be considered when examining the degradation of TDP-43 CTFs. Several studies have demonstrated enhanced turnover of exogenously expressed TDP-43 CTFs compared to full-length TDP-43 or a TDP-43 protein containing a mutated NLS that drives cytoplasmic expression, henceforth referred to as TDP-43 ΔNLS (Pesiridis et al., 2011; Zhang et al., 2011; Hans et al., 2014; Huang et al., 2014; Scotter et al., 2014). Although CTFs are often more prone to aggregation than the full-length protein, soluble CTF-25 typically exhibits lower steady-state levels. Critically, this may be impacted by experimental conditions; these levels are elevated by tagging with eGFP compared to small tags such as HA or Myc (Li et al., 2011; Zhang et al., 2011; Scotter et al., 2014). Furthermore, whereas CTF-25 is often less soluble than other TDP-43 variants, assays of cleavage of endogenous TDP-43 demonstrate higher levels of CTF-35. It is possible that the cell lines used in these experiments are inherently more adept at recognizing and degrading CTF-35 or maintaining its solubility, which may underlie the high aggregation propensity of CTF-25 in these models.

EXPRESSION OF TDP-43 CTFs IN CELL MODELS VARIABLY RECAPITULATES DISEASE

In addition to the observation that neurodegeneration can proceed in TDP-43 proteinopathies in the absence of detectable TDP-43 CTFs, the argument for a disease-causing role for these fragments is weakened by the disparate results yielded by investigations into the biochemical effects of TDP-43 CTFs using *in vitro* and cell-based assays. Despite forming disease-reminiscent inclusions upon exogenous expression, TDP-43 CTFs typically do not confer a toxic gain of function, leaving markers of cytotoxicity and apoptosis unaltered. However, there is some evidence that they disrupt RNA splicing by TDP-43.

Cytoplasmic Accumulation of Insoluble CTFs

TDP-43 CTFs accumulate in the cytoplasm of the cell, likely due to removal of the NLS during proteolytic cleavage (Winton et al., 2008; Lee et al., 2011). There is also evidence that CTFs form complexes with RNA transcripts to be transported out of the nucleus (Pesiridis et al., 2011). When expressed in cultured neuronal cells, fragments from the C-terminal portion of TDP-43 form ubiquitinated, phosphorylated inclusions that closely resemble human ALS and FTLD-TDP brain pathology (Igaz et al., 2009; Nonaka et al., 2009; Zhang et al., 2009, 2010; Yang et al., 2010; Fallini et al., 2012; Chou et al., 2015; Kitamura et al., 2016).

The propensity of TDP-43 to aggregate appears to be mediated by its C-terminal domain. Transduction of synthetic fibrils derived from short sequences within the TDP-43 C-terminal region has been shown to induce seed-dependent aggregation of full-length TDP-43 in neuroblastoma cells (Shimonaka et al., 2016). Deletion studies in yeast models determined that the presence of most of the TDP-43 C-terminal domain was necessary for aggregation to occur, and that aggregation increased according to how much of the RRM2 was included in the fragment (Johnson et al., 2008). Examination of recombinant TDP-43 *in vitro* revealed that amino acids 311–320 in the C-terminal domain were most critical for the formation of fibrils by TDP-43 CTFs (Saini and Chauhan, 2011). To complement these findings, removal of the glycine-rich domain (amino acids 265–319) in CTF-25 blocked heat shock-induced aggregation (Udan-Johns et al., 2014).

It is important to note that full-length TDP-43 is also inherently prone to aggregation and in the absence of mutations or modifications will spontaneously form aggregates that resemble those observed in ALS patients (Johnson et al., 2009). Moreover, neuroblastoma cells cultured with insoluble protein extracts from ALS brain tissue form aggregates of full-length TDP-43 prior to aggregates of CTFs (Nonaka et al., 2013). While aggregates of full-length TDP-43 are enriched for proteins involved in mRNA processing and RNA splicing, CTF-25 aggregates are enriched for proteins that moderate nucleocytoplasmic and intracellular transport (Chou et al., 2018), consistent with alterations to nuclear morphology observed following expression of this CTF (Walker et al., 2013). Thus, both full-length TDP-43 and its CTFs are prone to aggregation, and the aggregation of each may impact cellular functions via different mechanisms.

Factors That Modify TDP-43 CTF Aggregation

Cleavage of TDP-43 alone may not be sufficient to cause the insoluble inclusions that are characteristic of ALS and FTLD. Using an inducible form of the tobacco etch virus, it was shown that *de novo* cleavage of TDP-43 produced CTFs that were rapidly exported to the cytoplasm and cleared from the cell (Pesiridis et al., 2011). In this study, CTFs only formed inclusions when an additional insult occurred, such as microtubule transport disruption or depletion of RNA. RNA depletion has also been shown to exacerbate the sequestering of endogenous TDP-43 into CTF-25 aggregates (Kitamura et al., 2016). Phosphorylation may also modulate the solubility of TDP-43 CTFs. Indeed, the C-terminal domain of TDP-43 is enriched with serine residues, and phosphorylation of this region is widely observed in tissue from ALS and FTLD patients (Hasegawa et al., 2008; Inukai et al., 2008; Kametani et al., 2009; Neumann et al., 2009). Moreover, the majority of genetic mutations that map to the C-terminal domain of TDP-43 cause the abnormal creation or disturbance of serine or threonine residues, or the introduction of aspartic or glutamic acid phosphomimics (Buratti, 2018). TDP-43 CTFs transfected in immortalized cell lines were phosphorylated at the same or very similar sites to those seen in ALS and FTLD patient tissue and formed insoluble inclusions (Igaz et al., 2009; Zhang et al., 2010; Furukawa et al., 2011; Li et al., 2011). The effects of phosphorylation are likely dependent on the specific kinase involved and the site of phosphorylation.

Some studies suggest that phosphorylation has similar effects on both full-length TDP-43 and CTFs. For instance, inhibition of various kinase pathways, including c-Jun N-terminal kinase (JNK), cyclin-dependent kinase (CDK), and glycogen synthase

kinase 3 (GSK3), attenuates the aggregation of full-length and truncated forms of TDP-43 (Meyerowitz et al., 2011; Moujalled et al., 2013). However, there is also evidence that the solubility of TDP-43 and its lower molecular weight species may be differentially impacted by phosphorylation. In line with a pathogenic effect for phosphorylation, the degree of phosphorylation and associated insolubility of fragments cleaved within the RRM2 domain of TDP-43 has been shown to be dependent on the precise cleavage site; phosphorylation and insolubility of the fragment increased as the cleavage site moved closer to the C-terminus (Furukawa et al., 2011). On the other hand, phosphorylation of TDP-43 CTFs may be a protective phenomenon. Substitution of S409/410 for an aspartic acid phosphomimic in 15 kDa CTFs increased their solubility and decreased aggregation (Brady et al., 2011). Importantly, this mutation had no effect on full-length TDP-43, illustrating that a specific post-translational modification can have distinct effects on different TDP-43 species.

Aggregation of TDP-43 CTFs Does Not Necessitate Cell Death or Dysfunction

Continued debate surrounds the role of protein aggregation in neurodegeneration. It has been suggested that the large inclusions that characterize ALS and FTLD neuropathology may be the product of an adaptive response aimed at protecting cells from more toxic oligomers or diffusible assemblies that may not be readily detectable by standard biochemical or microscopy techniques (Polymenidou and Cleveland, 2011). Recent research has demonstrated that smaller soluble species of mutant SOD1 and dementia-associated forms of tau are more toxic to cells than large, mature fibrils (Ghag et al., 2018; Zhu et al., 2018). It is possible that TDP-43 aggregation functions in a similar manner; soluble TDP-43 monomers and oligomers as well as micro- and macro-aggregates have been identified in cellular models of TDP-43 proteinopathy (Scotter et al., 2014), and in another study, preventing TDP-43 self-aggregation did not prevent cell death (Liu et al., 2013).

Although CTFs expressed in cell culture reliably form disease-like cytoplasmic inclusions, this does not always induce cellular toxicity or apoptosis. For instance, exogenous expression of full-length TDP-43 induced programmed cell death more readily than CTF-35, whereas CTFs of 25–27 kDa had no effect, despite their cytoplasmic aggregation (Suzuki et al., 2011; Yamashita et al., 2014). By contrast, one study showed that CTF-25 triggered a greater degree of ER-stress mediated apoptosis than CTF-35 or full-length TDP-43 (Wang X. et al., 2015). Evidence for the toxicity of CTFs relative to full-length TDP-43 expressed in neuronal cell lines is also variable. Elevated levels of lactate dehydrogenase (LDH), indicating cell death, have been reported in M17 neuroblastoma cells following CTF-25 expression (Zhang et al., 2009). However, another study found that although longer CTFs (from residues 86–414 or 170–414) impaired neurite outgrowth, they did not impact LDH release or activated caspase-3 levels in NSC-34 cells, despite this fragment being more aggregation prone than full-length TDP-43 (Yang et al., 2010).

Evidence from studies of endogenous TDP-43 CTFs also calls into question the relationship between CTF aggregation and disease. In experiments using inducible pluripotent stem cells derived from a patient carrying an ALS-linked M337V TDP-43 mutation, some clones exhibited higher levels of insoluble CTFs but this was not associated with apoptosis (Bilican et al., 2012). Thus, a critical finding from cell biology studies is that, regardless of cytoplasmic redistribution and aggregation propensity, TDP-43 CTFs do not reliably induce a toxic "gain of function" via cellular toxicity or activation of apoptotic pathways. Further, these studies highlight the need to assay factors additional to aggregation. For example, cellular atrophy, necrosis and the activation of cell stress responses may also contribute to the functional failure of specific neuronal populations in TDP-43 proteinopathies (Bodansky et al., 2010; Liachko et al., 2010; Matus et al., 2013).

The Role of Phase Transition in TDP-43 Accumulation

Emerging research into the effects of TDP-43 liquid–liquid phase separation on the dynamics of membraneless organelles such as stress granules offers an alternative way of viewing TDP-43 accumulation in ALS and FTLD. The role of the TDP-43 C-terminal domain in liquid–liquid phase separation has been well established (Dewey et al., 2011; Li et al., 2018a,b). However, recent research suggests that the N-terminal domain also contributes to this phenomenon (Wang A. et al., 2018; Wang L. et al., 2018). In cell culture, TDP-43 CTF-35 is recruited to stress granules when ectopically expressed (Nishimoto et al., 2010; Nihei et al., 2012) or when fragmentation is induced by chronic oxidative stress (Meyerowitz et al., 2011). However, CTF-25 formed fewer stress granules than CTF-35 or full-length TDP-43 (Liu-Yesucevitz et al., 2010). Stress granule markers have been shown to co-localize with TDP-43-positive inclusions in the ALS spinal cord (Liu-Yesucevitz et al., 2010; Bentmann et al., 2012), or partially colocalize with smaller punctate forms of TDP-43 (Colombrita et al., 2009). However, in the cortex of ALS and FTLD patients where CTFs predominate, stress granule markers do not co-localize with TDP-43 inclusions (Bentmann et al., 2012) or show a lower degree of specificity than in ALS spinal cord tissue (Liu-Yesucevitz et al., 2010). The fact that the RNA binding motifs of TDP-43 are intact in CTF-35 but not in CTF-25 (see **Figure 1**) (Wei et al., 2017) suggests that RNA-binding may be required for the formation of TDP-43-positive stress granules. Indeed, studies using deletion constructs have shown that both the RRM1 and C-terminal regions are necessary for the recruitment of TDP-43 to stress granules (Colombrita et al., 2009).

Cell-to-Cell Propagation of TDP-43

The C-terminal region of TDP-43 shares moderate sequence homology with prion proteins (Guo et al., 2011). Given this structural similarity, a prion-like mechanism of self-templating propagation has been proposed to explain the focal onset and subsequent spread of dysfunction in ALS patients (Cushman et al., 2010; Polymenidou and Cleveland, 2011; Jucker and Walker, 2013; Ludolph and Brettschneider, 2015; Brauer et al., 2018). Consistent with this, mammalian cells incubated with

protein or exosomes extracted from ALS and FTLD brain homogenates formed TDP-43 CTFs of the same molecular weight as those detected by immunoblotting of the brain lysates (Nonaka et al., 2009; Furukawa et al., 2011; Iguchi et al., 2016; Smethurst et al., 2016). In a similar manner, ALS spinal cord homogenates, which do not contain CTFs, induced the formation of aggregates of full-length TDP-43 in cell culture (Smethurst et al., 2016). The capacity to induce *de novo* pathology suggests that TDP-43 is capable of being transmitted to nearby or interconnected cells, where it may corrupt endogenous TDP-43 to adopt pathological, aggregation-prone conformations (Irwin et al., 2015). While the C-terminal domain has been postulated to mediate self-templating of TDP-43 (Mompean et al., 2016), the regional spreading of TDP-43 is not unique to CTFs, and the inoculation studies described above do not indicate exacerbated propagation of pathology by brain extracts containing CTFs compared to spinal cord extracts containing the full-length protein (Smethurst et al., 2016). Further, it has been proposed that the prion-like architecture of the C-terminal domain enables TDP-43 to form structurally flexible aggregates under physiological conditions (Wang et al., 2012). In this study, ALS-linked mutations to this region, such as G348C and R361S, decreased the prion-like activity of TDP-43, thereby triggering the formation of rigid pathological inclusions. Overall, despite the prion-like structure of the TDP-43 C-terminal domain, there is no evidence from cell assays that the templated inter-cellular transmission of TDP-43 pathology is impacted by the cleavage of TDP-43 into CTFs.

Effects of CTFs on Endogenous Full-Length TDP-43

C-terminal fragments of approximately 30–35 kDa have been shown to sequester endogenous TDP-43 from the nucleus, resembling the clearance of nuclear TDP-43 seen in people with ALS and FTLD-TDP (Nonaka et al., 2009; Nishimoto et al., 2010; Che et al., 2011, 2015). On the other hand, co-immunoprecipitation experiments have demonstrated that TDP-43 CTF-25 binds weakly to native full-length TDP-43 (Nonaka et al., 2009; Zhang et al., 2009). Although this resulted in depletion of nuclear TDP-43 in one study (Nonaka et al., 2009), another study reported no sequestration of endogenous TDP-43 (Zhang et al., 2009).

CTFs May Impair RNA Processing by TDP-43

Evidence for perturbation of RNA metabolism following cleavage of TDP-43 is more consistent. Impairment of skipping of exon 9 of the cystic fibrosis transmembrane conductance regulator (CFTR) pre-mRNA, used as a model of TDP-43 function, has been observed for both CTF-25 (Igaz et al., 2009; Nonaka et al., 2009; Zhang et al., 2009; Nishimoto et al., 2010; Udan-Johns et al., 2014) and CTF-35 (Nishimoto et al., 2010; Che et al., 2011, 2015). However, one study reported no effect on exon skipping following expression of a CTF from residues 220–414 in neuroblastoma cells, corresponding to the caspase-cleaved CTF-25 identified in human disease (Zhang et al., 2009). This may be because the glycine/asparagine-rich region of the TDP-43 C-terminal domain contributes to exon skipping activity and other aspects of gene transcription (Wang et al., 2004, 2012; Buratti et al., 2005). As a result, partial or total removal of the RNA recognition motifs of TDP-43 following cleavage of its N-terminal domain might not completely disrupt RNA processing. Thus, cell-based examinations suggest that TDP-43 CTFs may contribute to cellular dysfunction via a loss of normal function, impairing the ability of TDP-43 to regulate RNA splicing.

TDP-43 CTF EXPRESSION *IN VIVO* POORLY MODELS ALS AND FTLD PHENOTYPES

In both ALS and FTLD, TDP-43 pathology is observed in a range of cell types and may spread from a focal point of onset to affect other regions of the brain and spinal cord (Ravits and La Spada, 2009; Brettschneider et al., 2013, 2014). A key limitation of cellular models of ALS and FTLD is that they do not recapitulate the complex anatomy involved in TDP-43-driven neurodegeneration (Van Damme et al., 2017). For this reason, it is imperative that the validity of *in vitro* findings is confirmed in appropriate animal models. While simple model organisms such as *Drosophila melanogaster*, *Caenorhabditis elegans* and zebrafish are easily manipulated for microscopy and offer well-characterized genomes, rodent models more faithfully reproduce the cellular and behavioral or motor phenotypes that typify TDP-43 proteinopathies (Dayton et al., 2013). Accordingly, rodent models are particularly useful for illuminating disease mechanisms and for pre-clinical testing of potential therapeutics (Van Damme et al., 2017), and are the most broadly employed *in vivo* models of ALS and FTD (Tan et al., 2017a).

In order to examine the contribution of truncated forms of TDP-43 to motor or cognitive decline in ALS and FTD, several transgenic rodent models expressing TDP-43 CTFs of approximately 25 kDa have been developed. These models have typically used broad neuronal promoters such as *Thy1.2*, mouse prion protein (*PrP*) and neurofilament heavy chain (*NEFH*) to direct selective transgene expression in neurons of the brain and spinal cord. Some models have employed the Ca^{2+}/calmodulin-dependent kinase II α (*CaMKIIα*) promoter to restrict expression to forebrain neurons, primarily in the cortex, hippocampus, and striatum (Cannon et al., 2012), making them particularly relevant for the investigation of FTLD. When modeling ALS and FTLD, the choice of gene promoter is pertinent as CTFs are rarely detected in the spinal cord of patients, regardless of which disease is manifested.

Transgenic TDP-43 CTF Expression Modestly Affects Motor Performance and Cognition

Numerous animal models have considered the role of TDP-43 CTF-25 in the onset and progression of ALS and FTD, summarized in **Table 2**. Remarkably, transgenic overexpression of TDP-43 CTFs in behaving animals consistently fails to recapitulate the key behavioral features of these diseases.

TABLE 2 | Few overt effects on neuropathology and motor and behavioral phenotypes are seen in overexpression studies of TDP-43 CTFs in mouse, rat, *Drosophila*, and *C. elegans* models.

Model organism	Amino acid sequence of TDP-43 CTF transgene	Promoter/ driver	Additional study details	Controls and comparisons	Phenotype measure	Phenotype outcome	Neuropathology	References
Mouse	208–414	*CaMKIIα*	Dox-suppressible expression. Transgene induced at 1 month of age. Mice examined up to 24 months of age.	NT and monogenic littermates	Rotarod Wirehang Y-maze	No gross motor or cognitive deficits.	CTFs localized to cytoplasm but no large inclusions. CTFs phosphorylated in hippocampal CA1 region but no neurodegeneration. Minimal phosphorylation of CTFs in the dentate gyrus but progressive death of granule cells in mice 10 months and older.	Walker et al., 2015b
			Insoluble protein extracted from FTLD-TDP brains injected into mouse cortex.	NT and ΔNLS mice		n/a	Mice demonstrated less spread of TDP-43 pathology throughout the brain compared to ΔNLS mice.	Porta et al., 2018
		NEFH	Dox-suppressible expression. Transgene induced at 1 month of age. Mice examined up to 19 months of age.	NT and monogenic littermates		n/a	No overt neurodegeneration. TDP-43 phosphorylated in CA1 region of hippocampus, and ubiquitinated in SLM.	Walker et al., 2015b
			Dox-suppressible expression. Transgene induced for 6 weeks in adult mice.	NT	No gross motor defects observed (data not shown).		No motor neuron degeneration, clearance of nuclear TDP-43 or large cytoplasmic inclusions detected in lumbar SC.	Spiller et al., 2018
		PrP	Animals examined at 8, 13, and 18 months of age.	FL-TDP-43 and NT	Rotarod Y-maze Contextual and cued fear conditioning	No motor or behavioral phenotype. Mild memory and motor deficits were observed in mice that overexpressed FL-TDP-43.	No change in endogenous TDP-43 levels.	Tsuiji et al., 2017
	216–414	*Thy1.2*	Animals examined at 2 or 6 months of age.	NT littermates	Novel object recognition test T-maze Open field locomotion test Rotarod	No significant difference in any behavior or motor tests.	Soluble CTFs detected in cytoplasm and nucleus, by long exposure of immunoblot. No change in endogenous TDP-43 levels and no inclusions or neurodegeneration.	Caccamo et al., 2012
			Mice treated with the glucocorticoid dexamethasone at 6 months of age.	NT	Spatial version of Morris water maze	Dexamethasone treatment worsened memory deficits but had no effect on swim speed or distance traveled, indicating no motor impairment.	In mice expressing CTF-25, dexamethasone treatment impaired autophagy (indicated by lower levels of Atg7 and LC3-II) and increased soluble CTF-25 levels in the nucleus and cytoplasm but no change to endogenous FL-TDP-43 levels.	Caccamo et al., 2013

(Continued)

TABLE 2 | Continued

Model organism	Amino acid sequence of TDP-43 CTF transgene	Promoter/ driver	Additional study details	Controls and comparisons	Phenotype measure	Phenotype outcome	Neuropathology	Reference
			Hemizygous and homozygous mice examined at 15 months of age.	NT	Radial arm water Maze Morris water maze Rotarod	Hemizygous mice exhibited motor dysfunction and impaired spatial and working memory, exacerbated in homozygous mice.	Impaired autophagy and proteosomal function in both lines. Soluble and insoluble CTF-25 detected in the nucleus and cytoplasm, but FL-TDP-43 only detected in the nucleus. Homozygous mice showed lower levels of endogenous FL TDP-43.	Caccamo et al., 2015
	219–414	CMV/chicken β-actin	*In utero* electroporation of construct into embryonic motor cortex.	FL-TDP-43 and TDP-43^{M337V}		n/a	CTFs formed ubiquitinated, phosphorylated aggregates in nucleus and cytoplasm, detected up to 21 days post-natal.	Akamatsu et al., 2013
Rat	220–414	CMV/chicken β-actin	IV injection of AAV9 in WT neonatal rats. Animals phenotyped from 2 to 24 weeks of age.	ΔNLS and GFP	Rotarod Open field test Hindlimb extension Locomotor Scoring of rearing behavior	CTF and ΔNLS rats showed equivalent motor dysfunction in rotarod and open field tests. Deficient forelimb use during rearing in seven of 13 CTF and two of 16 ΔNLS rats tested.	No neurodegeneration or muscle atrophy in any of the models examined.	Dayton et al., 2013
Drosophila	174–414 and 206–414	*elav/Gal4* for pan-neuronal expression, *D42/Gal4* for MN expression, *DaG32/Gal4* for ubiquitous expression		FL-TDP-43, ΔNLS, and disease-linked mutants (TDP-43^{A315T}, TDP-43^{G287S}, TDP-43^{A382T}, and TDP-43^{N390D})	Climbing assay Longevity assay	Pan-neuronal or MN specific CTF expression caused a milder reduction in locomotion and lifespan compared to ΔNLS and disease-linked mutants. CTF had no impact on lifespan while other mutants caused premature death.	n/a	Voigt et al., 2010
	202–414	*GMR-Gal4* for expression in retinal photoreceptors		FL-TDP-43 and RFP		n/a	FL-TDP-43 associated with progressive degeneration and ultrastructural vacuoles in retinal cells, while CTF expression had no effect.	Li et al., 2010

(Continued)

TABLE 2 | Continued

Model organism	Amino acid sequence of TDP-43 CTF transgene	Promoter/ driver	Additional study details	Controls and comparisons	Phenotype measure	Phenotype outcome	Neuropathology	Reference
				NT and FL-TDP-43	Climbing assay Longevity assay	Compared to FL-TDP-43, expression of CTF caused later onset of motor deficits, which was rescued by treatment with the small heat shock protein CG14207.	CTF-25 was less toxic than FL-TDP-43, produced a milder rough eye phenotype and was cleared more efficiently by CG14207.	Gregory et al., 2012
		OK107-Gal4 for expression in mushroom bodies		FL-TDP-43 and RFP		n/a	FL-TDP-43 was associated with neuronal death and loss of axons. No effect of CTF expression.	Li et al., 2010
		OK371-Gal4 for MN expression		FL-TDP-43 and RFP		n/a	CTF expression had no effect. Regions where FL-TDP-43 had accumulated in the cytoplasm showed axonal swelling, inclusion formation in soma and axons and fragmentation of the nucleus.	Li et al., 2010
C. elegans	219–411	*snb-1* for pan-neuronal expression		FL-TDP-43, disease-linked TDP-43^{Q331K} and TDP-43^{M337V} mutants	Fly motility assay	FL-TDP-43 and disease mutants produced more severe motor deficits than expression of the CTF.	CTF formed cytoplasmic aggregates but less toxic to neurons than FL-TDP-43.	Zhang et al., 2011
	220–411	*snb-1*		Constructs with RMM1, RMM2 or C-terminal deleted		n/a	CTF formed large cytoplasmic inclusions whereas RMM1 and RMM2 mutants had a granular appearance and C-terminal deletion mutant formed a singular aggregate in the cytoplasm.	Ash et al., 2010

AAV9, adeno-associated virus serotype 9; Atg7, autophagy-related protein 7; C. elegans, Caenorhabditis elegans; CA1, cornu ammonis field 1; CaMKIIα, Ca^{2+}/calmodulin-dependent kinase II α; CMV, cytomegalovirus; CTF, C-terminal fragment; Dox, doxycycline; FL-TDP-43, full-length TDP-43; GFP, green fluorescent protein; IV, intravenous; LC3, microtubule-associated protein 1A/1B-light chain 3; LC3-II, LC3-phosphatidylethanolamine conjugate; MN, motor neuron; NT, non-transgenic; RFP, red fluorescent protein; RRM1, RNA recognition motif 1; RRM2, RNA recognition motif 2; SC, spinal cord; SLM, stratum lacunosum-moleculare; snb-1, synaptobrevin-1; WT, wild-type.

Moreover, the neuropathology observed following CTF expression in animals is incongruent with findings in cell and human post-mortem studies. These animal models therefore provide the most compelling evidence that TDP-43 CTFs alone are unlikely to be prime triggers of neurodegenerative disease.

In transgenic mice, using the *CaMKIIα* promoter for forebrain expression or the *NEFH* promoter to direct expression of CTF-25 (spanning amino acids 208–414) to the neurons of the brain and spinal cord does not induce motor or cognitive defects (Walker et al., 2015b; Spiller et al., 2018). The same CTF has been expressed in mice using the *PrP* promoter (for brain and spinal cord distribution) and again, no behavioral phenotype was reported (Tsuiji et al., 2017). By contrast, pan-neuronal expression of TDP-43 ΔNLS, for example, generates a dramatic and progressive motor phenotype akin to ALS (Walker et al., 2015a). Therefore, the inability of TDP-43 CTF-25 to induce behavioral alterations in mice cannot be explained by the choice of promoter.

In a different mouse model, CTF-25 (TDP-43 amino acids 216–414) was expressed in neurons using a *Thy1.2* promoter system (Caccamo et al., 2010, 2012, 2013, 2015). However, transgenic animals did not display any significant disease phenotype at 2 or 6 months of age on tests of motor function or measures of behavioral changes associated with FTD, such as the novel object recognition test (Caccamo et al., 2012, 2013). Performance of these animals on tests of working and spatial memory, such as the radial arm water maze and the Morris water maze, indicated memory impairments under specific conditions, such as aging and stress hormone modulation (Caccamo et al., 2013, 2015). However, changes to memory are rarely detected in the early stages of FTD (Bang et al., 2015). Hippocampal-dependent tasks, such as those used in these studies, are more appropriate measures of Alzheimer's disease and dementia subtypes characterized by memory loss (Roberson, 2012; Vernay et al., 2016). Consistent with the memory impairments observed in these mouse models, TDP-43 CTFs arising from caspase cleavage at residue 219 have been detected in neurofibrillary tangles, Hirano bodies and reactive astrocytes in the hippocampus and entorhinal cortex of people with Alzheimer's disease at post-mortem (Rohn, 2008). At 15 months of age, but not at earlier timepoints, *Thy1.2* CTF-25 mice performed significantly worse on rotarod test of motor co-ordination but showed no difference in swim speed in the Morris water maze (Caccamo et al., 2015). Overall, these studies indicate that under certain conditions, CTF-25 may cause some neuronal dysfunction, but this is not dramatic and is not highly reminiscent of ALS or FTD.

A rat model of TDP-43 CTF-25 (amino acids 220–414) has been produced using a viral-mediated strategy, resulting in highest expression in the spinal cord, cerebellum, muscle, heart, and liver (Dayton et al., 2013). Approximately half of the animals tested displayed mild forelimb impairment but exhibited no evidence of neuron loss or muscle wasting, in stark contrast to the widespread muscle atrophy and rapidly progressing motor dysfunction that is characteristic of people with ALS. It is also unclear how off-target effects due to heavy expression of the transgene outside the central nervous system (CNS) may have contributed to the results obtained. With regard to human pathology, it is critical to note that CTFs are rarely detected in the post-mortem ALS spinal cord and have not been reported in muscle (Weihl et al., 2008; Cykowski et al., 2018) or other peripheral tissues. The relevance of TDP-43 CTF expression outside the brain to the study of TDP-43 proteinopathies is therefore debateable.

Data from simple model organisms similarly suggest that TDP-43 CTFs are not key drivers of disease. In *Drosophila*, transgenic expression of full-length TDP-43 or ALS/FTLD-linked mutations has been shown to shorten overall lifespan (Voigt et al., 2010) and exacerbate age-dependent reductions in fly motility (Li et al., 2010) more dramatically than expression of TDP-43 CTFs. Overall, transgenic expression of TDP-43 CTFs in a range of model organisms does not induce dramatic motor or behavioral alterations that resemble TDP-43 proteinopathies.

Neuropathology of CTFs in Animal Models Differs From Findings in Cell Culture

In addition to the poor recapitulation of disease-relevant behavioral and cognitive phenotypes in animal models of TDP-43 CTFs, the neuropathology in these animals also largely fails to capture that found in human ALS and FTD tissues. Perplexingly, the lack of clear TDP-43 pathology in animal models of TDP-43 CTFs differs from the consistent formation of TDP-43 inclusions that occur upon CTF overexpression in cell lines. Thus, data from animal models suggest that CTF expression alone is not sufficient to cause TDP-43 pathology *in vivo*, even when expression levels are several times greater than those of endogenous full-length TDP-43.

TDP-43 CTFs Rarely Form Inclusions in Animal Models

In contrast to the disease-reminiscent inclusions of TDP-43 CTFs observed in cell culture models, transgenic mice expressing TDP-43 CTFs exhibit microscopically diffuse CTFs with no evidence of large inclusions (Caccamo et al., 2012; Walker et al., 2015b; Spiller et al., 2018). In the human brain, antibodies against phosphorylated TDP-43 typically demonstrate high specificity when labeling TDP-43 macro-aggregates. However, in the mouse brain these antibodies indicate phosphorylation of diffuse CTF-25 (208–414). This occurs primarily in the CA1 region of the hippocampus despite expression of CTF-25 throughout the entire forebrain brain (Walker et al., 2015b). Likewise, phosphorylated but dispersed CTF-25 (220–414) has been detected in spinal cord motor neurons in virally transduced rats, without the presence of inclusions (Dayton et al., 2013), while *in utero* electroporation of CTF-25 (219–414) into the mouse motor cortex resulted in phosphorylated micro-aggregates detectable up to 3 weeks of age (Akamatsu et al., 2013). Although this discrepancy between inclusion formation and TDP-43 phosphorylation requires further study, these findings indicate that phosphorylation of TDP-43 CTFs can proceed even

when the protein is diffusely distributed and may not necessarily result in the formation of large inclusions that are reflective of TDP-43 proteinopathies.

Studies using TDP-43 CTF mice have yielded disparate results as to the solubility of TDP-43 CTFs. Immunoblotting of mouse brains expressing CTF-25 (216–414) detected the fragments as detergent-soluble in both nuclear and cytosolic fractions (Caccamo et al., 2012, 2013, 2015), whereas transgenic expression of CTF-25 (208–414) caused accumulation of the CTFs almost exclusively in the detergent-insoluble fraction of the mouse brain (Walker et al., 2015b), in line with human neuropathology studies (Neumann et al., 2006; Igaz et al., 2008). In *C. elegans*, ectopically expressed CTF-25 (219–411 or 220–411) forms cytoplasmic aggregates (Ash et al., 2010; Zhang et al., 2011). Importantly however, exogenous full-length TDP-43 was shown to be more toxic than CTF-25 (Zhang et al., 2011). Together, these studies demonstrate that in complex tissues such as the brain and spinal cord, expression of TDP-43 CTFs does not reliably induce disease-reminiscent inclusion morphology.

TDP-43 CTFs Cause No or Minimal Neurodegeneration in Animal Models

Converging evidence from various model organisms substantiates the argument that expression of TDP-43 CTFs does not effectively replicate the progressive neuronal dysfunction and degeneration that is observed in people with TDP-43 proteinopathies. Rodent models of TDP-43 CTFs generally do not exhibit overt neurodegeneration or cell death in relevant neuronal populations (Caccamo et al., 2012; Dayton et al., 2013; Spiller et al., 2018). Consistent with this, studies in *Drosophila* have repeatedly demonstrated that full-length or disease-associated TDP-43 mutants are more toxic to retinal and neuronal cells than CTFs (Li et al., 2010; Voigt et al., 2010; Gregory et al., 2012). In CTF-25 (208–414) mice that did show neuron loss, this occurred specifically in the dentate gyrus of the hippocampus in the absence of TDP-43 inclusions and was not found in the CA1 region that contained most of the phosphorylated CTF-25 (Walker et al., 2015b). This indicates that even if neurodegeneration occurs following TDP-43 CTF expression in rodents, it is not associated with key features of human ALS and FTLD-TDP neuropathology. While post-mortem analysis of neural tissue from people with TDP-43 proteinopathies demonstrates the sequestering of TDP-43 to the cytoplasm (Neumann et al., 2006), TDP-43 CTF expression does not impact the levels or localization of endogenous nuclear TDP-43 in mice (Walker et al., 2015b; Tsuiji et al., 2017). The lack of fundamental neuropathology signatures of TDP-43 proteinopathies following expression of TDP-43 CTFs in animals suggests that rather than being a central driver of disease, CTFs are instead a by-product or consequence of mechanisms that do not directly cause neurodegeneration.

TDP-43 CTFs Promote Cell-to-Cell Transmission of TDP-43 Pathology Less Readily Than Full-Length Cytoplasmic TDP-43

The propagation of pathogenic TDP-43 to interconnected cells has long been hypothesized based on staged immunohistochemical experiments in post-mortem tissue (Brettschneider et al., 2013, 2014), and has been demonstrated in cell culture (Furukawa et al., 2011; Nonaka et al., 2013; Smethurst et al., 2016). However, this phenomenon was only recently confirmed in behaving animals (Porta et al., 2018). In this seminal study, delivery of insoluble extracts from FTLD-TDP brains into the cerebral cortex of mice initiated the progressive spread of TDP-43 inclusion pathology to anatomically connected regions. Examination of this event in several transgenic mouse models revealed that TDP-43 CTFs provide a cellular environment that is less conducive to the self-templated aggregation of TDP-43; injected brain extracts seeded *de novo* pathology more rapidly and widely in mice expressing TDP-43 ΔNLS than in mice expressing a TDP-43 CTF (208–414) (Porta et al., 2018). TDP-43 CTFs do not therefore appear to be primarily responsible for the propagation of TDP-43 pathology throughout the CNS in ALS and FTLD.

The Presence of TDP-43 CTFs in Other Animal Models of ALS and FTLD Establishes TDP-43 CTFs as Disease-Associated Rather Than Disease-Causative

In **Table 3**, we present a comprehensive overview of the presence of TDP-43 CTFs in other animal models of TDP-43 proteinopathy which do not express TDP-43 CTFs alone. These models generally capture aspects of motor or behavioral dysfunction associated with ALS and FTLD more reliably than models of CTF overexpression, demonstrating more dramatic phenotypes and many of the neuropathological hallmarks of these diseases. Low levels of CTF-35, and even lower levels of CTF-25, are frequently observed in the brain and/or spinal cord of mice overexpressing wild-type TDP-43, or disease-associated mutations such as A315T, M337V and G348C amino acid substitutions (Wegorzewska et al., 2009; Stallings et al., 2010; Tsai et al., 2010; Wils et al., 2010; Xu et al., 2010, 2011; Swarup et al., 2011; Cannon et al., 2012; Janssens et al., 2013; D'Alton et al., 2014; Ke et al., 2015). In some of these models, TDP-43 CTFs are often difficult to detect by standard immunoblotting (Wegorzewska et al., 2009; Xu et al., 2011).

Numerous attempts have been made to correlate the abundance of TDP-43 CTFs with disease stage in animal models, in order to disentangle the functional relevance of CTFs to neurodegeneration. A study by Wegorzewska et al. (2009) provides the only compelling evidence that CTFs may contribute to the initiation of disease, demonstrating the presence of CTFs prior to symptom onset in TDP-43^{A315T} mice. However, this conflicts with studies in various other model organisms which found that CTFs were only detectable at later disease stages. These findings support the argument that CTFs accumulate as a consequence rather than cause of neurodegeneration (Zhou et al., 2010; Uchida et al., 2012). For instance, CTFs accumulated in the mouse brain and/or spinal cord as symptoms of motor dysfunction progressed (Wils et al., 2010; Swarup et al., 2011; Janssens et al., 2013). In a rat model, insoluble CTFs were detected in animals that had reached paralysis, but were not

TABLE 3 | Summary of studies examining the presence of TDP-43 CTF-25 and CTF-35 in transgenic mouse models of ALS/FTLD expressing wild-type or mutant forms of TDP-43.

Transgene	Promoter	Tissue analyzed	CTF-25	CTF-35	Other CTFs	Major findings	Reference
Wild-type hTDP-43	*PrP*	SC	+	+	–	Low levels of CTFs. Stronger labeling of FL-TDP-43 in nucleus and cytoplasm.	Stallings et al., 2010
		SC	+	+	–	Levels of FL-TDP-43 and CTFs was dose-dependent, with highest levels in homozygous mice.	Xu et al., 2010
	CaMKIIα	Brain	+	+	–	An antibody against total TDP-43 detected low levels of fragments in NT animals, and higher abundance in transgenic animals.	Cannon et al., 2012
		Brain	–	–	–	No CTFs detected despite progressive motor dysfunction.	Igaz et al., 2011
	Thy1.2	Brain	+	++	–	CTF-35 present from disease onset, CTF-25 increased by end stage.	Janssens et al., 2013
		Brain	+	++	–	Levels of soluble CTF-25 increased as disease progressed, whereas CTF-35 levels decreased. CTF-35 cytoplasmic, CTF-25 cytoplasmic and nuclear.	Wils et al., 2010
	Tardbp	Brain and SC	–	–	–	Very low or no CTF-35 and no CTF-25.	Swarup et al., 2011
Wild-type mTDP-43	*CaMKIIα*	Brain	+	++	–	Very low levels of fragments in transgenic animals aged to 6 months, but not animals aged to 2 months.	Tsai et al., 2010
hTDP-43^{A315T}		Brain	–	+	15 and 20 kDa	CTFs less abundant than FL-TDP-43. Insoluble fragments highly phosphorylated at serine 409/410, while only some phosphorylation of the FL-TDP-43 was detected.	Ke et al., 2015
	PrP	Brain	+	+	–	CTF-25 detected in cytosol of mutant mice and NT controls. CTF-35 detected in nucleus and cytosol of transgenic animals only. CTFs less abundant than FL-TDP-43.	Medina et al., 2014
		SC	+	+	–	CTFs present in cytosol. FL-TDP-43 detected in nuclear and cytosolic fractions, and more abundant than CTFs.	Stallings et al., 2010
		Brain and SC	+	++	–	Low level detection of soluble CTFs prior to symptom onset and as disease progressed.	Wegorzewska et al., 2009
	Tardbp	Brain and SC	+	++	–	Higher levels of CTFs in mice aged to 10 months, but FL-TDP-43 more abundant overall.	Swarup et al., 2011
hTDP-43^{M337V}	*PrP*	SC	+	+	–	Multiple faint bands between 25 and 35 kDa in cytosol, overall higher levels of FL-TDP-43 in nuclear and cytosolic fractions.	Stallings et al., 2010
		Brain	+	++	–	CTFs detected in both transgenic and NT mice by long exposure of immunoblot. FL-TDP-43 more abundant than CTFs.	Xu et al., 2011
	Thy1.2	Brain	+	++	–	CTF-35 present from disease onset, CTF-25 increased at end stage. Both lower than FL-TDP-43.	Janssens et al., 2013
	CaMKIIα	Cortex	+	++	–	Fragments were detected by antibodies against RRM2 of TDP-43 but not amino acids 3–12 or 404–414.	D'Alton et al., 2014
	TARDBP	Brain and SC	–	+	–	CTF-35 detected in cortex of transgenic and NT animals but not in SC.	Gordon et al., 2019
hTDP-43^{G348C}	*Tardbp*	Brain and SC	+	+	–	Higher levels of CTFs in mice aged to 10 months, but CTFs overall less abundant than FL-TDP-43.	Swarup et al., 2011
ΔNLS	*NEFH*	SC	–	+	–	Very low levels of CTF-35 in both transgenic and control animals.	Walker et al., 2015a
	CaMKIIα	Brain	–	–	–	No detection of CTFs.	Igaz et al., 2011

"+" indicates that the fragment was present, "–" indicates that it was not detected, and "++" indicates higher abundance of one fragment relative to the other. CA3, cornu ammonis field 3; CTF, C-terminal fragment; CTF-25, TDP-43 CTF of 25 kDa; CTF-35, TDP-43 CTF of 35 kDa; Dox, doxycycline; FL-TDP-43, full-length TDP-43; hTDP-43, human TDP-43; NT, non-transgenic; RRM2, RNA recognition motif 2; SC, spinal cord.

detected at disease onset (Zhou et al., 2010). In a cynomolgus monkey, viral mediated delivery of wild-type TDP-43 to the cervical spinal cord induced motor dysfunction and muscle atrophy and, although low levels of CTF-25 was observed 4 weeks after injection, it was not present in early or mid-stage disease (Uchida et al., 2012).

Mice expressing TDP-43 ΔNLS show no or minimal TDP-43 fragmentation, despite a robust motor phenotype (Igaz et al., 2011; Walker et al., 2015a). The same observations have been made in mice that express ALS-linked TDP-43 mutations to levels equivalent to endogenous TDP-43, diminishing the status of CTFs as either disease-causing or disease-associated (Arnold et al., 2013). Moreover, some experiments have detected equivalent levels of CTFs in both transgenic animals and non-transgenic controls (Xu et al., 2011; D'Alton et al., 2014; Medina et al., 2014; Gordon et al., 2019). These studies provide convincing evidence that CTFs are not necessary to induce neurodegeneration, even in models that successfully phenocopy multiple aspects of human disease. However, it is interesting to note that although CTFs are present in low levels in both the brain and spinal cord of mice, transgenic expression of TDP-43 in pigs was associated with more prominent fragment pathology in the brain compared to the spinal cord (Wang G. et al., 2015), similar to the distribution seen in humans. In line with this, CTFs were more abundant than full length TDP-43 in M337V transgenic macaques, whereas mice expressing the same transgene showed lower relative abundance of fragments (Yin et al., 2019). This was replicated *in vitro*; recombinant TDP-43 M337V was cleaved into C-terminal fragments when incubated with monkey but not mouse brain extracts. This points to potential species-specific differences in the way that TDP-43 is processed. Indeed, the *TARDBP* gene of mammals is highly homologous with that of *Drosophila* and *C. elegans* from the N-terminal to RRM2, and diverges toward the C-terminus (Wang et al., 2004). Closer investigation is required to determine any differences in the C-terminal structure of primate and rodent TDP-43, and whether species differences affect TDP-43 processing.

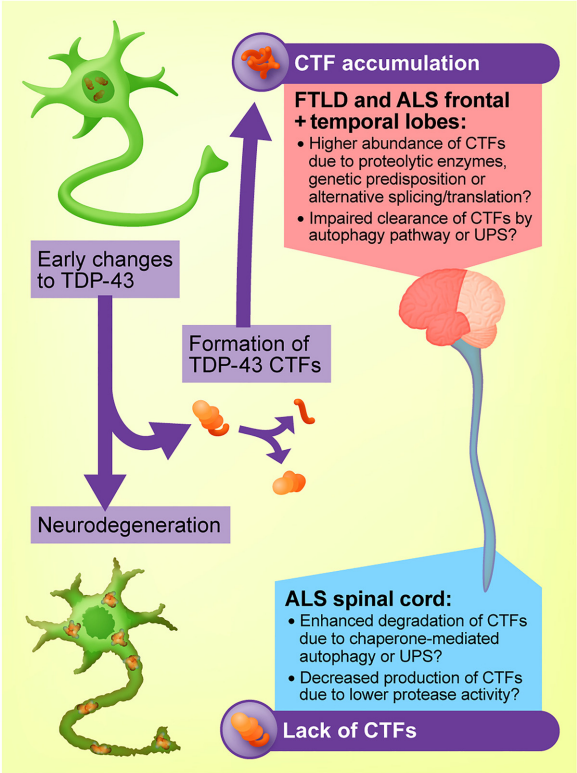

FIGURE 2 | Proposed model for the regional heterogeneity of TDP-43 C-terminal fragments (CTFs). CTFs may accumulate in the brains of people with ALS and FTLD-TDP due to elevated activity of proteases such as caspases and calpains, genetic predisposition, or upregulation of alternative TARDBP transcripts that produce a truncated protein. The lack of CTFs in the ALS spinal cord may arise from mechanisms including enhanced CTF clearance by chaperone-mediated autophagy or the ubiquitin-proteasome system (UPS).

CELL-TYPE-SPECIFIC DIFFERENCES IN THE GENERATION AND CLEARANCE OF TDP-43 CTFs: A POTENTIAL EXPLANATION FOR REGIONAL HETEROGENEITY

The mechanism through which TDP-43 drives neurodegeneration may differ between the brain and the spinal cord. A prime example of this is the pathological acetylation of TDP-43, which has been detected in the ALS spinal cord but not the brain, likely due to removal of the targeted lysine residues in the N-terminal domain upon cleavage of TDP-43 in the brain (Cohen et al., 2015). The evidence from cell and animal models reviewed above strongly suggests that TDP-43 CTFs are not responsible for neurodegeneration in the brains of people with ALS and FTLD. However, differences in the burden of TDP-43 CTFs across the human CNS is nonetheless interesting as it points to cell-type-specific differences in the way that the TDP-43 protein is modified, which may ultimately determine the cellular effects of TDP-43. It is possible that differences in the ability of distinct groups of cells in the brain and spinal cord to cleave TDP-43, or to clear the resultant fragments, represents a molecular mechanism underpinning the varying abundance of CTFs across the CNS (see **Figure 2**). In the case of ALS and FTLD, the elevated levels of CTFs in the brain may arise from increased activation of proteases responsible for TDP-43 cleavage, translation of genes that promote cleavage or upregulation of transcripts that produce a truncated TDP-43 protein. By the same principle, it is possible that the relative absence of TDP-43 CTFs in the ALS spinal cord is due to enhanced activity of degradation pathways specific to particular TDP-43 fragments, or decreased activity of the proteases responsible for CTF formation.

Neurons are particularly diverse cells with highly specialized functions. With regard to motor neurons, subtypes vary dramatically in terms of neurotransmitter secretion, excitability and cytoarchitecture (Stifani, 2014), as well as the molecules that regulate cellular stress tolerance (Simandi et al., 2018).

Factors such as these may influence cellular responses to TDP-43 and protein accumulation in general. Epigenetic mechanisms also differ according to cell type and CNS sub-region (Davies et al., 2012) and may underlie the regional heterogeneity of CTF distribution by regulating the silencing and transcription of different genes responsible for the formation or degradation of TDP-43 CTFs. Indeed, DNA methylation patterns vary greatly between motor neurons of the cortex and spinal cord in tissue samples from both people with ALS and healthy controls (Chestnut et al., 2011), which could potentially allow TDP-43 CTFs to accumulate in select groups of cells.

Experimental data also indicate that alterations to TDP-43, such as its cleavage into CTFs, may proceed in a cell-type-specific manner. For instance, in people with inclusion body myopathy, an inflammatory muscle disease, TDP-43 is ubiquitinated and translocated to the cytoplasm of the muscle cells but does not appear to be cleaved into CTFs (Weihl et al., 2008). In cell culture, CTF-25 is more prone to aggregation and less readily degraded when transfected into NSC-34 cells in comparison with a muscle cell line (Cicardi et al., 2018). These studies suggest that the formation and aggregation of TDP-43 CTFs is a CNS-specific phenomenon. It has recently been demonstrated that the specific intracellular environment can influence the conformation of α-synuclein and its biological actions, ultimately creating distinct α-synuclein strains that distinguish dementia with Lewy bodies from multiple system atrophy (Peng et al., 2018). This may also hold true for TDP-43, whereby the unique molecular composition of the cell determines how the TDP-43 protein is modified, impacting its resultant biochemical actions.

The distinct features of certain cell populations may also confer vulnerability to TDP-43 pathology. This was recently demonstrated in mice, whereby intra-cortical injection of insoluble protein extracted from FTLD-TDP brains led to a selective spread of pathology to deeper structures that have previously been shown to be affected in the FTLD-TDP brain, such as the nucleus accumbens and basolateral amygdala (Porta et al., 2018). Determining how the distinct gene and protein profiles of various classes of neurons renders certain populations susceptible to TDP-43 pathology or specific post-translational TDP-43 modifications may assist in understanding the complex biology of TDP-43 in diseases such as ALS and FTD that are characterized by dramatic genetic, neuropathological and phenotypic heterogeneity (Simon et al., 2014), and elucidate protective molecular and cellular factors for therapeutic targeting.

FINAL REMARKS AND CONCLUSION

Amyotrophic lateral sclerosis is a rapidly progressing and debilitating disease, and currently available treatments offer only modest benefits. Riluzole may extend survival by 2–3 months, potentially via attenuation of glutamate excitotoxicity (Bellingham, 2011; Miller et al., 2012). The more recently available edaravone, a free radical scavenger, appears to have a small impact on lifespan and quality of life for a select population of people living with ALS, with results from phase II clinical trials not always reaching significance (Sawada, 2017). Pharmaceutical interventions for FTD are equally disappointing, with no treatments available to alter the rate of disease progression, and the repurposing of existing anti-psychotic medications showing limited efficacy in symptom management (Tsai and Boxer, 2016). TDP-43 pathology has dramatic impacts on the CNS, triggering a multitude of cellular alterations and disease cascades in both neurons and glial cells. To develop new disease-modifying treatments targeted at the underlying pathology, it is critical that research attention is focused on changes to TDP-43-affected cells that have a clear, causal connection to disease.

TDP-43 CTFs are considered a pathological hallmark in the brains of people with ALS and FTLD-TDP. However, these fragments are rarely detected in the ALS spinal cord, despite the dramatic death of lower motor neurons. Exogenous expression of these fragments in cultured cells has provided mixed results and whether CTFs are more toxic to cells than full-length TDP-43 remains debateable. Critically, transgenic animals expressing TDP-43 CTFs do not exhibit a robust ALS-like phenotype of motor dysfunction, and only display mild deficits that potentially resemble broader aspects of neurodegeneration, but not specifically ALS or FTD, in aged animals. Given the low-level detection of these fragments in ALS cerebrospinal fluid (Ding et al., 2015) and FTD plasma (Foulds et al., 2009), further investigation of their efficacy as a biomarker of disease is warranted. However, our evaluation of evidence across cell and animal models and human post-mortem tissue illustrates that TDP-43 CTFs are unlikely to be a primary cause of neurodegeneration in ALS and FTD. For this reason, therapeutics specifically targeted against TDP-43 CTFs are unlikely to modify disease, and further investigation of other potential disease-modifying strategies is warranted.

AUTHOR CONTRIBUTIONS

BB and AW conceived and wrote the manuscript and compiled the tables.

FUNDING

This work and related studies in the Neurodegeneration Pathobiology Laboratory was supported by an Australian Government Research Training Program Scholarship to BB, the MND Research Institute of Australia (Ph.D. top-up scholarship to BB and grant 1727 to AW), the Australian National Health and Medical Research Council (Project Grant GNT1124005 and RD Wright Career Development Fellowship GNT1140386 to AW), the MonSTaR Foundation, the Ross Maclean Fellowship, and the Brazil Family Program for Neurology.

ACKNOWLEDGMENTS

We thank Dr. Rebecca San Gil, Dr. Joshua H. K. Tam, and Rowan Tweedale for critical reading of the manuscript, and Dr. Nick Valmas for figure design.

REFERENCES

Ahmed, Z., Sheng, H., Xu, Y. F., Lin, W. L., Innes, A. E., Gass, J., et al. (2010). Accelerated lipofuscinosis and ubiquitination in granulin knockout mice suggest a role for progranulin in successful aging. *Am. J. Pathol.* 177, 311–324. doi: 10.2353/ajpath.2010.090915

Akamatsu, M., Takuma, H., Yamashita, T., Okada, T., Keino-Masu, K., Ishii, K., et al. (2013). A unique mouse model for investigating the properties of amyotrophic lateral sclerosis-associated protein TDP-43, by in utero electroporation. *Neurosci. Res.* 77, 234–241. doi: 10.1016/j.neures.2013.09.009

Arai, T., Hasegawa, M., Akiyama, H., Ikeda, K., Nonaka, T., Mori, H., et al. (2006). TDP-43 is a component of ubiquitin-positive tau-negative inclusions in frontotemporal lobar degeneration and amyotrophic lateral sclerosis. *Biochem. Biophys. Res. Commun.* 351, 602–611. doi: 10.1016/j.bbrc.2006.10.093

Arai, T., Hasegawa, M., Nonoka, T., Kametani, F., Yamashita, M., Hosokawa, M., et al. (2010). Phosphorylated and cleaved TDP-43 in ALS, FTLD and other neurodegenerative disorders and in cellular models of TDP-43 proteinopathy. *Neuropathology* 30, 170–181. doi: 10.1111/j.1440-1789.2009.01089.x

Arnold, E. S., Ling, S. C., Huelga, S. C., Lagier-Tourenne, C., Polymenidou, M., Ditsworth, D., et al. (2013). ALS-linked TDP-43 mutations produce aberrant RNA splicing and adult-onset motor neuron disease without aggregation or loss of nuclear TDP-43. *Proc. Natl. Acad. Sci. U.S.A.* 110, E736–E745. doi: 10.1073/pnas.1222809110

Ash, P. E., Zhang, Y. J., Roberts, C. M., Saldi, T., Hutter, H., Buratti, E., et al. (2010). Neurotoxic effects of TDP-43 overexpression in *C. elegans*. *Hum. Mol. Genet.* 19, 3206–3218. doi: 10.1093/hmg/ddq230

Ayala, V., Granado-Serrano, A. B., Cacabelos, D., Naudi, A., Ilieva, E. V., Boada, J., et al. (2011). Cell stress induces TDP-43 pathological changes associated with ERK1/2 dysfunction: implications in ALS. *Acta Neuropathol.* 122, 259–270. doi: 10.1007/s00401-011-0850-y

Ayala, Y. M., De Conti, L., Avendano-Vazquez, S. E., Dhir, A., Romano, M., D'Ambrogio, A., et al. (2011). TDP-43 regulates its mRNA levels through a negative feedback loop. *Embo J.* 30, 277–288. doi: 10.1038/emboj.2010.310

Ayala, Y. M., Zago, P., D'Ambrogio, A., Xu, Y. F., Petrucelli, L., Buratti, E., et al. (2008). Structural determinants of the cellular localization and shuttling of TDP-43. *J. Cell Sci.* 121(Pt 22), 3778–3785. doi: 10.1242/jcs.038950

Bang, J., Spina, S., and Miller, B. L. (2015). Frontotemporal dementia. *Lancet* 386, 1672–1682. doi: 10.1016/S0140-6736(15)00461-4

Baudry, M., and Bi, X. (2016). Calpain-1 and Calpain-2: the yin and yang of synaptic plasticity and neurodegeneration. *Trends Neurosci.* 39, 235–245. doi: 10.1016/j.tins.2016.01.007

Becker, L. A., Huang, B., Bieri, G., Ma, R., Knowles, D. A., Afar-Nejad, P. J., et al. (2017). Therapeutic reduction of ataxin-2 extends lifespan and reduces pathology in TDP-43 mice. *Nature* 544, 367–371. doi: 10.1038/nature22038

Bellingham, M. C. (2011). A review of the neural mechanisms of action and clinical efficiency of riluzole in treating amyotrophic lateral sclerosis: What have we learned in the last decade? *CNS Neurosci. Ther.* 17, 4–31. doi: 10.1111/j.1755-5949.2009.00116.x

Bentmann, E., Neumann, M., Tahirovic, S., Rodde, R., Dormann, D., and Haass, C. (2012). Requirements for stress granule recruitment of fused in sarcoma (FUS) and TAR DNA-binding protein of 43 kDa (TDP-43). *J. Biol. Chem.* 287, 23079–23094. doi: 10.1074/jbc.M111.328757

Bilican, B., Serio, A., Barmada, S. J., Nishimura, A. L., Sullivan, G. J., Carrasco, M., et al. (2012). Mutant induced pluripotent stem cell lines recapitulate aspects of TDP-43 proteinopathies and reveal cell-specific vulnerability. *Proc. Natl. Acad. Sci. U.S.A.* 109, 5803–5808. doi: 10.1073/pnas.1202922109

Bodansky, A., Kim, J. M., Tempest, L., Velagapudi, A., Libby, R., and Ravits, J. (2010). TDP-43 and ubiquitinated cytoplasmic aggregates in sporadic ALS are low frequency and widely distributed in the lower motor neuron columns independent of disease spread. *Amyotroph. Lateral Scler.* 11, 321–327. doi: 10.3109/17482961003602363

Boeve, B. F., Boylan, K. B., Graff-Radford, N. R., DeJesus-Hernandez, M., Knopman, D. S., Pedraza, O., et al. (2012). Characterization of frontotemporal dementia and/or amyotrophic lateral sclerosis associated with the GGGGCC repeat expansion in C9ORF72. *Brain* 135(Pt 3), 765–783. doi: 10.1093/brain/aws004

Brady, O. A., Meng, P., Zheng, Y., Mao, Y., and Hu, F. (2011). Regulation of TDP-43 aggregation by phosphorylation and p62/SQSTM1. *J. Neurochem.* 116, 248–259. doi: 10.1111/j.1471-4159.2010.07098.x

Branco, L. M., De, Albuquerque M, De, Andrade HM, Bergo, F. P., Nucci, A., and França, M. C. Jr. (2014). Spinal cord atrophy correlates with disease duration and severity in amyotrophic lateral sclerosis. *Amyotroph. Lateral Scler. Frontotemporal Degener.* 15, 93–97. doi: 10.3109/21678421.2013.852589

Brauer, S., Zimyanin, V., and Hermann, A. (2018). Prion-like properties of disease-relevant proteins in amyotrophic lateral sclerosis. *J. Neural Transm.* 125, 591–613. doi: 10.1007/s00702-018-1851-y

Brettschneider, J., Del Tredici, K., Irwin, D. J., Grossman, M., Robinson, J. L., Toledo, J. B., et al. (2014). Sequential distribution of pTDP-43 pathology in behavioral variant frontotemporal dementia (bvFTD). *Acta Neuropathol.* 127, 423–439. doi: 10.1007/s00401-013-1238-y

Brettschneider, J., Del Tredici, K., Toledo, J. B., Robinson, J. L., Irwin, D. J., Grossman, M., et al. (2013). Stages of pTDP-43 pathology in amyotrophic lateral sclerosis. *Ann. Neurol.* 74, 20–38. doi: 10.1002/ana.23937

Broe, M., Hodges, J. R., Schofield, E., Shepherd, C. E., Kril, J. J., and Halliday, G. M. (2003). Staging disease severity in pathologically confirmed cases of frontotemporal dementia. *Neurology* 60, 1005–1011. doi: 10.1212/01.WNL.0000052685.09194.39

Brower, C. S., Piatkov, K. I., and Varshavsky, A. (2013). Neurodegeneration-associated protein fragments as short-lived substrates of the N-end rule pathway. *Mol. Cell* 50, 161–171. doi: 10.1016/j.molcel.2013.02.009

Bryson, K., McGuffin, L. J., Marsden, R. L., Ward, J. J., Sodhi, J. S., and Jones, D. T. (2005). Protein structure prediction servers at University College London. *Nucleic Acids Res.* 33, W36–W38. doi: 10.1093/nar/gki410

Buratti, E. (2018). TDP-43 post-translational modifications in health and disease. *Expert Opin. Ther. Targets* 22, 279–293. doi: 10.1080/14728222.2018.1439923

Buratti, E., and Baralle, F. E. (2001). Characterization and functional implications of the RNA binding properties of nuclear factor TDP-43, a novel splicing regulator of CFTR exon 9. *J. Biol. Chem.* 276, 36337–36343. doi: 10.1074/jbc.M104236200

Buratti, E., and Baralle, F. E. (2008). Multiple roles of TDP-43 in gene expression, splicing regulation, and human disease. *Front. Biosci.* 13, 867–878. doi: 10.2741/2727

Buratti, E., Brindisi, A., Giombi, M., Tisminetzky, S., Ayala, Y. M., and Baralle, F. E. (2005). TDP-43 binds heterogeneous nuclear ribonucleoprotein A/B through its C-terminal tail: an important region for the inhibition of cystic fibrosis transmembrane conductance regulator exon 9 splicing. *J. Biol. Chem.* 280, 37572–37584. doi: 10.1074/jbc.M505557200

Caccamo, A., Magri, A., and Oddo, S. (2010). Age-dependent changes in TDP-43 levels in a mouse model of Alzheimer disease are linked to Abeta oligomers accumulation. *Mol. Neurodegener.* 5:51. doi: 10.1186/1750-1326-5-51

Caccamo, A., Majumder, S., and Oddo, S. (2012). Cognitive decline typical of frontotemporal lobar degeneration in transgenic mice expressing the 25-kDa C-terminal fragment of TDP-43. *Am. J. Pathol.* 180, 293–302. doi: 10.1016/j.ajpath.2011.09.022

Caccamo, A., Medina, D. X., and Oddo, S. (2013). Glucocorticoids exacerbate cognitive deficits in TDP-25 transgenic mice via a glutathione-mediated mechanism: implications for aging, stress and TDP-43 proteinopathies. *J. Neurosci.* 33, 906–913. doi: 10.1523/JNEUROSCI.3314-12.2013

Caccamo, A., Shaw, D. M., Guarino, F., Messina, A., Walker, A. W., and Oddo, S. (2015). Reduced protein turnover mediates functional deficits in transgenic mice expressing the 25 kDa C-terminal fragment of TDP-43. *Hum. Mol. Genet.* 24, 4625–4635. doi: 10.1093/hmg/ddv193

Cai, M., Lee, K. W., Choi, S. M., and Yang, E. J. (2015). TDP-43 modification in the hSOD1(G93A) amyotrophic lateral sclerosis mouse model. *Neurol. Res.* 37, 253–262. doi: 10.1179/1743132814Y.0000000443

Cannon, A., Yang, B., Knight, J., Farnham, I. M., Zhang, Y., Wuertzer, C. A., et al. (2012). Neuronal sensitivity to TDP-43 overexpression is dependent on timing of induction. *Acta Neuropathol.* 123, 807–823. doi: 10.1007/s00401-012-0979-3

Caragounis, A., Price, K. A., Soon, C. P., Filiz, G., Masters, C. L., Li, Q. X., et al. (2010). Zinc induces depletion and aggregation of endogenous TDP-43. *Free Radic. Biol. Med.* 48, 1152–1161. doi: 10.1016/j.freeradbiomed.2010.01.035

Cassel, J. A., McDonnell, M. E., Velvadapu, V., Andrianov, V., and Reitz, A. B. (2012). Characterization of a series of 4-aminoquinolines that stimulate

caspase-7 mediated cleavage of TDP-43 and inhibit its function. *Biochimie* 94, 1974–1981. doi: 10.1016/j.biochi.2012.05.020

Cassel, J. A., and Reitz, A. B. (2013). Ubiquilin-2 (UBQLN2) binds with high affinity to the C-terminal region of TDP-43 and modulates TDP-43 levels in H4 cells: characterization of inhibition by nucleic acids and 4-aminoquinolines. *Biochim. Biophys. Acta* 1834, 964–971. doi: 10.1016/j.bbapap.2013.03.020

Che, M. X., Jiang, L. L., Li, H. Y., Jiang, Y. J., and Hu, H. Y. (2015). TDP-35 sequesters TDP-43 into cytoplasmic inclusions through binding with RNA. *FEBS Lett.* 589, 1920–1928. doi: 10.1016/j.febslet.2015.06.009

Che, M. X., Jiang, Y. J., Xie, Y. Y., Jiang, L. L., and Hu, H. Y. (2011). Aggregation of the 35-kDa fragment of TDP-43 causes formation of cytoplasmic inclusions and alteration of RNA processing. *Faseb J.* 25, 2344–2353. doi: 10.1096/fj.10-174482

Chen, Z., and Ma, L. (2010). Grey matter volume changes over the whole brain in amyotrophic lateral sclerosis: A voxel-wise meta-analysis of voxel based morphometry studies. *Amyotroph. Lateral Scler.* 11, 549–554. doi: 10.3109/17482968.2010.516265

Chestnut, B. A., Chang, Q., Price, A., Lesuisse, C., Wong, M., and Martin, L. J. (2011). Epigenetic regulation of motor neuron cell death through DNA methylation. *J. Neurosci.* 31, 16619–16636. doi: 10.1523/JNEUROSCI.1639-11.2011

Chiang, C. H., Grauffel, C., Wu, L. S., Kuo, P. H., Doudeva, L. G., Lim, C., et al. (2016). Structural analysis of disease-related TDP-43 D169G mutation: linking enhanced stability and caspase cleavage efficiency to protein accumulation. *Sci. Rep.* 6:21581. doi: 10.1038/srep21581

Chou, C. C., Alexeeva, O. M., Yamada, S., Pribadi, A., Zhang, Y., Mo, B., et al. (2015). PABPN1 suppresses TDP-43 toxicity in ALS disease models. *Hum. Mol. Genet.* 24, 5154–5173. doi: 10.1093/hmg/ddv238

Chou, C. C., Zhang, Y., Umoh, M. E., Vaughan, S. W., Lorenzini, I., Liu, F., et al. (2018). TDP-43 pathology disrupts nuclear pore complexes and nucleocytoplasmic transport in ALS/FTD. *Nat. Neurosci.* 21, 228–239. doi: 10.1038/s41593-017-0047-3

Cicardi, M. E., Cristofani, R., Rusmini, P., Meroni, M., Ferrari, V., Vezzoli, G., et al. (2018). Tdp-25 routing to autophagy and proteasome ameliorates its aggregation in amyotrophic lateral sclerosis target cells. *Sci. Rep.* 8:12390. doi: 10.1038/s41598-018-29658-2

Cohen, T. J., Hwang, A. W., Restrepo, C. R., Yuan, C. X., Trojanowski, J. Q., and Lee, V. M. (2015). An acetylation switch controls TDP-43 function and aggregation propensity. *Nat. Commun.* 6:5845. doi: 10.1038/ncomms6845

Colombrita, C., Onesto, E., Megiorni, F., Pizzuti, A., Baralle, F. E., Buratti, E., et al. (2012). TDP-43 and FUS RNA-binding proteins bind distinct sets of cytoplasmic messenger RNAs and differently regulate their post-transcriptional fate in motoneuron-like cells. *J. Biol. Chem.* 287, 15635–15647. doi: 10.1074/jbc.M111.333450

Colombrita, C., Zennaro, E., Fallini, C., Weber, M., Sommacal, A., Buratti, E., et al. (2009). TDP-43 is recruited to stress granules in conditions of oxidative insult. *J. Neurochem.* 111, 1051–1061. doi: 10.1111/j.1471-4159.2009.06383.x

Conicella, A. E., Zerze, G. H., Mittal, J., and Fawzi, N. L. (2016). ALS mutations disrupt phase separation mediated by alpha-helical structure in the TDP-43 low-complexity C-terminal domain. *Structure* 24, 1537–1549. doi: 10.1016/j.str.2016.07.007

Consonni, M., Contarino, V. E., Catricala, E., Dalla Bella, E., Pensato, V., Gellera, C., et al. (2018). Cortical markers of cognitive syndromes in amyotrophic lateral sclerosis. *Neuroimage Clin.* 19, 675–682. doi: 10.1016/j.nicl.2018.05.020

Corrado, L., Ratti, A., Gellera, C., Buratti, E., Castellotti, B., Carlomagno, Y., et al. (2009). High frequency of TARDBP gene mutations in Italian patients with amyotrophic lateral sclerosis. *Hum. Mutat.* 30, 688–694. doi: 10.1002/humu.20950

Crippa, V., Cicardi, M. E., Ramesh, N., Seguin, S. J., Ganassi, M., Bigi, I., et al. (2016). The chaperone HSPB8 reduces the accumulation of truncated TDP-43 species in cells and protects against TDP-43-mediated toxicity. *Hum. Mol. Genet.* 25, 3908–3924. doi: 10.1093/hmg/ddw232

Crockford, C., Newton, J., Lonergan, K., Chiwera, T., Booth, T., Chandran, S., et al. (2018). ALS-specific cognitive and behavior changes associated with advancing disease stage in ALS. *Neurology* 91, e1370–e1380. doi: 10.1212/WNL.0000000000006317

Cushman, M., Johnson, B. S., King, O. D., Gitler, A. D., and Shorter, J. (2010). Prion-like disorders: blurring the divide between transmissibility and infectivity. *J. Cell Sci.* 123(Pt 8), 1191–1201. doi: 10.1242/jcs.051672

Cykowski, M. D., Powell, S. Z., Appel, J. W., Arumanayagam, A. S., Rivera, A. L., and Appel, S. H. (2018). Phosphorylated TDP-43 (pTDP-43) aggregates in the axial skeletal muscle of patients with sporadic and familial amyotrophic lateral sclerosis. *Acta Neuropathol. Commun.* 6:28. doi: 10.1186/s40478-018-0528-y

D'Alton, S., Altshuler, M., Cannon, A., Dickson, D. W., Petrucelli, L., and Lewis, J. (2014). Divergent phenotypes in mutant TDP-43 transgenic mice highlight potential confounds in TDP-43 transgenic modeling. *PLoS One* 9:e86513. doi: 10.1371/journal.pone.0086513

D'Alton, S., Altshuler, M., and Lewis, J. (2015). Studies of alternative isoforms provide insight into TDP-43 autoregulation and pathogenesis. *RNA* 21, 1419–1432. doi: 10.1261/rna.047647.114

Davies, M. N., Volta, M., Pidsley, R., Lunnon, K., Dixit, A., Lovestone, S., et al. (2012). Functional annotation of the human brain methylome identifies tissue-specific epigenetic variation across brain and blood. *Genome Biol.* 13:R43. doi: 10.1186/gb-2012-13-6-r43

Dayton, R. D., Gitcho, M. A., Orchard, E. A., Wilson, J. D., Wang, D. B., Cain, C. D., et al. (2013). Selective forelimb impairment in rats expressing a pathological TDP-43 25 kDa C-terminal fragment to mimic amyotrophic lateral sclerosis. *Mol. Ther.* 21, 1324–1334. doi: 10.1038/mt.2013.88

De Marco, G., Lomartire, A., Mandili, G., Lupino, E., Buccinna, B., Ramondetti, C., et al. (2014). Reduced cellular Ca2+ availability enhances TDP-43 cleavage by apoptotic caspases. *Biochim. Biophys. Acta* 1843, 725–734. doi: 10.1016/j.bbamcr.2014.01.010

DeJesus-Hernandez, M., Mackenzie, I. R., Boeve, B. F., Boxer, A. L., Baker, M., Rutherford, N. J., et al. (2011). Expanded GGGGCC hexanucleotide repeat in noncoding region of C9ORF72 causes chromosome 9p-linked FTD and ALS. *Neuron* 72, 245–256. doi: 10.1016/j.neuron.2011.09.011

Dewey, C. M., Cenik, B., Sephton, C. F., Dries, D. R., Mayer, P. III, Good, S. K., et al. (2011). TDP-43 is directed to stress granules by sorbitol, a novel physiological osmotic and oxidative stressor. *Mol. Cell Biol.* 31, 1098–1108. doi: 10.1128/MCB.01279-10

Ding, X., Ma, M., Teng, J., Teng, R. K., Zhou, S., Yin, J., et al. (2015). Exposure to ALS-FTD-CSF generates TDP-43 aggregates in glioblastoma cells through exosomes and TNTs-like structure. *Oncotarget* 6, 24178–24191. doi: 10.18632/oncotarget.4680

Dix, M. M., Simon, G. M., and Cravatt, B. F. (2008). Global mapping of the topography and magnitude of proteolytic events in apoptosis. *Cell* 134, 679–691. doi: 10.1016/j.cell.2008.06.038

Dormann, D., Capell, A., Carlson, A. M., Shankaran, S. S., Rodde, R., Neumann, M., et al. (2009). Proteolytic processing of TAR DNA binding protein-43 by caspases produces C-terminal fragments with disease defining properties independent of progranulin. *J. Neurochem.* 110, 1082–1094. doi: 10.1111/j.1471-4159.2009.06211.x

Ederle, H., Funk, C., Abou-Ajram, C., Hutten, S., Funk, E. B. E., Kehlenbach, R. H., et al. (2018). Nuclear egress of TDP-43 and FUS occurs independently of Exportin-1/CRM1. *Sci. Rep.* 8:7084. doi: 10.1038/s41598-018-25007-5

Elden, A. C., Kim, H. J., Hart, M. P., Chen-Plotkin, A. S., Johnson, B. S., Fang, X., et al. (2010). Ataxin-2 intermediate-length polyglutamine expansions are associated with increased risk for ALS. *Nature* 466, 1069–1075. doi: 10.1038/nature09320

Fallini, C., Bassell, G. J., and Rossoll, W. (2012). The ALS disease protein TDP-43 is actively transported in motor neuron axons and regulates axon outgrowth. *Hum. Mol. Genet.* 21, 3703–3718. doi: 10.1093/hmg/dds205

Fang, M. Y., Markmiller, S., Dowdle, W. E., Vu, A. Q., Bushway, P. J., Ding, S., et al. (2018). Modulation of RNA-dependent interactions in stress granules prevents persistent TDP-43 accumulation in ALS/FTD. *bioRxiv* Available at: https://doi.org/10.1101/474577. doi: 10.1101/474577

Foulds, P. G., Davidson, Y., Mishra, M., Hobson, D. J., Humphreys, K. M., Taylor, M., et al. (2009). Plasma phosphorylated-TDP-43 protein levels correlate with brain pathology in frontotemporal lobar degeneration. *Acta Neuropathol.* 118, 647–658. doi: 10.1007/s00401-009-0594-0

Freibaum, B. D., Chitta, R. K., High, A. A., and Taylor, J. P. (2010). Global analysis of TDP-43 interacting proteins reveals strong association with RNA splicing and translation machinery. *J. Proteome Res.* 9, 1104–1120. doi: 10.1021/pr901076y

Furukawa, Y., Kaneko, K., Watanabe, S., Yamanaka, K., and Nukina, N. (2011). A seeding reaction recapitulates intracellular formation of Sarkosyl-insoluble transactivation response element (TAR) DNA-binding protein-43 inclusions. *J. Biol. Chem.* 286, 18664–18672. doi: 10.1074/jbc.M111.231209

Galiano, M. R., Goitea, V. E., and Hallak, M. E. (2016). Post-translational protein arginylation in the normal nervous system and in neurodegeneration. *J. Neurochem.* 138, 506–517. doi: 10.1111/jnc.13708

Geser, F., Lee, V. M., and Trojanowski, J. Q. (2010). Amyotrophic lateral sclerosis and frontotemporal lobar degeneration: a spectrum of TDP-43 proteinopathies. *Neuropathology* 30, 103–112. doi: 10.1111/j.1440-1789.2009.01091.x

Ghag, G., Bhatt, N., Cantu, D. V., Guerrero-Munoz, M. J., Ellsworth, A., Sengupta, U., et al. (2018). Soluble tau aggregates, not large fibrils, are the toxic species that display seeding and cross-seeding behavior. *Protein Sci.* 27, 1901–1909. doi: 10.1002/pro.3499

Giordana, M. T., Piccinini, M., Grifoni, S., De Marco, G., Vercellino, M., Magistrello, M., et al. (2010). TDP-43 redistribution is an early event in sporadic amyotrophic lateral sclerosis. *Brain Pathol.* 20, 351–360. doi: 10.1111/j.1750-3639.2009.00284.x

Gitcho, M. A., Baloh, R. H., Chakraverty, S., Mayo, K., Norton, J. B., Levitch, D., et al. (2008). TDP-43 A315T mutation in familial motor neuron disease. *Ann. Neurol.* 63, 535–538. doi: 10.1002/ana.21344

Gitcho, M. A., Bigio, E. H., Mishra, M., Johnson, N., Weintraub, S., Mesulam, M., et al. (2009a). TARDBP 3'-UTR variant in autopsy-confirmed frontotemporal lobar degeneration with TDP-43 proteinopathy. *Acta Neuropathol.* 118, 633–645. doi: 10.1007/s00401-009-0571-7

Gitcho, M. A., Strider, J., Carter, D., Taylor-Reinwald, L., Forman, M. S., Goate, A. M., et al. (2009b). VCP mutations causing frontotemporal lobar degeneration disrupt localization of TDP-43 and induce cell death. *J. Biol. Chem.* 284, 12384–12398. doi: 10.1074/jbc.M900992200

Goh, C. W., Lee, I. C., Sundaram, J. R., George, S. E., Yusoff, P., Brush, M. H., et al. (2018). Chronic oxidative stress promotes GADD34-mediated phosphorylation of the TAR DNA-binding protein TDP-43, a modification linked to neurodegeneration. *J. Biol. Chem.* 293, 163–176. doi: 10.1074/jbc.M117.814111

Gordon, D., Dafinca, R., Scaber, J., Alegre-Abarrategui, J., Farrimond, L., Scott, C., et al. (2019). Single-copy expression of an amyotrophic lateral sclerosis-linked TDP-43 mutation (M337V) in BAC transgenic mice leads to altered stress granule dynamics and progressive motor dysfunction. *Neurobiol. Dis.* 121, 148–162. doi: 10.1016/j.nbd.2018.09.024

Gregory, J. M., Barros, T. P., Meehan, S., Dobson, C. M., and Luheshi, L. M. (2012). The aggregation and neurotoxicity of TDP-43 and its ALS-associated 25 kDa fragment are differentially affected by molecular chaperones in Drosophila. *PLoS One* 7:e31899. doi: 10.1371/journal.pone.0031899

Guo, W., Chen, Y., Zhou, X., Kar, A., Ray, P., Chen, X., et al. (2011). An ALS-associated mutation affecting TDP-43 enhances protein aggregation, fibril formation and neurotoxicity. *Nat. Struct. Mol. Biol.* 18, 822–830. doi: 10.1038/nsmb.2053

Hans, F., Fiesel, F. C., Strong, J. C., Jackel, S., Rasse, T. M., Geisler, S., et al. (2014). UBE2E ubiquitin-conjugating enzymes and ubiquitin isopeptidase Y regulate TDP-43 protein ubiquitination. *J. Biol. Chem.* 289, 19164–19179. doi: 10.1074/jbc.M114.561704

Hart, M. P., and Gitler, A. D. (2012). ALS-associated ataxin 2 polyQ expansions enhance stress-induced caspase 3 activation and increase TDP-43 pathological modifications. *J. Neurosci.* 32, 9133–9142. doi: 10.1523/JNEUROSCI.0996-12.2012

Hasegawa, M., Arai, T., Nonaka, T., Kametani, F., Yoshida, M., Hashizume, Y., et al. (2008). Phosphorylated TDP-43 in frontotemporal lobar degeneration and amyotrophic lateral sclerosis. *Ann. Neurol.* 64, 60–70. doi: 10.1002/ana.21425

Hasegawa, M., Nonaka, T., Tsuji, H., Tamaoka, A., Yamashita, M., Kametani, F., et al. (2011). Molecular dissection of TDP-43 proteinopathies. *J. Mol. Neurosci.* 45, 480–485. doi: 10.1007/s12031-011-9571-x

Herskowitz, J. H., Gozal, Y. M., Duong, D. M., Dammer, E. B., Gearing, M., Ye, K., et al. (2012). Asparaginyl endopeptidase cleaves TDP-43 in brain. *Proteomics* 12, 2455–2463. doi: 10.1002/pmic.201200006

Huang, C. C., Bose, J. K., Majumder, P., Lee, K. H., Huang, J. T., Huang, J. K., et al. (2014). Metabolism and mis-metabolism of the neuropathological signature protein TDP-43. *J. Cell Sci.* 127(Pt 14), 3024–3038. doi: 10.1242/jcs.136150

Igaz, L. M., Kwong, L. K., Chen-Plotkin, A., Winton, M. J., Unger, T. L., Xu, Y., et al. (2009). Expression of TDP-43 C-terminal fragments in vitro recapitulates pathological features of TDP-43 proteinopathies. *J. Biol. Chem.* 284, 8516–8524. doi: 10.1074/jbc.M809462200

Igaz, L. M., Kwong, L. K., Lee, E. B., Chen-Plotkin, A., Swanson, E., Unger, T., et al. (2011). Dysregulation of the ALS-associated gene TDP-43 leads to neuronal death and degeneration in mice. *J. Clin. Invest.* 121, 726–738. doi: 10.1172/JCI44867

Igaz, L. M., Kwong, L. K., Xu, Y., Truax, A. C., Uryu, K., Neumann, M., et al. (2008). Enrichment of C-terminal fragments in TAR DNA-binding protein-43 cytoplasmic inclusions in brain but not in spinal cord of frontotemporal lobar degeneration and amyotrophic lateral sclerosis. *Am. J. Pathol.* 173, 182–194. doi: 10.2353/ajpath.2008.080003

Iguchi, Y., Eid, L., Parent, M., Soucy, G., Bareil, C., Riku, Y., et al. (2016). Exosome secretion is a key pathway for clearance of pathological TDP-43. *Brain* 139(Pt 12), 3187–3201. doi: 10.1093/brain/aww237

Inukai, Y., Nonaka, T., Arai, T., Yoshida, M., Hashizume, Y., Beach, T. G., et al. (2008). Abnormal phosphorylation of Ser409/410 of TDP-43 in FTLD-U and ALS. *FEBS Lett.* 582, 2899–2904. doi: 10.1016/j.febslet.2008.07.027

Irwin, D. J., Cairns, N. J., Grossman, M., McMillan, C. T., Lee, E. B., Van Deerlin, V. M., et al. (2015). Frontotemporal lobar degeneration: defining phenotypic diversity through personalized medicine. *Acta Neuropathol.* 129, 469–491. doi: 10.1007/s00401-014-1380-1

Ishii, T., Kawakami, E., Endo, K., Misawa, H., and Watabe, K. (2017). Formation and spreading of TDP-43 aggregates in cultured neuronal and glial cells demonstrated by time-lapse imaging. *PLoS One* 12:e0179375. doi: 10.1371/journal.pone.0179375

Janssens, J., Wils, H., Kleinberger, G., Joris, G., Cuijt, I., Ceuterick-de Groote, C., et al. (2013). Overexpression of ALS-associated p.*M337V* human TDP-43 in mice worsens disease features compared to wild-type human TDP-43 mice. *Mol. Neurobiol.* 48, 22–35. doi: 10.1007/s12035-013-8427-5

Jeon, G. S., Shim, Y. M., Lee, D. Y., Kim, J. S., Kang, M., Ahn, S. H., et al. (2018). Pathological Modification of TDP-43 in Amyotrophic Lateral Sclerosis with SOD1 Mutations. *Mol. Neurobiol.* 56, 2007–2021. doi: 10.1007/s12035-018-1218-2

Johnson, B. S., McCaffery, J. M., Lindquist, S., and Gitler, A. D. (2008). A yeast TDP-43 proteinopathy model: exploring the molecular determinants of TDP-43 aggregation and cellular toxicity. *Proc. Natl. Acad. Sci. U.S.A.* 105, 6439–6444. doi: 10.1073/pnas.0802082105

Johnson, B. S., Snead, D., Lee, J. J., McCaffery, J. M., Shorter, J., and Gitler, A. D. (2009). TDP-43 is intrinsically aggregation-prone, and amyotrophic lateral sclerosis-linked mutations accelerate aggregation and increase toxicity. *J. Biol. Chem.* 284, 20329–20339. doi: 10.1074/jbc.M109.010264

Josephs, K. A., Murray, M. E., Whitwell, J. L., Tosakulwong, N., Weigand, S. D., Petrucelli, L., et al. (2016). Updated TDP-43 in Alzheimer's disease staging scheme. *Acta Neuropathol.* 131, 571–585. doi: 10.1007/s00401-016-1537-1

Ju, J. S., Fuentealba, R. A., Miller, S. E., Jackson, E., Piwnica-Worms, D., Baloh, R. H., et al. (2009). Valosin-containing protein (VCP) is required for autophagy and is disrupted in VCP disease. *J. Cell Biol.* 187, 875–888. doi: 10.1083/jcb.200908115

Jucker, M., and Walker, L. C. (2013). Self-propagation of pathogenic protein aggregates in neurodegenerative diseases. *Nature* 501, 45–51. doi: 10.1038/nature12481

Kabashi, E., Valdmanis, P. N., Dion, P., Spiegelman, D., McConkey, B. J., Vande Velde, C., et al. (2008). TARDBP mutations in individuals with sporadic and familial amyotrophic lateral sclerosis. *Nat. Genet.* 40, 572–574. doi: 10.1038/ng.132

Kametani, F., Nonaka, T., Suzuki, T., Arai, T., Dohmae, N., Akiyama, H., et al. (2009). Identification of casein kinase-1 phosphorylation sites on TDP-43. *Biochem. Biophys. Res. Commun.* 382, 405–409. doi: 10.1016/j.bbrc.2009.03.038

Kametani, F., Obi, T., Shishido, T., Akatsu, H., Murayama, S., Saito, Y., et al. (2016). Mass spectrometric analysis of accumulated TDP-43 in amyotrophic lateral sclerosis brains. *Sci. Rep.* 6:23281. doi: 10.1038/srep23281

Kanazawa, M., Kakita, A., Igarashi, H., Takahashi, T., Kawamura, K., Takahashi, H., et al. (2011). Biochemical and histopathological alterations in TAR DNA-binding protein-43 after acute ischemic stroke in rats. *J. Neurochem.* 116, 957–965. doi: 10.1111/j.1471-4159.2010.06860.x

Kasu, Y. A. T., Alemu, S., Lamari, A., Loew, N., and Brower, C. S. (2018). The N-termini of TAR DNA-binding protein-43 (TDP43) C-terminal fragments influence degradation, aggregation propensity and morphology. *Mol. Cell Biol.* 38:e00243-18. doi: 10.1128/MCB.00243-18

Kawahara, Y., and Mieda-Sato, A. (2012). TDP-43 promotes microRNA biogenesis as a component of the Drosha and Dicer complexes. *Proc. Natl. Acad. Sci. U.S.A.* 109, 3347–3352. doi: 10.1073/pnas.1112427109

Ke, Y. D., van Hummel, A., Stevens, C. H., Gladbach, A., Ippati, S., Bi, M., et al. (2015). Short-term suppression of A315T mutant human TDP-43 expression improves functional deficits in a novel inducible transgenic mouse model of FTLD-TDP and ALS. *Acta Neuropathol.* 130, 661–678. doi: 10.1007/s00401-015-1486-0

Kirshner, H. S. (2014). Frontotemporal dementia and primary progressive aphasia, a review. *Neuropsychiatr. Dis. Treat.* 10, 1045–1055. doi: 10.2147/NDT.S38821

Kitamura, A., Nakayama, Y., Shibasaki, A., Taki, A., Yuno, S., Takeda, K., et al. (2016). Interaction of RNA with a C-terminal fragment of the amyotrophic lateral sclerosis-associated TDP43 reduces cytotoxicity. *Sci. Rep.* 6:19230. doi: 10.1038/srep19230

Kleinberger, G., Wils, H., Ponsaerts, P., Joris, G., Timmermans, J. P., Van Broeckhoven, C., et al. (2010). Increased caspase activation and decreased TDP-43 solubility in progranulin knockout cortical cultures. *J. Neurochem.* 115, 735–747. doi: 10.1111/j.1471-4159.2010.06961.x

Kraemer, B. C., Schuck, T., Wheeler, J. M., Robinson, L. C., Trojanowski, J. Q., Lee, V. M., et al. (2010). Loss of murine TDP-43 disrupts motor function and plays an essential role in embryogenesis. *Acta Neuropathol.* 119, 409–419. doi: 10.1007/s00401-010-0659-0

Kwong, L. K., Irwin, D. J., Walker, A. K., Xu, Y., Riddle, D. M., Trojanowski, J. Q., et al. (2014). Novel monoclonal antibodies to normal and pathologically altered human TDP-43 proteins. *Acta Neuropathol. Commun.* 2:33. doi: 10.1186/2051-5960-2-33

Laferriere, F., Maniecka, Z., Perez-Berlanga, M., Hruska-Plochan, M., Gilhespy, L., Hock, E. M., et al. (2019). TDP-43 extracted from frontotemporal lobar degeneration subject brains displays distinct aggregate assemblies and neurotoxic effects reflecting disease progression rates. *Nat. Neurosci.* 22, 65–77. doi: 10.1038/s41593-018-0294-y

Lee, E. B., Lee, V. M., and Trojanowski, J. Q. (2011). Gains or losses: molecular mechanisms of TDP43-mediated neurodegeneration. *Nat. Rev. Neurosci.* 13, 38–50. doi: 10.1038/nrn3121

Lee, E. B., Porta, S., Michael Baer, G., Xu, Y., Suh, E., Kwong, L. K., et al. (2017). Expansion of the classification of FTLD-TDP: distinct pathology associated with rapidly progressive frontotemporal degeneration. *Acta Neuropathol.* 134, 65–78. doi: 10.1007/s00401-017-1679-9

Lee, Y. B., Baskaran, P., Gomez, J., Chen, H. J., Nishimura, A., Smith, B., et al. (2017). C9orf72 poly GA RAN-translated protein plays a key role in Amyotrophic Lateral Sclerosis via aggregation and toxicity. *Hum. Mol. Genet.* 26, 4765–4777. doi: 10.1093/hmg/ddx350

Li, H. R., Chen, T. C., Hsiao, C. L., Shi, L., Chou, C. Y., and Huang, J. R. (2018a). The physical forces mediating self-association and phase-separation in the C-terminal domain of TDP-43. *Biochim. Biophys. Acta* 1866, 214–223. doi: 10.1016/j.bbapap.2017.10.001

Li, H. R., Chiang, W. C., Chou, P. C., Wang, W. J., and Huang, J. R. (2018b). TAR DNA-binding protein 43 (TDP-43) liquid-liquid phase separation is mediated by just a few aromatic residues. *J. Biol. Chem.* doi: 10.1074/jbc.AC117.001037

Li, H. Y., Yeh, P. A., Chiu, H. C., Tang, C. Y., and Tu, B. P. (2011). Hyperphosphorylation as a defense mechanism to reduce TDP-43 aggregation. *PLoS One* 6:e23075. doi: 10.1371/journal.pone.0023075

Li, Q., Yokoshi, M., Okada, H., and Kawahara, Y. (2015). The cleavage pattern of TDP-43 determines its rate of clearance and cytotoxicity. *Nat. Commun.* 6:6183. doi: 10.1038/ncomms7183

Li, Y., Ray, P., Rao, E. J., Shi, C., Guo, W., Chen, X., et al. (2010). A Drosophila model for TDP-43 proteinopathy. *Proc. Natl. Acad. Sci. U.S.A.* 107, 3169–3174. doi: 10.1073/pnas.0913602107

Liachko, N. F., Guthrie, C. R., and Kraemer, B. C. (2010). Phosphorylation promotes neurotoxicity in a *Caenorhabditis elegans* model of TDP-43 proteinopathy. *J. Neurosci.* 30, 16208–16219. doi: 10.1523/JNEUROSCI.2911-10.2010

Lin, P. Y., Folorunso, O., Taglialatela, G., and Pierce, A. (2016). Overexpression of heat shock factor 1 maintains TAR DNA binding protein 43 solubility via induction of inducible heat shock protein 70 in cultured cells. *J. Neurosci. Res.* 94, 671–682. doi: 10.1002/jnr.23725

Ling, S. C., Albuquerque, C. P., Han, J. S., Lagier-Tourenne, C., Tokunaga, S., Zhou, H., et al. (2010). ALS-associated mutations in TDP-43 increase its stability and promote TDP-43 complexes with FUS/TLS. *Proc. Natl. Acad. Sci. U.S.A.* 107, 13318–13323. doi: 10.1073/pnas.1008227107

Ling, S. C., Polymenidou, M., and Cleveland, D. W. (2013). Converging mechanisms in ALS and FTD: disrupted RNA and protein homeostasis. *Neuron* 79, 416–438. doi: 10.1016/j.neuron.2013.07.033

Liu, R., Yang, G., Nonaka, T., Arai, T., Jia, W., and Cynader, M. S. (2013). Reducing TDP-43 aggregation does not prevent its cytotoxicity. *Acta Neuropathol. Commun.* 1:49. doi: 10.1186/2051-5960-1-49

Liu-Yesucevitz, L., Bilgutay, A., Zhang, Y. J., Vanderweyde, T., Citro, A., Mehta, T., et al. (2010). Tar DNA binding protein-43 (TDP-43) associates with stress granules: analysis of cultured cells and pathological brain tissue. *PLoS One* 5:e13250. doi: 10.1371/journal.pone.0013250

Lopez de Munain, A., Alzualde, A., Gorostidi, A., Otaegui, D., Ruiz-Martinez, J., Indakoetxea, B., et al. (2008). Mutations in progranulin gene: clinical, pathological, and ribonucleic acid expression findings. *Biol. Psychiatry* 63, 946–952. doi: 10.1016/j.biopsych.2007.08.015

Ludolph, A. C., and Brettschneider, J. (2015). TDP-43 in amyotrophic lateral sclerosis - is it a prion disease? *Eur. J. Neurol.* 22, 753–761. doi: 10.1111/ene.12706

Mackenzie, I. R., Baborie, A., Pickering-Brown, S., Du Plessis, D., Jaros, E., Perry, R. H., et al. (2006). Heterogeneity of ubiquitin pathology in frontotemporal lobar degeneration: classification and relation to clinical phenotype. *Acta Neuropathol.* 112, 539–549. doi: 10.1007/s00401-006-0138-9

Mackenzie, I. R., Bigio, E. H., Ince, P. G., Geser, F., Neumann, M., Cairns, N. J., et al. (2007). Pathological TDP-43 distinguishes sporadic amyotrophic lateral sclerosis from amyotrophic lateral sclerosis with SOD1 mutations. *Ann. Neurol.* 61, 427–434. doi: 10.1002/ana.21147

Mackenzie, I. R., Neumann, M., Baborie, A., Sampathu, D. M., Du Plessis, D., Jaros, E., et al. (2011). A harmonized classification system for FTLD-TDP pathology. *Acta Neuropathol.* 122, 111–113. doi: 10.1007/s00401-011-0845-8

Mackenzie, I. R., Nicholson, A. M., Sarkar, M., Messing, J., Purice, M. D., Pottier, C., et al. (2017). TIA1 mutations in amyotrophic lateral sclerosis and frontotemporal dementia promote phase separation and alter stress granule dynamics. *Neuron* 95, 808–816.e9. doi: 10.1016/j.neuron.2017.07.025

Martin, L. J. (1999). Neuronal death in amyotrophic lateral sclerosis is apoptosis: possible contribution of a programmed cell death mechanism. *J. Neuropathol. Exp. Neurol.* 58, 459–471. doi: 10.1097/00005072-199905000-00005

Matus, S., Valenzuela, V., Medinas, D. B., and Hetz, C. (2013). ER dysfunction and protein folding stress in ALS. *Int J. Cell Biol.* 2013:674751. doi: 10.1155/2013/674751

McCann, E. P., Williams, K. L., Fifita, J. A., Tarr, I. S., O'Connor, J., Rowe, D. B., et al. (2017). The genotype-phenotype landscape of familial amyotrophic lateral sclerosis in Australia. *Clin. Genet.* 92, 259–266. doi: 10.1111/cge.12973

Medina, D. X., Orr, M. E., and Oddo, S. (2014). Accumulation of C-terminal fragments of transactive response DNA-binding protein 43 leads to synaptic loss and cognitive deficits in human TDP-43 transgenic mice. *Neurobiol. Aging* 35, 79–87. doi: 10.1016/j.neurobiolaging.2013.07.006

Mercado, P. A., Ayala, Y. M., Romano, M., Buratti, E., and Baralle, F. E. (2005). Depletion of TDP 43 overrides the need for exonic and intronic splicing enhancers in the human apoA-II gene. *Nucleic Acids Res.* 33, 6000–6010. doi: 10.1093/nar/gki897

Meyerowitz, J., Parker, S. J., Vella, L. J., Ng, D., Price, K. A., Liddell, J. R., et al. (2011). C-Jun N-terminal kinase controls TDP-43 accumulation in stress granules induced by oxidative stress. *Mol. Neurodegener.* 6:57. doi: 10.1186/1750-1326-6-57

Miller, R. G., Mitchell, J. D., and Moore, D. H. (2012). Riluzole for amyotrophic lateral sclerosis (ALS)/motor neuron disease (MND). *Cochrane Database Syst. Rev.* 3:Cd001447. doi: 10.1002/14651858.CD001447.pub3

Moisse, K., Mepham, J., Volkening, K., Welch, I., Hill, T., and Strong, M. J. (2009). Cytosolic TDP-43 expression following axotomy is associated with caspase 3 activation in NFL-/- mice: support for a role for TDP-43 in the physiological response to neuronal injury. *Brain Res.* 1296, 176–186. doi: 10.1016/j.brainres.2009.07.023

Molliex, A., Temirov, J., Lee, J., Coughlin, M., Kanagaraj, A. P., Kim, H. J., et al. (2015). Phase separation by low complexity domains promotes stress granule assembly and drives pathological fibrillization. *Cell* 163, 123–133. doi: 10.1016/j.cell.2015.09.015

Mompean, M., Baralle, M., Buratti, E., and Laurents, D. V. (2016). An amyloid-like pathological conformation of TDP-43 is stabilized by hypercooperative hydrogen bonds. *Front. Mol. Neurosci.* 9:125. doi: 10.3389/fnmol.2016.00125

Moujalled, D., James, J. L., Parker, S. J., Lidgerwood, G. E., Duncan, C., Meyerowitz, J., et al. (2013). Kinase inhibitor screening identifies cyclin-dependent kinases and glycogen synthase kinase 3 as potential modulators of TDP-43 cytosolic accumulation during cell stress. *PLoS One* 8:e67433. doi: 10.1371/journal.pone.0067433

Murley, A. G., and Rowe, J. B. (2018). Neurotransmitter deficits from frontotemporal lobar degeneration. *Brain* 141, 1263–1285. doi: 10.1093/brain/awx327

Nakashima-Yasuda, H., Uryu, K., Robinson, J., Xie, S. X., Hurtig, H., Duda, J. E., et al. (2007). Co-morbidity of TDP-43 proteinopathy in Lewy body related diseases. *Acta Neuropathol.* 114, 221–229. doi: 10.1007/s00401-007-0261-2

Nan, Y., Wang, S., and Jia, W. (2018). Caspase independent cleavages of TDP-43 generates 35kD fragment that cause apoptosis of breast cancer cells. *Biochem. Biophys. Res. Commun.* 497, 51–57. doi: 10.1016/j.bbrc.2018.01.190

Narayanan, R. K., Mangelsdorf, M., Panwar, A., Butler, T. J., Noakes, P. G., and Wallace, R. H. (2013). Identification of RNA bound to the TDP-43 ribonucleoprotein complex in the adult mouse brain. *Amyotroph. Lateral Scler. Frontotemporal Degener.* 14, 252–260. doi: 10.3109/21678421.2012.734520

Neudert, C., Oliver, D., Wasner, M., and Borasio, G. D. (2001). The course of the terminal phase in patients with amyotrophic lateral sclerosis. *J. Neurol.* 248, 612–616. doi: 10.1007/s004150170140

Neumann, M., Kwong, L. K., Lee, E. B., Kremmer, E., Flatley, A., Xu, Y., et al. (2009). Phosphorylation of S409/410 of TDP-43 is a consistent feature in all sporadic and familial forms of TDP-43 proteinopathies. *Acta Neuropathol.* 117, 137–149. doi: 10.1007/s00401-008-0477-9

Neumann, M., Mackenzie, I. R., Cairns, N. J., Boyer, P. J., Markesbery, W. R., Smith, C. D., et al. (2007). TDP-43 in the ubiquitin pathology of frontotemporal dementia with VCP gene mutations. *J. Neuropathol. Exp. Neurol.* 66, 152–157. doi: 10.1097/nen.0b013e31803020b9

Neumann, M., Sampathu, D. M., Kwong, L. K., Truax, A. C., Micsenyi, M. C., Chou, T. T., et al. (2006). Ubiquitinated TDP-43 in frontotemporal lobar degeneration and amyotrophic lateral sclerosis. *Science* 314, 130–133. doi: 10.1126/science.1134108

Nihei, Y., Ito, D., and Suzuki, N. (2012). Roles of ataxin-2 in pathological cascades mediated by TAR DNA-binding protein 43 (TDP-43) and Fused in Sarcoma (FUS). *J. Biol. Chem.* 287, 41310–41323. doi: 10.1074/jbc.M112.398099

Nishimoto, Y., Ito, D., Yagi, T., Nihei, Y., Tsunoda, Y., and Suzuki, N. (2010). Characterization of alternative isoforms and inclusion body of the TAR DNA-binding protein-43. *J. Biol. Chem.* 285, 608–619. doi: 10.1074/jbc.M109.022012

Nonaka, T., Kametani, F., Arai, T., Akiyama, H., and Hasegawa, M. (2009). Truncation and pathogenic mutations facilitate the formation of intracellular aggregates of TDP-43. *Hum. Mol. Genet.* 18, 3353–3364. doi: 10.1093/hmg/ddp275

Nonaka, T., Masuda-Suzukake, M., Arai, T., Hasegawa, Y., Akatsu, H., Obi, T., et al. (2013). Prion-like properties of pathological TDP-43 aggregates from diseased brains. *Cell Rep.* 4, 124–134. doi: 10.1016/j.celrep.2013.06.007

Peng, C., Gathagan, R. J., Covell, D. J., Medellin, C., Stieber, A., Robinson, J. L., et al. (2018). Cellular milieu imparts distinct pathological alpha-synuclein strains in alpha-synucleinopathies. *Nature* 557, 558–563. doi: 10.1038/s41586-018-0104-4

Pesiridis, G. S., Lee, V. M., and Trojanowski, J. Q. (2009). Mutations in TDP-43 link glycine-rich domain functions to amyotrophic lateral sclerosis. *Hum. Mol. Genet.* 18, R156–R162. doi: 10.1093/hmg/ddp303

Pesiridis, G. S., Tripathy, K., Tanik, S., Trojanowski, J. Q., and Lee, V. M. (2011). A two-hit hypothesis for inclusion formation by carboxyl-terminal fragments of TDP-43 protein linked to RNA depletion and impaired microtubule-dependent transport. *J. Biol. Chem.* 286, 18845–18855. doi: 10.1074/jbc.M111.231118

Pinarbasi, E. S., Cagatay, T., Fung, H. Y. J., Li, Y. C., Chook, Y. M., and Thomas, P. J. (2018). Active nuclear import and passive nuclear export are the primary determinants of TDP-43 localization. *Sci. Rep.* 8:7083. doi: 10.1038/s41598-018-25008-4

Polymenidou, M., and Cleveland, D. W. (2011). The seeds of neurodegeneration: prion-like spreading in ALS. *Cell* 147, 498–508. doi: 10.1016/j.cell.2011.10.011

Polymenidou, M., Lagier-Tourenne, C., Hutt, K. R., Huelga, S. C., Moran, J., Liang, T. Y., et al. (2011). Long pre-mRNA depletion and RNA missplicing contribute to neuronal vulnerability from loss of TDP-43. *Nat. Neurosci.* 14, 459–468. doi: 10.1038/nn.2779

Porta, S., Xu, Y., Restrepo, C. R., Kwong, L. K., Zhang, B., Brown, H. J., et al. (2018). Patient-derived frontotemporal lobar degeneration brain extracts induce formation and spreading of TDP-43 pathology in vivo. *Nat. Commun.* 9:4220. doi: 10.1038/s41467-018-06548-9

Ravits, J. M., and La Spada, A. R. (2009). ALS motor phenotype heterogeneity, focality, and spread: deconstructing motor neuron degeneration. *Neurology* 73, 805–811. doi: 10.1212/WNL.0b013e3181b6bbbd

Renton, A. E., Majounie, E., Waite, A., Simon-Sanchez, J., Rollinson, S., Gibbs, J. R., et al. (2011). A hexanucleotide repeat expansion in C9ORF72 is the cause of chromosome 9p21-linked ALS-FTD. *Neuron* 72, 257–268. doi: 10.1016/j.neuron.2011.09.010

Robberecht, W., and Philips, T. (2013). The changing scene of amyotrophic lateral sclerosis. *Nat. Rev. Neurosci.* 14, 248–264. doi: 10.1038/nrn3430

Roberson, E. D. (2012). Mouse models of frontotemporal dementia. *Ann. Neurol.* 72, 837–849. doi: 10.1002/ana.23722

Roccatagliata, L., Bonzano, L., Mancardi, G., Canepa, C., and Caponnetto, C. (2009). Detection of motor cortex thinning and corticospinal tract involvement by quantitative MRI in amyotrophic lateral sclerosis. *Amyotroph. Lateral Scler.* 10, 47–52. doi: 10.1080/17482960802267530

Rohn, T. T. (2008). Caspase-cleaved TAR DNA-binding protein-43 is a major pathological finding in Alzheimer's disease. *Brain Res.* 1228, 189–198. doi: 10.1016/j.brainres.2008.06.094

Rosen, D. R., Siddique, T., Patterson, D., Figlewicz, D. A., Sapp, P., Hentati, A., et al. (1993). Mutations in Cu/Zn superoxide dismutase gene are associated with familial amyotrophic lateral sclerosis. *Nature* 362, 59–62. doi: 10.1038/362059a0

Rutherford, N. J., Zhang, Y. J., Baker, M., Gass, J. M., Finch, N. A., Xu, Y. F., et al. (2008). Novel mutations in TARDBP (TDP-43) in patients with familial amyotrophic lateral sclerosis. *PLoS Genet.* 4:e1000193. doi: 10.1371/journal.pgen.1000193

Saini, A., and Chauhan, V. S. (2011). Delineation of the core aggregation sequences of TDP-43 C-terminal fragment. *Chembiochem* 12, 2495–2501. doi: 10.1002/cbic.201100427

Sambataro, F., and Pennuto, M. (2017). Post-translational modifications and protein quality control in motor neuron and polyglutamine diseases. *Front. Mol. Neurosci.* 10:82. doi: 10.3389/fnmol.2017.00082

Sampathu, D. M., Neumann, M., Kwong, L. K., Chou, T. T., Micsenyi, M., Truax, A., et al. (2006). Pathological heterogeneity of frontotemporal lobar degeneration with ubiquitin-positive inclusions delineated by ubiquitin immunohistochemistry and novel monoclonal antibodies. *Am. J. Pathol.* 169, 1343–1352. doi: 10.2353/ajpath.2006.060438

Santamaria, N., Alhothali, M., Alfonso, M. H., Breydo, L., and Uversky, V. N. (2017). Intrinsic disorder in proteins involved in amyotrophic lateral sclerosis. *Cell Mol. Life Sci.* 74, 1297–1318. doi: 10.1007/s00018-016-2416-6

Sawada, H. (2017). Clinical efficacy of edaravone for the treatment of amyotrophic lateral sclerosis. *Expert Opin. Pharmacother.* 18, 735–738. doi: 10.1080/14656566.2017.1319937

Schwab, C., Arai, T., Hasegawa, M., Yu, S., and McGeer, P. L. (2008). Colocalization of transactivation-responsive DNA-binding protein 43 and huntingtin in inclusions of Huntington disease. *J. Neuropathol. Exp. Neurol.* 67, 1159–1165. doi: 10.1097/NEN.0b013e31818e8951

Scotter, E. L., Vance, C., Nishimura, A. L., Lee, Y. B., Chen, H. J., Urwin, H., et al. (2014). Differential roles of the ubiquitin proteasome system and autophagy in the clearance of soluble and aggregated TDP-43 species. *J. Cell Sci.* 127(Pt 6), 1263–1278. doi: 10.1242/jcs.140087

Sellami, L., Bocchetta, M., Masellis, M., Cash, D. M., Dick, K. M., van Swieten, J., et al. (2018). Distinct neuroanatomical correlates of neuropsychiatric symptoms in the three main forms of genetic frontotemporal dementia in the GENFI cohort. *J. Alzheimers Dis.* 65, 147–163. doi: 10.3233/JAD-180053

Sephton, C. F., Good, S. K., Atkin, S., Dewey, C. M., Mayer, P. III, Herz, J., et al. (2010). TDP-43 is a developmentally regulated protein essential for early embryonic development. *J. Biol. Chem.* 285, 6826–6834. doi: 10.1074/jbc.M109.061846

Shan, X., Vocadlo, D., and Krieger, C. (2009). Mislocalization of TDP-43 in the G93A mutant SOD1 transgenic mouse model of ALS. *Neurosci. Lett.* 458, 70–74. doi: 10.1016/j.neulet.2009.04.031

Shankaran, S. S., Capell, A., Hruscha, A. T., Fellerer, K., Neumann, M., Schmid, B., et al. (2008). Missense mutations in the progranulin gene linked to frontotemporal lobar degeneration with ubiquitin-immunoreactive inclusions reduce progranulin production and secretion. *J. Biol. Chem.* 283, 1744–1753. doi: 10.1074/jbc.M705115200

Shimonaka, S., Nonaka, T., Suzuki, G., Hisanaga, S., and Hasegawa, M. (2016). Templated aggregation of TAR DNA-binding Protein of 43 kDa (TDP-43) by seeding with TDP-43 peptide fibrils. *J. Biol. Chem.* 291, 8896–8907. doi: 10.1074/jbc.M115.713552

Simandi, Z., Pajer, K., Karolyi, K., Sieler, T., Jiang, L. L., Kolostyak, Z., et al. (2018). Arginine methyltransferase PRMT8 provides cellular stress tolerance in aging motoneurons. *J. Neurosci.* 38, 7683–7700. doi: 10.1523/JNEUROSCI.3389-17.2018

Simon, N. G., Turner, M. R., Vucic, S., Al-Chalabi, A., Shefner, J., Lomen-Hoerth, C., et al. (2014). Quantifying disease progression in amyotrophic lateral sclerosis. *Ann. Neurol.* 76, 643–657. doi: 10.1002/ana.24273

Smethurst, P., Newcombe, J., Troakes, C., Simone, R., Chen, Y. R., Patani, R., et al. (2016). In vitro prion-like behaviour of TDP-43 in ALS. *Neurobiol. Dis.* 96, 236–247. doi: 10.1016/j.nbd.2016.08.007

Spiller, K. J., Restrepo, C. R., Khan, T., Dominique, M. A., Fang, T. C., Canter, R. G., et al. (2018). Microglia-mediated recovery from ALS-relevant motor neuron degeneration in a mouse model of TDP-43 proteinopathy. *Nat. Neurosci.* 21, 329–340. doi: 10.1038/s41593-018-0083-7

Sreedharan, J., Blair, I. P., Tripathi, V. B., Hu, X., Vance, C., Rogelj, B., et al. (2008). TDP-43 mutations in familial and sporadic amyotrophic lateral sclerosis. *Science* 319, 1668–1672. doi: 10.1126/science.1154584

Stallings, N. R., Puttaparthi, K., Luther, C. M., Burns, D. K., and Elliott, J. L. (2010). Progressive motor weakness in transgenic mice expr D. K. essing human TDP-43. *Neurobiol. Dis.* 40, 404–414. doi: 10.1016/j.nbd.2010.06.017

Stifani, N. (2014). Motor neurons and the generation of spinal motor neuron diversity. *Front. Cell Neurosci.* 8:293. doi: 10.3389/fncel.2014.00293

Su, J. H., Nichol, K. E., Sitch, T., Sheu, P., Chubb, C., Miller, B. L., et al. (2000). DNA damage and activated caspase-3 expression in neurons and astrocytes: evidence for apoptosis in frontotemporal dementia. *Exp. Neurol.* 163, 9–19. doi: 10.1006/exnr.2000.7340

Suzuki, H., Lee, K., and Matsuoka, M. (2011). TDP-43-induced death is associated with altered regulation of BIM and Bcl-xL and attenuated by caspase-mediated TDP-43 cleavage. *J. Biol. Chem.* 286, 13171–13183. doi: 10.1074/jbc.M110.197483

Swarup, V., Phaneuf, D., Bareil, C., Robertson, J., Rouleau, G. A., Kriz, J., et al. (2011). Pathological hallmarks of amyotrophic lateral sclerosis/frontotemporal lobar degeneration in transgenic mice produced with TDP-43 genomic fragments. *Brain* 134(Pt 9), 2610–2626. doi: 10.1093/brain/awr159

Tan, C. F., Eguchi, H., Tagawa, A., Onodera, O., Iwasaki, T., Tsujino, A., et al. (2007). TDP-43 immunoreactivity in neuronal inclusions in familial amyotrophic lateral sclerosis with or without SOD1 gene mutation. *Acta Neuropathol.* 113, 535–542. doi: 10.1007/s00401-007-0206-9

Tan, R. H., Ke, Y. D., Ittner, L. M., and Halliday, G. M. (2017a). ALS/FTLD: experimental models and reality. *Acta Neuropathol.* 133, 177–196. doi: 10.1007/s00401-016-1666-6

Tan, R. H., Shepherd, C. E., Kril, J. J., McCann, H., McGeachie, A., McGinley, C., et al. (2013). Classification of FTLD-TDP cases into pathological subtypes using antibodies against phosphorylated and non-phosphorylated TDP43. *Acta Neuropathol. Commun.* 1:33. doi: 10.1186/2051-5960-1-33

Tan, R. H., Yang, Y., Kim, W. S., Dobson-Stone, C., Kwok, J. B., Kiernan, M. C., et al. (2017b). Distinct TDP-43 inclusion morphologies in frontotemporal lobar degeneration with and without amyotrophic lateral sclerosis. *Acta Neuropathol. Commun.* 5:76. doi: 10.1186/s40478-017-0480-2

Tanji, K., Zhang, H. X., Mori, F., Kakita, A., Takahashi, H., and Wakabayashi, K. (2012). p62/sequestosome 1 binds to TDP-43 in brains with frontotemporal lobar degeneration with TDP-43 inclusions. *J. Neurosci. Res.* 90, 2034–2042. doi: 10.1002/jnr.23081

Thiede, B., Treumann, A., Kretschmer, A., Sohlke, J., and Rudel, T. (2005). Shotgun proteome analysis of protein cleavage in apoptotic cells. *Proteomics* 5, 2123–2130. doi: 10.1002/pmic.200401110

Tollervey, J. R., Curk, T., Rogelj, B., Briese, M., Cereda, M., Kayikci, M., et al. (2011). Characterizing the RNA targets and position-dependent splicing regulation by TDP-43. *Nat. Neurosci.* 14, 452–458. doi: 10.1038/nn.2778

Tsai, K. J., Yang, C. H., Fang, Y. H., Cho, K. H., Chien, W. L., Wang, W. T., et al. (2010). Elevated expression of TDP-43 in the forebrain of mice is sufficient to cause neurological and pathological phenotypes mimicking FTLD-U. *J. Exp. Med.* 207, 1661–1673. doi: 10.1084/jem.20092164

Tsai, R. M., and Boxer, A. L. (2016). Therapy and clinical trials in frontotemporal dementia: past, present, and future. *J. Neurochem.* 138(Suppl. 1), 211–221. doi: 10.1111/jnc.13640

Tsuiji, H., Inoue, I., Takeuchi, M., Furuya, A., Yamakage, Y., Watanabe, S., et al. (2017). TDP-43 accelerates age-dependent degeneration of interneurons. *Sci. Rep.* 7:14972. doi: 10.1038/s41598-017-14966-w

Tsuji, H., Arai, T., Kametani, F., Nonaka, T., Yamashita, M., Suzukake, M., et al. (2012a). Molecular analysis and biochemical classification of TDP-43 proteinopathy. *Brain* 135(Pt 11), 3380–3391. doi: 10.1093/brain/aws230

Tsuji, H., Nonaka, T., Yamashita, M., Masuda-Suzukake, M., Kametani, F., Akiyama, H., et al. (2012b). Epitope mapping of antibodies against TDP-43 and detection of protease-resistant fragments of pathological TDP-43 in amyotrophic lateral sclerosis and frontotemporal lobar degeneration. *Biochem. Biophys. Res. Commun.* 417, 116–121. doi: 10.1016/j.bbrc.2011.11.066

Uchida, A., Sasaguri, H., Kimura, N., Tajiri, M., Ohkubo, T., Ono, F., et al. (2012). Non-human primate model of amyotrophic lateral sclerosis with cytoplasmic mislocalization of TDP-43. *Brain* 135(Pt 3), 833–846. doi: 10.1093/brain/awr348

Uchida, T., Tamaki, Y., Ayaki, T., Shodai, A., Kaji, S., Morimura, T., et al. (2016). CUL2-mediated clearance of misfolded TDP-43 is paradoxically affected by VHL in oligodendrocytes in ALS. *Sci. Rep.* 6:19118. doi: 10.1038/srep19118

Udan-Johns, M., Bengoechea, R., Bell, S., Shao, J., Diamond, M. I., True, H. L., et al. (2014). Prion-like nuclear aggregation of TDP-43 during heat shock is regulated by HSP40/70 chaperones. *Hum. Mol. Genet.* 23, 157–170. doi: 10.1093/hmg/ddt408

Uversky, V. N. (2015). Intrinsically disordered proteins and their (disordered) proteomes in neurodegenerative disorders. *Front. Aging Neurosci.* 7:18. doi: 10.3389/fnagi.2015.00018

Uversky, V. N. (2017). The roles of intrinsic disorder-based liquid-liquid phase transitions in the Dr. Jekyll-Mr. Hyde behavior of proteins involved in amyotrophic lateral sclerosis and frontotemporal lobar degeneration. *Autophagy* 13, 2115–2162. doi: 10.1080/15548627.2017.1384889

Van Damme, P., Martens, L., Van Damme, J., Hugelier, K., Staes, A., Vandekerckhove, J., et al. (2005). Caspase-specific and nonspecific in vivo protein processing during Fas-induced apoptosis. *Nat. Methods* 2, 771–777. doi: 10.1038/nmeth792

Van Damme, P., Robberecht, W., and Van Den Bosch, L. (2017). Modelling amyotrophic lateral sclerosis: progress and possibilities. *Dis. Model Mech.* 10, 537–549. doi: 10.1242/dmm.029058

Van Den Bosch, L., Van Damme, P., Bogaert, E., and Robberecht, W. (2006). The role of excitotoxicity in the pathogenesis of amyotrophic lateral sclerosis. *Biochim. Biophys. Acta* 1762, 1068–1082. doi: 10.1016/j.bbadis.2006.05.002

van der Zee, J., Le Ber, I., Maurer-Stroh, S., Engelborghs, S., Gijselinck, I., Camuzat, A., et al. (2007). Mutations other than null mutations producing a pathogenic loss of progranulin in frontotemporal dementia. *Hum. Mutat.* 28, 416. doi: 10.1002/humu.9484

van Eersel, J., Ke, Y. D., Gladbach, A., Bi, M., Gotz, J., Kril, J. J., et al. (2011). Cytoplasmic accumulation and aggregation of TDP-43 upon proteasome inhibition in cultured neurons. *PLoS One* 6:e22850. doi: 10.1371/journal.pone.0022850

Van Mossevelde, S., Engelborghs, S., van der Zee, J., and Van Broeckhoven, C. (2018). Genotype-phenotype links in frontotemporal lobar degeneration. *Nat. Rev. Neurol.* 14, 363–378. doi: 10.1038/s41582-018-0009-8

Vernay, A., Sellal, F., and Rene, F. (2016). Evaluating behavior in mouse models of the behavioral variant of frontotemporal dementia: Which test for which symptom? *Neurodegener. Dis.* 16, 127–139. doi: 10.1159/000439253

Verstraete, E., Veldink, J. H., Hendrikse, J., Schelhaas, H. J., van den Heuvel, M. P., and van den Berg, L. H. (2012). Structural MRI reveals cortical thinning in amyotrophic lateral sclerosis. *J. Neurol. Neurosurg. Psychiatry* 83, 383–388. doi: 10.1136/jnnp-2011-300909

Voigt, A., Herholz, D., Fiesel, F. C., Kaur, K., Muller, D., Karsten, P., et al. (2010). TDP-43-mediated neuron loss in vivo requires RNA-binding activity. *PLoS One* 5:e12247. doi: 10.1371/journal.pone.0012247

Walker, A. K., Daniels, C. M., Goldman, J. E., Trojanowski, J. Q., Lee, V. M., and Messing, A. (2014). Astrocytic TDP-43 pathology in Alexander disease. *J. Neurosci.* 34, 6448–6458. doi: 10.1523/JNEUROSCI.0248-14.2014

Walker, A. K., Soo, K. Y., Sundaramoorthy, V., Parakh, S., Ma, Y., Farg, M. A., et al. (2013). ALS-associated TDP-43 induces endoplasmic reticulum stress, which drives cytoplasmic TDP-43 accumulation and stress granule formation. *PLoS One* 8:e81170. doi: 10.1371/journal.pone.0081170

Walker, A. K., Spiller, K. J., Ge, G., Zheng, A., Xu, Y., Zhou, M., et al. (2015a). Functional recovery in new mouse models of ALS/FTLD after clearance of pathological cytoplasmic TDP-43. *Acta Neuropathol.* 130, 643–660. doi: 10.1007/s00401-015-1460-x

Walker, A. K., Tripathy, K., Restrepo, C. R., Ge, G., Xu, Y., Kwong, L. K., et al. (2015b). An insoluble frontotemporal lobar degeneration-associated TDP-43 C-terminal fragment causes neurodegeneration and hippocampus pathology in transgenic mice. *Hum Mol Genet* 24, 7241–7254. doi: 10.1093/hmg/ddv424

Wang, A., Conicella, A. E., Schmidt, H. B., Martin, E. W., Rhoads, S. N., Reeb, A. N., et al. (2018). A single N-terminal phosphomimic disrupts TDP-43 polymerization, phase separation, and RNA splicing. *Emboj* 37:e97452. doi: 10.15252/embj.201797452

Wang, L., Kang, J., Lim, L., Wei, Y., and Song, J. (2018). TDP-43 NTD can be induced while CTD is significantly enhanced by ssDNA to undergo liquid-liquid phase separation. *Biochem. Biophys. Res. Commun.* 499, 189–195. doi: 10.1016/j.bbrc.2018.03.121

Wang, H. Y., Wang, I. F., Bose, J., and Shen, C. K. (2004). Structural diversity and functional implications of the eukaryotic TDP gene family. *Genomics* 83, 130–139. doi: 10.1016/S0888-7543(03)00214-3

Wang, I. F., Chang, H. Y., Hou, S. C., Liou, G. G., Way, T. D., and James Shen, C. K. (2012). The self-interaction of native TDP-43 C terminus inhibits its degradation and contributes to early proteinopathies. *Nat. Commun.* 3:766. doi: 10.1038/ncomms1766

Wang, G., Yang, H., Yan, S., Wang, C. E., Liu, X., Zhao, B., et al. (2015). Cytoplasmic mislocalization of RNA splicing factors and aberrant neuronal gene splicing in TDP-43 transgenic pig brain. *Mol. Neurodegener.* 10:42. doi: 10.1186/s13024-015-0036-5

Wang, X., Ma, M., Teng, J., Che, X., Zhang, W., Feng, S., et al. (2015). Valproate attenuates 25-kDa C-terminal fragment of TDP-43-induced neuronal toxicity via suppressing endoplasmic reticulum stress and activating autophagy. *Int. J. Biol. Sci.* 11, 752–761. doi: 10.7150/ijbs.11880

Watanabe, R., Kawakami, I., Onaya, M., Higashi, S., Arai, N., Akiyama, H., et al. (2018). Frontotemporal dementia with trans-activation response DNA-binding protein 43 presenting with catatonic syndrome. *Neuropathology* 38, 281–287. doi: 10.1111/neup.12442

Wegorzewska, I., Bell, S., Cairns, N. J., Miller, T. M., and Baloh, R. H. (2009). TDP-43 mutant transgenic mice develop features of ALS and frontotemporal lobar degeneration. *Proc. Natl. Acad. Sci. U.S.A.* 106, 18809–18814. doi: 10.1073/pnas.0908767106

Wei, Y., Lim, L., Wang, L., and Song, J. (2017). ALS-causing cleavages of TDP-43 abolish its RRM2 structure and unlock CTD for enhanced aggregation and toxicity. *Biochem. Biophys. Res. Commun.* 485, 826–831. doi: 10.1016/j.bbrc.2017.02.139

Weihl, C. C., Temiz, P., Miller, S. E., Watts, G., Smith, C., Forman, M., et al. (2008). TDP-43 accumulation in inclusion body myopathy muscle suggests a common pathogenic mechanism with frontotemporal dementia. *J. Neurol. Neurosurg. Psychiatry* 79, 1186–1189. doi: 10.1136/jnnp.2007.131334

Wennberg, A. M., Tosakulwong, N., Lesnick, T. G., Murray, M. E., Whitwell, J. L., Liesinger, A. M., et al. (2018). Association of apolipoprotein E ε4 with Transactive Response DNA-Binding Protein 43. *JAMA Neurol.* 75, 1347–1354. doi: 10.1001/jamaneurol.2018.3139

Wils, H., Kleinberger, G., Janssens, J., Pereson, S., Joris, G., Cuijt, I., et al. (2010). TDP-43 transgenic mice develop spastic paralysis and neuronal inclusions characteristic of ALS and frontotemporal lobar degeneration. *Proc. Natl. Acad. Sci. U.S.A.* 107, 3858–3863. doi: 10.1073/pnas.0912417107

Wilson, R. S., Yang, J., Yu, L., Leurgans, S. E., Capuano, A. W., Schneider, J. A., et al. (2019). Postmortem neurodegenerative markers and trajectories of decline in cognitive systems. *Neurology* 92, e831–e840. doi: 10.1212/WNL.0000000000006949

Winton, M. J., Igaz, L. M., Wong, M. M., Kwong, L. K., Trojanowski, J. Q., and Lee, V. M. (2008). Disturbance of nuclear and cytoplasmic TAR DNA-binding protein (TDP-43) induces disease-like redistribution, sequestration, and aggregate formation. *J. Biol. Chem.* 283, 13302–13309. doi: 10.1074/jbc.M800342200

Wobst, H. J., Delsing, L., Brandon, N. J., and Moss, S. J. (2017). Truncation of the TAR DNA-binding protein 43 is not a prerequisite for cytoplasmic relocalization, and is suppressed by caspase inhibition and by introduction of the A90V sequence variant. *PLoS One* 12:e0177181. doi: 10.1371/journal.pone.0177181

Wu, L. S., Cheng, W. C., Hou, S. C., Yan, Y. T., Jiang, S. T., and Shen, C. K. (2010). TDP-43, a neuro-pathosignature factor, is essential for early mouse embryogenesis. *Genesis* 48, 56–62. doi: 10.1002/dvg.20584

Xiao, S., Sanelli, T., Chiang, H., Sun, Y., Chakrabartty, A., Keith, J., et al. (2015). Low molecular weight species of TDP-43 generated by abnormal splicing form inclusions in amyotrophic lateral sclerosis and result in motor neuron death. *Acta Neuropathol.* 130, 49–61. doi: 10.1007/s00401-015-1412-5

Xiao, S., Sanelli, T., Dib, S., Sheps, D., Findlater, J., Bilbao, J., et al. (2011). RNA targets of TDP-43 identified by UV-CLIP are deregulated in ALS. *Mol. Cell Neurosci.* 47, 167–180. doi: 10.1016/j.mcn.2011.02.013

Xu, Y. F., Gendron, T. F., Zhang, Y. J., Lin, W. L., D'Alton, S., Sheng, H., et al. (2010). Wild-type human TDP-43 expression causes TDP-43 phosphorylation, mitochondrial aggregation, motor deficits, and early mortality in transgenic mice. *J. Neurosci.* 30, 10851–10859. doi: 10.1523/JNEUROSCI.1630-10.2010

Xu, Y. F., Zhang, Y. J., Lin, W. L., Cao, X., Stetler, C., Dickson, D. W., et al. (2011). Expression of mutant TDP-43 induces neuronal dysfunction in transgenic mice. *Mol. Neurodegener.* 6:73. doi: 10.1186/1750-1326-6-73

Yamashita, M., Nonaka, T., Hirai, S., Miwa, A., Okado, H., Arai, T., et al. (2014). Distinct pathways leading to TDP-43-induced cellular dysfunctions. *Hum. Mol. Genet.* 23, 4345–4356. doi: 10.1093/hmg/ddu152

Yamashita, T., Hideyama, T., Hachiga, K., Teramoto, S., Takano, J., Iwata, N., et al. (2012). A role for calpain-dependent cleavage of TDP-43 in amyotrophic lateral sclerosis pathology. *Nat. Commun.* 3:1307. doi: 10.1038/ncomms2303

Yamashita, T., Teramoto, S., and Kwak, S. (2016). Phosphorylated TDP-43 becomes resistant to cleavage by calpain: a regulatory role for phosphorylation in TDP-43 pathology of ALS/FTLD. *Neurosci. Res.* 107, 63–69. doi: 10.1016/j.neures.2015.12.006

Yang, C., Tan, W., Whittle, C., Qiu, L., Cao, L., Akbarian, S., et al. (2010). The C-terminal TDP-43 fragments have a high aggregation propensity and harm neurons by a dominant-negative mechanism. *PLoS One* 5:e15878. doi: 10.1371/journal.pone.0015878

Yang, Z., Lin, F., Robertson, C. S., and Wang, K. K. (2014). Dual vulnerability of TDP-43 to calpain and caspase-3 proteolysis after neurotoxic conditions and traumatic brain injury. *J. Cereb. Blood Flow Metab.* 34, 1444–1452. doi: 10.1038/jcbfm.2014.105

Yerbury, J. J., Ooi, L., Dillin, A., Saunders, D. N., Hatters, D. M., Beart, P. M., et al. (2016). Walking the tightrope: proteostasis and neurodegenerative disease. *J. Neurochem.* 137, 489–505. doi: 10.1111/jnc.13575

Yin, P., Guo, X., Yang, W., Yan, S., Yang, S., Zhao, T., et al. (2019). Caspase-4 mediates cytoplasmic accumulation of TDP-43 in the primate brains. *Acta Neuropathol.* doi: 10.1007/s00401-019-01979-0 [Epub ahead of print].

Yokoseki, A., Shiga, A., Tan, C. F., Tagawa, A., Kaneko, H., Koyama, A., et al. (2008). TDP-43 mutation in familial amyotrophic lateral sclerosis. *Ann. Neurol.* 63, 538–542. doi: 10.1002/ana.21392

Zeineddine, R., Farrawell, N. E., Lambert-Smith, I. A., and Yerbury, J. J. (2017). Addition of exogenous SOD1 aggregates causes TDP-43 mislocalisation and aggregation. *Cell Stress Chaperones* 22, 893–902. doi: 10.1007/s12192-017-0804-y

Zhang, T., Mullane, P. C., Periz, G., and Wang, J. (2011). TDP-43 neurotoxicity and protein aggregation modulated by heat shock factor and insulin/IGF-1 signaling. *Hum. Mol. Genet.* 20, 1952–1965. doi: 10.1093/hmg/ddr076

Zhang, Y. J., Gendron, T. F., Xu, Y. F., Ko, L. W., Yen, S. H., and Petrucelli, L. (2010). Phosphorylation regulates proteasomal-mediated degradation and solubility of TAR DNA binding protein-43 C-terminal fragments. *Mol. Neurodegener.* 5:33. doi: 10.1186/1750-1326-5-33

Zhang, Y. J., Jansen-West, K., Xu, Y. F., Gendron, T. F., Bieniek, K. F., Lin, W. L., et al. (2014). Aggregation-prone c9FTD/ALS poly(GA) RAN-translated proteins cause neurotoxicity by inducing ER stress. *Acta Neuropathol.* 128, 505–524. doi: 10.1007/s00401-014-1336-5

Zhang, Y. J., Xu, Y. F., Cook, C., Gendron, T. F., Roettges, P., Link, C. D., et al. (2009). Aberrant cleavage of TDP-43 enhances aggregation and cellular toxicity. *Proc. Natl. Acad. Sci. U.S.A.* 106, 7607–7612. doi: 10.1073/pnas.0900688106

Zhang, Y. J., Xu, Y. F., Dickey, C. A., Buratti, E., Baralle, F., Bailey, R., et al. (2007). Progranulin mediates caspase-dependent cleavage of TAR DNA binding protein-43. *J. Neurosci.* 27, 10530–10534. doi: 10.1523/JNEUROSCI.3421-07.2007

Zhou, H., Huang, C., Chen, H., Wang, D., Landel, C. P., Xia, P. Y., et al. (2010). Transgenic rat model of neurodegeneration caused by mutation in the TDP gene. *PLoS Genet.* 6:e1000887. doi: 10.1371/journal.pgen.1000887

Zhu, C., Beck, M. V., Griffith, J. D., Deshmukh, M., and Dokholyan, N. V. (2018). Large SOD1 aggregates, unlike trimeric SOD1, do not impact cell viability in a model of amyotrophic lateral sclerosis. *Proc. Natl. Acad. Sci. U.S.A.* 115, 4661–4665. doi: 10.1073/pnas.1800187115

Conflict of Interest Statement: The authors declare that the research was conducted in the absence of any commercial or financial relationships that could be construed as a potential conflict of interest.

frontiers in Neuroscience

OPINION
published: 25 April 2019
doi: 10.3389/fnins.2019.00395

Granulin in Frontotemporal Lobar Degeneration: Molecular Mechanisms of the Disease

Zemfira N. Karamysheva[1]*, *Elena B. Tikhonova*[2] and *Andrey L. Karamyshev*[2]*

[1] Department of Biological Sciences, Texas Tech University, Lubbock, TX, United States, [2] Department of Cell Biology and Biochemistry, Texas Tech University Health Sciences Center, Lubbock, TX, United States

Keywords: frontotemporal lobar degeneration (FTLD), granulin, disease-causing mutations, protein quality control, protein targeting and transport, signal peptide, signal recognition particle (SRP), RNA degradation

OPEN ACCESS

Edited by:
Alberto Lleo, Hospital de la Santa Creu i Sant Pau, Spain

Reviewed by:
Marc Suárez-Calvet, BarcelonaBeta Brain Research Center, Spain

***Correspondence:**
Zemfira N. Karamysheva
zemfira.karamysheva@ttu.edu
Andrey L. Karamyshev
andrey.karamyshev@ttuhsc.edu

Specialty section:
This article was submitted to Neurodegeneration, a section of the journal Frontiers in Neuroscience

Received: *15 February 2019*
Accepted: *08 April 2019*
Published: *25 April 2019*

Citation:
Karamysheva ZN, Tikhonova EB and Karamyshev AL (2019) Granulin in Frontotemporal Lobar Degeneration: Molecular Mechanisms of the Disease. Front. Neurosci. 13:395. doi: 10.3389/fnins.2019.00395

Frontotemporal lobar degeneration (FTLD) is a pathological process characterized by severe atrophy in the frontal and temporal lobes of the brain (Mackenzie et al., 2011). There are three major clinical syndromes in FTLD: behavioral variant of frontotemporal dementia (bvFTD), nonfluent variant of primary progressive aphasia (nfvPPA), and semantic variant of PPA (svPPA) (Gorno-Tempini et al., 2011; Rascovsky et al., 2011). bvFTD is the most common among three (Hernandez et al., 2018). It is associated with changes in personality and behavior accompanied with language deficits at later stages. In rare cases, FTLD subtypes may be associated with motor neuron disease worsening the patient survival time (Olney et al., 2005). FTLD also includes the clinical presentations of progressive supranuclear palsy (PSP) and corticobasal degeneration (CBD), that are associated with parkinsonism, and other clinical features. PSP and CBD account for about 20–30% of patients in FTLD (Park and Chung, 2013). Unfortunately, there is no significant progress achieved in development of effective treatments for FTLD and current treatment options are purely symptomatic (Hodges and Piguet, 2018).

The pathological changes found in FTLD are very heterogenous in their nature. FTLD can be divided in three main histological subtypes according to the accumulation of neuronal protein inclusions (Mackenzie et al., 2011). The most common disease is characterized by the presence of inclusions containing the trans-activation response DNA-binding protein-43 (TDP-43) which is found to be abnormally phosphorylated and ubiquitinated in patients (Neumann et al., 2006). This subtype of pathology is classified as FTLD-TDP (Mackenzie et al., 2011). The second pathological subtype, FTLD-tau, includes cases with inclusions consisting of abnormally phosphorylated microtubule associated protein tau (Cairns et al., 2007). The third subtype, FTLD-FET, contains fused in sarcoma (FUS) RNA-binding protein, Ewing's sarcoma protein (EWS), and TATA-binding protein associated factor 15 (TAF15) in the pathological inclusions (Mackenzie and Neumann, 2012). About 40% of FTLD cases are familial and about 10% of cases exhibit autosomal dominant inheritance (Bang et al., 2015). Mutations in *GRN* (Baker et al., 2006; Cruts et al., 2006), *MAPT* (Hutton et al., 1998), *CHMP2B* (Skibinski et al., 2005), *VCP* (Watts et al., 2004), and *C9orf72* (Renton et al., 2011) have been found associated with the disease. The most common known genetic causes of FTLD are connected with mutations in *GRN*, *MAPT*, and *C9orf72* genes (Cruts et al., 2006; Gass et al., 2006, 2012; Mori et al., 2013; Hodges and Piguet, 2018). In this article we focus on progranulin (PGRN protein encoded by *GRN* gene) role in FTLD. Patients with progranulin mutations have ubiquitin and TDP-43 positive pathological inclusions (Baker et al., 2006; Cruts et al., 2006). In addition to its role in neurodegenerative diseases PGRN is also implicated in epithelial ovarian cancer and its level is highly elevated in various tumors (He and Bateman, 2003). It also has a role in metabolic diseases and its excess is associated with obesity and insulin resistance (Matsubara et al., 2012). PRGN is a multifunctional protein involved in regulation of many cellular processes including angiogenesis, cell proliferation, inflammation, tissue remodeling, and wound repair (Nguyen et al., 2013).

PRGN is encoded by *GRN* gene that is located on chromosome 17q21 and consists of 13 exons with the Kozak sequence present in the second exon (Bhandari et al., 1992; Cruts and Van Broeckhoven, 2008) (**Figure 1A**). It encodes 593 amino acid long precursor protein with a predicted molecular mass of 63.5 kDa. PRGN contains a signal peptide (also known as a signal sequence) at the N-terminus to mediate its secretion, followed by 7.5 highly conserved cysteine-rich tandem repeats called granulins. Granulins are separated by divergent linker sequences. Cleavage of the signal peptide generates mature protein that is heavily glycosylated and migrates as 88 kDa protein. This protein is further processed by the cleavage at the linker regions to produce 6 kDa granulins or linked combinations of granulins (Cenik et al., 2012; Gass et al., 2012) (**Figure 1B**). PGRN does not have clear consensus sequence for protease cleavage and is cleaved by multiple intracellular and extracellular proteases such as elastase, proteinase 3, matrix metallopeptidase 12, or by cathepsins in the lysosomes (Gass et al., 2012; Nguyen et al., 2013; Zhou et al., 2017a). Both progranulin and 6 kDa granulins are shown to exist *in viv*o, however, their biological functions in the cell are not very clear. Recent data suggest that progranulin may be involved in anti-inflammatory activities through modulation of the TNF signaling while granulins are proinflammatory (Tang et al., 2011; Hu et al., 2014). The C-terminus of PRGN is necessary to bind sortilin, a receptor protein regulating intracellular protein trafficking in the Golgi (Hu et al., 2010). Lysosomal targeting of PGRN is carried out by two independent and complementary pathways. The first utilizes sortilin protein, protein trafficking receptor, located in Golgi and cell surface (Hu et al., 2010). The second, sortilin-independent pathway, is mediated by prosaposin (PSAP) through its interaction with mannose 6-phosphate receptor (M6PR) and low-density lipoprotein receptor-related protein 1 (LRP1) (Zhou et al., 2015). PSAP is the precursor of saposin protein essential for lysosomal degradation of glycosphingolipids. The role of PRGN and granulins in lysosome function is poorly understood, however, it has been recently revealed that deficiencies in granulins caused by mutations may play a role in lysosome dysfunction (Holler et al., 2017). Complete loss of PGRN due to homozygous *GRN* mutations was reported as a cause for neuronal ceroid lipofuscinosis (NCL) linking rare lysosomal impairment to neurodegeneration in FTLD (Smith et al., 2012; Gotzl et al., 2016). This disease leads to progressive degeneration of brain and loss of vision due to accumulation of ceroid lipofuscin, a lipid-containing pigment, associated with lysosome dysfunction (Kohlschutter and Schulz, 2009). It was shown that a lack of PGRN leads to decreased level of PSAP in neurons causing NCL (Zhou et al., 2017b). These discoveries suggested that PRGN and PSAP facilitate each other's lysosomal trafficking. Furthermore, studies of lysosome storage diseases from different groups suggested that PRGN might acts as a chaperone of lysosomal enzymes (Jian et al., 2016; Beel et al., 2017). Chaperone functions required direct association of PRGN with lysosomal proteins through granulin E domain and also involved recruitment of HSP70.

Loss of the PGRN function can occur on the genomic, transcriptional, and posttranscriptional levels (Kleinberger et al., 2013). Mutations in *GRN* are one of the major causes of FTLD and found in 11.2% of patients, therefore progranulin is an important emerging target to develop better treatments (Abella et al., 2017). More than 100 different mutations were identified in the *GRN* gene, and at least 79 pathogenic mutations in 259 families have been associated with FTLD (Cruts et al., 2012) (http://www.molgen.ua.ac.be/FTDmutations/). Most common mutations include nonsense, frameshift and splice site mutations leading to generation of a premature stop codon that activate nonsense-mediated decay (NMD) (Baker et al., 2006; Cruts et al., 2006). Therefore, majority of the mutations are believed to act through a haploinsufficiency mechanism due to mutant mRNA degradation of the one allele and as a result reduced progranulin protein level (Cruts and Van Broeckhoven, 2008). Other mutations include genomic deletions or elimination of the initiation codon for protein synthesis. Loss of the PGRN function can also be mediated by mutations affecting the protein sorting, secretion, proteolytic processing, association with sortilin and cyclin T1, neurite outgrowth, and proinflammatory response (Kleinberger et al., 2013). Some missense and intronic mutations in *GRN* also contribute to the pathogenicity connected to FTLD due to the loss of functional protein (Abella et al., 2017).

Unusual and intriguing molecular mechanism of FTLD that is associated with mutations in progranulin signal sequences was recently discovered (Pinarbasi et al., 2018). Progranulin is a secreted protein and it is synthesized as a precursor with signal peptide (**Figure 1A**). Signal Recognition Particle (SRP) recognizes signal peptides co-translationally during protein synthesis at the ribosome and targets ribosome nascent complexes to endoplasmic reticulum (ER) membrane for the protein translocation to the ER lumen and further processing and transport outside of the cells (**Figure 1B**). It is well-established that integrity of the signal peptides is important for protein targeting and transport (Karamyshev et al., 1998; Kalinin et al., 1999; Karamyshev and Johnson, 2005; Nilsson et al., 2015). Despite the absence of the strong amino acid homology between signal peptides of different proteins they have similar organization and contain n-terminal, hydrophobic core or h-region, and c-terminal parts (von Heijne, 1985). Amino acid substitutions that decrease hydrophobicity of the h-region inhibit interaction with SRP (Nilsson et al., 2015). As we recently discovered, the loss of SRP interaction activates the protein quality control pathway named RAPP (regulation of aberrant protein production) leading to mRNA degradation of the defective proteins (Karamyshev et al., 2014; Karamyshev and Karamysheva, 2018). Among more than 100 of different mutations in the progranulin three missense mutations lead to amino acid alterations in the signal peptide hydrophobic core; they are V5L, W7R, and A9D (Gass et al., 2006; Mukherjee et al., 2006; Lopez de Munain et al., 2008; Cruts et al., 2012) (**Figure 1A**). While V5L and W7R mutations are not well-studied in patients, it was demonstrated that the A9D mutation resulted in decreased *GRN* mRNA and protein levels (Mukherjee et al., 2006, 2008). However, the mechanism of the reduced mRNA level was not clear at that time. Further detailed experimental examination of the PGRN signal peptide mutations showed that W7R and A9D inhibited signal peptide interaction with

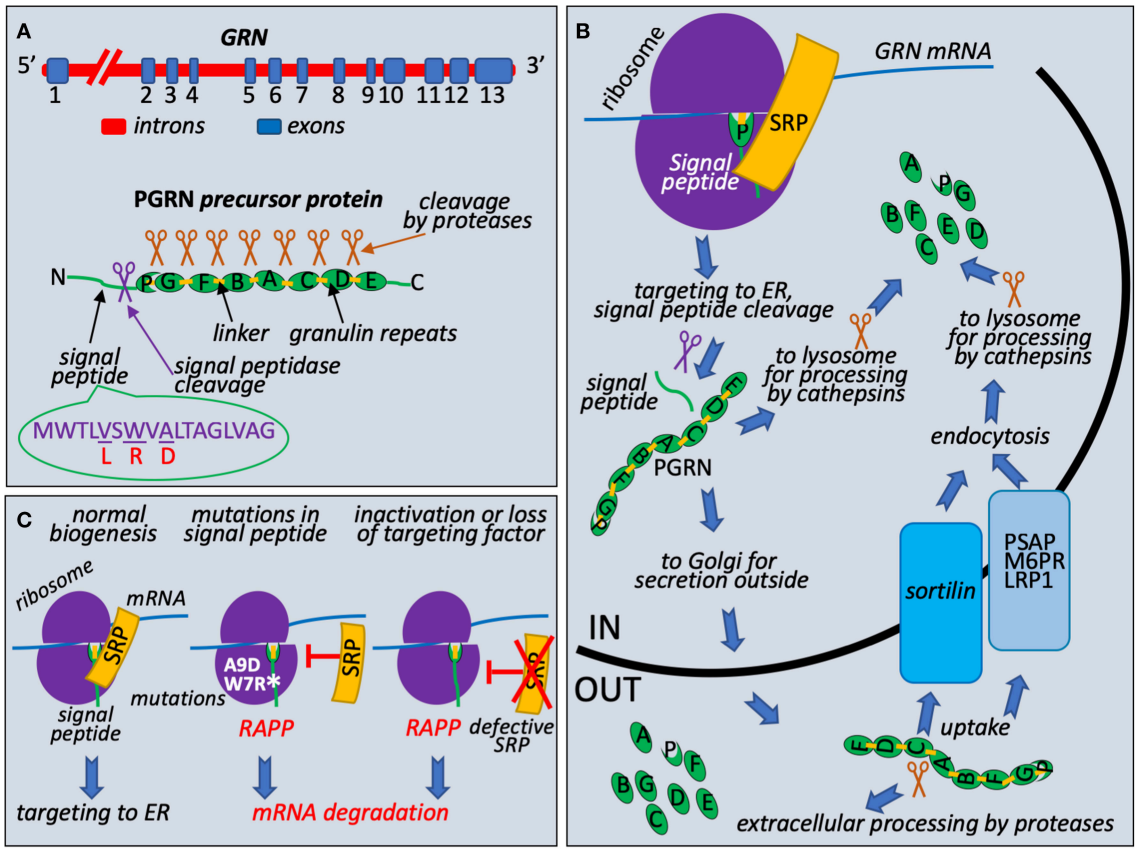

FIGURE 1 | Granulin biogenesis, quality control at the ribosome during its synthesis, and molecular mechanism of FTLD associated with mutations in the signal peptide of the granulin precursor. **(A)** Schematic presentation of *GRN*, precursor protein structure, and known missense mutations in the signal peptide. Progranulin pre-mRNA transcript is synthesized in the nucleus from *GRN* gene in the chromosome 17. It has 13 exons with exons 2–13 containing protein coding region. After splicing, mRNA is exported to cytoplasm for translation. Progranulin precursor (63.5 kDa protein) consists of N-terminal cleavable signal peptide (green line with indicated position of the cleavage by the signal peptidase shown as purple scissors) and 7.5 repeats (green ovals): P (half-repeat, paragranulin), G (granulin 1), F (granulin 2), B (granulin 3), A (granulin 4), C (granulin 5), D (granulin 6), and E (granulin 7). Repeats are connected by linker sequences (light orange boxes). Proteases are shown as brown scissors. Signal peptide sequence presented with known missense mutations L (V5L), R (W7R), D (A9D), corresponding amino acid residues in the wild-type signal peptide are underlined. **(B)** PGRN protein trafficking and processing. During early translation step on the ribosome (purple hemispheres), N-terminal signal peptide of progranulin (green line) is recognized by Signal Recognition Particle (SRP) (shown in orange) and ribosome-nascent chain complex is targeted to ER for signal peptide cleavage (purple scissors), posttranslational modifications, and further processing and transport. Full length protein could be processed to 6 kDa granulins in lysosomes by cathepsins (brown scissors are symbols for all proteases involved in posttranslational processing) or secreted outside and undergo extracellular processing. Uptake of full-length protein is governed by endocytosis with the help of sortilin receptor (blue box) or through alternative PSAP (prosaposin)-dependent pathway with involvement of mannose 6-phosphate receptor (M6PR) and low density lipoprotein receptor-related protein 1 (LRP1) (gray blue box). **(C)** Loss of interaction with targeting factor, SRP, activates RAPP pathway. During normal translational event, PGRN with N-terminal signal sequence is targeted to ER through interaction with SRP. Amino acid sequence of signal peptide and location of reported clinical mutations are shown on **(A)**. When A9D or W7R mutations in signal peptide is detected or SRP is defective or lost, nascent chain is no longer targeted to ER by SRP. It leads to the RAPP pathway activation and degradation of the *GRN* mRNA.

SRP and pathologically activated the RAPP pathway leading to degradation of the defective *GRN* mRNAs establishing the molecular mechanism of the familial FTLD through mRNA degradation (Pinarbasi et al., 2018) (**Figure 1C**). Remarkably, the mechanism of *GRN* mRNA degradation was specific to the mutated mRNAs only and did not affect the wild-type *GRN* mRNA when they were co-expressed. The mRNA degradation was initiated by the loss of SRP interaction with the signal peptide due to W7R or A9D mutation. RAPP activation is a unique feature of the pathway—it recognizes defective proteins and degrades their mRNA templates. Interestingly, V5L mutation did not interfere with SRP interactions and did not induce the RAPP pathway, and the mutated mRNA did not degrade, suggesting that the V5L is a benign polymorphism and most likely does not lead to a disease. Analysis of the signal peptide hydrophobicity profiles revealed that W7R or A9D mutations decreased hydrophobicity while V5L did not. This observation may be used for theoretical prediction of the impact of the uncharacterized mutations for RAPP activation and mRNA degradation. Noteworthy, the depletion of SRP54 (one of the six SRP subunits) led to mRNA degradation of the wild-type protein (**Figure 1C**). This fact suggests that defects in SRP

subunits may be a molecular basis of sporadic human diseases. Indeed, it was found recently that several mutations in SRP54 are associated with inherited neutropenia and Shwachman-Diamond-like syndrome (Carapito et al., 2017).

Polypeptide nascent chain interactions at the ribosome are important for proper protein folding, transport, and modification. As it is discussed above, the loss of the SRP signal peptide interaction leads to dramatic consequences: elimination of the defective protein mRNA in the RAPP pathway and as a result to decrease of PGRN protein level and finally to FTLD. Most likely, the induction of the RAPP pathway is not limited to the mutant PGRNs, and may be associated with signal peptide mutations in other secretory proteins leading to the diverse group of the human diseases caused by the pathological RAPP activation.

In conclusion, it seems that the decrease or loss of *GRN* expression in many different familial FTLDs is associated with mRNA degradation, although the nature of the mutations is different. The nonsense, frameshift, and splice site mutations generate premature stop codons that induce NMD, while the mutations in the signal peptide activate RAPP. Regardless of the pathway engaged, the *GRN* mRNA is degraded that may lead to PGRN haploinsufficiency and the disease. These observations open the necessity of deep exploration of the molecular mechanisms of mRNA degradation pathways in neurodegenerative diseases that may eventually lead to development better pharmacological treatments in the future.

AUTHOR CONTRIBUTIONS

AK and ZK wrote the manuscript. ET designed and prepared the figure, all authors discussed and edited the manuscript.

FUNDING

This work was supported by the National Institute of Neurological Disorders and Stroke of the National Institutes of Health under award number R03NS102645 to AK. The content is solely the responsibility of the authors and does not necessarily represent the official views of the National Institutes of Health.

REFERENCES

Abella, V., Pino, J., Scotece, M., Conde, J., Lago, F., Gonzalez-Gay, M. A., et al. (2017). Progranulin as a biomarker and potential therapeutic agent. *Drug Discov. Today* 22, 1557–1564. doi: 10.1016/j.drudis.2017.06.006

Baker, M., Mackenzie, I. R., Pickering-Brown, S. M., Gass, J., Rademakers, R., Lindholm, C., et al. (2006). Mutations in progranulin cause tau-negative frontotemporal dementia linked to chromosome 17. *Nature* 442, 916–919. doi: 10.1038/nature05016

Bang, J., Spina, S., and Miller, B. L. (2015). Frontotemporal dementia. *Lancet* 386, 1672–1682. doi: 10.1016/S0140-6736(15)00461-4

Beel, S., Moisse, M., Damme, M., De Muynck, L., Robberecht, W., Van Den Bosch, L., et al. (2017). Progranulin functions as a cathepsin D chaperone to stimulate axonal outgrowth *in vivo*. *Hum. Mol. Genet.* 26, 2850–2863. doi: 10.1093/hmg/ddx162

Bhandari, V., Palfree, R. G., and Bateman, A. (1992). Isolation and sequence of the granulin precursor cDNA from human bone marrow reveals tandem cysteine-rich granulin domains. *Proc Natl Acad Sci U.S.A.* 89, 1715–1719.

Cairns, N. J., Bigio, E. H., Mackenzie, I. R., Neumann, M., Lee, V. M., Hatanpaa, K. J., et al. (2007). Neuropathologic diagnostic and nosologic criteria for frontotemporal lobar degeneration: consensus of the Consortium for Frontotemporal Lobar Degeneration. *Acta Neuropathol.* 114, 5–22. doi: 10.1007/s00401-007-0237-2

Carapito, R., Konantz, M., Paillard, C., Miao, Z., Pichot, A., Leduc, M. S., et al. (2017). Mutations in signal recognition particle SRP54 cause syndromic neutropenia with Shwachman-Diamond-like features. *J. Clin. Invest.* 127, 4090–4103. doi: 10.1172/JCI92876

Cenik, B., Sephton, C. F., Kutluk Cenik, B., Herz, J., and Yu, G. (2012). Progranulin: a proteolytically processed protein at the crossroads of inflammation and neurodegeneration. *J. Biol. Chem.* 287, 32298–32306. doi: 10.1074/jbc.R112.399170

Cruts, M., Gijselinck, I., van der Zee, J., Engelborghs, S., Wils, H., Pirici, D., et al. (2006). Null mutations in progranulin cause ubiquitin-positive frontotemporal dementia linked to chromosome 17q21. *Nature* 442, 920–924. doi: 10.1038/nature05017

Cruts, M., Theuns, J., and Van Broeckhoven, C. (2012). Locus-specific mutation databases for neurodegenerative brain diseases. *Hum. Mutat.* 33, 1340–1344. doi: 10.1002/humu.22117

Cruts, M., and Van Broeckhoven, C. (2008). Loss of progranulin function in frontotemporal lobar degeneration. *Trends Genet.* 24, 186–194. doi: 10.1016/j.tig.2008.01.004

Gass, J., Cannon, A., Mackenzie, I. R., Boeve, B., Baker, M., Adamson, J., et al. (2006). Mutations in progranulin are a major cause of ubiquitin-positive frontotemporal lobar degeneration. *Hum. Mol. Genet.* 15, 2988–3001. doi: 10.1093/hmg/ddl241

Gass, J., Prudencio, M., Stetler, C., and Petrucelli, L. (2012). Progranulin: an emerging target for FTLD therapies. *Brain Res.* 1462, 118–128. doi: 10.1016/j.brainres.2012.01.047

Gorno-Tempini, M. L., Hillis, A. E., Weintraub, S., Kertesz, A., Mendez, M., Cappa, S. F., et al. (2011). Classification of primary progressive aphasia and its variants. *Neurology* 76, 1006–1014. doi: 10.1212/WNL.0b013e3182 1103e6

Gotzl, J. K., Lang, C. M., Haass, C., and Capell, A. (2016). Impaired protein degradation in FTLD and related disorders. *Ageing Res. Rev.* 32, 122–139. doi: 10.1016/j.arr.2016.04.008

He, Z., and Bateman, A. (2003). Progranulin (granulin-epithelin precursor, PC-cell-derived growth factor, acrogranin) mediates tissue repair and tumorigenesis. *J. Mol. Med.* 81, 600–612. doi: 10.1007/s00109-003-0474-3

Hernandez, I., Fernandez, M. V., Tarraga, L., Boada, M., and Ruiz, A. (2018). Frontotemporal lobar degeneration (FTLD): review and update for clinical neurologists. *Curr. Alzheimer Res.* 15, 511–530. doi: 10.2174/1567205014666170725130819.

Hodges, J. R., and Piguet, O. (2018). Progress and challenges in frontotemporal dementia research: a 20-year review. *J. Alzheimers Dis.* 62, 1467–1480. doi: 10.3233/JAD-171087

Holler, C. J., Taylor, G., Deng, Q., and Kukar, T. (2017). Intracellular proteolysis of progranulin generates stable, lysosomal granulins that are haploinsufficient in patients with frontotemporal dementia caused by GRN mutations. *eNeuro* 4:ENEURO.0100-17.2017. doi: 10.1523/ENEURO.0100-17.2017

Hu, F., Padukkavidana, T., Vaegter, C. B., Brady, O. A., Zheng, Y., Mackenzie, I. R., et al. (2010). Sortilin-mediated endocytosis determines levels of the frontotemporal dementia protein, progranulin. *Neuron* 68, 654–667. doi: 10.1016/j.neuron.2010.09.034

Hu, Y., Xiao, H., Shi, T., Oppenheim, J. J., and Chen, X. (2014). Progranulin promotes tumour necrosis factor-induced proliferation of suppressive mouse CD4(+) Foxp3(+) regulatory T cells. *Immunology* 142, 193–201. doi: 10.1111/imm.12241

Hutton, M., Lendon, C. L., Rizzu, P., Baker, M., Froelich, S., Houlden, H., et al. (1998). Association of missense and 5'-splice-site mutations in tau with the inherited dementia FTDP-17. *Nature* 393, 702–705. doi: 10.1038/31508

Jian, J., Tian, Q. Y., Hettinghouse, A., Zhao, S., Liu, H., Wei, J., et al. (2016). Progranulin recruits HSP70 to beta-glucocerebrosidase and

is therapeutic against gaucher disease. *EBioMedicine* 13, 212–224. doi: 10.1016/j.ebiom.2016.10.010

Kalinin, A. E., Mikhaleva, N. I., Karamyshev, A. L., Karamysheva, Z. N., and Nesmeyanova, M. A. (1999). Interaction of mutant alkaline phosphatase precursors with membrane phospholipids *in vivo* and *in vitro*. *Biochemistry* 64, 1021–1029.

Karamyshev, A. L., and Johnson, A. E. (2005). Selective SecA association with signal sequences in ribosome-bound nascent chains: a potential role for SecA in ribosome targeting to the bacterial membrane. *J. Biol. Chem.* 280, 37930–37940. doi: 10.1074/jbc.M509100200

Karamyshev, A. L., and Karamysheva, Z. N. (2018). Lost in translation: ribosome-associated mRNA and protein quality controls. *Front. Genet.* 9:431. doi: 10.3389/fgene.2018.00431

Karamyshev, A. L., Karamysheva, Z. N., Kajava, A. V., Ksenzenko, V. N., and Nesmeyanova, M. A. (1998). Processing of *Escherichia coli* alkaline phosphatase: role of the primary structure of the signal peptide cleavage region. *J. Mol. Biol.* 277, 859–870. doi: 10.1006/jmbi.1997.1617

Karamyshev, A. L., Patrick, A. E., Karamysheva, Z. N., Griesemer, D. S., Hudson, H., Tjon-Kon-Sang, S., et al. (2014). Inefficient SRP interaction with a nascent chain triggers a mRNA quality control pathway. *Cell* 156, 146–157. doi: 10.1016/j.cell.2013.12.017

Kleinberger, G., Capell, A., Haass, C., and Van Broeckhoven, C. (2013). Mechanisms of granulin deficiency: lessons from cellular and animal models. *Mol. Neurobiol.* 47, 337–360. doi: 10.1007/s12035-012-8380-8

Kohlschutter, A., and Schulz, A. (2009). Towards understanding the neuronal ceroid lipofuscinoses. *Brain Dev.* 31, 499–502. doi: 10.1016/j.braindev.2008.12.008

Lopez de Munain, A., Alzualde, A., Gorostidi, A., Otaegui, D., Ruiz-Martinez, J., Indakoetxea, B., et al. (2008). Mutations in progranulin gene: clinical, pathological, and ribonucleic acid expression findings. *Biol. Psychiatry* 63, 946–952. doi: 10.1016/j.biopsych.2007.08.015

Mackenzie, I. R., and Neumann, M. (2012). FET proteins in frontotemporal dementia and amyotrophic lateral sclerosis. *Brain Res.* 1462, 40–43. doi: 10.1016/j.brainres.2011.12.010

Mackenzie, I. R., Neumann, M., Baborie, A., Sampathu, D. M., Du Plessis, D., Jaros, E., et al. (2011). A harmonized classification system for FTLD-TDP pathology. *Acta Neuropathol.* 122, 111–113. doi: 10.1007/s00401-011-0845-8

Matsubara, T., Mita, A., Minami, K., Hosooka, T., Kitazawa, S., Takahashi, K., et al. (2012). PGRN is a key adipokine mediating high fat diet-induced insulin resistance and obesity through IL-6 in adipose tissue. *Cell Metab.* 15, 38–50. doi: 10.1016/j.cmet.2011.12.002

Mori, K., Weng, S. M., Arzberger, T., May, S., Rentzsch, K., Kremmer, E., et al. (2013). The C9orf72 GGGGCC repeat is translated into aggregating dipeptide-repeat proteins in FTLD/ALS. *Science* 339, 1335–1338. doi: 10.1126/science.1232927

Mukherjee, O., Pastor, P., Cairns, N. J., Chakraverty, S., Kauwe, J. S., Shears, S., et al. (2006). HDDD2 is a familial frontotemporal lobar degeneration with ubiquitin-positive, tau-negative inclusions caused by a missense mutation in the signal peptide of progranulin. *Ann. Neurol.* 60, 314–322. doi: 10.1002/ana.20963

Mukherjee, O., Wang, J., Gitcho, M., Chakraverty, S., Taylor-Reinwald, L., Shears, S., et al. (2008). Molecular characterization of novel progranulin (GRN) mutations in frontotemporal dementia. *Hum. Mutat.* 29, 512–521. doi: 10.1002/humu.20681

Neumann, M., Sampathu, D. M., Kwong, L. K., Truax, A. C., Micsenyi, M. C., Chou, T. T., et al. (2006). Ubiquitinated TDP-43 in frontotemporal lobar degeneration and amyotrophic lateral sclerosis. *Science* 314, 130–133. doi: 10.1126/science.1134108

Nguyen, A. D., Nguyen, T. A., Martens, L. H., Mitic, L. L., and Farese, R. V. Jr., (2013). Progranulin: at the interface of neurodegenerative and metabolic diseases. *Trends Endocrinol. Metab.* 24, 597–606. doi: 10.1016/j.tem.2013.08.003

Nilsson, I., Lara, P., Hessa, T., Johnson, A. E., von Heijne, G., and Karamyshev, A. L. (2015). The code for directing proteins for translocation across ER membrane: SRP cotranslationally recognizes specific features of a signal sequence. *J. Mol. Biol.* 427 (6 Pt A), 1191–1201. doi: 10.1016/j.jmb.2014.06.014.

Olney, R. K., Murphy, J., Forshew, D., Garwood, E., Miller, B. L., Langmore, S., et al. (2005). The effects of executive and behavioral dysfunction on the course of ALS. *Neurology* 65, 1774–1777. doi: 10.1212/01.wnl.0000188759.87240.8b

Park, H. K., and Chung, S. J. (2013). New perspective on parkinsonism in frontotemporal lobar degeneration. *J Mov Disord* 6, 1–8. doi: 10.14802/jmd.13001

Pinarbasi, E. S., Karamyshev, A. L., Tikhonova, E. B., Wu, I. H., Hudson, H., and Thomas, P. J. (2018). Pathogenic signal sequence mutations in progranulin disrupt SRP interactions required for mRNA stability. *Cell Rep.* 23, 2844–2851. doi: 10.1016/j.celrep.2018.05.003

Rascovsky, K., Hodges, J. R., Knopman, D., Mendez, M. F., Kramer, J. H., Neuhaus, J., et al. (2011). Sensitivity of revised diagnostic criteria for the behavioural variant of frontotemporal dementia. *Brain* 134 (Pt 9), 2456–2477. doi: 10.1093/brain/awr179

Renton, A. E., Majounie, E., Waite, A., Simon-Sanchez, J., Rollinson, S., Gibbs, J. R., et al. (2011). A hexanucleotide repeat expansion in C9ORF72 is the cause of chromosome 9p21-linked ALS-FTD. *Neuron* 72, 257–268. doi: 10.1016/j.neuron.2011.09.010

Skibinski, G., Parkinson, N. J., Brown, J. M., Chakrabarti, L., Lloyd, S. L., Hummerich, H., et al. (2005). Mutations in the endosomal ESCRTIII-complex subunit CHMP2B in frontotemporal dementia. *Nat. Genet.* 37, 806–808. doi: 10.1038/ng1609

Smith, K. R., Damiano, J., Franceschetti, S., Carpenter, S., Canafoglia, L., Morbin, M., et al. (2012). Strikingly different clinicopathological phenotypes determined by progranulin-mutation dosage. *Am. J. Hum. Genet.* 90, 1102–1107. doi: 10.1016/j.ajhg.2012.04.021

Tang, W., Lu, Y., Tian, Q. Y., Zhang, Y., Guo, F. J., Liu, G. Y., et al. (2011). The growth factor progranulin binds to TNF receptors and is therapeutic against inflammatory arthritis in mice. *Science* 332, 478–484. doi: 10.1126/science.1199214

von Heijne, G. (1985). Signal sequences. The limits of variation. *J. Mol. Biol.* 184, 99–105.

Watts, G. D., Wymer, J., Kovach, M. J., Mehta, S. G., Mumm, S., Darvish, D., et al. (2004). Inclusion body myopathy associated with Paget disease of bone and frontotemporal dementia is caused by mutant valosin-containing protein. *Nat. Genet.* 36, 377–381. doi: 10.1038/ng1332

Zhou, X., Paushter, D. H., Feng, T., Sun, L., Reinheckel, T., and Hu, F. (2017a). Lysosomal processing of progranulin. *Mol. Neurodegener.* 12:62. doi: 10.1186/s13024-017-0205-9.

Zhou, X., Sun, L., Bastos de Oliveira, F., Qi, X., Brown, W. J., Smolka, M. B., et al. (2015). Prosaposin facilitates sortilin-independent lysosomal trafficking of progranulin. *J. Cell Biol.* 210, 991–1002. doi: 10.1083/jcb.201502029.

Zhou, X., Sun, L., Bracko, O., Choi, J. W., Jia, Y., Nana, A. L., et al. (2017b). Impaired prosaposin lysosomal trafficking in frontotemporal lobar degeneration due to progranulin mutations. *Nat. Commun.* 8:15277. doi: 10.1038/ncomms15277

Conflict of Interest Statement: The authors declare that the research was conducted in the absence of any commercial or financial relationships that could be construed as a potential conflict of interest.

frontiers in Neurology

ORIGINAL RESEARCH
published: 10 May 2019
doi: 10.3389/fneur.2019.00485

Clinical Correlates of Alzheimer's Disease Cerebrospinal Fluid Analytes in Primary Progressive Aphasia

*Catherine Norise, Molly Ungrady, Amy Halpin, Charles Jester, Corey T. McMillan, David J. Irwin, Katheryn A. Cousins and Murray Grossman**

Department of Neurology and Penn FTD Center, University of Pennsylvania, Philadelphia, PA, United States

Background: While primary progressive aphasia (PPA) is associated with frontotemporal lobar degeneration (FTLD) pathology due to tau or TDP, clinical-pathological studies also demonstrate many cases have Alzheimer's disease (AD) pathology. The logopenic variant of PPA (lvPPA) is most often associated with AD pathology, but this has proven to be the least reliable PPA to diagnose using published clinical criteria. In this study, we used cerebrospinal fluid (CSF) analytes to identify patients with likely AD pathology, and relate phenotypic features of lvPPA to CSF.

Methods: We studied 46 PPA patients who had available CSF analytes, including 26 with a clinical diagnosis of lvPPA, 9 with non-fluent/agrammatic variant (naPPA), and 11 with semantic variant (svPPA). We identified patients with likely AD pathology using amyloid-beta 1–42 ($A\beta_{1-42}$) <192 pg/ml and assessed MRI gray matter atrophy in these patients.

Results: We found that 23 (49%) of 46 PPA patients have a low CSF $A\beta_{1-42}$ level consistent with AD pathology. Twenty-one (91%) of 23 patients had a lvPPA phenotype, and 18 (79%) of 23 cases with an elevated CSF $A\beta_{1-42}$ level did not have a lvPPA phenotype. Patients with a lvPPA phenotype demonstrated GM atrophy in the left lateral temporal lobe, and this was also seen in those with a CSF $A\beta_{1-42}$ level <192 pg/ml.

Conclusion: The lvPPA clinical phenotype may be a useful screen for CSF analytes that are a surrogate for likely AD pathology, and may help establish eligibility of these patients for disease-modifying treatment trials.

Keywords: primary progressive aphasia (ppa), PPA, lvPPA, logopenic variant primary progressive aphasia, CSF, logopenic primary progressive aphasia, cerebrospinal fluid

OPEN ACCESS

Edited by:
Anne Marja Remes, University of Oulu, Finland

Reviewed by:
Romina Vuono, University of Cambridge, United Kingdom
Antonio Lucio Teixeira, University of Texas Health Science Center at Houston, United States
Norbert Zilka, Institute of Neuroimmunology (SAS), Slovakia

****Correspondence:***
Murray Grossman
mgrossma@pennmedicine.upenn.edu

Specialty section:
This article was submitted to Neurodegeneration, a section of the journal Frontiers in Neurology

Received: *22 October 2018*
Accepted: *23 April 2019*
Published: *10 May 2019*

Citation:
Norise C, Ungrady M, Halpin A, Jester C, McMillan CT, Irwin DJ, Cousins KA and Grossman M (2019) Clinical Correlates of Alzheimer's Disease Cerebrospinal Fluid Analytes in Primary Progressive Aphasia. Front. Neurol. 10:485. doi: 10.3389/fneur.2019.00485

INTRODUCTION

Primary progressive aphasia (PPA) refers to a syndrome of declining language ability that results from a neurodegenerative disease. Three variants of PPA have been identified: non-fluent/agrammatic (naPPA), semantic (svPPA), and logopenic (lvPPA) (1). It is valuable to identify these variants of PPA because there is a statistical association of a PPA variant with a specific underlying pathology (2, 3). There is broad agreement on the clinical characteristics that distinguish naPPA and svPPA (4–7). The typical clinical presentation of naPPA involves effortful speech, agrammatism, and motor speech errors known as apraxia of speech (6, 8, 9), and autopsy studies

have indicated that naPPA is often associated with frontotemporal lobar degeneration (FTLD) with underlying FTLD-tau pathology (2, 3). svPPA is characterized by impairments in naming and single-word comprehension (9, 10), and svPPA is often associated with underlying FTLD-TDP pathology (3, 11). However, compared to naPPA and svPPA, lvPPA cases are more challenging to identify clinically (4–7, 12). lvPPA is said to be characterized by difficulty with repetition and lexical retrieval (1, 13), but criteria for a repetition impairment have been challenging to identify and lexical retrieval deficits are ubiquitous among patients with PPA. Correspondingly, there has been some variability in the pathology found in patients with a clinical diagnosis of lvPPA, although lvPPA is often associated with Alzheimer's disease (AD) pathology (2, 3, 11, 14).

Since cerebrospinal fluid (CSF) analytes have been shown to serve as a sensitive biomarker for AD pathology (15), this study examined the usefulness of CSF markers in identifying likely AD pathology in individuals with PPA. Specifically, we used the CSF level of beta-amyloid 1–42 ($A\beta_{1-42}$) to identify PPA patients with likely AD pathology, and assessed whether this corresponds to PPA patients with a lvPPA phenotype. Several previous studies have examined $A\beta_{1-42}$ in PPA. In one study, patients with a clinical diagnosis of lvPPA had lower $A\beta_{1-42}$ levels than controls and naPPA patients (16). In a large, multi-center cohort of PPA patients with pathology determined by CSF or positron emission tomography (PET) molecular markers or autopsy findings, 86% of lvPPA patients had findings consistent with Aß pathology (17). Here we contrasted PPA patients with low $A\beta_{1-42}$ relative to those with elevated $A\beta_{1-42}$ levels, and independently verified diagnosis in the PPA patient groups with MRI analyses consistent with published imaging data.

TABLE 1 | Patient demographic characteristics and cerebrospinal fluid analyte levels.

	lvPPA	naPPA	svPPA
Gender (F/M)	16/10	2/7	7/4
Age at CSF (years)	62.6 (8.2)	64.2 (9.4)	63.1 (5.6)
Education (years)	15.8 (3.4)	15.3 (3.2)	16.7 (2.5)
Disease duration AT CSF (years)	2.7 (1.6)	2.7 (2.1)	2.4 (1.9)
$A\beta_{1-42}$ pg/mL[a]	175.8 (105.0)	341.3 (176.3)[b]	323.2 (122.0)[b]
Phosphorylated tau pg/mL[a]	38.7 (24.4)	22.6 (20.1)[b]	18.1 (16.9)[b]
Total tau pg/mL	137.8 (139.1)	118.3 (143.5)	85.7 (104.8)
Total tau/$A\beta_{1-42}$ pg/mL[a]	0.005 (0.004)	0.001 (0.001)[b]	0.001 (0.000)[b]

lvPPA, logopenic variant primary progressive aphasia; naPPA, non-fluent/ agrammatic variant primary progressive aphasia; svPPA, semantic variant primary progressive aphasia; Low Abeta ($A\beta_{42}$ level <192 pg/mL); High Abeta ($A\beta_{42}$ level >192 pg/mL).
[a] Significant difference between groups, according to Kruskal-Wallis test (all $p \leq 0.02$).
[b] Differ significantly from lvPPA group (all $p \leq 0.017$).

METHODS

Patients

Patients included for this study were seen in the Department of Neurology out-patient clinic of the Penn FTD Center and data were retrieved from The Integrated Neurodegenerative Disease Database (INDD) (18) at the University of Pennsylvania. All patients had a clinical diagnosis of PPA involving prominent language difficulty and minimal evidence of impairment in other cognitive domains (19) based on a semi-structured clinical history, a complete neurological evaluation, and a detailed mental status assessment. From among 131 individuals with a diagnosis of PPA in INDD who also had CSF data, we restricted participants in the current study to those that met strict clinical diagnostic criteria for a specific variant of PPA (1) as adapted recently for lvPPA (14). In this study, a diagnosis of lvPPA included deficits of word-finding difficulty in continuous speech with impaired phonological loop functioning measured by a short forward digit span. Using these criteria, 46 patients were included for analysis (lvPPA: $n = 26$, svPPA: $n = 11$, naPPA: $n = 9$) (**Table 1**). All patients were native English-speakers with a high school education, and were matched for age, education, and disease duration at lumbar puncture. Patients were excluded if elementary neurological features such as bulbar motor weakness or extrapyramidal disease suggesting a likely pathologic diagnosis were present or other medical, psychiatric, or neurological conditions (e.g., head trauma, stroke, hydrocephalus) were present that could clinically resemble PPA. Al MRIs were clinically inspected to insure that there was minimal small vessel ischemic disease (Fazekas $\leq$ grade 1), and there was no evidence of cerebral microbleeds on any of the MRIs. All mutation carriers were excluded. An autopsy evaluation was available for three cases. Two cases with an lvPPA phenotype had a CSF $A\beta_{1-42}$ level that was <192 pg/mL and AD pathology. One autopsy case with FTLD-Tau pathology had a CSF of $A\beta_{1-42}$ level that was >192 pg/mL and did not have a lvPPA phenotype. Some of these cases have participated in other CSF biomarker studies.

We assessed the neuropsychological profile for each subtype of PPA (**Table 2**). We evaluated the patients' performance on naming by using the Boston Naming Test (BNT) (20), function of the phonologic loop using forward digit span {Antonio:to}, executive functioning as determined by the amount of words beginning with the letter "F" in 1 min {Tombaugh:tg}, and episodic memory by the immediate and delayed recall of the Craft story {Monsell:uu}. Shapiro tests were used to check for a normal or abnormal distribution of the data. The lvPPA group had neuropsychological data that was not normally distributed, so we performed Kruskal–Wallis tests to assess the differences of each group. Analyses showed a significant difference in BNT, forward digit span, and memory. No significant differences were observed between groups for words per minute or F words per minute. Pair-wise group differences with Mann–Whitney U are summarized in **Table 2**.

Standard Protocol Approvals, Registrations, and Patient Consents

All procedures, including CSF collection and MRI, involved participation in an informed consent procedure, and were performed in accordance with the Helsinki Agreement and

TABLE 2 | Patient neuropsychological profiles by phenotype.

	lvPPA			naPPA			svPPA		
Neuropsychological tasks	**Score (SD)**	***N***	**Time from CSF (SD) (m)**	**Score (SD)**	***N***	**Time from CSF (SD) (m)**	**Score (SD)**	***N***	**Time from CSF (SD) (m)**
Boston naming test[a]	19.95 (9.29)	19	0.73 (2.31)	23.78 (6.03)	9	0.11 (0.33)	6.63 (6.12)[b]	11	3.82 (11.70)
Digit span forward[a]	4.1 (0.88)	10	2.9 (6.15)	3.2 (1.92)	5	16 (22.31)	6.86 (1.46)[b]	7	5.57 (9.73)
F Words/minute	6.39 (4.77)	18	7.63 (12.54)	6.13 (3.14)	8	0.5 (0.76)	9 (5.42)	11	3.27 (6.90)
Craft story Immediate recall[a]	4.00 (2.45)	7	26.57 (19.15)	18.33 (0.07)[b]	3	47.67 (0.58)	5.50 (3.51)	6	39.83 (18.11)
Craft story delayed recall[a]	4.43 (2.30)	7	26.57 (19.15)	13.33 (9.29)[b]	3	47.67 (0.58)	5.33 (2.88)	6	39.83 (18.11)

lvPPA, logopenic variant primary progressive aphasia; naPPA, non-fluent agrammatic variant primary progressive aphasia; svPPA, semantic variant primary progressive aphasia.
[a] *Significant Kruskal–Wallis test ($p<0.02$);*
[b] *Significant Mann–Whitney U group difference relative to lvPPA ($p <= 0.017$).*

the rules of the Institutional Review Board at the University of Pennsylvania.

Cerebrospinal Fluid Analyses

CSF samples were obtained by routine lumbar puncture according to standard operating procedures of the Alzheimer's Disease Neuroimaging Initiative (ADNI) (15). In brief, baseline CSF samples were obtained in the morning typically after an overnight fast. Lumbar punctures were performed with a 20- or 24-gauge spinal needle. CSF was collected into polypropylene transfer tubes, 0.5 ml aliquots were prepared from these samples, and then frozen within 1 h. The aliquots were stored in barcode–labeled polypropylene vials at −80°C. Samples were assayed via Luminex for $A\beta_{1-42}$, p-tau, and t-tau levels, as previously described (15), and a small number of samples were analyzed by ELISA and transformed to Luminex equivalents using an autopsy-confirmed formula (21).

Statistical Analysis

In the first analysis, we grouped patients according to the predefined cut-point of 192 pg/ml. Since the cut-point based on an AD phenotype may not generalize to non-amnestic cases with AD pathology, we also implemented a second analytic approach. Here we used a k-means cluster analysis with a two-group solution to identify the groups among all PPA patients in our cohort according to their CSF $A\beta_{1-42}$ level, and examined this cut-point in our cohort. The variables utilized in this analysis were the categorical variable "clinical phenotype" and the continuous variable "CSF $A\beta_{1-42}$ level." A receiver operating characteristic (ROC) curve analysis used sensitivity and specificity to define the cut-point between these groups, and provided the area under the curve (AUC). In both the analysis using the predetermined cut-point and the empirically determined cut-point in our cohort, we tabulated the frequency of patients with lvPPA compared to PPA patients with another phenotype in the two CSF-determined groups, and used chi-squared analyses to assess whether there was a statistically significant difference between phenotypes within and between CSF-defined groups.

MRI Analysis

High resolution T1-weighted MRI scans were available for 20 lvPPA, 10 naPPA, and 11 svPPA, and we compared these PPA patients with 69 demographically matched control participants. The PPA patients with MRI matched the clinical and demographic characteristics of those without MRI (all $p > 0.1$). MRI exclusion criteria included poor-quality MRI at visual inspection (e.g., distortion, excessive motion, or processing failure due to image distortion/artifact). Briefly, participants underwent a structural T1-weighted MPRAGE MRI acquired from a SIEMENS 3.0T Trio scanner with an eight-channel coil using the following parameters: repetition time (TR) = 1,620 ms; echo time (TE) = 3 ms; 160 1.0 mm slices; flip angle = 15°; matrix = 192 × 256; and in-plane resolution = 0.9766 × 0.9766 mm. T1 MRI images were preprocessed using antsCorticalThickness (22). Each individual dataset was deformed into a standard local template space in a canonical stereotactic coordinate system. Registration was performed using a diffeomorphic deformation that is symmetric to minimize bias toward the reference space for computing the mappings and topology-preserving to capture the large deformation necessary to aggregate images in a common space. The ANTs Atropos tool used template-based priors to segment images into 6 tissue classes (cortical gray matter, white matter, CSF, deep gray structures, midbrain, and cerebellum), and generated the probability images of each tissue class (23). Here we focused on cortical gray matter probability (GMP) images that were transformed into MNI space, and downsampled to 2 mm isotropic voxels. This voxel size approximates the true thickness of cortex, although at the cost of less robust *p*-values due to a larger number of comparisons. We smoothed the data using a 2 sigma full-width half-maximum Gaussian kernel before analysis. Voxelwise analyses of GMP were performed using the non-parametric randomize tool implemented in the FMRIB Software Library (FSL: http://fsl.fmrib.ox.ac.uk) with 10,000 permutations that is equivalent to an analysis protecting

for multiple comparisons. We report clusters that survived $p < 0.01$ with a minimum of 150 adjacent voxels. We report two sets of *t*-tests: First, we examined each patient group (lvPPA, naPPA, svPPA) relative to controls; and second, we examined each CSF-subgroup relative to controls (low-Aβ_{1-42}, hi-Aβ_{1-42}).

RESULTS

Identifying Groups Based on CSF Aβ_{1-42} Level

A summary of CSF analyte values is provided in **Table 1**. Twenty-three patients had a low CSF Aβ_{1-42} level consistent with likely AD pathology, and 21 (91.3%) of these cases had an lvPPA phenotype, revealing significantly more cases of clinically diagnosed lvPPA than non-lvPPA among PPA patients with a lower CSF Aβ_{1-42} level ($p < 0.001$). The sensitivity for low CSF Aβ_{1-42} level to identify lvPPA compared to non-lvPPA is 91%; the specificity is 89%; the positive predictive value is 87%; and the negative predictive value is 92%. Of the 2 non-lvPPA cases with a lower Aβ_{1-42} level, one had an svPPA phenotype (CSF Aβ_{1-42} level = 167 pg/ml) and the other had a naPPA phenotype (CSF Aβ_{1-42} level = 183 pg/ml). The svPPA patient with CSF Aβ_{1-42} level <192 pg/mL had an age at onset of 68. Not only was this well-above the mean age of onset of lvPPA patients with CSF Aβ_{1-42} <192 pg/mL, but it was also well above the mean age at onset of the svPPA patients with CSF Aβ_{1-42} level > 192 pg/mL ($M = 60.18$ years, SD = 7.45), suggesting the possibility of AD co-pathology. Duration of disease at the time of obtaining CSF was shorter in this svPPA patient (1 year) and longer in this naPPA patient (7 years), and differed from the mean disease duration of lvPPA patients with CSF Aβ_{1-42} <192 pg/mL ($M = 2.7$ years, SD = 1.6) and from that of PPA patients with CSF Aβ_{1-42} level >192 pg/mL ($M = 2.57$ years, SD = 1.65). The svPPA and naPPA patients with CSF Aβ_{1-42} <192 pg/mL levels did not differ from lvPPA patients with CSF Aβ_{1-42} <192 pg/mL, and did not differ from PPA patients with CSF Aβ_{1-42} level >192 pg/mL with regards to education level.

Twenty-one (80.8%) of 26 cases with a clinical diagnosis of lvPPA had a CSF Aβ_{1-42} level <192 pg/mL, significantly greater than the number of lvPPA cases with CSF >192 pg/mL ($p < 0.001$). The sensitivity for lvPPA to identify low CSF Aβ_{1-42} level compared to elevated CSF Aβ_{1-42} level is 81%; the specificity is 75%; the positive predictive value is 91%; and the negative predictive value is 78%. The mean CSF Aβ_{1-42} level of the 5 lvPPA cases with CSF >192 pg/mL was 317 pg/mL (SD = 186). The lvPPA patients with CSF Aβ_{1-42} <192 pg/mL did not differ significantly from those with CSF Aβ_{1-42} level >192 pg/mL with regards to education level and disease duration at the time that CSF was obtained. The age at onset, however, differed significantly [$t_{(22)} = 4.20$, $p < 0.001$], with the 5 lvPPA patients with an elevated CSF Aβ_{1-42} level having an older age at onset ($M = 65.2$ years, SD = 9.36) than lvPPA cases with CSF Aβ_{1-42} <192 pg/ml ($M = 58.87$, SD = 7.23).

Since CSF Aβ_{1-42} level in non-amnestic AD with early-onset disease may differ from the CSF Aβ_{1-42} level associated with later-onset amnestic AD, we also used a cluster analysis to partition the entire cohort of PPA patients ($n = 46$) according to the CSF Aβ_{1-42} level. One cluster included PPA patients with a lower Aβ_{1-42} level ($n = 23$, $M = 145.2$ pg/ml; SD =27.8), and the second cluster included PPA patients with a higher Aβ_{1-42} level ($n = 23$, $M = 344.1$ pg/ml; SD = 159.4). A ROC curve analysis in this sample defined a cutpoint at 204.2 pg/mL, yielding 91% sensitivity, 89% specificity, and an area under the curve = 0.914. Independent samples *t*-test showed that the Aβ_{1-42} level of the cohort with likely AD pathology to be significantly lower than that of the cohort less likely to have AD pathology [$t_{(44)} = 6.6$, $p < 0.001$].

MRI Imaging

The imaging analysis evaluated the anatomic distribution of disease in the cohort of subjects with a low Aβ_{1-42} level and a high Aβ_{1-42} level. This demonstrated distinct areas of atrophy that stratified the two groups (**Figure 1**; **Table 3**). Significant areas of GM atrophy for the low Aβ_{1-42} cohort were in the left middle-superior temporal gyrus, left parietal region, and left precuneus (**Figure 1A**). This overlapped substantially with the analysis of the cohort with a lvPPA phenotype where significant atrophy was found in the left middle-superior temporal gyrus, left parietal region, and left occipital region (**Figure 1B**). Neither group had significant hippocampal atrophy, emphasizing the PPA phenotype as opposed to a language-dominant syndrome of clinical AD. By comparison, in the high Aβ_{1-42} cohort, significant atrophy was found in the left anterior temporal region and left inferior frontal-insula region $p < 0.01$, k = 150 (**Figure 1C**), anatomic areas associated with svPPA and naPPA, respectively.

DISCUSSION

Autopsy studies have demonstrated that the three PPA variants—lvPPA, svPPA, and naPPA—are often associated with distinct underlying pathology (2, 3). In an era of expensive diagnostic markers such as molecular PET and the advent of disease-modifying treatment trials targeting a specific pathology, it is valuable to have less expensive biomarkers that can screen for underlying pathology. However, identifying patients with likely AD pathology during life has been particularly challenging: While the lvPPA phenotype was developed in part to identify the subgroup of PPA patients with likely AD pathology, the clinical criteria for lvPPA have proven to be relatively less reliable (4–7, 12). Here we examined the usefulness of a reliable and valid proxy of AD pathology—CSF analytes—to identify a subset of PPA cases with a phenotype that may be associated with AD pathology. Our findings suggest that many PPA patients with a low CSF Aβ_{1-42} level have a lvPPA phenotype.

We found that a low Aβ_{1-42} level (<192 pg/mL) is present in the CSF of many PPA patients, suggesting that these PPA patients may have AD pathology (15). It is potentially valuable that most of these patients had a phenotype most consistent with lvPPA. The criteria defining lvPPA have been controversial (4–7). In our study, we accepted a lvPPA phenotype as defined by a clinical-pathological study (14), which included word-finding difficulty together with a deficit of repetition marked by a low forward

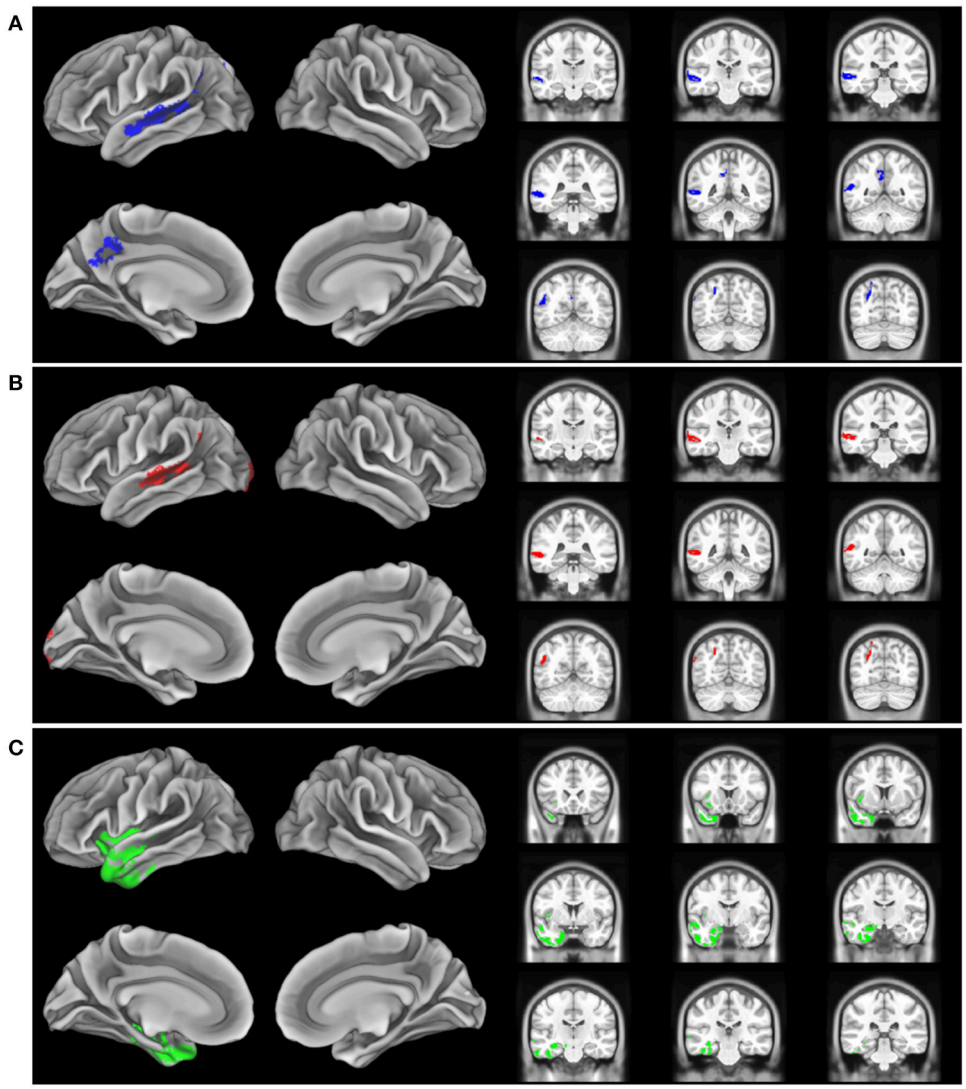

FIGURE 1 | Distribution of significant gray matter atrophy in T1-weighted MRI scans. **(A)** low CSF Aß1-42 (<192 pg/mL) vs. controls, **(B)** logopenic variant PPA vs. controls, **(C)** High CSF Aß1-42 (>192 pg/mL) vs. controls.

digit span score. We found that a very large proportion of cases with a CSF $A\beta_{1-42}$ level in the range consistent with likely AD pathology have a clinical phenotype of lvPPA.

While a large majority of cases with a low CSF $A\beta_{1-42}$ level had lvPPA, this phenotype alone cannot be used reliably to identify patients with likely AD pathology. For example, in our cohort we found two patients with a low CSF $A\beta_{1-42}$ level who did not have a lvPPA phenotype: One patient had svPPA and another had naPPA. Without autopsy evidence, we can only speculate about the basis for this discrepancy. One possibility is that these cases in fact have AD pathology but in an anatomic distribution more consistent with these non-lvPPA phenotypes. Several patients with atypical presentations of AD pathology have been reported with svPPA or naPPA phenotypes (24, 25). A second possibility is that these cases may have secondary AD co-pathology in the context of primary FTLD pathologies causing these syndromes. Co-pathology is not uncommon in neurodegenerative disease (26), and we found in our autopsy series that CSF analytes for AD are significantly biased by the presence of AD co-pathology even in individuals where the primary pathology is consistent with an FTLD spectrum pathology (23).

Another important consideration is that 26 cases in our cohort had a lvPPA phenotype, but only 21 of these cases with a lvPPA phenotype had low CSF $A\beta_{1-42}$. The five lvPPA cases with elevated CSF $A\beta_{1-42}$ levels had an age of onset that was older than that of the lvPPA patients with lower CSF $A\beta_{1-42}$ levels. With the caveat that we did not have a pathologic diagnosis in our cases, our findings are consistent with the claim that a clinical evaluation for lvPPA can be an inexpensive way to screen

TABLE 3 | MRI atrophy in patient groups relative to healthy controls, and in comparisons of patient groups, including cluster size, coordinates, anatomic location, and Brodmann area.

Cluster size	Peak x-coord	Peak y-coord	Peak z-coord	Anatomical location	BA
Low Abeta < Controls					
912	−50	−4	−16	Left superior temporal gyrus	22
206	−28	−84	20	Left superior occiptal gyrus	19
150	−4	−56	28	Left posterior cingulate	31
LvPPA subgroup-Low Abeta < Controls					
772	−50	−24	−8	Left middle temporal gyrus	21
189	−20	−98	−16	Left lateral occiptal gyrus	18
183	−32	−90	20	Left superior occiptal gyrus	19
High Abeta < Controls					
2,067	−38	−6	−48	Left inferior temporal gyrus	20
158	−30	20	−12	Left inferior orbitofrontal gyrus	47

lvPPA, logopenic variant primary progressive aphasia; naPPA, non-fluent/ agrammatic variant primary progressive aphasia; svPPA, semantic variant primary progressive aphasia; low $A\beta_{42}$ = $A\beta_{42}$ level <192 pg/mL); high $A\beta_{42}$ = $A\beta_{42}$ level >192 pg/mL). All analyses $p < 0.01$, $k = 150$; please see text for details.

PPA patients for those who may be eligible for participation in disease-modifying therapies targeting the misfolded proteins contributing to AD pathology. Additional biomarker data would be helpful to confirm the diagnosis of PPA associated with likely AD such as amyloid-PET, although it should be noted that amyloid-PET is also associated with false-positive and false-negative findings (27).

The MRI analysis was consistent with the finding that the lvPPA phenotype is most prominent in the low $A\beta_{1-42}$ level cohort by showing nearly identical areas of reduced GMP in the lvPPA cohort and the low $A\beta_{1-42}$ level cohort (**Figures 1A,B**). The pattern of atrophy of the cohort with the lvPPA phenotype included in the left middle-superior temporal gyrus, left parietal region, and left occipital region. This resembles the distribution of MRI atrophy seen in other MRI studies of lvPPA (13, 14, 26, 28). Atrophy in the left lateral temporal lobe is associated with lexical retrieval (29) and auditory-verbal short-term memory (13) that are compromised in lvPPA. Moreover, this closely resembles the areas of GM atrophy in the low $A\beta_{1-42}$ cohort, including the left middle-superior temporal gyrus, left parietal region, and left precuneus. This anatomic distribution of atrophy is a subset of regions typically affected in clinical AD. Importantly, our cohort did not have significant medial temporal lobe atrophy, emphasizing that these patients had PPA and not a language-dominant variant of AD. Despite the small cohort of PPA patients with elevated CSF $A\beta_{1-42}$ consistent with a non-AD form of PPA, the pattern of atrophy in this group is distinctly different from that of the low CSF $A\beta_{1-42}$ cohort with lvPPA. The areas of atrophy found in the group with elevated CSF $A\beta_{1-42}$ include the left anterior temporal region, and the left inferior frontal-insula region. These are areas associated with svPPA and naPPA, respectively (28, 30).

Other groups have explored the utility of using CSF analytes to differentiate PPA phenotypes. One study evaluated CSF levels of $A\beta_{1-42}$, t-tau, and p-tau_{181} in a small cohort of PPA patients, AD patients, and healthy controls (16). They found that the ratio of p-tau_{181}/$A\beta_{1-42}$ ratio allowed separating AD and non-AD patients, although there was no available converging evidence such as imaging or autopsy to support this finding. Another study also found lower levels of CSF $A\beta_{1-42}$ in clinically-diagnosed lvPPA compared to other PPA patients, discriminating between lvPPA and naPPA/svPPA with 86% sensitivity and 69% specificity (22). In a small autopsy series from Northwestern University, six of nine autopsied PPA cases with AD pathology had an antemortem proprietary CSF ATI score in the range consistent with Alzheimer's disease pathology (23). In a large, multi-center cohort of PPA patients with pathology determined by CSF or PET molecular markers or autopsy findings, 86% of lvPPA patients had biomarker findings consistent with Aß pathology (17). An important challenge to the use of CSF or PET biomarkers in the present study and this previously published work is that co-pathology is frequently present in neurodegenerative disease (26, 31). In particular, AD co-pathology may be present in cases with other primary pathologies, and thus give the false impression that a patient's primary pathologic diagnosis is AD. In the study of Bergeron et al. (17), for example, primary AD pathology was present only in 76% of cases, and the discrepancy between pathology ascertained at autopsy compared to pathology estimated by biomarkers may have been due in part to the sensitivity to secondary AD co-pathology in CSF biomarker-ascertained cases with non-AD primary pathologies. Neurogranin (Ng) also has been identified as a CSF biomarker associated with AD pathology, and we found that Ng is significantly elevated in a clinical cohort of lvPPA patients that partially overlaps with the cohort presented in the current study (24). Serum neurofilament light chain (NfL) also may be useful for discriminating between lvPPA and non-lvPPA with 81% sensitivity and 67% specificity (22), and others have shown elevated NfL in svPPA and naPPA relative to a small number of lvPPA (25) [also see (31)], although others have found CSF NfL elevated in AD (32, 33). Considerable caution must be adopted in concluding from screening studies that lvPPA may be a marker for AD pathology: Our study and others suggest that lvPPA may be associated with a CSF surrogate for AD pathology, but this does not exclude the possibility that other pathologies may be contributing to a patient's difficulties.

Several caveats should be kept in mind when considering our results. First, a relatively small number of patients participated in our study, although PPA is a relatively rare condition, and we adhered narrowly to the published criteria for PPA to determine the usefulness of AD CSF analytes within the scope of these criteria. Other CSF analytes may be informative

in PPA and have been reported in some patients from this cohort elsewhere (24), and additional work is needed to assess these other analytes. Very few autopsy-validated studies of CSF analytes have been reported including some of the patients from this study (17, 23), and although we used autopsy-validated CSF analytes, another limitation is that we knew the true pathologic diagnosis in only a very small number of these PPA cases. Additional work is needed with an autopsy-defined cohort (14). lvPPA has been associated with cerebral microbleeds {Mendes:vv}, although there were no cerebral microbleeds in our cohort. Generalizeability of our findings may be limited since this is a single-center study. With these caveats in mind, this study demonstrated that low CSF $A\beta_{1-42}$ is not uncommon in patients with PPA, and that there is a statistical association between a low CSF $A\beta_{1-42}$ level and the lvPPA phenotype. The link between lvPPA phenotype and a surrogate marker of AD pathology was further supported by MRI imaging. The potential use of the lvPPA clinical phenotype to screen for CSF analytes as a surrogate for likely AD pathology may help establish eligibility of these patients for disease-modifying treatment trials.

ETHICS STATEMENT

This study was carried out in accordance with the recommendations of the Institutional Review Board of the University of Pennsylvania with written informed consent from all subjects and witnessed by a responsible caregiver. All subjects gave written informed consent in accordance with the Declaration of Helsinki. The protocol was approved by the Institutional Review Board of the University of Pennsylvania.

AUTHOR CONTRIBUTIONS

AH, CJ, MU, DI, and MG data collection. CN, CJ, CM, and KC data analysis. CN, CM, DI, KC, and MG manuscript writing and editing.

FUNDING

This work was supported by National Institutes of Health (AG017586, AG054519, AG052943, AG010124), Wyncote Foundation, and an anonymous donor.

REFERENCES

1. Gorno-Tempini ML, Hillis AE, Weintraub S, Kertesz A, Mendez M, Cappa SF, et al. Classification of primary progressive aphasia and its variants. *Neurology*. (2011) 76:1006–14. doi: 10.1212/WNL.0b013e31821103e6
2. Spinelli EG, Mandelli ML, Miller ZA, Santos-Santos MA, Wilson SM, Agosta F, et al. Typical and atypical pathology in primary progressive aphasia variants. *Ann Neurol.* (2017) 81:430–43. doi: 10.1002/ana.24885
3. Grossman M. Primary progressive aphasia: clinicopathological correlations. *Nat Rev Neurol.* (2010) 6:88–97. doi: 10.1038/nrneurol.2009.216
4. Sajjadi SA, Patterson K, Arnold RJ, Watson PC, Nestor PJ. Primary progressive aphasia: a tale of two syndromes and the rest. *Neurology.* (2012) 78:1670–7. doi: 10.1212/WNL.0b013e3182574f79
5. Mesulam MM, Wieneke C, Thompson C, Rogalski E, Weintraub S. Quantitative classification of primary progressive aphasia at early and mild impairment stages. *Brain.* (2012) 135:1537–53. doi: 10.1093/brain/aws080
6. Croot K, Ballard K, Leyton CE, Hodges JR. Apraxia of speech and phonological errors in the diagnosis of nonfluent/agrammatic and logopenic variants of primary progressive aphasia. *J Speech Lang Hear Res.* (2012) 55:S1562–72. doi: 10.1044/1092-4388(2012/11-0323)
7. Leyton CE, Hodges JR. Differential diagnosis of primary progressive aphasia variants using the international criteria. *Aphasiology.* (2014) 28:909–21. doi: 10.1080/02687038.2013.869306
8. Grossman M. The non-fluent/agrammatic variant of primary progressive aphasia. *Lancet Neurol.* (2012) 11:545–55. doi: 10.1016/S1474-4422(12)70099-6
9. Grossman M. Linguistic aspects of primary progressive aphasia. *Annu Rev Linguist.* (2018) 4:377–403. doi: 10.1146/annurev-linguistics-011516-034253
10. Hodges JR, Patterson K. Semantic dementia: a unique clinicopathological syndrome. *Lancet Neurol.* (2007) 6:1004–14. doi: 10.1016/S1474-4422(07)70266-1
11. Leyton CE, Britton AK, Hodges JR, Halliday GM, Kril JJ. Distinctive pathological mechanisms involved in primary progressive aphasias. *Neurobiol Aging.* (2016) 38:82–92. doi: 10.1016/j.neurobiolaging.2015.10.017
12. Mesulam MM, Weintraub S, Rogalski EJ, Wieneke C, Geula C, Bigio EH. Asymmetry and heterogeneity of Alzheimer's and frontotemporal pathology in primary progressive aphasia. *Brain.* (2014) 137:1176–92. doi: 10.1093/brain/awu024
13. Gorno-Tempini ML, Brambati SM, Ginex V, Ogar J, Dronkers NF, Marcone A, et al. The logopenic/phonological variant of primary progressive aphasia. *Neurology.* (2008) 71:1227–34. doi: 10.1212/01.wnl.0000320506.79811.da
14. Giannini LAA, Irwin DJ, McMillan CT, Ash S, Rascovsky K, Wolk DA, et al. Clinical marker for Alzheimer disease pathology in logopenic primary progressive aphasia. *Neurology.* (2017) 88:2276–84. doi: 10.1212/WNL.0000000000004034
15. Shaw LM, Vanderstichele H, Knapik-Czajka M, Clark CM, Aisen PS, Petersen RC, et al. Cerebrospinal fluid biomarker signature in Alzheimer's disease neuroimaging initiative subjects. *Ann Neurol.* (2009) 65:403–13. doi: 10.1002/ana.21610
16. Paraskevas GP, Kasselimis D, Kourtidou E, Constantinides V, Bougea A, Potagas C, et al. Cerebrospinal fluid biomarkers as a diagnostic tool of the underlying pathology of primary progressive aphasia. *J Alzheimers Dis.* (2017) 55:1453–61. doi: 10.3233/JAD-160494
17. Bergeron D, Gorno-Tempini ML, Rabinovici GD, Santos-Santos MA, Seeley W, Miller BL, et al. Prevalence of amyloid-β pathology in distinct variants of primary progressive aphasia. *Ann Neurol.* (2018) 729–40. doi: 10.1002/ana.25333
18. Toledo JB, Van Deerlin VM, Lee EB, Suh E, Baek Y, Robinson JL, et al. A platform for discovery: The university of pennsylvania integrated neurodegenerative disease *Biobank. Alzheimers Dement.* (2013) (2013) 10:477–84.e1. doi: 10.1016/j.jalz.2013.06.003
19. Mesulam MM. Primary progressive aphasia - a language-based dementia. *N Engl J Med.* (2003) 349:1535–42. doi: 10.1056/NEJMra022435
20. Goodglass H, Kaplan E, Weintraub S. *Boston Naming Test*. Philadelphia, PA: Lea & Febiger (1983).
21. Irwin DJ, McMillan CT, Toledo JB, Arnold SE, Shaw LM, Wang LS, et al. Comparison of cerebrospinal fluid levels of tau and Aβ 1-42 in Alzheimer disease and frontotemporal degeneration using 2 analytical platforms. *Arch Neurol.* (2012) 69:1018–25. doi: 10.1001/archneurol.2012.26
22. Steinacker P, Semler E, Anderl-Straub S, Diehl-Schmid J, Schroeter ML, Uttner I, et al. Neurofilament as a blood marker for diagnosis and monitoring of primary progressive aphasias. *Neurology.* (2017) 88:961–9. doi: 10.1212/WNL.0000000000003688
23. Oboudiyat C, Gefen T, Varelas E, Weintraub S, Rogalski E, Bigio EH, et al. Cerebrospinal fluid markers detect Alzheimer's disease in nonamnestic dementia. *Alzheimers Dement.* (2017) 13:598–601. doi: 10.1016/j.jalz.2017.01.006

24. Portelius E, Olsson B, Höglund K, Cullen NC, Kvartsberg H, Andreasson U, et al. Cerebrospinal fluid neurogranin concentration in neurodegeneration: relation to clinical phenotypes and neuropathology. *Acta Neuropathol.* (2018) 136:363–76. doi: 10.1007/s00401-018-1851-x
25. Meeter LHH, Vijverberg EG, Del Campo M, Rozemuller AJM, Donker Kaat L, de Jong FJ, et al. Clinical value of neurofilament and phospho-tau/tau ratio in the frontotemporal dementia spectrum. *Neurology.* (2018) 90:e1231–9. doi: 10.1212/WNL.0000000000005261
26. Rogalski E, Cobia D, Martersteck A, Rademaker A, Wieneke C, Weintraub S, et al. Asymmetry of cortical decline in subtypes of primary progressive aphasia. *Neurology.* (2014) 83:1184–91. doi: 10.1212/WNL.0000000000000824
27. Ossenkoppele R, Jansen WJ, Rabinovici GD, Knol DL, van der Flier WM, van Berckel BN, et al. Prevalence of amyloid PET positivity in dementia syndromes: a meta-analysis. *JAMA.* (2015) 313:1939–49. doi: 10.1001/jama.2015.4669
28. Gorno-Tempini ML, Dronkers NF, Rankin KP, Ogar JM, Phengrasamy L, Rosen HJ, et al. Cognition and anatomy in three variants of primary progressive aphasia. *Ann Neurol.* (2004) 55:335–46. doi: 10.1002/ana.10825
29. Hillis AE, Tuffiash E, Wityk RJ, Barker PB. Regions of neural dysfunction associated with impaired naming of actions and objects in acute stroke. *Cogn Neuropsychol.* (2002) 19:523–34. doi: 10.1080/02643290244000077
30. Giannini LAA, Xie SX, McMillan CT, Liang M, Williams A, Jester C, et al. Divergent patterns of TDP-43 and tau pathologies in primary progressive aphasia. *Ann Neurol.* (2019) 85:630–43. doi: 10.1002/ana.25465
31. Scherling CS, Hall T, Berisha F, Klepac K, Karydas A, Coppola G, et al. Cerebrospinal fluid neurofilament concentration reflects disease severity in frontotemporal degeneration. *Ann Neurol.* (2014) 75:116–26. doi: 10.1002/ana.24052
32. Mattsson N, Insel PS, Palmqvist S, Portelius E, Zetterberg H, Weiner M, et al. Cerebrospinal fluid tau, neurogranin, and neurofilament light in Alzheimer's disease. *EMBO Mol Med.* (2016) 8:1184–96. doi: 10.15252/emmm.201606540
33. Zetterberg H, Skillbäck T, Mattsson N, Trojanowski JQ, Portelius E, Shaw LM, et al. Association of cerebrospinal fluid neurofilament light concentration with alzheimer disease progression. *JAMA Neurol.* (2016) 73:60–7. doi: 10.1001/jamaneurol.2015.3037

Conflict of Interest Statement: MG is an Associate Editor of Neurology, participates in clinical trials sponsored by Biogen, Alector, and Eisai, and receives support for his role as a consultant for Biogen, UCB, Ionis and Bracco.

The remaining authors declare that the research was conducted in the absence of any commercial or financial relationships that could be construed as a potential conflict of interest.

frontiers in Neuroscience

MINI REVIEW
published: 15 May 2019
doi: 10.3389/fnins.2019.00486

Astrocytes and Microglia as Potential Contributors to the Pathogenesis of *C9orf72* Repeat Expansion-Associated FTLD and ALS

*Hannah Rostalski[1], Stina Leskelä[1], Nadine Huber[1], Kasper Katisko[2], Antti Cajanus[2], Eino Solje[2,3], Mikael Marttinen[4], Teemu Natunen[4], Anne M. Remes[5,6], Mikko Hiltunen[4] and Annakaisa Haapasalo[1]**

[1] A.I. Virtanen Institute for Molecular Sciences, University of Eastern Finland, Kuopio, Finland, [2] Institute of Clinical Medicine – Neurology, University of Eastern Finland, Kuopio, Finland, [3] Neuro Center, Neurology, Kuopio University Hospital, Kuopio, Finland, [4] Institute of Biomedicine, University of Eastern Finland, Kuopio, Finland, [5] Medical Research Center, Oulu University Hospital, Oulu, Finland, [6] Research Unit of Clinical Neuroscience, Neurology, University of Oulu, Oulu, Finland

OPEN ACCESS

Edited by:
Jean-Marc Gallo, King's College London, United Kingdom

Reviewed by:
Laura Ferraiuolo, University of Sheffield, United Kingdom
Chiara F. Valori, German Center for Neurodegenerative Diseases (DZNE), Germany

***Correspondence:**
Annakaisa Haapasalo
annakaisa.haapasalo@uef.fi

Specialty section:
This article was submitted to Neurodegeneration, a section of the journal Frontiers in Neuroscience

Received: *28 February 2019*
Accepted: *29 April 2019*
Published: *15 May 2019*

Citation:
Rostalski H, Leskelä S, Huber N, Katisko K, Cajanus A, Solje E, Marttinen M, Natunen T, Remes AM, Hiltunen M and Haapasalo A (2019) Astrocytes and Microglia as Potential Contributors to the Pathogenesis of C9orf72 Repeat Expansion-Associated FTLD and ALS. Front. Neurosci. 13:486. doi: 10.3389/fnins.2019.00486

Frontotemporal lobar degeneration (FTLD) and amyotrophic lateral sclerosis (ALS) are neurodegenerative diseases with a complex, but often overlapping, genetic and pathobiological background and thus they are considered to form a disease spectrum. Although neurons are the principal cells affected in FTLD and ALS, increasing amount of evidence has recently proposed that other central nervous system-resident cells, including microglia and astrocytes, may also play roles in neurodegeneration in these diseases. Therefore, deciphering the mechanisms underlying the disease pathogenesis in different types of brain cells is fundamental in order to understand the etiology of these disorders. The major genetic cause of FTLD and ALS is a hexanucleotide repeat expansion (HRE) in the intronic region of the *C9orf72* gene. In neurons, specific pathological hallmarks, including decreased expression of the *C9orf72* RNA and proteins and generation of toxic RNA and protein species, and their downstream effects have been linked to *C9orf72* HRE-associated FTLD and ALS. In contrast, it is still poorly known to which extent these pathological changes are presented in other brain cells. Here, we summarize the current literature on the potential role of astrocytes and microglia in *C9orf72* HRE-linked FTLD and ALS and discuss their possible phenotypic alterations and neurotoxic mechanisms that may contribute to neurodegeneration in these diseases.

Keywords: amyotrophic lateral sclerosis, astrocyte, *C9orf72*, *C9orf72* expansion, frontotemporal lobar degeneration, microglia, neurodegeneration

INTRODUCTION

Frontotemporal lobar degeneration (FTLD) is a group of neurodegenerative disorders affecting predominantly the frontal and temporal lobes of the brain (Gorno-Tempini et al., 2011; Rascovsky et al., 2011) and the second most prevalent early-onset dementia (Onyike and Diehl-Schmid, 2013). FTLD clinical syndromes are characterized by changes in behavior, personality, and executive functions or deterioration of language functions. *GGGGCC* hexanucleotide repeat expansion (HRE) in the non-coding region of *chromosome 9 open reading frame 72* (*C9orf72*) (C9-HRE) is

the major genetic cause of familial FTLD (12–48%) and amyotrophic lateral sclerosis (ALS) (24–46%) cases and 6–20% of sporadic cases for both diseases (DeJesus-Hernandez et al., 2011; Renton et al., 2011; Majounie et al., 2012). C9-HRE may also lead to concomitant FTLD and ALS. The pathobiology of C9-HRE-associated FTLD and ALS (C9-FTLD or C9-ALS) is complex. Neurons in the C9-HRE carriers display specific pathological hallmarks, including toxic RNA and proteins derived from the expanded C9-HRE and decreased expression of *C9orf72* due to haploinsufficiency (see reviews Gitler and Tsuiji, 2016; Freibaum and Taylor, 2017; Balendra and Isaacs, 2018). However, recently the potential role of other central nervous system (CNS)-resident cells, especially astrocytes and microglia, has also started to gain attention.

Glial cells are essential for brain homeostasis, but they also may mediate neuroinflammation (Jang et al., 2013; Franco and Fernández-Suárez, 2015; Shinozaki et al., 2017). Chronic changes in their physiological functions may contribute to neurodegeneration via both cell autonomous and non-cell autonomous mechanisms in neurodegenerative diseases, including ALS and FTLD. Whereas, most of the early findings on glial involvement in ALS pathogenesis derived from studies on mutant superoxide dismutase 1 (SOD1), there is accumulating evidence for glial contribution in other subtypes of ALS as well (Broe et al., 2004; Haidet-Phillips et al., 2011; Minami et al., 2015; Radford et al., 2015; Chen et al., 2016; Lee et al., 2016; Taylor et al., 2016; Cooper-Knock et al., 2017; Hallmann et al., 2017; Krabbe et al., 2017; Bachiller et al., 2018; Deczkowska et al., 2018); for a recent review on the role of neuroinflammation and complement system in ALS see also (Parker et al., 2019). Communication between neurons and glia via secreted factors and membrane-bound receptors is crucial for e.g., regulation of synaptic pruning and detection and clearance of apoptotic cells, and alterations in this crosstalk are suggested to contribute to the pathogenesis of neurodegenerative diseases (Rama Rao and Kielian, 2015; Szepesi et al., 2018). For example, complement 3 (C3) levels are increased, whereas the levels of signal regulatory protein (SIRP) α, a protein negatively regulating phagocytosis, and its corresponding receptor on microglia, cluster of differentiation (CD) 47, are reduced in the frontal cortex of FTLD patients compared to healthy controls or ALS and FTLD/ALS patients (Gitik et al., 2011; Umoh et al., 2018). Also, levels of CD200, expressed on neurons and restricting microglial activation (Barclay et al., 2002), are reduced in the frontal cortex of FTLD compared to FTLD/ALS patients (Umoh et al., 2018). These findings imply that microglia-mediated synaptic pruning and phagocytosis might be enhanced in FTLD brains. RNA expression analyses have indicated that pathways including the complement system, antigen presentation, and interferon (IFN) γ and interleukin (IL) 1-β signaling are significantly upregulated in the brains of C9-ALS patients compared to sporadic ALS patients (Prudencio et al., 2015; O'Rourke et al., 2016). Also transcription factors of the nuclear factor kappa B (NFκB) pathway were differentially expressed in C9-ALS and non-C9-ALS patients compared to healthy subjects (Ismail et al., 2013), but it is unclear in which cells these alterations occur. Lower levels of C-X-C motif chemokine ligand 10 protein, a microglial chemoattractant, in the cerebrospinal fluid (CSF) of C9-ALS patients were observed compared to non-C9-ALS cases (Ismail et al., 2013), but the physiological consequences of this are unknown. Astrocytes from C9-ALS patients show glucose hypermetabolism as compared to non-C9-ALS cases and controls, possibly as a consequence of astrogliosis (Cistaro et al., 2014). Decreased levels of excitatory amino acid transporter (EAAT) 2 in the frontal cortex of FTLD patients compared to controls (Umoh et al., 2018) and in C9-ALS compared to sporadic ALS patients (Fomin et al., 2018) suggest that astrocytes in both C9-HRE carriers and non-carriers might show defective uptake of glutamate, which could lead to excitotoxicity. Thus, mounting evidence points to a potentially altered physiology of microglia and astrocytes in FTLD and ALS associated with C9-HRE.

PATHOLOGICAL HALLMARKS OF C9-HRE IN GLIAL CELLS

RNA Foci Are Less Abundant in Glial Cells Compared to Neurons

Sense and antisense RNA foci, formed by aggregated C9-HRE-containing RNA, represent a unique pathological feature of C9-FTLD and C9-ALS. RNA foci have mainly been reported in neurons (DeJesus-Hernandez et al., 2011; Renton et al., 2011; Gendron et al., 2013; Mizielinska et al., 2013; Dafinca et al., 2016), but also in non-neuronal cells, such as fibroblasts and lymphoblasts (Donnelly et al., 2013; Lagier-Tourenne et al., 2013; Cooper-Knock et al., 2014). Interestingly, glial fibrillary acidic protein (GFAP)-positive and negative glial cells in the cerebellum of C9-ALS and C9-FTLD cases (Gendron et al., 2013) and induced pluripotent stem cell (iPSC)-derived astroglia have also been confirmed to contain sense foci (Sareen et al., 2013). However, compared to neurons, RNA foci have only been detected in a small fraction of microglia and astrocytes in *post-mortem* C9-ALS frontal cortex (Mizielinska et al., 2013) and/or cerebellum of C9-HRE carrying FTLD, ALS and FTLD/ALS patients (DeJesus-Hernandez et al., 2017). Furthermore, the number of RNA foci per cell was lower in microglia and astrocytes compared to neurons (Mizielinska et al., 2013). Whereas, neurons may exhibit nuclear and, to a lower extent, cytoplasmic RNA foci, microglia, and astrocytes showed only intranuclear RNA foci (Lagier-Tourenne et al., 2013; Mizielinska et al., 2013). This may suggest that (i) glial cells might not express C9-HRE to the same extent as neurons; (ii) expression of RNA-binding proteins, known to stabilize RNA foci, and/or proteins involved in cytoplasmic translocation of C9-HRE RNA are less abundant; (iii) glial cells can better clear C9-HRE-containing RNA (Peters et al., 2015); or (iv) somatic heterogeneity of the C9-HRE length, which can occur in different cells within the same tissue of C9-HRE carriers (DeJesus-Hernandez et al., 2011; Almeida et al., 2013; van Blitterswijk et al., 2013; Nordin et al., 2015), might underlie the lower prevalence of RNA foci in glial cells compared to neurons. The RNA foci in neurons are suggested to cause disturbances in RNA metabolism through sequestration of RNA-binding proteins (Donnelly et al., 2013; Mori et al., 2013a; Sareen et al., 2013; Cooper-Knock et al., 2014).

Similar effects might occur in glial cells exhibiting RNA foci, but further investigations are required to ascertain this.

Dipeptide Repeat Proteins Appear Less Frequent in Glial Cells Than Neurons

In addition to the RNA foci, five dipeptide repeat protein (DRP) species, namely poly-glycine-alanine (poly-GA), poly-glycine-proline (poly-GP), poly-glycine-arginine (poly-GR), poly-proline-arginine (poly-PR), and poly-proline-alanine (poly-PA) are directly derived via repeat-associated non-AUG (RAN) translation from the C9-HRE-containing RNA and represent additional pathological hallmarks unique to C9-FTLD and C9-ALS (Zu et al., 2011, 2013; Ash et al., 2013; Gendron et al., 2013; Mori et al., 2013b). Consistent with the low prevalence of RNA foci in glia, poly-GA inclusions were not detected in microglia or astrocytes of *post-mortem* C9-FTLD or C9-ALS brains (Mackenzie et al., 2013) or in astrocytes in the hippocampus of a C9-ALS patient (Ash et al., 2013). Also, poly-GP inclusions were undetectable in glial cells of C9-ALS and C9-FTLD patients showing sense RNA foci in cerebellar astrocytes (Gendron et al., 2013). Another study on C9-ALS *post-mortem* brains could not detect any of the DRPs in glial cells in subcortical white matter, hippocampus or white matter in the spinal cord, where glial cells are abundant (Saberi et al., 2018). However, poly-GA, poly-GP and poly-GR inclusions were detected in the ependymal cells of the spinal cord central canal of C9-FTLD and C9-FTLD/ALS cases. Poly-GA inclusions were also observed in ependymal and subependymal cells of the lateral ventricular wall (Schludi et al., 2015). These results suggest that DRP inclusions might be present in glial cells, but to a lower extent than in neurons and in defined CNS areas. Use of cell type-specific antibodies may help to decipher which glial cell types exhibit DRP inclusions and whether they, if present, compromise glial cell function. The lower prevalence of DRPs in glia as compared to neurons could mean that (i) less C9-HRE-containing RNA is translocated into the cytosol; ii) it undergoes RAN translation less efficiently; (iii) and/or DRPs are degraded before they can accumulate. These might be supported by the finding that adeno-associated virus (AAV)-mediated expression of DRPs in mice leads to DRP accumulation in neurons but not glial cells (Chew et al., 2015). However, it cannot be excluded that glial DRPs might in fact derive from DRPs secreted by neurons, since neuron-to-glia transmission has been shown to occur *in vitro* (Westergard et al., 2016) (**Figures 1**, **2**).

Glial Cells of C9-ALS and C9-FTLD Brain Present TDP-43 Pathology and p62 Inclusions

Transactive response DNA binding protein 43 (TDP-43) phosphorylation, cytoplasmic translocation, and truncation are pathological hallmarks of FTLD and ALS, including C9-FTLD and C9-ALS (Cooper-Knock et al., 2012), and potential contributors to disturbed RNA metabolism (Gendron et al., 2010). Neuronal TDP-43-negative, but p62-positive inclusions containing DRPs, represent another unique hallmark of C9-HRE (Mahoney et al., 2012). It has been suggested that TDP-43 aggregation can be caused by *C9orf72* haploinsufficiency, formation of RNA foci, or DRP toxicity (Cooper-Knock et al., 2015; Sellier et al., 2016; Nonaka et al., 2018), whereas p62 accumulation might result from *C9orf72* haploinsufficiency via impairment of autophagy (Sellier et al., 2016) or DRP expression (May et al., 2014). Cytoplasmic p62 and (phospho)-TDP-43-positive inclusions have been reported in glia in frontal, parietal, temporal, and motor cortex, hippocampus, brainstem, cerebellum, and spinal cord of C9-FTLD, C9-FTLD/ALS, and C9-ALS cases (Al-Sarraj et al., 2011; Cooper-Knock et al., 2012; Schipper et al., 2016), but it was not specified in which glial cell types the inclusions were detected. Some studies have reported phospho-TDP-43-positive inclusions in oligodendrocytes (Murray et al., 2011; Brettschneider et al., 2014; Fatima et al., 2015) and p62-positive inclusions in astrocytes (Simón-Sánchez et al., 2012). Co-immunostaining with cell type-specific antibodies would provide clarification to which extent astrocytes and microglia display p62 and TDP-43 inclusions. Understanding how the accumulation and aggregation of these proteins affect glial cell function could yield mechanistic insights into their potential contribution to disease pathogenesis. In conclusion, so far C9-HRE-associated pathological hallmarks have been detected to a lower extent in glial cells than in neurons in human *post-mortem* brains. In addition to the abovementioned potential reasons underlying the lower prevalence of these hallmarks in glial cells, yet one other option might be that glial cells can undergo extensive proliferation (Michell-Robinson et al., 2015; Verkhratsky and Nedergaard, 2018), which could either prevent the formation or dilute the amount of already existing RNA foci, DRPs, protein aggregates, or inclusions.

ASTROCYTES IN MODEL SYSTEMS OF C9-FTLD AND C9-ALS

C9-HRE Might Cause Astrogliosis

Increased chitinase-3-like protein 1 (CHI3L1) and GFAP expression are considered as indicators of astrogliosis (Sofroniew and Vinters, 2010; Zamanian et al., 2012), and both proteins show increased levels in the frontal cortex and CSF of FTLD patients (Umoh et al., 2018; Oeckl et al., 2019). Interestingly, elevated GFAP expression was detected in mice upon AAV-mediated C9-HRE expression and in one bacterial artificial chromosome (BAC) C9-HRE mouse model (Liu et al., 2016). However, in two other BAC mice, signs of astrogliosis or microgliosis were not detected (Peters et al., 2015; Jiang et al., 2016). It should be noted that these mice did not concomitantly model haploinsufficiency. Astrocytes of *C9orf72*$^{-/-}$ mice did not show enhanced GFAP immunoreactivity, indicating that lack of *C9orf72* does not cause astrogliosis (Koppers et al., 2015). Increased GFAP levels do not always correlate with enhanced ionized calcium-binding adapter molecule (Iba)1 levels (Zhang et al., 2016; Schludi et al., 2017), suggesting that trigger(s) for astro- and microgliosis are different.

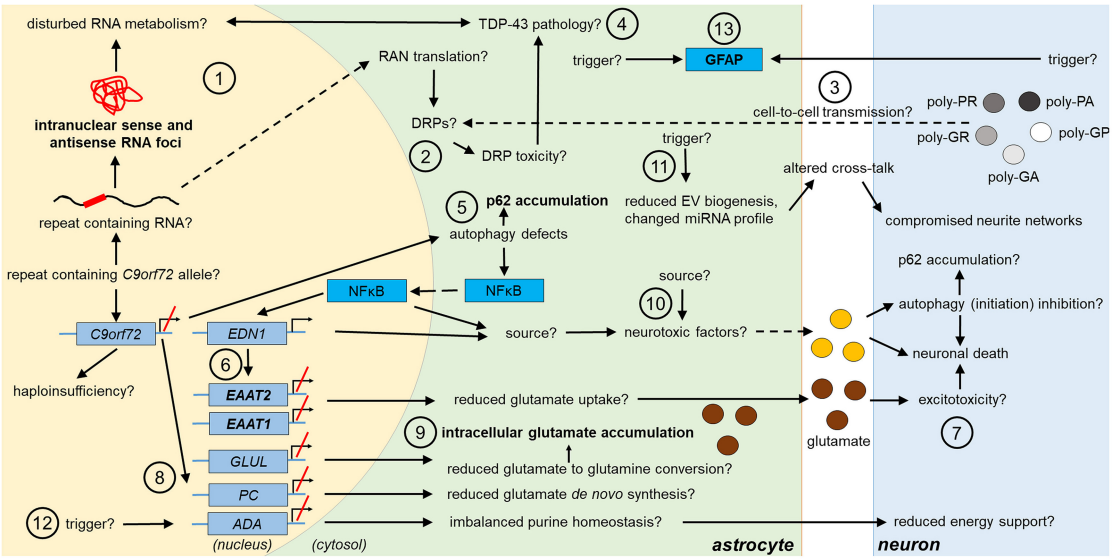

FIGURE 1 | Potential and confirmed phenotypic features of *C9orf72* HRE-associated astrocytes in FTLD/ALS. Features detected in the astrocytes of FTLD or ALS patient *post-mortem* brain are indicated in bold text. The presence of the typical C9-HRE-associated pathological hallmarks, which have previously been observed mainly in neurons, as well as other potential mechanisms, which still need to be confirmed in human patient astrocytes, are indicated with a question mark. Directions of sequential events are visualized with arrows. Steps requiring intracellular or intercellular translocation of molecules are indicated by dashed arrows. The different events are indicated by numbers as follows: **(1)** C9-HRE-containing RNA might be transcribed in astrocytes, forming intranuclear sense and antisense RNA foci, which may disturb RNA metabolism. **(2)** C9-HRE-containing RNA might be translocated into the cytosol of astrocytes, where it could undergo RAN translation creating potentially toxic DRPs. **(3)** DRPs might also be transmitted from other cell types, such as neurons, to astrocytes. **(4)** Potential disturbances in RNA metabolism as well as DRP toxicity might lead to TDP-43 pathology, which in turn could lead to defects in RNA processing in astrocytes. **(5)** Reduced C9orf72 levels in astrocytes might cause defects in autophagy, resulting in p62 accumulation and increase of NFκB levels in the cytosol and nucleus. **(6)** Enhanced NFκB levels with simultaneously decreased C9orf72 levels might enhance *EDN1* expression, which suppresses *EAAT1* and 2 expression in astrocytes. **(7)** As a result, astrocytic uptake of extracellular glutamate might be diminished, which might lead to excitotoxicity. **(8)** Reduced *C9orf72* levels might lead to decreased expression of genes involved in glutamate *de novo* synthesis (e.g., *PC*) and glutamate to glutamine conversion (e.g., *GLUL*). **(9)** Reduced conversion of glutamate to glutamine might underlie intracellular glutamate accumulation. **(10)** Neurotoxic factors, which partly might be created through the altered NFκB signaling, cause neuronal death. Neurotoxic factors might cause autophagy inhibition in neurons, which might lead to p62 accumulation. **(11)** Reduced EV synthesis, which might lead to decreased EV secretion, and an altered miRNA expression profile, might influence the crosstalk between astrocytes and neurons, which could lead to disturbed neurite growth and networks. **(12)** Decreased expression of *ADA* might disrupt purine metabolism and lead to decreased energy support of neurons by astrocytes. **(13)** Enhanced GFAP expression might derive from endogenous or exogenous triggers. ADA, adenosine deaminase; DRP, dipeptide repeat protein; EAAT1/2, excitatory amino acid transporter1/2; EDN1, endothelin 1; EV, extracellular vesicle; GFAP, glial fibrillary acidic protein; GLUL, glutamate-ammonia ligase; HRE, hexanucleotide repeat expansion; miRNA, micro ribonucleic acid; NFκB, nuclear factor "kappa-light-chain-enhancer" of activated B-cells; PC, pyruvate carboxylase; RAN, repeat-associated non-AUG; TDP-43, Transactive response DNA-binding protein 43.

Identification of such triggers might be essential for elucidating pathogenic disease mechanisms.

Neurotoxicity Mediated by Astrocytes Containing C9-HRE

Recent studies suggest that astrocytes from C9-HRE carriers with ALS can mediate neurotoxicity. Murine embryonic stem cell-derived motor neurons co-cultured with fibroblast-derived astrocytes from sporadic ALS or C9-ALS patients underwent extensive cell death within 4 days. Partial replacement of the culture medium by control astrocyte conditioned medium (ACM) did not prevent cell death, suggesting involvement of a gain-of-toxic-function mechanism rather than insufficient trophic support by the C9-HRE astrocytes (Meyer et al., 2014). Moreover, iPSC-derived motor neurons from control subjects or C9-ALS patients cultured in C9-ALS ACM showed dramatically decreased viability after 5 days (Madill et al., 2017). These studies indicate that direct physical contact between C9-HRE astrocytes and neurons as well as secretion of neurotoxicants might mediate neuronal cell death in a non-cell autonomous manner. Varcianna et al. showed that extracellular vesicles (EVs) secreted by induced astrocytes from C9-ALS patients decreased motor neuron survival. Also, C9-HRE astrocytes revealed a profile of increased or decreased expression of certain microRNAs compared to healthy controls, of which many are involved in axonal guidance and maintenance. Among these, miRNA-494-3p, which was recently shown to protect against lipopolysaccharide-induced cell death by targeting IL-13 expression (Geng and Liu, 2019), was significantly reduced in EVs secreted by C9-HRE astrocytes. Treatment with miRNA-494-3p mimic restored neurite length and number of nodes, and promoted motor neuron survival, suggesting that C9-HRE astrocytes might have impaired capacity to support neurons. This lack of support might also partially involve impaired EV biogenesis in astrocytes, which has also been shown to take place in fibroblasts and motor neurons derived from C9-HRE carriers (Aoki et al., 2017; Varcianna et al., 2019).

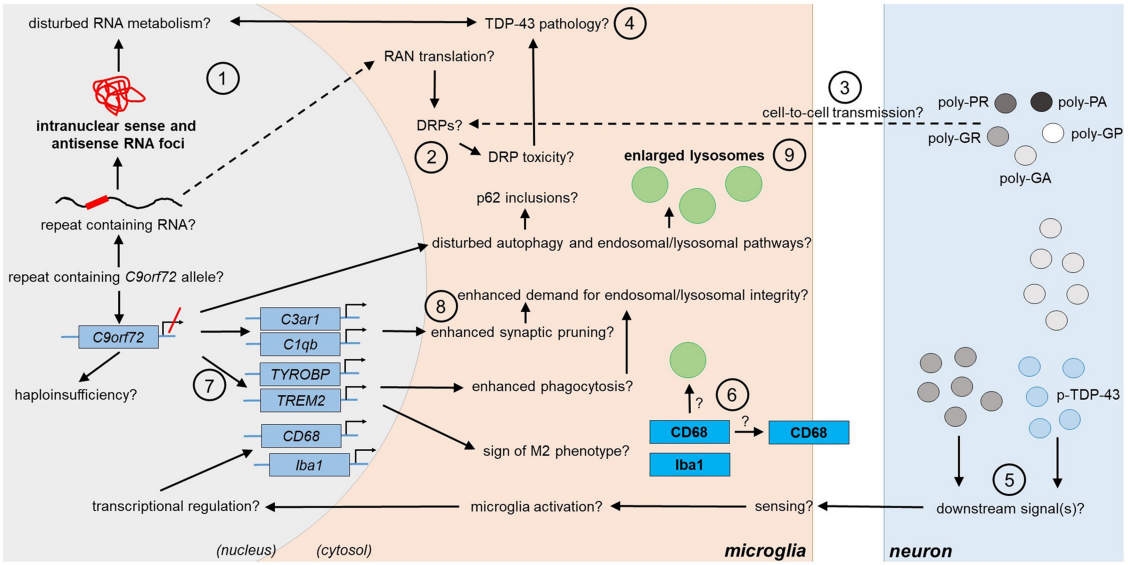

FIGURE 2 | Potential and confirmed phenotypic features of *C9orf72* HRE-associated microglia in FTLD/ALS. Features detected in the microglia of FTLD or ALS patient *post-mortem* brain are indicated in bold text. The presence of the typical C9-HRE-associated pathological hallmarks, which have previously been observed mainly in neurons, as well as other potential mechanisms, which still need to be confirmed in human patient microglia, are indicated with a question mark. Directions of sequential events are visualized with arrows. Steps requiring intracellular or intercellular translocation of molecules are indicated by dashed arrows. The different events are indicated by numbers as follows: **(1)** C9-HRE-containing RNA might be transcribed in microglia, forming intranuclear sense and antisense RNA foci, which may disturb RNA metabolism. **(2)** C9-HRE-containing RNA might be translocated into the cytosol of microglia, where it could undergo RAN translation creating potentially toxic DRPs. **(3)** DRPs might also be transmitted from other cell types, such as neurons, to microglia. **(4)** Potential disturbances in RNA metabolism as well as DRP toxicity might lead to TDP-43 pathology, which in turn could lead to defects in RNA processing in microglia. **(5)** Expression of poly-GA in combination with enhanced TDP-43 phosphorylation (p-TDP-43) or poly-GR expression alone in neurons might lead to downstream signals, which are recognized by adjacent microglia, leading first to enhanced *CD68* and later *Iba1* expression. **(6)** CD68 could serve as a receptor on the cell surface or localize in lysosomes. **(7)** Downregulation of *C9orf72* might increase *TREM2* and *TYROBP* expression, which might be a sign of M2 microglial phenotype switching and result in increased phagocytic activity. **(8)** Microglial *C3ar1* and *C1qb* expression might be increased through decreased expression of *C9orf72* and lead to enhanced synaptic pruning. **(9)** Decreased *C9orf72* expression might disturb autophagy pathway, resulting in p62 accumulation and enlarged lysosomes in microglia. C1qb, complement subcomponent C1q chain B; C3ar1, complement C3a Receptor 1; CD68, cluster of differentiation 68; DRP, dipeptide repeat protein; HRE, hexanucleotide repeat expansion; Iba1, ionized calcium-binding adapter molecule 1; RAN, repeat-associated non-AUG; TDP-43, Transactive response DNA binding protein 43; TREM2, Triggering receptor expressed on myeloid cells 2; TYROBP, tyrosine kinase binding protein.

Addition of the ACM from the same C9-HRE astrocytes led to slightly decreased cell survival compared to EVs only, indicating that in addition to EVs, also other astrocyte-derived soluble factors might cause neurotoxicity (Varcianna et al., 2019). In addition, impaired autophagy initiation and increased levels of SOD1 in neurons have been proposed as possible underlying mechanisms of the neurotoxicity mediated by C9-HRE-containing astrocytes through secreted factors (Madill et al., 2017), but require further investigations. Since SOD1 is regulated by transcription factors, such as NFκB (Milani et al., 2011), which in turn are controlled by environmental stimuli, investigating the mechanism behind increased SOD1 levels might yield better understanding on mechanisms of astrocyte-mediated neurotoxicity. Since autophagy can be regulated via microRNAs (Shah et al., 2018), investigating whether microRNAs secreted by C9-HRE astrocytes are the underlying mechanism of the inhibition of autophagy initiation in co-cultured cells would be interesting in order to find therapeutic targets.

Notably, under stress conditions, such as increased extracellular adenosine levels, neurotoxicity might be even enhanced. This idea is supported by the finding that induced sporadic as well as C9-HRE astrocytes and neurons harbor lower levels of adenosine deaminase (ADA), which normally deaminates adenosine to inosine. This predisposition has been shown to lead to enhanced death of the induced astrocytes themselves as well as motor neurons when cultured together with C9-HRE or sporadic induced astrocytes. Several conditions can lead to elevated adenosine triphosphate (ATP) levels in the brain and these can be sensed by and activate microglia and astrocytes. Under normal conditions, excessive ATP can be metabolized. However, defective ATP metabolism, as e.g., during ADA deficiency, could lead to excessive glial activation and subsequent neuroinflammation. In addition, decreased ADA levels could disturb energy metabolism in astrocytes and result in impaired nutritional support for neurons by C9-HRE astrocytes (Allen et al., 2019).

Haploinsufficiency as a Potential Mechanism of Astrocyte-Mediated Neurotoxicity

In humans, two C9orf72 protein isoforms, long (∼50 kDa) and short (∼25 kDa), have been described. The levels of

both protein isoforms are reduced in C9-HRE carrier tissues, including brain areas affected by neurodegeneration (Saberi et al., 2018). siRNA-mediated knockdown of both C9orf72 isoforms in U87 glioblastoma cells or normal human astrocytes has been shown to lead to the accumulation of p62 inclusions (Fomin et al., 2018), supporting the idea that loss of *C9orf72* may lead to their formation. Also, reduced expression of *pyruvate carboxylase* (*PC*), *EAAT1* and *2*, and *glutamine synthetase* (*GLUL*) together with intracellular glutamate accumulation was observed, implying that disturbed glutamate *de novo* synthesis, uptake and conversion into glutamine, all crucial functions in astrocytes, may take place upon *C9orf72* knockdown (Fomin et al., 2018). Decreased *EAAT1* and *EAAT2* levels suggest that C9-HRE astrocytes may not be able to efficiently take up excessive glutamate from synaptic cleft, which might lead to glutamate excitotoxicity, especially as induced motor neurons of C9-HRE ALS patients and *C9orf72*-deficient motor neurons have higher levels of glutamate receptors in neurites and dendritic spines (Shi et al., 2018). It was also observed that expression of *endothelin* (*EDN*) *1* as well as the levels of cytosolic and nuclear NFκB p65 were increased. The authors showed that the short C9orf72 isoform can bind to the predicted NFκB promoter binding site in *EDN1* and further suggested that in *C9orf72* knockdown cells, increased NFκB expression could lead to increased expression of *EDN1*, a negative regulator of *EAAT2* expression (Fomin et al., 2018). Therefore, the mechanisms underlying C9-HRE astrocyte-mediated neurotoxicity might involve *C9orf72* haploinsufficiency and p62 accumulation, and enhanced *EDN1* expression and NFκB signaling, known to induce the expression of nitric oxide synthase (Fomin et al., 2018).

Knockdown of both C9orf72 isoforms in U251 human astroglioma cells increased transmembrane protein 106b (TMEM106b) and progranulin but not lysosomal-associated membrane protein (LAMP) 1 and cathepsin D protein levels (similar to microglia in *C9orf72*-deficient mice Sullivan et al., 2016, see below). Similar effect was not detected when the cells were only expressing C9-HRE (Nicholson et al., 2018). These findings implicate that *C9orf72* haploinsufficiency may cause changes in astrocytic lysosomal pathways. Whether such effects can be observed in C9-HRE carriers and how they might affect astrocytic function still remains unknown. Taken together, these studies suggest that *C9orf72* haploinsufficiency, resulting from the C9-HRE, may lead to p62 accumulation, which could also propagate to other cells (Madill et al., 2017). Additionally, changes in NFκB and EDN1 signaling, disturbed glutamate metabolism, and lysosomal alterations might be phenotypic features of C9-HRE astrocytes with potentially altered physiological functions (**Figure 1**).

MICROGLIA IN C9-FTLD AND C9-ALS MODELS

Features of C9-HRE-Expressing Microglia

Depending on environmental cues, microglia can switch from resting to activated phenotype, characterized by elevated expression of CD68 (Choi et al., 2017; Hendrickx et al., 2017). Studies on *post-mortem* brains have shown increased microglial activation based on cell morphology and Iba1 and CD68 immunoreactivity in C9-FTLD and C9-ALS *vs.* sporadic FTLD and ALS cases. Significantly increased microglial activation according to number and morphology (ramified *vs.* ameoboid) of CD68-positive cells in frontal and temporal gray and white matter was detected in FTLD cases compared to controls, although there were no differences between C9-FTLD and sporadic FTLD cases (Lant et al., 2014). Also, augmented microglial activation based on CD68 immunoreactivity and cell morphology in the white matter of medulla and motor cortex of C9-ALS patients compared to non-C9-ALS cases has been reported. Iba1 immunoreactivity was also increased, indicating potentially increased number of microglia (Brettschneider et al., 2012). Higher CD68 immunoreactivity in the white matter of motor cortex, medulla, mid-crus cerebri, and lateral and anterior corticospinal tracts of C9-ALS patients (Cooper-Knock et al., 2012) and in the body and genu of corpus callosum of C9-HRE-carrying vs. non-carrying ALS patients has been detected (Cardenas et al., 2017), suggesting that microglial activation and infiltration in the brain might take place at least in late stages of C9-FTLD and C9-ALS. It would be crucial to assess at different stages of the disease process whether the phenotype of C9-HRE-carrying activated microglia is pro- or anti-inflammatory.

Iba1-positive microglia of C9-ALS patient *post-mortem* motor cortex and spinal cord contained enlarged lysosomes based on LAMP1 immunoreactivity compared to sporadic ALS cases (O'Rourke et al., 2016), suggesting lysosomal alterations in C9-HRE carriers. Total LAMP1 levels were not significantly changed in the frontal cortex of C9-ALS cases compared to sporadic ALS nor between FTLD and ALS and control samples (Umoh et al., 2018). This might suggest that (i) altered lysosomal morphology does not correlate with total LAMP1 levels or (ii) that microglia from spinal cord and frontal cortex show different lysosomal features. Enlarged microglial lysosomes may emerge under different conditions, such as cathepsin B and L inhibition and subsequent prevention of autophagosome-lysosome fusion (Jung et al., 2015), defects in lysosomal fission (Durchfort et al., 2012), progranulin deficiency (Evers et al., 2017) or TMEM106b overexpression (Nicholson and Rademakers, 2016), resulting in decreased lysosomal degradation capacity (Jung et al., 2015; Nicholson and Rademakers, 2016), and upon phagocytosis of fibrillar amyloid β, resulting in cathepsin B release (Halle et al., 2008). Further investigations are warranted related to the number of microglia with enlarged lysosomes and factors triggering such a phenotype, as well as understanding whether the enlarged lysosomes reflect dysfunction or improved function. Nevertheless, enhanced Iba1 and CD68 immunoreactivity and enlarged lysosomes may be considered as typical features of late stage C9-FTLD or C9-ALS microglia (**Figure 2**).

Neuron-Microglia Crosstalk Might Contribute to C9-HRE Microglia Phenotype

Expression of pathological C9-HRE in mouse cortex has been shown to upregulate *Iba1* expression, but it is unclear

whether this is due to cell-autonomous or non-cell autonomous effects (Nicholson et al., 2018). Significantly enhanced CD68 and Iba1 expression was detected at 6 months of age in the spinal cord of transgenic mice expressing poly-GA_{149} specifically in neurons. Increased microglial activation was absent in brain areas where the neurons did not exhibit poly-GA pathology. At this time point, no significant neuronal loss could be detected. However, the mice demonstrated enhanced TDP-43 phosphorylation, but no translocation or inclusions, and mild behavioral deficits, indicating that microglial activation might precede severe neuronal dysfunction. Interestingly, 1 month-old mice did not exhibit elevated Iba1 but already elevated CD68 expression (Schludi et al., 2017), implicating that enhanced CD68 expression in microglia may precede increased Iba1 expression. In contrast, expression of poly-GA_{50} did not increase Iba1 levels or cause TDP-43 pathology at 6 months of age, but the mice showed behavioral impairments and neurodegeneration (Zhang et al., 2016). Expression of poly-GR_{100} led to elevated Iba1 levels in mouse cortex and hippocampus, which peaked at 1.5 months of age. Notably, at this time, neuronal loss and brain atrophy, but no TDP-43 pathology, were already detectable in hippocampus and cortex (Zhang et al., 2018). These studies suggest that DRP length or type and/or concomitant additional factors, such as TDP-43 phosphorylation, might differentially regulate microglial Iba1 levels and activation. Also, neuron-microglia crosstalk might contribute to the activation of microglia.

Decreased C9orf72 Levels May Influence C9-HRE Microglia Phenotype

Human *C9orf72* and its mouse ortholog 3110043O21Rik are strongly expressed in myeloid cells, including microglia (O'Rourke et al., 2016; Rizzu et al., 2016; Iyer et al., 2018). *C9orf72*$^{-/-}$ mice show severe autoimmune phenotypes, elevated levels of inflammatory cytokines [IL-12, IL-10, tumor necrosis factor (TNF) α, IL-17] and monocyte chemoattractant protein 1 in serum and pro-inflammatory macrophage polarization (Atanasio et al., 2016; O'Rourke et al., 2016; Sullivan et al., 2016). Microglia of *C9orf72*$^{-/-}$ mice showed phenotypes ranging from accumulation of enlarged lysosomes and enhanced LAMP1 immunoreactivity, strongly increased expression of IL-6 and IL-1β under basal conditions (O'Rourke et al., 2016) to no changes in LAMP1 or cathepsin D immunoreactivity (Sullivan et al., 2016). However, microglia from hemizygous mice were not reported to show significant increases in pro-inflammatory cytokine levels or lysosomal changes (O'Rourke et al., 2016). Furthermore, even in *C9orf72*$^{-/-}$ mice, no increase in Iba1 immunoreactivity or changes in the morphology, number, or distribution of microglia were detected in contrast to human *post-mortem* brain as described above (Koppers et al., 2015; Sullivan et al., 2016). On the other hand, antisense oligonucleotides targeting *C9orf72* transcripts induced the mRNA levels of *triggering receptor expressed on myeloid cells* (*TREM*) *2, tyrosine kinase binding protein* (*TYROBP*), *C1q B chain* (*C1qb*) and *C3a receptor 1* (*C3ar1*), all predominantly expressed in microglia and regulating central microglial functions, including activation, pruning, and phagocytosis (Lagier-Tourenne et al., 2013), suggesting that reduced *C9orf72* levels associate with alterations in these microglial functions. Altogether, the current data suggest that *C9orf72* haploinsufficiency might not underlie the C9-ALS and C9-FTLD microglial phenotypes as assessed by Iba1 and CD68 immunoreactivity. Whether lysosomal changes resulting from reduced *C9orf72* levels occur in microglia needs further investigation. *C9orf72* knockout in HEK293T cells leads to enlarged lysosomes, suggesting that similar effects might also occur in other cell types (Amick et al., 2016). However, enhanced *TREM2*, *TYROBP, C1qb,* and *C3ar1* expression might represent additional phenotypic features of C9-HRE microglia (**Figure 2**). Interestingly, also progranulin-deficient mice show enlarged lysosomes, increased *CD68*, *TYROBP*, *TREM*2 and complement factor expression (Evers et al., 2017) and Iba1 immunoreactivity (Tanaka et al., 2014).

CONCLUSIONS AND FUTURE PERSPECTIVES

Here, we have discussed the potential phenotypes of C9-HRE astrocytes and microglia based on the current literature. In general, FTLD and ALS are complex multifactorial diseases involving multi-cellular components. Thus, dysfunction of one cell type only might not be enough to trigger neurodegeneration but different cell types and their crosstalk are likely to contribute. Regarding C9-HRE-associated FTLD and ALS, astrocytes are suggested to mediate neurotoxic effects, but so far there is no conclusive experimental evidence of direct contribution of microglia to neurodegeneration in C9-FTLD and C9-ALS models. The reason for this might be that the current approaches have focused mostly on *C9orf72* haploinsufficiency when modeling the C9-HRE-related effects in microglia. These studies have suggested that *C9orf72* depletion, which leads to severe dysfunction of the immune system, might affect macrophages and microglia differently. Since neurons with C9-HRE-associated pathological features rather than *C9orf72* haploinsufficiency might cause microglia activation, concomitant modeling of the loss-of-function and gain-of-toxic function mechanisms might help to decipher whether and how microglia may take part in C9-FTLD and C9-ALS pathogenesis. Also, since loss of *C9orf72* has been linked to autoimmune phenotypes, it would be important to also investigate the crosstalk between the peripheral immune system and CNS-resident cells in the future. While the C9-HRE microglial phenotypes might result, at least partially, from neuron-microglia crosstalk, astrocytic neurotoxicity appears to derive from intrinsic factors, which then display non-cell autonomous deleterious effects on neurons. Since C9-HRE astrocytes show defects in EV-based communication with neurons, investigating whether the crosstalk between astrocytes and microglia of C9-HRE carriers is changed as well, would reveal further insights into mechanisms potentially underlying C9-HRE-associated ALS and FTLD. Future investigations are warranted to uncover

potential spatial and temporal contributions of glia to onset and progression of C9-FTLD and C9-ALS. Also, even though C9-FTLD and C9-ALS share overlapping genetic background and pathological features, it will be interesting to find out the similarities and potential differences in the effects of microglia and astrocytes on the pathogenesis of these two diseases. As the presently available literature on glia in the context of C9-HRE is still limited, we hope that this summary of the current knowledge and the hypotheses presented will help to design future experiments for deciphering the so far poorly understood role of astrocytes and microglia in disease pathogenesis and for identifying potential novel biomarker and/or therapeutic target candidates for FTLD and ALS.

AUTHOR CONTRIBUTIONS

HR and AH outlined and drafted the manuscript. HR, SL, NH, KK, AC, ES, MM, TN, AR, MH, and AH participated in the writing and editing the manuscript. All authors have accepted the contents of the submitted manuscript.

FUNDING

This study was supported by grants from the Academy of Finland, grant nos. 315459 (AH), 315460 (AR), 288659 (TN), and 307866 (MH); Yrjö Jahnsson Foundation, grant no. 20187070 (AH); ALS tutkimuksen tuki ry. registered association (HR, SL, NH); Sigrid Jusélius Foundation (MH); Maire Taponen Foundation (AC); Finnish Cultural Foundation (AC); Finnish Brain Foundation (KK); Finnish Medical Foundation (KK); Päivikki and Sakari Sohlberg Foundation (KK); the Strategic Neuroscience Funding of the University of Eastern Finland (AH, MH); and Neurocenter Finland—AlzTrans pilot project (MH).

ACKNOWLEDGMENTS

HR, SL, and NH are supported by the University of Eastern Finland Doctoral Program in Molecular Medicine (DPMM) and GenomMed. This publication is part of a project that has received funding from the European Union's Horizon 2020 research and innovation programme under the Marie Skłodowska-Curie grant agreement No 740264.

REFERENCES

Allen, S. P., Hall, B., Castelli, L. M., Francis, L., Woof, R., Siskos, A. P., et al. (2019). Astrocyte adenosine deaminase loss increases motor neuron toxicity in amyotrophic lateral sclerosis. *Brain* 142, 586–605. doi: 10.1093/brain/awy353

Almeida, S., Gascon, E., Tran, H., Chou, H. J., Gendron, T. F., DeGroot, S., et al. (2013). Modeling key pathological features of frontotemporal dementia with C9ORF72 repeat expansion in iPSC-derived human neurons. *Acta Neuropathol.* 126, 385–399. doi: 10.1007/s00401-013-1149-y

Al-Sarraj, S., King, A., Troakes, C., Smith, B., Maekawa, S., Bodi, I., et al. (2011). p62 positive, TDP-43 negative, neuronal cytoplasmic and intranuclear inclusions in the cerebellum and hippocampus define the pathology of C9orf72-linked FTLD and MND/ALS. *Acta Neuropathol.* 122, 691–702. doi: 10.1007/s00401-011-0911-2

Amick, J., Roczniak-Ferguson, A., and Ferguson, S. M. (2016). C9orf72 binds SMCR8, localizes to lysosomes, and regulates mTORC1 signaling. *Mol. Biol. Cell* 27, 3040–3051. doi: 10.1091/mbc.e16-01-0003

Aoki, Y., Manzano, R., Lee, Y., Dafinca, R., Aoki, M., Douglas, A. G. L., et al. (2017). C9orf72 and RAB7L1 regulate vesicle trafficking in amyotrophic lateral sclerosis and frontotemporal dementia. *Brain* 140, 887–897. doi: 10.1093/brain/awx024

Ash, P. E., Bieniek, K. F, Gendron, T. F., Caulfield, T., Lin, W. L., DeJesus-Hernandez, M., et al. (2013). Unconventional translation of C9ORF72 GGGGCC expansion generates insoluble polypeptides specific to c9FTD/ALS. *Neuron* 77, 639–646. doi: 10.1016/j.neuron.2013.02.004

Atanasio, A., Decman, V., White, D., Ramos, M., Ikiz, B., Lee, H., et al. (2016). C9orf72 ablation causes immune dysregulation characterized by leukocyte expansion, autoantibody production, and glomerulonephropathy in mice. *Sci. Rep.* 6:23204. doi: 10.1038/srep23204

Bachiller, S., Jiménez-Ferrer, I., Paulus, A., Yang, Y., Swanberg, M., Deierborg, T., et al. (2018). Microglia in neurological diseases: a road map to brain-disease dependent-inflammatory response. *Front. Cell. Neurosci.* 12:488. doi: 10.3389/fncel.2018.00488

Balendra, R., and Isaacs, A. M. (2018). C9orf72-mediated ALS and FTD: multiple pathways to disease. *Nat. Rev. Neurol.* 14, 544–558. doi: 10.1038/s41582-018-0047-2

Barclay, A. N., Wright, G. J., Brooke, G., and Brown, M. H. (2002). CD200 and membrane protein interactions in the control of myeloid cells. *Trends Immunol.* 23, 285–290. doi: 10.1016/S.1471-4906(02)02223-8

Brettschneider, J., Arai, K., Del Tredici, K., Toledo, J. B., Robinson, J. L., Lee, E. B., et al. (2014). TDP-43 pathology and neuronal loss in amyotrophic lateral sclerosis spinal cord. *Acta Neuropathol.* 128, 423–437. doi: 10.1007/s00401-014-1299-6

Brettschneider, J., Toledo, J. B., Van Deerlin, V. M., Elman, L., McCluskey, L., Lee, V. M., et al. (2012). Microglial activation correlates with disease progression and upper motor neuron clinical symptoms in amyotrophic lateral sclerosis. *PLoS ONE* 7:e39216. doi: 10.1371/journal.pone.0039216

Broe, M., Kril, J., and Halliday, G. M. (2004). Astrocytic degeneration relates to the severity of disease in frontotemporal dementia. *Brain J. Neurol.* 127, 2214–2220. doi: 10.1093/brain/awh250

Cardenas, A. M., Sarlls, J. E., Kwan, J. Y., Bageac, D., Gala, Z. S., Danielian, L. E., et al. (2017). Pathology of callosal damage in ALS: an *ex-vivo*, 7T diffusion tensor MRI study. *NeuroImage Clin.* 15, 200–208. doi: 10.1016/j.nicl.2017.04.024

Chen, W. W., Zhang, X., and Huang, W. J. (2016). Role of neuroinflammation in neurodegenerative diseases (Review). *Mol. Med. Rep.* 13, 3391–3396. doi: 10.3892/mmr.2016.4948

Chew, J., Gendron, T. F., Prudencio, M., Sasaguri, H., Zhang, Y. J., Castanedes-Casey, M., et al. (2015). Neurodegeneration. C9ORF72 repeat expansions in mice cause TDP-43 pathology, neuronal loss, and behavioral deficits. *Science* 348, 1151–1154. doi: 10.1126/science.aaa9344

Choi, J. Y., Kim, J. Y., Kim, J. Y., Park, J., Lee, W. T., and Lee, J. E. (2017). M2 phenotype microglia-derived cytokine stimulates proliferation and neuronal differentiation of endogenous stem cells in ischemic brain. *Exp. Neurobiol.* 26, 33–41. doi: 10.5607/en.2017.26.1.33

Cistaro, A., Pagani, M., Montuschi, A., Calvo, A., Moglia, C., Canosa, A., et al. (2014). The metabolic signature of C9ORF72-related ALS: FDG PET comparison with nonmutated patients. *Eur. J. Nucl. Med. Mol. Imaging* 41, 844–852. doi: 10.1007/s00259-013-2667-5

Cooper-Knock, J., Green, C., Altschuler, G., Wei, W., Bury, J. J., Heath, P. R., et al. (2017). A data-driven approach links microglia to pathology and prognosis in amyotrophic lateral sclerosis. *Acta Neuropathol Commun* 5:23. doi: 10.1186/s40478-017-0424-x

Cooper-Knock, J., Hewitt, C., Highley, J. R., Brockington, A., Milano, A., Man, S., et al. (2012). Clinico-pathological features in amyotrophic lateral

sclerosis with expansions in C9ORF72. *Brain J. Neurol.* 135, 751–764. doi: 10.1093/brain/awr365

Cooper-Knock, J., Higginbottom, A., Stopford, M. J., Highley, J. R., Ince, P. G., Wharton, S. B., et al. (2015). Antisense RNA foci in the motor neurons of C9ORF72-ALS patients are associated with TDP-43 proteinopathy. *Acta Neuropathol.* 130, 63–75. doi: 10.1007/s00401-015-1429-9

Cooper-Knock, J., Walsh, M. J., Higginbottom, A., Robin Highley, J., Dickman, M. J., Edbauer, D., et al. (2014). Sequestration of multiple RNA recognition motif-containing proteins by C9orf72 repeat expansions. *Brain* 137, 2040–2051. doi: 10.1093/brain/awu120

Dafinca, R., Scaber, J., Ababneh, N., Lalic, T., Weir, G., Christian, H., et al. (2016). C9orf72 hexanucleotide expansions are associated with altered endoplasmic reticulum calcium homeostasis and stress granule formation in induced pluripotent stem cell-derived neurons from patients with amyotrophic lateral sclerosis and frontotemporal dementia. *Stem Cells* 34, 2063–2078. doi: 10.1002/stem.2388

Deczkowska, A., Keren-Shaul, H., Weiner, A., Colonna, M., Schwartz, M., and Amit, I. (2018). Disease-associated microglia: a universal immune sensor of neurodegeneration. *Cell* 173, 1073–1081. doi: 10.1016/j.cell.2018.05.003

DeJesus-Hernandez, M., Finch, N. A., Wang, X., Gendron, T. F., Bieniek, K. F., Heckman, M. G., et al. (2017). In-depth clinico-pathological examination of RNA foci in a large cohort of C9ORF72 expansion carriers. *Acta Neuropathol.* 134, 255–269. doi: 10.1007/s00401-017-1725-7

DeJesus-Hernandez, M., Mackenzie, I., Boeve, B., Boxer, A., Baker, M., Rutherford, N., et al. (2011). Expanded GGGGCC hexanucleotide repeat in noncoding region of C9ORF72 causes chromosome 9p-linked FTD and ALS. *Neuron* 72, 245–256. doi: 10.1016/j.neuron.2011.09.011

Donnelly, C. J., Zhang, P. W., Pham, J. T., Haeusler, A. R., Mistry, N. A., Vidensky, S., et al. (2013). RNA toxicity from the ALS/FTD C9ORF72 expansion is mitigated by antisense intervention. *Neuron* 80, 415–428. doi: 10.1016/j.neuron.2013.10.015

Durchfort, N., Verhoef, S., Vaughn, M. B., Shrestha, R., Adam, D., Kaplan, J., et al. (2012). The enlarged lysosomes in beigej cells result from decreased lysosome fission and not increased lysosome fusion. *Traffic* 13, 108–119. doi: 10.1111/j.1600-0854.2011.01300.x

Evers, B. M., Rodriguez-Navas, C., Tesla, R. J., Prange-Kiel, J., Wasser, C. R., Yoo, K. S., et al. (2017). Lipidomic and transcriptomic basis of lysosomal dysfunction in progranulin deficiency. *Cell Rep.* 20, 2565–2574. doi: 10.1016/j.celrep.2017.08.056

Fatima, M., Tan, R., Halliday, G. M., and Kril, J. J. (2015). Spread of pathology in amyotrophic lateral sclerosis: assessment of phosphorylated TDP-43 along axonal pathways. *Acta Neuropathol. Commun.* 3:47. doi: 10.1186/s40478-015-0226-y

Fomin, V., Richard, P., Hoque, M., Li, C., Gu, Z., Fissore-O'Leary, M., et al. (2018). The C9ORF72 gene, implicated in amyotrophic lateral sclerosis and frontotemporal dementia, encodes a protein that functions in control of endothelin and glutamate signaling. *Mol. Cell. Biol.* 38:e00155-18. doi: 10.1128/MCB.00155-18

Franco, R., and Fernández-Suárez, D. (2015). Alternatively activated microglia and macrophages in the central nervous system. *Prog. Neurobiol.* 131, 65–86. doi: 10.1016/j.pneurobio.2015.05.003

Freibaum, B. D., and Taylor, J. P. (2017). The role of dipeptide repeats in C9ORF72-related ALS-FTD. *Front. Mol. Neurosci.* 10:35. doi: 10.3389/fnmol.2017.00035

Gendron, T. F., Bieniek, K. F., Zhang, Y. J., Jansen-West, K., Ash, P. E., Caulfield, T., et al. (2013). Antisense transcripts of the expanded C9ORF72 hexanucleotide repeat form nuclear RNA foci and undergo repeat-associated non-ATG translation in c9FTD/ALS. *Acta Neuropathol.* 126, 829–844. doi: 10.1007/s00401-013-1192-8

Gendron, T. F., Josephs, K. A., and Petrucelli, L. (2010). Review: transactive response DNA-binding protein 43 (TDP-43): mechanisms of neurodegeneration. *Neuropathol. Appl. Neurobiol.* 36, 97–112. doi: 10.1111/j.1365-2990.2010.01060.x

Geng, W., and Liu, L. (2019). MiR-494 alleviates lipopolysaccharide (LPS)-induced autophagy and apoptosis in PC-12 cells by targeting IL-13. *Adv. Clin. Exp. Med.* 28, 85–94. doi: 10.17219/acem/76749

Gitik, M., Liraz-Zaltsman, S., Oldenborg, P., Reichert, F., and Rotshenker, S. (2011). Myelin down-regulates myelin phagocytosis by microglia and macrophages through interactions between CD47 on myelin and SIRPα (signal regulatory protein-α) on phagocytes. *J. Neuroinflammation* 8:24. doi: 10.1186/1742-2094-8-24

Gitler, A. D., and Tsuiji, H. (2016). There has been an awakening: emerging mechanisms of C9orf72 mutations in FTD/ALS. *Brain Res.* 1647, 19–29. doi: 10.1016/j.brainres.2016.04.004

Gorno-Tempini, M. L., Hillis, A. E., Weintraub, S., Kertesz, A., Mendez, M., Cappa, S. F., et al. (2011). Classification of primary progressive aphasia and its variants. *Neurology* 76, 1006–1014. doi: 10.1212/WNL.0b013e31821103e6

Haidet-Phillips, A. M., Hester, M. E., Miranda, C. J., Meyer, K., Braun, L., Frakes, A., et al. (2011). Astrocytes from familial and sporadic ALS patients are toxic to motor neurons. *Nat. Biotechnol.* 29, 824–828. doi: 10.1038/nbt.1957

Halle, A., Hornung, V., Petzold, G. C., Stewart, C. R., Monks, B. G., Reinheckel, T., et al. (2008). The NALP3 inflammasome is involved in the innate immune response to amyloid-b. *Nat. Immunol.* 9, 857–865. doi: 10.1038/ni.1636

Hallmann, A. L., Araúzo-Bravo, M. J., Mavrommatis, L., Ehrlich, M., Röpke, A., Brockhaus, J., et al. (2017). Astrocyte pathology in a human neural stem cell model of frontotemporal dementia caused by mutant TAU protein. *Sci. Rep.* 7:42991. doi: 10.1038/srep42991

Hendrickx, D. A. E., van Eden, C. G., Schuurman, K. G., Hamann, J., and Huitinga, I. (2017). Staining of HLA-DR, Iba1 and CD68 in human microglia reveals partially overlapping expression depending on cellular morphology and pathology. *J. Neuroimmunol.* 309, 12–22. doi: 10.1016/j.jneuroim.2017.04.007

Ismail, A., Cooper-Knock, J., Highley, J. R., Milano, A., Kirby, J., Goodall, E., et al. (2013). Concurrence of multiple sclerosis and amyotrophic lateral sclerosis in patients with hexanucleotide repeat expansions of C9ORF72. *J. Neurol. Neurosurg. Psychiatr.* 84, 79–87. doi: 10.1136/jnnp-2012-303326

Iyer, S., Acharya, K. R., and Subramanian, V. (2018). A comparative bioinformatic analysis of C9orf72. *Peer J.* 6:e4391. doi: 10.7717/peerj.4391

Jang, E., Kim, J. H., Lee, S., Kim, J. H., Seo, J. W., Jin, M., et al. (2013). Phenotypic polarization of activated astrocytes: the critical role of lipocalin-2 in the classical inflammatory activation of astrocytes. *J. Immunol.* 191, 5204–5219. doi: 10.4049/jimmunol.1301637

Jiang, J., Zhu, Q., Gendron, T. F., Saberi, S., McAlonis-Downes, M., Seelman, A., et al. (2016). Gain of toxicity from ALS/FTD-linked repeat expansions in C9ORF72 Is alleviated by antisense oligonucleotides targeting GGGGCC-containing RNAs. *Neuron* 90, 535–550. doi: 10.1016/j.neuron.2016.04.006

Jung, M., Lee, J., Seo, H. Y., Lim, J. S., and Kim, E. K. (2015). Cathepsin inhibition-induced lysosomal dysfunction enhances pancreatic beta-cell apoptosis in high glucose. *PLoS ONE* 10:e0116972. doi: 10.1371/journal.pone.0116972

Koppers, M., Blokhuis, A. M., Westeneng, H. J., Terpstra, M. L., Zundel, C. A., Vieira de Sa, R., et al. (2015). C9orf72 ablation in mice does not cause motor neuron degeneration or motor deficits. *Ann. Neurol.* 78, 426–438. doi: 10.1002/ana.24453

Krabbe, G., Minami, S. S., Etchegaray, J. I., Taneja, P., Djukic, B., Davalos, D., et al. (2017). Microglial NFκB-TNFα hyperactivation induces obsessive–compulsive behavior in mouse models of progranulin-deficient frontotemporal dementia. *Proc. Natl. Acad. Sci. U S A.* 114, 5029–5034. doi: 10.1073/pnas.1700477114

Lagier-Tourenne, C., Baughn, M., Rigo, F., Sun, S., Liu, P., Li, H. R., et al. (2013). Targeted degradation of sense and antisense C9orf72 RNA foci as therapy for ALS and frontotemporal degeneration. *Proc. Natl. Acad. Sci. U S A.* 110, E4530–E4539. doi: 10.1073/pnas.1318835110

Lant, S. B., Robinson, A. C., Thompson, J. C., Rollinson, S., Pickering-Brown, S., Snowden, J. S., et al. (2014). Patterns of microglial cell activation in frontotemporal lobar degeneration. *Neuropathol. Appl. Neurobiol.* 40, 686–696. doi: 10.1111/nan.12092

Lee, J., Hyeon, S. J., Im, H., Ryu, H., Kim, Y., and Ryu, H. (2016). Astrocytes and microglia as non-cell autonomous players in the pathogenesis of ALS. *Exp. Neurobiol.* 25, 233–240. doi: 10.5607/en.2016.25.5.233

Liu, Y., Pattamatta, A., Zu, T., Reid, T., Bardhi, O., Borchelt, D., et al. (2016). C9orf72 BAC mouse model with motor deficits and neurodegenerative features of ALS/FTD. *Neuron* 90, 521–534. doi: 10.1016/j.neuron.2016.04.005

Mackenzie, I. R., Arzberger, T., Kremmer, E., Troost, D., Lorenzl, S., Mori, K., et al. (2013). Dipeptide repeat protein pathology in C9ORF72 mutation cases: clinico-pathological correlations. *Acta Neuropathol.* 126, 859–879. doi: 10.1007/s00401-013-1181-y

Madill, M., McDonagh, K., Ma, J., Vajda, A., McLoughlin, P., O'Brien, T., et al. (2017). Amyotrophic lateral sclerosis patient iPSC-derived astrocytes

impair autophagy via non-cell autonomous mechanisms. *Mol. Brain* 10, 22–12. doi: 10.1186/s13041-017-0300-4

Mahoney, C. J., Beck, J., Rohrer, J. D., Lashley, T., Mok, K., Shakespeare, T., et al. (2012). Frontotemporal dementia with the C9ORF72 hexanucleotide repeat expansion: clinical, neuroanatomical and neuropathological features. *Brain* 135, 736–750. doi: 10.1093/brain/awr361

Majounie, E., Renton, A. E., Mok, K., Dopper, E. G., Waite, A., Rollinson, S., et al. (2012). Frequency of the C9orf72 hexanucleotide repeat expansion in patients with amyotrophic lateral sclerosis and frontotemporal dementia: a cross-sectional study. *Lancet Neurol.* 11, 323–330. doi: 10.1016/S1474-4422(12)70043-1

May, S., Hornburg, D., Schludi, M. H., Arzberger, T., Rentzsch, K., Schwenk, B. M., et al. (2014). C9orf72 FTLD/ALS-associated Gly-Ala dipeptide repeat proteins cause neuronal toxicity and Unc119 sequestration. *Acta Neuropathol.* 128, 485–503. doi: 10.1007/s00401-014-1329-4

Meyer, K., Ferraiuolo, L., Miranda, C. J., Likhite, S., McElroy, S., Renusch, S., et al. (2014). Direct conversion of patient fibroblasts demonstrates non-cell autonomous toxicity of astrocytes to motor neurons in familial and sporadic ALS. *Proc. Natl. Acad. Sci. U S A.* 111, 829–832. doi: 10.1073/pnas.1314085111

Michell-Robinson, M. A., Touil, H., Healy, L. M., Owen, D. R., Durafourt, B. A., Bar-Or, A., et al. (2015). Roles of microglia in brain development, tissue maintenance and repair. *Brain* 138, 1138–1159. doi: 10.1093/brain/awv066

Milani, P., Gagliardi, S., Cova, E., and Cereda, C. (2011). SOD1 transcriptional and posttranscriptional regulation and its potential implications in ALS. *Neurol. Res. Int.* 2011:458427. doi: 10.1155/2011/458427

Minami, S. S., Shen, V., Le, D., Krabbe, G., Asgarov, R., Perez-Celajes, L., et al. (2015). Reducing inflammation and rescuing FTD-related behavioral deficits in progranulin-deficient mice with α7 nicotinic acetylcholine receptor agonists. *Biochem. Pharmacol.* 97, 454–462. doi: 10.1016/j.bcp.2015.07.016

Mizielinska, S., Lashley, T., Norona, F. E., Clayton, E. L., Ridler, C. E., Fratta, P., et al. (2013). C9orf72 frontotemporal lobar degeneration is characterised by frequent neuronal sense and antisense RNA foci. *Acta Neuropathol.* 126, 845–857. doi: 10.1007/s00401-013-1200-z

Mori, K., Arzberger, T., Grässer, F. A., Gijselinck, I., May, S., Rentzsch, K., et al. (2013b). Bidirectional transcripts of the expanded C9orf72 hexanucleotide repeat are translated into aggregating dipeptide repeat proteins. *Acta Neuropathol.* 126, 881–893. doi: 10.1007/s00401-013-1189-3

Mori, K., Lammich, S., Mackenzie, I. R., Forné, I., Zilow, S., Kretzschmar, H., et al. (2013a). hnRNP A3 binds to GGGGCC repeats and is a constituent of p62-positive/TDP43-negative inclusions in the hippocampus of patients with C9orf72 mutations. *Acta Neuropathol.* 125, 413–423. doi: 10.1007/s00401-013-1088-7

Murray, M. E., DeJesus-Hernandez, M., Rutherford, N. J., Baker, M., Duara, R., Graff-Radford, N. R., et al. (2011). Clinical and neuropathologic heterogeneity of c9FTD/ALS associated with hexanucleotide repeat expansion in C9ORF72. *Acta Neuropathol.* 122, 673–690. doi: 10.1007/s00401-011-0907-y

Nicholson, A. M., and Rademakers, R. (2016). What we know about TMEM106B in neurodegeneration. *Acta Neuropathol.* 132, 639–651. doi: 10.1007/s00401-016-1610-9

Nicholson, A. M., Zhou, X., Perkerson, R. B., Parsons, T. M., Chew, J., Brooks, M., et al. (2018). Loss of Tmem106b is unable to ameliorate frontotemporal dementia-like phenotypes in an AAV mouse model of C9ORF72-repeat induced toxicity. *Acta Neuropathol. Commun.* 6:42. doi: 10.1186/s40478-018-0545-x

Nonaka, T., Masuda-Suzukake, M., Hosokawa, M., Shimozawa, A., Hirai, S., Okado, H., et al. (2018). C9ORF72 dipeptide repeat poly-GA inclusions promote intracellular aggregation of phosphorylated TDP-43. *Hum. Mol. Genet.* 27, 2658–2670. doi: 10.1093/hmg/ddy174

Nordin, A., Akimoto, C., Wuolikainen, A., Alstermark, H., Jonsson, P., Birve, A., et al. (2015). Extensive size variability of the GGGGCC expansion in C9orf72 in both neuronal and non-neuronal tissues in 18 patients with ALS or FTD. *Hum. Mol. Genet.* 24, 3133–3142. doi: 10.1093/hmg/ddv064

Oeckl, P., Weydt, P., Steinacker, P., Anderl-Straub, S., Nordin, F., Volk, A. E., et al. (2019). Different neuroinflammatory profile in amyotrophic lateral sclerosis and frontotemporal dementia is linked to the clinical phase. *J. Neurol. Neurosurg. Psychiatr.* 90, 4–10. doi: 10.1136/jnnp-2018-318868

Onyike, C. U., and Diehl-Schmid, J. (2013). The epidemiology of frontotemporal dementia. *Int. Rev. Psychiatry* 25, 130–137. doi: 10.3109/09540261.2013.776523

O'Rourke, J. G., Bogdanik, L., Yáñez, A., Lall, D., Wolf, A. J., Muhammad, A. K., et al. (2016). C9orf72 is required for proper macrophage and microglial function in mice. *Science* 351, 1324–1329. doi: 10.1126/science.aaf1064

Parker, S. E., Hanton, A. M., Stefanou, S. N., Noakes, P. G., Woodruff, T. M., and Lee, J. D. (2019). Revisiting the role of the innate immune complement system in ALS. *Neurobiol. Dis.* 127, 223–232. doi: 10.1016/j.nbd.2019.03.003

Peters, O., Cabrera, G., Tran, H., Gendron, T., McKeon, J., Metterville, J., et al. (2015). Human C9ORF72 hexanucleotide expansion reproduces RNA foci and dipeptide repeat proteins but not neurodegeneration in BAC transgenic mice. *Neuron* 88, 902–909. doi: 10.1016/j.neuron.2015.11.018

Prudencio, M., Belzil, V. V., Batra, R., Ross, C. A., Gendron, T. F., Pregent, L. J., et al. (2015). Distinct brain transcriptome profiles in C9orf72-associated and sporadic ALS. *Nat. Neurosci.* 18, 1175–1182. doi: 10.1038/nn.4065

Radford, R. A., Morsch, M., Rayner, S. L., Cole, N. J., Pountney, D. L., and Chung, R. S. (2015). The established and emerging roles of astrocytes and microglia in amyotrophic lateral sclerosis and frontotemporal dementia. *Front. Cell. Neurosci.* 9:414. doi: 10.3389/fncel.2015.00414

Rama Rao, K. V., and Kielian, T. (2015). Neuron–astrocyte interactions in neurodegenerative diseases: role of neuroinflammation. *Clin. Exp. Neuroimmunol.* 6, 245–263. doi: 10.1111/cen3.12237

Rascovsky, K., Hodges, J. R., Knopman, D., Mendez, M. F., Kramer, J. H., Neuhaus, J., et al. (2011). Sensitivity of revised diagnostic criteria for the behavioural variant of frontotemporal dementia. *Brain* 134, 2456–2477. doi: 10.1093/brain/awr179

Renton, A. E., Majounie, E., Waite, A., Simón-Sánchez, J., Rollinson, S., Gibbs, J. R., et al. (2011). A hexanucleotide repeat expansion in C9ORF72 is the cause of chromosome 9p21-linked ALS-FTD. *Neuron* 72, 257–268. doi: 10.1016/j.neuron.2011.09.010

Rizzu, P., Blauwendraat, C., Heetveld, S., Lynes, E. M., Castillo-Lizardo, M., Dhingra, A., et al. (2016). C9orf72 is differentially expressed in the central nervous system and myeloid cells and consistently reduced in C9orf72, MAPT and GRN mutation carriers. *Acta Neuropathol. Commun.* 4:37. doi: 10.1186/s40478-016-0306-7

Saberi, S., Stauffer, J. E., Jiang, J., Garcia, S. D., Taylor, A. E., Schulte, D., et al. (2018). Sense-encoded poly-GR dipeptide repeat proteins correlate to neurodegeneration and uniquely co-localize with TDP-43 in dendrites of repeat-expanded C9orf72 amyotrophic lateral sclerosis. *Acta Neuropathol.* 135, 459–474. doi: 10.1007/s00401-017-1793-8

Sareen, D., O'Rourke, J. G., Meera, P., Muhammad, A. K., Grant, S., Simpkinson, M., et al. (2013). Targeting RNA foci in iPSC-derived motor neurons from ALS patients with a C9ORF72 repeat expansion. *Sci. Transl. Med.* 5:208ra149. doi: 10.1126/scitranslmed.3007529

Schipper, L. J., Raaphorst, J., Aronica, E., Baas, F., de Haan, R., de Visser, M., et al. (2016). Prevalence of brain and spinal cord inclusions, including dipeptide repeat proteins, in patients with the C9ORF72 hexanucleotide repeat expansion: a systematic neuropathological review. *Neuropathol. Appl. Neurobiol.* 42, 547–560. doi: 10.1111/nan.12284

Schludi, M., May, S., Grässer, F., Rentzsch, K., Kremmer, E., Küpper, C., et al. (2015). Distribution of dipeptide repeat proteins in cellular models and C9orf72 mutation cases suggests link to transcriptional silencing. *Acta Neuropathol.* 130, 537–555. doi: 10.1007/s00401-015-1450-z

Schludi, M. H., Becker, L., Garrett, L., Gendron, T. F., Zhou, Q., Schreiber, F., et al. (2017). Spinal poly-GA inclusions in a C9orf72 mouse model trigger motor deficits and inflammation without neuron loss. *Acta Neuropathol.* 134, 241–254. doi: 10.1007/s00401-017-1711-0

Sellier, C., Campanari, M. L., Julie Corbier, C., Gaucherot, A., Kolb-Cheynel, I., Oulad-Abdelghani, M., et al. (2016). Loss of C9ORF72 impairs autophagy and synergizes with polyQ Ataxin-2 to induce motor neuron dysfunction and cell death. *EMBO J.* 35, 1276–1297. doi: 10.15252/embj.201593350

Shah, S. Z. A., Zhao, D., Hussain, T., Sabir, N., and Yang, L. (2018). Regulation of MicroRNAs-mediated autophagic flux: a new regulatory avenue for neurodegenerative diseases with focus on prion diseases. *Front. Aging Neurosci.* 10:139. doi: 10.3389/fnagi.2018.00139

Shi, Y., Lin, S., Staats, K. A., Li, Y., Chang, W. H., Hung, S. T., et al. (2018). Haploinsufficiency leads to neurodegeneration in C9ORF72 ALS/FTD human induced motor neurons. *Nat. Med.* 24, 313–325. doi: 10.1038/nm.4490

Shinozaki, Y., Shibata, K., Yoshida, K., Shigetomi, E., Gachet, C., Ikenaka, K., et al. (2017). Transformation of astrocytes to a neuroprotective phenotype by microglia via P2Y1 receptor downregulation. *Cell Rep.* 19, 1151–1164. doi: 10.1016/j.celrep.2017.04.047

Simón-Sánchez, J., Dopper, E. G., Cohn-Hokke, P. E., Hukema, R. K., Nicolaou, N., Seelaar, H., et al. (2012). The clinical and pathological phenotype of C9ORF72 hexanucleotide repeat expansions. *Brain* 135, 723–35. doi: 10.1093/brain/awr353

Sofroniew, M. V., and Vinters, H. V. (2010). Astrocytes: biology and pathology. *Acta Neuropathol.* 119, 7–35. doi: 10.1007/s00401-009-0619-8

Sullivan, P. M., Zhou, X., Robins, A. M., Paushter, D. H., Kim, D., Smolka, M. B., et al. (2016). The ALS/FTLD associated protein C9orf72 associates with SMCR8 and WDR41 to regulate the autophagy-lysosome pathway. *Acta Neuropathol. Commun.* 4:51. doi: 10.1186/s40478-016-0324-5

Szepesi, Z., Manouchehrian, O., Bachiller, S., and Deierborg, T. (2018). Bidirectional microglia-neuron communication in health and disease. *Front. Cell. Neurosci.* 12:323. doi: 10.3389/fncel.2018.00323

Tanaka, Y., Chambers, J. K., Matsuwaki, T., Yamanouchi, K., and Nishihara, M. (2014). Possible involvement of lysosomal dysfunction in pathological changes of the brain in aged progranulin-deficient mice. *Acta Neuropathol. Commun.* 2:78. doi: 10.1186/s40478-014-0078-x

Taylor, J. P., Brown, R. H. Jr., and Cleveland, D. W. (2016). Decoding ALS: from genes to mechanism. *Nature* 539, 197–206. doi: 10.1038/nature20413

Umoh, M. E., Dammer, E. B., Dai, J., Duong, D. M., Lah, J. J., Levey, A. I., et al. (2018). A proteomic network approach across the ALS-FTD disease spectrum resolves clinical phenotypes and genetic vulnerability in human brain. *EMBO Mol. Med.* 10, 48–62. doi: 10.15252/emmm.201708202

van Blitterswijk, M., DeJesus-Hernandez, M., Niemantsverdriet, E., Murray, M. E., Heckman, M. G., Diehl, N. N., et al. (2013). Association between repeat sizes and clinical and pathological characteristics in carriers of C9ORF72 repeat expansions (Xpansize-72): a cross-sectional cohort study. *Lancet Neurol.* 12, 978–988. doi: 10.1016/S1474-4422(13)70210-2

Varcianna, A., Myszczynska, M. A., Castelli, L. M., O'Neill, B., Kim, Y., Talbot, J., et al. (2019). Micro-RNAs secreted through astrocyte-derived extracellular vesicles cause neuronal network degeneration in C9orf72 ALS. *EBioMedicine* 40, 626–635. doi: 10.1016/j.ebiom.2018.11.067

Verkhratsky, A., and Nedergaard, M. (2018). Physiology of astroglia. *Physiol. Rev.* 98, 239–389. doi: 10.1152/physrev.00042.2016

Westergard, T., Jensen, B. K., Wen, X., Cai, J., Kropf, E., Iacovitti, L., et al. (2016). Cell-to-cell transmission of dipeptide repeat proteins linked to C9orf72-ALS/FTD. *Cell Rep.* 17, 645–652. doi: 10.1016/j.celrep.2016.09.032

Zamanian, J. L., Xu, L., Foo, L. C., Nouri, N., Zhou, L., Giffard, R. G., et al. (2012). Genomic analysis of reactive astrogliosis. *J. Neurosci.* 32, 6391–6410. doi: 10.1523/JNEUROSCI.6221-11.2012

Zhang, Y. J, Gendron, T. F., Grima, J. C., Sasaguri, H., Jansen-West, K., Xu, Y. F., et al. (2016). C9ORF72 poly(GA) aggregates sequester and impair HR23 and nucleocytoplasmic transport proteins. *Nat. Neurosci.* 19, 668– 677. doi: 10.1038/nn.4272

Zhang, Y. J., Gendron, T. F., Ebbert, M. T. W., O'Raw, A. D., Yue, M., Jansen-West, K., et al. (2018). Poly(GR) impairs protein translation and stress granule dynamics in C9orf72-associated frontotemporal dementia and amyotrophic lateral sclerosis. *Nat. Med.* 24, 1136–1142. doi: 10.1038/s41591-018-0071-1

Zu, T., Gibbens, B., Doty, N. S., Gomes-Pereira, M., Huguet, A., Stone, M. D., et al. (2011). Non-ATG-initiated translation directed by microsatellite expansions. *Proc. Natl. Acad. Sci. U S A.* 108, 260–265. doi: 10.1073/pnas.1013343108

Zu, T., Liu, Y., Bañez-Coronel, M., Reid, T., Pletnikova, O., Lewis, J., et al. (2013). RAN proteins and RNA foci from antisense transcripts in C9ORF72 ALS and frontotemporal dementia. *Proc. Natl. Acad. Sci. U S A.* 110, E4968–E4977. doi: 10.1073/pnas.1315438110

Conflict of Interest Statement: The authors declare that the research was conducted in the absence of any commercial or financial relationships that could be construed as a potential conflict of interest.

frontiers in Neuroscience

MINI REVIEW
published: 16 May 2019
doi: 10.3389/fnins.2019.00506

Genome Wide Association Study and Next Generation Sequencing: A Glimmer of Light Toward New Possible Horizons in Frontotemporal Dementia Research

Miriam Ciani[1,2†], Luisa Benussi[1†], Cristian Bonvicini[1] and Roberta Ghidoni[1]*

[1] Molecular Markers Laboratory, IRCCS Istituto Centro San Giovanni di Dio Fatebenefratelli, Brescia, Italy, [2] Department of Molecular and Translational Medicine, University of Brescia, Brescia, Italy

Frontotemporal Dementia (FTD) is a focal neurodegenerative disease, with a strong genetic background, that causes early onset dementia. The present knowledge about the risk loci and causative mutations of FTD mainly derives from genetic linkage analysis, studies of candidate genes, Genome-Wide Association Studies (GWAS) and Next-Generation Sequencing (NGS) applications. In this review, we report recent insights into the genetics of FTD, and, specifically, the results achieved thanks to GWAS and NGS approaches. Linkage studies of large FTD pedigrees have prompted the identification of causal mutations in different genes: mutations in *C9orf72*, *MAPT*, and *GRN* genes explain the large majority of cases with a high family history of the disease. In cases with a less clear inheritance, GWAS and NGS have contributed to further understand the genetic picture of FTD. GWAS identified several common genetic variants with a modest risk effect. Of interest, many of these variants are in genes belonging to the endo-lysosomal pathway, the immune response and neuronal survival. On the opposite, the NGS approach allowed the identification of rare variants with a strong risk effect. These variants were identified in known FTD-associated genes and again in genes involved in the endo-lysosomal pathway and in the immune response. Interestingly, both approaches demonstrated that several genes are associated to multiple neurodegenerative disorders including FTD. Thanks to these complementary approaches, the genetic picture of FTD is becoming more clear and novel key molecular processes are emerging. This will foster opportunities to move toward prevention and therapy for this incurable disease.

Keywords: frontotemporal dementia, genome wide association study, next generation sequencing, genetic mutations, genetic rare variants, genetic common variants

OPEN ACCESS

Edited by:
Annakaisa Haapasalo,
University of Eastern Finland, Finland

Reviewed by:
Romina Vuono,
University of Cambridge, United Kingdom
Serena Stanga,
University of Turin, Italy

****Correspondence:***
Luisa Benussi
lbenussi@fatebenefratelli.eu

† These authors have contributed equally to this work

Specialty section:
This article was submitted to Neurodegeneration, a section of the journal Frontiers in Neuroscience

Received: *29 January 2019*
Accepted: *02 May 2019*
Published: *16 May 2019*

Citation:
Ciani M, Benussi L, Bonvicini C and Ghidoni R (2019) Genome Wide Association Study and Next Generation Sequencing: A Glimmer of Light Toward New Possible Horizons in Frontotemporal Dementia Research. Front. Neurosci. 13:506. doi: 10.3389/fnins.2019.00506

INTRODUCTION

Genetic understanding of neurodegenerative diseases has considerably increased over the years, favoring the identification of possible targets for new potential therapies.

In this review, we report the most recent genetic insights regarding Frontotemporal Dementia (FTD), a focal neurodegenerative disease affecting the frontal and temporal lobes of the brain.

FTD has a heterogeneous clinical presentation: behavioral abnormalities are prominent in the behavioral variant FTD (bvFTD) (Rascovsky et al., 2011), while language disabilities characterize the Primary Progressive Aphasias (PPAs) (Gorno-Tempini et al., 2011). In addition, the FTD clinical presentation may include movement disorders, such as Progressive Supranuclear Palsy (PSP) and Corticobasal Syndrome (Litvan et al., 1996; Armstrong et al., 2013). Once considered a rare disorder, nowadays FTD is considered a common form of early-onset dementia, with a mean age of presentation under 65 years old (Ratnavalli et al., 2002; Knopman et al., 2004; Coyle-Gilchrist et al., 2016).

Frontotemporal Dementia has a strong genetic background: 30–40% of FTD patients have a positive family history and, even if a clear autosomal dominant inheritance pattern is often difficult to trace, a high family history is present in roughly 15% of FTD patients (Rohrer et al., 2009; Wood et al., 2013; Fostinelli et al., 2018). Linkage studies of large families with dominant inheritance pattern for FTD have led to the identification of causative mutations in different genes. Mutations in the microtubule associated protein tau gene (*MAPT*), located on chromosome 17 and encoding for tau protein, were first identified in 1998 in FTD patients with tau-positive brain inclusions (Hutton et al., 1998; Poorkaj et al., 1998). Genetic research in FTD remained almost silent till 2006, when null mutations in the *GRN* gene, encoding for progranulin, were found in FTD families with a positive linkage on chromosome 17, in the proximity of *MAPT* (Baker et al., 2006; Cruts et al., 2006). So far, all identified pathogenic *GRN* mutations exert a null effect on progranulin protein: therefore, mutations can be easily captured by plasma/serum dosage (Ghidoni et al., 2008, 2012; Finch et al., 2009; Sleegers et al., 2009). In 2011, an additional major genetic determinant was found in families with FTD and Amyotrophic lateral sclerosis (ALS): an intronic expansion of a hexanucleotide repeat in the *C9orf72* gene, located on chromosome 9, where previous linkage studies had had identified an FTD/ALS locus (DeJesus-Hernandez et al., 2011; Renton et al., 2011). *MAPT*, *GRN*, and *C9orf72* mutations, detected in up to 74% of patients with high family history, represent the most frequent genetic cause of FTD; nowadays 54 and 79 mutations have been described for *MAPT* and *GRN*, respectively.[1,2] Of note, a compound heterozygosity of two *MAPT* mutations (transmitted by the unaffected parents) was found in a sporadic case, thus highlighting that mutations can be found also in sporadic cases (Anfossi et al., 2011). However, considering FTD patients with lower family history and apparently sporadic cases, mutations in these genes are found in roughly 15% of cases (Wood et al., 2013; Fostinelli et al., 2018). Additionally, rare FTD-causing mutations have been found in: the Valosin gene (*VCP*), that was first reported to be mutated in families with hereditary inclusion body myopathy with Paget disease of the bone and FTD; the Charged multivesicular body protein 2B (*CHMP2B*), with only one proven pathogenic mutation described in 2005 and segregating with FTD; the TAR DNA binding protein (*TARDP*) and the Fused in Sarcoma (*FUS*) genes, two well established ALS-associated genes, playing a minor role also in FTD (Pottier et al., 2015). Together, mutations in these genes account for a large proportion of FTD pedigrees with a high family history of the disease, but only a minority of apparently sporadic patients or patients with a less clear family history.

Thus, deciphering the "missing heritability" of the remaining FTD cases represents one of the main challenges in FTD research. In this direction, Genome-Wide Association Studies (GWAS) and Next-Generation Sequencing (NGS) technologies represent a great potential.

GENOME WIDE ASSOCIATION STUDIES AND THE "COMMON-VARIANTS THEORY"

For many years, the candidate-gene hypothesis and genetic linkage studies have been the predominant approaches to guide the discovery of FTD-associated genes (Loy et al., 2014). However, these approaches were not enough to fill the gap regarding the missing heritability of most cases. Thus, the candidate-gene studies have been completed with hypothesis-free approaches like GWAS studies, which are based on the analysis of common variants widely distributed in the genome, with a modest effect (Yang et al., 2010; Weiner et al., 2017). Here, the "common-variants theory," which claims that common disease-causing variants can be identified in every human population that manifest a given disease, became the predominant molecular paradigm. GWAS is based on the use of specific genotyping arrays that interrogate an independent set of variants within the whole genome in related/unrelated individuals, identifying an association between one/more variants and pathological traits (Mishra et al., 2017). This approach has allowed the identification of genetic alterations conferring disease risk revealing that susceptibility factors can be enriched in genes clumped into disease-relevant pathways, offering new angles for research and therapeutic intervention (Ferrari et al., 2015).

A number of genomic regions that may increase the FTD risk has been identified (**Table 1**).

The importance of the transmembrane protein 106B (*TMEM106B*) gene, identified by the first GWAS on FTD patients (Van Deerlin et al., 2010), has been confirmed in different studies (Busch et al., 2016; Nicholson and Rademakers, 2016; Gallagher et al., 2017; Rhinn and Abeliovich, 2017). In Van Deerlin et al. (2010), the first team recognized *TMEM106B* as genetic risk factor in patients with a specific neuropathology. However, when the authors tried to validate this result in a more heterogeneous group of probable FTD cases, lacking post-mortem confirmation, the association of *TMEM106B* with FTD was lost. Interestingly, van Blitterswijk et al. (2014) identified *TMEM106B* variants which appeared to alter the *C9orf72* phenotype and cause later disease onset. Similarly, specific variants in this gene influence *GRN*-associated FTD risk, reducing the disease penetrance in *GRN* mutation carriers (Finch et al., 2011). Latecomer, the FTD risk linked to *TMEM106B* variants seems to be associated to lysosomal

[1] http://www.molgen.ua.ac.be/ADMutations/

[2] https://www.alzforum.org

dysfunctions, being *TMEM106B* a lysosomal protein (Nicholson and Rademakers, 2016; Klein et al., 2017). Recently, Pottier replicated the previously reported *TMEM106B* association and identified a novel genome-wide significant locus at the GDNF family receptor alpha 2 (*GFRA2*) gene, which encodes for a neurotropic factor with a key role involved in neuron survival and differentiation (Pottier et al., 2018). Moreover, in a recent GWAS study, a link between the C6orf10/LOC101929163 locus and the age of onset in *C9orf72* mutation-carriers was identified, supporting the involvement of autophagy in modulating *C9orf72* disease (Zhang et al., 2018).

In the largest FTD-GWAS so far, the *HLA*, *RAB38*, and Cathepsin C (*CTSC*) genes were recognized as FTD risk loci, suggesting alterations in immune system, lysosomal and autophagic pathways (Ferrari et al., 2014). An immune-related genetic enrichment in FTD was also described in a very exhaustive study in which a systematic investigation of genetic overlap between immune-mediated diseases and the spectrum of FTD-related disorders was performed. In addition, the authors identified novel susceptibility loci within the Leucine rich repeat kinase 2 (*LRRK2*), the TBK1 binding protein 1 (*TBKBP1*), and the PiggyBac transposable element derived (*5PGBD5*) genes, involved in cell survival, immunity processes and genomic rearrangements, respectively (Broce et al., 2018). Interestingly, GWAS was also used to evaluate shared pathobiology between neurodegenerative disorders. Recently, Karch et al. (2018) highlighted a genetic overlap between FTD and ALS, identifying shared common variants near *C9orf72* and the Unc-13 homolog A (*UNC13A*) genes, linked to neuronal vitality. Additionally, the Major histocompatibility complex (*HLA*), the *MAPT*, and the Apolipoprotein E (*APOE*) regions were associated to FTD, Alzheimer's disease (AD) and Parkinson's Disease (PD) risk, supporting a genetic pleiotropy in these neurodegenerative diseases (Ferrari et al., 2017). Furthermore, the Elongator acetyltransferase complex subunit 2 (*ELP2*) gene, a component of the Elongator complex which regulates the activity of RNA polymerase II, was identified as susceptible gene in patients with FTD and FTD-ALS (Dong et al., 2015; Taskesen et al., 2018). Additionally, Mishra et al. (2017) reported an association of *APOE* and the Translocase of outer mitochondrial membrane 40 (*TOMM40*) genes with bvFTD, and the Rho GTPase activating protein 35 (*ARHGAP35*) and the Serpin family A member 1 (*SERPINA1*) genes with progressive non-fluent aphasia. Further, they found the ε2 and ε4 alleles of *APOE* harboring protective and risk increasing effects, respectively, in FTD clinical subtypes (Mishra et al., 2017). *TOMM40* provided insight into a metabolic mitochondrial basis for the etiology of FTD (Roses et al., 2016); instead, the novel associations of *ARHGAP35* and *SERPINA1* with PNFA revealed a potential role of the stress-signaling pathway in FTD pathophysiology (Mishra et al., 2017). In 2015, the RFNG O-fucosylpeptide 3-beta-N-acetylglucosaminyltransferase (RFNG) and the Apoptosis-associated tyrosine kinase (AATK) genes, involved in neuronal genesis and differentiation and axon outgrowth, were recognized as genetic risk factors in an Italian FTD cohort (Ferrari et al., 2015). A GWAS on AD, FTD, and PSP evidenced the ATP binding cassette subfamily A member 7 (*ABCA7*), the Dysferlin (*DYSF*), and the PAX interacting protein 1 (*PAXIP1*) as susceptibility genes (Chen et al., 2015), known to be implicated in lipid metabolism, immune

TABLE 1 | Genome-Wide Association Studies (GWAS) mediated identification of potential pathways contributing to FTD.

Genes	Pathways	References
TMEM106B	Lysosomal function	Van Deerlin et al., 2010; Finch et al., 2011; Busch et al., 2016; Nicholson and Rademakers, 2016; Gallagher et al., 2017; Rhinn and Abeliovich, 2017; Pottier et al., 2018
HLA	Immune response	Ferrari et al., 2014; Broce et al., 2018
RAB38, CTSC	Vesicle-trafficking; lysosomal function	Ferrari et al., 2014
C9orf72, UNC13A	Neuronal survival	Karch et al., 2018
HLA, MAPT, APOE	Intracellular vesicular trafficking; immune response; endo/lysosomal processes	Ferrari et al., 2017
GFRA2	Neuron survival and differentiation	Pottier et al., 2018
C6orf10/LOC101929163	Microglial/autophagy pathways	Zhang et al., 2018
LRRK2, TBKBP1 5PGBD5	Enzyme function; immune response; sequence-specific genomic rearrangements	Broce et al., 2018
ELP2	RNA transcription	Taskesen et al., 2018
APOE, TOMM40 SERPINA1, ARHGAP35	Lipid metabolism; metabolic and mitochondrial pathways Stress-signaling pathway Stress-signaling pathway	Mishra et al., 2017
RFNG, AATK	Neuronal genesis and differentiation; axon outgrowth	Ferrari et al., 2015
ABCA7, DYSF, PAXIP1	Lipid metabolism; immune response; membrane regeneration and repair: genome stability; Cell survival	Chen et al., 2015

processes, mitochondrial abnormalities, and genome stability, respectively (Muñoz and Rouse, 2009; Vincent et al., 2016; Aikawa et al., 2018).

Although GWAS has played an important role in the discovery of risk variants for a specific trait, the identified loci are able to explain only a modest fraction of the predicted genetic variance. Technological limits, including small sample size, allelic heterogeneity and small effect sizes of these genetic variants, in addition to conceptual limitations, once again linked to the inability of common variants in explaining all the still remaining forms without an identified genetic factor, have again influenced the transition to a new approach: from common variants with small effect sizes to rare variants with a higher penetrance.

NEXT-GENERATION SEQUENCING AND THE "RARE-VARIANTS THEORY"

A further significant contribution toward the knowledge of genetic FTD background came from the "rare-variants theory": rare variants widespread in the genome could represent the missing genetic components for complex diseases. Interestingly, these variants can have determining effects on clinical phenotype, in terms of severity and earlier onset (Xu et al., 2018).

In this scenario, novel methodological issues have raised, due to the unavailability of suitable technologies to unravel the huge number of rare variants throughout the genome. The development of NGS has revolutionized the genetic research, allowing: the analysis of entire genomes (Whole Genome Sequencing, WGS); specific loci or selected candidate genes Targeted Sequencing (TS), or sequencing of exons of all coding genes (Whole Exome Sequencing, WES) (Pottier et al., 2015; Williams et al., 2016; Bonvicini et al., 2019). Thus, in this technological Era, a new opportunity is offered: the genetic analysis is no longer limited to the sequencing of the whole coding sequence of genes known for their implication in a disease, but it is also extended to the parallel analysis of groups of genes acting together in disease-relevant pathways (Boyle et al., 2017).

Thanks to NGS, the "rare variants hypothesis" has been explored also in FTD: discoveries achieved in this field in the last years are reported in **Table 2**.

Interestingly, a rare variant in the Alpha-synuclein (*SNCA*) gene, cause of autosomal dominant PD, was observed in

TABLE 2 | NGS mediated identification of rare variants associated with FTD.

Mutated gene	Main results	Approaches	References
PSEN1, MAPT, APP	- Identification of known and novel variants in *PSEN1*, *MAPT*, and *APP* - FTD mutation carriers: low age of onset; more rapid progression	WES	Xu et al., 2018
SNCA	- Identification of a rare variant in *SNCA* in a bvFTD patient - Pleiotropic effect of *SNCA* - Alterations of mitochondrial processes in FTD	NGS	Breza et al., 2018
VCP	- Identification of known and novel variants in *VCP* both in family members and unrelated cases - Pleiotropic effect of *VCP*→ heterogeneous clinical features - FTD associated with alterations of ubiquitin system, vesicle transport, proteostasis, neural vitality, and stress response	WES	Abrahao et al., 2016; Saracino et al., 2018; Wong et al., 2018
SORT1	- Identification of rare known and novel variants in *SORT1* in Belgian, Spanish, Italian, and Portuguese cohorts - *SORT1* further confirmed as genetic risk factor for FTD - Defects in protein transport and cellular transduction	NGS	Philtjens et al., 2018
GRN, CSF1R	- Identification of a *GRN* known pathogenic variant in a bvFTD case	NGS	Kim et al., 2018
AARS2	- Identification of novel variants in two dementia-related genes as *CSF1R* and *AARS2* in bvFTD patients - Immunity response, inflammatory processes and mitochondrial function involvement in FTD etiology confirmed		
TREM2, GRN	- Identification of a rare variant in *TREM2* - Identification of two novel nonsense *GRN* mutations - *TREM2* and *GRN* further confirmed as FTD risk genes - Immune pathways and inflammatory responses are altered in FTD	TS	Ng et al., 2018
TYROBP	- Identification of a rare variant in *TYROBP* - Immune pathway and inflammatory response involvement in FTD etiology confirmed	NGS	Giannoccaro et al., 2017
TBKBP1	- Identification of novel deletions and missense mutations - Immune response involvement in FTD etiology confirmed	TS	van der Zee et al., 2017
SQSTM1	- Identification of rare variants in an extended cohort of FTD patients - Autophagy-lysosomal alterations in FTD	WES	van der Zee et al., 2014
CCNF	- NGS allowed to reveal, in a locus previously identified, a missense mutation in *CCNF* - Combined technologies for a better understanding of diseases - Impairment of protein homeostasis mediated by *CCNF*	NGS, linkage analysis	Williams et al., 2016

a bvFTD patient, suggesting alterations in mitochondrial processes also in FTD (Mullin and Schapira, 2013; Breza et al., 2018). A WES study was conducted to perform a genetic exploration in patients with early onset forms of dementia, including FTD. Specifically, Xu et al. (2018) focused on 89 dementia-related causing and susceptible genes, identifying known pathogenic mutations in *PSEN1* (Presenilin 1) and *MAPT*, and one novel pathogenic variant in the Amyloid beta precursor protein (*APP*) gene. The authors also revealed that all the identified mutations caused dementia with an earlier age of onset and a more rapid disease progression (Xu et al., 2018).

Recently, a group of FTD subjects was screened for different known FTD genes through a WES approach: this study identified two novel and one already known *VCP* mutations in three patients with a clinical diagnosis of FTD (Wong et al., 2018). In addition, Saracino et al. (2018) analyzed *VCP* in an FTD cohort, observing seven mutations in unrelated families, including three novel mutations segregating with dementia. Interestingly, a novel rare missense variant in *VCP* was also described in a FTD subject, member of a family presenting an unusual intra-familiar association of a specific myopathy with ALS and FTD (Abrahao et al., 2016). In all these cases, NGS has permitted to reveal interesting mutations in *VCP*, implicated in ubiquitin pathways, vesicle transport, proteostasis, neural vitality and stress response (Meyer and Weihl, 2014; Rainero et al., 2017).

By gene target re-sequencing, rare variants within the Sortilin 1 (*SORT1*) gene were identified in a Belgian FTD cohort. A subsequent study of cohorts sampled in Spain, Italy and Portugal revealed additional non-synonymous variants in European patients. Specifically, *SORT1* is a known FTD risk factor: the encoded protein is a neuronal receptor involved in intracellular protein transport and cellular signal transduction (Philtjens et al., 2018).

In sporadic FTD patients without a recognized genetic cause in the well-known FTD related genes (*MAPT*, *GRN*, and *C9orf72*), novel variants were identified in two dementia-related genes, the Colony stimulating factor 1 receptor (*CSF1R*) and the Mitochondrial alanyl-tRNA synthetase 2 (*AARS2*), suggesting new genes to be considered for a genetic FTD diagnosis. *CSF1R*, which shows important role in innate immunity and inflammatory processes, and *AARS2*, involved in mitochondrial functions, highlight alterations of these processes in the FTD etiology (Kim et al., 2018).

Recently, a TS of 12 FTD-associated genes was performed: this study revealed a rare variant in the Triggering receptor expressed on myeloid cells 2 (*TREM2*) and two nonsense *GRN* mutations (Ng et al., 2018).

In Giannoccaro et al. (2017), a panel of dementia-associated genes was explored in an Italian group of ALS/FTD pedigrees by using a TS approach: genetic variants in additional ALS and dementia-related genes were found in four pedigrees, including a rare variant in the Tyrosine kinase binding protein (*TYROBP*) gene. The *TYROBP* protein, which interacts with several other proteins like *TREM2*, is specifically involved in immune pathway and inflammatory response (Giannoccaro et al., 2017).

In addition, the TBK1 binding protein 1 (*TBKBP1*) was screened in a wide cohort of FTD, ALS, FTD-ALS subjects through a TS approach, identifying deletions and missense mutations in this gene involved in immune response (van der Zee et al., 2017).

In van der Zee et al. (2014), rare variants in the Sequestosome 1 (*SQSTM1*) gene were identified in a cohort of FTD patients, suggesting a role of this gene in the etiology of disease.

Next-Generation Sequencing coupled with conventional approaches is considered the cutting-edge approach for a better understanding of the genetic underpinnings of complex diseases: studies employing NGS have identified rare variants within regions previously prioritized by GWAS, along with novel variants in previously unidentified genes (Williams et al., 2016; Patel et al., 2017). As for GWAS, the linkage analysis has again emerged as an extremely powerful method for the identification of variants implicated in disease in conjunction with WGS filtering approaches (Ott et al., 2015). As regards, in Williams et al. (2016) a genome-wide linkage analysis identified a novel disease locus on chromosome 16p13.3 in a large ALS/FTD cohort. NGS allowed to reveal at this locus a novel missense mutation in Cyclin F (*CCNF*) gene, in which specific mutations have been subsequently described in FTD-ALS subjects (Lee et al., 2018), pointing toward an impairment of protein homeostasis in this complex disorder (Williams et al., 2016; Pan et al., 2017).

CONCLUDING REMARKS

Overall, this mini-review points up that GWAS and NGS, based on the analysis of different variants with moderate-to-strong effect, have concurrently revealed the implication of common molecular pathways in FTD. In particular, these approaches revealed genetic alterations in genes acting together in molecular pathways involved in neuronal-viability and survival, vesicle trafficking, immune and inflammatory response, and energy metabolism. Noteworthy, it has been suggested that defects of all these primary processes could be interrelated at different levels, leading to the degeneration of the whole system and, thus, causing the disease (Ramanan and Saykin, 2013). In particular, multiple studies consolidate the view that immune and endo/lysosomal processes are key players in the pathobiology of these disorders. In future studies, the combination of different molecular approaches also at protein and metabolic levels will definitely help in further clarifying the role of these pathways in FTD pathogenesis and their possible interconnection. In this way, we will foster our potential to move toward effective prevention and therapy for this incurable neurodegenerative disease.

AUTHOR CONTRIBUTIONS

MC, LB, CB, and RG gave their substantial contribution to conception and design of the manuscript and drafting

the manuscript, revising it critically for important intellectual content. All authors have approved the manuscript in its present form for publication. All authors agreed to be accountable for all aspects of the work in ensuring that questions related to the accuracy or integrity of any part of the work are appropriately investigated and resolved.

FUNDING

This work was supported by the Italian Ministry of Health (Ricerca Corrente) and the EU Joint Programme – Neurodegenerative Disease Research (JPND2013 www.jpnd.eu) – Funding organization Italy, Italian Ministry of Health.

REFERENCES

Abrahao, A., Abath, N. O., Kok, F., Zanoteli, E., Santos, B., Pinto, W. B., et al. (2016). One family, one gene and three phenotypes: A novel VCP (valosin-containing protein) mutation associated with myopathy with rimmed vacuoles, amyotrophic lateral sclerosis and frontotemporal dementia. *J. Neurol. Sci.* 368, 352–358. doi: 10.1016/j.jns.2016.07.048

Aikawa, T., Holm, M. L., and Kanekiyo, T. (2018). ABCA7 and pathogenic pathways of alzheimer's disease. *Brain Sci.* 8:E27. doi: 10.3390/brainsci8020027

Anfossi, M., Vuono, R., Maletta, R., Virdee, K., Mirabelli, M., Colao, R., et al. (2011). Compound heterozygosity of 2 novel MAPT mutations in frontotemporal dementia. *Neurobiol. Aging* 32, 757.e1–757.e11. doi: 10.1016/j.neurobiolaging.2010.12.013

Armstrong, M. J., Litvan, I., Lang, A. E., Bak, T. H., Bhatia, K. P., Borroni, B., et al. (2013). Criteria for the diagnosis of corticobasal degeneration. *Neurology* 80, 496–503. doi: 10.1212/WNL.0b013e31827f0fd1

Baker, M., Mackenzie, I. R., Pickering-Brown, S. M., Gass, J., Rademakers, R., Lindholm, C., et al. (2006). Mutations in progranulin cause tau-negative frontotemporal dementia linked to chromosome 17. *Nature* 442, 916–919. doi: 10.1038/nature05016

Bonvicini, C., Scassellati, C., Benussi, L., Di Maria, E., Maj, C., Ciani, M., et al. (2019). Next generation sequencing analysis in early onset dementia patients. *J. Alzheimers Dis.* 67, 243–256. doi: 10.3233/JAD-180482

Boyle, E. A., Li, Y. I., and Pritchard, J. K. (2017). An expanded view of complex traits: from polygenic to omnigenic. *Cell* 169, 1177–1186. doi: 10.1016/j.cell.2017.05.038

Breza, M., Koutsis, G., Karadima, G., Potagas, C., Kartanou, C., Papageorgiou, S. G., et al. (2018). The different faces of the p. A53T alpha-synuclein mutation: a screening of Greek patients with parkinsonism and/or dementia. *Neurosci. Lett.* 672, 136–139. doi: 10.1016/j.neulet.2017.12.015

Broce, I., Karch, C. M., Wen, N., Fan, C. C., Wang, Y., Tan, C. H., et al. (2018). Immune-related genetic enrichment in frontotemporal dementia: An analysis of genome-wide association studies. *PLoS. Med.* 15:e1002487. doi: 10.1371/journal.pmed.1002504

Busch, J. I., Unger, T. L., Jain, N., Tyler, S. R., Charan, R. A., and Chen-Plotkin, A. S. (2016). Increased expression of the frontotemporal dementia risk factor TMEM106B causes C9orf72-dependent alterations in lysosomes. *Hum. Mol. Genet.* 25, 2681–2697. doi: 10.1093/hmg/ddw127

Chen, J. A., Wang, Q., Davis-Turak, J., Li, Y., Karydas, A. M., Hsu, S. C., et al. (2015). A multiancestral genome-wide exome array study of Alzheimer disease, frontotemporal dementia, and progressive supranuclear palsy. *JAMA Neurol.* 72, 414–422. doi: 10.1001/jamaneurol.2014.4040

Coyle-Gilchrist, I. T., Dick, K. M., Patterson, K., Vázquez Rodríquez, P., Wehmann, E., Wilcox, A., et al. (2016). Prevalence, characteristics, and survival of frontotemporal lobar degeneration syndromes. *Neurology* 86, 1736–1743. doi: 10.1212/WNL.0000000000002638

Cruts, M., Gijselinck, I., van der Zee, J., Engelborghs, S., Wils, H., Pirici, D., et al. (2006). Null mutations in progranulin cause ubiquitin-positive frontotemporal dementia linked to chromosome 17q21. *Nature* 442, 920–924. doi: 10.1038/nature05017

DeJesus-Hernandez, M., Mackenzie, I. R., Boeve, B. F., Boxer, A. L., Baker, M., Rutherford, N. J. et al. (2011). Expanded GGGGCC hexanucleotide repeat in noncoding region of C9ORF72 causes chromosome 9p-linked FTD and ALS. *Neuron* 72, 245–256. doi: 10.1016/j.neuron.2011.09.011

Dong, C., Lin, Z., Diao, W., Li, D., Chu, X., Wang, Z., et al. (2015). The Elp2 subunit is essential for elongator complex assembly and functional regulation. *Structure* 23, 1078–1086. doi: 10.1016/j.str.2015.03.018

Ferrari, R., Grassi, M., Salvi, E., Borroni, B., Palluzzi, F., Pepe, D., et al. (2015). A genome-wide screening and SNPs-to-genes approach to identify novel genetic risk factors associated with frontotemporal dementia. *Neurobiol. Aging* 36:2904. doi: 10.1016/j.neurobiolaging.2015.06.005

Ferrari, R., Hernandez, D. G., Nalls, M. A., Rohrer, J. D., Ramasamy, A., Kwok, J. B., et al. (2014). Frontotemporal dementia and its subtypes: a genome-wide association study. *Lancet Neurol.* 13, 686–699. doi: 10.1016/S1474-4422(14)70065-1

Ferrari, R., Wang, Y., Vandrovcova, J., Guelfi, S., Witeolar, A., Karch, C. M., et al. (2017). Genetic architecture of sporadic frontotemporal dementia and overlap with Alzheimer's and Parkinson's diseases. *J. Neurol. Neurosurg. Psychiatry* 88, 152–164. doi: 10.1136/jnnp-2016-314411

Finch, N., Baker, M., Crook, R., Swanson, K., Kuntz, K., Surtees, R., et al. (2009). Plasma progranulin levels predict progranulin mutation status in frontotemporal dementia patients and asymptomatic family members. *Brain* 132, 583–591. doi: 10.1093/brain/awn352

Finch, N., Carrasquillo, M. M., Baker, M., Rutherford, N. J., Coppola, G., Dejesus-Hernandez, M., et al. (2011). TMEM106B regulates progranulin levels and the penetrance of FTLD in GRN mutation carriers. *Neurology* 76, 467–474. doi: 10.1212/WNL.0b013e31820a0e3b

Fostinelli, S., Ciani, M., Zanardini, R., Zanetti, O., Binetti, G., Ghidoni, R. et al. (2018). The heritability of frontotemporal lobar degeneration: validation of pedigree classification criteria in a Northern Italy cohort. *J. Alzheimers Dis.* 61, 753–760. doi: 10.3233/JAD-170661

Gallagher, M. D., Posavi, M., Huang, P., Unger, T. L., Berlyand, Y., Gruenewald, A. L., et al. (2017). A dementia-associated risk variant near TMEM106B alters chromatin architecture and gene expression. *Am. J. Hum. Genet.* 101, 643–663. doi: 10.1016/j.ajhg.2017.09.004

Ghidoni, R., Benussi, L., Glionna, M., Franzoni, M., and Binetti, G. (2008). Low plasma progranulin levels predict progranulin mutations in frontotemporal lobar degeneration. *Neurology* 71, 1235–1239. doi: 10.1212/01.wnl.0000325058.10218.fc

Ghidoni, R., Stoppani, E., Rossi, G., Piccoli, E., Albertini, V., Paterlini, A., et al. (2012). Optimal plasma progranulin cutoff value forpredicting null progranulin mutations in neurodegenerative diseases: a multicenter Italian study. *Neurodegener. Dis.* 9, 121–127. doi: 10.1159/000333132

Giannoccaro, M. P., Bartoletti-Stella, A., Piras, S., Pession, A., De Massis, P., Oppi, F., et al. (2017). Multiple variants in families with amyotrophic lateral sclerosis and frontotemporal dementia related to C9orf72 repeat expansion: further observations on their oligogenic nature. *J. Neurol.* 264, 1426–1433. doi: 10.1007/s00415-017-8540-x

Gorno-Tempini, M. L., Hillis, A. E., Weintraub, S., Kertesz, A., Mendez, M., Cappa, S. F., et al. (2011). Classification of primary progressive aphasia and its variants. *Neurology* 76, 1006–1014. doi: 10.1212/WNL.0b013e31821103e6

Hutton, M., Lendon, C. L., Rizzu, P., Baker, M., Froelich, S., Houlden, H., et al. (1998). Association of missense and 5′-splice-site mutations in tau with the inherited dementia FTDP-17. *Nature* 393, 702–705. doi: 10.1038/31508

Karch, C. M., Wen, N., Fan, C. C., Yokoyama, J. S., Kouri, N., Ross, O. A., et al. (2018). Selective genetic overlap between amyotrophic lateral sclerosis and diseases of the frontotemporal dementia spectrum. *JAMA Neurol.* 75, 860–875. doi: 10.1001/jamaneurol.2018.0372

Kim, E. J., Kim, Y. E., Jang, J. H., Cho, E. H., Na, D. L., Seo, S. W., et al. (2018). Analysis of frontotemporal dementia, amyotrophic lateral sclerosis, and other dementia-related genes in 107 Korean patients with frontotemporal dementia. *Neurobiol. Aging* 72:186. doi: 10.1016/j.neurobiolaging.2018.06.031

Klein, Z. A., Takahashi, H., Ma, M., Stagi, M., Zhou, M., Lam, T. T., et al. (2017). Loss of TMEM106B ameliorates lysosomal and frontotemporal dementia-related phenotypes in progranulin-deficient mice. *Neuron* 95, 281–296. doi: 10.1016/j.neuron.2017.06.026

Knopman, D. S., Petersen, R. C., Edland, S. D., Cha, R. H., and Rocca, W. A. (2004). The incidence of frontotemporal lobar degeneration in Rochester, Minnesota, 1990 through 1994. *Neurology* 62, 506–508. doi: 10.1212/01.WNL.0000106827.39764.7E

Lee, A., Rayner, S. L., Gwee, S. S. L., De Luca, A., Shahheydari, H., Sundaramoorthy, V., et al. (2018). Pathogenic mutation in the ALS/FTD gene, CCNF, causes elevated Lys48-linked ubiquitylation and defective autophagy. *Cell. Mol. Life Sci.* 75, 335–354. doi: 10.1007/s00018-017-2632-8

Litvan, I., Agid, Y., Calne, D., Campbell, G., Dubois, B., Duvoisin, R. C., et al. (1996). Clinical research criteria for the diagnosis of progressive supranuclear palsy (Steele-Richardson-Olszewski syndrome): report of the NINDS-SPSP international workshop. *Neurology* 47, 1–9. doi: 10.1212/wnl.47.1.1

Loy, C. T., Schofield, P. R., Turner, A. M., and Kwok, J. B. (2014). Genetics of dementia. *Lancet* 383, 828–840. doi: 10.1016/S0140-6736(13)60630-3

Meyer, H., and Weihl, C. C. (2014). The VCP/p97 system at a glance: connecting cellular function to disease pathogenesis. *J. Cell. Sci.* 127, 3877–3883. doi: 10.1242/jcs.093831

Mishra, A., Ferrari, R., Heutink, P., Hardy, J., Pijnenburg, Y., Posthuma, D., et al. (2017). Gene-based association studies report genetic links for clinical subtypes of frontotemporal dementia. *Brain* 140, 1437–1446. doi: 10.1093/brain/awx066

Mullin, S., and Schapira, A. (2013). α-synuclein and mitochondrial dysfunction in parkinson's disease. *Mol. Neurobiol.* 47, 587–597. doi: 10.1007/s12035-013-8394-x

Muñoz, I. M., and Rouse, J. (2009). Control of histone methylation and genome stability by PTIP. *EMBO Rep.* 10, 239–245. doi: 10.1038/embor.2009.21

Ng, A. S. L., Tan, Y. J., Yi, Z., Tandiono, M., Chew, E., Dominguez, J., et al. (2018). Targeted exome sequencing reveals homozygous TREM2 R47C mutation presenting with behavioral variant frontotemporal dementia without bone involvement. *Neurobiol. Aging* 68:160. doi: 10.1016/j.neurobiolaging.2018.04.003

Nicholson, A. M., and Rademakers, R. (2016). What we know about TMEM106B in neurodegeneration. *Acta Neuropathol.* 132, 639–651. doi: 10.1007/s00401-016-1610-9

Ott, J., Wang, J., and Leal, S. M. (2015). Genetic linkage analysis in the age of whole-genome sequencing. *Nat. Rev. Genet.* 16, 275–284. doi: 10.1038/nrg3908

Pan, C., Jiao, B., Xiao, T., Hou, L., Zhang, W., Liu, X., et al. (2017). Mutations of CCNF gene is rare in patients with amyotrophic lateral sclerosis and frontotemporal dementia from Mainland China. *Amyotroph. Lateral. Scler. Frontotemporal Degener.* 18, 265–268. doi: 10.1080/21678421.2017.1293111

Patel, T., Brookes, K. J., Turton, J., Chaudhury, S., Guetta-Baranes, T., Guerreiro, R., et al. (2017). Whole-exome sequencing of the BDR cohort: evidence to support the role of the PILRA gene in Alzheimer's disease. *Neuropathol. Appl. Neurobiol.* 44, 506–521. doi: 10.1111/nan.12452

Philtjens, S., Van Mossevelde, S., van der Zee, J., Wauters, E., Dillen, L., Vandenbulcke, M., et al. (2018). Rare nonsynonymous variants in SORT1 are associated with increased risk for frontotemporal dementia. *Neurobiol. Aging* 66:181. doi: 10.1016/j.neurobiolaging.2018.02.011

Poorkaj, P., Bird, T. D., Wijsman, E., Nemens, E., Garruto, R. M., Anderson, L., et al. (1998). Tau is a candidate gene for chromosome 17 frontotemporal dementia. *Ann. Neurol.* 43, 815–825. doi: 10.1002/ana.410430617

Pottier, C., Bieniek, K. F., Finch, N., van de Vorst, M., Baker, M., Perkersen, R., et al. (2015). Whole-genome sequencing reveals important role for TBK1 and OPTN mutations in frontotemporal lobar degeneration without motor neuron disease. *Acta Neuropathol.* 30, 77–92. doi: 10.1007/s00401-015-1436-x

Pottier, C., Zhou, X., Perkerson, R. B., Baker, M., Jenkins, G. D., Serie, D. J., et al. (2018). Potential genetic modifiers of disease risk and age at onset in patients with frontotemporal lobar degeneration and GRN mutations: a genome-wide association study. *Lancet Neurol.* 17, 548–558. doi: 10.1016/S1474-4422(18)30126-1

Rainero, I., Rubino, E., Michelerio, A., D'Agata, F., Gentile, S., and Pinessi, L. (2017). Recent advances in the molecular genetics of frontotemporal lobar degeneration. *Funct. Neurol.* 32, 7–16. doi: 10.11138/FNeur/2017.32.1.007

Ramanan, V. K., and Saykin, A. J. (2013). Pathways to neurodegeneration: mechanistic insights from GWAS in Alzheimer's disease, Parkinson's disease, and related disorders. *Am. J. Neurodegener. Dis.* 2, 145–175.

Rascovsky, K., Hodges, J. R., Knopman, D., Mendez, M. F., Kramer, J. H., Neuhaus, J., et al. (2011). Sensitivity of revised diagnostic criteria for the behavioural variant of frontotemporal dementia. *Brain* 134, 2456–2477. doi: 10.1093/brain/awr179

Ratnavalli, E., Brayne, C., Dawson, K., and Hodges, J. R. (2002). The prevalence of frontotemporal dementia. *Neurology* 58, 1615–1621.

Renton, A. E., Majounie, E., Waite, A., Simon-Sanchez, J., Rollinson, S., Gibbs, J. R., et al. (2011). A hexanucleotide repeat expansion in C9ORF72 is the cause of chromosome 9p21-linked ALS-FTD. *Neuron* 72, 257–268. doi: 10.1016/j.neuron.2011.09.010

Rhinn, H., and Abeliovich, A. (2017). Differential aging analysis in human cerebral cortex identifies variants in TMEM106B and GRN that regulate aging phenotypes. *Cell. Syst.* 4, 404–415. doi: 10.1016/j.cels.2017.02.009

Rohrer, J. D., Guerreiro, R., Vandrovcova, J., Uphill, J., Reiman, D., Beck, J., et al. (2009). The heritability and genetics of frontotemporal lobar degeneration. *Neurology* 73, 1451–1456. doi: 10.1212/WNL.0b013e3181bf997a

Roses, A., Sundseth, S., Saunders, A., Gottschalk, W., Burns, D., and Lutz, M. (2016). Understanding the genetics of APOE and TOMM40 and role of mitochondrial structure and function in clinical pharmacology of Alzheimer's disease. *Alzheimers Dem.* 12, 687–694. doi: 10.1016/j.jalz.2016.03.015

Saracino, D., Clot, F., Camuzat, A., Anquetil, V., Hannequin, D., Guyant-Maréchal, L., et al. (2018). Novel VCP mutations expand the mutational spectrum of frontotemporal dementia. *Neurobiol. Aging* 72:187. doi: 10.1016/j.neurobiolaging.2018.06.037

Sleegers, K., Brouwers, N., Van Damme, P., Engelborghs, S., Gijselinck, I., van der Zee, J., et al. (2009). Serum biomarker for progranulin-associated frontotemporal lobar degeneration. *Ann. Neurol.* 65, 603–609. doi: 10.1002/ana.21621

Taskesen, E., Mishra, A., van der Sluis, S., Ferrari, R., International Ftd-Genomics Consortium, Veldink, J. H., et al. (2018). Susceptible genes and disease mechanisms identified in frontotemporal dementia and frontotemporal dementia with amyotrophic lateral sclerosis by DNA-methylation and GWAS. *Sci. Rep.* 8:7789. doi: 10.1038/s41598-018-21308-x

van Blitterswijk, M., Mullen, B., Nicholson, A. M., Bieniek, K. F., Heckman, M. G., Baker, M. C., et al. (2014). TMEM106B protects C9ORF72 expansion carriers against frontotemporal dementia. *Acta Neuropathol.* 127, 397–406. doi: 10.1007/s00401-013-1240-4

Van Deerlin, V. M., Sleiman, P. M., Martinez-Lage, M., Chen-Plotkin, A., Wang, L. S., Graff-Radford, N. R., et al. (2010). Common variants at 7p21 are associated with frontotemporal lobar degeneration with TDP-43 inclusions. *Nat. Genet.* 42, 234–239. doi: 10.1038/ng.536

van der Zee, J., Gijselinck, I., Van Mossevelde, S., Perrone, F., Dillen, L., Heeman, B., et al. (2017). TBK1 mutation spectrum in an extended european patient cohort with frontotemporal dementia and amyotrophic lateral sclerosis. *Hum. Mutat.* 38, 297–309. doi: 10.1002/humu.23161

van der Zee, J., Van Langenhove, T., Kovacs, G. G., Dillen, L., Deschamps, W., Engelborghs, S., et al. (2014). Rare mutations in SQSTM1 modify susceptibility to frontotemporal lobar degeneration. *Acta. Neuropathol.* 128, 397–410. doi: 10.1007/s00401-014-1298-7

Vincent, A. E., Rosa, H. S., Alston, C. L., Grady, J. P., Rygiel, K. A., Rocha, M. C., et al. (2016). Dysferlin mutations and mitochondrial dysfunction. *Neuromuscul. Disord.* 26, 782–788. doi: 10.1016/j.nmd.2016.08.008

Weiner, D. J., Wigdor, E. M., Ripke, S., Walters, R. K., Kosmicki, J. A., Grove, J., et al. (2017). Polygenic transmission disequilibrium confirms that common and rare variation act additively to create risk for autism spectrum disorders. *Nat. Genet.* 49, 978–985. doi: 10.1038/ng.3863

Williams, K. L., Topp, S., Yang, S., Smith, B., Fifita, J., Warraich, S. T., et al. (2016). CCNF mutations in amyotrophic lateral sclerosis and frontotemporal dementia. *Nat. Commun.* 7:11253. doi: 10.1038/ncomms11253

Wong, T. H., Pottier, C., Hondius, D. C., Meeter, L. H. H., van Rooij, J. G. J., Melhem, S., et al. (2018). Three VCP mutations in patients with frontotemporal dementia. *J. Alzheimers Dis.* 65, 1139–1146. doi: 10.3233/JAD-180301

Wood, E. M., Falcone, D., Suh, E., Irwin, D. J., Chen-Plotkin, A. S., Lee, E. B., et al. (2013). Development and validation of pedigree classification criteria for frontotemporal lobar degeneration. *JAMA Neurol.* 70, 1411–1417. doi: 10.1001/jamaneurol.2013.3956

Xu, Y., Liu, X., Shen, J., Tian, W., Fang, R., Li, B., et al. (2018). The Whole exome sequencing clarifies the genotype- phenotype correlations in patients with early-onset dementia. *Aging Dis.* 9, 696–705. doi: 10.14336/AD.2018.0208

Yang, J., Benyamin, B., McEvoy, B. P., Gordon, S., Henders, A. K., Nyholt, D. R., et al. (2010). Common SNPs explain a large proportion of the heritability for human height. *Nat. Genet.* 42, 565–569. doi: 10.1038/ng.608

Zhang, M., Ferrari, R., Tartaglia, M. C., Keith, J., Surace, E. I., Wolf, U., et al. (2018). A C6orf10/LOC101929163 locus is associated with age of onset in C9orf72 carriers. *Brain* 141, 2895–2907. doi: 10.1093/brain/awy238

Conflict of Interest Statement: The authors declare that the research was conducted in the absence of any commercial or financial relationships that could be construed as a potential conflict of interest.

frontiers in Neuroscience

ORIGINAL RESEARCH
published: 04 June 2019
doi: 10.3389/fnins.2019.00551

Heterogeneous Nuclear Ribonucleoprotein E2 (hnRNP E2) Is a Component of TDP-43 Aggregates Specifically in the A and C Pathological Subtypes of Frontotemporal Lobar Degeneration

Wejdan Kattuah[1,2], Boris Rogelj[3,4,5], Andrew King[1,6], Christopher E. Shaw[7], Tibor Hortobágyi[8,9,10†] and Claire Troakes[1†]*

[1] London Neurodegenerative Diseases Brain Bank, Department of Basic and Clinical Neuroscience, Institute of Psychiatry, Psychology and Neuroscience, King's College London, London, United Kingdom, [2] Department of Physiological Sciences, College of Medicine, Alfaisal University, Riyadh, Saudi Arabia, [3] Department of Biotechnology, Jozef Stefan Institute, Ljubljana, Slovenia, [4] Biomedical Research Institute BRIS, Ljubljana, Slovenia, [5] Faculty of Chemistry and Chemical Technology, University of Ljubljana, Ljubljana, Slovenia, [6] Department of Clinical Neuropathology, King's College Hospital NHS Foundation Trust, London, United Kingdom, [7] UK Dementia Research Institute, Department of Basic and Clinical Neuroscience, Maurice Wohl Clinical Neuroscience Institute, Institute of Psychiatry, Psychology and Neuroscience, King's College London, London, United Kingdom, [8] Department of Old Age Psychiatry, Institute of Psychiatry, Psychology and Neuroscience, King's College London, London, United Kingdom, [9] Department of Pathology, University of Szeged, Szeged, Hungary, [10] MTA-DE Cerebrovascular and Neurodegenerative Research Group, Department of Neurology, University of Debrecen, Debrecen, Hungary

OPEN ACCESS

Edited by:
Annakaisa Haapasalo, University of Eastern Finland, Finland

Reviewed by:
Cintia Roodveldt, Centro Andaluz de Biología Molecular y Medicina Regenerativa (CABIMER), Spain
Savina Apolloni, Fondazione Santa Lucia (IRCCS), Italy

***Correspondence:**
Claire Troakes
claire.troakes@kcl.ac.uk

† These authors have contributed equally to this work

Specialty section:
This article was submitted to Neurodegeneration, a section of the journal Frontiers in Neuroscience

Received: *29 January 2019*
Accepted: *13 May 2019*
Published: *04 June 2019*

Citation:
Kattuah W, Rogelj B, King A, Shaw CE, Hortobágyi T and Troakes C (2019) Heterogeneous Nuclear Ribonucleoprotein E2 (hnRNP E2) Is a Component of TDP-43 Aggregates Specifically in the A and C Pathological Subtypes of Frontotemporal Lobar Degeneration. Front. Neurosci. 13:551. doi: 10.3389/fnins.2019.00551

TAR DNA-binding protein 43 (TDP-43) is the major component of the ubiquitin-positive protein aggregates seen in the majority of frontotemporal lobar degeneration and amyotrophic lateral sclerosis cases. TDP-43 belongs to the heterogeneous nuclear ribonucleoprotein (hnRNP) family that is involved in the regulation of RNA transcription, splicing, transport and translation. There are a great many hnRNPs, which often have overlapping functions and act cooperatively in RNA processing. Here we demonstrate that another hnRNP family member, hnRNP E2, shows a striking accumulation within dystrophic neurites and cytoplasmic inclusions in the frontal cortex and hippocampus of a subset of FTLD-TDP cases belonging to pathological subtypes A and C, where hnRNP E2 was found to co-localize with 87% of TDP-43 immunopositive inclusions. hnRNP E2-positive inclusions were not seen in FTLD-TDP cases with the *C9orf72* expansion or in any other neurodegenerative disorders examined. This interaction with TDP-43 in specific FTLD subtypes suggests different underlying neurodegenerative pathways.

Keywords: FTLD, ALS, TDP-43, hnRNP, hnRNP E2

INTRODUCTION

Frontotemporal lobar degeneration (FTLD) refers to a group of neurodegenerative disorders predominantly affecting the frontal and temporal lobes. The group is clinically, pathologically and genetically heterogeneous. Typically, patients initially present with behavioral dysfunction and changes in personal and social conduct (behavioral variant) or with disorders of speech and

language (semantic dementia and progressive non-fluent aphasia). FTLD can occur alone or, as seen in approximately 15% of cases, accompanied by amyotrophic lateral sclerosis (ALS) with progressive upper and lower motor neuron degeneration.

Approximately 30–50% of FTLD cases are familial with an autosomal dominant pattern of inheritance. Reported mutations include *MAPT*, *GRN*, *VCP* and the GGGGCC repeat expansion in the *C9orf72* gene (Watts et al., 2004; Baker et al., 2006; DeJesus-Hernandez et al., 2011).

Pathologically, FTLD cases exhibit intraneuronal (and in some cases glial) inclusions formed of abnormally aggregated proteins. Cases can be classified according to the type of hallmark protein accumulated in the neuronal inclusions, with most cases showing inclusions positive for either tau (FTLD-tau) or TDP-43 (FTLD-TDP) and, less frequently, FUS (FTLD-FUS).

Since 2011, a harmonized classification has been used in FTLD-TDP cases based on the morphology and neuroanatomical distribution of inclusions (Mackenzie et al., 2011). Briefly, FTLD-TDP type A is characterized by crescentic or oval neuronal cytoplasmic inclusions (NCI) and numerous short dystrophic neurites (DN), primarily in layer 2 of the neocortex. Lentiform neuronal intranuclear inclusions (NII) can sometimes be seen, however, they are not a consistent feature of this subtype. Type B is characterized by a moderate number of NCI in all cortical layers and very few DN. Type C have numerous elongated DN in the upper cortical layers but very few NCI. Type D FTLD-TDP refers to the pathology associated with *VCP* mutations and is characterized by frequent lentiform NII and numerous short DN. The pathological subtypes of FTLD-TDP cases have some correlation to the clinical phenotypes, subtype A being associated with behavioral variant of frontotemporal dementia (bvFTD) or progressive non-fluent aphasia (PFNA), subtype B with bvFTD and often combined with ALS and subtype C with semantic dementia. Subtype D is often associated with Paget's disease of bone and hereditary inclusion body myopathy

Normally TDP-43 is predominantly localized to the nucleus, however, it is continuously shuttling between the nucleus and the cytoplasm (Ayala et al., 2008; Prpar Mihevc et al., 2017). It is capable of binding to nucleic acids, with involvement in RNA splicing, stability, transcription and translation (Da Cruz and Cleveland, 2011; Tollervey et al., 2011; Buratti and Baralle, 2012). TDP-43 is a member of the heterogeneous ribonucleoprotein (hnRNP) family and interacts with a number of other members, mainly through its C-terminal tail (Romano et al., 2014). Mutations in TDP-43 have been associated with ALS, but not FTLD (Sreedharan et al., 2008).

Other hnRNPs have previously been reported to be associated with pathology in FTLD-TDP. hnRNP A3 was identified as a component of some of the p62-positive and TDP-43-negative hippocampal inclusions seen in a subset of FTLD/ALS cases with the *C9orf72* expansion; it was also shown to be a component of "RNA foci" and it has been suggested that it binds to the GGGGCC repeats in *C9orf72* transcripts (Mori et al., 2013); however, its pathogenic role has not yet been determined. In addition, the recent implication of hnRNP A2/B1 and hnRNP A1 in ALS and multisystem proteinopathy supports the hypothesis of a physical and functional interaction between TDP-43 and other hnRNPs (Calini et al., 2013; Kim et al., 2013; Romano et al., 2014). The relative expression of a specific protein within the TDP-43 interaction network may have a significant impact on the function of TDP-43, either through direct interaction or independently by acting on the same cellular targets (Hanson et al., 2010; Buratti and Baralle, 2012; Mohagheghi et al., 2016).

hnRNP E2 is an RNA-binding protein that belongs to the hnRNP K family of proteins. They are characterized by triple K Homology (KH) domains that can interact independently with target RNA sequences, which allows this protein family to potentially form highly complex-specific RNA interactions. hnRNP E2 has been reported to incorporate into stress granules alongside TDP-43 (Fujimura et al., 2008; Liu-Yesucevitz et al., 2010) and in a recent pathological study hnRNP E2 was shown to colocalise with TDP-43 inclusions in FTLD cases which presented with the semantic dementia clinical phenotype (Davidson et al., 2017).

Here we examined the expression of hnRNP E2 in a large cohort of cases, including a FTLD-TDP cohort comprising cases from all 4 pathological subtypes, cases with and without the *C9orf72* expansion, controls, and a number of other neurodegenerative diseases.

MATERIALS AND METHODS

Case Selection and Tissue Preparation

Post-mortem brain tissue samples in 10% formalin-fixed paraffin embedded blocks were obtained from the MRC London Neurodegenerative Diseases Brain Bank at the Institute of Psychiatry, Psychology and Neuroscience, King's College London. Consent for autopsy, neuropathological assessment and research was obtained for all cases and the study was carried out under the ethical approval of the tissue bank. Block taking and neuropathological assessment was performed according to standard criteria.

Tissue samples were selected from a total of 108 cases. 30 cases of FTLD-TDP without the *C9orf72* expansion (FTLD-TDP) were examined (comprising 15 classified as pathological subtype A, four subtype B, nine subtype C, one subtype D case and one which could not be definitively classified due to atypical inclusions). Additionally, 24 FTLD-TDP cases with *C9orf72* expansion were investigated (FTLD-TDP-*C9orf72*) (of which three were identified as subtype A, 16 as subtype B, and five which could not be definitively subtyped).

To investigate the specificity of hnRNP E2 to FTLD-TDP, seven FTLD with tau aggregates (FTLD-Tau), 14 sporadic ALS (sALS), three ALS with *SOD1* mutations (ALS-*SOD*), three ALS with *FUS* mutations (ALS-*FUS*) and one ALS with a *TARDBP* mutation were examined.

To determine the specificity of hnRNP E2 to FTLD, seven Alzheimer's disease, two Dementia with Lewy bodies (DLB), one argyrophilic grain disease (AGD), one spinocerebellar ataxia

(SCA) and one Huntington's disease case were examined. Fourteen healthy controls without a history of neurological problems or psychiatric disorders and without any significant pathology (matched for gender, age and post-mortem delay) were also investigated (see **Table 1** for details).

In each case frontal and temporal lobe (containing the hippocampus) were examined. In some cases (where available) the spinal cord was also studied.

Immunohistochemistry

Seven micrometer thick, formalin fixed, paraffin embedded sections were cut from the middle frontal gyrus, hippocampus and, in some cases, the spinal cord. Immunohistochemistry was conducted as per previously published protocols (Maekawa et al., 2009). In brief, sections were deparaffinised in xylene and endogenous peroxidase was blocked by immersion in 2.5% H_2O_2 in methanol. Antigen retrieval was enhanced using an extended microwave citrate buffer treatment. After blocking in normal swine serum (DAKO, Cambridgeshire, United Kingdom) 1:10 for 20 min, hnRNP E2 antibody (hnRNP E2-23G, sc-101136, Santa Cruz) was applied at 1:500 overnight at 4°C. Following washes, the sections were incubated with biotinylated secondary antibody (DAKO), followed by avidin:biotinylated enzyme complex (Vectastain Elite ABC kit, Vector Laboratories, Peterborough, United Kingdom). The sections were then incubated for 10–15 min with 0.5 mg/mL 3,3′-diaminobenzidine chromogen (Sigma-Aldrich Company Ltd., Dorset, United Kingdom) in Tris-buffered saline (pH 7.6) containing 0.05% H_2O_2. The sections were counterstained with Harris' haematoxylin and immunostaining analyzed using a Leica microscope.

Double Immunofluorescence

To investigate co-localisation of hnRNP E2 with ubiquitin and TDP-43, double immunofluorescence was carried out on a subset of the FTLD-TDP cases. Seven micrometer sections cut from formalin-fixed paraffin-embedded blocks were deparaffinised in xylene and dehydrated in 99% industrial methylated spirit. Sections were pre-treated with microwave heating in citrate buffer and normal serum blocking was performed using normal goat serum (1:10 for 45 min). Sections were incubated overnight at 4°C with hnRNP E2 (hnRNP E2-23G: sc-101136, Santa Cruz) at 1:200 with either TDP-43 (Proteintech, 10782-2-AP) at 1:250 or anti-ubiquitin (Dako, Z045801) at 1:100.

After washes, sections were incubated with AlexaFluor secondary antibodies (goat anti-mouse 488 and goat anti-rabbit 568, Invitrogen, Paisley, United Kingdom). Sections were treated with Sudan Black for 10 min to quench autofluorescence. Following numerous washes in phosphate buffered saline, sections were mounted with Vectashield hard set media containing DAPI. Sections were visualized using a fluorescent microscope (Zeiss Axiovert S 100, Gottingen, Germany) and images captured using ImagePro Express (v6) (Meyer Instruments, Houston, TX, United States). Sections were also examined using confocal microscopy (Leica confocal SP system) and captured images analyzed using ImageJ 1.47v software.

Statistical Analysis of hnRNP-E2 Pathology and Demographic Data

A Chi-square test of independence was performed to examine the relationship between gender, age at death, post-mortem delay and fixation time with presence of hnRNP E2 pathology.

RESULTS

Immunohistochemistry for hnRNP E2 showed striking inclusions in 17 FTLD-TDP cases, specifically those with subtype A and C pathology (see **Table 1**). The inclusions showed a similar pattern to that of the TDP-43 pathology. In subtype A FTLD-TDP cases six out of 15 cases showed hnRNP E2 inclusions in the frontal cortex with two of these also showing inclusions in the hippocampus and in the spinal cord. Within the frontal cortex hnRNP E2 inclusions were predominant in the superficial layers, mainly in layer 2 of the neocortex, with numerous perinuclear cytoplasmic neuronal inclusions and frequent dystrophic neurites (**Figure 1B**). Similar inclusions were detected within the hippocampus granular cells (**Figure 1C**). In the spinal cord, sparse inclusions were detected in the anterior horn of the thoracic spinal cord in the two cases (**Figure 1D**). All nine subtype C cases showed hnRNP E2 inclusions in the frontal cortex; long dystrophic neurites were predominantly detected in the superficial layers of the frontal cortex (**Figure 1E**) and in the hippocampus (**Figure 1F**). In all nine cases round intracellular inclusions were also detected in the granular cells of dentate fascia (**Figure 1G**) and in one case inclusions were seen in the spinal cord. hnRNP E2-positive inclusions were seen in both the frontal cortex and the spinal cord of an additional FTLD-TDP case that, due to atypical p62 positive, TDP negative intranuclear inclusions, could not be definitively classified into a sub-group. No hnRNP E2 positive inclusions were seen in either the frontal cortex or hippocampus of the FTLD-TDP subtype D case (**Figure 1H**). Inclusions were seen in just one of the FTLD-TDP C9orf72 expansion positive cases (classified as a subtype B). Within control cases, the hnRNP E2 immunohistochemistry showed weak diffuse staining in the cytoplasm and stronger nuclear staining (**Figure 1A**). No hnRNP E2 aggregates were seen in the brain or spinal cord in any disease other than FTLD-TDP, with staining appearing similar to the control cases.

Co-localisation of TDP-43 and hnRNP E2

Double immunofluorescence revealed a strong relationship between TDP-43 and hnRNP E2, in both the frontal cortex (**Figures 2A1–A3**) and hippocampus (**Figures 2B1–B3**) with 87% of the TDP-43-positive inclusions being found to co-localize with hnRNP E2 (a total of 583 TDP-43 positive inclusions and 507 hnRNP E2 positive inclusions were counted in three FTLD-TDP type A cases and four FTLD-TDP type C cases). Higher magnification images of individual cells were obtained using a confocal microscope, which showed

TABLE 1 | List of cases used in the study, showing demographic details and hnRNP E2 immunohistochemistry positivity.

MRC ID	Diagnosis	TDP-Subtype	Sex	Age at death	PMD	Fixation time	hnRNP E2 positivity		
							Frontal	H/C	SC
BBN_1085	FTLD-TDP	A	M	87	41	12	N	N	N/A
BBN_15298	FTLD-TDP (?ALS)	A	M	69	42	5	**Y**	**Y**	**Y**
BBN_10599	FTLD-TDP	A	F	79	56	6	**Y**	N	N/A
BBN_4568	FTLD-TDP	A	M	59	36	4	**Y**	**Y**	**Y**
BBN_15299	FTLD-TDP	A	M	88	31	8	**Y**	N	N/A
BBN_15306	FTLD-TDP	A	M	71	14	8	N	N	N
BBN_10245	FTLD-TDP	A	M	87	31	10	**Y**	N	N
BBN_9863	FTLD-TDP	A	M	73	25	8	N	N	N/A
BBN_15281	FTLD-TDP	A	F	67	15	7	N	N	N/A
BBN_19697	FTLD-TDP	A	F	78	72	8	N	N	N/A
BBN_15302	FTLD-TDP	A	M	81	11	24	N	N	N/A
BBN_16282	FTLD-TDP	A	M	78	>100	4	N	N	N/A
BBN_15292	FTLD-TDP	A	F	56	35	10	**Y**	N	N/A
BBN_15287	FTLD-TDP	A	F	74	70	8	N	N	N/A
BBN_15283	FTLD-TDP	A	M	70	57	22	N	N	N/A
BBN_9950	FTLD-TDP	B	M	72	38	12	N	N	N/A
BBN_4590	FTLD-TDP	B	F	73	54	8	N	N	N
BBN_15289	FTLD-TDP	B	M	68	46	4	N	N	N
BBN_11067	FTLD-TDP	B	M	81	31	8	N	N	N/A
BBN_15303	FTLD-TDP	C	M	69	6	12	**Y**	**Y**	N
BBN_15286	FTLD-TDP	C	M	68	120	7	**Y**	**Y**	N
BBN_15200	FTLD-TDP	C	M	69	16	11	**Y**	**Y**	N
BBN_15294	FTLD-TDP	C	F	85	24	11	**Y**	**Y**	N/A
BBN_15304	FTLD-TDP	C	M	80	45	20	**Y**	**Y**	N
BBN_15295	FTLD-TDP	C	M	82	14	16	**Y**	**Y**	**Y**
BBN_15297	FTLD-TDP	C	M	78	24	12	**Y**	**Y**	N/A
BBN_15288	FTLD-TDP	C	M	80	7	12	**Y**	**Y**	N/A
BBN_15290	FTLD-TDP	C	M	66	54	8	**Y**	**Y**	N
N/A	FTLD-TDP	D	M	61	3	14	N	N	N
BBN_4249	FTLD-TDP	NC	M	86	45	6	**Y**	N	N
BBN_15300	FTLD-ALS *C9orf72*	A	M	79	35	5	N	N	N/A
BBN_15291	FTLD-ALS *C9orf72*	A	M	56	19	11	N	N	N/A
BBN_16438	FTLD-ALS *C9orf72*	A	F	58	12	61	N	N	N/A
BBN_15279	FTLD-*C9orf72*	B	F	57	16	18	N	N	N
BBN_6230	FTLD-ALS *C9orf72*	B	M	71	44	17	**Y**	N	**Y**
BBN_15296	FTLD-*C9orf72*	B	F	70	16	12	N	N	N
BBN_16615	FTLD-ALS *C9orf72*	B	F	64	44	4	N	N	N/A
BBN_15713	FTLD-ALS *C9orf72*	B	M	57	23	35	N	N	N/A
BBN_6252	FTLD-ALS *C9orf72*	B	F	43	69	14	N	N	N/A
BBN_6254	FTLD-ALS *C9orf72*	B	M	53	82	10	N	N	N/A
BBN_16304	FTLD-ALS *C9orf72*	B	M	59	46	10	N	N	N/A
BBN_16651	FTLD-ALS *C9orf72*	B	M	51	64	7	N	N	N/A
BBN_16458	FTLD-ALS *C9orf72*	B	M	70	40	8	N	N	N/A
BBN_6227	FTLD-ALS *C9orf72*	B	M	55	76	31	N	N	N/A
BBN_6198	FTLD-ALS *C9orf72*	B	M	58	11	15	N	N	N/A
BBN_10306	FTLD-ALS *C9orf72*	B	M	64	68	11	N	N	N/A
BBN_16969	FTLD-ALS *C9orf72*	B	F	57	12	12	N	N	N/A
BBN_4253	FTLD-ALS *C9orf72*	B	F	59	21	10	N	N	N/A
BBN_6251	FTLD-ALS *C9orf72*	B	M	62	74	14	N	N	N/A

(Continued)

TABLE 1 | Continued

MRC ID	Diagnosis	TDP-Subtype	Sex	Age at death	PMD	Fixation time	hnRNP E2 positivity		
							Frontal	H/C	SC
BBN_16380	FTLD-ALS *C9orf72*	NC	F	59	35	17	N	N	N/A
BBN_16223	FTLD-ALS *C9orf72*	NC	M	55	19	17	N	N	N/A
BBN_6242	FTLD-ALS *C9orf72*	NC	F	39	70	18	N	N	N/A
BBN_6232	FTLD-ALS *C9orf72*	NC	M	70	38	12	N	N	N/A
BBN_15641	FTLD-ALS *C9orf72*	NC	F	70	60	37	N	N	N/A
BBN_15268	FTLD-Tau		F	58	31	13	N	N	N/A
BBN_15269	FTLD-Tau		M	67	35	9	N	N	N/A
BBN_15284	FTLD-Tau		F	62	31	9	N	N	N/A
BBN_10282	FTLD-Tau		M	72	6	19	N	N	N/A
BBN_10281	FTLD-Tau		M	61	23	21	N	N	N/A
BBN_15776	FTLD-Tau		M	66	17	3	N	N	N/A
BBN_15285	FTLD-Tau		M	67	17	7	N	N	N/A
BBN_6244	sALS		M	55	33	22	N	N	N/A
BBN_6187	sALS		M	70	73	75	N	N	N/A
BBN_10272	sALS		M	87	70	22	N	N	N/A
BBN_6248	sALS		M	66	38	8	N	N	N/A
BBN_15715	sALS		M	74	34	40	N	N	N/A
BBN_6219	sALS		M	49	33	33	N	N	N/A
BBN_6267	sALS		M	68	5	18	N	N	N/A
BBN_6257	sALS		F	69	64	14	N	N	N/A
BBN_6243	sALS		M	67	70	11	N	N	N/A
BBN_6217	sALS		F	56	39	56	N	N	N/A
BBN_6268	sALS		M	78	2	18	N	N	N/A
BBN_6280	sALS		M	75	38	9	N	N	N/A
BBN_10285	sALS		M	42	41	23	N	N	N/A
BBN_16384	sALS		F	57	15	23	N	N	N/A
BBN_16392	ALS-*SOD*		F	61	14	21	N	N	N/A
BBN_10276	ALS-*SOD*		M	47	14	18	N	N	N/A
BBN_16553	ALS-*SOD*		F	46	5	14	N	N	N/A
BBN_6245	ALS-*FUS*		F	35	13	5	N	N	N/A
BBN_6189	ALS-*FUS*		F	35	24	39	N	N	N/A
BBN_10244	ALS-*FUS*		F	23	37	12	N	N	N/A
BBN_19995	ALS-*TARDBP*		M	57	48	9	N	N	N/A
BBN_9933	Alzheimer's Disease		F	98	25	9	N	N	N/A
BBN_9934	Alzheimer's Disease		M	70	60	19	N	N	N/A
BBN_4182	Alzheimer's Disease		F	81	23	18	N	N	N/A
BBN_4183	Alzheimer's Disease		F	79	40	8	N	N	N/A
BBN_9801	Alzheimer's Disease		F	90	23	20	N	N	N/A
BBN_9927	Alzheimer's Disease		F	90	35	18	N	N	N/A
BBN_9930	Alzheimer's Disease		M	101	48	12	N	N	N/A
BBN_16337	DLB		M	85	30	18	N	N	N/A
BBN_10290	DLB		M	78	41	25	N	N	N/A
BBN_2924	Agyrophilic Grain Disease		M	82	20	8	N	N	N/A
BBN_15766	SCA		F	74	33	53	N	N	N/A
BBN_11070	Huntington's disease		M	65	36	8	N	N	N/A
BBN_15777	Control		F	87	22	150	N	N	N/A
BBN_15753	Control		M	64	71	53	N	N	N/A
BBN_16291	Control		M	81	18	17	N	N	N/A

(Continued)

TABLE 1 | Continued

MRC ID	Diagnosis	TDP-Subtype	Sex	Age at death	PMD	Fixation time	hnRNP E2 positivity		
							Frontal	H/C	SC
BBN_16242	Control		F	90	50	19	N	N	N/A
BBN_15621	Control		M	61	53	14	N	N	N/A
BBN_16429	Control		M	68	53	4	N	N	N/A
BBN_16280	Control		M	78	24	8	N	N	N/A
BBN_16277	Control		M	54	30	8	N	N	N/A
BBN_15791	Control		M	95	44	20	N	N	N/A
BBN_15790	Control		M	40	40	25	N	N	N/A
BBN_16256	Control		M	62	80	18	N	N	N/A
BBN_16251	Control		M	66	52	7	N	N	N/A
BBN_22991	Control		F	73	27	6	N	N	N/A
BBN_16525	Control		F	77	29	14	N	N	N/A

PMD (post-mortem delay), H/C (hippocampus), SC (spinal cord) ?ALS (sparse pathology seen in cord but no clinical symptoms reported), sALS (sporadic ALS), DLB (Dementia with Lewy bodies), SCA (Spinocerebellar ataxia), NC (non-classifiable), N/A (not available). Y (hnRNP-E2 positive aggregates).

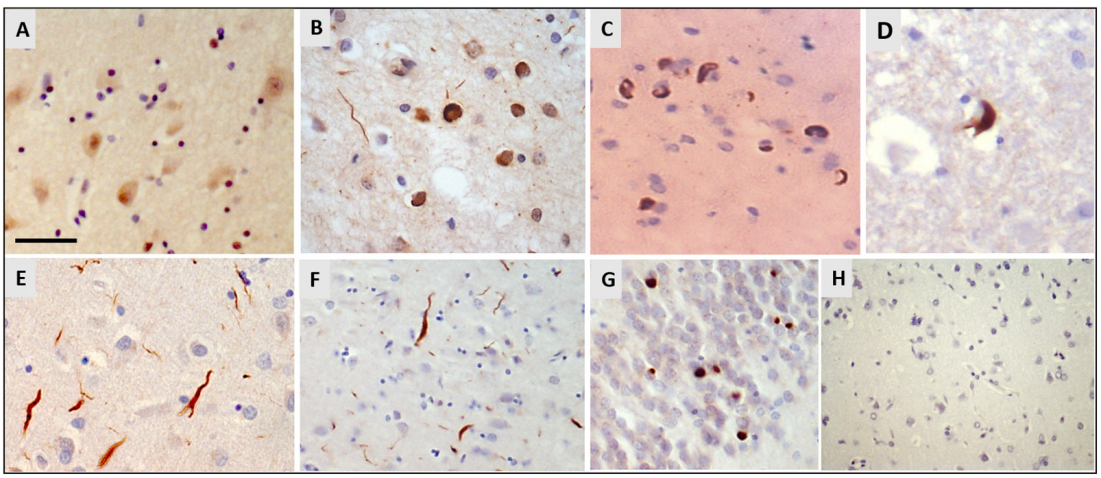

FIGURE 1 | Immunohistochemistry for hnRNP E2. **(A)** Weak cytoplasmic staining and stronger nuclear staining is seen in the frontal cortex of a control case (case ID BBN_16256). **(B–D)** Sections from a FTLD-TDP subtype A case showed numerous perinuclear cytoplasmic neuronal inclusions and frequent dystrophic neurites, mainly in layer 2 of the frontal cortex **(B)**. Similar cytoplasmic inclusions were detected in hippocampal neurons **(C)** and sparsely in the anterior horn of the spinal cord **(D)** (case ID BBN_15298). **(E–G)** In FTLD-TDP subtype C there were frequent long dystrophic neurites in the superficial layers of the frontal cortex **(E)** and in the hippocampus **(F)**. Within the granular cells of the dentate fascia round intracellular inclusions were seen **(G)** (case ID BBN_15303). **(H)** No inclusions were seen in the frontal cortex of the subtype D case **(H)**. Scale bar represents 20 μm in panels **(A,B,E)**; 80 μm in panels **(C,D,G)**; 100 μm in panel **(F,H)**.

the complete co-localisation of both TDP-43 and hnRNP E2 in the perinuclear inclusions and dystrophic neurites, respectively (**Figures 2C1–C3**). Images were also obtained from a type C FTLD-TDP case where mainly TDP-43 dystrophic neurites are detected in the frontal cortex, again, complete co-localisation of hnRNP E2 with TDP-43 was detected (**Figures 2D1–D3**). Interestingly the *C9orf72* positive case showed little co-localisation between hnRNP E2 and TDP-43 (image not shown).

Co-localisation of Ubiquitin and hnRNP-E2

hnRNP E2 was also present in 70% of the ubiquitin-positive inclusions in the frontal cortex (**Figures 3A1–A3**) and hippocampus (**Figures 3B1–B3**) of the same cases (with a total of 810 ubiquitin positive inclusions and 571 hnRNP-E2 positive inclusions being counted from three FTLD-TDP type A cases and four FTLD-TDP type C cases). High resolution images of the hnRNP E2/ubiquitin inclusions appear to show hnRNP E2 is partially ubiquitinated (**Figures 3C1–C3,D1–D3**).

Effects of Gender, Age, PMD and Fixation Time

hnRNP E2 pathology was found to be independent of both gender and age. There was also no significant effect of PMD or fixation time on the presence of hnRNP E2 pathology in the FTLD-TDP cases (**Table 2**).

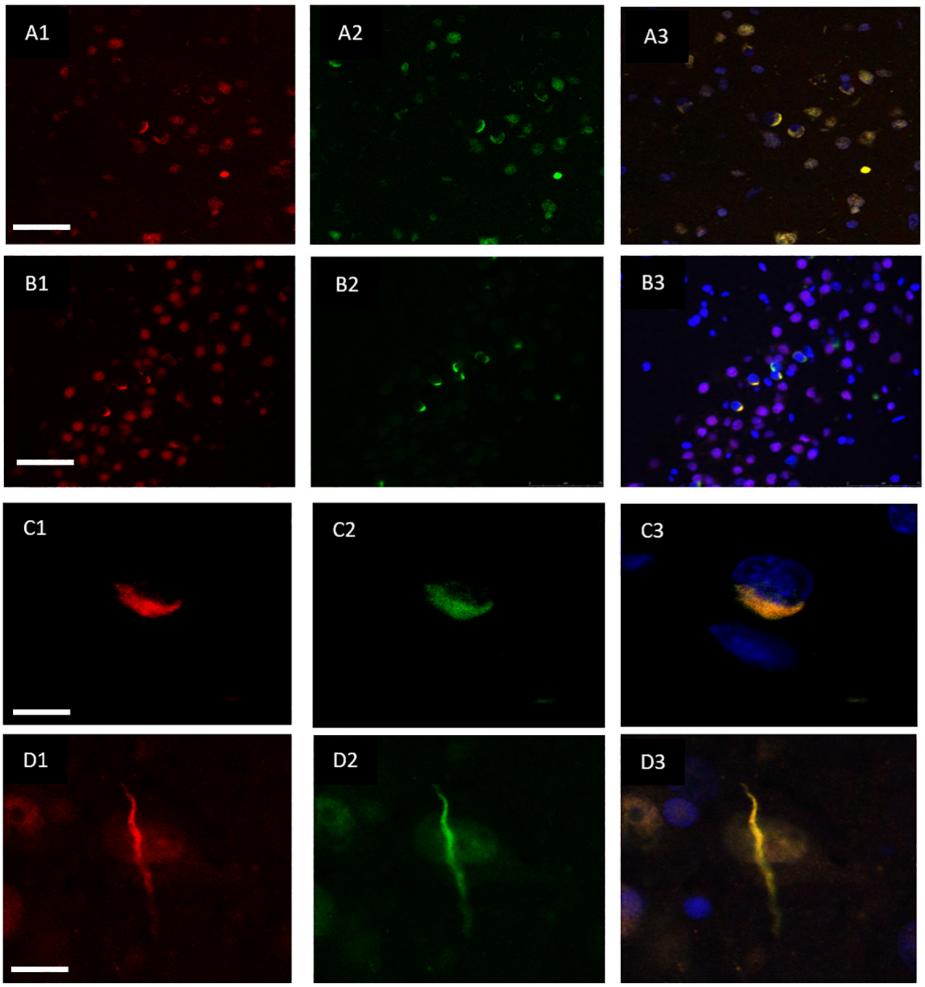

FIGURE 2 | Co-localisation of TDP-43 and hnRNP E2. Double-labeling immunofluorescence shows inclusions positive for TDP-43 (red) **(A1)** and hnRNP E2 (green) **(A2)** in the frontal cortex of a subtype A case, the merged image **(A3)** shows numerous areas of co-localisation (case ID BBN_15298). Co-localisation is also seen in the hippocampus, panels **(B1–B3)** show a subtype A case (case ID 482 BBN_4568). Higher magnification images demonstrate the complete co-localisation of the TDP-43 and hnRNP E2 in a perinuclear inclusion from the subtype A case **(C1–C3)** and along a dystrophic neurite in a subtype C case **(D1–D3)** (case ID BBN_15303). Scale bar represents 100 μm in panels **(A1–A3,B1–B3)**, 25 μm in panels **(C1–C3,D1–D3)**.

DISCUSSION

Since its identification as the major component of the protein aggregates in the majority of ALS and FTLD cases, TDP-43 has been subject to much investigation. However, its mechanistic role in neuronal degeneration has not yet been fully characterized. Identifying proteins that interact with TDP-43 would represent a major step forward in understanding the pathological mechanism and pathways.

In this study we report that immunohistochemistry for hnRNP E2 revealed prominent perinuclear cytoplasmic inclusions and dystrophic neurites in FTLD-TDP patient tissue – specifically in those classified as pathological subtypes A (6/15) and C (9/9). Positive inclusions were also seen in an additional FTLD-TDP case which was unable to be exactly classified, as well as in just a single *C9orf72* expansion positive case [classed as subtype B – although it should be noted that the classification of *C9orf72* cases can sometimes be difficult (Mackenzie and Neumann, 2017)]. Inclusions were not seen in subtype B or D FTLD-TDP or in the majority of *C9orf72* expansion-positive cases, despite the presence of TDP-43 inclusions. This adds to the increasing evidence for differences in the underlying mechanisms driving TDP-43 aggregation in different subtypes of FTLD-TDP. It has been proposed that TDP-43 may not be the driving force behind the neurodegeneration seen in *C9orf72* expansion cases (Leko et al., 2019) although this remains controversial (Mackenzie et al., 2015). No inclusions were seen in control cases or in any other neurodegenerative condition investigated.

Further insight into the functions of hnRNP E2 within the nervous system could provide an explanation for the co-localisation of hnRNP E2 with TDP-43 in the inclusions. Recent evidence suggests one explanation could be the role of hnRNP E2 in the regulation of apoptosis. Evidence of neuronal apoptosis has been reported in ALS and FTLD-TDP cases, with elevated

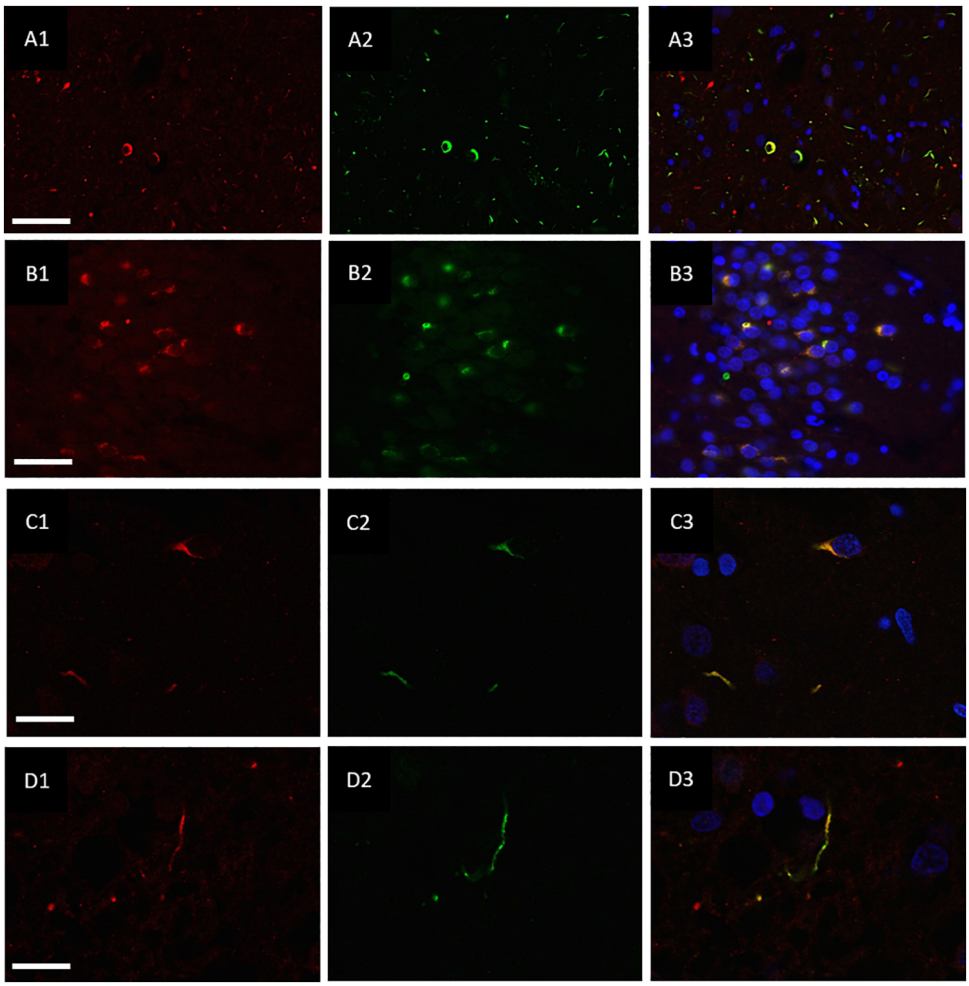

FIGURE 3 | Co-localisation of ubiquitin and hnRNP E2. Double-labeling immunofluorescence of Ubiquitin (red) and hnRNP E2 (green) shows high levels of co-localisation within the frontal cortex **(A1–A3)** and hippocampus **(B1–B3)** of a subtype A case (case ID BBN_4568). Strong co-localisation can be seen within the inclusions in a subtype A case **(C1–C3)** (case ID BBN_15298). In a subtype C case, some inclusions show only ubiquitin positivity **(D1)** and some only hnRNP-E2 positivity **(D2)**. Within inclusions showing both proteins, the co-localisation is not absolute **(D3)** (case ID BBN_15303). Scale bar represents 80 μm in panel **(A1–A3)**, 50 μm in panel **(B1–B3)**, 20 μm in panels **(C1–C3,D1–D3)**.

levels of activated caspase-3 seen in the spinal cord and brain (Martin, 1999; Su et al., 2000) and caspase-3 being identified as the protease responsible for TDP-43 fragmentation (Zhang et al., 2007). Interestingly, caspase-3 downregulates TDP-43 in glioma cells (Nan et al., 2014). Previous studies have linked hnRNP E2 to caspase-3 activation; hnRNP E2 is upregulated in human glioma tissue, while hnRNP E2 knockdown inhibited glioma growth through the induction of caspase-3-mediated apoptosis and the inhibition of cell-cycle progression (Han et al., 2013). Additionally, it has been reported that the overexpression of hnRNP E2 induces apoptosis in human oral cancer cells (Roychoudhury et al., 2007). Following spinal cord injury, both hnRNP E2 and caspase-3 were upregulated in neurons (Mao et al., 2016) and knockdown of hnRNP E2 decreased the expression of caspase-3 in primary neuronal cultures. However, the levels of cyclin D1 did not change after hnRNP E2 knockdown, which suggested that hnRNP E2-induced neuronal apoptosis is independent of cell cycle activation (Mao et al., 2016). The detailed mechanism of how hnRNP E2 may modulate caspase-3 activity and apoptosis has not yet been clarified but it is possible that this mechanism may mediate TDP-43 aggregation in some FTLD-TDP cases.

TABLE 2 | No significant effect of gender, age, post-mortem delay or fixation time was seen on hnRNP E2 positivity in FTLD-TDP cases using a Pearson's Chi-squared test (for gender) or Welch Two Sample *t*-test (for age, post-mortem delay and fixation time) df = degrees of freedom.

Variable	Test	Df	*p*-value
Gender	X-squared = 0.4026	1	0.5257
Age	$t = -0.3908$	26.293	0.6991
Post-mortem delay	$t = 0.5136$	26.736	0.6118
Fixation time	$t = 0.3276$	22.793	0.7462

A further possible explanation for the co-localisation of hnRNP E2 and TDP-43 in the FTLD-TDP brain is their role in the stress response. It has been shown that TDP-43 and hnRNP E2 are both recruited into stress granules under stress conditions (Fujimura et al., 2008; Monahan et al., 2016). Following oxidative stress, endogenous TDP-43 and hnRNP E2 colocalised within stress granules as well as with the stress granule marker PABP1, an effect that was greatly enhanced by the sequential addition of an osmotic challenge. hnRNP E2 has been identified as a facilitator of internal ribosome entry site-mediated translation and to have an important role in remodeling mRNAs in the stress granules and in transferring specific mRNAs from stress granules to P-bodies for degradation (Fujimura et al., 2008, 2009).

Another possible link could be established through microRNAs (miRNA). Nuclear and cytoplasmic TDP-43 were identified as modulators of miRNA maturation and, by facilitating miRNA production, to be essential for neuronal outgrowth (Kawahara and Mieda-Sato, 2012). Interestingly, hnRNP E2 expression was found to be regulated by miRNA-214; however, the regulatory pathway still needs to be determined (Tang et al., 2015).

Both TDP-43 and hnRNP E2 are present alongside ubiquitin in FTLD-TDP cases, thus, it is possible that ubiquitin could act as the link between TDP-43 and hnRNP E2. Scotter et al. (2014) suggested that an impaired ubiquitin proteasome system (UPS) contributes to elevated TDP-43 levels. The cascade of ubiquitin-mediated protein degradation involves the stepwise action of three enzymes, namely the ubiquitin-activating enzyme (E1), the ubiquitin-conjugating enzyme (E2) and the ubiquitin ligase enzyme (E3), which provide substrate specificity. E3 ubiquitin ligase recruits the ubiquitin-loaded conjugating enzyme E2, recognizes a protein substrate and either directly catalyzes or assists with the transfer of ubiquitin from E2 to the protein substrate (Hershko and Ciechanover, 1998). hnRNP E2 was identified as an adapter between the ubiquitin ligase E3 and the mitochondrial antiviral-signaling protein (MAVS) in cellular studies (You et al., 2009). The overexpression of hnRNP E2 led to the degradation of MAVS and abolished the cellular response to viral infection, while the knockdown of hnRNP E2 had the opposite effect. hnRNP E2 is not a ligase enzyme; however, it performs a ligase-enzyme-adapting activity, which recruits the conjugating enzyme to its substrate (You et al., 2009). Moreover, a ubiquitin ligase complex has been recently identified that is involved in TDP-43 degradation (Uchida et al., 2016). The ligase complex consists of the von Hippel-Lindau protein (VHL) and the cullin-2 (CUL2) RING, which belongs to the hydrophobic family of proteins that provides a temporary complex for ubiquitin ligase E3. VHL preferential binds to the RRM2 of misfolded TDP-43. Interestingly, when VHL is overloaded in the cytoplasm, it tends to stabilize and aggregate with TDP-43. VHL was detected in TDP-43 inclusions in spinal cord motor neurons of ALS patients, suggesting that the imbalance between VHL and CUL2 is the key to TDP-43 aggregation and highlighted the CUL2 E3 ligase as a potential therapeutic target for TDP-43 proteinopathies (Uchida et al., 2016). Determining whether hnRNP E2 could be a component or an adaptor of this ligase complex requires further investigation.

Our work corroborates the findings of a recent study by Davidson et al. (2017), where hnRNP E2 inclusions were reported in a subset of FTLD-TDP subtype C only. The authors suggested that long-term storage of tissue in formalin might have been the cause of variations in hnRNP E2 staining among the FTLD-TDP type C group. Our study showed inclusions in all type C cases examined (9/9) as well as a proportion of type A (6/16). Statistical analysis did not find any significant effect of fixation time on presence of hnRNP E2 staining, nor was there any relationship between gender, age or post-mortem delay in the FTLD-TDP cases.

Our findings highlight the importance of characterizing the protein composition of aggregates in order to understand the underlying pathological mechanisms and suggest that the co-localisation of hnRNP E2 with TDP-43 in inclusions may have implications in the pathogenesis of a subset of FTLD-TDP cases - which could even be considered as a subtype in future classifications of FTLD-TDP-43 proteinopathies.

ETHICS STATEMENT

This study was carried out in accordance with the Tissue Bank ethical approval for the London Neurodegenerative Diseases Brain Bank (18/WA/0206, Wales REC 3) with written informed consent from all subjects. All subjects gave written informed consent in accordance with the Declaration of Helsinki. The protocol was approved by the Wales REC 3.

AUTHOR CONTRIBUTIONS

WK and CT conducted the immunohistochemical and immunofluorescent staining. CT, TH, and CS designed the project. AK and TH conducted neuropathological assessment and subtyping of FTLD-TDP-43 cases. WK and CT wrote the manuscript. All authors reviewed and approved the final manuscript.

FUNDING

This study represents independent research partly funded by the National Institute for Health Research (NIHR) Biomedical Research Centre at South London and Maudsley NHS Foundation Trust and King's College London. Tissue samples were supplied by The London Neurodegenerative Diseases Brain Bank, which receives funding from the UK Medical Research Council (MR/L016397/1) and as part of the Brains for Dementia Research programme, jointly funded by Alzheimer's Research UK and the Alzheimer's Society. The views expressed are those of the authors and not necessarily those of the NHS, the NIHR or the Department of Health. The datasets used and/or analyzed during the current study are available from the corresponding author on reasonable request. WK was supported by the Saudi Arabian Ministry of Education under King Abdullah's

Scholarships Program. BR received funding from Slovenian Research Agency grants (P4-0127, J3-9263, J3-8201, and J3-6789). TH received funding from the Hungarian Brain Research Program (2017-1.2.1-NKP-2017-00002) and SZTE ÁOK-KKA.

ACKNOWLEDGMENTS

We would like to thank Professor Dennis Dickson for providing the FTLD-TDP subtype D tissue samples.

REFERENCES

Ayala, Y. M., Zago, P., D'Ambrogio, A., Xu, Y. F., Petrucelli, L., Buratti, E., et al. (2008). Structural determinants of the cellular localization and shuttling of TDP-43. *J. Cell Sci.* 121(Pt 22), 3778–3785. doi: 10.1242/jcs.038950

Baker, M., Mackenzie, I. R., Pickering-Brown, S. M., Gass, J., Rademakers, R., Lindholm, C., et al. (2006). Mutations in progranulin cause tau-negative frontotemporal dementia linked to chromosome 17. *Nature* 442, 916–919. doi: 10.1038/nature05016

Buratti, E., and Baralle, F. E. (2012). TDP-43: gumming up neurons through protein-protein and protein-RNA interactions. *Trends Biochem. Sci.* 37, 237–247. doi: 10.1016/j.tibs.2012.03.003

Calini, D., Corrado, L., Del Bo, R., Gagliardi, S., Pensato, V., Verde, F., et al. (2013). Analysis of hnRNPA1. A2/B1, and A3 genes in patients with amyotrophic lateral sclerosis. *Neurobiol. Aging* 34, e11–e12.

Da Cruz, S., and Cleveland, D. W. (2011). Understanding the role of TDP-43 and FUS/TLS in ALS and beyond. *Curr. Opin. Neurobiol.* 21, 904–919. doi: 10.1016/j.conb.2011.05.029

Davidson, Y. S., Flood, L., Robinson, A. C., Nihei, Y., Mori, K., Rollinson, S., et al. (2017). Heterogeneous ribonuclear protein A3 (hnRNP A3) is present in dipeptide repeat protein containing inclusions in Frontotemporal Lobar Degeneration and Motor Neurone disease associated with expansions in C9orf72 gene. *Acta Neuropathol. Commun.* 5:31. doi: 10.1186/s40478-017-0437-5

DeJesus-Hernandez, M., Mackenzie, I. R., Boeve, B. F., Boxer, A. L., Baker, M., Rutherford, N. J., et al. (2011). Expanded GGGGCC hexanucleotide repeat in noncoding region of C9ORF72 causes chromosome 9p-linked FTD and ALS. *Neuron* 72, 245–256. doi: 10.1016/j.neuron.2011.09.011

Fujimura, K., Kano, F., and Murata, M. (2008). Identification of PCBP2, a facilitator of IRES-mediated translation, as a novel constituent of stress granules and processing bodies. *RNA* 14, 425–431. doi: 10.1261/rna.780708

Fujimura, K., Katahira, J., Kano, F., Yoneda, Y., and Murata, M. (2009). Selective localization of PCBP2 to cytoplasmic processing bodies. *Biochim. Biophys. Acta* 1793, 878–887. doi: 10.1016/j.bbamcr.2009.02.002

Han, W., Xin, Z., Zhao, Z., Bao, W., Lin, X., Yin, B., et al. (2013). RNA-binding protein PCBP2 modulates glioma growth by regulating FHL3. *J. Clin. Invest.* 123, 2103–2118. doi: 10.1172/JCI61820

Hanson, K. A., Kim, S. H., Wassarman, D. A., and Tibbetts, R. S. (2010). Ubiquilin modifies TDP-43 toxicity in a Drosophila model of amyotrophic lateral sclerosis (ALS). *J. Biol. Chem.* 285, 11068–11072. doi: 10.1074/jbc.C109.078527

Hershko, A., and Ciechanover, A. (1998). The ubiquitin system. *Annu. Rev. Biochem.* 67, 425–479.

Kawahara, Y., and Mieda-Sato, A. (2012). TDP-43 promotes microRNA biogenesis as a component of the Drosha and Dicer complexes. *Proc. Natl. Acad. Sci. U.S.A.* 109, 3347–3352. doi: 10.1073/pnas.1112427109

Kim, H. J., Kim, N. C., Wang, Y. D., Scarborough, E. A., Moore, J., Diaz, Z., et al. (2013). Mutations in prion-like domains in hnRNPA2B1 and hnRNPA1 cause multisystem proteinopathy and ALS. *Nature* 495, 467–473. doi: 10.1038/nature11922

Leko, M. B., Župunski, V., Kirincich, J., Smilović, D., Hortobágyi, T., Hof, P. R., et al. (2019). Molecular mechanisms of neurodegeneration related to C9orf72 hexanucleotide repeat expansion. *Behav. Neurol.* 2019:2909168. doi: 10.1155/2019/2909168

Liu-Yesucevitz, L., Bilgutay, A., Zhang, Y. J., Vanderweyde, T., Citro, A., Mehta, T., et al. (2010). Tar DNA binding protein-43 (TDP-43) associates with stress granules: analysis of cultured cells and pathological brain tissue. *PLoS One* 5:e13250. doi: 10.1371/journal.pone.0013250

Mackenzie, I. R., Frick, P., Grasser, F. A., Gendron, T. F., Petrucelli, L., Cashman, N. R., et al. (2015). Quantitative analysis and clinico-pathological correlations of different dipeptide repeat protein pathologies in C9ORF72 mutation carriers. *Acta Neuropathol.* 130, 845–861. doi: 10.1007/s00401-015-1476-2

Mackenzie, I. R., and Neumann, M. (2017). Reappraisal of TDP-43 pathology in FTLD-U subtypes. *Acta Neuropathol.* 134, 79–96. doi: 10.1007/s00401-017-1716-8

Mackenzie, I. R., Neumann, M., Baborie, A., Sampathu, D. M., Du Plessis, D., Jaros, E., et al. (2011). A harmonized classification system for FTLD-TDP pathology. *Acta Neuropathol.* 122, 111–113. doi: 10.1007/s00401-011-0845-8

Maekawa, S., Leigh, P. N., King, A., Jones, E., Steele, J. C., Bodi, I., et al. (2009). TDP-43 is consistently co-localized with ubiquitinated inclusions in sporadic and Guam amyotrophic lateral sclerosis but not in familial amyotrophic lateral sclerosis with and without SOD1 mutations. *Neuropathology* 29, 672–683. doi: 10.1111/j.1440-1789.2009.01029.x

Mao, X., Liu, J., Chen, C., Zhang, W., Qian, R., Chen, X., et al. (2016). PCBP2 modulates neural apoptosis and astrocyte proliferation after spinal cord injury. *Neurochem. Res.* 41, 2401–2414. doi: 10.1007/s11064-016-1953-6

Martin, L. J. (1999). Neuronal death in amyotrophic lateral sclerosis is apoptosis: possible contribution of a programmed cell death mechanism. *J. Neuropathol. Exp. Neurol.* 58, 459–471. doi: 10.1097/00005072-199905000-00005

Mohagheghi, F., Prudencio, M., Stuani, C., Cook, C., Jansen-West, K., Dickson, D. W., et al. (2016). TDP-43 functions within a network of hnRNP proteins to inhibit the production of a truncated human SORT1 receptor. *Hum. Mol. Genet.* 25, 534–545. doi: 10.1093/hmg/ddv491

Monahan, Z., Shewmaker, F., and Pandey, U. B. (2016). Stress granules at the intersection of autophagy and ALS. *Brain Res.* 1649(Pt B), 189–200. doi: 10.1016/j.brainres.2016.05.022

Mori, K., Lammich, S., Mackenzie, I. R., Forne, I., Zilow, S., Kretzschmar, H., et al. (2013). hnRNP A3 binds to GGGGCC repeats and is a constituent of p62-positive/TDP43-negative inclusions in the hippocampus of patients with C9orf72 mutations. *Acta Neuropathol.* 125, 413–423. doi: 10.1007/s00401-013-1088-7

Nan, Y. N., Zhu, J. Y., Tan, Y., Zhang, Q., Jia, W., and Hua, Q. (2014). Staurosporine induced apoptosis rapidly downregulates TDP- 43 in glioma cells. *Asian Pac. J. Cancer Prev.* 15, 3575–3579. doi: 10.7314/apjcp.2014.15.8.3575

Prpar Mihevc, S., Darovic, S., Kovanda, A., Bajc Cesnik, A., Zupunski, V., and Rogelj, B. (2017). Nuclear trafficking in amyotrophic lateral sclerosis and frontotemporal lobar degeneration. *Brain* 140, 13–26. doi: 10.1093/brain/aww197

Romano, M., Buratti, E., Romano, G., Klima, R., Del Bel Belluz, L., Stuani, C., et al. (2014). Evolutionarily conserved heterogeneous nuclear ribonucleoprotein (hnRNP) A/B proteins functionally interact with human and Drosophila TAR DNA-binding protein 43 (TDP-43). *J. Biol. Chem.* 289, 7121–7130. doi: 10.1074/jbc.M114.548859

Roychoudhury, P., Paul, R. R., Chowdhury, R., and Chaudhuri, K. (2007). HnRNP E2 is downregulated in human oral cancer cells and the overexpression of hnRNP E2 induces apoptosis. *Mol. Carcinog.* 46, 198–207. doi: 10.1002/mc.20265

Scotter, E. L., Vance, C., Nishimura, A. L., Lee, Y. B., Chen, H. J., Urwin, H., et al. (2014). Differential roles of the ubiquitin proteasome system and autophagy in the clearance of soluble and aggregated TDP-43 species. *J. Cell Sci.* 127(Pt 6), 1263–1278. doi: 10.1242/jcs.140087

Sreedharan, J., Blair, I. P., Tripathi, V. B., Hu, X., Vance, C., Rogelj, B., et al. (2008). TDP-43 mutations in familial and sporadic amyotrophic lateral sclerosis. *Science* 319, 1668–1672. doi: 10.1126/science.1154584

Su, J. H., Nichol, K. E., Sitch, T., Sheu, P., Chubb, C., Miller, B. L., et al. (2000). DNA damage and activated caspase-3 expression in neurons and astrocytes: evidence for apoptosis in frontotemporal dementia. *Exp. Neurol.* 163, 9–19. doi: 10.1006/exnr.2000.7340

Tang, S. L., Gao, Y. L., and Chen, X. B. (2015). MicroRNA-214 targets PCBP2 to suppress the proliferation and growth of glioma cells. *Int. J. Clin. Exp. Pathol.* 8, 12571–12576.

Tollervey, J. R., Curk, T., Rogelj, B., Briese, M., Cereda, M., Kayikci, M., et al. (2011). Characterizing the RNA targets and position-dependent splicing regulation by TDP-43. *Nat. Neurosci.* 14, 452–458. doi: 10.1038/nn.2778

Uchida, T., Tamaki, Y., Ayaki, T., Shodai, A., Kaji, S., Morimura, T., et al. (2016). CUL2-mediated clearance of misfolded TDP-43 is paradoxically affected by VHL in oligodendrocytes in ALS. *Sci. Rep.* 6:19118. doi: 10.1038/srep19118

Watts, G. D., Wymer, J., Kovach, M. J., Mehta, S. G., Mumm, S., Darvish, D., et al. (2004). Inclusion body myopathy associated with paget disease of bone and frontotemporal dementia is caused by mutant valosin-containing protein. *Nat. Genet.* 36, 377–381. doi: 10.1038/ng1332

You, F., Sun, H., Zhou, X., Sun, W., Liang, S., Zhai, Z., et al. (2009). PCBP2 mediates degradation of the adaptor MAVS via the HECT ubiquitin ligase AIP4. *Nat. Immunol.* 10, 1300–1308. doi: 10.1038/ni.1815

Zhang, Y. J., Xu, Y. F., Dickey, C. A., Buratti, E., Baralle, F., Bailey, R., et al. (2007). Progranulin mediates caspase-dependent cleavage of TAR DNA binding protein-43. *J. Neurosci.* 27, 10530–10534. doi: 10.1523/jneurosci.3421-07.2007

Conflict of Interest Statement: The authors declare that the research was conducted in the absence of any commercial or financial relationships that could be construed as a potential conflict of interest.

frontiers in Neuroscience

MINI REVIEW
published: 21 June 2019
doi: 10.3389/fnins.2019.00658

Prodromal and Early bvFTD: Evaluating Clinical Features and Current Biomarkers

Kasper Katisko[1†], Antti Cajanus[1†], Titta Korhonen[1], Anne M. Remes[1,2,3,4], Annakaisa Haapasalo[5] and Eino Solje[1,2]*

[1] Institute of Clinical Medicine – Neurology, University of Eastern Finland, Kuopio, Finland, [2] Neuro Center, Neurology, Kuopio University Hospital, Kuopio, Finland, [3] Research Unit of Clinical Neuroscience, Neurology, University of Oulu, Oulu, Finland, [4] Medical Research Center, Oulu University Hospital, Oulu, Finland, [5] A.I. Virtanen Institute for Molecular Sciences, University of Eastern Finland, Kuopio, Finland

Despite the current diagnostic criteria, early diagnostics of behavioral variant of frontotemporal dementia (bvFTD) has remained challenging. Patients with bvFTD often present with misleading psychiatric phenotype, and, on the other hand, impairment in memory functions have increasingly been reported. However, impaired episodic memory is currently considered as an exclusion criterion for bvFTD. Single biofluid-based or imaging biomarkers do not currently provide sufficient sensitivity or specificity for early bvFTD diagnosis at single-subject level, although studies have suggested improved accuracy with different biomarker combinations. In this mini review, we evaluate the core clinical features of early bvFTD and summarize the most potential imaging and fluid biomarkers for bvFTD diagnostics.

Keywords: frontotemporal dementia, frontotemporal lobar degeneration, diagnostics, differential diagnostics, biomarker, neuroimaging, GRN, *C9orf72*

OPEN ACCESS

Edited by:
Antonio Lucio Teixeira, The University of Texas Health Science Center at Houston, United States

Reviewed by:
Olivier Piguet, University of Sydney, Australia
Laura Pasetto, Istituto Di Ricerche Farmacologiche Mario Negri, Italy

***Correspondence:**
Eino Solje
eino.solje@uef.fi

† These authors have contributed equally to this work

***Received:** 26 February 2019*
***Accepted:** 07 June 2019*
***Published:** 21 June 2019*

Citation:
Katisko K, Cajanus A, Korhonen T, Remes AM, Haapasalo A and Solje E (2019) Prodromal and Early bvFTD: Evaluating Clinical Features and Current Biomarkers. Front. Neurosci. 13:658. doi: 10.3389/fnins.2019.00658

INTRODUCTION

Frontotemporal lobar degeneration (FTLD) is the second most common early onset memory disorder (Ratnavalli et al., 2002), accounting for approximately 10 % of all progressive neurodegenerative memory diseases. FTLD has a substantial hereditary nature, and the most common genetic causes are the hexanucleotide repeat expansion in *C9orf72* gene (later *C9orf72*-RE) and mutations in *MAPT* or *GRN* genes. The most common clinical subtype of FTLD is the behavioral variant frontotemporal dementia (bvFTD), covering over half of the FTLD cases (Johnson et al., 2005). The diagnostics of bvFTD is challenging. In bvFTD, deterioration of episodic memory functions are not typically observed similarly to other neurodegenerative memory disorders and the patients are mainly characterized by altered personality and behavior (Rascovsky et al., 2011). Thus, the correct diagnosis is often delayed and misdiagnoses as psychiatric disorders are frequent (Galimberti et al., 2015; Solje et al., 2015).

The main inadequacy of the current diagnostic criteria is the lack of specificity. The *possible bvFTD* criteria include only behavioral symptoms and thus bvFTD can be easily confused with psychiatric disorders. The *probable bvFTD* criteria include also atrophy or hypoperfusion in frontal and/or temporal lobes and significant functional decline in addition to behavioral symptoms. Visual assessment of brain MRI results requires an experienced neuroradiologist and is time consuming, yet it provides only moderate sensitivity and specificity (Harper et al., 2016). Furthermore, as brain

atrophy develops slowly, the observation of subtle brain changes in the early phase of the disease can be even more difficult.

Currently there are no routinely used and validated specific CSF or blood biomarkers for the diagnostics of bvFTD. However, there is an urgent need for such biomarkers for differential diagnostics, disease monitoring, and assessment of the effects of potential therapeutic treatments in FTLD patients. Biomarkers showing specific changes already at the presymptomatic or prodromal phase of the disease would be especially valuable for disease prediction and intervention when pharmacological, lifestyle, or psychosocial interventions become available. They would also be very useful for patient stratification in drug trials and would allow personalized medicine approaches for treatment and managing FTLD patients in the future.

In this minireview, we summarize core clinical features of early bvFTD and recent findings from studies examining novel brain imaging methods and biofluid biomarkers focusing on the early alterations in prodromal bvFTD. We attempt to provide some answers to the following questions. What are the most promising biomarkers for early bvFTD diagnostics? Is it possible to develop more sensitive multimodal diagnostic criteria or instruments to detect bvFTD during the early stages of the disease compared to the prevailing (Rascovsky et al., 2011) diagnostic criteria?

Early Clinical Features in bvFTD Patients

The characteristic behavioral features in bvFTD patients may be measured with scales such as frontal behavioral inventory (FBI), neuropsychiatric inventory (NPI), Cambridge behavioral inventory (CBI) or other similar ratings that are preferably based on overt behaviors rather than inferences about the patient's cognitive state (Rascovsky et al., 2011). Presymptomatic familial FTLD patients with known mutations have been reported to present cognitive changes in neuropsychological testing up to eight years before the estimated onset of symptoms (Geschwind et al., 2001; Janssen et al., 2005; Rohrer et al., 2008, 2015; Dopper et al., 2013; Jiskoot et al., 2016, 2018b). Changes in attention, executive function, and social cognition have been found particularly in presymptomatic *MAPT* and *GRN* mutation carriers (Geschwind et al., 2001; Dopper et al., 2013; Rohrer et al., 2015; Jiskoot et al., 2016, 2018b). Neuropsychological tools assessing ventromedial prefrontal cortex dysfunction, such as theory of mind (ToM) tasks (Poletti et al., 2012; Pardini et al., 2013; Dodich et al., 2016) and social cognition and emotional assessment (SEA), have been demonstrated to be able to detect and distinguish bvFTD at the very early stage from Alzheimer's disease (AD), and amnestic mild cognitive impairment (MCI) (Funkiewiez et al., 2012; Bertoux et al., 2013). Early decline in both affective and cognitive ToM component tasks has been noted in bvFTD patients, suggesting that impaired ventromedial prefrontal cortex function may explain the characteristic symptoms of bvFTD, such as early behavioral dysfunction, and loss of empathy (Gregory et al., 2002; Adenzato et al., 2010; Poletti et al., 2012).

Early neuropsychiatric symptoms and early contacts to psychiatric services are characteristic features in especially the inherited bvFTD associated with the *C9orf72-RE* (Boeve et al., 2012; Mahoney et al., 2012; Snowden et al., 2012; Devenney et al., 2014; Solje et al., 2015). In particular, delusions and hallucinations are prevalent (Omar et al., 2009; Boeve et al., 2012; Kertesz et al., 2013), and predominantly the patients with a concomitant motoneuron disease (MND) may experience psychotic symptoms in the prodromal stages of the disease (Velakoulis et al., 2009; Lillo et al., 2010). In a Finnish study, up to 60% of bvFTD patients carrying the *C9orf72*-RE presented with psychiatric symptoms on average 4.6 years prior to diagnosis of bvFTD (Solje et al., 2015). Also, criminal behavior has been identified in about 30% bvFTD (Diehl-Schmid et al., 2013; Liljegren et al., 2015; Shinagawa et al., 2017). According to these studies, the most common criminal acts include theft, traffic violations, trespassing, willful damage to property, housebreaking, assault, sexual advances, and indecent behavior.

Impaired episodic memory has been considered as an exclusion criterion for bvFTD in the current diagnostic criteria (Rascovsky et al., 2011), but increasing evidence has suggested impairment of memory functions and subjective memory complaints in early stages of bvFTD (Hodges et al., 2004; Pijnenburg et al., 2004; Hornberger et al., 2010; Hornberger and Piguet, 2012). In approximately 60% of cases, bvFTD patients and their caregivers report episodic memory disturbances in the initial stages of the disease (Hodges et al., 2004). Recent studies have also demonstrated that episodic memory impairments in bvFTD patients in neuropsychological tests may even be as severe as in patients with AD (Irish et al., 2011, 2014; Pennington et al., 2011; Bertoux et al., 2013; Frisch et al., 2013; Fernández-Matarrubia et al., 2017; Jiskoot et al., 2019).

Early Imaging Findings in bvFTD Patients

The typical neuroimaging findings in bvFTD patients are atrophy and/or hypoperfusion of anterior temporal and frontal lobes, and these are included in the diagnostic criteria of probable bvFTD (Rascovsky et al., 2011). In the past 5–10 years, early structural and functional brain changes of bvFTD patients and presymptomatic carriers of the three main bvFTD-associated genetic mutations have been a target of intensive research. The focus of the studies has partially shifted from the conventional structural volumetric measures to measurements that are more novel, such as estimates of white matter tract integrity or functional network connectivity using diffusion weighted imaging and functional magnetic resonance imaging (MRI) methods and their quantification.

The earliest structural changes in presymptomatic mutation carriers can be detected in the insula and temporal and frontal areas as early as 10 years before the expected onset of the symptoms (Rohrer et al., 2015). Similar to symptomatic patients, the pattern of brain atrophy in the presymptomatic subjects varies depending on the mutation they carry (Lee et al., 2017; Bertrand et al., 2018; Cash et al., 2018; Olm et al., 2018; Wen et al., 2018). The characteristic brain changes according to predisposing genes are listed in **Table 1**. Presymptomatic *C9orf72*-RE carriers show earlier and more profound changes than *GRN* and *MAPT* carriers. However, similar findings are not evident in the offspring of MND patients carrying the *C9orf72*-RE (Walhout et al., 2015). In addition, a recent study with symptomatic bvFTD

patients reported that increased cortical mean diffusivity is detected earlier than decreased cortical thickness, suggesting that diffusion-weighted imaging could be a preferable imaging modality also for detecting presymptomatic bvFTD patients (Illán-Gala et al., 2019).

According to the recent guidelines of European panel of experts (EANM-EAN), fluorodeoxyglucose positron emission tomography (FDG-PET) should be used in the early diagnosis of bvFTD, particularly because of its high negative predictive value (Grimmer et al., 2016; Arbizu et al., 2018; Caminiti et al., 2018). Characteristically bvFTD presents as uni- or bilateral hypometabolism in the prefrontal cortex, anterior temporal lobe, anterior cingulate, and basal ganglia (Morbelli et al., 2016; Krämer et al., 2018). However, the changes vary between individual patients, as some patients show a more prominent frontal hypometabolism, while the others present with a more prominent temporal lobe hypometabolism (Cerami et al., 2016). In patients with MCI, FDG-PET is useful in distinguishing patients with a progressive neurodegenerative disease from subjects with subjective symptoms or non-progressive conditions. However, at early stage, FDG-PET lacks specificity in differentiating between various neurodegenerative diseases (Arbizu et al., 2018).

The changes in spatially distinct, but functionally connected networks in cortical and subcortical areas in presymptomatic bvFTD patients have been evaluated using functional MRI (fMRI) methods. The main functional networks associated with bvFTD are the salience network (SN) and the default mode network (DMN) (Greicius et al., 2003; Menon and Uddin, 2010; Pievani et al., 2011; Farb et al., 2013; Lee et al., 2014). In symptomatic bvFTD patients, atrophy and hypoconnectivity in SN related areas is detected regardless of genetic etiology or neuropathologic presentation (Seeley et al., 2009; Zhou et al., 2010; Whitwell et al., 2011; Farb et al., 2013). Considering DMN, the studies show contradictory results, varying from hyper- to hypoconnectivity compared to healthy controls (Zhou et al., 2010; Whitwell et al., 2011; Farb et al., 2013; Rytty et al., 2013; Lee et al., 2014). In the presymptomatic *C9orf72*-RE carriers, there is hypoconnectivity in the SN compared to healthy controls, and this can be already distinguished in persons younger than 40 years of age (Lee et al., 2017).

Even though the results of recent neuroimaging studies appear promising in differentiating presymptomatic bvFTD from healthy controls, the imaging modalities and analysis methods need to be validated to obtain uniform protocols. In addition, also electro encephalogram and transcranial magnetic stimulation have been studied for diagnostic and even therapeutic purposes for bvFTD, but the results remain contradictory (Chan et al., 2004; Pijnenburg et al., 2008; Moretti et al., 2016; Carlino et al., 2014; Benussi et al., 2018). Moreover, large prospective studies are needed to validate the predictive value of different brain imaging techniques. Today, group level differences of presymptomatic bvFTD and healthy controls can be detected, but the predictive value of multimodal imaging at single-subject level can be considered suggestive at the most (Feis et al., 2018). Summary of the early imaging findings in bvFTD is provided in **Table 1**.

TABLE 1 | Summary of the early imaging findings of bvFTD according to different mutation carriers compared to non-carrying healthy controls.

Group	Early imaging findings	References
Presymptomatic C9ORF72-RE	Reduced volume in thalamus, cerebellum, parietal and frontal lobes. Reduced WM tracts connecting frontal lobes, thalamic radiation, corticospinal tracts.	Lee et al., 2017; Papma et al., 2017; Bertrand et al., 2018; Cash et al., 2018; Floeter et al., 2018; Jiskoot et al., 2018a; Popuri et al., 2018; Wen et al., 2018
Presymptomatic GRN	Reduced volume in insula, orbitofrontal, posterior frontal and anterior temporal lobes, and striatum. Reduced WM tracts in corpus callosum, superior longitudinal fasciculus and internal capsule.	Borroni et al., 2008; Pievani et al., 2014; Cash et al., 2018; Jiskoot et al., 2018a; Olm et al., 2018
Presymptomatic MAPT	Reduced volume in anterior and medial temporal lobes and the orbitofrontal lobe. Reduced WM tracts connecting frontal lobes.	Cash et al., 2018; Jiskoot et al., 2018a

Early Biological Fluid Biomarkers of bvFTD

The most studied biomarkers in the cerebrospinal fluid (CSF) of bvFTD patients have been phospho-tau, total tau, amyloid-β_{1-42} (and their ratios), and, more recently, neuronal cytoskeletal protein neurofilament light chain (NfL). Tau, phospho-tau and amyloid-β_{1-42} are validated biomarkers primarily in the diagnostics of AD. A few studies have shown that high CSF ratio of tau/amyloid-β_{1-42} or phospho-tau/amyloid-β_{1-42} can discriminate patients with AD from those with bvFTD (or FTLD in general) (Rivero-Santana et al., 2017; Paterson et al., 2018). However, decreased amyloid-β_{1-42} levels have been found in 25% of definite FTLD cases without any signs of AD (Kämäläinen et al., 2015). Similarly to other neuronal cytoskeletal proteins like tau and phospho-tau, NfL release into the CSF is considered as a marker for neuronal injury and neurodegeneration. Altered levels of NfL can be detected in the CSF of patients with different brain diseases, suggesting that NfL may represent a general, rather unspecific marker for neurodegeneration. On the other hand, several studies have suggested that FTLD patients (including bvFTD) display higher levels of CSF NfL and/or lower ratio of phospho-tau/tau compared to healthy controls or patients with other neurodegenerative or psychiatric diseases, including e.g., AD (Skillbäck et al., 2014; Meeter et al., 2016; Vijverberg et al., 2017; Abu-Rumeileh et al., 2018; Goossens et al., 2018; Meeter L.H.H. et al., 2018; Niikado et al., 2018). Notably, combined assessment of NfL levels with the AD biomarkers in the CSF could provide additional value in the differentiation diagnostics of AD and bvFTD (de Jong et al., 2007). Additionally, concomitantly increased NfL levels and reduced phospho-tau/tau ratio in the CSF, and increased NfL levels in serum might show potential as biomarkers discriminating bvFTD from psychiatric disorders (Vijverberg et al., 2017; Al Shweiki et al., 2019).

It has been reported that elevated NfL levels and low phospho-tau/tau ratio in the CSF associate with poorer survival and

especially with manifestation as motoneuron disease (FTLD-MND), suggesting that these biomarkers may be useful in disease monitoring in FTLD patients (Meeter et al., 2016; Ljubenkov et al., 2018; Meeter L.H.H. et al., 2018). In the same study, longitudinal data on CSF NfL levels did not indicate differences between control subjects and presymptomatic carriers of *GRN* or *MAPT* mutations or *C9orf72*-RE. However, the NfL levels showed a substantial increase after disease onset in all these patients, with the *GRN* mutation carriers showing the highest levels (Meeter et al., 2016). These data suggest that at individual level, NfL-test, with particular cut-off based reference values, may not necessarily be suitable in the very early stages of the disease when the neuropathological changes have already started to take place, but when there is not yet detectable neurodegeneration in the CNS. On the other hand, repeated analysis of CSF NfL levels at different time points during the very early stages of the disease in a patient could provide information about whether the NfL levels remain stable over time or show a rapid increase, allowing prediction of a potentially progressive neurodegenerative disease.

Reliable discrimination between FTLD-tau and FTLD-TDP, the two most common neuropathological subtypes of bvFTD patients (Perry et al., 2017), has remained challenging. Tau or TDP-43 levels in the CSF of neuropathologically confirmed FTLD-TDP and FTLD-tau cases were reported to show a great overlap (Kuiperij et al., 2017). Another study with neuropathologically confirmed FTLD-TDP and FTLD-tau patients suggested some other analytes, such as IL-17, IL-23, eotaxin-3 (CCL26), and macrophage-derived chemokine (MDC), as potential diagnostic biomarkers distinguishing between FTLD-TDP and FTLD-tau cases (Hu et al., 2010), and possibly reflecting involvement of different immunological processes in these neuropathological FTLD subtypes.

Investigations in FTLD patients with different genetic backgrounds have revealed that detection of CSF levels of dipeptide repeat proteins (DPR), namely poly-GP, in the *C9orf72*-RE carriers and progranulin in the *GRN* mutation carriers enables rather reliable separation of these patients from patients who do not carry these mutations (Ghidoni et al., 2012; Meeter et al., 2016; Gendron et al., 2017; Lehmer et al., 2017). On the other hand, poly-GP and progranulin levels in the CSF were increased already in the presymptomatic phase and did not show further significant increases during the symptomatic phase, thus suggesting that they do not predict disease onset or progression, but might be suitable for evaluating therapeutic effects (Meeter et al., 2016; Gendron et al., 2017; Lehmer et al., 2017). Furthermore, the poly-GP DPRs could be detected in the peripheral blood mononuclear cells (PBMCs) of the *C9orf72*-RE carriers, indicating that detection of poly-GP proteins in blood or other patient-derived cells might also be utilized in the diagnosis or therapy trials (Gendron et al., 2017). Also nuclear RNA foci, another pathological hallmark directly and specifically generated from the *C9orf72*-RE, can be detected for example in lymphocytes from the *C9orf72*-RE-carrying patients, and thus could potentially be exploited as biomarkers in assessing the effects of potential therapeutic substances, e.g., antisense oligonucleotides or small molecules (Su et al., 2014). However, it is still unclear at which point during the disease course these pathological hallmarks become detectable in different types of cells, and thus further studies are needed to evaluate their potential as early or prognostic peripheral biomarkers in *C9orf72*-RE carriers. Recent investigations have also suggested that decreased levels of *GRN* mRNA and progranulin in the serum can be used to identify affected and at-risk presymptomatic *GRN* mutation carriers from controls, suggesting potential as peripherally measurable biomarkers for these patients (Guven et al., 2019). Future longitudinal data on serum *GRN* mRNA or progranulin levels at different time points during the disease course would provide insights into their potential use as prognostic biomarkers.

Increasing amount of recent reports indicate a potential association between FTLD and inflammation. Therefore, assessing different inflammatory biomarkers in FTLD could provide diagnostic and/or prognostic value. Autoantibodies against AMPA receptor and antinuclear autoantibodies (ANA) were detected significantly more often in the sera of sporadic FTLD patients compared to control subjects (Borroni et al., 2017; Cavazzana et al., 2018). Levels of glial cell-derived inflammatory mediator YKL-40 (Chitinase 3-like 1) have been shown to be elevated in the CSF of both FTLD and AD patients compared to controls (Janelidze et al., 2016; Alcolea et al., 2017). On the other hand, similarly to several other biomarkers, also YKL-40 levels provide poor specificity between different neurodegenerative diseases (Alcolea et al., 2014; Janelidze et al., 2016). However, YKL-40 was found useful in the differential diagnostics between FTLD and psychiatric diseases, as higher YKL-40 levels in combination with higher NfL levels and reduced p-tau/tau ratio in the CSF could be used to distinguish FTLD patients from those with a psychiatric disease (Vijverberg et al., 2017). A key question considering the early diagnostics of FTLD is at which point during the disease course the inflammation occurs and can be detected. One of the important proteins related to inflammation is the triggering receptor expressed in myeloid cells 2 (TREM2), expressed in microglia. So far, only *GRN* mutations have been associated with elevated CSF soluble TREM2 (sTREM2) levels in FTLD (Woollacott et al., 2018). These data altogether thus suggest that specific inflammatory markers or a specific combination of them could have potential as early biomarkers of neurodegeneration and perhaps specifically also FTLD. The current CSF- or blood-derived biomarkers and their feasibility in the diagnostics of bvFTD are summarized in **Table 2**.

DISCUSSION

Despite recent advances in the early characterization of bvFTD, early clinical diagnosis is still a challenge. The primary symptoms of bvFTD include apathy, changes in personality, executive function deficits, and abnormal social behavior. According to current criteria, memory performance is not impaired at the early stage of the bvFTD, whereas memory loss and visuospatial problems are often the early symptoms in patients with AD (Dubois et al., 2007; Rascovsky et al., 2011; Ranasinghe et al., 2016). In contrast, patients with bvFTD may present with early neuropsychiatric symptoms, such as depression and

TABLE 2 | Current CSF- or blood-derived biomarkers and their feasibility in the diagnostics of bvFTD.

Biomarker	In clinical use (currently; yes/no)	Potential utility value	References
CSF amyloid-β1–42	Yes; AD diagnostics	Useful in differentiating AD vs. bvFTD (decreased in AD).	Rivero-Santana et al., 2017; Paterson et al., 2018
CSF tau	Yes; AD diagnostics	Combined with decreased amyloid-β1–42 (tau/amyloid-β1–42 ratio), high levels indicate AD over other neurodegenerative diseases, including bvFTD.	Rivero-Santana et al., 2017; Paterson et al., 2018
CSF phospho-tau	Yes; AD diagnostics	Combined with decreased amyloid-β1–42, high levels indicate AD over other neurodegenerative diseases.	Rivero-Santana et al., 2017
CSF phospho-tau/tau ratio	No; Not routinely used	Especially low values observed in Creutzfeldt-Jakob disease. In general, lower values indicate more severe neurodegeneration (for example ALS or rapidly progressive FTLD), and indicate FTLD over psychiatric disorders or AD.	Riemenschneider et al., 2003; Pijnenburg et al., 2015; Vijverberg et al., 2017
CSF and blood NfL	No	Disease severity assessment and diagnostics between bvFTD and non-neurodegenerative diseases (psychiatric). Higher levels in bvFTD compared to AD have been observed. Similar results found in both blood and CSF.	Vijverberg et al., 2017; Steinacker et al., 2018; Abu-Rumeileh et al., 2018; Al Shweiki et al., 2019
Specific markers for genetic forms of FTLD - CSF/blood poly-GP - Nuclear RNA foci from C9orf72-RE - CSF/blood progranulin	No	Detectable in presymptomatic phase. Potentially useful in the future when evaluating the effects of therapeutic interventions in genetic bvFTD.	Ghidoni et al., 2012; Su et al., 2014; Gendron et al., 2017
Inflammatory markers - anti-AMPA GluA3 - ANA - YKL-40 - sTREM2	Yes; ANA detection is used in diagnostics of several systemic and especially rheumatic autoimmune conditions	Diagnostics between FTLD and non-neurodegenerative diseases. Might indicate inflammation as a potential target for therapeutic approach.	Vijverberg et al., 2017; Borroni et al., 2017; Cavazzana et al., 2018; Woollacott et al., 2018

psychosis, that are compatible with a range of neurologic and psychiatric disorders. Those patients, who lack the key symptoms for the clinical diagnosis of bvFTD and do not meet full diagnostic criteria, are initially often misdiagnosed as psychiatric disorders, and other neurological diseases, most often AD. Therefore, misrecognition of symptoms in the early stages of bvFTD frequently delays a correct diagnosis (Mendez and Perryman, 2002; Rosness et al., 2008; Landqvist Waldö et al., 2015; Bertoux et al., 2016). Despite the significant clinical overlap between bvFTD, other neurodegenerative diseases and psychiatric disorders, the clinical phenotype has a great emphasis in the current diagnostic criteria as the clinical phenotype solely forms the first level (possible bvFTD) of the diagnosis. Additionally, the further criteria require positive imaging findings (for probable bvFTD) and genetic confirmation (for definite bvFTD), although the imaging findings may be absent especially in the early stages of bvFTD. Moreover, most of the cases are sporadic without a known genetic alteration underlying the disease. Thus, diagnosing bvFTD solely based on the "possible bvFTD" criteria lacks specificity, but on the other hand it is often not possible to increase the diagnostic certainty to the "probable" or "definite" levels.

Due to the limitations in the current criteria, more sensitive and specific neuroimaging and biomarker assessments are needed for early and more accurate diagnosis. On the other hand, the current criteria should remain as the clinical gold standard at least until bvFTD-specific biological markers become available. Future biomarkers should ideally be able to differentiate FTLD patients with different underlying pathological processes or genetic backgrounds, as potential treatment strategies will likely be targeted for specific patients or group of patients in a more personalized manner. Additionally, identifying individuals at increased risk for FTLD before disease onset and at still early stages of neurodegeneration could enable earlier diagnostics and increase potential for interventions.

To date, individual imaging or biomarker analysis tools do not yet provide sufficient sensitivity and/or specificity. On the other hand, combining different diagnostic instruments (neuroimaging, serum NfL measurement, immunological/metabolic biomarkers, and neuropathological biomarkers) could result in greater applicability to clinical diagnostics, compared to the prevailing diagnostic criteria. For instance, combination of serum NfL and diffusion weighted MRI scans could provide greater sensitivity and specificity in differentiating bvFTD from other neurodegenerative and psychiatric disorders and could possibly be included in the diagnostic criteria in the future. However, the biomarkers considered in this review still require extensive research as the current literature for them in FTLD or bvFTD rests on only a few suggestive findings. As bvFTD can be considered a clinically, genetically and pathologically heterogenous disease, the composition of large and well-defined cohorts is necessary. This emphasizes the need of multicenter, international collaboration,

as larger study populations are needed to validate and screen the existing and upcoming diagnostic tools for clinical use.

AUTHOR CONTRIBUTIONS

ES, AR, and AH contributed to the conception and design of the study. All authors wrote the sections, edited, read, and approved the final version of the manuscript for submission.

FUNDING

This work was supported by the Academy of Finland, grant numbers 315459 and 315460, Finnish Medical Foundation, Finnish Brain Foundation, Päivikki and Sakari Sohlberg Foundation, Finnish Alzheimer's Disease Research Society, Maire Taponen Foundation, Finnish Cultural Foundation, Olvi Foundation, and Yrjö Jahnsson Foundation, grant number 20187070.

REFERENCES

Abu-Rumeileh, S., Mometto, N., Bartoletti-Stella, A., Polischi, B., Oppi, F., Poda, R., et al. (2018). Cerebrospinal fluid biomarkers in patients with frontotemporal dementia spectrum: a single-center study. *J. Alzheimers Dis.* 66, 551–563. doi: 10.3233/jad-180409

Adenzato, M., Cavallo, M., and Enrici, I. (2010). Theory of mind ability in the behavioural variant of frontotemporal dementia: an analysis of the neural, cognitive, and social levels. *Neuropsychologia* 48, 2–12. doi: 10.1016/j.neuropsychologia.2009.08.001

Al Shweiki, M., Steinacker, P., Oeckl, P., Hengerer, P., Danek, A., Fassbender, K., et al. (2019). Neurofilament light chain as a blood biomarker to differentiate psychiatric disorders from behavioural variant frontotemporal dementia. *J. Psychiatr. Res.* 113, 137–140. doi: 10.1016/j.jpsychires.2019.03.019

Alcolea, D., Carmona-Iragui, M., Suárez-Calvet, M., Sánchez-Saudinós, M. B., Sala, I., Antón-Aguirre, S., et al. (2014). Relationship between β-secretase, inflammation and core cerebrospinal fluid biomarkers for alzheimer's disease. *J. Alzheimer's Dis.* 42, 157–167. doi: 10.3233/JAD-140240

Alcolea, D., Vilaplana, E., Suárez-Calvet, M., Illán-Gala, I., Blesa, R., Clarimón, J., et al. (2017). CSF sAPPβ, YKL-40, and neurofilament light in frontotemporal lobar degeneration. *Neurology* 89, 178–188. doi: 10.1212/WNL.0000000000004088

Arbizu, J., Festari, C., Altomare, D., Walker, Z., Bouwman, F., Rivolta, J., et al. (2018). Clinical utility of FDG-PET for the clinical diagnosis in MCI. *Eur. J. Nucl. Med. Mol. Imaging* 45, 1497–1508. doi: 10.1007/s00259-018-4039-7

Benussi, A., Alberici, A., Ferrari, C., Cantoni, V., Dell'Era, V., Turrone, R., et al. (2018). The impact of transcranial magnetic stimulation on diagnostic confidence in patients with Alzheimer disease. *Alzheimers Res. Ther.* 10:94. doi: 10.1186/s13195-018-0423-6

Bertoux, M., de Souza, L. C., O'Callaghan, C., Greve, A., Sarazin, M., Dubois, B., et al. (2016). Social cognition deficits: the key to discriminate behavioral variant frontotemporal dementia from alzheimer's disease regardless of amnesia? *J. Alzheimers Dis.* 49, 1065–1074. doi: 10.3233/JAD-150686

Bertoux, M., Funkiewiez, A., O'Callaghan, C., Dubois, B., and Hornberger, M. (2013). Sensitivity and specificity of ventromedial prefrontal cortex tests in behavioral variant frontotemporal dementia. *Alzheimers Dement.* 9, S84–S94. doi: 10.1016/j.jalz.2012.09.010

Bertrand, A., Wen, J., Rinaldi, D., Houot, M., Sayah, S., Camuzat, A., et al. (2018). Early cognitive, structural, and microstructural changes in presymptomatic C9orf72 carriers younger than 40 years. *JAMA Neurol.* 75, 236–245. doi: 10.1001/jamaneurol.2017.4266

Boeve, B. F., Boylan, K. B., Graff-Radford, N. R., DeJesus-Hernandez, M., Knopman, D. S., Pedraza, O., et al. (2012). Characterization of frontotemporal dementia and/or amyotrophic lateral sclerosis associated with the GGGGCC repeat expansion in C9ORF72. *Brain* 135, 765–783. doi: 10.1093/brain/aws004

Borroni, B., Alberici, A., Premi, E., Archetti, S., Garibotto, V., Agosti, C., et al. (2008). Brain magnetic resonance imaging structural changes in a pedigree of asymptomatic progranulin mutation carriers. *Rejuven. Res.* 11, 585–595. doi: 10.1089/rej.2007.0623

Borroni, B., Stanic, J., Verpelli, C., Mellone, M., Bonomi, E., Alberici, A., et al. (2017). Anti-AMPA GluA3 antibodies in frontotemporal dementia: a new molecular target. *Sci. Rep.* 7:6723. doi: 10.1038/s41598-017-06117-y

Caminiti, S. P., Ballarini, T., Sala, A., Cerami, C., Presotto, L., Santangelo, R., et al. (2018). FDG-PET and CSF biomarker accuracy in prediction of conversion to different dementias in a large multicentre MCI cohort. *NeuroImage. Clin.* 18, 167–177. doi: 10.1016/j.nicl.2018.01.019

Carlino, E., Frisaldi, E., Rainero, I., Asteggiano, G., Cappa, G., Tarenzi, L., et al. (2014). Nonlinear analysis of electroencephalogram in frontotemporal lobar degeneration. *Neuroreport* 25, 496–500. doi: 10.1097/WNR.0000000000000123

Cash, D. M., Bocchetta, M., Thomas, D. L., Dick, K. M., van Swieten, J. C., Borroni, B., et al. (2018). Patterns of gray matter atrophy in genetic frontotemporal dementia: results from the GENFI study. *Neurobiol. Aging* 62, 191–196. doi: 10.1016/j.neurobiolaging.2017.10.008

Cavazzana, I., Alberici, A., Bonomi, E., Ottaviani, R., Kumar, R., Archetti, S., et al. (2018). Antinuclear antibodies in frontotemporal dementia: the tip's of autoimmunity iceberg? *J. Neuroimmunol.* 325, 61–63. doi: 10.1016/j.jneuroim.2018.10.006

Cerami, C., Dodich, A., Lettieri, G., Iannaccone, S., Magnani, G., Marcone, A., et al. (2016). Different FDG-PET metabolic patterns at single-subject level in the behavioral variant of fronto-temporal dementia. *Cortex* 83, 101–112. doi: 10.1016/j.cortex.2016.07.008

Chan, D., Walters, R. J., Sampson, E. L., Schott, J. M., Smith, S. J., and Rossor, M. N. (2004). EEG abnormalities in frontotemporal lobar degeneration. *Neurology* 62, 1628–1630. doi: 10.1212/01.wnl.0000123103.89419.b7

de Jong, D., Jansen, R. W., Pijnenburg, Y. A. L., van Geel, W. J. A., Borm, G. F., Kremer, H. P. H., et al. (2007). CSF neurofilament proteins in the differential diagnosis of dementia. *J. Neurol. Neurosurg. Psychiatry* 78, 936–938. doi: 10.1136/jnnp.2006.107326

Devenney, E., Hornberger, M., Irish, M., Mioshi, E., Burrell, J., Tan, R., et al. (2014). Frontotemporal dementia associated with the *C9ORF72* Mutation. *JAMA Neurol.* 71:331. doi: 10.1001/jamaneurol.2013.6002

Diehl-Schmid, J., Perneczky, R., Koch, J., Nedopil, N., and Kurz, A. (2013). Guilty by suspicion? criminal behavior in frontotemporal lobar degeneration. *Cogn. Behav. Neurol.* 26, 73–77. doi: 10.1097/WNN.0b013e31829cff11

Dodich, A., Cerami, C., Crespi, C., Canessa, N., Lettieri, G., Iannaccone, S., et al. (2016). Differential impairment of cognitive and affective mentalizing abilities in neurodegenerative dementias: evidence from behavioral variant of frontotemporal dementia, alzheimer's disease, and mild cognitive impairment. *J. Alzheimers Dis.* 50, 1011–1022. doi: 10.3233/JAD-150605

Dopper, E. G., Rombouts, S. A., Jiskoot, L. C., den Heijer, T., de Graaf, J. R., de Koning, I., et al. (2013). Structural and functional brain connectivity in presymptomatic familial frontotemporal dementia. *Neurology* 80, 814–823. doi: 10.1212/WNL.0b013e31828407bc

Dubois, B., Feldman, H. H., Jacova, C., Dekosky, S. T., Barberger-Gateau, P., Cummings, J., et al. (2007). Research criteria for the diagnosis of Alzheimer's disease: revising the NINCDS-ADRDA criteria. *Lancet Neurol.* 6, 734–746. doi: 10.1016/S1474-4422(07)70178-3

Farb, N. A. S., Grady, C. L., Strother, S., Tang-Wai, D. F., Masellis, M., Black, S., et al. (2013). Abnormal network connectivity in frontotemporal dementia: evidence for prefrontal isolation. *Cortex* 49, 1856–1873. doi: 10.1016/j.cortex.2012.09.008

Feis, R. A., Bouts, M. J. R. J., Panman, J. L., Jiskoot, L. C., Dopper, E. G. P., Schouten, T. M., et al. (2018). Single-subject classification of presymptomatic frontotemporal dementia mutation carriers using multimodal MRI. *NeuroImage Clin.* 20, 188–196. doi: 10.1016/j.nicl.2018.07.014

Fernández-Matarrubia, M., Matías-Guiu, J. A., Cabrera-Martín, M. N., Moreno-Ramos, T., Valles-Salgado, M., Carreras, J. L., et al. (2017). Episodic memory dysfunction in behavioral variant frontotemporal dementia: a clinical and FDG-PET study. *J. Alzheimers Dis.* 57, 1251–1264. doi: 10.3233/JAD-160874

Floeter, M. K., Danielian, L. E., Braun, L. E., and Wu, T. (2018). Longitudinal diffusion imaging across the C9orf72 clinical spectrum. *J. Neurol. Neurosurg. Psychiatry* 89, 53–60. doi: 10.1136/jnnp-2017-316799

Frisch, S., Dukart, J., Vogt, B., Horstmann, A., Becker, G., Villringer, A., et al. (2013). Dissociating memory networks in early Alzheimer's disease and frontotemporal lobar degeneration - a combined study of hypometabolism and atrophy. *PLoS One* 8:e55251. doi: 10.1371/journal.pone.0055251

Funkiewiez, A., Bertoux, M., de Souza, L. C., Lévy, R., and Dubois, B. (2012). The SEA (social cognition and emotional assessment): a clinical neuropsychological tool for early diagnosis of frontal variant of frontotemporal lobar degeneration. *Neuropsychology* 26, 81–90. doi: 10.1037/a0025318

Galimberti, D., Dell'Osso, B., Altamura, A. C., and Scarpini, E. (2015). Psychiatric symptoms in frontotemporal dementia: epidemiology, phenotypes, and differential diagnosis. *Biol. Psychiatry* 78, 684–692. doi: 10.1016/j.biopsych.2015.03.028

Gendron, T. F., Chew, J., Stankowski, J. N., Hayes, L. R., Zhang, Y. J., Prudencio, M., et al. (2017). Poly(GP) proteins are a useful pharmacodynamic marker for C9ORF72-associated amyotrophic lateral sclerosis. *Sci. Transl. Med.* 9:eaai7866. doi: 10.1126/scitranslmed.aai7866

Geschwind, D. H., Robidoux, J., Alarcón, M., Miller, B. L., Wilhelmsen, K. C., Cummings, J. L., et al. (2001). Dementia and neurodevelopmental predisposition: cognitive dysfunction in presymptomatic subjects precedes dementia by decades in frontotemporal dementia. *Ann. Neurol.* 50, 741–746. doi: 10.1002/ana.10024

Ghidoni, R., Stoppani, E., Rossi, G., Piccoli, E., Albertini, V., Paterlini, A., et al. (2012). Optimal plasma progranulin cutoff value for predicting null progranulin mutations in neurodegenerative diseases: a multicenter italian study. *Neurodegener. Dis.* 9, 121–127. doi: 10.1159/000333132

Goossens, J., Bjerke, M., Mossevelde, S., Van den Bossche, T., Goeman, J., De Vil, B., et al. (2018). Diagnostic value of cerebrospinal fluid tau, neurofilament, and progranulin in definite frontotemporal lobar degeneration. *Alzheimers Res. Ther.* 10:31. doi: 10.1186/s13195-018-0364-0

Gregory, C., Lough, S., Stone, V., Erzinclioglu, S., Martin, L., Baron-Cohen, S., et al. (2002). Theory of mind in patients with frontal variant frontotemporal dementia and alzheimer's disease: theoretical and practical implications. *Brain* 125, 752–764. doi: 10.1093/brain/awf079

Greicius, M. D., Krasnow, B., Reiss, A. L., and Menon, V. (2003). Functional connectivity in the resting brain: A network analysis of the default mode hypothesis. *Proc. Natl. Acad. Sci. U.S.A.* 100, 253–258. doi: 10.1073/pnas.0135058100

Grimmer, T., Wutz, C., Alexopoulos, P., Drzezga, A., Förster, S., Förstl, H., et al. (2016). Visual versus fully automated analyses of 18F-FDG and amyloid PET for prediction of dementia due to alzheimer disease in mild cognitive impairment. *J. Nucl. Med.* 57, 204–207. doi: 10.2967/jnumed.115.163717

Guven, G., Bilgic, B., Tufekcioglu, Z., Erginel Unaltuna, N., Hanagasi, H., Gurvit, H., et al. (2019). Peripheral GRN mRNA and serum progranulin levels as a potential indicator for both the presence of splice site mutations and individuals at risk for frontotemporal dementia. *J. Alzheimer's Dis.* 67, 159–167. doi: 10.3233/JAD-180599

Harper, L., Fumagalli, G. G., Barkhof, F., Scheltens, P., O'Brien, J. T., Bouwman, F., et al. (2016). MRI visual rating scales in the diagnosis of dementia: evaluation in 184 post-mortem confirmed cases. *Brain* 139, 1211–1225. doi: 10.1093/brain/aww005

Hodges, J. R., Davies, R. R., Xuereb, J. H., Casey, B., Broe, M., Bak, T. H., et al. (2004). Clinicopathological correlates in frontotemporal dementia. *Ann. Neurol.* 56, 399–406. doi: 10.1002/ana.20203

Hornberger, M., and Piguet, O. (2012). Episodic memory in frontotemporal dementia: a critical review. *Brain* 135, 678–692. doi: 10.1093/brain/aws011

Hornberger, M., Piguet, O., Graham, A. J., Nestor, P. J., and Hodges, J. R. (2010). How preserved is episodic memory in behavioral variant frontotemporal dementia? *Neurology* 74, 472–479. doi: 10.1212/WNL.0b013e3181cef85d

Hu, W. T., Chen-Plotkin, A., Grossman, M., Arnold, S. E., Clark, C. M., Shaw, L. M., et al. (2010). Novel CSF biomarkers for frontotemporal lobar degenerations. *Neurology* 75, 2079–2086. doi: 10.1212/WNL.0b013e318200d78d

Illán-Gala, I., Montal, V., Borrego-Écija, S., Vilaplana, E., Pegueroles, J., Alcolea, D., et al. (2019). Cortical microstructure in the behavioural variant of frontotemporal dementia: looking beyond atrophy. *Brain* 142, 1121–1133. doi: 10.1093/brain/awz031

Irish, M., Hornberger, M., Lah, S., Miller, L., Pengas, G., Nestor, P. J., et al. (2011). Profiles of recent autobiographical memory retrieval in semantic dementia, behavioural-variant frontotemporal dementia, and Alzheimer's disease. *Neuropsychologia* 49, 2694–2702. doi: 10.1016/j.neuropsychologia.2011.05.017

Irish, M., Piguet, O., Hodges, J. R., and Hornberger, M. (2014). Common and unique gray matter correlates of episodic memory dysfunction in frontotemporal dementia and Alzheimer's disease. *Hum. Brain Mapp.* 35, 1422–1435. doi: 10.1002/hbm.22263

Janelidze, S., Hertze, J., Zetterberg, H., Landqvist Waldö, M., Santillo, A., Blennow, K., et al. (2016). Cerebrospinal fluid neurogranin and YKL-40 as biomarkers of Alzheimer's disease. *Ann. Clin. Transl. Neurol.* 3, 12–20. doi: 10.1002/acn3.266

Janssen, J. C., Schott, J. M., Cipolotti, L., Fox, N. C., Scahill, R. I., Josephs, K. A., et al. (2005). Mapping the onset and progression of atrophy in familial frontotemporal lobar degeneration. *J. Neurol. Neurosurg. Psychiatry* 76, 162–168. doi: 10.1136/jnnp.2003.032201

Jiskoot, L. C., Bocchetta, M., Nicholas, J. M., Cash, D. M., Thomas, D., Modat, M., et al. (2018a). Presymptomatic white matter integrity loss in familial frontotemporal dementia in the GENFI cohort: a cross-sectional diffusion tensor imaging study. *Ann. Clin. Transl. Neurol.* 5, 1025–1036. doi: 10.1002/acn3.601

Jiskoot, L. C., Dopper, E. G. P., Heijer, T., den Timman, R., van Minkelen, R., van Swieten, J. C., et al. (2016). Presymptomatic cognitive decline in familial frontotemporal dementia: a longitudinal study. *Neurology* 87, 384–391. doi: 10.1212/WNL.0000000000002895

Jiskoot, L. C., Panman, J. L., Meeter, L. H., Dopper, E. G. P., Donker Kaat, L., Franzen, S., et al. (2019). Longitudinal multimodal MRI as prognostic and diagnostic biomarker in presymptomatic familial frontotemporal dementia. *Brain* 142, 193–208. doi: 10.1093/brain/awy288

Jiskoot, L. C., Panman, J. L., van Asseldonk, L., Franzen, S., Meeter, L. H. H., Donker Kaat, L., et al. (2018b). Longitudinal cognitive biomarkers predicting symptom onset in presymptomatic frontotemporal dementia. *J. Neurol.* 265, 1381–1392. doi: 10.1007/s00415-018-8850-7

Johnson, J. K., Diehl, J., Mendez, M. F., Neuhaus, J., Shapira, J. S., Forman, M., et al. (2005). Frontotemporal lobar degeneration. *Arch. Neurol.* 62, 925–930. doi: 10.1001/archneur.62.6.925

Kertesz, A., Ang, L. C., Jesso, S., MacKinley, J., Baker, M., Brown, P., et al. (2013). Psychosis and hallucinations in frontotemporal dementia with the C9ORF72 mutation: a detailed clinical cohort. *Cogn. Behav. Neurol.* 26, 146–154. doi: 10.1097/WNN.0000000000000008

Krämer, J., Lueg, G., Schiffler, P., Vrachimis, A., Weckesser, M., Wenning, C., et al. (2018). Diagnostic value of diffusion tensor imaging and positron emission tomography in early stages of frontotemporal dementia. *J. Alzheimers Dis.* 63, 239–253. doi: 10.3233/JAD-170224

Kuiperij, H. B., Versleijen, A. A. M., Beenes, M., Verwey, N. A., Benussi, L., Paterlini, A., et al. (2017). Tau rather than TDP-43 proteins are potential cerebrospinal fluid biomarkers for frontotemporal lobar degeneration subtypes: a pilot study. *J. Alzheimer's Dis.* 55, 19–35. doi: 10.3233/JAD-160386

Kämäläinen, A., Herukka, S. K., Hartikainen, P., Helisalmi, S., Moilanen, V., Knuuttila, A., et al. (2015). Cerebrospinal fluid biomarkers for Alzheimer's disease in patients with frontotemporal lobar degeneration and amyotrophic lateral sclerosis with the C9ORF72 repeat expansion. *Dement. Geriatr. Cogn. Disord.* 39, 287–293. doi: 10.1159/000371704

Landqvist Waldö, M., Gustafson, L., Passant, U., and Englund, E. (2015). Psychotic symptoms in frontotemporal dementia: a diagnostic dilemma? *Int. Psychogeriatr.* 27, 531–539. doi: 10.1017/S1041610214002580

Lee, S. E., Khazenzon, A. M., Trujillo, A. J., Guo, C. C., Yokoyama, J. S., Sha, S. J., et al. (2014). Altered network connectivity in frontotemporal dementia with C9orf72 hexanucleotide repeat expansion. *Brain* 137, 3047–3060. doi: 10.1093/brain/awu248

Lee, S. E., Sias, A. C., Mandelli, M. L., Brown, J. A., Brown, A. B., Khazenzon, A. M., et al. (2017). Network degeneration and dysfunction in presymptomatic C9ORF72 expansion carriers. *NeuroImage Clin.* 14, 286–297. doi: 10.1016/j.nicl.2016.12.006

Lehmer, C., Oeckl, P., Weishaupt, J. H., Volk, A. E., Diehl-Schmid, J., Schroeter, M. L., et al. (2017). Poly-GP in cerebrospinal fluid links C9orf72 -associated

dipeptide repeat expression to the asymptomatic phase of ALS/FTD. *EMBO Mol. Med.* 9, 859–868. doi: 10.15252/emmm.201607486

Liljegren, M., Naasan, G., Temlett, J., Perry, D. C., Rankin, K. P., Merrilees, J., et al. (2015). Criminal behavior in frontotemporal dementia and Alzheimer disease. *JAMA Neurol.* 72, 295–300. doi: 10.1001/jamaneurol.2014.3781

Lillo, P., Garcin, B., Hornberger, M., Bak, T. H., and Hodges, J. R. (2010). Neurobehavioral features in frontotemporal dementia with amyotrophic lateral sclerosis. *Arch. Neurol.* 67, 826–830. doi: 10.1001/archneurol.2010.146

Ljubenkov, P. A., Staffaroni, A. M., Rojas, J. C., Allen, I. E., Wang, P., Heuer, H., et al. (2018). Cerebrospinal fluid biomarkers predict frontotemporal dementia trajectory. *Ann. Clin. Transl. Neurol.* 5, 1250–1263. doi: 10.1002/acn3.643

Mahoney, C. J., Beck, J., Rohrer, J. D., Lashley, T., Mok, K., Shakespeare, T., et al. (2012). Frontotemporal dementia with the C9ORF72 hexanucleotide repeat expansion: clinical, neuroanatomical and neuropathological features. *Brain* 135, 736–750. doi: 10.1093/brain/awr361

Meeter, L. H., Dopper, E. G., Jiskoot, L. C., Sanchez-Valle, R., Graff, C., Benussi, L., et al. (2016). Neurofilament light chain: a biomarker for genetic frontotemporal dementia. *Ann. Clin. Transl. Neurol.* 3, 623–636. doi: 10.1002/acn3.325

Meeter, L. H. H., Patzke, H., Loewen, G., Dopper, E. G. P., Pijnenburg, Y. A. L., van Minkelen, R., et al. (2016). Progranulin levels in plasma and cerebrospinal fluid in granulin mutation carriers. *Dement. Geriatr. Cogn. Dis. Extra.* 6, 330–340. doi: 10.1159/000447738

Meeter, L. H. H., Vijverberg, E. G., Campo, M., Del Rozemuller, A. J. M., Kaat, L. D., de Jong, F. J., et al. (2018). Clinical value of neurofilament and phospho-tau/tau ratio in the frontotemporal dementia spectrum. *Neurology* 90, e1231–e1239. doi: 10.1212/wnl.0000000000005261

Mendez, M. F., and Perryman, K. M. (2002). Neuropsychiatric features of frontotemporal dementia: evaluation of consensus criteria and review. *J. Neuropsychiatry Clin. Neurosci.* 14, 424–429. doi: 10.1176/jnp.14.4.424

Menon, V., and Uddin, L. Q. (2010). Saliency, switching, attention and control: a network model of insula function. *Brain Struct. Funct.* 214, 655–667. doi: 10.1007/s00429-010-0262-0

Morbelli, S., Ferrara, M., Fiz, F., Dessi, B., Arnaldi, D., Picco, A., et al. (2016). Mapping brain morphological and functional conversion patterns in predementia late-onset bvFTD. *Eur. J. Nucl. Med. Mol. Imaging* 43, 1337–1347. doi: 10.1007/s00259-016-3335-3

Moretti, D. V., Benussi, L., Fostinelli, S., Ciani, M., Binetti, G., and Ghidoni, R. (2016). Progranulin mutations affects brain oscillatory activity in frontotemporal dementia. *Front. Aging Neurosci.* 8:35. doi: 10.3389/fnagi.2016.00035

Niikado, M., Chrem-Méndez, P., Itzcovich, T., Barbieri-Kennedy, M., Calandri, I., Martinetto, H., et al. (2018). Evaluation of cerebrospinal fluid neurofilament light chain as a routine biomarker in a memory clinic. *J. Gerontol. Ser. A* 74, 442–445. doi: 10.1093/gerona/gly179

Olm, C. A., McMillan, C. T., Irwin, D. J., Van Deerlin, V. M., Cook, P. A., Gee, J. C., et al. (2018). Longitudinal structural gray matter and white matter MRI changes in presymptomatic progranulin mutation carriers. *NeuroImage Clin.* 19, 497–506. doi: 10.1016/j.nicl.2018.05.017

Omar, R., Sampson, E. L., Loy, C. T., Mummery, C. J., Fox, N. C., Rossor, M. N., et al. (2009). Delusions in frontotemporal lobar degeneration. *J. Neurol.* 256, 600–607. doi: 10.1007/s00415-009-0128-7

Papma, J. M., Jiskoot, L. C., Panman, J. L., Dopper, E. G., den Heijer, T., Donker Kaat, L., et al. (2017). Cognition and gray and white matter characteristics of presymptomatic C9orf72 repeat expansion. *Neurology* 89, 1256–1264. doi: 10.1212/WNL.0000000000004393

Pardini, M., Emberti Gialloreti, L., Mascolo, M., Benassi, F., Abate, L., Guida, S., et al. (2013). Isolated theory of mind deficits and risk for frontotemporal dementia: a longitudinal pilot study. *J. Neurol. Neurosurg. Psychiatry* 84, 818–821. doi: 10.1136/jnnp-2012-303684

Paterson, R. W., Slattery, C. F., Poole, T., Nicholas, J. M., Magdalinou, N. K., Toombs, J., et al. (2018). Cerebrospinal fluid in the differential diagnosis of Alzheimer's disease: clinical utility of an extended panel of biomarkers in a specialist cognitive clinic. *Alzheimers Res. Ther.* 10:32. doi: 10.1186/s13195-018-0361-3

Pennington, C., Hodges, J. R., and Hornberger, M. (2011). Neural correlates of episodic memory in behavioral variant frontotemporal dementia. *J. Alzheimer's Dis.* 24, 261–268. doi: 10.3233/JAD-2011-101668

Perry, D. C., Brown, J. A., Possin, K. L., Datta, S., Trujillo, A., Radke, A., et al. (2017). Clinicopathological correlations in behavioural variant frontotemporal dementia. *Brain* 140, 3329–3345. doi: 10.1093/brain/awx254

Pievani, M., de Haan, W., Wu, T., Seeley, W. W., and Frisoni, G. B. (2011). Functional network disruption in the degenerative dementias. *Lancet Neurol.* 10, 829–843. doi: 10.1016/S1474-4422(11)70158-2

Pievani, M., Paternicò, D., Benussi, L., Binetti, G., Orlandini, A., Cobelli, M., et al. (2014). Pattern of structural and functional brain abnormalities in asymptomatic granulin mutation carriers. *Alzheimers Dement.* 10, S354–S363. doi: 10.1016/j.jalz.2013.09.009

Pijnenburg, Y. A. L., Gillissen, F., Jonker, C., and Scheltens, P. (2004). Initial complaints in frontotemporal lobar degeneration. *Dement. Geriatr. Cogn. Disord.* 17, 302–306. doi: 10.1159/000077159

Pijnenburg, Y. A. L., Strijers, R. L. M., Made, Y. V., van der Flier, W. M., Scheltens, P., and Stam, C. J. (2008). Investigation of resting-state EEG functional connectivity in frontotemporal lobar degeneration. *Clin. Neurophysiol.* 119, 1732–1738. doi: 10.1016/j.clinph.2008.02.024

Pijnenburg, Y. A. L., Verwey, N. A., van der Flier, W. M., Scheltens, P., and Teunissen, C. E. (2015). Discriminative and prognostic potential of cerebrospinal fluid phosphoTau/tau ratio and neurofilaments for frontotemporal dementia subtypes. *Alzheimer's Dement. Diagn. Assess. Dis. Monit.* 1, 505–512. doi: 10.1016/j.dadm.2015.11.001

Poletti, M., Enrici, I., and Adenzato, M. (2012). Cognitive and affective Theory of Mind in neurodegenerative diseases: neuropsychological, neuroanatomical and neurochemical levels. *Neurosci. Biobehav. Rev.* 36, 2147–2164. doi: 10.1016/j.neubiorev.2012.07.004

Popuri, K., Dowds, E., Beg, M. F., Balachandar, R., Bhalla, M., Jacova, C., et al. (2018). Gray matter changes in asymptomatic C9orf72 and GRN mutation carriers. *NeuroImage Clin.* 18, 591–598. doi: 10.1016/j.nicl.2018.02.017

Ranasinghe, K. G., Rankin, K. P., Lobach, I. V., Kramer, J. H., Sturm, V. E., Bettcher, B. M., et al. (2016). Cognition and neuropsychiatry in behavioral variant frontotemporal dementia by disease stage. *Neurology* 86, 600–610. doi: 10.1212/WNL.0000000000002373

Rascovsky, K., Hodges, J. R., Knopman, D., Mendez, M. F., Kramer, J. H., Neuhaus, J., et al. (2011). Sensitivity of revised diagnostic criteria for the behavioural variant of frontotemporal dementia. *Brain* 134, 2456–2477. doi: 10.1093/brain/awr179

Ratnavalli, E., Brayne, C., Dawson, K., and Hodges, J. R. (2002). The prevalence of frontotemporal dementia. *Neurology* 58, 1615–1621.

Riemenschneider, M., Wagenpfeil, S., Vanderstichele, H., Otto, M., Wiltfang, J., Kretzschmar, H., et al. (2003). Phospho-tau/total tau ratio in cerebrospinal fluid discriminates creutzfeldt-Jakob disease from other dementias. *Mol. Psychiatry* 8, 343–347. doi: 10.1038/sj.mp.4001220

Rivero-Santana, A., Ferreira, D., Perestelo-Pérez, L., Westman, E., Wahlund, L. O., Sarría, A., et al. (2017). Cerebrospinal fluid biomarkers for the differential diagnosis between alzheimer's disease and frontotemporal lobar degeneration: systematic review, HSROC analysis, and confounding factors. *J. Alzheimer's Dis.* 55, 625–644. doi: 10.3233/JAD-160366

Rohrer, J. D., Nicholas, J. M., Cash, D. M., van Swieten, J., Dopper, E., Jiskoot, L., et al. (2015). Presymptomatic cognitive and neuroanatomical changes in genetic frontotemporal dementia in the genetic frontotemporal dementia initiative (GENFI) study: a cross-sectional analysis. *Lancet Neurol.* 14, 253–262. doi: 10.1016/S1474-4422(14)70324-2

Rohrer, J. D., Warren, J. D., Barnes, J., Mead, S., Beck, J., Pepple, T., et al. (2008). Mapping the progression of progranulin-associated frontotemporal lobar degeneration. *Nat. Clin. Pract. Neurol.* 4, 455–460. doi: 10.1038/ncpneuro0869

Rosness, T. A., Haugen, P. K., Passant, U., and Engedal, K. (2008). Frontotemporal dementia: a clinically complex diagnosis. *Int. J. Geriatr. Psychiatry* 23, 837–842. doi: 10.1002/gps.1992

Rytty, R., Nikkinen, J., Paavola, L., Abou Elseoud, A., Moilanen, V., Visuri, A., et al. (2013). GroupICA dual regression analysis of resting state networks in a behavioral variant of frontotemporal dementia. *Front. Hum. Neurosci.* 7:461. doi: 10.3389/fnhum.2013.00461

Seeley, W. W., Crawford, R. K., Zhou, J., Miller, B. L., and Greicius, M. D. (2009). Neurodegenerative diseases target large-scale human brain networks. *Neuron* 62, 42–52. doi: 10.1016/j.neuron.2009.03.024

Shinagawa, S., Shigenobu, K., Tagai, K., Fukuhara, R., Kamimura, N., Mori, T., et al. (2017). Violation of laws in frontotemporal dementia: a multicenter study in Japan. *J. Alzheimers Dis.* 57, 1221–1227. doi: 10.3233/JAD-170028

Skillbäck, T., Farahmand, B., Bartlett, J. W., Rosén, C., Mattsson, N., Nägga, K., et al. (2014). CSF neurofilament light differs in neurodegenerative diseases and predicts severity and survival. *Neurology* 83, 1945–1953. doi: 10.1212/WNL.0000000000001015

Snowden, J. S., Rollinson, S., Thompson, J. C., Harris, J. M., Stopford, C. L., Richardson, A. M. T., et al. (2012). Distinct clinical and pathological characteristics of frontotemporal dementia associated with C9ORF72 mutations. *Brain* 135, 693–708. doi: 10.1093/brain/awr355

Solje, E., Aaltokallio, H., Koivumaa-Honkanen, H., Suhonen, N. M., Moilanen, V., Kiviharju, A., et al. (2015). The phenotype of the C9ORF72 expansion carriers according to revised criteria for bvFTD. *PLoS One* 10:E131817. doi: 10.1371/journal.pone.0131817

Steinacker, P., Anderl-Straub, S., Diehl-Schmid, J., Semler, E., Uttner, I., von Arnim, C. A. F., et al. (2018). Serum neurofilament light chain in behavioral variant frontotemporal dementia. *Neurology* 91, e1390–e1401. doi: 10.1212/wnl.0000000000006318

Su, Z., Zhang, Y., Gendron, T. F., Bauer, P. O., Chew, J., Yang, W. Y., et al. (2014). Discovery of a biomarker and lead small molecules to target r(GGGGCC)-associated defects in c9FTD/ALS. *Neuron* 83, 1043–1050. doi: 10.1016/j.neuron.2014.07.041

Velakoulis, D., Walterfang, M., Mocellin, R., Pantelis, C., and McLean, C. (2009). Frontotemporal dementia presenting as schizophrenia-like psychosis in young people: clinicopathological series and review of cases. *Br. J. Psychiatry* 194, 298–305. doi: 10.1192/bjp.bp.108.057034

Vijverberg, E. G. B., Dols, A., Krudop, W. A., Milan, M. D. C., Kerssens, C. J., Gossink, F., et al. (2017). Cerebrospinal fluid biomarker examination as a tool to discriminate behavioral variant frontotemporal dementia from primary psychiatric∼disorders. *Alzheimers Dement. Diagn. Assess. Dis. Monit.* 7, 99–106. doi: 10.1016/j.dadm.2017.01.009

Walhout, R., Schmidt, R., Westeneng, H.-J., Verstraete, E., Seelen, M., van Rheenen, W., et al. (2015). Brain morphologic changes in asymptomatic C9orf72 repeat expansion carriers. *Neurology* 85, 1780–1788. doi: 10.1212/WNL.0000000000002135

Wen, J., Zhang, H., Alexander, D. C., Durrleman, S., Routier, A., Rinaldi, D., et al. (2018). Neurite density is reduced in the presymptomatic phase of C9orf72 disease. *J. Neurol. Neurosurg. Psychiatry* 90, 387–394. doi: 10.1136/jnnp-2018-318994

Whitwell, J. L., Josephs, K. A., Avula, R., Tosakulwong, N., Weigand, S. D., Senjem, M. L., et al. (2011). Altered functional connectivity in asymptomatic MAPT subjects a comparison to bvFTD. *Neurology* 77, 866–874. doi: 10.1212/WNL.0b013e31822c61f2

Woollacott, I. O. C., Nicholas, J. M., Heslegrave, A., Heller, C., Foiani, M. S., Dick, K. M., et al. (2018). Cerebrospinal fluid soluble TREM2 levels in frontotemporal dementia differ by genetic and pathological subgroup. *Alzheimers Res. Ther.* 10:79. doi: 10.1186/s13195-018-0405-8

Zhou, J., Greicius, M. D., Gennatas, E. D., Growdon, M. E., Jang, J. Y., Rabinovici, G. D., et al. (2010). Divergent network connectivity changes in behavioural variant frontotemporal dementia and Alzheimer's disease. *Brain* 133, 1352–1367. doi: 10.1093/brain/awq075

Conflict of Interest Statement: The authors declare that the research was conducted in the absence of any commercial or financial relationships that could be construed as a potential conflict of interest.

frontiers in Neuroscience

REVIEW
published: 27 June 2019
doi: 10.3389/fnins.2019.00532

Motor Neuron Susceptibility in ALS/FTD

*Audrey M. G. Ragagnin[1], Sina Shadfar[1], Marta Vidal[1], Md Shafi Jamali[1] and Julie D. Atkin[1,2]**

[1] Centre for Motor Neuron Disease Research, Department of Biomedical Sciences, Faculty of Medicine and Health Sciences, Macquarie University, Sydney, NSW, Australia, [2] Department of Biochemistry and Genetics, La Trobe Institute for Molecular Science, La Trobe University, Melbourne, VIC, Australia

Amyotrophic lateral sclerosis (ALS) is a neurodegenerative disease characterized by the death of both upper and lower motor neurons (MNs) in the brain, brainstem and spinal cord. The neurodegenerative mechanisms leading to MN loss in ALS are not fully understood. Importantly, the reasons why MNs are specifically targeted in this disorder are unclear, when the proteins associated genetically or pathologically with ALS are expressed ubiquitously. Furthermore, MNs themselves are not affected equally; specific MNs subpopulations are more susceptible than others in both animal models and human patients. Corticospinal MNs and lower somatic MNs, which innervate voluntary muscles, degenerate more readily than specific subgroups of lower MNs, which remain resistant to degeneration, reflecting the clinical manifestations of ALS. In this review, we discuss the possible factors intrinsic to MNs that render them uniquely susceptible to neurodegeneration in ALS. We also speculate why some MN subpopulations are more vulnerable than others, focusing on both their molecular and physiological properties. Finally, we review the anatomical network and neuronal microenvironment as determinants of MN subtype vulnerability and hence the progression of ALS.

Keywords: amyotrophic lateral sclerosis, neurodegeneration, selective vulnerability, fast and slow motor units, frontotemporal dementia

OPEN ACCESS

Edited by:
Alberto Lleo, Hospital de la Santa Creu i Sant Pau, Spain

Reviewed by:
Mamede De Carvalho, Universidade de Lisboa, Portugal
Adrian Israelson, Ben-Gurion University of the Negev, Israel

***Correspondence:**
Julie D. Atkin
julie.atkin@mq.edu.au

Specialty section:
This article was submitted to Neurodegeneration, a section of the journal Frontiers in Neuroscience

Received: *06 March 2019*
Accepted: *08 May 2019*
Published: *27 June 2019*

Citation:
Ragagnin AMG, Shadfar S, Vidal M, Jamali MS and Atkin JD (2019) Motor Neuron Susceptibility in ALS/FTD. Front. Neurosci. 13:532. doi: 10.3389/fnins.2019.00532

INTRODUCTION

Amyotrophic lateral sclerosis (ALS) is a late-onset, progressive and fatal neurodegenerative disease which primarily affects motor neurons (MNs) of the motor cortex of the brain, brainstem motor nuclei and anterior horn of the spinal cord (Kiernan et al., 2011; Renton et al., 2014; Al Sultan et al., 2016; Taylor et al., 2016). ALS commonly begins in late-adulthood, when patients first experience focal symptoms, such as weakness in the limb or bulbar muscles, as well as widespread fasciculations. The disease then usually progresses in an organized way to adjacent areas of the central nervous system (CNS), and consequently symptoms appear in other regions of the body. Several clinical subsets of ALS can be distinguished by the anatomical location first affected (Renton et al., 2014; Taylor et al., 2016). This includes bulbar onset, where symptoms first appear in the muscles controlling speech, mastication and swallowing; and limb onset, where symptoms present initially in the upper (arm or hand) or lower limbs (leg or foot). Bulbar onset patients face a much worse prognosis than those with spinal onset ALS, where the average survival time following diagnosis is less than 2 years. However, in patients with the much rarer respiratory onset form (3–5%), the prognosis is even worse as the

survival time following diagnosis is only 1.4 years (Swinnen and Robberecht, 2014). At disease end stage, only support and palliation are available, and patients usually die from respiratory failure, typically 3–5 years after diagnosis (Taylor et al., 2016). There are currently few effective treatments. Hence there is an urgent need to understand the underlying causes and risk factors for ALS to discover new therapeutic targets.

Neurons have complex and extended morphologies compared to other cell types, and within the CNS, neurons can vary greatly in their properties. MNs are unique cells amongst neurons because they are large, even by neuronal standards, with very long axons, up to 1 m in length in an adult human. MNs can be distinguished into two main categories according to their location in the CNS: upper MNs (UMNs) located in the cortex, and lower MNs (LMNs) located in the brainstem and spinal cord. The spinal MNs comprise both visceral MNs of the thoracic and sacral regions, which control autonomic functions, and somatic MNs, which regulate the contraction of skeletal muscles and thus control movement. The diversity of MNs reflects the variety of targets they innervate, including a wide range of muscle fiber types. UMNs and LMNs differ in the location of their cell bodies, the neurotransmitters released, their targeting and symptoms resulting from their injury.

It is unknown why MNs are specifically targeted in ALS and remarkably, MNs are not equally affected (Rochat et al., 2016; Nijssen et al., 2017). Whilst both UMNs and LMNs are involved, some LMN subtypes are relatively resistant to neurodegeneration. Spinal cord and hypoglossal MNs are amongst the first to degenerate, hence the ability to speak, breath and move is lost early in disease course. As ALS progresses, specific MN subtypes then preferentially deteriorate. However, some MNs are spared until disease end stage, such as oculomotor neurons and Onuf's nuclei MNs, and as a result, patients retain normal visual, sexual and bladder function throughout the disease course. The resistant MNs differ significantly from the vulnerable MNs anatomically and functionally, and they possess distinct transcriptomes, metabolic and developmental profiles. Surprisingly, there are also differences in vulnerability amongst spinal MNs, because those that are part of the faster motor units degenerate before those in the slower motor units (Frey et al., 2000; Pun et al., 2006; Hegedus et al., 2007; Hadzipasic et al., 2014; Sharma et al., 2016; Spiller et al., 2016a), thus adding further complexity to the question of MN vulnerability.

ALS shares clinical and pathological features with frontotemporal dementia (FTD), a type of dementia that involves impaired judgment and executive skills. In FTD, the loss of cortical MNs is accompanied by loss of neurons in the frontal and temporal cortices, which correlates clinically with the symptoms of FTD (Neumann et al., 2006; Burrell et al., 2016). The relationship between ALS and FTD has been confirmed through genetic studies, and these two conditions are now considered to be at opposite ends of the same disease continuum (Taylor et al., 2016; Shahheydari et al., 2017). Hence, while ALS was historically judged as a disorder affecting the motor system only, it is now recognized that non-motor features are present (Fang et al., 2017). A wealth of evidence also demonstrates that ALS is a heterogeneous disorder. The clinical symptoms, including the proportion of UMN and LMN signs, age of onset, disease duration, and association with other conditions, are major features contributing to its highly variable phenotypes. As well as the development of FTD (Strong and Yang, 2011), ALS can also involve cognitive impairment in up to 50% of patients (Tsermentseli et al., 2012), the autonomic nervous system (Piccione et al., 2015), supranuclear gaze systems (van der Graaff et al., 2009; Donaghy et al., 2011), and extrapyramidal motor signs (Pradat et al., 2002). Sensory, olfactory and visual dysfunction have also been described in some patients (Bede et al., 2016). In addition, there are also other conditions affecting MNs that share similarities, but also striking differences, to ALS. In particular, primary lateral sclerosis (PLS) affects UMNs but it progresses much slowly than ALS. It also has a significantly lower mortality rate (Tartaglia et al., 2007), consistent with the relative resistant of LMNs in ALS.

One of the main pathological characteristics of ALS is the presence of insoluble protein inclusions in the soma of MNs. TAR DNA binding protein-43 (TDP-43) is the major component of these inclusions (Arai et al., 2006; Neumann et al., 2006) in almost all (∼97%) ALS patients and ∼50% FTD patients (Arai et al., 2006; Neumann et al., 2006; Mackenzie et al., 2007; Scotter et al., 2015; Le et al., 2016). Loss of TDP-43 from the nucleus is evident in MNs from ALS/FTD patient tissues, concomitant with the formation of TDP-43 inclusions in the cytoplasm of both MNs and glia. Neuropathological studies have also revealed that the clinical course of ALS reflects the presence of TDP-43 pathology, from its deposition at an initial site of onset, to its spread to contiguous regions of the CNS (Brettschneider et al., 2013). Mutations in TDP-43 are also present in 5% of familial forms of ALS (Sreedharan et al., 2008). In the genetic types of ALS, it remains unclear why MNs are specifically affected when the mutant proteins are ubiquitously expressed. Males are affected more by ALS than females, and ethnic populations show differences in the incidence rates of ALS, further highlighting the contribution of genetics to ALS.

Whilst our understanding of the etiology of ALS has increased significantly in recent years, major gaps in our knowledge remain. In this review, we address several unanswered questions regarding the unique susceptibility of specific types of MNs in ALS: Why does neurodegeneration spread throughout specific neural networks? How can ubiquitously expressed genes be selectively toxic to MNs? Why are some MN subtypes more vulnerable to degeneration than others? We also discuss the role of the neuronal network and the specific cellular microenvironment in driving cell-to-cell disease progression, plus the importance of genetics in influencing susceptibility of specific neuronal subpopulations. Finally, we discuss the role of aging as a potential risk factor for the susceptibility of specific MN subtypes. A thorough comprehension of why specific cell types degenerate is imperative to our understanding of ALS because it provides important clues as to what initiates neurodegeneration, and how this knowledge may be harnessed therapeutically.

ANATOMY OF THE MOTOR SYSTEM

In the CNS, the motor cortex, basal ganglia, cerebellum, and parts of the brainstem, are directly involved in the planning and initiation of movement. In contrast, the precise timing and pattern of movement is generated by MNs located in the spinal cord (**Figure 1**; Kiehn, 2016). The corticospinal (anterior and lateral) tract is the largest descending tract in humans. The lateral corticospinal tract originates in the primary motor cortex, which lies in the precentral gyrus and sends fibers to muscles in the extremity. This is via contralateral cortical innervation, so that the left motor cortex controls the right extremities and vice versa, to control the voluntary movement of contralateral limbs (Javed and Lui, 2018). MNs outputs are not confined to the peripheral muscles however, but also include excitatory terminals to a group of interneurons, Renshaw cells, and also to other MNs.

Glutamate (cortex, spinal cord) and acetylcholine (spinal cord) modulate excitatory input within neurons, whereas GABA and glycine facilitate inhibitory neurotransmission (Ramírez-Jarquín et al., 2014). At the neuromuscular junction (NMJ), only acetylcholine acts at the synapse but interestingly, synaptic transmission between MNs in the spinal cord involves both acetylcholine and glutamate (Bhumbra and Beato, 2018). Renshaw cells are excited through both acetylcholine and glutamate receptors and spinal MNs co-release glutamate to excite Renshaw cells and other MNs, but not to excite muscles (Nishimaru et al., 2005; Bories et al., 2007; Bhumbra and Beato, 2018). Hence, different synaptic transmission systems are present at different postsynaptic targets of MNs (Bhumbra and Beato, 2018).

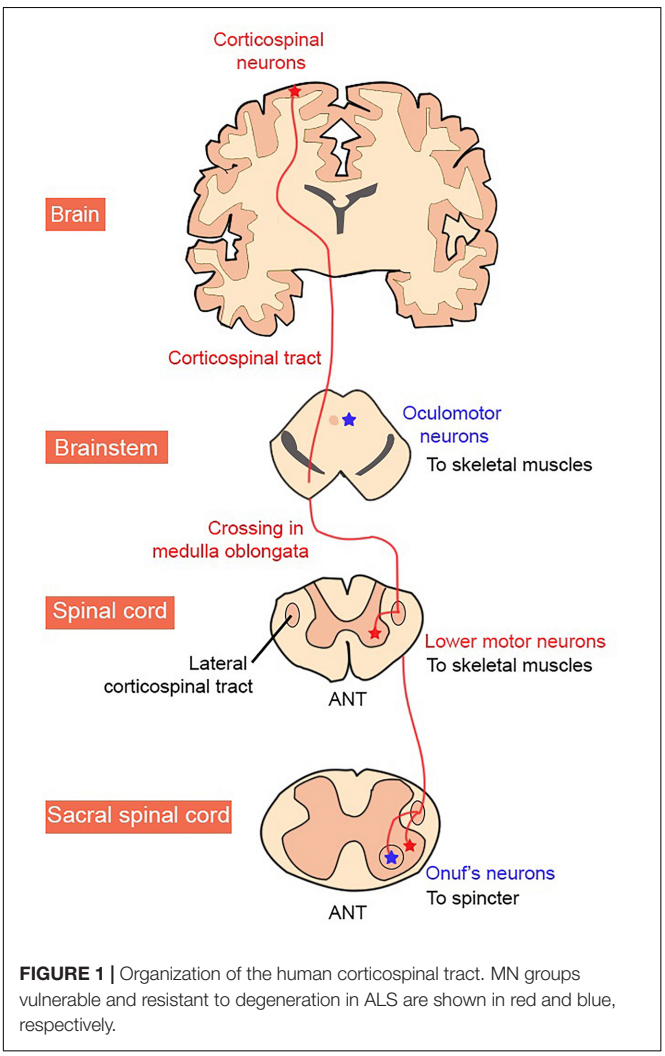

FIGURE 1 | Organization of the human corticospinal tract. MN groups vulnerable and resistant to degeneration in ALS are shown in red and blue, respectively.

However, MNs are not homogeneous throughout the CNS because they exhibit distinct morphologies and patterns of connectivity, which underlie their different physiological functions. Hence, within a single region, MNs that perform closely related functions can be further subdivided, both anatomically and physiologically. The identities of specific MN subtypes and their target projections are controlled by selective cell-type expression of transcription factors, notably members of the Hox, LIM, Nkx6, and ETS families (Stifani, 2014). This provides the fundamental mechanism for spinal MN diversification and connectivity to specific peripheral muscle targets. Thus, to generate movement, MNs integrate information from sensory structures and transform it into precise temporal and magnitudal activation of muscles.

A MN located in the spinal cord innervates up to several hundred fibers within one muscle, which together form the motor unit. Trains of action potentials within the axon cause the release of acetylcholine at the NMJ, which activates nicotinic receptors on the muscle fibers the MN innervates. This initiates a cascade of signaling events in the muscle fiber that leads to its contraction. A motor pool consists of all the individual MNs that innervate a single muscle. A muscle unit (one muscle and its motor pool) is composed of three different types of functional motor units consisting of alpha (α), beta (β), and gamma (γ) MNs, which are classified according to the contractile activity of the muscle fiber innervated. We will now discuss in more detail the anatomy of those structures involved in movement.

The Spinal Cord

In the spinal cord, MNs are organized into columns (**Table 1**) based on the location of their target muscle [reviewed in Matise and Sharma (2013) and Stifani (2014)]. Within each column, the MNs innervating each muscle are clustered into motor pools, each containing of 20–300 cells depending on the muscle (Bryan et al., 1972; McHanwell and Biscoe, 1981). α-MNs located in the spinal cord are archetypal MNs that innervate extrafusal muscle fibers, thus creating force to move the skeleton (**Table 2**). In contrast, γ-MNs innervate intrafusal fibers, which modulate the sensitivity of muscle spindles to stretch (**Table 2**) (Hunt and Kuffler, 1951; Kuffler et al., 1951; Kanning et al., 2010). β-MNs are not as well characterized as α-MNs but they innervate both intrafusal and extrafusal muscle fibers (Bessou et al., 1965). Both α and γ-MNs have large dendritic trees but γ-MNs have fewer large dendrites than α-MNs (7–11) and they also branch less (Westbury, 1982). The somas of γ-MNs are smaller than those of α-MNs and they also possess thinner axons, which

TABLE 1 | Segmental organization of spinal cord columns.

Segment	CERVICAL								THORACIC							LUMBAR					SACRAL				
Vertebrae	1	2	3	4	5	6	7	8	1	2	3	...	10	11	12	1	2	3	4	5	1	2	3	4	5
Median motor column																									
Spinal accessory column																									
Phrenic motor column																									
Preganglionic column																					*	*	*		
Hypaxial motor column																									
Lateral motor column																									

Pools of MNs that innervate muscles of similar embryonic origin are stereotypically localized within the ventral spinal cord, known as motor columns. The medial motor column (brown) is present in the whole spinal cord and it comprises MNs that innervate the long muscles of the back and the body wall musculature. The spinal accessory column (purple) and the phrenic column (red) are found along the five first cervical segments (C1 to C5) and between C3 and C5, respectively. The preganglionic column (yellow) extends from the first thoracic segment (T1) to the second lumbar segment (L2), and between sacral segments 2 and 4 (S2 to S4) where the Onuf's nuclei (*) are found. MNs in the preganglionic column innervate neurons of the sympathetic ganglia. The hypaxial motor column (blue) is restricted to the thoracic spinal cord (T1 to T12). The lateral motor column (green), connected to the limbs, comprises the cervical and thoracic spinal cord (from C5 to T1) and the lumbar spinal cord (L1 to L5).

TABLE 2 | Comparison of α- and γ-spinal motor neurons.

	Spinal α-MN	Spinal γ-MN
Target muscle fiber	Extrafusal[1]	Intrafusal[1]
Soma size	Larger[2,3,4,5]	Smaller[2,3,4,5]
Axon diameter	Larger[2]	Thinner[2]
Dendrite branching	More[2]	Less[2]
Motor unit size (innervation ratio)	Larger[6]	Smaller[6]
Membrane input resistance	Larger[7]	Smaller[7]
Firing	Subtype-dependent[8]	Subtype-dependent[8]
Axon conduction velocity	Faster[2,7,9]	Slower[2,7,9]
Afterhyperpolarization duration	Subtype-dependent[7,9]	Variable[7,9]
Spinal reflex	Yes[10]	No[10]
Affected in ALS	Yes[11,12]	Less[11,12]
Affected in aging	Yes[13,14]	No[13,14]
Markers	Osteopontin[15] RBFOX3/NeuN[16] Hb9::GFP[5] NKAα1[17] (adult)	Err3[16] Weak NeuN[5,16] NKAα3[17] (adult) ESRRG[16] GFRα1[5] HTR1D[18] (early marker) WNT7A[19] (late embryonic stage)

ESRRG, estrogen-related receptor gamma; GFRα1, GDNF family receptor alpha 1; HTR1D, serotonin receptor 1D; NAKα1/3, Na^+/K^+-ATPases 1/3; RBFOX3, RNA binding protein fox-1 homolog 3. [1](Kuffler et al., 1951), [2](Burke et al., 1977), [3](Westbury, 1982), [4](Friese et al., 2009), [5](Shneider et al., 2009), [6](Adal and Barker, 1965), [7](Kemm and Westbury, 1978), [8](Murphy and Martin, 1993), [9](Gustafsson and Lipski, 1979), [10](Eccles et al., 1960), [11](Mohajeri et al., 1998), [12](Lalancette-Hebert et al., 2016), [13](Swash and Fox, 1972), [14](Hashizume et al., 1988), [15](Misawa et al., 2012), [16](Friese et al., 2009), [17](Edwards et al., 2013), [18](Enjin et al., 2012), [19](Ashrafi et al., 2012).

reflects their slower conduction velocity (<55 m/s in γ-MN vs. ∼70–90 m/s in α-MNs in cats) (**Table 2**) (Westbury, 1982). γ-MNs receive only indirect sensory inputs. Therefore, γ-MNs do not directly participate in spinal reflexes (Eccles et al., 1960; Stifani, 2014), but they contribute to the modulation of muscle contraction instead.

A distinct group of MNs in the sacral spinal cord termed 'Onuf's' neurons, innervate the striated muscles of the external urethra, external anal sphincter via the pudental nerve, and the ischiocavernosus and bulbocavernosus muscles in males (Sato et al., 1978; Nagashima et al., 1979; Kuzuhara et al., 1980; Roppolo et al., 1985). These MNs are histologically similar to limb α-MNs (Mannen et al., 1977) and they are located anteromedial to the anterolateral nucleus and extend between the distal part of the S1 segment and the proximal part of S3.

α-motor units can be subdivided according to their contractile properties, into fast-twitch (F) and slow-twitch (S) fatigue-resistant types (**Table 3**) (Burke et al., 1973). In addition, fast-twitch α-motor units can be further categorized into fast-twitch fatigable [FF] and fast-twitch fatigue-resistant [FR] types, based on the length of time they sustain contraction. The basis of this classification is the duration of the twitch contraction time (Burke et al., 1973). F- and S-MNs also exhibit different afterhyperpolarization duration (AHP) properties. AHP is the phenomenon by which the membrane potential undershoots the resting potential following an action potential. S-MNs have a longer AHP than F-MNs, indicating that S-MNs have a longer "waiting period" before they can be stimulated by an action potential. Thus, they cannot fire at the same frequency as F-MNs (Eccles et al., 1957), so the larger FF-MNs take longer to reach an activation threshold. Similarly, other electrical properties differ between S- and F-MNs (**Table 3**), including their input resistance (a measure of resistance over the plasma membrane) and rheobase (a measure of the current needed to generate an action potential). S-MNs have a higher input resistance than F-MNs, underlying Hennenman's size principle which postulates that S-motor units are the first to be recruited during movement, followed by FR and then FF units (Henneman, 1957; Mendell, 2005). Hence, a slow movement generating a small force will only recruit S-MNs, whereas a quick and strong movement will also recruit F-MNs, as well as S-MNs.

In addition, at least eleven types of interneurons are involved in the control of movement, as part of central pattern generators in the spinal cord. Interneurons arise from five progenitor cells and, according to the expression

of distinct transcription factors, they mature into different lineages. This includes excitatory V2a, V3, MN and Hb9 neurons and inhibitory V0C/G,$V0_D$, $V0_V$, V1, V2b, Ia and Renshaw cells (belonging to the V1 interneuron subclass), which display specific locations and projections within the spinal cord (Ramírez-Jarquín et al., 2014).

The Brainstem

Cranial nerve nuclei are populations of neurons in the brainstem that are associated with one or more cranial nerves. They provide afferent and efferent (sensory, motor, and autonomic) innervation to the structures of the head and neck (Sonne and Lopez-Ojeda, 2018). The more posterior and lateral nuclei tend to be sensory, and the more anterior nuclei are usually motor nuclei. Trigeminal MNs innervate the muscles of mastication, whereas facial MNs supply the superficial muscles of the face, and ambiguous MNs supply the muscles of the soft palate, pharynx, and larynx. The oculomotor (III), trochlear (IV) and abducens (VI) nuclei are somatic efferents innervating the extraocular muscles within the orbit. The oculomotor nucleus contains MNs that innervate four of the six extraocular muscles (superior, medial and inferior recti, inferior oblique), plus the levator palpebrae superioris muscle. These muscles display a unique composition of six fiber types, distinct from other skeletal muscles that possess marked fatigue resistance (**Table 4**). Oculomotor units are amongst the smallest of the motor units, in contrast to skeletal muscle motor units that have higher maximum MN discharge rates. Furthermore, α-MNs in oculomotor units have higher resting membrane potentials (∼61 mV) than spinal cord α-MNs (∼70 mV), and they also discharge at higher frequencies (∼100 Hz during steady state and ∼600 Hz during saccadic eye movements, compared to ∼100 Hz for spinal cord α-MNs) (**Table 4**) (Robinson, 1970; Fuchs et al., 1988; Torres-Torrelo et al., 2012). Oculomotor neurons are almost continually active at high frequencies when maintaining eye position (Fuchs et al., 1988; De La Cruz et al., 1989), and this level of activity places high metabolic demand on these cells (Robinson, 1970; Porter and Baker, 1996; Brockington et al., 2013).

The Cortical Motor System

The motor cortex is the region of the cerebral cortex responsible for mediating voluntary movements. In rodents, the primary cortex (M1) is large and comprises almost all of the frontal cortex (Gioanni and Lamarche, 1985; Neafsey et al., 1986; Brecht et al., 2004; Yu et al., 2008; Hira et al., 2013; Paxinos, 2014), whereas in primates, the frontal cortex is compartmentalized into specialized premotor subfields and M1 is relatively small in comparison (Ferrier, 1875; Leyton and Sherrington, 1917; Asanuma and Rosén, 1972; Dickey et al., 2013; Riehle et al., 2013; Young et al., 2013; Ebbesen and Brecht, 2017). M1 plays a central role in controlling movement. This involves specialized UMNs located in layer V of this region (Broadman area 4), the giant Betz cells or corticospinal MNs. These MNs are the cortical components of the MN circuit that initiates and modulates precise voluntary movement, through long-range projections to the spinal cord. Approximately ∼30–50% of corticospinal projections originate from M1 MNs and they begin modulating their firing rate several hundred ms before movement of the limb is initiated (Georgopoulos et al., 1982; Porter and Lemon, 1993). In most mammals, the axons of cortical MNs terminate at spinal interneurons, but they also make direct connections to MNs (Lemon, 2008; Rathelot and Strick, 2009). This constitutes the final efferent pathway to the muscle to generate or suppress movement (Ramírez-Jarquín and Tapia, 2018).

TABLE 3 | Comparison of fast (FF, fast-fatigable; FR, fast-resistant) and slow (S) spinal α-motor neurons.

	Spinal α-MN	
	F	**S**
Target muscle fiber	IIb (FF), IIa (FR)[1]	I[1]
Soma size	Similar[2,3,4,5,6]	Similar[2,3,4,5,6]
Axon diameter	Larger[7,8]	Thinner[7,8]
Dendrite branching	More[4,9]	Less[4,9]
Motor unit size (innervation ratio)	Larger[1,10]	Smaller[1,10]
Membrane input resistance	Smaller[11,12,13]	Larger[11,12,13]
Firing	Phasic[14,15]	Tonic[14,15]
Axon conduction velocity	Faster[1,13]	Slower[1,13]
Afterhyperpolarization duration	Shorter[14]	Longer[14]
Recruitment	Late[15]	Early[15]
Affected in ALS	Early[16,17,18]	Late[16,17,18]
Affected in aging	Early[19,20,21]	Late[19,20,21]
Markers	CHODL[22] CALCA[22]	SV2a[23] SK3[24] ESRRB[22] (adult)

CALCA, calcitonin-related polypeptide alpha; CHODL, chondrolectin; SV2A, synaptic vesicle glycoprotein 2a; SK3, postsynaptic Ca^{2+}-activated K^+ 3; ESRRB, estrogen-related receptor beta. [1]*(Burke et al., 1973),* [2]*(Kernell and Zwaagstra, 1981),* [3]*(Burke et al., 1982),* [4]*(Cullheim et al., 1987),* [5]*(Vinsant et al., 2013),* [6]*(Hadzipasic et al., 2014),* [7]*(Burke et al., 1977),* [8]*(Dukkipati et al., 2018),* [9]*(Ulfhake and Kellerth, 1981),* [10]*(Burke and Tsairis, 1973),* [11]*(Bakels and Kernell, 1993),* [12]*(Gardiner, 1993),* [13]*(Zengel et al., 1985),* [14]*(Eccles et al., 1957),* [15]*(Zajac and Faden, 1985),* [16]*(Frey et al., 2000),* [17]*(Hegedus et al., 2007),* [18]*(Pun et al., 2006),* [19]*(Hashizume et al., 1988),* [20]*(Kadhiresan et al., 1996),* [21]*(Kanda and Hashizume, 1989),* [22]*(Enjin et al., 2010),* [23]*(Chakkalakal et al., 2010),* [24]*(Deardorff et al., 2013).*

Motor Neurons Selectively Degenerate in ALS Patients

Lesions to motor structures in humans and experimental animals lead to impairments in normal movement. In ALS, as MNs degenerate, the ability to control movement of the muscles is progressively lost. Specific MNs in the brain, brainstem and spinal cord are selectively targeted, and pathology appears first in these restricted MN populations. In fact, the name "Amyotrophic Lateral Sclerosis" reflects the strikingly selective degeneration of MNs in ALS. It is derived from a combination of three words; "Lateral" refers to the lateral spinal cord, given that corticospinal MNs are particularly vulnerable to degeneration; "Amyotrophic" is from the Greek "amyotrophia," meaning lacking muscle nourishment; and "Sclerosis" (fibrosis) refers to gliosis of the crossed corticospinal tract in the dorsolateral

TABLE 4 | Comparison of α-spinal motor neurons and oculomotor neurons.

	Spinal α-MN	Oculomotor neuron
Target muscle fiber	Single fiber type[1]	Multiple fiber types[1]
Soma size	Larger[2,3]	Smaller[2,3]
Dendrite branching	Larger[2]	Smaller[2]
Motor unit size (innervation ratio)	Larger[4,5,6,7]	Smaller[4,5,6,7]
Resting potential	Smaller[8,9,10]	Higher[8,9,10]
Discharge frequency	100 Hz[8,9,10]	100–600 Hz[8,9,10]
Affected in ALS	Yes[11,12,13,14]	No[11,12,13,14]
Affected in aging	Yes[15,16]	No[15,16]

[1](Zhou et al., 2011), [2](Durand, 1989), [3](Shoenfeld et al., 2014), [4](Burke et al., 1971), [5](Burke and Tsairis, 1973), [6](Enoka, 1995), [7](Guéritaud et al., 1985), [8](Robinson, 1970), [9](Fuchs et al., 1988), [10](Torres-Torrelo et al., 2012), [11](Nimchinsky et al., 2000), [12](Hedlund et al., 2010), [13](Valdez et al., 2012), [14](Comley et al., 2016), [15](Hashizume et al., 1988), [16](Swash and Fox, 1972).

quadrant of the spinal cord (Charcot, 1874; Frey et al., 2000; Pun et al., 2006). In the brain, UMNs in the primary cortex are also amongst the first to degenerate in ALS, and similarly, in the brainstem, the hypoglossal MNs that innervate the muscles of the tongue involved in swallowing and breathing, are also targeted early in disease course. In the brainstem, ALS can also affect trigeminal MNs, the facial MNs and ambiguous MNs. However, other MN subgroups within this region are relatively resistant to degeneration, including MNs of the oculomotor (III), trochlear (IV) and abducens (VI) nuclei, innervating the extraocular muscles (Mannen et al., 1977; Schrøder and Reske-Nielsen, 1984). Hence, eye movements remain relatively preserved throughout disease course (Kanning et al., 2010) and as a consequence, eye tracking devices are often used to aid communication in the later stages of ALS (Caligari et al., 2013). Whilst it has been reported that oculomotor neurons may be affected at disease end stage, this was recently attributed to dysfunction of the dorsolateral prefrontal cortex, the frontal eye field and the supplementary eye field, confirming the relative resistance of pure oculomotor functions in ALS (Shaunak et al., 1995; Proudfoot et al., 2015). Widespread loss of GABAergic interneurons has also been described in ALS, in both the cortex (Stephens et al., 2001; Maekawa et al., 2004) and the spinal cord (Stephens et al., 2006; Hossaini et al., 2011).

MRI studies of ALS patients has revealed that very specific neuronal networks are vulnerable to degeneration in ALS (Bede et al., 2016). However, whilst TDP-43 pathology is the signature pathological hallmark of almost all ALS cases, it can arise in areas of the CNS that are not particularly vulnerable to degeneration (Geser et al., 2008). Significant TDP-43 pathology is present in the substantia nigra and basal ganglia, which are not affected in ALS, as well as in the motor gyrus, midbrain and spinal cord. Curiously, pathological forms of TDP-43 are also detectable in the occipital lobe, amygdala, orbital gyrus and hippocampus (Geser et al., 2008). Hence, whilst major degeneration of corticobulbar, LMN, pyramidal and frontotemporal networks underlie the widespread clinical symptoms of ALS, it remains unclear how other circuits, such as the visual, sensory, autonomic and auditory systems, remain relatively protected in ALS. These unaffected networks, however, have not been well studied in ALS patients.

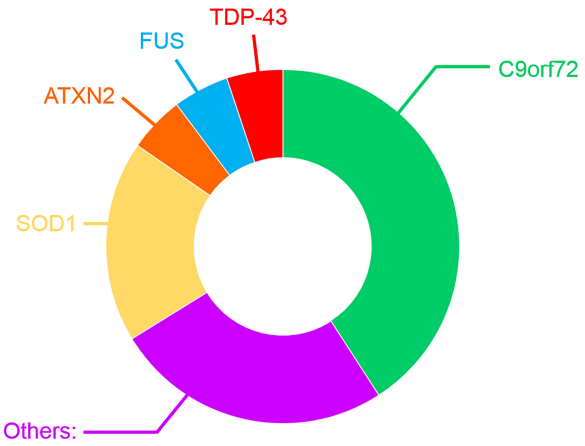

FIGURE 2 | Frequency of mutated genes in FALS patients.

GENETIC MUTATIONS AND RISK FACTORS IN ALS

Genetics of ALS

Most ALS cases occur without a clearly identified cause and are therefore referred to as sporadic ALS (SALS). In contrast, a positive family history is present in ∼10% of all patients (familial ALS; FALS) (van Blitterswijk et al., 2012; Nguyen et al., 2018) and these genetic mutations cause ALS in a mostly autosomal-dominant manner (**Supplementary Table 1** and **Figure 2**). However, several recently discovered mutations have been described in patients diagnosed with SALS (Renton et al., 2014; Al Sultan et al., 2016; Taylor et al., 2016). The patterns of selective MN degeneration and vulnerability are similar between FALS and SALS (Comley et al., 2015), implying that shared molecular mechanisms exist between the two conditions.

The first gene found to harbor mutations causing FALS encodes Cu/Zn superoxide dismutase (*SOD1*), an enzyme that detoxifies superoxide radicals (Rosen et al., 1993). Mutations in *SOD1* account for 12–23.5% of FALS cases, representing 1–2.5% of all ALS, and 186 ALS mutations have now been described[1]. Since then, mutations in approximatively 26 genes have been identified (**Supplementary Table 1** and **Figure 2**) using genome-wide or exome-wide association studies combined with segregation analysis. Hexanucleotide repeat expansions (GGGGCC) within the first intron of the chromosome 9 open reading frame 72 (*C9orf72*) gene are the most common cause of FALS and FTD (∼30–50% of FALS, ∼10% of SALS 25% of familial FTD and ∼5% of apparently sporadic ALS and

[1]http://alsod.iop.kcl.ac.uk/

FTD) (DeJesus-Hernandez et al., 2011b; Renton et al., 2011; Majounie et al., 2012; Devenney et al., 2014) (**Supplementary Table 1** and **Figure 2**), in both Europe and North America (DeJesus-Hernandez et al., 2011b; Renton et al., 2011). However, this mutation is much rarer in Asian and Middle Eastern populations (Majounie et al., 2012; Woollacott and Mead, 2014). Healthy individuals possess $\leq$ 11 GGGGCC repeats in *C9orf72* (Rutherford et al., 2012; Harms et al., 2013; van der Zee et al., 2013), whereas hundreds to thousands of repeats are present in ALS/FTD patients (Beck et al., 2013; Harms et al., 2013; van Blitterswijk et al., 2013; Suh et al., 2015). After *C9orf72*, mutations in *SOD1* (20% of FALS), *TARDPB* encoding TDP-43 (5% of FALS, >50% of FTD) (Rutherford et al., 2008; Sreedharan et al., 2008; Borroni et al., 2010; Kirby et al., 2010), *Fused in sarcoma* encoding FUS (*FUS*, 5% of FALS) (Belzil et al., 2009; Blair et al., 2009; Chiò et al., 2009; Kwiatkowski et al., 2009; Neumann et al., 2009; Vance et al., 2009), and *CCNF* encoding cyclin F (0.6–3.3% of FALS-FTD) are more frequent than the remaining 20 genes mutated in the much rarer forms of FALS (**Supplementary Table 1**). The physiological functions and properties of the proteins encoded by these genes can be grouped according to their involvement in protein quality control, cytoskeletal dynamics, RNA homeostasis and the DNA damage response. However, it is possible that genetic inheritance could sometimes be missed, due to incomplete penetrance or an oligogenic mode of inheritance, whereby more than one mutated gene is necessary to fully present disease (Nguyen et al., 2018). Consistent with this notion, the frequency of ALS patients carrying two or more mutations in ALS-associated genes is in excess of what would be expected by chance (van Blitterswijk et al., 2012; Veldink, 2017; Zou et al., 2017; Nguyen et al., 2018).

TDP-43 is an ubiquitously expressed RNA-binding protein belonging to the heterogeneous nuclear ribonucleoprotein (hnRNP) family. Fifty three mutations in *TARDBP* have now been associated with FALS, located within all but one reside of the C-terminal domain of TDP-43 [Gitcho et al., 2008; Kabashi et al., 2008; Van Deerlin et al., 2008; http://alsod.iop.kcl.ac.uk/]. Pathological forms of TDP-43 – phosphorylated, fragmented, aggregated, ubiquitinated TDP-43 – were identified as the major component of MN inclusions (Neumann et al., 2006) in almost all ALS cases, including SALS (97%) (Arai et al., 2006; Neumann et al., 2006; Mackenzie et al., 2007; Scotter et al., 2015; Le et al., 2016). TDP-43 pathology is also observed in *C9orf72* mutation cases in several brain regions, including the frontal, temporal and primary motor cortices, hippocampus, basal ganglia, amygdala, thalamus and midbrain (Murray et al., 2011; Hsiung et al., 2012; Mahoney et al., 2012; Irwin et al., 2013; Mackenzie et al., 2013; Balendra and Isaacs, 2018), highlighting an important role for TDP-43 in neurodegeneration in both SALS and FALS. Moreover, ALS and FTD cases bearing TDP-43 pathology are often referred to "TDP-43 proteinopathies" (Mackenzie et al., 2009). TDP-43 shares similar functional roles in RNA-binding, splicing and nucleocytosolic RNA transport as FUS. Fifty nine mutations in FUS have been identified in both SALS and FALS patients (Lattante et al., 2013; http://alsod.iop.kcl.ac.uk/) and FUS colocalises with TDP-43 in protein aggregates in MNs of a proportion of SALS and FALS patients (Kwiatkowski et al., 2009; Deng et al., 2010).

Disease Mechanisms Implicated in ALS

A wide range of cellular pathways have been implicated in ALS pathogenesis, as reviewed recently (Shin and Lee, 2013; Taylor et al., 2016; Balendra and Isaacs, 2018). These include altered RNA processing/metabolism, nucleolar dysfunction, RNA splicing transcriptional defects (Barmada, 2015; Fratta and Isaacs, 2018) and DNA damage (Konopka and Atkin, 2018; Penndorf et al., 2018). Proteostasis pathways have also been implicated, with impairments in autophagy and lysosomal function, the endoplasmic reticulum (ER), mitochondrial and the ubiquitin–proteasome systems described (Maharjan and Saxena, 2016; Ruegsegger and Saxena, 2016). Furthermore, several modes of vesicular trafficking are impaired in ALS, including nucleocytoplasmic (Kim and Taylor, 2017), ER-Golgi (Soo et al., 2015), and axonal forms of transport (De Vos and Hafezparast, 2017). In addition, defects in neuronal-specific processes, including hyper-excitability and hypo-excitability, glutamate excitotoxicity, and neuronal branching defects, have also been described in ALS (Fogarty, 2018).

Mouse Models of ALS

Over the last 20 years, several transgenic mouse strains expressing human mutant SOD1 have been generated. These mice have been used to either examine disease mechanisms or trial potential therapeutic strategies for ALS, although the latter has led to questionable success (Perrin, 2014) (**Tables 5**, **6**). The transgenic line harboring the Gly93 $\rightarrow$ Ala substitution ($SOD1^{G93A}$) has been used most extensively (Gurney et al., 1994), followed by the $SOD1^{G37R}$ (Wong et al., 1995), $SOD1^{G85R}$ (Bruijn et al., 1997), $SOD1^{G86R}$ (Ripps et al., 1995) and $SOD1^{D90A}$ (Jonsson et al., 2006) models.

The B6SJL-TgN(SOD1-G93A)1Gur mouse (Gurney et al., 1994) carries 25 $\pm$ 1.5 copies of the transgene within chromosome 12 and as a result, it expresses very high levels of human mutant $SOD1^{G93A}$ (Alexander et al., 2004). Whilst these significant levels of overexpression are criticized as a major limitation (Alexander et al., 2004), these animals remain the most widely used mouse model for therapeutic studies in ALS (Gurney et al., 1994). These $SOD1^{G93A}$ mice become paralyzed in the hindlimbs as a result of MN loss from the spinal cord, resulting in death by 5 months of age. Another variant of this model, B6SJL-TgN(SOD1-G93A)^{dl}1Gur, possesses fewer copies of the transgene; 8 $\pm$ 1.5 (Gurney, 1997; Alexander et al., 2004)[2]. This "low-copy" mouse, hereafter referred to as "G93A-slow" (s-$SOD1^{G93A}$), develops a slower disease course in comparison, where paralysis begins at 6–8.5 months of age (Alexander et al., 2004; Muller et al., 2008; Acevedo-Arozena et al., 2011). In addition, several other "low-copy" mouse lines

[2]https://www.jax.org/strain/002300

TABLE 5 | SOD1, TDP-43 and FUS mouse models of ALS.

Mouse models		Promotor	CNS over-expression (fold)	Survival (months)	Inclusions	Motor Phenotype	MN loss	Denervation	References
SOD1	G93A	hSOD1	17	3.5–4.5	SOD1(+)	Yes	Yes	Yes	Gurney et al., 1994
	s-G93A	hSOD1	8–10	8.3	hyaline	Yes	Yes	Yes	Gurney, 1997
	G37R	hSOD1	4–12	5	SOD1(+)	Yes	Yes	Yes	Wong et al., 1995
	G85R	hSOD1	0.2–1	8.5	SOD1(+) Ub(+)	Yes	Yes	Yes	Bruijn et al., 1997
TDP-43	A315T	*PrP*	3	5	TDP-43(–) Ub(+)	Yes	Yes	Yes	Wegorzewska et al., 2009
	rNLS8	*NEFH*	–	2.6 off Dox	TDP-43(+)	Yes	Yes	Yes	Walker et al., 2015; Spiller et al., 2016a
	$M337V^{KNOCK-IN}$	–	No	24.5	No	No	No	Yes	Ebstein et al., 2019
	$G298S^{KNOCK-IN}$	–	No	24.5	No	No	Yes	Yes	Ebstein et al., 2019
	TDP-43 KO	–	–	ns	No	Yes	Yes	Yes	Iguchi et al., 2013
FUS	$hFUS^{WT}$	*MAPT*		2.6	No	No	No	Yes	Sharma et al., 2016
	$hFUS^{R521C}$	*MAPT*	4	12	No	No	Yes	Yes	Sharma et al., 2016
	$hFUS^{P525L}$	*MAPT*	4	12	No	Yes	Yes	Yes	Sharma et al., 2016

TABLE 6 | Commonly used SOD1-transgenic mouse models of ALS and their phenotypes in relation to transgenic expression.

SOD1 mouse models	Transgene copies	SOD1 protein levels in the CNS (human/mouse)	Disease onset (days)	Survival (months)	References
B6SJL-TgN(SOD1-G93A)1Gur	34	17	90	3.5–4.5	Gurney et al., 1994; Alexander et al., 2004
SOD1-G93A Drop Copy#3	13	–	–	6	Alexander et al., 2004
SOD1-G93A Drop Copy#4	11	–	–	6.5	Alexander et al., 2004
B6SJL-TgN(SOD1-G93A)^{dl}1Gur	10	8–10	168	8.3	Gurney, 1997
SOD1-G93A Drop Copy#1	4	–	–	21	Alexander et al., 2004
G37R	–	4–12	105	5	Wong et al., 1995; Haenggeli et al., 2007
G85R	–	0.2–1	240	8.5	Bruijn et al., 1997
G86R (M1 line)	–	–	90–120	4	Ripps et al., 1995
D90A	–	–	350	13.5	Jonsson et al., 2006

(–), unknown.

have subsequently been generated, with even fewer copies of the human $SOD1^{G93A}$ transgene. These models also exhibit greater life spans compared to the higher copy lines (Alexander et al., 2004) (**Table 6**). Similarly, four lines of mice expressing another SOD1 mutant, $SOD1^{G37R}$, at different levels (5–14 times) have been produced, with variable phenotypes (Wong et al., 1995). Multiple mouse models based on transgenic expression of wild type or mutant TDP-43 have also been generated (Philips and Rothstein, 2015) (**Table 5**). Overexpressing human TDP-43 with a defective nuclear localization signal (NLS) in mice – in the absence of an ALS mutation – results in cytoplasmic expression of hTDP-43 and nuclear TDP-43 clearance. This results in a severe motor phenotype and reduced survival in the resulting 'rNLS8' mice compared to littermate controls (Walker et al., 2015). Several mouse models also exist based on transgenic expression of mutant FUS (**Table 5**). These mice display progressive, age- and mutation-dependent degeneration that also model aspects of ALS (Sharma et al., 2016). Furthermore, several newer models based on the C9orf72 repeat expansion have also been produced, although the phenotypes are more reminiscent of FTD rather than ALS (Batra and Lee, 2017).

Misfolded Protein Expression Level Influences Susceptibility

The expression of specific proteins can vary between MN subpopulations and this may be linked to their vulnerability to degenerate. Evidence for this hypothesis comes from the existing mouse models of ALS. Whilst mutant $SOD1^{G93A}$ is expressed in all MNs in these mice (Jaarsma et al., 2008), its propensity to induce neurodegeneration and disease is proportional to its expression level (**Table 6**) (Gurney et al., 1994; Bruijn et al., 1997; Alexander et al., 2004). At lower levels of expression, pathology is restricted to MNs in the spinal cord and brainstem only, whereas higher expression levels also induce severe abnormalities in the brain. Fewer copies of the $SOD1^{G37R}$ transgene correlate with delayed disease progression and a significant increase in lifespan compared to animals with higher copy numbers (**Table 6**) (Zwiegers et al., 2014). Similarly, in TDP-43 models, higher

levels of overexpression are associated with a worse phenotype (Philips and Rothstein, 2015). Moreover, disease is evident in both wildtype and mutant TDP-43 models, indicating that the expression levels of TDP-43, rather than the presence of a mutation *per se*, induces neurodegeneration. Hence, the effect of the TDP-43 mutation can be difficult to segregate from the effects of overexpression in these models (Philips and Rothstein, 2015). Both retaining the physiological expression levels and normal nuclear localization of TDP-43 have been linked to maintaining cellular homeostasis (Swarup et al., 2011; Philips and Rothstein, 2015). These studies together highlight the role of differing protein expression levels in the development and progression of ALS. However, further work is required to determine whether the expression levels of mutant ALS-associated proteins are different among MN subtypes, and whether this can differentially sensitize specific MNs to neurodegeneration and stress in ALS.

Selectivity in MN Degeneration in Mouse Models of ALS

Rodent disease models are also useful in studies examining the selective vulnerability of specific MNs within an individual motor pool in ALS. Similar to human ALS, in mouse models based on mutant SOD1^{G93A}, TDP-43^{A315T} and FUS^{P525L}, α-MNs selectively degenerate, while γ-MNs and MNs in the Onuf's nucleus are spared (Mannen et al., 1977; Lalancette-Hebert et al., 2016). Also, as in ALS patients, the oculomotor MNs are spared in SOD1^{G93A} (Niessen et al., 2006) and SOD1^{G86R} (Nimchinsky et al., 2000) mice, whereas spinal cord MNs, trigeminal, facial and hypoglossal MNs are targeted (Niessen et al., 2006). In rNLS8 mice, MNs in the hypoglossal nucleus and the spinal cord are also involved, whereas those in the oculomotor, trigeminal, and facial nuclei are spared, despite widespread neuronal expression of cytoplasmic hTDP-43 (Spiller et al., 2016a). Atrophy of MNs in the trigeminal motor, facial and hypoglossal nuclei are also significantly smaller in TDP-43 knock-out mice, whereas MNs in the oculomotor nuclei are preserved (Iguchi et al., 2013). In addition, in another TDP-43 model, Prp-TDP43^{A315T} mice, degeneration of specific neuronal populations occurs (Wegorzewska et al., 2009). Cytoplasmic ubiquitinated proteins accumulate in neurons of cortical layer V and in large neurons of the ventral horn and scattered interneurons, despite expression of the Prp-TDP-43^{A315T} transgene in all neurons and glia (Wegorzewska et al., 2009). In a knock-in TDP-43 mouse model bearing a G298S mutation, MN loss was restricted to large-diameter α-MNs (Ebstein et al., 2019). Furthermore, in FUS^{P525L} and FUS^{R521C} mouse models, no significant MN loss was detected in oculomotor neurons, whereas spinal cord MNs were progressively lost during disease course (Sharma et al., 2016).

In mutant SOD1^{G93A} mice, FF α-MNs are more susceptible to degenerate than FR α-MNs, resulting in the FF muscles becoming paralyzed before FR muscles (Hegedus et al., 2007). Furthermore, tonic S-units only disconnect from the muscle at disease end stage, meaning that S α-MNs are the least vulnerable within motor pools in SOD1^{G93A}, SOD1^{G85R} (Frey et al., 2000; Pun et al., 2006; Hegedus et al., 2007; Hadzipasic et al., 2014), TDP-43 rNLS8 (Spiller et al., 2016a), FUS^{R521C} and FUS^{P525L} transgenic models (Sharma et al., 2016). These findings together therefore provide strong evidence that there is a gradient of vulnerability amongst spinal MNs, whereby the faster, less excitable motor units are affected before the slower, more excitable types, at least in mouse models. Interestingly, selective denervation of MN subtypes occurs at the NMJ. Less denervation of the relatively resistant slow-twitch soleus muscle (Frey et al., 2000), compared to the vulnerable fast-twitch tibialis anterior muscle, occurs in TDP-43^{M337V}, TDP-43^{G298S}, FUS^{P525L}, FUS^{R521C} and TDP-43 rNLS8 mouse models (Sharma et al., 2016; Spiller et al., 2016a; Ebstein et al., 2019). In both the low- and high-copy s-SOD1^{G93A} and SOD1^{G93A} mice, the onset of interneuron degeneration also precedes the onset of behavioral motor manifestations and most MN degeneration (Chang and Martin, 2009; Jiang et al., 2009; Pullen and Athanasiou, 2009). Subtle changes to inhibitory synaptic inputs to MNs may therefore modulate MN excitability, leading to degeneration and motor symptoms in ALS/FTD.

NETWORK-DRIVEN MN VULNERABILITY

Genetic mutations are present throughout life in ALS patients (summarized in **Supplementary Table 1**), but as only specific cellular populations are affected, this implies that the vulnerability of MN subtypes in ALS is not caused wholly by genetic factors. Hence, environmental or extrinsic factors, such as the neuronal circuitry or the microenvironment surrounding MNs, may explain the selective vulnerability of MNs in ALS/FTD.

Site-Specific Onset and Spread of Neurodegeneration in ALS

The pattern of neurodegeneration in ALS/FTD is not random; it targets specific large-scale distributed networks in the brain and spinal cord. Motor manifestations begin in one region of the body in ∼98% of patients (Ravits et al., 2007) accompanied by unilateral, focal damage to MNs in the motor cortex or spinal cord, that innervate the corresponding peripheral body regions. It has been previously suggested that ALS targets specific evolutionarily linked, interdependent functions, and as the disease progresses these deficits combine into failure of specific networks (Eisen et al., 2014). More recently, several clinical studies have revealed that neurodegeneration and TDP-43 pathology spread to continuous anatomical regions during disease course (Ravits et al., 2007; Brettschneider et al., 2013; Walhout et al., 2018), and symptoms arise in the contralateral regions following a unilateral limb onset (Walhout et al., 2018). This also implies that neuronal circuitry might drive disease progression to specific MN populations in ALS/FTD. The spread of misfolded proteins from cell-to-cell, particularly TDP-43, provides a molecular explanation for the specific network and anatomical vulnerability observed in ALS. However, it must be noted that whilst contiguous spread is observed for most patients, this is not the case for all (Ravits and La Spada, 2009).

Increasing evidence suggests that ALS begins in the cortical regions of the brain, which is referred to as the "dying-forward hypothesis." Features of cortical hyperexcitability – heralded by reduction in short interval intracortical inhibition – have been

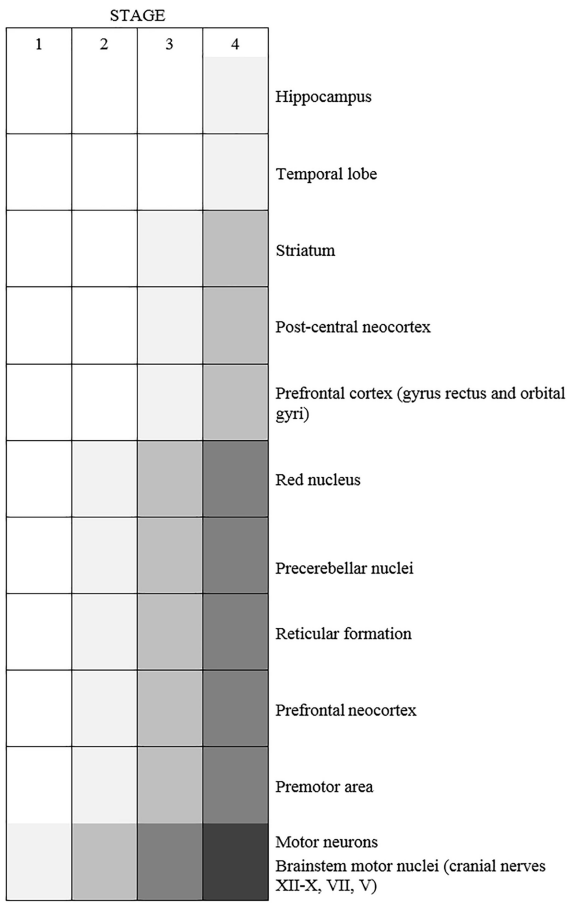

FIGURE 3 | Schematic diagram representing the typical spread of neurodegeneration following an initial onset in motor neurons in ALS patients (n = 76 patients) (Brettschneider et al., 2013). Shading represents TDP-43 pathology.

detected during the early phases of ALS in transcranial magnetic stimulation studies (Thomsen et al., 2014; Menon et al., 2015). This can precede the clinical onset of bulbar/spinal motor dysfunction by ∼3–6 months (Vucic et al., 2008; Bakulin et al., 2016). The dying forward hypothesis is consistent with Charcot, who first postulated that ALS begins in the cortex (Charcot, 1874). Clinical observations that MNs without monosynaptic connections to cortical MNs, such as the oculomotor, abducens, and Onuf's nuclei, are spared in ALS, and that pure LMN forms of ALS are rare, also support this hypothesis. Further evidence is provided by the observation that MNs receiving direct, monosynaptic cortical input also predominantly develop TDP-43 pathology, while subcortical MNs do not (Eisen et al., 2017). Similarly, TDP-43 pathology develops in patients only in structures under the control of corticofugal projections (Brettschneider et al., 2013; Menon et al., 2015; Eisen et al., 2017)

TDP-43 pathology may then propagate through corticofugal axons to the spinal cord and regions of the brain (Braak et al., 2013; Eisen et al., 2017) in a time-dependant and region-specific manner (Brettschneider et al., 2013), consistent with the dying forward hypothesis (**Figure 3**). This sequential pattern of TDP-43 dissemination is consistent with the hypothesis that TDP-43 pathology is propagated synaptically from cell to cell (Brundin et al., 2010; Maniecka and Polymenidou, 2015), in a similar way to the pathogenic prion protein, a concept known as the "prion-like mechanism" (Lee and Kim, 2015; Ayers and Cashman, 2018). In this model, misfolded proteins act as template seeds to trigger aggregation of their natively folded counterparts. This results in the propagation of protein misfolding, leading to its orderly spread through the CNS (Soto, 2012; Maniecka and Polymenidou, 2015). However, the question of where disease begins remains controversial because many researchers still favor the "dying-back" hypothesis, in which ALS begins within the muscle cells or at the NMJ. This hypothesis proposes that there is a spread of pathology from LMNs to UMNs (Chou and Norris, 1993; Fischer et al., 2004; Pun et al., 2006; Turner et al., 2018), or else, a simultaneous involvement of both UMNS and LMNs (Turner et al., 2018). Whilst most of the evidence for the dying-back mechanism comes from animal models, studies of muscle biopsies from early stage ALS patients and long-term survivors have demonstrated significant morphological abnormalities and major denervation/re-innervation at the NMJ, implying that this region is targeted early in disease (Millecamps et al., 2010; reviewed in Arbour et al., 2017).

There is evidence to support the prion-like model in ALS. The spread of neurodegeneration through adjacent anatomical regions of the CNS resembles the orderly spread of protein misfolding in prion disease. The *in vitro* cell-to-cell transmission of misfolded SOD1, TDP-43 and C9orf72 di-peptide repeat proteins has been demonstrated (Grad et al., 2011, 2014; Münch et al., 2011; Nonaka et al., 2013; Feiler et al., 2015; Porta et al., 2018). Similarly, the addition of cerebrospinal fluid from ALS/FTD patients (Ding et al., 2015), detergent-insoluble fractions of ALS-disease brains (Nonaka et al., 2013) or insoluble phosphorylated TDP-43 from post-mortem brain and spinal cord tissue (Smethurst et al., 2016), results in misfolding of TDP-43 when added to human cell lines. However, so far, only misfolded SOD1 and TDP-43 transmissibility has been demonstrated *in vivo* (Ayers et al., 2014, 2016; Porta et al., 2018). A recent study demonstrated that injection of brain-derived extracts from FTD patients into mice promoted the spatio-temporal transmission of TDP-43 pathology via the neuroanatomical connectome, suggesting that TDP-43 travels via axonal transport through connected regions of the CNS (Porta et al., 2018). Similarly, axonal transport is implicated in the spread of mutant SOD1 in mice (Ayers et al., 2016). Overexpression of misfolded TDP-43 or SOD1 facilitated the seeding ability of each inoculum, consistent with results obtained *in vitro* (Nonaka et al., 2013; Feiler et al., 2015; Smethurst et al., 2016).

Whilst these animal studies demonstrate that ALS spreads within MNs that are connected synaptically, a small portion of patients do not display this contiguous spreading of pathology, however. This implies the existence of alternative mechanisms of disease progression (Fujimura-Kiyono et al., 2011; Gargiulo-Monachelli et al., 2012), such as the transfer of misfolded proteins in nanotubules or exosomes (Nonaka et al., 2013; Sundaramoorthy et al., 2013; Grad et al., 2014; Ding et al.,

2015; Feiler et al., 2015; Westergard et al., 2016). Interestingly, it has been suggested that the vulnerability of specific MN populations is associated with the spread of neurodegeneration in ALS (Fu et al., 2018).

Role of Glial Cells in Driving Disease Progression

There is increasing evidence for a role of the neighboring non-neuronal cells in ALS. Under normal conditions, glial cells provide nutritional and trophic support to MNs, but in ALS, they appear to exacerbate neurodegeneration in a non-cell autonomous fashion. These cells include microglia, astrocytes, oligodendrocytes and Schwann cells. Limiting the expression of mutant SOD1 to MNs only does not lead to neurodegeneration in mice (Pramatarova et al., 2001; Lino et al., 2002), and chimeric mouse studies have established that the presence of mutant $SOD1^{G93A}$ in glial cells induces neurodegeneration and MN loss (Papadeas et al., 2011). Both microglia and astrocytes appear to enhance disease progression by inducing neuroinflammation, whereas oligodendrocytes drive disease initiation. Non-neuronal cells may also be involved in the spread of pathological proteins in ALS (Thomas et al., 2017; Porta et al., 2018). However, whilst misfolded proteins released by MNs can be taken up by glial cells, they may be less toxic to these cells than to MNs (Benkler et al., 2018).

Microglia

Microglia are the main immune cells of the CNS (Fujita and Kitamura, 1975; Hickey and Kimura, 1988; Lawson et al., 1990). In ALS patients, activated microglia increase in CNS regions that are susceptible to neurodegeneration (Kawamata et al., 1992) and in $SOD1^{G93A}$ mice, enhanced microglial reactivity precedes nerve denervation at the NMJ (Alexianu et al., 2001; Saxena et al., 2009). Microglia exist in both resting and activated states [reviewed in Perry and Holmes (2014)] and in ALS, activated microglia display two distinct phenotypes. The neuroprotective M2 phenotype promotes tissue repair and supports MN survival by releasing neuroprotective factors, and the toxic M1 phenotype produces cytokines, enhances inflammation, and induces cell death (Liao et al., 2012). Studies in mutant SOD1 mice reveal that the numbers of microglia increase during disease progression, but they vary between the neuroprotective M2 and toxic M1 phenotypes (Liao et al., 2012; Chiu et al., 2013). In lumbar spinal cords of pre-symptomatic $SOD1^{G93A}$ mice, the anti-inflammatory M2 microglia predominate (Gravel et al., 2016), whereas at disease onset and during progression, the proinflammatory M1 type is more common (Beers et al., 2011). Microglial-specific ablation of mutant $SOD1^{G37R}$ in mice does not affect disease initiation, but it significantly slows disease progression (Boillée et al., 2006b), indicating that microglia enhance the progression, but not the onset, of disease in transgenic mutant SOD1 mice. However, contradictory findings were obtained in the TDP-43 rNLS8 model, where microglia were neuroprotective and not neurotoxic (Spiller et al., 2018). Interestingly, knockdown of C9orf72 in mice alters microglial function and induces age-related neuroinflammation, but not neurodegeneration (Lall and Baloh, 2017). Further investigations are required to examine the role of microglia in other ALS disease models, and to determine whether MN subtypes display different vulnerabilities to microglia-mediated protective and/or toxicity in ALS.

Astrocytes

Astrocytes perform multiple homeostatic functions in the CNS; they regulate the plasticity of synapses and synthesis of neurotransmitters (Ullian et al., 2004; Volterra and Meldolesi, 2005; Sloan and Barres, 2014), they maintain the blood brain barrier, and they provide neurotrophic support to MNs by releasing glial-derived neurotrophic factor (GDNF) and transforming growth factor β1 (TGF-β1) amongst others. Like microglia, during the neurodegenerative process, astrocytes can exist in two states, either reactive or activated, and activated astrocytes lose their neuroprotective functions and become neurotoxic during disease (Yamanaka et al., 2008; Ilieva et al., 2009; Valori et al., 2014; Das and Svendsen, 2015). Also, like microglia, astrocytes are implicated in the progression rather than onset of ALS. Deletion of SOD1 from astrocytes slowed disease progression, but not disease onset, in $SOD1^{G93A}$ mice (Yamanaka et al., 2008; Wang L. et al., 2011), whereas deletion of mutant SOD1 from MNs did delay onset (Boillée et al., 2006a; Wang L. et al., 2009). Furthermore, gene expression changes in MNs, astrocytes and oligodendrocytes start just before disease onset in $SOD1^{G37R}$ mice, but these alterations are first observed in MNs (Sun et al., 2015). Recently, two different subsets of reactive astrocytes were described in the adult CNS, A1 and A2 (Liddelow et al., 2017; Clarke et al., 2018; Miller, 2018) and the A1 reactive astrocytes were associated with the death of both neurons and oligodendrocytes (Liddelow et al., 2017).

There is increasing evidence that astrocytes mediate MN degeneration via the release of neurotoxic factors. Soluble toxic compounds produced by astrocytes expressing mutant SOD1 trigger the selective loss of spinal MNs (Nagai et al., 2007), but not spinal GABAergic neurons, consistent with the specific vulnerability of these cells in ALS (Nagai et al., 2007). Astrocytes in the ventral spinal cord can be distinguished from astrocytes in the dorsal spinal cord by expression of semaphorin A3 (Sema3a), which is implicated in the specific vulnerability to FF-MNs in ALS (see section "Neuroprotective and Neurotoxic Factor Expression in MN Subpopulations" below). Furthermore, astrocytes are also implicated in MN loss and disease progression by mediating AMPA receptor-induced excitotoxicity via EAAT2/GLT-1, as discussed below (section "Neuronal Excitability"). Expression of mutant $TDP\text{-}43^{M337V}$ in rat astrocytes led to down-regulation of neurotrophic genes, up-regulation of neurotoxic genes and progressive MN degeneration (Tong et al., 2013; Huang et al., 2014). Conditioned medium from primary astrocyte cultures of $SOD1^{G86R}$ and $TDP\text{-}43^{A315T}$ mice also induces MN death through activation of sodium channels and nitro-oxidative stress (Rojas et al., 2014). Furthermore, astrocytes expressing mutant FUS^{R521G} trigger MN death by secreting pro-inflammatory tumor necrosis factor (TNF)-α (Kia et al., 2018). $SOD1^{G93A}$ aggregates in astrocytes appear in late disease stages, selectively in regions with extensive neuronal degeneration and prominent

astrogliosis (Jaarsma et al., 2008). This raises the possibility that astroglial aggregate formation is triggered by MN degeneration, implying that disease may spread from neurons to glia (Jaarsma et al., 2008; Sun et al., 2015).

Together these studies suggest the involvement of astrocytes in the selective degeneration of MNs in ALS. Under normal conditions, astrocytes may be able to cope with the expression of low levels of misfolded proteins, but, during cell stress or in the context of MN degeneration, they become more vulnerable, and release factors toxic to MNs, thus producing a vicious cycle. However, the relative resistance of neuronal populations surrounded by reactive astrocytes indicates that the vulnerability of MNs is also determined by cell-autonomous components, such as their genetic background and transcriptional/translational profiles (Boillée et al., 2006a; Sun et al., 2015).

Oligodendrocytes and Schwann Cells

The two glial cell types responsible for myelination of axons have also been investigated in the context of ALS. Oligodendrocytes myelinate axons in the CNS whereas Schwann cells are responsible for myelination in the peripheral nervous system (PNS). Whilst they perform similar functions, there are also important differences between these two cell types. Schwann cells form a single myelin sheath around one single axon, whereas oligodendrocytes myelinate many different axons. Furthermore, there are differences in the protein composition of CNS and PNS myelin.

In ALS, TDP-43 pathology has been detected in oligodendrocytes in the motor cortex and spinal cord of both SALS and FALS patients (Arai et al., 2006; Mackenzie et al., 2007; Tan et al., 2007; Zhang et al., 2008; Seilhean et al., 2009; Murray et al., 2011; Philips et al., 2013). In addition, FUS forms cytoplasmic aggregates in oligodendrocytes from ALS patients bearing FUS^{R521C} or FUS^{P525L} mutations (Mackenzie et al., 2011). Degeneration of oligodendrocytes and their precursors was also linked with axon demyelination in both SALS and FALS patients (Kang et al., 2013). In $SOD1^{G93A}$ mice, oligodendrocyte loss in the spinal cord occurs before symptoms appear and importantly, before MN loss, implying that oligodendrocytes are associated with disease onset. This MN loss increases with disease progression, resulting in MNs with only partially myelinated axons in $SOD1^{G93A}$ mice and $SOD1^{G93A}$ rats (Niebroj-Dobosz et al., 2007; Kang et al., 2013; Philips et al., 2013). Whilst the proliferation of oligodendrocyte precursors may compensate for this loss, newly synthetized oligodendrocytes failed to mature and remain dysfunctional in $SOD1^{G93A}$ mice (Magnus et al., 2008; Philips et al., 2013). Recently, $SOD1^{G85R}$ was able to transfer from MNs to nearby oligodendrocytes (Thomas et al., 2017). The selective removal of mutant SOD1 from NG2+ oligodendrocyte progenitors, but not mature oligodendrocytes in $SOD1^{G37R}$ mice, leads to delayed disease onset and prolonged survival (Kang et al., 2013), further suggesting that mutant SOD1-induced oligodendrocyte defects are detrimental to MNs in ALS.

Schwann cells are required for the long-term maintenance of synapses at the NMJ (Reynolds and Woolf, 1992; Son and Thompson, 1995; Reddy et al., 2003). Early studies demonstrated that myelin is altered along peripheral nerves in ALS patients, implying that Schwann cells are involved in disease (Perrie et al., 1993). However, unlike the other glial cell types, more recent studies on the role of Schwann cells in ALS have reached conflicting conclusions. Knockdown of $SOD1^{G37R}$ within Schwann cells significantly accelerates disease progression, concomitant with a specific reduction in insulin-like growth factor (IGF-I), which is protective to MNs (see section "Neuroprotective and Neurotoxic Factor Expression in MN Subpopulations" below) (Lobsiger et al., 2009). This surprising finding, implying that $SOD1^{G37R}$ is protective in Schwann cells, could be linked to the dismutase activity of SOD1. Whereas $SOD1^{G37R}$ retains its enzymatic activity, $SOD1^{G85R}$ does not, and similar experiments performed in $SOD1^{G85R}$ mice resulted in opposite findings; Schwann cell specific knock-down of $SOD1^{G85R}$ delayed disease onset and extended survival (Wang et al., 2012). Furthermore, TGF-β1 produced by Schwann cells promotes synaptogenesis by increasing nerve-muscle contacts (Feng and Ko, 2008), in contrast to TGF-β1 expression in astrocytes which accelerates disease progression in SOD1 mice (Endo et al., 2015). Hence, the role of Schwann cells in ALS remains unclear.

INTRINSIC FACTORS SPECIFIC TO MN SUBPOPULATIONS

Multiple cellular pathways are now implicated in the etiology of ALS, but it remains unclear how dysfunction of these diverse processes can result in the same disease phenotype. Furthermore, the same genetic mutation can result in either ALS, FTD or both conditions, implying that specific disease modifiers exist. Studies using *in vivo* and *in vitro* models of FALS suggest that the intrinsic properties of MNs are crucial for degeneration and/or protection (Boillée et al., 2006a). Importantly, resistant MN subtypes appear to display diverse gene expression profiles from susceptible MNs. Microarray analysis and laser capture microdissection of MNs isolated from oculomotor/trochlear nuclei, the hypoglossal nucleus and the lateral column of the cervical spinal cord in $SOD1^{G93A}$ rats (Hedlund et al., 2010), or in human brain and spinal cords (Brockington et al., 2013), have revealed marked differences between these subpopulations. Importantly, many of the genes that were differentially expressed encode proteins that function in pathways implicated in ALS pathogenesis, such as ER function, calcium regulation, mitochondrial function, ubiquitination, apoptosis, nitrogen metabolism, transport and cellular growth. Interestingly, oculomotor neurons possess a specific and relatively conserved protein signature between humans and rodents, implying that this contributes to the relative resistance of these MNs in ALS/FTD (Hedlund et al., 2010; Comley et al., 2015). Several of these proteins are known to be protective against MN neurodegeneration, such as insulin-like growth factors (IGF) and their receptors (see section "Neuroprotective and Neurotoxic Factor Expression in MN Subpopulations" below). Similarly, other genes highly expressed in vulnerable MNs are implicated in their susceptibility to degeneration, such as semaphorin A3 (Sema A3) and matrix metalloproteinase 9 (MMP-9) (see section "Neuroprotective and

TABLE 7 | Table with genes (described in this review) which are differently expressed among neuron subpopulations.

Gene	Gene acronym	Motor neurons						References
		Cortical	Oculomotor	Onuf's	Hypoglossal	Slow spinal cord	Fast spinal cord	
		Vulnerable	Resistant	Resistant	Vulnerable	Resistant	Vulnerable	
Insulin-like growth factor I receptor	*IGF-IR*		+			– (cervical spinal MNs)		Allodi et al., 2016
Insulin-like growth factor II	*IGF-II*		+			–		Hedlund et al., 2010; Allodi et al., 2016
Glial cell line-derived neurotrophic factor receptor subunit	*GFRα1*							Shneider et al., 2009
Semaphorin A3	*SemaA3*	+					+ (FF)	De Winter et al., 2006
Na^+/K^+ATPase-alpha3						–	+	Ruegsegger et al., 2016
AMPA receptor GluR2 subunits	*GluR2*		+					Brockington et al., 2013
calbindin—D28K	*CaBP*	–	+	+				Alexianu et al., 1994
Parvalbumin		–	+					Alexianu et al., 1994
Calreticulin	*CRT*						–	Bernard-Marissal et al., 2012
matrix metalloproteinase-9	*MMP-9*		–			–	+	Kaplan et al., 2014
Binding immunoglobulin protein co-chaperone	*SIL-1*					+	– (FF)	Filézac de L'Etang et al., 2015
Dynein			–		+	+ (spinal MNs)		Comley et al., 2015

(+), upregulation; (–), downregulation; gray, unknown.

Neurotoxic Factor Expression in MN Subpopulations" below). Recently, a comprehensive bioinformatics meta-analysis of ALS modifier genes was performed from 72 published studies (Yanagi et al., 2019). A total of 946 modifier genes were identified and of these, 43 genes were identified as modifiers in more than one ALS gene/model. These included TDP-43, SOD1, ATXN2 and MMP9. Intrinsic factors in MNs might therefore underlie their relative vulnerability or resistance to neurodegeneration in ALS. The two pioneering studies linking gene expression differences to MN vulnerability in ALS (Hedlund et al., 2010; Brockington et al., 2013) have led to several subsequent reports, where the role of specific genes were examined further (summarized in **Table 7**, and discussed further in the sections below). However, it is also possible that the differences in gene expression reflect the diverse embryological origins or milieu of resistant and susceptible MN groups, or simply the structural and functional differences between oculomotor units and motor units of other skeletal muscles. To date, no studies have extensively characterized the specific transcriptional profile of vulnerable vs. susceptible MNs in TDP-43, C9orf72 FUS or other models of ALS, similar to those performed in SOD1^{G93A} mice and ALS patients (Hedlund et al., 2010; Brockington et al., 2013).

In addition to alterations in gene expression profiles, it is also possible that the resistant MNs in ALS display differing functional or morphological properties to those more susceptible to degeneration. A recent study demonstrated that cultures obtained from surviving MNs of SOD1^{G93A} mice displayed more dendritic branching and axonal outgrowth, as well as increased actin based-growth cones, implying that they have more regenerative capacity (Osking et al., 2019).

RNA Homeostasis

Abnormal RNA homeostasis is increasingly implicated in the pathophysiology of ALS/FTD, consistent with the functions of TDP-43 and FUS in regulating RNA splicing and transport (Polymenidou et al., 2011; Tank et al., 2018). In the transgenic SOD1^{G93A} rat, differences in the number of genes involved in transcription, RNA metabolism, RNA binding and splicing, and regulation of translation, were evident between neuronal populations located in the oculomotor/trochlear nucleus, the hypoglossal nucleus and the lateral column of the cervical spinal cord (Hedlund et al., 2010). These results therefore suggest that RNA homeostatic processes are involved in the differential vulnerability of specific subtypes of MNs in ALS. However, further studies in this area are required to investigate this possibility, particularly in relation to TDP-43 and FUS.

Neuroprotective and Neurotoxic Factor Expression in MN Subpopulations

Differential expression of pro-survival or toxic factors is also implicated in the specific vulnerability of MN subtypes. The IGFs are proteins with high homology to insulin that form part of the IGF "axis" that promotes cell proliferation and inhibits apoptosis. In the normal rat, IGF-I is highly expressed in oculomotor neurons, where it is protective against glutamate-induced toxicity (Hedlund et al., 2010; Allodi et al., 2016). This may be due to activation of the PI3K/Akt and p44/42 MAPK pathways, which both inhibit apoptosis (Siddle et al., 2001; Sakowski et al., 2009). In addition, its associated receptor, IGF-I receptor (IGF-IR), is also highly expressed in oculomotor neurons and on the extraocular muscle endplate (Allodi et al., 2016). IGF-IR is important for the survival of neurons following hypoxic/ischemic injury (Vincent and Feldman, 2002; Liu et al., 2011) by upregulation of neuronal cellular inhibitor of apoptosis-1 (cIAP-1) and X-linked inhibitor of apoptosis (XIAP) (Liu et al., 2011). Delivery of IGF-II using AAV9 to the muscle of mutant SOD1^{G93A} mice extended life-span by 10%, prevented the loss of MNs and induced motor axon regeneration (Allodi et al., 2016). These findings indicate that differential expression of IGF-II and IGF-IR in oculomotor neurons might contribute to their relative resistance to degeneration in ALS/FTD.

Conversely, aberrant expression of axon repulsion factors near the NMJ may contribute to neurodegeneration in ALS. Sema3A and its receptor neuropilin 1 (Nrp1) are involved in axon guidance during neural development (Huber et al., 2005; Moret et al., 2007). Sema3A is specifically upregulated in terminal Schwann cells near NMJs of vulnerable FF muscle fibers in mutant SOD1^{G93A} mice (De Winter et al., 2006). Nrp1 is upregulated in axon terminals of the NMJ in this model and administration of an antibody against the Sema3A-binding domain of Nrp1 delayed the decline of motor functions while prolonging the lifespan of SOD1^{G93A} mice (Venkova et al., 2014). Furthermore, Sema3A is upregulated in the motor cortex of ALS patients (Körner et al., 2016; Birger et al., 2018), but not in the spinal cord. Sema3A induces death of sensory, sympathetic, retinal and cortical neurons (Shirvan et al., 2002; Ben-Zvi et al., 2008; Jiang et al., 2010; Wehner et al., 2016), but not spinal neurons (Molofsky et al., 2014; Birger et al., 2018). Similarly, Sema3A induces apoptosis of human cortical neurons but promotes survival of spinal MNs (Birger et al., 2018). Furthermore, loss of Sema3A-expressing astrocytes in the ventral spinal cord leads to selective degeneration of α-MNs, but not γ-MNs (Hochstim et al., 2008; Molofsky et al., 2014). These data indicate that whilst Sema3A and Nrp1 contribute to the loss of MNs in ALS, some neuronal subpopulations are more susceptible than others. There is also evidence that other axon guidance proteins are associated with the susceptibility of MNs in ALS. Increased expression of ephrin A1 has been demonstrated in the vulnerable spinal MNs of ALS patients (Jiang et al., 2005). *EPHA4,* which is a disease modifier in zebrafish, rodent models and human ALS, encodes an Eph receptor tyrosine kinase, which is involved in axonal repulsion during development and in synapse formation, plasticity and memory in adults (Van Hoecke et al., 2012). The more vulnerable MNs express higher levels of EPHA4, and neuromuscular re-innervation is inhibited by Epha4. In ALS patients, EPHA4 expression also inversely correlates with disease onset and survival (Van Hoecke et al., 2012).

Matrix Metalloproteinase (MMP9) has been recently identified as another determinant of selective neuronal vulnerability in SOD1^{G93A} mice (Kaplan et al., 2014). MMP-9 was strongly expressed by vulnerable FR spinal MNs, but not oculomotor, Onuf's nuclei or S α-MNs, and it enhanced ER stress and mediated muscle denervation in this model

(Kaplan et al., 2014). Delivery of MMP-9 into FF-MNs, but not in oculomotor neurons, accelerates denervation in SOD1^{G93A} mice (Kaplan et al., 2014). Similarly, another study demonstrated that reduction of MMP-9 expression attenuated neuromuscular defects in rNLS8 mice expressing cytoplasmic hTDP43$^{\Delta NLS}$ in neurons (Spiller et al., 2019). Edaravone, a free radical scavenger which inhibits MMP-9 expression, was recently approved for the treatment of ALS in Japan, South Korea, United States and Canada (Yoshino and Kimura, 2006; Ito et al., 2008; Yagi et al., 2009). Further molecular investigations into the differences and similarities between different motor units in ALS should yield additional insights into their vulnerability to neurodegeneration.

Polymorphisms in specific genes have also been linked to MN vulnerability. In SALS patients, variants in the gene encoding *UNC13A* are associated with greater susceptibility to disease and shorter survival (Diekstra et al., 2012). UNC13A functions in vesicle maturation during exocytosis and it regulates the release of neurotransmitters, including glutamate. Mutations in *EPHA4* are also associated with longer survival (Van Hoecke et al., 2012), implying that Epha4 modulates the vulnerability of MNs in ALS. Furthermore, repeat expansions in the gene encoding ataxin 2 (*ATXN2*), which cause spinocerebellar ataxia type 2 (SCA2), are also increased in ALS patients compared to healthy controls (Ross et al., 2011). This implies that *ATXN2* repeat expansions are also related to MN vulnerability to neurodegeneration in ALS.

Neuronal Excitability

The excitability properties of MNs are also implicated in the selective degeneration of specific MN subtypes in ALS. Alterations in MN excitability have been reported during the asymptomatic disease stage in the SOD1^{G93A} (Saxena et al., 2013), s-SOD1^{G93A} (Pambo-Pambo et al., 2009) and SOD1^{G85R} (Bories et al., 2007) mouse models, in iPSC-derived MNs (Vucic et al., 2008; Wainger et al., 2014) and in SALS and FALS patients (Vucic and Kiernan, 2010; Devlin et al., 2015). Specific isoforms of the sodium–potassium pump (Na^+/K^+ATPase), which generates the Na^+/K^+ gradients that drive the action potential, are associated with the specific vulnerability of MN subtypes. Misfolded mutant SOD1 forms a complex with the α3 isoform of Na^+/K^+ATPase, and this leads to impairment in its ATPase activity. Altered levels of this isoform were also observed in spinal cords of SALS and non-SOD1 FALS patients (Ruegsegger et al., 2016). Importantly, α3 is the major isoform in vulnerable FF-MNs, whereas both α1 and α3 predominate in FR-MNs, and S-MNs express only α2. Furthermore, viral-mediated expression of a mutant Na^+/K^+ATPase-α3 that cannot bind to mutant SOD1 restored Na^+/K^+ATPase-α3 activity, delayed disease manifestations and increased lifespan in two different mutant SOD1 mouse models (SOD1^{G93A} and SOD1^{G37R}) (Ruegsegger et al., 2016). This indicates that modulating the activity of the α3 isoform of the Na^+/K^+ATPase, and therefore modulating the excitability status of MNs, is important in neurodegeneration in ALS.

However, increasing MN excitability is also neuroprotective to MNs in ALS. Enhancing MN excitability by delivering AMPA receptor agonists to mutant SOD1^{G93A} mice reversed misfolded mutant protein accumulation, delayed pathology and extended survival, whereas reducing MN excitability by antagonist CNQX accelerated disease and induced early denervation, even in the more resistant S-MNs (Saxena et al., 2013). However, MN subpopulations can be differentially affected by changes in excitability. Disease resistant S-MNs exhibit hyper-excitability in ALS patients (de Carvalho and Swash, 2017) and early in disease in mutant SOD1^{G93A} mice, whereas disease vulnerable FF-MNs are not hyper-excitable, again highlighting increased excitability as a protective property in ALS (Leroy et al., 2014). Also, the vulnerable masticatory trigeminal MNs from SOD1^{G93A} mice exhibit a heterogeneous discharge pattern, unlike oculomotor neurons (Venugopal et al., 2015). However, MNs in FALS and SALS patients are hyperexcitable early in disease course, but then later become hypo-excitable (Vucic et al., 2008; Menon et al., 2015), indicating that modulation of neuronal excitability is a factor influencing the development of ALS.

Excitotoxicity

Excitotoxicity is the process by which neurons degenerate from excessive stimulation by neurotransmitters such as glutamate, due to overactivation of NMDA or AMPA receptors. This can result from pathologically high levels of glutamate, or from excitotoxins like NMDA and kainic acid, which allow high levels of Ca^{2+} to enter the cell. One line of evidence supporting a role for excitotoxicity in ALS is that riluzole, one of the only two drugs available for ALS patients, has anti-excitotoxic properties (Bensimon et al., 1994; Lacomblez et al., 1996). Riluzole inhibits the release of glutamate due to inactivation of voltage-dependant Na^+ channels on glutamatergic nerve terminals (Doble, 1996). Previous studies have suggested that MNs that are less susceptible to excitotoxicity are less prone to degenerate (Hedlund et al., 2010; Brockington et al., 2013).

Ca^{2+} enters neurons through ligand-gated channels or voltage-gated channels such as the voltage-gated-L-type Ca^{2+} channel (Cav1.3), which mediates the generation of persistent inward currents (Xu and Lipscombe, 2001). Cav1.3 is differentially expressed in MN subtypes, with more in the spinal cord compared to the oculomotor and hypoglossal nuclei (Shoenfeld et al., 2014). This Ca^{2+} inward current increases early in disease course in MNs of SOD1^{G93A} mice, which is associated with an increase in Cav1.3 expression.

In addition, the presence of atypical AMPA receptors in MNs compared to other neurons might render them more permeable to Ca^{2+}. Functional AMPA receptors normally form a tetrameric structure composed, in various combinations, of the four subunits, GluR1, GluR2, GluR3, and GluR4. The Ca^{2+} conductance of these receptors differs markedly depending on whether GluR2 is a component of the receptor. However, in MNs, AMPA receptors express proportionately fewer GluR2 subunits relative to other types (Kawahara et al., 2003; Sun et al., 2005), which may render them more permeable to Ca^{2+} and thus more vulnerable to excitotoxic injury than other cells. Consistent with this notion, more GluR1 and GluR2 subunits are present in oculomotor neurons compared to spinal MNs in humans (Brockington et al., 2013), and treatment with AMPA/kainate of slice preparations from the rat lumbar spinal cord and midbrain results in more Ca^{2+} influx in spinal cord MNs compared to oculomotor neurons (Brockington et al., 2013). MNs in culture or

in vivo are selectively vulnerable to glutamate receptor agonists, particularly those that stimulate AMPA receptors and induce excitotoxicity (Carriedo et al., 1996; Urushitani et al., 1998; Fryer et al., 1999; Van and Robberecht, 2000), whereas NMDA does not damage spinal cord MNs (Curtis and Malik, 1985; Pisharodi and Nauta, 1985; Hugon et al., 1989; Urca and Urca, 1990; Nakamura et al., 1994; Ikonomidou et al., 1996; Kruman et al., 1999). Moreover, ALS-vulnerable α-spinal cord MNs display greater AMPA receptor current density than other spinal neurons (Vandenberghe et al., 2000). Furthermore, when this density is reduced pharmacologically to levels similar to spinal neurons, these MNs are no longer vulnerable to activation of AMPA receptors. Similarly, when mutant $SOD1^{G93A}$ mice are crossed with mice overexpressing the GluR2 subunit in cholinergic neurons, the resulting progeny possess AMPA receptors with reduced permeability to Ca^{2+} and prolonged survival compared to $SOD1^{G93A}$ mice (Tateno et al., 2004), highlighting the importance of AMPA receptors and GluR2 in ALS.

Editing of mRNA controls the ability of the GluA2 subunit to regulate Ca^{2+}-permeability of AMPA receptors. RNA editing is a post-transcriptional modification (Gln; Q to Arg; R) in the GluA2 mRNA, and the AMPA receptor is Ca^{2+}-impermeable if it contains the edited GluA2(R) subunit. Conversely, the receptor is Ca^{2+}-permeable if it lacks GluA2 or if it contains the unedited GluA2(Q) subunit. Interestingly, spinal MNs in human ALS patients display less GluR2 Q/R site editing (Kawahara et al., 2004; Aizawa et al., 2010). GluR2 pre-mRNA is edited by the enzyme adenosine deaminase isoform 2 (ADAR2) (Kortenbruck et al., 2001) and reduced ADAR2 activity correlates with TDP-43 pathology in human MNs (Aizawa et al., 2010). Furthermore, when ADAR2 is conditionally knocked-down in MNs in mice, a decline in motor function and selective loss of MNs in the spinal cord and cranial motor nerve nuclei was observed (Hideyama et al., 2012). In contrast, MNs in the oculomotor nucleus were retained, despite a significant decrease in GluR2 Q/R site editing (Hideyama et al., 2010). Notably, cytoplasmic mislocalization of TDP-43 was present in the ADAR2-depleted MNs (Yamashita et al., 2012) and TDP-43 was also localized at the synapse, further highlighting a link between ADAR2, GluR2 and TDP-43 (Wang et al., 2008; Feiguin et al., 2009; Polymenidou et al., 2011; Gulino et al., 2015).

Motor neurons may be vulnerable to excitotoxicity because they possess a lower capacity than other neurons to buffer Ca^{2+} upon stimulation (Van Den Bosch et al., 2006). Several electrophysiological studies have demonstrated that susceptible MNs in ALS have a limited capacity to buffer Ca^{2+} compared to resistant MNs (Lips and Keller, 1998, 1999; Palecek et al., 1999; Vanselow and Keller, 2000). Ca^{2+}-binding proteins, such as calbindin D28K and parvalbumin, protect neurons from Ca^{2+}-mediated cell death by enhancing Ca^{2+} removal after stimulation (Chard et al., 1993). In human autopsy specimens, both proteins are absent in MN populations lost early in ALS (cortical, spinal and lower cranial MNs), whereas MNs targeted later in disease course (Onuf's nucleus, oculomotor, trochlear, and abducens MNs) expressed markedly more of each (Alexianu et al., 1994). Similarly, in pre-symptomatic $SOD1^{G93A}$ mice, lower levels of the Ca^{2+} binding ER chaperone calreticulin (CRT) were detected in vulnerable FF-MNs of the tibialis anterior muscle, compared to resistant MNs of the soleus (Bernard-Marissal et al., 2012). Knock-down of CRT *in vitro* was sufficient to trigger MN death by the Fas/NO pathway (Bernard-Marissal et al., 2012). Furthermore, reduced CRT levels and activation of Fas both trigger ER stress and cell death specifically in vulnerable $SOD1^{G93A}$-expressing MNs (Bernard-Marissal et al., 2012). These studies suggest that expression of Ca^{2+}-binding proteins may confer resistance to excitotoxic stimuli (Alexianu et al., 1994; Obál et al., 2006). However, overexpression of parvalbumin in high-copy $SOD1^{G93A}$ mice was beneficial (Laslo et al., 2000), although these findings have been challenged (Beers et al., 2001). Also, the loss or reduction of parvalbumin and calbindin D-28k immunoreactivity in large MNs at early stages in SOD1-transgenic mice suggest that these Ca^{2+}-binding proteins contribute to the selective vulnerability of MNs (Sasaki et al., 2006). Conversely, parvalbumin levels are significantly less in oculomotor neurons from $SOD1^{G93A}$ mice compared to spinal cord MNs (Comley et al., 2015). Hence, these conflicting data argue against the involvement of Ca^{2+}-binding proteins in oculomotor neuron resistance to degeneration. However, together these studies suggest that neuronal excitability and excitotoxicity are determinants of the selective vulnerability of spinal cord neurons, and the relative resistance of oculomotor neurons, in ALS.

Endoplasmic Reticulum Stress

The ER is responsible for the folding and quality control of virtually all proteins that transit through the secretory pathway. Hence it is a fundamental aspect of proteostasis. Unfolded or misfolded proteins are retained in the ER, which activates the unfolded protein response (UPR). This aims to improve the cellular protein folding capacity by inhibiting translation, upregulating ER chaperones – such as immunoglobulin binding protein (BiP) and protein disulfide isomerase (PDI) – and stimulating protein degradation (Walter and Ron, 2011; Rozas et al., 2017; Shahheydari et al., 2017). Numerous ALS-related proteins chronically active the UPR, including ALS-associated mutant forms of SOD1 (Nishitoh et al., 2008), TDP-43 (Walker et al., 2013), C9orf72 (Dafinca et al., 2016), Vesicle-associated membrane protein-associated protein B (VAPB) (Suzuki et al., 2009) and FUS (Farg et al., 2012). ER stress has also been detected in sporadic ALS patients (Ilieva et al., 2007; Atkin et al., 2008). Furthermore, ER stress is linked to excitability in ALS. Mutant SOD1 induces a transcriptional signature characteristic of ER stress, which also disrupts MN excitability (Kiskinis et al., 2014). Similarly, modulating the excitability properties of human iPSC-derived MNs alters the UPR (Kiskinis et al., 2014). Conversely, treatment of MNs with salubrinal, an inhibitor of ER stress which inhibits eIF2α dephosphorylation (Boyce et al., 2005), reduced the excitability of MNs (Kiskinis et al., 2014). Similar results were obtained in MNs from patients carrying C9orf72 repeat expansions or VCP mutations (Kiskinis et al., 2014; Dafinca et al., 2016; Hall et al., 2017). Moreover, pharmacological reduction of neuronal excitability in $SOD1^{G93A}$ mice specifically reduced BiP accumulation in ipsilateral FALS α-MNs (Saxena et al., 2013). Hence, together these findings

indicate that induction of the UPR and the electrical activity of MNs are both closely related in ALS.

An *in vivo* longitudinal analysis of MNs revealed that ER stress influences disease manifestations in $SOD1^{G93A}$ and $SOD1^{G85R}$ mouse models of FALS (Saxena et al., 2009). However, activation of the UPR is detrimental to mutant s-$SOD1^{G93A}$ mice, leading to failure to reinnervate NMJs. Conversely, treatment with salubrinal attenuated axon pathology and extended survival in mutant $SOD1^{G93A}$ mice (Saxena et al., 2009). Initiation of the UPR was detected specifically in FF-MNs in asymptomatic $SOD1^{G93A}$ mice, but not in S-MNs (Saxena et al., 2009). Hence these findings indicate that the more vulnerable MNs develop ER stress first, thus linking the UPR to MN susceptibility in ALS. FF-MNS may be more vulnerable to ER stress because they have much lower levels of BiP co-chaperone SIL1 compared to S-MNs (Filézac de L'Etang et al., 2015). SIL1 is protective against ER stress and reduces the formation of mutant SOD1 inclusions *in vitro*. Conversely SIL1 depletion leads to disturbed ER and nuclear envelope morphology, defective mitochondrial function, and ER stress, thus linking SIL1 to neurodegeneration (Roos et al., 2016). Furthermore, AAV-mediated overexpression of SIL1 in MNs of $SOD1^{G93A}$ mice preserves FF MN axons and prolongs survival by 25–30% compared to littermates (Filézac de L'Etang et al., 2015). In addition, SIL1 levels are reduced in MNs of mutant TDP-43^{A315T} mice, and are increased in the surviving MNs of SALS patients, also implying that SIL1 is protective in ALS (Filézac de L'Etang et al., 2015).

Consistent with these studies, ER stress is present specifically in anterior horn MNs in *knock-in* mice expressing BiP artificially retained in the ER. Furthermore, this was accompanied by the accumulation of ubiquitinated proteins and wild type SOD1 (Mimura et al., 2008; Jin et al., 2014), reminiscent of SALS (Bosco et al., 2010). Significant changes in mRNAs of ER stress genes were also detected in the cerebellum by transcriptome analysis (Prudencio et al., 2015). These studies together link SIL1 and BiP to neurodegeneration in both neuronal subpopulations in ALS/FTD.

PDI is also upregulated in SOD1 mice and human SALS spinal cord tissues (Ilieva et al., 2007; Atkin et al., 2008; Sasaki, 2010; Walker et al., 2010; Chen et al., 2015; Sun et al., 2015). Wild type PDI overexpression and related family member Erp57 are protective *in vitro* in neuronal cells expressing mutant SOD1 (Walker et al., 2010; Jeon et al., 2014; Parakh et al., 2018a). Interestingly, mutations in PDI and Erp57 have been identified in ALS patients, and expression in zebrafish induces motor defects (Woehlbier et al., 2016). Furthermore, the levels of PDI in MNs are lower than in astrocytes and oligodendrocytes in $SOD1^{G37R}$ mice (Sun et al., 2015). This implies that MNs are intrinsically more vulnerable to unfolded protein accumulation than other cell types, which may also contribute to their susceptibility in ALS.

It should also be noted, however, that the ER in neurons (and therefore MNs) is not as well characterized as other cell types. In fact, most studies examining UPR mechanisms have involved non-neuronal cells. Neurons possess extensive ER which is distributed continuously throughout the axonal, dendritic and somatic compartments, implying that neurons make unique demands on the ER compared to other cell types (Ramírez and Couve, 2011). Hence, our current soma-centric view of the ER does not consider its role in neuronal processes and how this might relate to their specific functions. This is particularly true for large neurons, such as MNs with their extended axons. The findings that the most susceptible MNs develop ER stress first implies that the ER in MNs may confer unique susceptibility on these cells compared to other MNs and non-neuronal cells. However, this idea requires validation experimentally.

Mitochondria and Energy Metabolism

Neurons utilize most of their energy at the synapse, which consumes more than a third of the overall cellular ATP (Harris et al., 2012; Niven, 2016). The properties and types of ion channels expressed in a MN influence the energy required to generate an action potential, and the Na^+/K^+ pump is estimated to account for 20–40% of the brain's energy consumption (Purves et al., 2001). The size and shape of a MN also affects its electrical properties, and the distance over which signals must spread. MNs have particularly high energetic demands, even compared to other neurons. They also have large numbers of NMJs as well as high intracellular Ca^{2+} flux as discussed above.

More than 90% of ATP generation in the CNS occurs via mitochondrial oxidative phosphorylation (Hyder et al., 2013; Vandoorne et al., 2018). Reductions in energy metabolism have been reported in ALS (Vandoorne et al., 2018) and mitochondrial abnormalities, such as swelling and morphological changes, are among the earliest signs of pathology in $SOD1^{G93A}$ and $SOD1^{G37R}$ mice (Wong et al., 1995; Kong and Xu, 1998), FUS^{R521C} rats (Huang et al., 2012; So et al., 2018) and wild type TDP-43 mice (Shan et al., 2010; Xu et al., 2010). Moreover, mitochondrial abnormalities are also present in MNs of ALS patient tissues (Fujita et al., 1996; Sasaki and Iwata, 1996; Swerdlow et al., 1998; Dhaliwal and Grewal, 2000; Sasaki et al., 2007). Furthermore, mutant SOD1 specifically associates with mitochondria and interferes with their function (Liu et al., 2004; Pasinelli et al., 2004; Ferri et al., 2006; Sotelo-Silveira et al., 2009; Vande Velde et al., 2011). Decreased activity of mitochondrial respiratory chain complexes was also present in spinal cord sections (Borthwick et al., 1999) and homogenates (Wiedemann et al., 2002) from ALS patients. Consistent with these findings, genes involved in mitochondrial function were upregulated in rat oculomotor neurons compared to hypoglossal and cervical spinal cord MNs. However, it should be noted that the higher firing rate of the former might confer some resistance to energy imbalance (Hedlund et al., 2010; Brockington et al., 2013).

In vulnerable MNs lacking Ca^{2+}-binding proteins calbindin and parvalbumin, Ca^{2+} is largely taken up by mitochondria (Lautenschläger et al., 2013). As a result, extensive mitochondrial transport to the dendritic space is required to maintain Ca^{2+} homeostasis. The normal distribution of mitochondria is also perturbed in ALS patient MNs. Whereas they are depleted in distal dendrites and axons, mitochondria also accumulate in the soma and proximal axon hillock (Sasaki et al., 2007). Disturbed mitochondrial dynamics were also described in MNs in mutant $SOD1^{G93A}$ (De Vos et al., 2007; Sotelo-Silveira et al., 2009; Bilsland et al., 2010; Magrané et al., 2014) and TDP-43^{A315T} (Magrané et al., 2014) mice. In addition, iPSC-derived A4V MNs

exhibit disturbances in mitochondrial morphology and motility within the axon (Kiskinis et al., 2014). Similarly, expression of mutant TDP-43 in spinal cord primary neurons leads to abnormal distribution of mitochondria (Wang et al., 2013). Dysfunctional Ca^{2+} uptake by mitochondria may therefore result in elevated intracellular Ca^{2+} levels, thus contributing to neurodegeneration.

Compared to FF-MNs, S-MNs have smaller soma and axons, less dendritic branching, and fewer neuromuscular terminals (Kanning et al., 2010). This results in higher input resistance and therefore less energy is required to initiate an action potential in comparison. Moreover, S-MNs contain more mitochondria compared to FF-MNs (Kanning et al., 2010). These two properties may therefore render FF-MNs more vulnerable to depletion of energy than S-MNs. Indeed, a computational analysis study estimated that the energy requirements of FF-MNs are considerably larger than S-MNs for a similar discharge (Le Masson et al., 2014), rendering the former more sensitive to ATP imbalance. Furthermore, the muscle fiber types associated with FF- and S-MNs differ in their major energy source. The slow twitch muscles use mainly oxidative metabolism, whereas the fast-twitch fibers use glycolysis. Hence, the heightened vulnerability of MN subpopulations may relate to their bioenergetic and morphological characteristics. Both the direct interaction of misfolded ALS mutant proteins with mitochondria and the secondary overload of ion uptake could account for mitochondrial metabolism failure, leading to reduced ATP availability (Israelson et al., 2010).

Motor Neuron Size

Motor neurons can vary widely in their size and this can impact on their physiological functions. There is also increasing evidence that vulnerability to degeneration is related to MN size. The disease-vulnerable FF-MNs somas are larger than the S-MN resistant types, and they possess larger motor units. Moreover, the size of a MN also correlates inversely with its excitability, discharge behavior, firing rate, recruitment during movement, and vulnerability to degeneration in ALS (Henneman, 1957; Le Masson et al., 2014). The soma of MNs from male $SOD1^{G93A}$ mice is larger than those of wild type male mice (Shoenfeld et al., 2014). Furthermore, a recent study demonstrated that not only are the larger MN subtypes more vulnerable to neurodegeneration in $SOD1^{G93A}$ mice, but MNs also increase in size during disease in multiple regions of the spinal cord. Interestingly, *in silico* modeling predicted that the excitability properties of these cells were also altered (Dukkipati et al., 2018). Hence, MN size may alter during disease progression, and this plasticity may impact on the vulnerability of MN subtypes.

Oxidative Stress

Oxidative stress arises when reactive oxygen species (ROS) or nitrogen species (RNS) accumulate within cells. This can lead to oxidative modifications and altered functional states of proteins, nucleic acids and lipids. Oxidative stress is linked to neurodegeneration in ALS (Carrí et al., 2003) and oxidation products, such as malondialdehyde, hydroxynonenal, and oxidized proteins, DNA or membrane phospholipids, are elevated in SALS and FALS patients (Shaw et al., 1995; Beal et al., 1997; Ferrante et al., 1997; Bogdanov et al., 2000; Shibata et al., 2001) and mouse models of ALS (Gurney et al., 1994; Andrus et al., 1998; Bogdanov et al., 1998; Hall et al., 1998; Liu et al., 1998, 1999; Rizzardini et al., 2003). Mitochondria damage in ALS has also been attributed to intracellular oxidative stress (Fujita et al., 1996). The normal physiological function of SOD1 is the detoxification of superoxide radicals, although loss of SOD1 function is no longer favored as a disease mechanism in ALS (Saccon et al., 2013). However, mutations in SOD1 increase neuronal vulnerability to oxidative stress (Franco et al., 2013; Tsang et al., 2014). Moreover, in response to elevated ROS, SOD1 relocates from the cytoplasm to the nucleus, where it regulates the expression of oxidative resistance and repair genes (Tsang et al., 2014).

Some neurons exhibit differential vulnerability to oxidative damage. Cerebellar granule and hippocampal CA1 neurons are more sensitive to oxidative stress than cerebral cortical and hippocampal CA3 neurons (Wang X. et al., 2009; Wang and Michaelis, 2010). Hence, it is possible that similar differences in vulnerability to oxidative stress might exist between MN populations. However, this possibility needs to be confirmed experimentally.

Protein Transport

Efficient intracellular trafficking is required to maintain the structure and function of MNs, particularly because MNs have very long axons that connect the soma with distant synaptic sites [reviewed in De Vos and Hafezparast (2017)]. Disorganization of the neuronal cytoskeleton and inhibition of axonal, ER-Golgi, endosomal and nucleocytoplasmic transport, are now widely reported features of ALS [reviewed in Parakh et al. (2018b) and Burk and Pasterkamp (2019)]. Importantly, defects in trafficking could reduce the supply of components necessary for synaptic and/or somal function, and prevent clearance of waste products from the synapse, together contributing to neurodegeneration in ALS.

The existence of mutations in genes encoding cytoskeletal proteins or the cellular transport machinery highlights the involvement of these processes in ALS/FTD. These include tubulin α4A (Smith et al., 2014a; Perrone et al., 2017), a major component of microtubules, neurofilament heavy chain (Figlewicz et al., 1994), a type of intermediate filament, and profilin-1 (Wu et al., 2012; Dillen et al., 2013; Smith et al., 2014b), which is involved in actin polymerization. Similarly, dynactin-1, involved in axonal transport (Puls et al., 2003; Münch et al., 2004; Münch et al., 2005; Liu et al., 2017) and SCFD1 (Sec1 family domain containing 1), involved in ER to Golgi transport (van Rheenen et al., 2016), are also mutated in a small proportion of patients, further implying that protein transport is impaired in ALS/FTD.

Axonal transport defects may be an important factor underlying the selective vulnerability of MNs or MN subtypes in ALS/FTD. Abnormal accumulation of phosphorylated neurofilaments, mitochondria and lysosomes in the proximal axon of large MNs and axonal spheroids, are present in SALS

and FALS patients (Hirano et al., 1984; Corbo and Hays, 1992; Okada et al., 1995; Rouleau et al., 1996; Sasaki and Iwata, 1996). Mutant SOD1 slows both anterograde (Williamson and Cleveland, 1999) and retrograde (Chen et al., 2007; Perlson et al., 2009) axonal transport. Cytoskeletal and motor proteins are differentially expressed in spinal MNs compared to oculomotor neurons. This includes peripherin (Hedlund et al., 2010; Comley et al., 2015), which is also found in ubiquitinated inclusions in the spinal cord of FALS (Robertson et al., 2003) and SALS patients (He and Hays, 2004). Overexpression of peripherin leads to defective axonal transport (Millecamps et al., 2006) and late-onset MN degeneration (Beaulieu et al., 1999), implying that differential expression of peripherin contributes to neurodegeneration.

Axonal transport requires the efficient regulation of both dynein and kinesin molecular motors (Melkov et al., 2016), which mediate transport in the retrograde and anterograde directions respectively. Dynein is differentially expressed in vulnerable and susceptible MNs because higher levels are present in spinal and hypoglossal MNs compared to oculomotor neurons (Ilieva et al., 2008). However, dynein levels were significantly decreased in motor nuclei in $SOD1^{G93A}$ mice compared to wild type mice although its expression in MNs was equivalent (Comley et al., 2015). Similar patterns were observed in ALS patients (Comley et al., 2015). Disruption of dynein inhibits axonal transport and results in abnormal redistribution of mitochondria (Varadi et al., 2004) and late-onset degeneration in mice (LaMonte et al., 2002). Several FALS-linked SOD1 mutants co-localize with dynein/dynactin *in vitro* and $SOD1^{G93A}$ mice (Ligon et al., 2005; Zhang et al., 2007; Shi et al., 2010), which perturbs axonal transport and synaptic mitochondrial content (De Vos et al., 2007). The lower expression of dynein in oculomotor neurons might therefore confer resistance to axonal transport defects in ALS. However, it is also possible that this simply reflects less need for retrograde transport in oculomotor neurons due to their smaller cell bodies, shorter axons and lower requirements for energy, compared to spinal and hypoglossal MNs. Nevertheless, the inefficient axonal transport of mitochondria may confer loss of energy at the synapse in vulnerable MN subpopulations. These MNs require more energy to function than other cells, leading to disturbed synaptic activity.

Kinesin-dependant axonal transport is also disrupted in ALS. Oxidized forms of wild type SOD1 immunopurified from SALS tissues inhibited kinesin-based fast axonal transport (Bosco et al., 2010). However, no interaction between members of the kinesin family (KIF5A, 5B or 5C) and SOD1 was detected in $SOD1^{G93A}$ mice. High expression of KIF proteins is also associated with neurodegeneration. KIF5C was abundantly expressed in vulnerable spinal MNs in $SOD1^{G93A}$ mice (Kanai et al., 2000), but a marked reduction in KIF3Aβ levels was detected in the motor cortex of SALS patients (Pantelidou et al., 2007). Furthermore, reduced kinesin-associated protein 3 (KIFAP3) expression was linked to an increase in the survival of ALS patients (Landers et al., 2009) and changes in the transport of choline acetyltransferase transporter (ChAT) along axons. KIF5C is expressed more in rat spinal MNs than oculomotor and hypoglossal MNs (Hedlund et al., 2010), However, further work is necessary to determine if this is related to ALS, and to examine whether KIFs are differentially expressed in neuronal subtypes.

Defects in the secretory pathway are also linked to ALS. Depletion of TDP-43 inhibits endosomal trafficking and results in lack of neurotrophic signaling and neurodegeneration (Schwenk et al., 2016). Similarly, inhibition of the first part of the classical secretory pathway, ER-Golgi transport, is also induced by mutant SOD1, TDP-43 and FUS (Sundaramoorthy et al., 2013; Soo et al., 2015). This mechanism has been described as a possible trigger for ER stress (Soo et al., 2015), which, as detailed above, is linked to neuronal susceptibility. Both endosomal and ER-Golgi transport are also linked to transport within the axon. However, it remains to be determined if these other forms of trafficking are directly associated with selective neuronal susceptibility in ALS.

Defective nucleocytoplasmic transport is emerging as an important cellular mechanism in the initiation or progression of ALS. Nuclear pore pathology is present in the brain of SALS and C9orf72 patients (Zhang K. et al., 2015; Chou et al., 2018). C9orf72 repeat expansions impair protein trafficking from the cytoplasm to the nucleus, and reduce the proportion of nuclear TDP-43 in patient-derived MNs (Zhang K. et al., 2015), thereby mimicking the nuclear depletion of TDP-43 in ALS patients (Neumann et al., 2006). Proteins involved in nucleocytoplasmic transport are abnormally localized in aggregates in the cortex of C9orf72 ALS patients, patient-derived MNs and the brain of C9orf72 mouse models (Zhang K. et al., 2015, Zhang et al., 2016). Similarly, TDP-43 pathology disrupts nuclear pore complexes and lamina morphology in cell lines and patient-derived MNs. Furthermore, insoluble TDP-43 aggregates also contain components of the nucleocytoplasmic machinery (Chou et al., 2018). Both protein import and RNA export were impaired by mutant TDP-43 in the brain of SALS mouse primary neurons (Chou et al., 2018). A recent meta-analysis of ALS modifier genes identified several genes encoding proteins involved in nucleocytoplasmic shuttling (Yanagi et al., 2019). In fact, the most enriched gene ontology term in this study was "protein import into the nucleus," and it included KPNB1, encoding importin subunit beta-1, which was identified as a genetic modifier in three separate ALS models. Interestingly, the gene encoding lamin B1 subunit 1, which is involved in nuclear stability, was upregulated in oculomotor neurons compared to hypoglossal MNs and spinal cord MNs (Hedlund et al., 2010). Furthermore, lamin B1 is also known to possess cellular protective functions such as controlling the cellular response to oxidative stress (Malhas et al., 2009), DNA repair (Butin-Israeli et al., 2015) and RNA synthesis (Tang et al., 2008). It is therefore tempting to speculate that lamin B1 confers resistance to specific MN populations when highly expressed. However, further work is necessary to examine this possibility.

AGING

Although genetic mutations are present throughout life, ALS most commonly develops in mid-adulthood (50–60 years), implying that the normal aging process renders MNs vulnerable to degeneration. However, there is considerable variability in disease progression amongst mutation carriers,

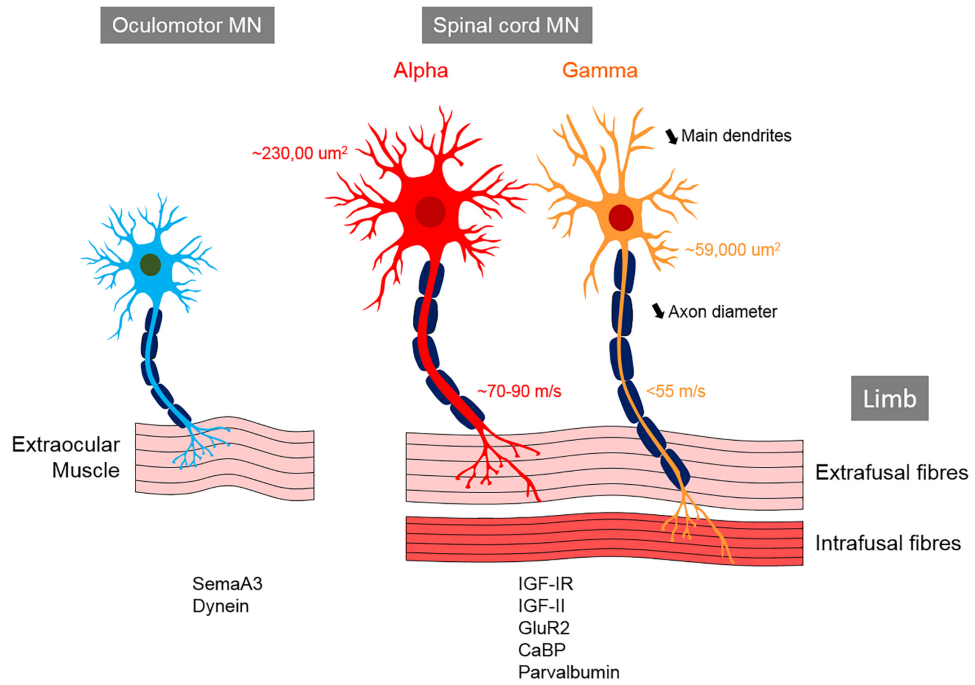

FIGURE 4 | Reported differences between the vulnerable (ventral spinal cord MNs) and resistant (oculomotor) motor neurons in ALS. The surface area and axonal conduction velocities referred to here were obtained from studies in cats (Westbury, 1982). The α-MNs innervate highly contracting extrafusal fibers, whereas γ-MNs innervate intrafusal fibers that contract much less; oculomotor neurons innervate the extraocular muscles in the orbit. α-MNs are larger than γ-MNs and oculomotor neurons and possess more dendritic trees. α-MNs are further subdivided based on their size and function. The proteins listed at the bottom of the figure are those enriched in each MN population.

even within the same families. Hence, this implies that there is no simple correlation between genetics and disease phenotypes, suggesting that environmental factors and the normal aging process are relevant to understand neuronal vulnerability in ALS/FTD.

Aging results in the accumulation of detrimental biological changes over time. The reduction of muscle mass and strength (sarcopenia) is one of the major causes of disability in older persons (Enoka et al., 2003; Lauretani et al., 2003; Delmonico et al., 2009; Clark and Manini, 2012), which affects gait speed, balance, and the command of fine motor skills (Fried et al., 2004; Sorond et al., 2015). The deterioration of motor functions with advancing age therefore increases the risk of injury and age-associated diseases such as ALS/FTD (Spiller et al., 2016b; Niccoli et al., 2017).

Aging-associated muscle weakness also results from impairment of the activity of MNs contacting skeletal muscles (Fiatarone and Evans, 1993; Manini et al., 2013). High resolution structural MRI imaging reveals prominent atrophy in the primary motor cortex (Salat et al., 2004), as early as middle life in humans. Age-related decreases in white matter mass and myelinated nerve fiber length also correlate with reductions in the size of the motor cortex (Marner et al., 2003). However, loss of neurons during normal human aging is restricted to specific regions of the CNS only, and the number of cells lost is only slight, contrary to previous convictions that significant loss of neurons occur in the human cortex (Pannese, 2011). Instead, age-related changes observed in aged rhesus monkeys and mice appear to involve loss of dendrites and axons, and demyelination, resulting in significant loss of synapses without loss of the neuronal soma (Pannese, 2011). Similarly, there are fewer cholinergic and glutamatergic synaptic inputs directly abutting α-MNs in aged animals, indicating that aging causes α-MNs to shed synaptic inputs. Thus, both impairment of axon function and substantial loss of synaptic inputs may contribute to age-related dysfunction of α-MNs, without loss of the soma (Maxwell et al., 2018). As a consequence, motor units are gradually lost over the first six decades of life, and this accelerates thereafter (Deschenes, 2011). These studies together indicate that neuronal atrophy and axonal impairment, with reduced neuromuscular activity in the absence of MN loss, occur with normal aging.

A major component of aging-related muscle weakness is breakdown in communication between the brain and NMJ. This is related to increased neural noise which reduces the accuracy of neural transmission (Manini et al., 2013). This can result in activation of the motor unit, so that it becomes erratic, and together with diminished glutamate uptake into MNs, leads to an inability to exert muscle force and motor control (Manini et al., 2013). Furthermore, susceptibility of neurons to cellular stress, due to impairment of proteostasis and/or increased oxidative or metabolic stress during normal aging, may render MNs vulnerable to degeneration. Hence, genetic and environmental factors may combine to determine whether

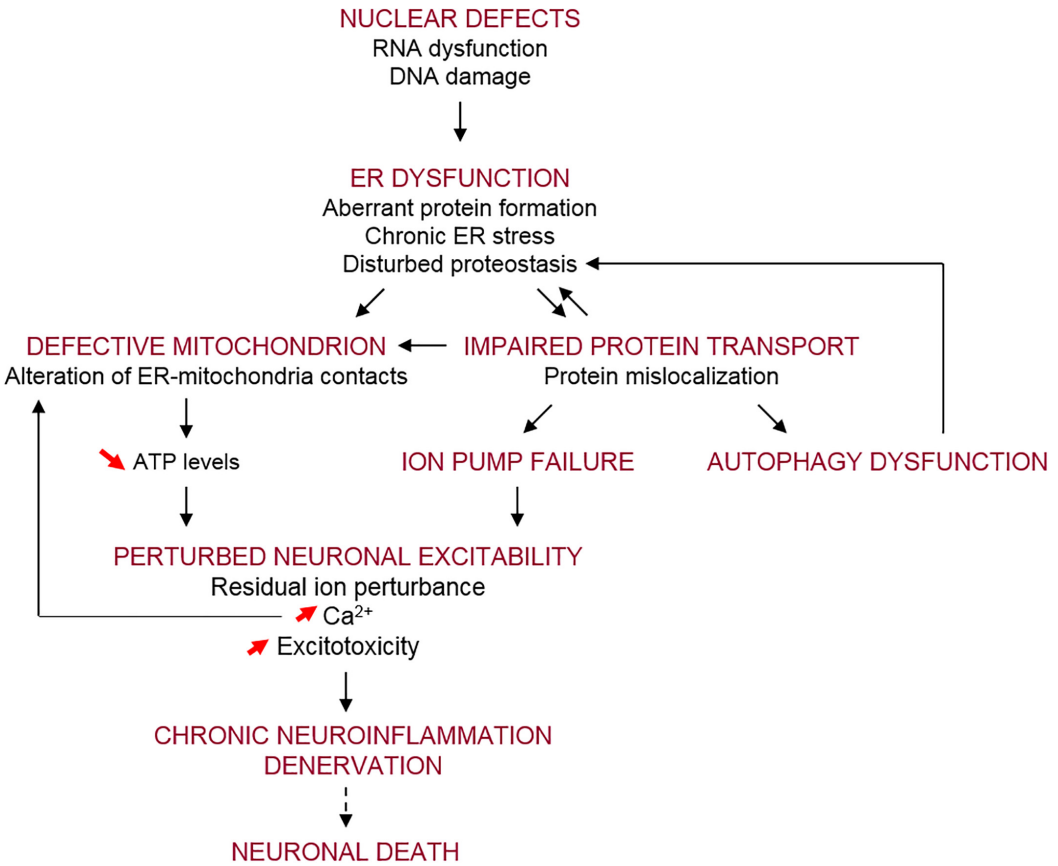

FIGURE 5 | Diagram showing a hypothetic cascade of cellular events leading to neurodegeneration and neuronal death in motor neurons in ALS/FTD. This schematic diagram summarizes the key features occurring in vulnerable MNs. Resistant MNs are protected by the expression of a genes controlling cellular mechanisms that are defective in ALS/FTD (RNA dysfunction, ER stress, mitochondrial defects, protein transport dysfunction, dysregulation of neuronal excitability and excitotoxicity). These processes can be exacerbated by age, environmental and genetic mutations.

a MN can withstand an age-related disease such as ALS or not (Mattson and Magnus, 2006).

Age-Related Proteostasis Disturbance

During the aging process, a decline in the normal cellular ability to maintain proteostasis is observed and, as a result, damaged proteins accumulate (Kikis et al., 2010). Thus the normal aging process in MNs that are already weakened by ALS-associated insults, such as the presence of misfolded proteins or environmental factors, may combine to induce neurodegeneration. MN populations that are more susceptible in ALS may therefore be less able to tolerate disturbances in proteostasis than the more resistant populations (Neumann et al., 2006; Kikis et al., 2010).

Mitochondria play a crucial role in neuronal aging. Normal features observed in the aging brain include the accumulation of mutations in mitochondrial DNA, the production of ROS, mitochondrial metabolic abnormalities and altered Ca^{2+} storage (Sun et al., 2016). Remarkably, mitochondria in different regions of the CNS are not equally affected during aging. The sensitivity of the mitochondrial permeability transition pore to Ca^{2+} in the cortex and hippocampus is greater than that of the striatum and the cerebellum in aged rats (LaFrance et al., 2005; Brown et al., 2006). The cellular location of mitochondria is also relevant to the aging processes. Synaptic mitochondria are more prone to oxidative stress-induced damage than mitochondria located in the soma (Brown et al., 2006; Reddy and Beal, 2008). In addition, synaptic mitochondria display a limited capacity to accumulate Ca^{2+}, unlike those located in the soma (Brown et al., 2006). Furthermore, marked differences have been described between mitochondria located in the spinal cord and those found in distal axons of MNs from aged rats. In the axon termini at the NMJ, mitochondria swelling, fusion and an abundance of megamitochondria (giant mitochondria) during aging have been reported (García et al., 2013). These studies therefore imply that mitochondria become dysfunctional in aged MNs, which might sensitize vulnerable MN populations to ALS/FTD. Mitochondria located at the synapse may also be particularly vulnerable to these age-related processes.

Age-Related DNA Damage

The mammalian genome is under constant attack from both endogenous and exogenous sources. This can result in DNA

damage, mutations and impaired cellular viability if not repaired correctly (Madabhushi et al., 2014). There is a significant increase in DNA damage during aging due to reduced capacity of DNA repair. Moreover, erroneous repair of DNA lesions can result in further mutations in the aged brain (Vijg and Suh, 2013). DNA damage is increasingly implicated in neurodegenerative disorders, including ALS, where it is induced by the C9orf72 repeat expansion (Farg et al., 2017; Walker et al., 2017). Interestingly, there is also evidence that both FUS and TDP-43 function in the DNA damage response, in either prevention of damage or repair of R loop-associated DNA damage (Hill et al., 2016). In addition, impairment of the DNA damage response due to the presence of ALS/FTD-associated FUS mutations induces neurodegeneration (Higelin et al., 2016; Naumann et al., 2018). It is therefore possible that the normal aging process results in an impaired ability to repair DNA in MNs. This may be an important source of cellular stress that precipitates neurodegeneration in cells already exposed to pathological events throughout life. However, recent work suggests that mutant $SOD1^{G93A}$ does not impact on DNA strand integrity, implying that DNA damage is not present in all forms of ALS (Penndorf et al., 2017).

CONCLUSION

Motor neurons are unique cells compared to other neurons. They are large cells, with extraordinarily long axons, and very high energetic requirements, which may render them uniquely susceptible to degeneration in ALS. Remarkably, however, not all MNs are equally affected, and there are marked differences in vulnerabilities between MN subtypes, even within the same motor unit. The resistant MNs possess distinct morphological and functional characteristics, as well as different gene expression profiles, compared to the more vulnerable groups (**Figure 4**). Importantly, the oculomotor neurons continue to function, even in the late stages of ALS when the vulnerable spinal and other MNs are significantly depleted. These oculomotor neurons are anatomically and functionally very different from all other motor units: they are much smaller, and their function involves sensing rather than movement, hence different circuits are involved. In contrast, spinal MNs are more prone to hyperexcitation and they express high levels of AMPA receptors, they are more prone to develop ER stress, and they do not buffer Ca^{2+} as well as the more resistant MN types. These properties may confer unique sensitivity to neurodegeneration in ALS. Interestingly, even within spinal MNs, there are distinct differences in vulnerability, because FF-MNs degenerate first, followed by FR-MNs, and the more resistant S-MNs degenerate later. Similarly, these cells also display differences in excitability and ER stress.

A hypothetical model is presented in **Figure 5**, summarizing the possible molecular mechanisms involved in MN vulnerability in ALS. The regulation of synaptic plasticity and neuronal excitability may underlie susceptibility in ALS involving nuclear-cytoplasmic defects, ER stress, transport dysfunction and mitochondrial alterations. From an initial site of onset, neurodegeneration begins in susceptible MN groups, and then spreads contiguously throughout the neuroanatomy, in a defined pattern, to the surrounding cells. This therefore highlights the role of impaired neurotransmission in triggering and propagating neurodegeneration in ALS. Glial cells are involved in both the onset and progression of ALS.

The susceptibility of specific MN groups, however, is further complicated by the heterogeneous nature of ALS, even within the same families, and the different patterns of motor involvement. Stratification of ALS patients into distinct subtypes and investigations into MNs susceptibilities may reveal more insights why specific groups of MNs degenerate first in ALS in the future. However, the blurring of some neurodegenerative disorders, including ALS and FTD, and the presence of C9orf72 mutations in several other neurodegenerative conditions as well as ALS, is another confounding factor. Understanding the fundamental mechanisms dictating MN vulnerability in ALS is central to our understanding of this devastating disorder. Hence, studies in this area may lead to novel therapeutic insights in the future.

AUTHOR CONTRIBUTIONS

MV wrote the "Site-Specific Onset and Spread of Neurodegeneration in ALS" section. MJ wrote the "Role of Glial Cells in Driving Disease Progression" section. SS wrote the "Aging" section. AR conceived and prepared the figures, and wrote the "Introduction," and "Anatomy of the Motor System," "Genetic Mutations and Risk Factors in ALS," and "Intrinsic Factors Specific to MN Subpopulations" sections. JA conceived the article, wrote the "Conclusion" section, contributed text in numerous sections, and edited the manuscript throughout for content and style consistency.

FUNDING

This work was supported by the Australian National Health and Medical Research Council, FightMND Foundation, and Motor Neuron Disease Research Institute of Australia. SS was supported by an International Research Training Program Scholarship (iRTP). MJ was supported by the International Macquarie University Research Excellence Scholarship (iMQRES).

SUPPLEMENTARY MATERIAL

The Supplementary Material for this article can be found online at: https://www.frontiersin.org/articles/10.3389/fnins.2019.00532/full#supplementary-material

REFERENCES

Acevedo-Arozena, A., Kalmar, B., Essa, S., Ricketts, T., Joyce, P., Kent, R., et al. (2011). A comprehensive assessment of the SOD1G93A low-copy transgenic mouse, which models human amyotrophic lateral sclerosis. *Dis. Model Mech.* 4, 686–700. doi: 10.1242/dmm.00723

Adal, M. N., and Barker, D. (1965). Intramuscular branching of fusimotor fibres. *J. Physiol.* 177, 288–299. doi: 10.1113/jphysiol.1965.sp007592

Aizawa, H., Sawada, J., Hideyama, T., Yamashita, T., Katayama, T., Hasebe, N., et al. (2010). TDP-43 pathology in sporadic ALS occurs in motor neurons lacking the RNA editing enzyme ADAR2. *Acta Neuropathol.* 120, 75–84. doi: 10.1007/s00401-010-0678-x

Al Sultan, A., Waller, R., Heath, P., and Kirby, J. (2016). The genetics of amyotrophic lateral sclerosis: current insights. *Degen. Neurol. Neuromusc. Dis.* 2016, 49–64.

Alexander, G. M., Erwin, K. L., Byers, N., Deitch, J. S., Augelli, B. J., Blankenhorn, E. P., et al. (2004). Effect of transgene copy number on survival in the G93A SOD1 transgenic mouse model of ALS. *Brain Res. Mol. Brain Res.* 130, 7–15. doi: 10.1016/j.molbrainres.2004.07.002

Alexianu, M. E., Ho, B. K., Mohamed, A. H., La Bella, V., Smith, R. G., and Appel, S. H. (1994). The role of calcium-binding proteins in selective motoneuron vulnerability in amyotrophic lateral sclerosis. *Ann. Neurol.* 36, 846–858. doi: 10.1002/ana.410360608

Alexianu, M. E., Kozovska, M., and Appel, S. H. (2001). Immune reactivity in a mouse model of familial ALS correlates with disease progression. *Neurology* 57, 1282–1289. doi: 10.1212/wnl.57.7.1282

Allodi, I., Comley, L., Nichterwitz, S., Nizzardo, M., Simone, C., Benitez, J. A., et al. (2016). Differential neuronal vulnerability identifies IGF-2 as a protective factor in ALS. *Sci. Rep.* 6:25960. doi: 10.1038/srep25960

Andersen, P. M., Sims, K. B., Xin, W. W., Kiely, R., O'Neill, G., Ravits, J., et al. (2003). Sixteen novel mutations in the Cu/Zn superoxide dismutase gene in amyotrophic lateral sclerosis: a decade of discoveries, defects and disputes. *Amyotroph. Lateral Scler. Other Motor Neuron Disord.* 4, 62–73. doi: 10.1080/14660820310011700

Andrus, P. K., Fleck, T. J., Gurney, M. E., and Hall, E. D. (1998). Protein oxidative damage in a transgenic mouse model of familial amyotrophic lateral sclerosis. *J. Neurochem.* 71, 2041–2048. doi: 10.1046/j.1471-4159.1998.71052041.x

Arai, T., Hasegawa, M., Akiyama, H., Ikeda, K., Nonaka, T., Mori, H., et al. (2006). TDP-43 is a component of ubiquitin-positive tau-negative inclusions in frontotemporal lobar degeneration and amyotrophic lateral sclerosis. *Biochem. Biophys. Res. Commun.* 351, 602–611. doi: 10.1016/j.bbrc.2006.10.093

Arbour, D., Vande Velde, C., and Robitaille, R. (2017). New perspectives on amyotrophic lateral sclerosis: the role of glial cells at the neuromuscular junction. *J. Physiol.* 595, 647–661. doi: 10.1113/JP270213

Asanuma, H., and Rosén, I. (1972). Topographical organization of cortical efferent zones projecting to distal forelimb muscles in the monkey. *Exp. Brain Res.* 14, 243–256. doi: 10.1007/BF00816161

Ashrafi, S., Lalancette-Hébert, M., Friese, A., Sigrist, M., Arber, S., Shneider, N. A., et al. (2012). Wnt7A identifies embryonic γ-motor neurons and reveals early postnatal dependence of γ-motor neurons on a muscle spindle-derived signal. *J. Neurosci.* 32, 8725–8731. doi: 10.1523/JNEUROSCI.1160-12.2012

Atkin, J. D., Farg, M. A., Walker, A. K., McLean, C., Tomas, D., and Horne, M. K. (2008). Endoplasmic reticulum stress and induction of the unfolded protein response in human sporadic amyotrophic lateral sclerosis. *Neurobiol. Dis.* 30, 400–407. doi: 10.1016/j.nbd.2008.02.009

Ayers, J. I., and Cashman, N. R. (2018). Prion-like mechanisms in amyotrophic lateral sclerosis. *Handb. Clin. Neurol.* 153, 337–354. doi: 10.1016/B978-0-444-63945-5.00018-0

Ayers, J. I., Fromholt, S., Koch, M., DeBosier, A., McMahon, B., Xu, G., et al. (2014). Experimental transmissibility of mutant SOD1 motor neuron disease. *Acta Neuropathol.* 128, 791–803. doi: 10.1007/s00401-014-1342-7

Ayers, J. I., Fromholt, S. E., O'Neal, V. M., Diamond, J. H., and Borchelt, D. R. (2016). Prion-like propagation of mutant SOD1 misfolding and motor neuron disease spread along neuroanatomical pathways. *Acta Neuropathol.* 131, 103–114. doi: 10.1007/s00401-015-1514-0

Bakels, R., and Kernell, D. (1993). Matching between motoneurone and muscle unit properties in rat medial gastrocnemius. *J. Physiol.* 463, 307–324. doi: 10.1113/jphysiol.1993.sp019596

Bakulin, I. S., Chervyakov, A. V., Suponeva, N. A., Zakharova, M. N., and Piradov, M. A. (2016). *Motor Cortex Hyperexcitability, Neuroplasticity, and Degeneration in Amyotrophic Lateral Sclerosis. Update on Amyotrophic Lateral Sclerosis*. London: Intechopen.

Balendra, R., and Isaacs, A. M. (2018). C9orf72 -mediated ALS and FTD: multiple pathways to disease. *Nat. Rev. Neurol.* 14:544. doi: 10.1038/s41582-018-0047-2

Bannwarth, S., Ait-El-Mkadem, S., Chaussenot, A., Genin, E. C., Lacas-Gervais, S., Fragaki, K., et al. (2014). A mitochondrial origin for frontotemporal dementia and amyotrophic lateral sclerosis through CHCHD10 involvement. *Brain* 137, 2329–2345. doi: 10.1093/brain/awu138

Barmada, S. J. (2015). Linking RNA dysfunction and neurodegeneration in amyotrophic lateral sclerosis. *Neurotherapeutics* 12, 340–351. doi: 10.1007/s13311-015-0340-3

Batra, R., and Lee, C. W. (2017). Mouse models of C9orf72 hexanucleotide repeat expansion in amyotrophic lateral sclerosis/ frontotemporal dementia. *Front. Cell Neurosci.* 11:196. doi: 10.3389/fncel.2017.00196

Beal, M. F., Ferrante, R. J., Browne, S. E., Matthews, R. T., Kowall, N. W., and Brown, R. H. (1997). Increased 3-nitrotyrosine in both sporadic and familial amyotrophic lateral sclerosis. *Ann. Neurol.* 42, 644–654. doi: 10.1002/ana.410420416

Beaulieu, J. M., Nguyen, M. D., and Julien, J. P. (1999). Late onset of motor neurons in mice overexpressing wild-type peripherin. *J. Cell Biol.* 147, 531–544. doi: 10.1083/jcb.147.3.531

Beck, J., Poulter, M., Hensman, D., Rohrer, J. D., Mahoney, C. J., Adamson, G., et al. (2013). Large C9orf72 hexanucleotide repeat expansions are seen in multiple neurodegenerative syndromes and are more frequent than expected in the UK population. *Am. J. Hum. Genet.* 92, 345–353. doi: 10.1016/j.ajhg.2013.01.011

Bede, P., Iyer, P. M., Schuster, C., Elamin, M., Mclaughlin, R. L., Kenna, K., et al. (2016). The selective anatomical vulnerability of ALS: "disease-defining" and "disease-defying" brain regions. *Amyotroph. Lateral Scler. Frontotemporal Degener.* 17, 561–570. doi: 10.3109/21678421.2016.1173702

Beers, D. R., Henkel, J. S., Zhao, W., Wang, J., Huang, A., Wen, S., et al. (2011). Endogenous regulatory T lymphocytes ameliorate amyotrophic lateral sclerosis in mice and correlate with disease progression in patients with amyotrophic lateral sclerosis. *Brain J. Neurol.* 134, 1293–1314. doi: 10.1093/brain/awr074

Beers, D. R., Ho, B.-K., Siklós, L., Alexianu, M. E., Mosier, D. R., Mohamed, A. H., et al. (2001). Parvalbumin overexpression alters immune-mediated increases in intracellular calcium, and delays disease onset in a transgenic model of familial amyotrophic lateral sclerosis. *J. Neurochem.* 79, 499–509. doi: 10.1046/j.1471-4159.2001.00582.x

Belzil, V. V., Valdmanis, P. N., Dion, P. A., Daoud, H., Kabashi, E., Noreau, A., et al. (2009). Mutations in FUS cause FALS and SALS in French and French Canadian populations. *Neurology* 73, 1176–1179. doi: 10.1212/WNL.0b013e3181bbfeef

Benkler, C., O'Neil, A. L., Slepian, S., Qian, F., Weinreb, P. H., and Rubin, L. L. (2018). Aggregated SOD1 causes selective death of cultured human motor neurons. *Sci. Rep.* 8:16393. doi: 10.1038/s41598-018-34759-z

Bensimon, G., Lacomblez, L., and Meininger, V. (1994). A controlled trial of riluzole in amyotrophic lateral sclerosis. ALS/Riluzole study group. *N. Engl. J. Med.* 330, 585–591. doi: 10.1056/NEJM199403033300901

Ben-Zvi, A., Manor, O., Schachner, M., Yaron, A., Tessier-Lavigne, M., and Behar, O. (2008). The Semaphorin receptor PlexinA3 mediates neuronal apoptosis during dorsal root ganglia development. *J. Neurosci.* 28, 12427–12432. doi: 10.1523/JNEUROSCI.3573-08.2008

Bernard-Marissal, N., Moumen, A., Sunyach, C., Pellegrino, C., Dudley, K., Henderson, C. E., et al. (2012). Reduced calreticulin levels link endoplasmic reticulum stress and Fas-triggered cell death in motoneurons vulnerable to ALS. *J. Neurosci.* 32, 4901–4912. doi: 10.1523/JNEUROSCI.5431-11.2012

Bessou, P., Emonet-Dénand, F., and Laporte, Y. (1965). Motor fibres innervating extrafusal and intrafusal muscle fibres in the cat. *J. Physiol.* 180, 649–672. doi: 10.1113/jphysiol.1965.sp007722

Bhumbra, G. S., and Beato, M. (2018). Recurrent excitation between motoneurones propagates across segments and is purely glutamatergic. *PLoS Biol.* 16:e2003586. doi: 10.1371/journal.pbio.2003586

Bilsland, L. G., Sahai, E., Kelly, G., Golding, M., Greensmith, L., and Schiavo, G. (2010). Deficits in axonal transport precede ALS symptoms in vivo. *Proc. Natl. Acad. Sci. U.S.A.* 107, 20523–20528. doi: 10.1073/pnas.1006869107

Birger, A., Ottolenghi, M., Perez, L., Reubinoff, B., and Behar, O. (2018). ALS-related human cortical and motor neurons survival is differentially affected by Sema3A. *Cell Death Dis.* 9:256. doi: 10.1038/s41419-018-0294-6

Blair, I. P., Williams, K. L., Warraich, S. T., Durnall, J. C., Thoeng, A. D., Manavis, J., et al. (2009). FUS mutations in amyotrophic lateral sclerosis: clinical, pathological, neurophysiological and genetic analysis. *J. Neurol. Neurosurg. Psychiatry* 81, 639–645. doi: 10.1136/jnnp.2009.194399

Boehringer, A., Garcia-Mansfield, K., Singh, G., Bakkar, N., Pirrotte, P., and Bowser, R. (2017). ALS associated mutations in matrin 3 alter protein-protein interactions and impede mRNA nuclear export. *Sci. Rep.* 7:14529. doi: 10.1038/s41598-017-14924-6

Bogdanov, M., Brown, R. H., Matson, W., Smart, R., Hayden, D., O'Donnell, H., et al. (2000). Increased oxidative damage to DNA in ALS patients. *Free Radic. Biol. Med.* 29, 652–658.

Bogdanov, M. B., Ramos, L. E., Xu, Z., and Beal, M. F. (1998). Elevated "hydroxyl radical" generation in vivo in an animal model of amyotrophic lateral sclerosis. *J. Neurochem.* 71, 1321–1324. doi: 10.1046/j.1471-4159.1998.71031321.x

Boillée, S., Vande Velde, C., and Cleveland, D. W. (2006a). ALS: a disease of motor neurons and their nonneuronal neighbors. *Neuron* 52, 39–59. doi: 10.1016/j.neuron.2006.09.018

Boillée, S., Yamanaka, K., Lobsiger, C. S., Copeland, N. G., Jenkins, N. A., Kassiotis, G., et al. (2006b). Onset and progression in inherited ALS determined by motor neurons and microglia. *Science* 312, 1389–1392. doi: 10.1126/science.1123511

Bories, C., Amendola, J., Lamotte d'Incamps, B., and Durand, J. (2007). Early electrophysiological abnormalities in lumbar motoneurons in a transgenic mouse model of amyotrophic lateral sclerosis. *Eur. J. Neurosci.* 25, 451–459. doi: 10.1111/j.1460-9568.2007.05306.x

Borroni, B., Archetti, S., Del Bo, R., Papetti, A., Buratti, E., Bonvicini, C., et al. (2010). TARDBP mutations in frontotemporal lobar degeneration: frequency, clinical features, and disease course. *Rejuven. Res* 13, 509–517. doi: 10.1089/rej.2010.1017

Borthwick, G. M., Johnson, M. A., Ince, P. G., Shaw, P. J., and Turnbull, D. M. (1999). Mitochondrial enzyme activity in amyotrophic lateral sclerosis: implications for the role of mitochondria in neuronal cell death. *Ann. Neurol.* 46, 787–790. doi: 10.1002/1531-8249(199911)46:5<787::aid-ana17>3.0.co;2-8

Bosco, D. A., Morfini, G., Karabacak, N. M., Song, Y., Gros-Louis, F., Pasinelli, P., et al. (2010). Wild-type and mutant SOD1 share an aberrant conformation and a common pathogenic pathway in ALS. *Nat. Neurosci.* 13, 1396–1403. doi: 10.1038/nn.2660

Boyce, M., Bryant, K. F., Jousse, C., Long, K., Harding, H. P., Scheuner, D., et al. (2005). A selective inhibitor of eIF2alpha dephosphorylation protects cells from ER stress. *Science* 307, 935–939. doi: 10.1126/science.1101902

Braak, H., Brettschneider, J., Ludolph, A. C., Lee, V. M., Trojanowski, J. Q., and Del Tredici, K. (2013). Amyotrophic lateral sclerosis–a model of corticofugal axonal spread. *Nat. Rev. Neurol.* 9, 708–714. doi: 10.1038/nrneurol.2013.221

Bradshaw, W. J., Rehman, S., Pham, T. T. K., Thiyagarajan, N., Lee, R. L., Subramanian, V., et al. (2017). Structural insights into human angiogenin variants implicated in Parkinson's disease and amyotrophic lateral sclerosis. *Sci. Rep.* 7:41996. doi: 10.1038/srep41996

Brecht, M., Krauss, A., Muhammad, S., Sinai-Esfahani, L., Bellanca, S., and Margrie, T. W. (2004). Organization of rat vibrissa motor cortex and adjacent areas according to cytoarchitectonics, microstimulation, and intracellular stimulation of identified cells. *J. Comp. Neurol.* 479, 360–373. doi: 10.1002/cne.20306

Brenner, D., Müller, K., Wieland, T., Weydt, P., Böhm, S., Lulé, D., et al. (2016). NEK1 mutations in familial amyotrophic lateral sclerosis. *Brain* 139:e28. doi: 10.1093/brain/aww033

Brettschneider, J., Del Tredici, K., Toledo, J. B., Robinson, J. L., Irwin, D. J., Grossman, M., et al. (2013). Stages of pTDP-43 pathology in amyotrophic lateral sclerosis. *Ann. Neurol.* 74, 20–38. doi: 10.1002/ana.23937

Brockington, A., Ning, K., Heath, P. R., Wood, E., Kirby, J., Fusi, N., et al. (2013). Unravelling the enigma of selective vulnerability in neurodegeneration: motor neurons resistant to degeneration in ALS show distinct gene expression characteristics and decreased susceptibility to excitotoxicity. *Acta Neuropathol.* 125, 95–109. doi: 10.1007/s00401-012-1058-5

Brown, M. R., Sullivan, P. G., and Geddes, J. W. (2006). Synaptic mitochondria are more susceptible to ca2+overload than nonsynaptic mitochondria. *J. Biol. Chem.* 281, 11658–11668. doi: 10.1074/jbc.M510303200

Bruijn, L. I., Becher, M. W., Lee, M. K., Anderson, K. L., Jenkins, N. A., Copeland, N. G., et al. (1997). ALS-linked SOD1 mutant G85R mediates damage to astrocytes and promotes rapidly progressive disease with SOD1-containing inclusions. *Neuron* 18, 327–338. doi: 10.1016/s0896-6273(00)80272-x

Brundin, P., Melki, R., and Kopito, R. (2010). Prion-like transmission of protein aggregates in neurodegenerative diseases. *Nat. Rev. Mol. Cell Biol.* 11, 301–307. doi: 10.1038/nrm2873

Bryan, R. N., Trevino, D. L., and Willis, W. D. (1972). Evidence for a common location of alpha and gamma motoneurons. *Brain Res.* 38, 193–196. doi: 10.1016/0006-8993(72)90602-6

Burk, K., and Pasterkamp, R. J. (2019). Disrupted neuronal trafficking in amyotrophic lateral sclerosis. *Acta Neuropathol.* doi: 10.1007/s00401-019-01964-7 [Epub ahead of print].

Burke, R. E., Dum, R. P., Fleshman, J. W., Glenn, L. L., Lev-Tov, A., O'Donovan, M. J., et al. (1982). A HRP study of the relation between cell size and motor unit type in cat ankle extensor motoneurons. *J. Comp. Neurol.* 209, 17–28. doi: 10.1002/cne.902090103

Burke, R. E., Levine, D. N., Tsairis, P., and Zajac, F. E. (1973). Physiological types and histochemical profiles in motor units of the cat gastrocnemius. *J. Physiol.* 234, 723–748. doi: 10.1113/jphysiol.1973.sp010369

Burke, R. E., Levine, D. N., and Zajac, F. E. (1971). Mammalian motor units: physiological-histochemical correlation in three types in cat gastrocnemius. *Science* 174, 709–712. doi: 10.1126/science.174.4010.709

Burke, R. E., Strick, P. L., Kanda, K., Kim, C. C., and Walmsley, B. (1977). Anatomy of medial gastrocnemius and soleus motor nuclei in cat spinal cord. *J. Neurophysiol.* 40, 667–680. doi: 10.1152/jn.1977.40.3.667

Burke, R. E., and Tsairis, P. (1973). Anatomy and innervation ratios in motor units of cat gastrocnemius. *J. Physiol.* 234, 749–765. doi: 10.1113/jphysiol.1973.sp010370

Burrell, J. R., Halliday, G. M., Kril, J. J., Ittner, L. M., Götz, J., Kiernan, M. C., et al. (2016). The frontotemporal dementia-motor neuron disease continuum. *Lancet* 388, 919–931. doi: 10.1016/S0140-6736(16)00737-6

Butin-Israeli, V., Adam, S. A., Jain, N., Otte, G. L., Neems, D., Wiesmüller, L., et al. (2015). Role of lamin B1 in chromatin instability. *Mol. Cell Biol.* 35, 884–898. doi: 10.1128/MCB.01145-14

Caligari, M., Godi, M., Guglielmetti, S., Franchignoni, F., and Nardone, A. (2013). Eye tracking communication devices in amyotrophic lateral sclerosis: impact on disability and quality of life. *Amyotroph. Lateral Scler. Frontotemporal Degen.* 14, 546–552. doi: 10.3109/21678421.2013.803576

Carrí, M. T., Ferri, A., Cozzolino, M., Calabrese, L., and Rotilio, G. (2003). Neurodegeneration in amyotrophic lateral sclerosis: the role of oxidative stress and altered homeostasis of metals. *Brain Res. Bull.* 61, 365–374. doi: 10.1016/s0361-9230(03)00179-5

Carriedo, S. G., Yin, H. Z., and Weiss, J. H. (1996). Motor neurons are selectively vulnerable to AMPA/Kainate receptor-mediated injury in vitro. *J. Neurosci.* 16, 4069–4079. doi: 10.1523/JNEUROSCI.16-13-04069.1996

Chakkalakal, J. V., Nishimune, H., Ruas, J. L., Spiegelman, B. M., and Sanes, J. R. (2010). Retrograde influence of muscle fibers on their innervation revealed by a novel marker for slow motoneurons. *Development* 137, 3489–3499. doi: 10.1242/dev.053348

Chang, Q., and Martin, L. J. (2009). Glycinergic innervation of motoneurons is deficient in amyotrophic lateral sclerosis mice: a quantitative confocal analysis. *Am. J. Pathol.* 174, 574–585. doi: 10.2353/ajpath.2009.080557

Charcot, J.-M. (1874). De la sclérose latérale amyotrophique. *Prog. Med.* 2, 325–327, 341–342, 453–455.

Chard, P. S., Bleakman, D., Christakos, S., Fullmer, C. S., and Miller, R. J. (1993). Calcium buffering properties of calbindin D28k and parvalbumin in rat sensory neurones. *J. Physiol.* 472, 341–357. doi: 10.1113/jphysiol.1993.sp019950

Chen, D., Wang, Y., and Chin, E. R. (2015). Activation of the endoplasmic reticulum stress response in skeletal muscle of G93A*SOD1 amyotrophic lateral sclerosis mice. *Front. Cell Neurosci.* 9:170. doi: 10.3389/fncel.2015.00170

Chen, X.-J., Levedakou, E. N., Millen, K. J., Wollmann, R. L., Soliven, B., and Popko, B. (2007). Proprioceptive sensory neuropathy in mice with a mutation in the cytoplasmic dynein heavy chain 1 gene. *J. Neurosci.* 27, 14515–14524. doi: 10.1523/JNEUROSCI.4338-07.2007

Chiò, A., Restagno, G., Brunetti, M., Ossola, I., Calvo, A., Mora, G., et al. (2009). Two Italian kindreds with familial amyotrophic lateral sclerosis due to FUS mutation. *Neurobiol. Aging* 30, 1272–1275. doi: 10.1016/j.neurobiolaging.2009.05.001

Chiu, I. M., Morimoto, E. T. A., Goodarzi, H., Liao, J. T., O'Keeffe, S., Phatnani, H. P., et al. (2013). A neurodegeneration-specific gene expression signature and immune profile of acutely isolated microglia from an ALS mouse model. *Cell Rep.* 4, 385–401. doi: 10.1016/j.celrep.2013.06.018

Chou, C.-C., Zhang, Y., Umoh, M. E., Vaughan, S. W., Lorenzini, I., Liu, F., et al. (2018). TDP-43 pathology disrupts nuclear pore complexes and nucleocytoplasmic transport in ALS/FTD. *Nat. Neurosci.* 21, 228–239. doi: 10.1038/s41593-017-0047-3

Chou, S. M., and Norris, F. H. (1993). Amyotrophic lateral sclerosis: lower motor neuron disease spreading to upper motor neurons. *Muscle Nerve* 16, 864–869. doi: 10.1002/mus.880160810

Cirulli, E. T., Lasseigne, B. N., Petrovski, S., Sapp, P. C., Dion, P. A., Leblond, C. S., et al. (2015). Exome sequencing in amyotrophic lateral sclerosis identifies risk genes and pathways. *Science* 347, 1436–1441. doi: 10.1126/science.aaa3650

Clark, B. C., and Manini, T. M. (2012). What is dynapenia? *Nutrition* 28, 495–503. doi: 10.1016/j.nut.2011.12.002

Clarke, L. E., Liddelow, S. A., Chakraborty, C., Münch, A. E., Heiman, M., and Barres, B. A. (2018). Normal aging induces A1-like astrocyte reactivity. *PNAS* 115, E1896–E1905. doi: 10.1073/pnas.1800165115

Comley, L., Allodi, I., Nichterwitz, S., Nizzardo, M., Simone, C., Corti, S., et al. (2015). Motor neurons with differential vulnerability to degeneration show distinct protein signatures in health and ALS. *Neuroscience* 291, 216–229. doi: 10.1016/j.neuroscience.2015.02.013

Comley, L. H., Nijssen, J., Frost-Nylen, J., and Hedlund, E. (2016). Cross-disease comparison of amyotrophic lateral sclerosis and spinal muscular atrophy reveals conservation of selective vulnerability but differential neuromuscular junction pathology. *J. Comp. Neurol.* 524, 1424–1442. doi: 10.1002/cne.23917

Corbo, M., and Hays, A. P. (1992). Peripherin and neurofilament protein coexist in spinal spheroids of motor neuron disease. *J. Neuropathol. Exp. Neurol.* 51, 531–537. doi: 10.1097/00005072-199209000-00008

Cullheim, S., Fleshman, J. W., Glenn, L. L., and Burke, R. E. (1987). Membrane area and dendritic structure in type-identified triceps surae alpha motoneurons. *J. Comp. Neurol.* 255, 68–81. doi: 10.1002/cne.902550106

Curtis, D. R., and Malik, R. (1985). A neurophysiological analysis of the effect of kainic acid on nerve fibres and terminals in the cat spinal cord. *J. Physiol.* 368, 99–108. doi: 10.1113/jphysiol.1985.sp015848

Dafinca, R., Scaber, J., Ababneh, N., Lalic, T., Weir, G., Christian, H., et al. (2016). C9orf72 hexanucleotide expansions are associated with altered endoplasmic reticulum calcium homeostasis and stress granule formation in induced pluripotent stem cell-derived neurons from patients with amyotrophic lateral sclerosis and frontotemporal dementia. *Stem Cells* 34, 2063–2078. doi: 10.1002/stem.2388

Das, M. M., and Svendsen, C. N. (2015). Astrocytes show reduced support of motor neurons with aging that is accelerated in a rodent model of ALS. *Neurobiol. Aging* 36, 1130–1139. doi: 10.1016/j.neurobiolaging.2014.09.020

de Carvalho, M., and Swash, M. (2017). Physiology of the fasciculation potentials in amyotrophic lateral sclerosis: which motor units fasciculate? *J. Physiol. Sci.* 67, 569–576. doi: 10.1007/s12576-016-0484-x

De La Cruz, R. R., Escudero, M., and Delgado-García, J. M. (1989). Behaviour of medial rectus motoneurons in the alert cat. *Eur. J. Neurosci.* 1, 288–295. doi: 10.1111/j.1460-9568.1989.tb00796.x

De Vos, K. J., Chapman, A. L., Tennant, M. E., Manser, C., Tudor, E. L., Lau, K.-F., et al. (2007). Familial amyotrophic lateral sclerosis-linked SOD1 mutants perturb fast axonal transport to reduce axonal mitochondria content. *Hum. Mol. Genet.* 16, 2720–2728. doi: 10.1093/hmg/ddm226

De Vos, K. J., and Hafezparast, M. (2017). Neurobiology of axonal transport defects in motor neuron diseases: opportunities for translational research? *Neurobiol. Dis.* 105, 283–299. doi: 10.1016/j.nbd.2017.02.004

De Winter, F., Vo, T., Stam, F. J., Wisman, L. A. B., Bär, P. R., Niclou, S. P., et al. (2006). The expression of the chemorepellent Semaphorin 3A is selectively induced in terminal Schwann cells of a subset of neuromuscular synapses that display limited anatomical plasticity and enhanced vulnerability in motor neuron disease. *Mol. Cell. Neurosci.* 32, 102–117. doi: 10.1016/j.mcn.2006.03.002

Deardorff, A. S., Romer, S. H., Deng, Z., Bullinger, K. L., Nardelli, P., Cope, T. C., et al. (2013). Expression of postsynaptic Ca2+-activated K+ (SK) channels at C-bouton synapses in mammalian lumbar α-motoneurons. *J. Physiol.* 591, 875–897. doi: 10.1113/jphysiol.2012.240879

DeJesus-Hernandez, M., Desaro, P., Johnston, A., Ross, O. A., Wszolek, Z. K., Ertekin-Taner, N., et al. (2011a). Novel p.I*le*151Val mutation in VCP in a patient of African American descent with sporadic ALS. *Neurology* 77, 1102–1103. doi: 10.1212/WNL.0b013e31822e563c

DeJesus-Hernandez, M., Mackenzie, I. R., Boeve, B. F., Boxer, A. L., Baker, M., Rutherford, N. J., et al. (2011b). Expanded GGGGCC hexanucleotide repeat in noncoding region of C9ORF72 causes chromosome 9p-Linked FTD and ALS. *Neuron* 72, 245–256. doi: 10.1016/j.neuron.2011.09.011

Delmonico, M. J., Harris, T. B., Visser, M., Park, S. W., Conroy, M. B., Velasquez-Mieyer, P., et al. (2009). Longitudinal study of muscle strength, quality, and adipose tissue infiltration. *Am. J. Clin. Nutr.* 90, 1579–1585. doi: 10.3945/ajcn.2009.28047

Deng, H.-X., Chen, W., Hong, S.-T., Boycott, K. M., Gorrie, G. H., Siddique, N., et al. (2011). Mutations in UBQLN2 cause dominant X-linked juvenile and adult onset ALS and ALS/dementia. *Nature* 477, 211–215. doi: 10.1038/nature10353

Deng, H.-X., Zhai, H., Bigio, E. H., Yan, J., Fecto, F., Ajroud, K., et al. (2010). FUS-immunoreactive inclusions are a common feature in sporadic and non-SOD1 familial amyotrophic lateral sclerosis. *Ann. Neurol.* 67, 739–748. doi: 10.1002/ana.22051

Deschenes, M. R. (2011). Motor unit and neuromuscular junction remodeling with aging. *Curr. Aging Sci.* 4, 209–220. doi: 10.2174/1874609811104030209

Deshaies, J.-E., Shkreta, L., Moszczynski, A. J., Sidibé, H., Semmler, S., Fouillen, A., et al. (2018). TDP-43 regulates the alternative splicing of hnRNP A1 to yield an aggregation-prone variant in amyotrophic lateral sclerosis. *Brain* 141, 1320–1333. doi: 10.1093/brain/awy062

Devenney, E., Hornberger, M., Irish, M., Mioshi, E., Burrell, J., Tan, R., et al. (2014). Frontotemporal dementia associated with the C9ORF72 mutation: a unique clinical profile. *JAMA Neurol.* 71, 331–339. doi: 10.1001/jamaneurol.2013.6002

Devlin, A.-C., Burr, K., Borooah, S., Foster, J. D., Cleary, E. M., Geti, I., et al. (2015). Human iPSC-derived motoneurons harbouring TARDBP or C9ORF72 ALS mutations are dysfunctional despite maintaining viability. *Nat. Commun.* 6:5999. doi: 10.1038/ncomms6999

Dhaliwal, G. K., and Grewal, R. P. (2000). Mitochondrial DNA deletion mutation levels are elevated in ALS brains. *Neuroreport* 11, 2507–2509. doi: 10.1097/00001756-200008030-00032

Dickey, A. S., Amit, Y., and Hatsopoulos, N. G. (2013). Heterogeneous neural coding of corrective movements in motor cortex. *Front. Neural Circ.* 7:51. doi: 10.3389/fncir.2013.00051

Diekstra, F. P., van Vught, P. W. J., van Rheenen, W., Koppers, M., Pasterkamp, R. J., van Es, M. A., et al. (2012). UNC13A is a modifier of survival in amyotrophic lateral sclerosis. *Neurobiol. Aging* 33, 630.e3–630.e8. doi: 10.1016/j.neurobiolaging.2011.10.029

Dillen, L., Van Langenhove, T., Engelborghs, S., Vandenbulcke, M., Sarafov, S., Tournev, I., et al. (2013). Explorative genetic study of UBQLN2 and PFN1 in an extended flanders-belgian cohort of frontotemporal lobar degeneration patients. *Neurobiol. Aging* 34, 1711.e1–1711.e5. doi: 10.1016/j.neurobiolaging.2012.12.007

Ding, X., Ma, M., Teng, J., Teng, R. K. F., Zhou, S., Yin, J., et al. (2015). Exposure to ALS-FTD-CSF generates TDP-43 aggregates in glioblastoma cells through exosomes and TNTs-like structure. *Oncotarget* 6, 24178–24191. doi: 10.18632/oncotarget.4680

Doble, A. (1996). The pharmacology and mechanism of action of riluzole. *Neurology* 47, S233–S241.

Dols-Icardo, O., Nebot, I., Gorostidi, A., Ortega-Cubero, S., Hernández, I., Rojas-García, R., et al. (2015). Analysis of the CHCHD10 gene in patients with

frontotemporal dementia and amyotrophic lateral sclerosis from Spain. *Brain* 138:e400. doi: 10.1093/brain/awv175

Donaghy, C., Thurtell, M. J., Pioro, E. P., Gibson, J. M., and Leigh, R. J. (2011). Eye movements in amyotrophic lateral sclerosis and its mimics: a review with illustrative cases. *J. Neurol. Neurosurg. Psychiatry* 82, 110–116. doi: 10.1136/jnnp.2010.212407

Dukkipati, S. S., Garrett, T. L., and Elbasiouny, S. M. (2018). The vulnerability of spinal motoneurons and soma size plasticity in a mouse model of amyotrophic lateral sclerosis. *J. Physiol.* 596, 1723–1745. doi: 10.1113/JP275498

Durand, J. (1989). Intracellular study of oculomotor neurons in the rat. *Neuroscience* 30, 639–649. doi: 10.1016/0306-4522(89)90157-7

Ebbesen, C. L., and Brecht, M. (2017). Motor cortex—to act or not to act? *Nat. Rev. Neurosci.* 18, 694–705. doi: 10.1038/nrn.2017.119

Ebstein, S. Y., Yagudayeva, I., and Shneider, N. A. (2019). Mutant TDP-43 causes early-stage dose-dependent motor neuron degeneration in a TARDBP knockin mouse model of ALS. *Cell Reports* 26, 364.e4–373.e4. doi: 10.1016/j.celrep.2018.12.045

Eccles, J. C., Eccles, R. M., Iggo, A., and Lundberg, A. (1960). Electrophysiological studies on gamma motoneurones. *Acta Physiol. Scand.* 50, 32–40. doi: 10.1111/j.1748-1716.1960.tb02070.x

Eccles, J. C., Eccles, R. M., and Lundberg, A. (1957). Durations of after-hyperpolarization of motoneurones supplying fast and slow muscles. *Nature* 179, 866–868. doi: 10.1038/179866b0

Edwards, I. J., Bruce, G., Lawrenson, C., Howe, L., Clapcote, S. J., Deuchars, S. A., et al. (2013). Na+/K+ ATPase α1 and α3 isoforms are differentially expressed in α- and γ-motoneurons. *J. Neurosci.* 33, 9913–9919. doi: 10.1523/JNEUROSCI.5584-12.2013

Eisen, A., Braak, H., Tredici, K. D., Lemon, R., Ludolph, A. C., and Kiernan, M. C. (2017). Cortical influences drive amyotrophic lateral sclerosis. *J. Neurol. Neurosurg. Psychiatry* 88, 917–924. doi: 10.1136/jnnp-2017-315573

Eisen, A., Turner, M. R., and Lemon, R. (2014). Tools and talk: an evolutionary perspective on the functional deficits associated with amyotrophic lateral sclerosis. *Muscle Nerve* 49, 469–477. doi: 10.1002/mus.24132

Elden, A. C., Kim, H.-J., Hart, M. P., Chen-Plotkin, A. S., Johnson, B. S., Fang, X., et al. (2010). Ataxin-2 intermediate-length polyglutamine expansions are associated with increased risk for ALS. *Nature* 466:1069. doi: 10.1038/nature09320

Endo, F., Komine, O., Fujimori-Tonou, N., Katsuno, M., Jin, S., Watanabe, S., et al. (2015). Astrocyte-derived TGF-β1 accelerates disease progression in ALS mice by interfering with the neuroprotective functions of microglia and T cells. *Cell Rep.* 11, 592–604. doi: 10.1016/j.celrep.2015.03.053

Enjin, A., Leão, K. E., Mikulovic, S., Le Merre, P., Tourtellotte, W. G., and Kullander, K. (2012). Sensorimotor function is modulated by the serotonin receptor 1d, a novel marker for gamma motor neurons. *Mol. Cell. Neurosci.* 49, 322–332. doi: 10.1016/j.mcn.2012.01.003

Enjin, A., Rabe, N., Nakanishi, S. T., Vallstedt, A., Gezelius, H., Memic, F., et al. (2010). Identification of novel spinal cholinergic genetic subtypes disclose Chodl and Pitx2 as markers for fast motor neurons and partition cells. *J. Comp. Neurol.* 518, 2284–2304. doi: 10.1002/cne.22332

Enoka, R. M. (1995). Morphological features and activation patterns of motor units. *J. Clin. Neurophysiol.* 12, 538–559. doi: 10.1097/00004691-199511000-00002

Enoka, R. M., Christou, E. A., Hunter, S. K., Kornatz, K. W., Semmler, J. G., Taylor, A. M., et al. (2003). Mechanisms that contribute to differences in motor performance between young and old adults. *J. Electromyogr. Kinesiol.* 13, 1–12. doi: 10.1016/s1050-6411(02)00084-6

Fang, T., Jozsa, F., and Al-Chalabi, A. (2017). Nonmotor symptoms in amyotrophic lateral sclerosis: a systematic review. *Int. Rev. Neurobiol.* 134, 1409–1441. doi: 10.1016/bs.irn.2017.04.009

Fang, X., Lin, H., Wang, X., Zuo, Q., Qin, J., and Zhang, P. (2015). The NEK1 interactor, C21ORF2, is required for efficient DNA damage repair. *Acta Biochim. Biophys. Sin.* 47, 834–841. doi: 10.1093/abbs/gmv076

Farg, M. A., Konopka, A., Soo, K. Y., Ito, D., and Atkin, J. D. (2017). The DNA damage response (DDR) is induced by the C9orf72 repeat expansion in amyotrophic lateral sclerosis. *Hum. Mol. Genet.* 26, 2882–2896. doi: 10.1093/hmg/ddx170

Farg, M. A., Soo, K. Y., Walker, A. K., Pham, H., Orian, J., Horne, M. K., et al. (2012). Mutant FUS induces endoplasmic reticulum stress in amyotrophic lateral sclerosis and interacts with protein disulfide-isomerase. *Neurobiol. Aging* 33, 2855–2868. doi: 10.1016/j.neurobiolaging.2012.02.009

Farg, M. A., Sundaramoorthy, V., Sultana, J. M., Yang, S., Atkinson, R. A., Levina, V., et al. (2014). C9ORF72, implicated in amytrophic lateral sclerosis and frontotemporal dementia, regulates endosomal trafficking. *Hum. Mol. Genet.* 23, 3579–3595. doi: 10.1093/hmg/ddu068

Fecto, F., Yan, J., Vemula, S. P., Liu, E., Yang, Y., Chen, W., et al. (2011). SQSTM1 mutations in familial and sporadic amyotrophic lateral sclerosis. *Arch. Neurol.* 68, 1440–1446. doi: 10.1001/archneurol.2011.250

Feiguin, F., Godena, V. K., Romano, G., D'Ambrogio, A., Klima, R., and Baralle, F. E. (2009). Depletion of TDP-43 affects Drosophila motoneurons terminal synapsis and locomotive behavior. *FEBS Lett.* 583, 1586–1592. doi: 10.1016/j.febslet.2009.04.019

Feiler, M. S., Strobel, B., Freischmidt, A., Helferich, A. M., Kappel, J., Brewer, B. M., et al. (2015). TDP-43 is intercellularly transmitted across axon terminals. *J. Cell Biol.* 211, 897–911. doi: 10.1083/jcb.201504057

Feit, H., Silbergleit, A., Schneider, L. B., Gutierrez, J. A., Fitoussi, R.-P., Réyes, C., et al. (1998). Vocal cord and pharyngeal weakness with autosomal dominant distal myopathy: clinical description and gene localization to 5q31. *Am. J. Hum. Genet.* 63, 1732–1742. doi: 10.1086/302166

Feng, Z., and Ko, C.-P. (2008). Schwann cells promote synaptogenesis at the neuromuscular junction via transforming growth factor-β1. *J. Neurosci.* 28, 9599–9609. doi: 10.1523/JNEUROSCI.2589-08.2008

Ferrante, R. J., Browne, S. E., Shinobu, L. A., Bowling, A. C., Baik, M. J., MacGarvey, U., et al. (1997). Evidence of increased oxidative damage in both sporadic and familial amyotrophic lateral sclerosis. *J. Neurochem.* 69, 2064–2074. doi: 10.1046/j.1471-4159.1997.69052064.x

Ferri, A., Cozzolino, M., Crosio, C., Nencini, M., Casciati, A., Gralla, E. B., et al. (2006). Familial ALS-superoxide dismutases associate with mitochondria and shift their redox potentials. *Proc. Natl. Acad. Sci. U.S.A.* 103, 13860–13865. doi: 10.1073/pnas.0605814103

Ferrier, D. (1875). Experiments on the brain of monkeys.—No. I. *Proc. R. Soc. Lond.* 23, 409–430. doi: 10.1098/rspl.1874.0058

Fiatarone, M. A., and Evans, W. J. (1993). The etiology and reversibility of muscle dysfunction in the aged. *J. Gerontol.* 48, 77–83. doi: 10.1093/geronj/48.special_issue.77

Figlewicz, D. A., Krizus, A., Martinoli, M. G., Meininger, V., Dib, M., Rouleau, G. A., et al. (1994). Variants of the heavy neurofilament subunit are associated with the development of amyotrophic lateral sclerosis. *Hum. Mol. Genet.* 3, 1757–1761. doi: 10.1093/hmg/3.10.1757

Filézac de L'Etang, A., Maharjan, N., Cordeiro Braña, M., Ruegsegger, C., Rehmann, R., Goswami, A., et al. (2015). Marinesco-Sjögren syndrome protein SIL1 regulates motor neuron subtype-selective ER stress in ALS. *Nat. Neurosci.* 18, 227–238. doi: 10.1038/nn.3903

Fischer, L. R., Culver, D. G., Tennant, P., Davis, A. A., Wang, M., Castellano-Sanchez, A., et al. (2004). Amyotrophic lateral sclerosis is a distal axonopathy: evidence in mice and man. *Exp. Neurol.* 185, 232–240. doi: 10.1016/j.expneurol.2003.10.004

Fogarty, M. J. (2018). Driven to decay: Excitability and synaptic abnormalities in amyotrophic lateral sclerosis. *Brain Res. Bull.* 140, 318–333. doi: 10.1016/j.brainresbull.2018.05.023

Franco, M. C., Dennys, C. N., Estévez, F. H. R., and Estévez, A. G. (2013). "Superoxide Dismutase and Oxidative Stress in Amyotrophic Lateral Sclerosis," in *Current Advances in Amyotrophic Lateral Sclerosis*, ed. A. Estévez (London: IntechOpen).

Fratta, P., and Isaacs, A. M. (2018). The snowball effect of RNA binding protein dysfunction in amyotrophic lateral sclerosis. *Brain* 141, 1236–1238. doi: 10.1093/brain/awy091

Freischmidt, A., Wieland, T., Richter, B., Ruf, W., Schaeffer, V., Müller, K., et al. (2015). Haploinsufficiency of TBK1 causes familial ALS and fronto-temporal dementia. *Nat. Neurosci.* 18, 631–636. doi: 10.1038/nn.4000

Frey, D., Schneider, C., Xu, L., Borg, J., Spooren, W., and Caroni, P. (2000). Early and selective loss of neuromuscular synapse subtypes with low sprouting competence in motoneuron diseases. *J. Neurosci.* 20, 2534–2542. doi: 10.1523/jneurosci.20-07-02534.2000

Fried, L. P., Ferrucci, L., Darer, J., Williamson, J. D., and Anderson, G. (2004). Untangling the concepts of disability, frailty, and comorbidity: implications for improved targeting and care. *J. Gerontol. A Biol. Sci. Med. Sci.* 59, 255–263.

Friese, A., Kaltschmidt, J. A., Ladle, D. R., Sigrist, M., Jessell, T. M., and Arber, S. (2009). Gamma and alpha motor neurons distinguished by expression of transcription factor Err3. *Proc. Natl. Acad. Sci. U.S.A.* 106, 13588–13593. doi: 10.1073/pnas.0906809106

Fryer, H. J., Knox, R. J., Strittmatter, S. M., and Kalb, R. G. (1999). Excitotoxic death of a subset of embryonic rat motor neurons in vitro. *J. Neurochem.* 72, 500–513. doi: 10.1046/j.1471-4159.1999.0720500.x

Fu, H., Hardy, J., and Duff, K. E. (2018). Selective vulnerability in neurodegenerative diseases. *Nat. Neurosci.* 21:1350. doi: 10.1038/s41593-018-0221-2

Fuchs, A. F., Scudder, C. A., and Kaneko, C. R. (1988). Discharge patterns and recruitment order of identified motoneurons and internuclear neurons in the monkey abducens nucleus. *J. Neurophysiol.* 60, 1874–1895. doi: 10.1152/jn.1988.60.6.1874

Fujimura-Kiyono, C., Kimura, F., Ishida, S., Nakajima, H., Hosokawa, T., Sugino, M., et al. (2011). Onset and spreading patterns of lower motor neuron involvements predict survival in sporadic amyotrophic lateral sclerosis. *J. Neurol. Neurosurg. Psychiatry* 82, 1244–1249. doi: 10.1136/jnnp-2011-300141

Fujita, K., Yamauchi, M., Shibayama, K., Ando, M., Honda, M., and Nagata, Y. (1996). Decreased cytochrome c oxidase activity but unchanged superoxide dismutase and glutathione peroxidase activities in the spinal cords of patients with amyotrophic lateral sclerosis. *J. Neurosci. Res.* 45, 276–281. doi: 10.1002/(sici)1097-4547(19960801)45:3<276::aid-jnr9>3.0.co;2-a

Fujita, S., and Kitamura, T. (1975). Origin of brain macrophages and the nature of the so-called microglia. *Acta Neuropathol. Suppl.* 6, 291–296. doi: 10.1007/978-3-662-08456-4_51

García, M. L., Fernández, A., and Solas, M. T. (2013). Mitochondria, motor neurons and aging. *J. Neurol. Sci.* 330, 18–26. doi: 10.1016/j.jns.2013.03.019

Gardiner, P. F. (1993). Physiological properties of motoneurons innervating different muscle unit types in rat gastrocnemius. *J. Neurophysiol.* 69, 1160–1170. doi: 10.1152/jn.1993.69.4.1160

Gargiulo-Monachelli, G. M., Janota, F., Bettini, M., Shoesmith, C. L., Strong, M. J., and Sica, R. E. P. (2012). Regional spread pattern predicts survival in patients with sporadic amyotrophic lateral sclerosis. *Eur. J. Neurol.* 19, 834–841. doi: 10.1111/j.1468-1331.2011.03616.x

Georgopoulos, A. P., Kalaska, J. F., Caminiti, R., and Massey, J. T. (1982). On the relations between the direction of two-dimensional arm movements and cell discharge in primate motor cortex. *J. Neurosci.* 2, 1527–1537. doi: 10.1523/jneurosci.02-11-01527.1982

Geser, F., Brandmeir, N. J., Kwong, L. K., Martinez-Lage, M., Elman, L., McCluskey, L., et al. (2008). Evidence of multisystem disorder in whole-brain map of pathological TDP-43 in amyotrophic lateral sclerosis. *Arch. Neurol.* 65, 636–641. doi: 10.1001/archneur.65.5.636

Gioanni, Y., and Lamarche, M. (1985). A reappraisal of rat motor cortex organization by intracortical microstimulation. *Brain Res.* 344, 49–61. doi: 10.1016/0006-8993(85)91188-6

Gitcho, M. A., Baloh, R. H., Chakraverty, S., Mayo, K., Norton, J. B., Levitch, D., et al. (2008). TDP-43 A315T mutation in familial motor neuron disease. *Ann. Neurol.* 63, 535–538. doi: 10.1002/ana.21344

Grad, L. I., Guest, W. C., Yanai, A., Pokrishevsky, E., O'Neill, M. A., Gibbs, E., et al. (2011). Intermolecular transmission of superoxide dismutase 1 misfolding in living cells. *PNAS* 108, 16398–16403. doi: 10.1073/pnas.1102645108

Grad, L. I., Yerbury, J. J., Turner, B. J., Guest, W. C., Pokrishevsky, E., O'Neill, M. A., et al. (2014). Intercellular propagated misfolding of wild-type Cu/Zn superoxide dismutase occurs via exosome-dependent and -independent mechanisms. *Proc. Natl. Acad. Sci. U.S.A.* 111, 3620–3625. doi: 10.1073/pnas.1312245111

Gravel, M., Béland, L.-C., Soucy, G., Abdelhamid, E., Rahimian, R., Gravel, C., et al. (2016). IL-10 controls early microglial phenotypes and disease onset in als caused by misfolded superoxide dismutase 1. *J. Neurosci.* 36, 1031–1048. doi: 10.1523/JNEUROSCI.0854-15.2016

Greenway, M. J., Andersen, P. M., Russ, C., Ennis, S., Cashman, S., Donaghy, C., et al. (2006). ANG mutations segregate with familial and "sporadic" amyotrophic lateral sclerosis. *Nat. Genet.* 38, 411–413. doi: 10.1038/ng1742

Guéritaud, J. P., Horcholle-Bossavit, G., Jami, L., Thiesson, D., and Tyc-Dumont, S. (1985). Resistance to glycogen depletion of motor units in the cat rectus lateralis muscle. *Exp. Brain Res.* 60, 542–550.

Gulino, R., Forte, S., Parenti, R., and Gulisano, M. (2015). TDP-43 as a modulator of synaptic plasticity in a mouse model of spinal motoneuron degeneration. *CNS Neurol. Disord. Drug Targets* 14, 55–60. doi: 10.2174/1871527314666150116115414

Gurney, M. E. (1997). The use of transgenic mouse models of amyotrophic lateral sclerosis in preclinical drug studies. *J. Neurol. Sci.* 152(Suppl. 1), S67–S73.

Gurney, M. E., Pu, H., Chiu, A. Y., Canto, M. D., Polchow, C. Y., Alexander, D. D., et al. (1994). Motor neuron degeneration in mice that express a human Cu,Zn superoxide dismutase mutation. *Science* 264, 1772–1775. doi: 10.1126/science.8209258

Gustafsson, B., and Lipski, J. (1979). Do γ-motoneurones lack a long-lasting afterhyperpolarization? *Brain Res.* 172, 349–353. doi: 10.1016/0006-8993(79)90545-6

Hadzipasic, M., Tahvildari, B., Nagy, M., Bian, M., Horwich, A. L., and McCormick, D. A. (2014). Selective degeneration of a physiological subtype of spinal motor neuron in mice with SOD1-linked ALS. *Proc. Natl. Acad. Sci. U.S.A.* 111, 16883–16888. doi: 10.1073/pnas.1419497111

Haenggeli, C., Julien, J.-P., Mosley, R. L., Perez, N., Dhar, A., Gendelman, H. E., et al. (2007). Therapeutic immunization with a glatiramer acetate derivative does not alter survival in G93A and G37R SOD1 mouse models of familial ALS. *Neurobiol. Dis.* 26, 146–152. doi: 10.1016/j.nbd.2006.12.013

Hall, C. E., Yao, Z., Choi, M., Tyzack, G. E., Serio, A., Luisier, R., et al. (2017). Progressive motor neuron pathology and the role of astrocytes in a human stem cell model of vcp-related ALS. *Cell Rep.* 19, 1739–1749. doi: 10.1016/j.celrep.2017.05.024

Hall, E. D., Andrus, P. K., Oostveen, J. A., Fleck, T. J., and Gurney, M. E. (1998). Relationship of oxygen radical-induced lipid peroxidative damage to disease onset and progression in a transgenic model of familial ALS. *J. Neurosci. Res.* 53, 66–77. doi: 10.1002/(sici)1097-4547(19980701)53:1<66::aid-jnr7>3.3.co;2-k

Harms, M. B., Cady, J., Zaidman, C., Cooper, P., Bali, T., Allred, P., et al. (2013). Lack of C9ORF72 coding mutations supports a gain of function for repeat expansions in amyotrophic lateral sclerosis. *Neurobiol. Aging* 34, 2234.e13–2234.e19. doi: 10.1016/j.neurobiolaging.2013.03.006

Harris, J. J., Jolivet, R., and Attwell, D. (2012). Synaptic energy use and supply. *Neuron* 75, 762–777. doi: 10.1016/j.neuron.2012.08.019

Hashizume, K., Kanda, K., and Burke, R. E. (1988). Medial gastrocnemius motor nucleus in the rat: age-related changes in the number and size of motoneurons. *J. Comp. Neurol.* 269, 425–430. doi: 10.1002/cne.902690309

He, C. Z., and Hays, A. P. (2004). Expression of peripherin in ubiquinated inclusions of amyotrophic lateral sclerosis. *J. Neurol. Sci.* 217, 47–54. doi: 10.1016/j.jns.2003.08.016

Hedlund, E., Karlsson, M., Osborn, T., Ludwig, W., and Isacson, O. (2010). Global gene expression profiling of somatic motor neuron populations with different vulnerability identify molecules and pathways of degeneration and protection. *Brain* 133, 2313–2330. doi: 10.1093/brain/awq167

Hegedus, J., Putman, C. T., and Gordon, T. (2007). Time course of preferential motor unit loss in the SOD1 G93A mouse model of amyotrophic lateral sclerosis. *Neurobiol. Dis.* 28, 154–164. doi: 10.1016/j.nbd.2007.07.003

Henneman, E. (1957). Relation between size of neurons and their susceptibility to discharge. *Science* 126, 1345–1347. doi: 10.1126/science.126.3287.1345

Hickey, W. F., and Kimura, H. (1988). Perivascular microglial cells of the CNS are bone marrow-derived and present antigen in vivo. *Science* 239, 290–292. doi: 10.1126/science.3276004

Hideyama, T., Yamashita, T., Aizawa, H., Tsuji, S., Kakita, A., Takahashi, H., et al. (2012). Profound downregulation of the RNA editing enzyme ADAR2 in ALS spinal motor neurons. *Neurobiol. Dis.* 45, 1121–1128. doi: 10.1016/j.nbd.2011.12.033

Hideyama, T., Yamashita, T., Suzuki, T., Tsuji, S., Higuchi, M., Seeburg, P. H., et al. (2010). Induced loss of ADAR2 engenders slow death of motor neurons from Q/R site-unedited GluR2. *J. Neurosci.* 30, 11917–11925. doi: 10.1523/JNEUROSCI.2021-10.2010

Higelin, J., Demestre, M., Putz, S., Delling, J. P., Jacob, C., Lutz, A.-K., et al. (2016). FUS mislocalization and vulnerability to DNA damage in ALS patients derived hiPSCs and aging motoneurons. *Front. Cell. Neurosci.* 10:290. doi: 10.3389/fncel.2016.00290

Hill, S. J., Mordes, D. A., Cameron, L. A., Neuberg, D. S., Landini, S., Eggan, K., et al. (2016). Two familial ALS proteins function in prevention/repair of transcription-associated DNA damage. *PNAS* 113, E7701–E7709. doi: 10.1073/pnas.1611673113

Hira, R., Ohkubo, F., Tanaka, Y. R., Masamizu, Y., Augustine, G. J., Kasai, H., et al. (2013). In vivo optogenetic tracing of functional corticocortical connections between motor forelimb areas. *Front. Neural Circ.* 7:55. doi: 10.3389/fncir.2013.00055

Hirano, A., Nakano, I., Kurland, L. T., Mulder, D. W., Holley, P. W., and Saccomanno, G. (1984). Fine structural study of neurofibrillary changes in a family with amyotrophic lateral sclerosis. *J. Neuropathol. Exp. Neurol.* 43, 471–480. doi: 10.1097/00005072-198409000-00002

Hochstim, C., Deneen, B., Lukaszewicz, A., Zhou, Q., and Anderson, D. J. (2008). Identification of positionally distinct astrocyte subtypes whose identities are specified by a homeodomain code. *Cell* 133, 510–522. doi: 10.1016/j.cell.2008.02.046

Hossaini, M., Cano, S. C., van Dis, V., Haasdijk, E. D., Hoogenraad, C. C., Holstege, J. C., et al. (2011). Spinal inhibitory interneuron pathology follows motor neuron degeneration independent of glial mutant superoxide dismutase 1 expression in SOD1-ALS Mice. *J. Neuropathol. Exp. Neurol.* 70, 662–677. doi: 10.1097/NEN.0b013e31822581ac

Hsiung, G.-Y. R., DeJesus-Hernandez, M., Feldman, H. H., Sengdy, P., Bouchard-Kerr, P., Dwosh, E., et al. (2012). Clinical and pathological features of familial frontotemporal dementia caused by C9ORF72 mutation on chromosome 9p. *Brain* 135, 709–722. doi: 10.1093/brain/awr354

Huang, C., Huang, B., Bi, F., Yan, L. H., Tong, J., Huang, J., et al. (2014). Profiling the genes affected by pathogenic TDP-43 in astrocytes. *J. Neurochem.* 129, 932–939. doi: 10.1111/jnc.12660

Huang, C., Tong, J., Bi, F., Wu, Q., Huang, B., Zhou, H., et al. (2012). Entorhinal cortical neurons are the primary targets of FUS mislocalization and ubiquitin aggregation in FUS transgenic rats. *Hum. Mol. Genet.* 21, 4602–4614. doi: 10.1093/hmg/dds299

Huber, A. B., Kania, A., Tran, T. S., Gu, C., De Marco Garcia, N., Lieberam, I., et al. (2005). Distinct roles for secreted semaphorin signaling in spinal motor axon guidance. *Neuron* 48, 949–964. doi: 10.1016/j.neuron.2005.12.003

Hugon, J., Vallat, J. M., Spencer, P. S., Leboutet, M. J., and Barthe, D. (1989). Kainic acid induces early and delayed degenerative neuronal changes in rat spinal cord. *Neurosci. Lett.* 104, 258–262. doi: 10.1016/0304-3940(89)90585-5

Hunt, C. C., and Kuffler, S. W. (1951). Further study of efferent small-nerve fibres to mammalian muscle spindles. multiple spindle innervation and activity during contraction. *J. Physiol.* 113, 283–297. doi: 10.1113/jphysiol.1951.sp004572

Hyder, F., Rothman, D. L., and Bennett, M. R. (2013). Cortical energy demands of signaling and nonsignaling components in brain are conserved across mammalian species and activity levels. *Proc. Natl. Acad. Sci. U.S.A.* 110, 3549–3554. doi: 10.1073/pnas.1214912110

Iguchi, Y., Katsuno, M., Niwa, J., Takagi, S., Ishigaki, S., Ikenaka, K., et al. (2013). Loss of TDP-43 causes age-dependent progressive motor neuron degeneration. *Brain* 136, 1371–1382. doi: 10.1093/brain/awt029

Ikonomidou, C., Qin Qin, Y., Labruyere, J., and Olney, J. W. (1996). Motor neuron degeneration induced by excitotoxin agonists has features in common with those seen in the SOD-1 transgenic mouse model of amyotrophic lateral sclerosis. *J. Neuropathol. Exp. Neurol.* 55, 211–224. doi: 10.1097/00005072-199602000-00010

Ilieva, E. V., Ayala, V., Jové, M., Dalfó, E., Cacabelos, D., Povedano, M., et al. (2007). Oxidative and endoplasmic reticulum stress interplay in sporadic amyotrophic lateral sclerosis. *Brain* 130, 3111–3123. doi: 10.1093/brain/awm190

Ilieva, H., Polymenidou, M., and Cleveland, D. W. (2009). Non-cell autonomous toxicity in neurodegenerative disorders: ALS and beyond. *J. Cell Biol.* 187, 761–772. doi: 10.1083/jcb.200908164

Ilieva, H. S., Yamanaka, K., Malkmus, S., Kakinohana, O., Yaksh, T., Marsala, M., et al. (2008). Mutant dynein (Loa) triggers proprioceptive axon loss that extends survival only in the SOD1 ALS model with highest motor neuron death. *Proc. Natl. Acad. Sci. U.S.A.* 105, 12599–12604. doi: 10.1073/pnas.0805422105

Irwin, D. J., McMillan, C. T., Brettschneider, J., Libon, D. J., Powers, J., Rascovsky, K., et al. (2013). Cognitive decline and reduced survival in C9orf72 expansion frontotemporal degeneration and amyotrophic lateral sclerosis. *J. Neurol. Neurosurg. Psychiatry* 84, 163–169. doi: 10.1136/jnnp-2012-303507

Israelson, A., Arbel, N., Da Cruz, S., Ilieva, H., Yamanaka, K., Shoshan-Barmatz, V., et al. (2010). Misfolded mutant SOD1 directly inhibits VDAC1 conductance in a mouse model of inherited ALS. *Neuron* 67, 575–587. doi: 10.1016/j.neuron.2010.07.019

Ito, H., Wate, R., Zhang, J., Ohnishi, S., Kaneko, S., Ito, H., et al. (2008). Treatment with edaravone, initiated at symptom onset, slows motor decline and decreases SOD1 deposition in ALS mice. *Exp. Neurol.* 213, 448–455. doi: 10.1016/j.expneurol.2008.07.017

Jaarsma, D., Teuling, E., Haasdijk, E. D., De Zeeuw, C. I., and Hoogenraad, C. C. (2008). Neuron-specific expression of mutant superoxide dismutase is sufficient to induce amyotrophic lateral sclerosis in transgenic mice. *J. Neurosci.* 28, 2075–2088. doi: 10.1523/JNEUROSCI.5258-07.2008

Javed, K., and Lui, F. (2018). "Neuroanatomy, Lateral Corticospinal Tract," in *StatPearls*, ed. M. Varacallo (Treasure Island FL: StatPearls Publishing).

Jeon, G. S., Nakamura, T., Lee, J.-S., Choi, W.-J., Ahn, S.-W., Lee, K.-W., et al. (2014). Potential effect of s-nitrosylated protein disulfide isomerase on mutant SOD1 aggregation and neuronal cell death in amyotrophic lateral sclerosis. *Mol. Neurobiol.* 49, 796–807. doi: 10.1007/s12035-013-8562-z

Jiang, M., Schuster, J. E., Fu, R., Siddique, T., and Heckman, C. J. (2009). Progressive changes in synaptic inputs to motoneurons in adult sacral spinal cord of a mouse model of amyotrophic lateral sclerosis. *J. Neurosci.* 29, 15031–15038. doi: 10.1523/JNEUROSCI.0574-09.2009

Jiang, S. X., Whitehead, S., Aylsworth, A., Slinn, J., Zurakowski, B., Chan, K., et al. (2010). Neuropilin 1 directly interacts with Fer kinase to mediate semaphorin 3A-induced death of cortical neurons. *J. Biol. Chem.* 285, 9908–9918. doi: 10.1074/jbc.M109.080689

Jiang, Y.-M., Yamamoto, M., Kobayashi, Y., Yoshihara, T., Liang, Y., Terao, S., et al. (2005). Gene expression profile of spinal motor neurons in sporadic amyotrophic lateral sclerosis. *Ann. Neurol.* 57, 236–251. doi: 10.1002/ana.20379

Jin, H., Mimura, N., Kashio, M., Koseki, H., and Aoe, T. (2014). Late-onset of spinal neurodegeneration in knock-in mice expressing a mutant biP. *PLoS One* 9:e112837. doi: 10.1371/journal.pone.0112837

Johnson, J. O., Glynn, S. M., Gibbs, J. R., Nalls, M. A., Sabatelli, M., Restagno, G., et al. (2014a). Mutations in the CHCHD10 gene are a common cause of familial amyotrophic lateral sclerosis. *Brain* 137:e311. doi: 10.1093/brain/awu265

Johnson, J. O., Pioro, E. P., Boehringer, A., Chia, R., Feit, H., Renton, A. E., et al. (2014b). Mutations in the Matrin 3 gene cause familial amyotrophic lateral sclerosis. *Nat. Neurosci.* 17:664.

Johnson, J. O., Mandrioli, J., Benatar, M., Abramzon, Y., Van Deerlin, V. M., Trojanowski, J. Q., et al. (2010). Exome sequencing reveals VCP mutations as a cause of familial ALS. *Neuron* 68, 857–864. doi: 10.1016/j.neuron.2010.11.036

Jonsson, P. A., Graffmo, K. S., Brännström, T., Nilsson, P., Andersen, P. M., and Marklund, S. L. (2006). Motor neuron disease in mice expressing the wild type-like D90A mutant superoxide dismutase-1. *J. Neuropathol. Exp. Neurol.* 65, 1126–1136. doi: 10.1097/01.jnen.0000248545.36046.3c

Kabashi, E., El Oussini, H., Bercier, V., Gros-Louis, F., Valdmanis, P. N., McDearmid, J., et al. (2013). Investigating the contribution of VAPB/ALS8 loss of function in amyotrophic lateral sclerosis. *Hum. Mol. Genet.* 22, 2350–2360. doi: 10.1093/hmg/ddt080

Kabashi, E., Valdmanis, P. N., Dion, P., Spiegelman, D., McConkey, B. J., Vande Velde, C., et al. (2008). TARDBP mutations in individuals with sporadic and familial amyotrophic lateral sclerosis. *Nat. Genet.* 40, 572–574. doi: 10.1038/ng.132

Kadhiresan, V. A., Hassett, C. A., and Faulkner, J. A. (1996). Properties of single motor units in medial gastrocnemius muscles of adult and old rats. *J. Physiol.* 493, 543–552. doi: 10.1113/jphysiol.1996.sp021402

Kanai, Y., Okada, Y., Tanaka, Y., Harada, A., Terada, S., and Hirokawa, N. (2000). KIF5C, a novel neuronal kinesin enriched in motor neurons. *J. Neurosci.* 20, 6374–6384. doi: 10.1523/JNEUROSCI.20-17-06374.2000

Kanda, K., and Hashizume, K. (1989). Changes in properties of the medial gastrocnemius motor units in aging rats. *J. Neurophysiol.* 61, 737–746. doi: 10.1152/jn.1989.61.4.737

Kang, S. H., Li, Y., Fukaya, M., Lorenzini, I., Cleveland, D. W., Ostrow, L. W., et al. (2013). Degeneration and impaired regeneration of gray matter oligodendrocytes in amyotrophic lateral sclerosis. *Nat. Neurosci.* 16, 571–579. doi: 10.1038/nn.3357

Kanning, K. C., Kaplan, A., and Henderson, C. E. (2010). Motor neuron diversity in development and disease. *Ann. Rev. Neurosci.* 33, 409–440. doi: 10.1146/annurev.neuro.051508.135722

Kaplan, A., Spiller, K. J., Towne, C., Kanning, K. C., Choe, G. T., Geber, A., et al. (2014). Neuronal matrix metalloproteinase-9 is a determinant of selective neurodegeneration. *Neuron* 81, 333–348. doi: 10.1016/j.neuron.2013.12.009

Kawahara, Y., Ito, K., Sun, H., Aizawa, H., Kanazawa, I., and Kwak, S. (2004). Glutamate receptors: RNA editing and death of motor neurons. *Nature* 427:801. doi: 10.1038/427801a

Kawahara, Y., Kwak, S., Sun, H., Ito, K., Hashida, H., Aizawa, H., et al. (2003). Human spinal motoneurons express low relative abundance of GluR2 mRNA: an implication for excitotoxicity in ALS. *J. Neurochem.* 85, 680–689. doi: 10.1046/j.1471-4159.2003.01703.x

Kawamata, T., Akiyama, H., Yamada, T., and McGeer, P. L. (1992). Immunologic reactions in amyotrophic lateral sclerosis brain and spinal cord tissue. *Am. J. Pathol.* 140, 691–707.

Kemm, R. E., and Westbury, D. R. (1978). Some properties of spinal gamma-motoneurones in the cat, determined by micro-electrode recording. *J. Physiol.* 282, 59–71. doi: 10.1113/jphysiol.1978.sp012448

Kernell, D., and Zwaagstra, B. (1981). Input conductance axonal conduction velocity and cell size among hindlimb motoneurones of the cat. *Brain Res.* 204, 311–326. doi: 10.1016/0006-8993(81)90591-6

Kia, A., McAvoy, K., Krishnamurthy, K., Trotti, D., and Pasinelli, P. (2018). Astrocytes expressing ALS-linked mutant FUS induce motor neuron death through release of tumor necrosis factor-alpha. *Glia* 66, 1016–1033. doi: 10.1002/glia.23298

Kiehn, O. (2016). Decoding the organization of spinal circuits that control locomotion. *Nat. Rev. Neurosci.* 17, 224–238. doi: 10.1038/nrn.2016.9

Kiernan, M. C., Vucic, S., Cheah, B. C., Turner, M. R., Eisen, A., Hardiman, O., et al. (2011). Amyotrophic lateral sclerosis. *Lancet* 377, 942–955. doi: 10.1016/S0140-6736(10)61156-7

Kikis, E. A., Gidalevitz, T., and Morimoto, R. I. (2010). Protein homeostasis in models of aging and age-related conformational disease. *Adv. Exp. Med. Biol.* 694, 138–159. doi: 10.1007/978-1-4419-7002-2_11

Kim, H. J., Kim, N. C., Wang, Y.-D., Scarborough, E. A., Moore, J., Diaz, Z., et al. (2013). Mutations in prion-like domains in hnRNPA2B1 and hnRNPA1 cause multisystem proteinopathy and ALS. *Nature* 495:467. doi: 10.1038/nature11922

Kim, H.-J., Kwon, M.-J., Choi, W.-J., Oh, K.-W., Oh, S.-I., Ki, C.-S., et al. (2014). Mutations in UBQLN2 and SIGMAR1 genes are rare in Korean patients with amyotrophic lateral sclerosis. *Neurobiol. Aging* 35, 1957.e7–1957.e8. doi: 10.1016/j.neurobiolaging.2014.03.001

Kim, H. J., and Taylor, J. P. (2017). Lost in transportation: nucleocytoplasmic transport defects in ALS and other neurodegenerative diseases. *Neuron* 96, 285–297. doi: 10.1016/j.neuron.2017.07.029

Kirby, J., Goodall, E. F., Smith, W., Highley, J. R., Masanzu, R., Hartley, J. A., et al. (2010). Broad clinical phenotypes associated with TAR-DNA binding protein (TARDBP) mutations in amyotrophic lateral sclerosis. *Neurogenetics* 11, 217–225. doi: 10.1007/s10048-009-0218-9

Kiskinis, E., Sandoe, J., Williams, L. A., Boulting, G. L., Moccia, R., Wainger, B. J., et al. (2014). Pathways disrupted in human ALS motor neurons identified through genetic correction of mutant SOD1. *Cell Stem Cell* 14, 781–795. doi: 10.1016/j.stem.2014.03.004

Kong, J., and Xu, Z. (1998). Massive mitochondrial degeneration in motor neurons triggers the onset of amyotrophic lateral sclerosis in mice expressing a mutant SOD1. *J. Neurosci.* 18, 3241–3250. doi: 10.1523/jneurosci.18-09-03241.1998

Konopka, A., and Atkin, J. D. (2018). The emerging role of DNA damage in the pathogenesis of the C9orf72 repeat expansion in amyotrophic lateral sclerosis. *Int. J. Mol. Sci.* 19:E3137. doi: 10.3390/ijms19103137

Körner, S., Böselt, S., Wichmann, K., Thau-Habermann, N., Zapf, A., Knippenberg, S., et al. (2016). The axon guidance protein semaphorin 3A is increased in the motor cortex of patients with amyotrophic lateral sclerosis. *J. Neuropathol. Exp. Neurol.* doi: 10.1093/jnen/nlw003 [Epub ahead of print].

Kortenbruck, G., Berger, E., Speckmann, E., and Musshoff, U. (2001). RNA editing at the Q/R site for the glutamate receptor subunits GLUR2, GLUR5, and GLUR6 in hippocampus and temporal cortex from epileptic patients - sciencedirect. *Neurobiol. Dis.* 8, 459–468. doi: 10.1006/nbdi.2001.0394

Kruman, I. I., Pedersen, W. A., Springer, J. E., and Mattson, M. P. (1999). ALS-linked Cu/Zn-SOD mutation increases vulnerability of motor neurons to excitotoxicity by a mechanism involving increased oxidative stress and perturbed calcium homeostasis. *Exp. Neurol.* 160, 28–39. doi: 10.1006/exnr.1999.7190

Kuffler, S. W., Hunt, C. C., and Quilliam, J. P. (1951). Function of medullated small-nerve fibers in mammalian ventral roots; efferent muscle spindle innervation. *J. Neurophysiol.* 14, 29–54. doi: 10.1152/jn.1951.14.1.29

Kuijpers, M., van Dis, V., Haasdijk, E. D., Harterink, M., Vocking, K., Post, J. A., et al. (2013). Amyotrophic lateral sclerosis (ALS)-associated VAPB-P56S inclusions represent an ER quality control compartment. *Acta Neuropathol. Commun.* 1:24. doi: 10.1186/2051-5960-1-24

Kuzuhara, S., Kanazawa, I., and Nakanishi, T. (1980). Topographical localization of the Onuf's nuclear neurons innervating the rectal and vesical striated sphincter muscles: a retrograde fluorescent double labeling in cat and dog. *Neurosci. Lett.* 16, 125–130. doi: 10.1016/0304-3940(80)90331-6

Kwiatkowski, T. J., Bosco, D. A., Leclerc, A. L., Tamrazian, E., Vanderburg, C. R., Russ, C., et al. (2009). Mutations in the FUS/TLS gene on chromosome 16 cause familial amyotrophic lateral sclerosis. *Science* 323, 1205–1208. doi: 10.1126/science.1166066

Lacomblez, L., Bensimon, G., Leigh, P. N., Guillet, P., and Meininger, V. (1996). Dose-ranging study of riluzole in amyotrophic lateral sclerosis. amyotrophic lateral sclerosis/riluzole study group II. *Lancet* 347, 1425–1431. doi: 10.1016/s0140-6736(96)91680-3

Laffita-Mesa, J. M., Pupo, J. M. R., Sera, R. M., Mojena, Y. V., Kourí, V., Laguna-Salvia, L., et al. (2013). De novo mutations in ataxin-2 gene and ALS risk. *PLoS One* 8:e70560. doi: 10.1371/journal.pone.0070560

LaFrance, R., Brustovetsky, N., Sherburne, C., Delong, D., and Dubinsky, J. M. (2005). Age-related changes in regional brain mitochondria from Fischer 344 rats. *Aging Cell* 4, 139–145. doi: 10.1111/j.1474-9726.2005.00156.x

Lalancette-Hebert, M., Sharma, A., Lyashchenko, A. K., and Shneider, N. A. (2016). Gamma motor neurons survive and exacerbate alpha motor neuron degeneration in ALS. *PNAS* 113, E8316–E8325. doi: 10.1073/pnas.1605210113

Lall, D., and Baloh, R. H. (2017). Microglia and C9orf72 in neuroinflammation and ALS and frontotemporal dementia. *J. Clin. Invest.* 127, 3250–3258. doi: 10.1172/JCI90607

LaMonte, B. H., Wallace, K. E., Holloway, B. A., Shelly, S. S., Ascaño, J., Tokito, M., et al. (2002). Disruption of dynein/dynactin inhibits axonal transport in motor neurons causing late-onset progressive degeneration. *Neuron* 34, 715–727. doi: 10.1016/s0896-6273(02)00696-7

Landers, J. E., Melki, J., Meininger, V., Glass, J. D., van den Berg, L. H., van Es, M. A., et al. (2009). Reduced expression of the kinesin-associated protein 3 (KIFAP3) gene increases survival in sporadic amyotrophic lateral sclerosis. *Proc. Natl. Acad. Sci. U.S.A.* 106, 9004–9009. doi: 10.1073/pnas.0812937106

Laslo, P., Lipski, J., Nicholson, L. F., Miles, G. B., and Funk, G. D. (2000). Calcium binding proteins in motoneurons at low and high risk for degeneration in ALS. *Neuroreport* 11, 3305–3308. doi: 10.1097/00001756-200010200-00009

Lattante, S., Rouleau, G. A., and Kabashi, E. (2013). TARDBP and FUS mutations associated with amyotrophic lateral sclerosis: summary and update. *Hum. Mutat.* 34, 812–826. doi: 10.1002/humu.22319

Lauretani, F., Russo, C. R., Bandinelli, S., Bartali, B., Cavazzini, C., Di Iorio, A., et al. (2003). Age-associated changes in skeletal muscles and their effect on mobility: an operational diagnosis of sarcopenia. *J. Appl. Physiol.* 95, 1851–1860. doi: 10.1152/japplphysiol.00246.2003

Lautenschläger, J., Prell, T., Ruhmer, J., Weidemann, L., Witte, O. W., and Grosskreutz, J. (2013). Overexpression of human mutated G93A SOD1 changes dynamics of the ER mitochondria calcium cycle specifically in mouse embryonic motor neurons. *Exp. Neurol.* 247, 91–100. doi: 10.1016/j.expneurol.2013.03.027

Lawson, L. J., Perry, V. H., Dri, P., and Gordon, S. (1990). Heterogeneity in the distribution and morphology of microglia in the normal adult mouse brain. *Neuroscience* 39, 151–170. doi: 10.1016/0306-4522(90)90229-w

Le, N. T. T., Chang, L., Kovlyagina, I., Georgiou, P., Safren, N., Braunstein, K. E., et al. (2016). Motor neuron disease, TDP-43 pathology, and memory deficits in mice expressing ALS-FTD-linked UBQLN2 mutations. *Proc. Natl. Acad. Sci. U.S.A.* 113, E7580–E7589. doi: 10.1073/pnas.1608432113

Le Ber, I., Camuzat, A., Guerreiro, R., Bouya-Ahmed, K., Bras, J., Nicolas, G., et al. (2013). SQSTM1 mutations in French patients with frontotemporal dementia or frontotemporal dementia with amyotrophic lateral sclerosis. *JAMA Neurol.* 70, 1403–1410. doi: 10.1001/jamaneurol.2013.3849

Le Masson, G., Przedborski, S., and Abbott, L. F. (2014). A computational model of motor neuron degeneration. *Neuron* 83, 975–988. doi: 10.1016/j.neuron.2014.07.001

Lee, S., and Kim, H.-J. (2015). Prion-like mechanism in amyotrophic lateral sclerosis: are protein aggregates the key? *Exp. Neurobiol.* 24, 1–7. doi: 10.5607/en.2015.24.1.1

Lemon, R. N. (2008). Descending pathways in motor control. *Annu. Rev. Neurosci.* 31, 195–218. doi: 10.1146/annurev.neuro.31.060407.125547

Leroy, F., Lamotte d'Incamps, B., Imhoff-Manuel, R. D., and Zytnicki, D. (2014). Early intrinsic hyperexcitability does not contribute to motoneuron degeneration in amyotrophic lateral sclerosis. *eLife* 3:e04046. doi: 10.7554/eLife.04046

Leyton, A. S. F., and Sherrington, C. S. (1917). Observations on the excitable cortex of the chimpanzee, orang-utan, and gorilla. *Q. J. Exp. Physiol.* 11, 135–222. doi: 10.1113/expphysiol.1917.sp000240

Liao, B., Zhao, W., Beers, D. R., Henkel, J. S., and Appel, S. H. (2012). Transformation from a neuroprotective to a neurotoxic microglial phenotype in a mouse model of ALS. *Exp. Neurol.* 237, 147–152. doi: 10.1016/j.expneurol.2012.06.011

Liddelow, S. A., Guttenplan, K. A., Clarke, L. E., Bennett, F. C., Bohlen, C. J., Schirmer, L., et al. (2017). Neurotoxic reactive astrocytes are induced by activated microglia. *Nature* 541, 481–487. doi: 10.1038/nature21029

Ligon, L. A., LaMonte, B. H., Wallace, K. E., Weber, N., Kalb, R. G., and Holzbaur, E. L. F. (2005). Mutant superoxide dismutase disrupts cytoplasmic dynein in motor neurons. *Neuroreport* 16, 533–536. doi: 10.1097/00001756-200504250-00002

Lin, F. R. (2011). Ataxin-2 intermediate-length polyglutamine expansions in European ALS patients. *Hum. Mol. Genet.* 20, 1697–1700. doi: 10.1093/hmg/ddr045

Lino, M. M., Schneider, C., and Caroni, P. (2002). Accumulation of SOD1 mutants in postnatal motoneurons does not cause motoneuron pathology or motoneuron disease. *J. Neurosci.* 22, 4825–4832. doi: 10.1523/jneurosci.22-12-04825.2002

Lips, M. B., and Keller, B. U. (1998). Endogenous calcium buffering in motoneurones of the nucleus hypoglossus from mouse. *J. Physiol.* 511, 105–117. doi: 10.1111/j.1469-7793.1998.105bi.x

Lips, M. B., and Keller, B. U. (1999). Activity-related calcium dynamics in motoneurons of the nucleus hypoglossus from mouse. *J. Neurophysiol.* 82, 2936–2946. doi: 10.1152/jn.1999.82.6.2936

Liu, D., Wen, J., Liu, J., and Li, L. (1999). The roles of free radicals in amyotrophic lateral sclerosis: reactive oxygen species and elevated oxidation of protein, DNA, and membrane phospholipids. *FASEB J.* 13, 2318–2328. doi: 10.1096/fasebj.13.15.2318

Liu, J., Lillo, C., Jonsson, P. A., Vande Velde, C., Ward, C. M., Miller, T. M., et al. (2004). Toxicity of familial ALS-linked SOD1 mutants from selective recruitment to spinal mitochondria. *Neuron* 43, 5–17. doi: 10.1016/j.neuron.2004.06.016

Liu, R., Althaus, J. S., Ellerbrock, B. R., Becker, D. A., and Gurney, M. E. (1998). Enhanced oxygen radical production in a transgenic mouse model of familial amyotrophic lateral sclerosis. *Ann. Neurol.* 44, 763–770. doi: 10.1002/ana.410440510

Liu, W., D'Ercole, J. A., and Ye, P. (2011). Blunting type 1 insulin-like growth factor receptor expression exacerbates neuronal apoptosis following hypoxic/ischemic injury. *BMC Neurosci.* 12:64. doi: 10.1186/1471-2202-12-64

Liu, X., Yang, L., Tang, L., Chen, L., Liu, X., and Fan, D. (2017). DCTN1 gene analysis in Chinese patients with sporadic amyotrophic lateral sclerosis. *PLoS One* 12:e0182572. doi: 10.1371/journal.pone.0182572

Lobsiger, C. S., Boillee, S., McAlonis-Downes, M., Khan, A. M., Feltri, M. L., Yamanaka, K., et al. (2009). Schwann cells expressing dismutase active mutant SOD1 unexpectedly slow disease progression in ALS mice. *Proc. Natl. Acad. Sci. U.S.A.* 106, 4465–4470. doi: 10.1073/pnas.0813339106

Mackenzie, I. R., Arzberger, T., Kremmer, E., Troost, D., Lorenzl, S., Mori, K., et al. (2013). Dipeptide repeat protein pathology in C9ORF72 mutation cases: clinico-pathological correlations. *Acta Neuropathol.* 126, 859–879. doi: 10.1007/s00401-013-1181-y

Mackenzie, I. R. A., Ansorge, O., Strong, M., Bilbao, J., Zinman, L., Ang, L.-C., et al. (2011). Pathological heterogeneity in amyotrophic lateral sclerosis with FUS mutations: two distinct patterns correlating with disease severity and mutation. *Acta Neuropathol.* 122, 87–98. doi: 10.1007/s00401-011-0838-7

Mackenzie, I. R. A., Bigio, E. H., Ince, P. G., Geser, F., Neumann, M., Cairns, N. J., et al. (2007). Pathological TDP-43 distinguishes sporadic amyotrophic lateral sclerosis from amyotrophic lateral sclerosis with SOD1 mutations. *Ann. Neurol.* 61, 427–434. doi: 10.1002/ana.21147

Mackenzie, I. R. A., Neumann, M., Bigio, E. H., Cairns, N. J., Alafuzoff, I., Kril, J., et al. (2009). Nomenclature for neuropathologic subtypes of frontotemporal lobar degeneration: consensus recommendations. *Acta Neuropathol.* 117, 15–18. doi: 10.1007/s00401-008-0460-5

Madabhushi, R., Pan, L., and Tsai, L.-H. (2014). DNA damage and its links to neurodegeneration. *Neuron* 83, 266–282. doi: 10.1016/j.neuron.2014.06.034

Maekawa, S., Al-Sarraj, S., Kibble, M., Landau, S., Parnavelas, J., Cotter, D., et al. (2004). Cortical selective vulnerability in motor neuron disease: a morphometric study. *Brain* 127, 1237–1251. doi: 10.1093/brain/awh132

Magnus, T., Carmen, J., Deleon, J., Xue, H., Pardo, A. C., Lepore, A. C., et al. (2008). Adult glial precursor proliferation in mutant SOD1G93A mice. *Glia* 56, 200–208. doi: 10.1002/glia.20604

Magrané, J., Cortez, C., Gan, W.-B., and Manfredi, G. (2014). Abnormal mitochondrial transport and morphology are common pathological denominators in SOD1 and TDP43 ALS mouse models. *Hum. Mol. Genet.* 23, 1413–1424. doi: 10.1093/hmg/ddt528

Maharjan, N., and Saxena, S. (2016). ER strikes again: proteostasis dysfunction in ALS. *EMBO J.* 35, 798–800. doi: 10.15252/embj.201694117

Mahoney, C. J., Beck, J., Rohrer, J. D., Lashley, T., Mok, K., Shakespeare, T., et al. (2012). Frontotemporal dementia with the C9ORF72 hexanucleotide repeat expansion: clinical, neuroanatomical and neuropathological features. *Brain* 135, 736–750. doi: 10.1093/brain/awr361

Majounie, E., Renton, A. E., Mok, K., Dopper, E. G. P., Waite, A., Rollinson, S., et al. (2012). Frequency of the C9orf72 hexanucleotide repeat expansion in patients with amyotrophic lateral sclerosis and frontotemporal dementia: a cross-sectional study. *Lancet Neurol.* 11, 323–330. doi: 10.1016/S1474-4422(12)70043-1

Malhas, A. N., Lee, C. F., and Vaux, D. J. (2009). Lamin B1 controls oxidative stress responses via Oct-1. *J. Cell Biol.* 184, 45–55. doi: 10.1083/jcb.200804155

Maniecka, Z., and Polymenidou, M. (2015). From nucleation to widespread propagation: a prion-like concept for ALS. *Virus Res.* 207, 94–105. doi: 10.1016/j.virusres.2014.12.032

Manini, T. M., Hong, S. L., and Clark, B. C. (2013). Aging and muscle: a neuron's perspective. *Curr. Opin. Clin. Nutr. Metab. Care* 16, 21–26. doi: 10.1097/MCO.0b013e32835b5880

Mannen, T., Iwata, M., Toyokura, Y., and Nagashima, K. (1977). Preservation of a certain motoneurone group of the sacral cord in amyotrophic lateral sclerosis: its clinical significance. *J. Neurol. Neurosurg. Psychiatry* 40, 464–469. doi: 10.1136/jnnp.40.5.464

Marner, L., Nyengaard, J. R., Tang, Y., and Pakkenberg, B. (2003). Marked loss of myelinated nerve fibers in the human brain with age. *J. Comp. Neurol.* 462, 144–152. doi: 10.1002/cne.10714

Maruyama, H., Morino, H., Ito, H., Izumi, Y., Kato, H., Watanabe, Y., et al. (2010). Mutations of optineurin in amyotrophic lateral sclerosis. *Nature* 465, 223–226. doi: 10.1038/nature08971

Matise, M., and Sharma, K. (2013). "Chapter 21 - The Specification and Generation of Neurons in the Ventral Spinal Cord," in *Patterning and Cell Type Specification in the Developing CNS and PNS*, eds J. L. R. Rubenstein and P. Rakic (Oxford: Academic Press), 401–415. doi: 10.1016/b978-0-12-397265-1.00101-5

Mattson, M. P., and Magnus, T. (2006). Ageing and neuronal vulnerability. *Nat. Rev. Neurosci.* 7, 278–294. doi: 10.1038/nrn1886

Maxwell, N., Castro, R. W., Sutherland, N. M., Vaughan, K. L., Szarowicz, M. D., de Cabo, R., et al. (2018). α-Motor neurons are spared from aging while their synaptic inputs degenerate in monkeys and mice. *Aging Cell* 17:e12726. doi: 10.1111/acel.12726

McHanwell, S., and Biscoe, T. J. (1981). The localization of motoneurons supplying the hindlimb muscles of the mouse. *Philos. Trans. R. Soc. Lond. B Biol. Sci.* 293, 477–508. doi: 10.1098/rstb.1981.0082

Melkov, A., Baskar, R., Alcalay, Y., and Abdu, U. (2016). A new mode of mitochondrial transport and polarized sorting regulated by Dynein,

Milton and Miro. *Development* 143, 4203–4213. doi: 10.1242/dev.138289

Mendell, L. M. (2005). The size principle: a rule describing the recruitment of motoneurons. *J. Neurophysiol.* 93, 3024–3026. doi: 10.1152/classicessays.00025.2005

Menon, P., Kiernan, M. C., and Vucic, S. (2015). Cortical hyperexcitability precedes lower motor neuron dysfunction in ALS. *Clin. Neurophysiol.* 126, 803–809. doi: 10.1016/j.clinph.2014.04.023

Millecamps, S., Da Barroca, S., Cazeneuve, C., Salachas, F., Pradat, P.-F., Danel-Brunaud, V., et al. (2010). Questioning on the role of D amino acid oxidase in familial amyotrophic lateral sclerosis. *Proc. Natl. Acad. Sci. U.S.A.* 107:E107. doi: 10.1073/pnas.1006190107

Millecamps, S., Robertson, J., Lariviere, R., Mallet, J., and Julien, J.-P. (2006). Defective axonal transport of neurofilament proteins in neurons overexpressing peripherin. *J. Neurochem.* 98, 926–938. doi: 10.1111/j.1471-4159.2006.03932.x

Miller, S. J. (2018). Astrocyte heterogeneity in the adult central nervous system. *Front. Cell Neurosci.* 12:401. doi: 10.3389/fncel.2018.00401

Mimura, N., Yuasa, S., Soma, M., Jin, H., Kimura, K., Goto, S., et al. (2008). Altered quality control in the endoplasmic reticulum causes cortical dysplasia in knock-in mice expressing a mutant BiP. *Mol. Cell. Biol.* 28, 293–301. doi: 10.1128/MCB.00473-07

Misawa, H., Hara, M., Tanabe, S., Niikura, M., Moriwaki, Y., and Okuda, T. (2012). Osteopontin is an alpha motor neuron marker in the mouse spinal cord. *J. Neurosci. Res.* 90, 732–742. doi: 10.1002/jnr.22813

Mitchell, J., Paul, P., Chen, H.-J., Morris, A., Payling, M., Falchi, M., et al. (2010). Familial amyotrophic lateral sclerosis is associated with a mutation in D-amino acid oxidase. *Proc. Natl. Acad. Sci. U.S.A.* 107, 7556–7561. doi: 10.1073/pnas.0914128107

Mohajeri, M. H., Figlewicz, D. A., and Bohn, M. C. (1998). Selective loss of alpha motoneurons innervating the medial gastrocnemius muscle in a mouse model of amyotrophic lateral sclerosis. *Exp. Neurol.* 150, 329–336. doi: 10.1006/exnr.1998.6758

Molofsky, A. V., Kelley, K. W., Tsai, H.-H., Redmond, S. A., Chang, S. M., Madireddy, L., et al. (2014). Astrocyte-encoded positional cues maintain sensorimotor circuit integrity. *Nature* 509, 189–194. doi: 10.1038/nature13161

Moret, F., Renaudot, C., Bozon, M., and Castellani, V. (2007). Semaphorin and neuropilin co-expression in motoneurons sets axon sensitivity to environmental semaphorin sources during motor axon pathfinding. *Development* 134, 4491–4501. doi: 10.1242/dev.011452

Muller, F. L., Liu, Y., Jernigan, A., Borchelt, D., Richardson, A., and Van Remmen, H. (2008). MnSOD deficiency has a differential effect on disease progression in two different ALS mutant mouse models. *Muscle Nerve* 38, 1173–1183. doi: 10.1002/mus.21049

Müller, T. J., Kraya, T., Stoltenburg-Didinger, G., Hanisch, F., Kornhuber, M., Stoevesandt, D., et al. (2014). Phenotype of matrin-3–related distal myopathy in 16 G erman patients. *Ann. Neurol.* 76, 669–680. doi: 10.1002/ana.24255

Münch, C., O'Brien, J., and Bertolotti, A. (2011). Prion-like propagation of mutant superoxide dismutase-1 misfolding in neuronal cells. *Proc. Natl. Acad. Sci. U.S.A.* 108, 3548–3553. doi: 10.1073/pnas.1017275108

Münch, C., Rosenbohm, A., Sperfeld, A.-D., Uttner, I., Reske, S., Krause, B. J., et al. (2005). Heterozygous R1101K mutation of the DCTN1 gene in a family with ALS and FTD. *Ann. Neurol.* 58, 777–780. doi: 10.1002/ana.20631

Münch, C., Sedlmeier, R., Meyer, T., Homberg, V., Sperfeld, A. D., Kurt, A., et al. (2004). Point mutations of the p150 subunit of dynactin (DCTN1) gene in ALS. *Neurology* 63, 724–726. doi: 10.1212/01.wnl.0000134608.83927.b1

Murphy, P. R., and Martin, H. A. (1993). Fusimotor discharge patterns during rhythmic movements. *Trends Neurosci.* 16, 273–278. doi: 10.1016/0166-2236(93)90181-K

Murray, M. E., DeJesus-Hernandez, M., Rutherford, N. J., Baker, M., Duara, R., Graff-Radford, N. R., et al. (2011). Clinical and neuropathologic heterogeneity of c9FTD/ALS associated with hexanucleotide repeat expansion in C9ORF72. *Acta Neuropathol.* 122, 673–690. doi: 10.1007/s00401-011-0907-y

Nagai, M., Re, D. B., Nagata, T., Chalazonitis, A., Jessell, T. M., Wichterle, H., et al. (2007). Astrocytes expressing ALS-linked mutated SOD1 release factors selectively toxic to motor neurons. *Nat. Neurosci.* 10, 615–622. doi: 10.1038/nn1876

Nagashima, T., Beppu, H., Uono, M., and Yamada, H. (1979). Demonstration of neuronal localization in Onufrowcz's group-X in rabbit by double labeling method. *Acta Histochem. Cytochem.* 12, 409–415. doi: 10.1267/ahc.12.409

Nakamura, R., Kamakura, K., and Kwak, S. (1994). Late-onset selective neuronal damage in the rat spinal cord induced by continuous intrathecal administration of AMPA. *Brain Res.* 654, 279–285. doi: 10.1016/0006-8993(94)90490-1

Naumann, M., Pal, A., Goswami, A., Lojewski, X., Japtok, J., Vehlow, A., et al. (2018). Impaired DNA damage response signaling by FUS-NLS mutations leads to neurodegeneration and FUS aggregate formation. *Nat. Commun.* 9:335. doi: 10.1038/s41467-017-02299-1

Neafsey, E. J., Bold, E. L., Haas, G., Hurley-Gius, K. M., Quirk, G., Sievert, C. F., et al. (1986). The organization of the rat motor cortex: a microstimulation mapping study. *Brain Res.* 396, 77–96. doi: 10.1016/s0006-8993(86)80191-3

Neumann, M., Rademakers, R., Roeber, S., Baker, M., Kretzschmar, H. A., and Mackenzie, I. R. (2009). A new subtype of frontotemporal lobar degeneration with FUS pathology. *Brain* 132, 2922–2931. doi: 10.1093/brain/awp214

Neumann, M., Sampathu, D. M., Kwong, L. K., Truax, A. C., Micsenyi, M. C., Chou, T. T., et al. (2006). Ubiquitinated TDP-43 in frontotemporal lobar degeneration and amyotrophic lateral sclerosis. *Science* 314, 130–133. doi: 10.1126/science.1134108

Nguyen, H. P., Broeckhoven, C. V., and van der Zee, J. (2018). ALS Genes in the genomic era and their implications for FTD. *Trends Genet.* 34, 404–423. doi: 10.1016/j.tig.2018.03.001

Niccoli, T., Partridge, L., and Isaacs, A. M. (2017). Ageing as a risk factor for ALS/FTD. *Hum. Mol. Genet.* 26, R105–R113. doi: 10.1093/hmg/ddx247

Niebroj-Dobosz, I., Rafałowska, J., Fidziańska, A., Gadamski, R., and Grieb, P. (2007). Myelin composition of spinal cord in a model of amyotrophic lateral sclerosis (ALS) in SOD1G93A transgenic rats. *Folia Neuropathol.* 45, 236–241.

Niessen, H. G., Angenstein, F., Sander, K., Kunz, W. S., Teuchert, M., Ludolph, A. C., et al. (2006). In vivo quantification of spinal and bulbar motor neuron degeneration in the G93A-SOD1 transgenic mouse model of ALS by T2 relaxation time and apparent diffusion coefficient. *Exp. Neurol.* 201, 293–300. doi: 10.1016/j.expneurol.2006.04.007

Nijssen, J., Comley, L. H., and Hedlund, E. (2017). Motor neuron vulnerability and resistance in amyotrophic lateral sclerosis. *Acta Neuropathol.* 133, 863–885. doi: 10.1007/s00401-017-1708-8

Nimchinsky, E. A., Young, W. G., Yeung, G., Shah, R. A., Gordon, J. W., Bloom, F. E., et al. (2000). Differential vulnerability of oculomotor, facial, and hypoglossal nuclei in G86R superoxide dismutase transgenic mice. *J. Comp. Neurol.* 416, 112–125. doi: 10.1002/(sici)1096-9861(20000103)416:1<112::aid-cne9>3.0.co;2-k

Nishimaru, H., Restrepo, C. E., Ryge, J., Yanagawa, Y., and Kiehn, O. (2005). Mammalian motor neurons corelease glutamate and acetylcholine at central synapses. *Proc. Natl. Acad. Sci. U.S.A.* 102, 5245–5249. doi: 10.1073/pnas.0501331102

Nishimura, A. L., Mitne-Neto, M., Silva, H. C. A., Richieri-Costa, A., Middleton, S., Cascio, D., et al. (2004). A mutation in the vesicle-trafficking protein VAPB causes late-onset spinal muscular atrophy and amyotrophic lateral sclerosis. *Am. J. Hum. Genet.* 75, 822–831. doi: 10.1086/425287

Nishitoh, H., Kadowaki, H., Nagai, A., Maruyama, T., Yokota, T., Fukutomi, H., et al. (2008). ALS-linked mutant SOD1 induces ER stress- and ASK1-dependent motor neuron death by targeting Derlin-1. *Genes Dev.* 22, 1451–1464. doi: 10.1101/gad.1640108

Niven, J. E. (2016). Neuronal energy consumption: biophysics, efficiency and evolution. *Curr. Opin. Neurobiol.* 41, 129–135. doi: 10.1016/j.conb.2016.09.004

Nonaka, T., Masuda-Suzukake, M., Arai, T., Hasegawa, Y., Akatsu, H., Obi, T., et al. (2013). Prion-like properties of pathological TDP-43 aggregates from diseased brains. *Cell Rep.* 4, 124–134. doi: 10.1016/j.celrep.2013.06.007

Obál, I., Engelhardt, J. I., and Siklós, L. (2006). Axotomy induces contrasting changes in calcium and calcium-binding proteins in oculomotor and hypoglossal nuclei of Balb/c mice. *J. Comp. Neurol.* 499, 17–32. doi: 10.1002/cne.21041

Okada, Y., Yamazaki, H., Sekine-Aizawa, Y., and Hirokawa, N. (1995). The neuron-specific kinesin superfamily protein KIF1A is a uniqye monomeric motor for anterograde axonal transport of synaptic

vesicle precursors. *Cell* 81, 769–780. doi: 10.1016/0092-8674(95)90538-3

Osking, Z., Ayers, J. I., Hildebrandt, R., Skruber, K., Brown, H., Ryu, D., et al. (2019). ALS-linked SOD1 mutants enhance neurite outgrowth and branching in adult motor neurons. *Science* 11, 294–304. doi: 10.1016/j.isci.2018.12.026

Palecek, J., Lips, M. B., and Keller, B. U. (1999). Calcium dynamics and buffering in motoneurones of the mouse spinal cord. *J. Physiol.* 520, 485–502. doi: 10.1111/j.1469-7793.1999.00485.x

Pambo-Pambo, A., Durand, J., and Gueritaud, J.-P. (2009). Early excitability changes in lumbar motoneurons of transgenic SOD1G85R and SOD1G(93A-Low) mice. *J. Neurophysiol.* 102, 3627–3642. doi: 10.1152/jn.00482.2009

Pannese, E. (2011). Morphological changes in nerve cells during normal aging. *Brain Struct. Funct.* 216, 85–89. doi: 10.1007/s00429-011-0308-y

Pantelidou, M., Zographos, S. E., Lederer, C. W., Kyriakides, T., Pfaffl, M. W., and Santama, N. (2007). Differential expression of molecular motors in the motor cortex of sporadic ALS. *Neurobiol. Dis.* 26, 577–589. doi: 10.1016/j.nbd.2007.02.005

Papadeas, S. T., Kraig, S. E., O'Banion, C., Lepore, A. C., and Maragakis, N. J. (2011). Astrocytes carrying the superoxide dismutase 1 (SOD1G93A) mutation induce wild-type motor neuron degeneration in vivo. *Proc. Natl. Acad. Sci. U.S.A.* 108, 17803–17808. doi: 10.1073/pnas.1103141108

Parakh, S., Jagaraj, C. J., Vidal, M., Ragagnin, A. M. G., Perri, E. R., Konopka, A., et al. (2018a). ERp57 is protective against mutant SOD1-induced cellular pathology in amyotrophic lateral sclerosis. *Hum. Mol. Genet.* 27, 1311–1331. doi: 10.1093/hmg/ddy041

Parakh, S., Perri, E. R., Jagaraj, C. J., Ragagnin, A. M. G., and Atkin, J. D. (2018b). Rab-dependent cellular trafficking and amyotrophic lateral sclerosis. *Crit. Rev. Biochem. Mol. Biol.* 53, 623–651. doi: 10.1080/10409238.2018.1553926

Pasinelli, P., Belford, M. E., Lennon, N., Bacskai, B. J., Hyman, B. T., Trotti, D., et al. (2004). Amyotrophic lateral sclerosis-associated SOD1 mutant proteins bind and aggregate with Bcl-2 in spinal cord mitochondria. *Neuron* 43, 19–30. doi: 10.1016/j.neuron.2004.06.021

Paxinos, G. (2014). *The Rat Nervous System,* 4th Edn. Amsterdam: Elsevier.

Penndorf, D., Tadiæ, V., Witte, O. W., Grosskreutz, J., and Kretz, A. (2017). DNA strand breaks and TDP-43 mislocation are absent in the murine hSOD1G93A model of amyotrophic lateral sclerosis in vivo and in vitro. *PLoS One* 12:e0183684. doi: 10.1371/journal.pone.0183684

Penndorf, D., Witte, O. W., and Kretz, A. (2018). DNA plasticity and damage in amyotrophic lateral sclerosis. *Neural Regen. Res.* 13, 173–180. doi: 10.4103/1673-5374.226377

Perlson, E., Jeong, G.-B., Ross, J. L., Dixit, R., Wallace, K. E., Kalb, R. G., et al. (2009). A switch in retrograde signaling from survival to stress in rapid-onset neurodegeneration. *J. Neurosci.* 29, 9903–9917. doi: 10.1523/JNEUROSCI.0813-09.2009

Perrie, W. T., Lee, G. T., Curtis, E. M., Sparke, J., Buller, J. R., and Rossi, M. L. (1993). Changes in the myelinated axons of femoral nerve in amyotrophic lateral sclerosis. *J. Neural Transm. Suppl.* 39, 223–233.

Perrin, S. (2014). Preclinical research: make mouse studies work. *Nature* 507, 423–425. doi: 10.1038/507423a

Perrone, F., Nguyen, H. P., Van Mossevelde, S., Moisse, M., Sieben, A., Santens, P., et al. (2017). Investigating the role of ALS genes CHCHD10 and TUBA4A in Belgian FTD-ALS spectrum patients. *Neurobiol. Aging* 51, 177.e9–177.e16. doi: 10.1016/j.neurobiolaging.2016.12.008

Perry, V. H., and Holmes, C. (2014). Microglial priming in neurodegenerative disease. *Nat. Rev. Neurol.* 10, 217–224. doi: 10.1038/nrneurol.2014.38

Philips, T., Bento-Abreu, A., Nonneman, A., Haeck, W., Staats, K., Geelen, V., et al. (2013). Oligodendrocyte dysfunction in the pathogenesis of amyotrophic lateral sclerosis. *Brain* 136, 471–482. doi: 10.1093/brain/aws339

Philips, T., and Rothstein, J. D. (2015). Rodent models of amyotrophic lateral sclerosis. *Curr. Protoc. Pharmacol.* 69, 5.67.1–5.67.21. doi: 10.1002/0471141755.ph0567s69

Piccione, E. A., Sletten, D. M., Staff, N. P., and Low, P. A. (2015). Autonomic system and ALS. *Muscle Nerve* 51, 676–679. doi: 10.1002/mus.24457

Pisharodi, M., and Nauta, H. J. (1985). An animal model for neuron-specific spinal cord lesions by the microinjection of N-methylaspartate, kainic acid, and quisqualic acid. *Appl. Neurophysiol.* 48, 226–233. doi: 10.1159/000101132

Polci, R., Peng, A., Chen, P.-L., Riley, D. J., and Chen, Y. (2004). NIMA-related protein kinase 1 is involved early in the ionizing radiation-induced DNA damage response. *Cancer Res.* 64, 8800–8803. doi: 10.1158/0008-5472.CAN-04-2243

Polymenidou, M., Lagier-Tourenne, C., Hutt, K. R., Huelga, S. C., Moran, J., Liang, T. Y., et al. (2011). Long pre-mRNA depletion and RNA missplicing contribute to neuronal vulnerability from loss of TDP-43. *Nat. Neurosci.* 14, 459–468. doi: 10.1038/nn.2779

Porta, S., Xu, Y., Restrepo, C. R., Kwong, L. K., Zhang, B., Brown, H. J., et al. (2018). Patient-derived frontotemporal lobar degeneration brain extracts induce formation and spreading of TDP-43 pathology in vivo. *Nat. Commun.* 9:4220. doi: 10.1038/s41467-018-06548-9

Porter, J. D., and Baker, R. S. (1996). Muscles of a different "color": the unusual properties of the extraocular muscles may predispose or protect them in neurogenic and myogenic disease. *Neurology* 46, 30–37. doi: 10.1212/wnl.46.1.30

Porter, R., and Lemon, R. (1993). *Corticospinal Function and Voluntary Movement*. Oxford: Clarendon Press.

Pottier, C., Bieniek, K. F., Finch, N., van de Vorst, M., Baker, M., Perkersen, R., et al. (2015). Whole-genome sequencing reveals important role for TBK1 and OPTN mutations in frontotemporal lobar degeneration without motor neuron disease. *Acta Neuropathol.* 130, 77–92. doi: 10.1007/s00401-015-1436-x

Pradat, P.-F., Salachas, F., Lacomblez, L., Patte, N., Leforestier, N., Gaura, V., et al. (2002). Association of chorea and motor neuron disease. *Mov. Disord.* 17, 419–420. doi: 10.1002/mds.10039

Pramatarova, A., Laganière, J., Roussel, J., Brisebois, K., and Rouleau, G. A. (2001). Neuron-specific expression of mutant superoxide dismutase 1 in transgenic mice does not lead to motor impairment. *J. Neurosci.* 21, 3369–3374. doi: 10.1523/jneurosci.21-10-03369.2001

Proudfoot, M., Menke, R. A. L., Sharma, R., Berna, C. M., Hicks, S. L., Kennard, C., et al. (2015). Eye-tracking in amyotrophic lateral sclerosis: a longitudinal study of saccadic and cognitive tasks. *Amyotroph. Lateral Scler. Frontotemporal Degener.* 17, 101–111. doi: 10.3109/21678421.2015.1054292

Prudencio, M., Belzil, V. V., Batra, R., Ross, C. A., Gendron, T. F., Pregent, L. J., et al. (2015). Distinct brain transcriptome profiles in C9orf72-associated and sporadic ALS. *Nat. Neurosci.* 18, 1175–1182. doi: 10.1038/nn.4065

Pullen, A. H., and Athanasiou, D. (2009). Increase in presynaptic territory of C-terminals on lumbar motoneurons of G93A SOD1 mice during disease progression. *Eur. J. Neurosci.* 29, 551–561. doi: 10.1111/j.1460-9568.2008.06602.x

Puls, I., Jonnakuty, C., LaMonte, B. H., Holzbaur, E. L. F., Tokito, M., Mann, E., et al. (2003). Mutant dynactin in motor neuron disease. *Nat. Genet.* 33, 455–456. doi: 10.1038/ng1123

Pun, S., Santos, A. F., Saxena, S., Xu, L., and Caroni, P. (2006). Selective vulnerability and pruning of phasic motoneuron axons in motoneuron disease alleviated by CNTF. *Nat. Neurosci.* 9, 408–419. doi: 10.1038/nn1653

Purves, D., Augustine, G. J., Fitzpatrick, D., Katz, L. C., LaMantia, A.-S., McNamara, J. O., et al. (2001). *Functional Properties of the Na+/K+ Pump*. Available at: https://www.ncbi.nlm.nih.gov/books/NBK10857/ (accessed December 14, 2018).

Ramírez, O. A., and Couve, A. (2011). The endoplasmic reticulum and protein trafficking in dendrites and axons. *Trends Cell Biol.* 21, 219–227. doi: 10.1016/j.tcb.2010.12.003

Ramírez-Jarquín, U. N., Lazo-Gómez, R., Tovar-Y-Romo, L. B., and Tapia, R. (2014). Spinal inhibitory circuits and their role in motor neuron degeneration. *Neuropharmacology* 82, 101–107. doi: 10.1016/j.neuropharm.2013.10.003

Ramírez-Jarquín, U. N., and Tapia, R. (2018). Excitatory and inhibitory neuronal circuits in the spinal cord and their role in the control of motor neuron function and degeneration. *ACS Chem. Neurosci.* 9, 211–216. doi: 10.1021/acschemneuro.7b00503

Rathelot, J.-A., and Strick, P. L. (2009). Subdivisions of primary motor cortex based on cortico-motoneuronal cells. *Proc. Natl. Acad. Sci. U.S.A.* 106, 918–923. doi: 10.1073/pnas.0808362106

Ravits, J., Paul, P., and Jorg, C. (2007). Focality of upper and lower motor neuron degeneration at the clinical onset of ALS. *Neurology* 68:1571. doi: 10.1212/01.wnl.0000260965.20021.47

Ravits, J. M., and La Spada, A. R. (2009). ALS motor phenotype heterogeneity, focality, and spread: deconstructing motor neuron degeneration. *Neurology* 73, 805–811. doi: 10.1212/WNL.0b013e3181b6bbbd

Reddy, L. V., Koirala, S., Sugiura, Y., Herrera, A. A., and Ko, C. P. (2003). Glial cells maintain synaptic structure and function and promote development of the neuromuscular junction in vivo. *Neuron* 40, 563–580. doi: 10.1016/s0896-6273(03)00682-2

Reddy, P. H., and Beal, M. F. (2008). Amyloid beta, mitochondrial dysfunction and synaptic damage: implications for cognitive decline in aging and Alzheimer's disease. *Trends Mol. Med.* 14, 45–53. doi: 10.1016/j.molmed.2007.12.002

Renton, A. E., Chiò, A., and Traynor, B. J. (2014). State of play in amyotrophic lateral sclerosis genetics. *Nat. Neurosci.* 17, 17–23. doi: 10.1038/nn.3584

Renton, A. E., Majounie, E., Waite, A., Simón-Sánchez, J., Rollinson, S., Gibbs, J. R., et al. (2011). A hexanucleotide repeat expansion in C9ORF72 is the cause of chromosome 9p21-Linked ALS-FTD. *Neuron* 72, 257–268. doi: 10.1016/j.neuron.2011.09.010

Reynolds, M. L., and Woolf, C. J. (1992). Terminal Schwann cells elaborate extensive processes following denervation of the motor endplate. *J. Neurocytol.* 21, 50–66. doi: 10.1007/bf01206897

Riehle, A., Wirtssohn, S., Grün, S., and Brochier, T. (2013). Mapping the spatio-temporal structure of motor cortical LFP and spiking activities during reach-to-grasp movements. *Front. Neural Circ.* 7:48. doi: 10.3389/fncir.2013.00048

Ripps, M. E., Huntley, G. W., Hof, P. R., Morrison, J. H., and Gordon, J. W. (1995). Transgenic mice expressing an altered murine superoxide dismutase gene provide an animal model of amyotrophic lateral sclerosis. *Proc. Natl. Acad. Sci. U.S.A.* 92, 689–693. doi: 10.1073/pnas.92.3.689

Rizzardini, M., Lupi, M., Bernasconi, S., Mangolini, A., and Cantoni, L. (2003). Mitochondrial dysfunction and death in motor neurons exposed to the glutathione-depleting agent ethacrynic acid. *J. Neurol. Sci.* 207, 51–58. doi: 10.1016/s0022-510x(02)00357-x

Robertson, J., Doroudchi, M. M., Nguyen, M. D., Durham, H. D., Strong, M. J., Shaw, G., et al. (2003). A neurotoxic peripherin splice variant in a mouse model of ALS. *J. Cell Biol.* 160, 939–949. doi: 10.1083/jcb.200205027

Robinson, D. A. (1970). Oculomotor unit behavior in the monkey. *J. Neurophysiol.* 33, 393–403. doi: 10.1152/jn.1970.33.3.393

Rochat, C., Bernard-Marissal, N., and Schneider, B. L. (2016). *Selective Vulnerability of Neuronal Subtypes in ALS: A Fertile Ground for the Identification of Therapeutic Targets*. London: IntechOpen.

Rojas, F., Cortes, N., Abarzua, S., Dyrda, A., and van Zundert, B. (2014). Astrocytes expressing mutant SOD1 and TDP43 trigger motoneuron death that is mediated via sodium channels and nitroxidative stress. *Front. Cell Neurosci.* 8:24. doi: 10.3389/fncel.2014.00024

Roos, A., Kollipara, L., Buchkremer, S., Labisch, T., Brauers, E., Gatz, C., et al. (2016). Cellular signature of SIL1 depletion: disease pathogenesis due to alterations in protein composition beyond the ER machinery. *Mol. Neurobiol.* 53, 5527–5541. doi: 10.1007/s12035-015-9456-z

Roppolo, J. R., Nadelhaft, I., and de Groat, W. C. (1985). The organization of pudendal motoneurons and primary afferent projections in the spinal cord of the rhesus monkey revealed by horseradish peroxidase. *J. Comp. Neurol.* 234, 475–488. doi: 10.1002/cne.902340406

Rosen, D. R., Siddique, T., Patterson, D., Figlewicz, D. A., Sapp, P., Hentati, A., et al. (1993). Mutations in Cu/Zn superoxide dismutase gene are associated with familial amyotrophic lateral sclerosis. *Nature* 362, 59–62. doi: 10.1038/362059a0

Ross, O. A., Rutherford, N. J., Baker, M., Soto-Ortolaza, A. I., Carrasquillo, M. M., DeJesus-Hernandez, M., et al. (2011). Ataxin-2 repeat-length variation and neurodegeneration. *Hum. Mol. Genet.* 20, 3207–3212. doi: 10.1093/hmg/ddr227

Rouleau, G. A., Clark, A. W., Rooke, K., Pramatarova, A., Krizus, A., Suchowersky, O., et al. (1996). SOD1 mutation is assosiated with accumulation of neurofilaments in amyotrophic lateral scelaries. *Ann. Neurol.* 39, 128–131. doi: 10.1002/ana.410390119

Rozas, P., Bargsted, L., Martínez, F., Hetz, C., and Medinas, D. B. (2017). The ER proteostasis network in ALS: determining the differential motoneuron vulnerability. *Neurosci. Lett.* 636, 9–15. doi: 10.1016/j.neulet.2016.04.066

Rubino, E., Rainero, I., Chiò, A., Rogaeva, E., Galimberti, D., Fenoglio, P., et al. (2012). SQSTM1 mutations in frontotemporal lobar degeneration and amyotrophic lateral sclerosis. *Neurology* 79, 1556–1562. doi: 10.1212/WNL.0b013e31826e25df

Ruegsegger, C., Maharjan, N., Goswami, A., Filézac de L'Etang, A., Weis, J., Troost, D., et al. (2016). Aberrant association of misfolded SOD1 with Na+/K+ATPase-α3 impairs its activity and contributes to motor neuron vulnerability in ALS. *Acta Neuropathol.* 131, 427–451. doi: 10.1007/s00401-015-1510-4

Ruegsegger, C., and Saxena, S. (2016). Proteostasis impairment in ALS. *Brain Res.* 1648, 571–579. doi: 10.1016/j.brainres.2016.03.032

Rutherford, N. J., Heckman, M. G., Dejesus-Hernandez, M., Baker, M. C., Soto-Ortolaza, A. I., Rayaprolu, S., et al. (2012). Length of normal alleles of C9ORF72 GGGGCC repeat do not influence disease phenotype. *Neurobiol. Aging* 33, 2950.e5–2950.e7. doi: 10.1016/j.neurobiolaging.2012.07.005

Rutherford, N. J., Zhang, Y.-J., Baker, M., Gass, J. M., Finch, N. A., Xu, Y.-F., et al. (2008). Novel mutations in TARDBP (TDP-43) in patients with familial amyotrophic lateral sclerosis. *PLoS Genet.* 4:e1000193. doi: 10.1371/journal.pgen.1000193

Saccon, R. A., Bunton-Stasyshyn, R. K. A., Fisher, E. M. C., and Fratta, P. (2013). Is SOD1 loss of function involved in amyotrophic lateral sclerosis? *Brain* 136, 2342–2358. doi: 10.1093/brain/awt097

Sakowski, S. A., Schuyler, A. D., and Feldman, E. L. (2009). Insulin-like growth factor-I for the treatment of amyotrophic lateral sclerosis. *Amyotroph. Lateral Scler.* 10, 63–73. doi: 10.1080/17482960802160370

Salat, D. H., Buckner, R. L., Snyder, A. Z., Greve, D. N., Desikan, R. S. R., Busa, E., et al. (2004). Thinning of the cerebral cortex in aging. *Cereb. Cortex* 14, 721–730. doi: 10.1093/cercor/bhh032

Sasaki, S. (2010). Endoplasmic reticulum stress in motor neurons of the spinal cord in sporadic amyotrophic lateral sclerosis. *J. Neuropathol. Exp. Neurol.* 69, 346–355. doi: 10.1097/NEN.0b013e3181d44992

Sasaki, S., Horie, Y., and Iwata, M. (2007). Mitochondrial alterations in dorsal root ganglion cells in sporadic amyotrophic lateral sclerosis. *Acta Neuropathol.* 114, 633–639. doi: 10.1007/s00401-007-0299-1

Sasaki, S., and Iwata, M. (1996). Dendritic synapses of anterior horn neurons in amyotrophic lateral sclerosis: an ultrastructural study. *Acta Neuropathol.* 91, 278–283. doi: 10.1007/s004010050426

Sasaki, S., Warita, H., Komori, T., Murakami, T., Abe, K., and Iwata, M. (2006). Parvalbumin and calbindin D-28k immunoreactivity in transgenic mice with a G93A mutant SOD1 gene. *Brain Res.* 1083, 196–203. doi: 10.1016/j.brainres.2006.01.129

Sato, M., Mizuno, N., and Konishi, A. (1978). Localization of motoneurons innervating perineal muscles: a HRP study in cat. *Brain Res.* 140, 149–154. doi: 10.1016/0006-8993(78)90244-5

Saxena, S., Cabuy, E., and Caroni, P. (2009). A role for motoneuron subtype–selective ER stress in disease manifestations of FALS mice. *Nat. Neurosci.* 12, 627–636. doi: 10.1038/nn.2297

Saxena, S., Roselli, F., Singh, K., Leptien, K., Julien, J.-P., Gros-Louis, F., et al. (2013). Neuroprotection through excitability and mTOR required in ALS motoneurons to delay disease and extend survival. *Neuron* 80, 80–96. doi: 10.1016/j.neuron.2013.07.027

Schrøder, H. D., and Reske-Nielsen, E. (1984). Preservation of the nucleus X-pelvic floor motosystem in amyotrophic lateral sclerosis. *Clin. Neuropathol.* 3, 210–216.

Schwenk, B. M., Hartmann, H., Serdaroglu, A., Schludi, M. H., Hornburg, D., Meissner, F., et al. (2016). TDP-43 loss of function inhibits endosomal trafficking and alters trophic signaling in neurons. *EMBO J.* 35, 2350–2370. doi: 10.15252/embj.201694221

Scotter, E. L., Chen, H.-J., and Shaw, C. E. (2015). TDP-43 Proteinopathy and ALS: insights into disease mechanisms and therapeutic targets. *Neurotherapeutics* 12, 352–363. doi: 10.1007/s13311-015-0338-x

Seilhean, D., Cazeneuve, C., Thuriès, V., Russaouen, O., Millecamps, S., Salachas, F., et al. (2009). Accumulation of TDP-43 and alpha-actin in an amyotrophic lateral sclerosis patient with the K17I ANG mutation. *Acta Neuropathol.* 118, 561–573. doi: 10.1007/s00401-009-0545-9

Shahheydari, H., Ragagnin, A., Walker, A. K., Toth, R. P., Vidal, M., Jagaraj, C. J., et al. (2017). Protein quality control and the amyotrophic lateral sclerosis/frontotemporal dementia continuum. *Front. Mol. Neurosci.* 10:119. doi: 10.3389/fnmol.2017.00119

Shan, X., Chiang, P.-M., Price, D. L., and Wong, P. C. (2010). Altered distributions of Gemini of coiled bodies and mitochondria in motor neurons of TDP-43 transgenic mice. *Proc. Natl. Acad. Sci. U.S.A.* 107, 16325–16330. doi: 10.1073/pnas.1003459107

Sharma, A., Lyashchenko, A. K., Lu, L., Nasrabady, S. E., Elmaleh, M., Mendelsohn, M., et al. (2016). ALS-associated mutant FUS induces selective motor neuron degeneration through toxic gain of function. *Nat. Commun.* 7:10465. doi: 10.1038/ncomms10465

Shaunak, S., Orrell, R. W., O'Sullivan, E., Hawken, M. B., Lane, R. J., Henderson, L., et al. (1995). Oculomotor function in amyotrophic lateral sclerosis: evidence for frontal impairment. *Ann. Neurol.* 38, 38–44. doi: 10.1002/ana.410380109

Shaw, P. J., Ince, P. G., Falkous, G., and Mantle, D. (1995). Oxidative damage to protein in sporadic motor neuron disease spinal cord. *Ann. Neurol.* 38, 691–695. doi: 10.1002/ana.410380424

Shi, P., Ström, A.-L., Gal, J., and Zhu, H. (2010). Effects of ALS-related SOD1 mutants on dynein- and KIF5-mediated retrograde and anterograde axonal transport. *Biochim. Biophys. Acta* 1802, 707–716. doi: 10.1016/j.bbadis.2010.05.008

Shibata, N., Nagai, R., Uchida, K., Horiuchi, S., Yamada, S., Hirano, A., et al. (2001). Morphological evidence for lipid peroxidation and protein glycoxidation in spinal cords from sporadic amyotrophic lateral sclerosis patients. *Brain Res.* 917, 97–104. doi: 10.1016/s0006-8993(01)02926-2

Shin, J. H., and Lee, J. K. (2013). "Multiple Routes of Motor Neuron Degeneration in ALS," in *Current Advances in Amyotrophic Lateral Sclerosis*, ed. A. Estévez (London: Intechopen). doi: 10.1080/14660820050515395

Shirvan, A., Kimron, M., Holdengreber, V., Ziv, I., Ben-Shaul, Y., Melamed, S., et al. (2002). Anti-semaphorin 3A antibodies rescue retinal ganglion cells from cell death following optic nerve axotomy. *J. Biol. Chem.* 277, 49799–49807. doi: 10.1074/jbc.M204793200

Shneider, N. A., Brown, M. N., Smith, C. A., Pickel, J., and Alvarez, F. J. (2009). Gamma motor neurons express distinct genetic markers at birth and require muscle spindle-derived GDNF for postnatal survival. *Neural Dev.* 4:42. doi: 10.1186/1749-8104-4-42

Shoenfeld, L., Westenbroek, R. E., Fisher, E., Quinlan, K. A., Tysseling, V. M., Powers, R. K., et al. (2014). Soma size and Cav1.3 channel expression in vulnerable and resistant motoneuron populations of the SOD1G93A mouse model of ALS. *Physiol. Rep.* 2:e12113. doi: 10.14814/phy2.12113

Siddle, K., Ursø, B., Niesler, C. A., Cope, D. L., Molina, L., Surinya, K. H., et al. (2001). Specificity in ligand binding and intracellular signalling by insulin and insulin-like growth factor receptors. *Biochem. Soc. Trans.* 29, 513–525. doi: 10.1042/bst0290513

Sloan, S. A., and Barres, B. A. (2014). Mechanisms of astrocyte development and their contributions to neurodevelopmental disorders. *Curr. Opin. Neurobiol.* 27, 75–81. doi: 10.1016/j.conb.2014.03.005

Smethurst, P., Newcombe, J., Troakes, C., Simone, R., Chen, Y.-R., Patani, R., et al. (2016). In vitro prion-like behaviour of TDP-43 in ALS. *Neurobiol. Dis.* 96, 236–247. doi: 10.1016/j.nbd.2016.08.007

Smith, B. N., Ticozzi, N., Fallini, C., Gkazi, A. S., Topp, S., Kenna, K. P., et al. (2014a). Exome-wide rare variant analysis identifies TUBA4A mutations associated with familial ALS. *Neuron* 84, 324–331. doi: 10.1016/j.neuron.2014.09.027

Smith, B. N., Vance, C., Scotter, E. L., Troakes, C., Wong, C. H., Topp, S., et al. (2014b). Novel mutations support a role for Profilin1 in the pathogenesis of ALS. *Neurobiol. Aging* 36, 1602.e17–1602.e27. doi: 10.1016/j.neurobiolaging.2014.10.032

So, E., Mitchell, J. C., Memmi, C., Chennell, G., Vizcay-Barrena, G., Allison, L., et al. (2018). Mitochondrial abnormalities and disruption of the neuromuscular junction precede the clinical phenotype and motor neuron loss in hFUSWT transgenic mice. *Hum. Mol. Genet.* 27, 463–474. doi: 10.1093/hmg/ddx415

Son, Y. J., and Thompson, W. J. (1995). Schwann cell processes guide regeneration of peripheral axons. *Neuron* 14, 125–132. doi: 10.1016/0896-6273(95)90246-5

Sonne, J., and Lopez-Ojeda, W. (2018). "Neuroanatomy, Cranial Nerve," in *StatPearls*, ed. M. Varacallo (Treasure Island FL: StatPearls Publishing).

Soo, K. Y., Halloran, M., Sundaramoorthy, V., Parakh, S., Toth, R. P., Southam, K. A., et al. (2015). Rab1-dependent ER-Golgi transport dysfunction is a common pathogenic mechanism in SOD1, TDP-43 and FUS-associated ALS. *Acta Neuropathol.* 130, 679–697. doi: 10.1007/s00401-015-1468-2

Sorond, F. A., Cruz-Almeida, Y., Clark, D. J., Viswanathan, A., Scherzer, C. R., De Jager, P., et al. (2015). Aging, the central nervous system, and mobility in older adults: neural mechanisms of mobility impairment. *J. Gerontol. A Biol. Sci. Med. Sci.* 70, 1526–1532. doi: 10.1093/gerona/glv130

Sotelo-Silveira, J. R., Lepanto, P., Elizondo, V., Horjales, S., Palacios, F., Martinez-Palma, L., et al. (2009). Axonal mitochondrial clusters containing mutant SOD1 in transgenic models of ALS. *Antioxid. Redox Signal.* 11, 1535–1545. doi: 10.1089/ars.2009.2614

Soto, C. (2012). Transmissible proteins: expanding the prion heresy. *Cell* 149, 968–977. doi: 10.1016/j.cell.2012.05.007

Spiller, K. J., Cheung, C. J., Restrepo, C. R., Kwong, L. K., Stieber, A. M., Trojanowski, J. Q., et al. (2016a). Selective motor neuron resistance and recovery in a new inducible mouse model of TDP-43 proteinopathy. *J. Neurosci.* 36, 7707–7717. doi: 10.1523/JNEUROSCI.1457-16.2016

Spiller, K. J., Restrepo, C. R., Khan, T., Stieber, A. M., Kwong, L. K., Trojanowski, J. Q., et al. (2016b). Progression of motor neuron disease is accelerated and the ability to recover is compromised with advanced age in rNLS8 mice. *Acta Neuropathol. Commun.* 4:105. doi: 10.1186/s40478-016-0377-5

Spiller, K. J., Khan, T., Dominique, M. A., Restrepo, C. R., Cotton-Samuel, D., Levitan, M., et al. (2019). Reduction of matrix metalloproteinase 9 (MMP-9) protects motor neurons from TDP-43-triggered death in rNLS8 mice. *Neurobiol. Dis.* 124, 133–140. doi: 10.1016/j.nbd.2018.11.013

Spiller, K. J., Restrepo, C. R., Khan, T., Dominique, M. A., Fang, T. C., Canter, R. G., et al. (2018). Microglia-mediated recovery from ALS-relevant motor neuron degeneration in a mouse model of TDP-43 proteinopathy. *Nat. Neurosci.* 21, 329–340. doi: 10.1038/s41593-018-0083-7

Sreedharan, J., Blair, I. P., Tripathi, V. B., Hu, X., Vance, C., Rogelj, B., et al. (2008). TDP-43 mutations in familial and sporadic amyotrophic lateral sclerosis. *Science* 319, 1668–1672. doi: 10.1126/science.1154584

Stephens, B., Guiloff, R. J., Navarrete, R., Newman, P., Nikhar, N., and Lewis, P. (2006). Widespread loss of neuronal populations in the spinal ventral horn in sporadic motor neuron disease. A morphometric study. *J. Neurol. Sci.* 244, 41–58. doi: 10.1016/j.jns.2005.12.003

Stephens, B., Navarrete, R., and Guiloff, R. J. (2001). Ubiquitin immunoreactivity in presumed spinal interneurones in motor neurone disease. *Neuropathol. Appl. Neurobiol.* 27, 352–361. doi: 10.1046/j.1365-2990.2001.00354.x

Stifani, N. (2014). Motor neurons and the generation of spinal motor neuron diversity. *Front. Cell Neurosci.* 8:293. doi: 10.3389/fncel.2014.00293

Strong, M. J., and Yang, W. (2011). The frontotemporal syndromes of ALS. clinicopathological correlates. *J. Mol. Neurosci.* 45, 648–655. doi: 10.1007/s12031-011-9609-0

Suga, A., Mizota, A., Kato, M., Kuniyoshi, K., Yoshitake, K., Sultan, W., et al. (2016). Identification of novel mutations in the LRR-Cap domain of C21orf2 in japanese patients with retinitis pigmentosa and cone-rod dystrophy. *Invest. Ophthalmol. Vis. Sci.* 57, 4255–4263. doi: 10.1167/iovs.16-19450

Suh, E., Lee, E. B., Neal, D., Wood, E. M., Toledo, J. B., Rennert, L., et al. (2015). Semi-automated quantification of C9orf72 expansion size reveals inverse correlation between hexanucleotide repeat number and disease duration in frontotemporal degeneration. *Acta Neuropathol.* 130, 363–372. doi: 10.1007/s00401-015-1445-9

Sun, H., Kawahara, Y., Ito, K., Kanazawa, I., and Kwak, S. (2005). Expression profile of AMPA receptor subunit mRNA in single adult rat brain and spinal cord neurons in situ. *Neurosci. Res.* 52, 228–234. doi: 10.1016/j.neures.2005.03.008

Sun, N., Youle, R. J., and Finkel, T. (2016). The mitochondrial basis of aging. *Mol. Cell* 61, 654–666. doi: 10.1016/j.molcel.2016.01.028

Sun, S., Sun, Y., Ling, S.-C., Ferraiuolo, L., McAlonis-Downes, M., Zou, Y., et al. (2015). Translational profiling identifies a cascade of damage initiated in motor neurons and spreading to glia in mutant SOD1-mediated ALS. *Proc. Natl. Acad. Sci. U.S.A.* 112, E6993–E7002. doi: 10.1073/pnas.1520639112

Sundaramoorthy, V., Walker, A. K., Yerbury, J., Soo, K. Y., Farg, M. A., Hoang, V., et al. (2013). Extracellular wildtype and mutant SOD1 induces ER-Golgi pathology characteristic of amyotrophic lateral sclerosis in neuronal cells. *Cell. Mol. Life Sci.* 70, 4181–4195. doi: 10.1007/s00018-013-1385-2

Suzuki, H., Kanekura, K., Levine, T. P., Kohno, K., Olkkonen, V. M., Aiso, S., et al. (2009). ALS-linked P56S-VAPB, an aggregated loss-of-function mutant of VAPB, predisposes motor neurons to ER stress-related death by inducing

aggregation of co-expressed wild-type VAPB. *J. Neurochem.* 108, 973–985. doi: 10.1111/j.0022-3042.2008.05857.x

Swarup, V., Phaneuf, D., Dupré, N., Petri, S., Strong, M., Kriz, J., et al. (2011). Deregulation of TDP-43 in amyotrophic lateral sclerosis triggers nuclear factor κB-mediated pathogenic pathways. *J. Exp. Med.* 208, 2429–2447. doi: 10.1084/jem.20111313

Swash, M., and Fox, K. P. (1972). The effect of age on human skeletal muscle. studies of the morphology and innervation of muscle spindles. *J. Neurol. Sci.* 16, 417–432. doi: 10.1016/0022-510x(72)90048-2

Swerdlow, R. H., Parks, J. K., Cassarino, D. S., Trimmer, P. A., Miller, S. W., Maguire, D. J., et al. (1998). Mitochondria in sporadic amyotrophic lateral sclerosis. *Exp. Neurol.* 153, 135–142. doi: 10.1006/exnr.1998.6866

Swinnen, B., and Robberecht, W. (2014). The phenotypic variability of amyotrophic lateral sclerosis. *Nat. Rev. Neurol.* 10, 661–670. doi: 10.1038/nrneurol.2014.184

Synofzik, M., Maetzler, W., Grehl, T., Prudlo, J., vom Hagen, J. M., Haack, T., et al. (2012). Screening in ALS and FTD patients reveals 3 novel UBQLN2 mutations outside the PXX domain and a pure FTD phenotype. *Neurobiol. Aging* 33:2949.e13–2949.e17. doi: 10.1016/j.neurobiolaging.2012.07.002

Tan, C.-F., Eguchi, H., Tagawa, A., Onodera, O., Iwasaki, T., Tsujino, A., et al. (2007). TDP-43 immunoreactivity in neuronal inclusions in familial amyotrophic lateral sclerosis with or without SOD1 gene mutation. *Acta Neuropathol.* 113, 535–542. doi: 10.1007/s00401-007-0206-9

Tang, C. W., Maya-Mendoza, A., Martin, C., Zeng, K., Chen, S., Feret, D., et al. (2008). The integrity of a lamin-B1-dependent nucleoskeleton is a fundamental determinant of RNA synthesis in human cells. *J. Cell Sci.* 121, 1014–1024. doi: 10.1242/jcs.020982

Tank, E. M., Figueroa-Romero, C., Hinder, L. M., Bedi, K., Archbold, H. C., Li, X., et al. (2018). Abnormal RNA stability in amyotrophic lateral sclerosis. *Nat. Commun.* 9:2845. doi: 10.1038/s41467-018-05049-z

Tartaglia, M. C., Rowe, A., Findlater, K., Orange, J. B., Grace, G., and Strong, M. J. (2007). Differentiation between primary lateral sclerosis and amyotrophic lateral sclerosis: examination of symptoms and signs at disease onset and during follow-up. *Arch. Neurol.* 64, 232–236. doi: 10.1001/archneur.64.2.232

Tateno, M., Sadakata, H., Tanaka, M., Itohara, S., Shin, R.-M., Miura, M., et al. (2004). Calcium-permeable AMPA receptors promote misfolding of mutant SOD1 protein and development of amyotrophic lateral sclerosis in a transgenic mouse model. *Hum. Mol. Genet.* 13, 2183–2196. doi: 10.1093/hmg/ddh246

Taylor, J. P., Brown, R. H., and Cleveland, D. W. (2016). Decoding ALS: from genes to mechanism. *Nature* 539, 197–206. doi: 10.1038/nature20413

Teyssou, E., Chartier, L., Amador, M.-D.-M., Lam, R., Lautrette, G., Nicol, M., et al. (2017). Novel UBQLN2 mutations linked to amyotrophic lateral sclerosis and atypical hereditary spastic paraplegia phenotype through defective HSP70-mediated proteolysis. *Neurobiol. Aging* 58, 239.e11–239.e20. doi: 10.1016/j.neurobiolaging.2017.06.018

Thomas, E. V., Fenton, W. A., McGrath, J., and Horwich, A. L. (2017). Transfer of pathogenic and nonpathogenic cytosolic proteins between spinal cord motor neurons in vivo in chimeric mice. *Proc. Natl. Acad. Sci. U.S.A.* 114, E3139–E3148. doi: 10.1073/pnas.1701465114

Thomsen, G. M., Gowing, G., Latter, J., Chen, M., Vit, J.-P., Staggenborg, K., et al. (2014). Delayed disease onset and extended survival in the SOD1G93A rat model of amyotrophic lateral sclerosis after suppression of mutant SOD1 in the motor cortex. *J. Neurosci.* 34, 15587–15600. doi: 10.1523/JNEUROSCI.2037-14.2014

Ticozzi, N., Vance, C., LeClerc, A. L., Keagle, P., Glass, J. D., McKenna-Yasek, D., et al. (2011). Mutational analysis reveals the FUS homolog TAF15 as a candidate gene for familial amyotrophic lateral sclerosis. *Am. J. Med. Genet.* 156, 285–290. doi: 10.1002/ajmg.b.31158

Tong, J., Huang, C., Bi, F., Wu, Q., Huang, B., Liu, X., et al. (2013). Expression of ALS-linked TDP-43 mutant in astrocytes causes non-cell-autonomous motor neuron death in rats. *EMBO J.* 32, 1917–1926. doi: 10.1038/emboj.2013.122

Torres-Torrelo, J., Rodríguez-Rosell, D., Nunez-Abades, P., Carrascal, L., and Torres, B. (2012). Glutamate modulates the firing rate in oculomotor nucleus motoneurons as a function of the recruitment threshold current. *J. Physiol.* 590, 3113–3127. doi: 10.1113/jphysiol.2011.226985

Tsang, C. K., Liu, Y., Thomas, J., Zhang, Y., and Zheng, X. F. S. (2014). Superoxide dismutase 1 acts as a nuclear transcription factor to regulate oxidative stress resistance. *Nat. Comm.* 5:3446. doi: 10.1038/ncomms4446

Tsermentseli, S., Leigh, P. N., and Goldstein, L. H. (2012). The anatomy of cognitive impairment in amyotrophic lateral sclerosis: more than frontal lobe dysfunction. *Cortex* 48, 166–182. doi: 10.1016/j.cortex.2011.02.004

Turner, M. R., Eisen, A., Kiernan, M. C., Ravits, J., and Swash, M. (2018). Kinnier Wilson's puzzling features of amyotrophic lateral sclerosis. *J. Neurol. Neurosurg. Psychiatry* 89, 657–666. doi: 10.1136/jnnp-2017-317217

Ulfhake, B., and Kellerth, J.-O. (1981). A quantitative light microscopic study of the dendrites of cat spinal α-motoneurons after intracellular staining with horseradish peroxidase. *J. Comp. Neurol.* 202, 571–583. doi: 10.1002/cne.902020409

Ullian, E. M., Christopherson, K. S., and Barres, B. A. (2004). Role for glia in synaptogenesis. *Glia* 47, 209–216. doi: 10.1002/glia.20082

Urca, G., and Urca, R. (1990). Neurotoxic effects of excitatory amino acids in the mouse spinal cord: quisqualate and kainate but not N-methyl-l-aspartate induce permanent neural damage. *Brain Res.* 529, 7–15. doi: 10.1016/0006-8993(90)90805-L

Urushitani, M., Shimohama, S., Kihara, T., Sawada, H., Akaike, A., Ibi, M., et al. (1998). Mechanism of selective motor neuronal death after exposure of spinal cord to glutamate: involvement of glutamate-induced nitric oxide in motor neuron toxicity and nonmotor neuron protection. *Ann. Neurol.* 44, 796–807. doi: 10.1002/ana.410440514

Valdez, G., Tapia, J. C., Lichtman, J. W., Fox, M. A., and Sanes, J. R. (2012). Shared resistance to aging and ALS in neuromuscular junctions of specific muscles. *PLoS One* 7:e34640. doi: 10.1371/journal.pone.0034640

Valori, C. F., Brambilla, L., Martorana, F., and Rossi, D. (2014). The multifaceted role of glial cells in amyotrophic lateral sclerosis. *Cell. Mol. Life Sci.* 71, 287–297. doi: 10.1007/s00018-013-1429-7

Van, L. D. B., and Robberecht, W. (2000). Different receptors mediate motor neuron death induced by short and long exposures to excitotoxicity. *Brain Res. Bull.* 53, 383–388. doi: 10.1016/S0361-9230(00)00371-3

van Blitterswijk, M., DeJesus-Hernandez, M., Niemantsverdriet, E., Murray, M. E., Heckman, M. G., Diehl, N. N., et al. (2013). Association between repeat sizes and clinical and pathological characteristics in carriers of C9ORF72 repeat expansions (Xpansize-72): a cross-sectional cohort study. *Lancet Neurol.* 12, 978–988. doi: 10.1016/S1474-4422(13)70210-2

van Blitterswijk, M., van Es, M. A., Hennekam, E. A. M., Dooijes, D., van Rheenen, W., Medic, J., et al. (2012). Evidence for an oligogenic basis of amyotrophic lateral sclerosis. *Hum. Mol. Genet.* 21, 3776–3784. doi: 10.1093/hmg/dds199

Van Deerlin, V. M., Leverenz, J. B., Bekris, L. M., Bird, T. D., Yuan, W., Elman, L. B., et al. (2008). TARDBP mutations in amyotrophic lateral sclerosis with TDP-43 neuropathology: a genetic and histopathological analysis. *Lancet Neurol.* 7, 409–416. doi: 10.1016/S1474-4422(08)70071-1

Van Den Bosch, L., Van Damme, P., Bogaert, E., and Robberecht, W. (2006). The role of excitotoxicity in the pathogenesis of amyotrophic lateral sclerosis. *Biochim. Biophys. Acta* 1762, 1068–1082. doi: 10.1016/j.bbadis.2006.05.002

van der Graaff, M. M., de Jong, J. M. B. V., Baas, F., and de Visser, M. (2009). Upper motor neuron and extra-motor neuron involvement in amyotrophic lateral sclerosis: a clinical and brain imaging review. *Neuromuscul. Disord.* 19, 53–58. doi: 10.1016/j.nmd.2008.10.002

van der Zee, J., Gijselinck, I., Dillen, L., Van Langenhove, T., Theuns, J., Engelborghs, S., et al. (2013). A pan-European study of the C9orf72 repeat associated with FTLD: geographic prevalence, genomic instability, and intermediate repeats. *Hum. Mutat.* 34, 363–373. doi: 10.1002/humu.22244

Van Hoecke, A., Schoonaert, L., Lemmens, R., Timmers, M., Staats, K. A., Laird, A. S., et al. (2012). EPHA4 is a disease modifier of amyotrophic lateral sclerosis in animal models and in humans. *Nat. Med.* 18, 1418–1422. doi: 10.1038/nm.2901

van Rheenen, W., Shatunov, A., Dekker, A. M., McLaughlin, R. L., Diekstra, F. P., Pulit, S. L., et al. (2016). Genome-wide association analyses identify new risk variants and the genetic architecture of amyotrophic lateral sclerosis. *Nat. Genet.* 48, 1043–1048. doi: 10.1038/ng.3622

Vance, C., Rogelj, B., Hortobágyi, T., De Vos, K. J., Nishimura, A. L., Sreedharan, J., et al. (2009). Mutations in FUS, an RNA processing protein, cause familial amyotrophic lateral sclerosis type 6. *Science* 323, 1208–1211. doi: 10.1126/science.1165942

Vande Velde, C., McDonald, K. K., Boukhedimi, Y., McAlonis-Downes, M., Lobsiger, C. S., Bel Hadj, S., et al. (2011). Misfolded SOD1 associated with motor neuron mitochondria alters mitochondrial shape and distribution

prior to clinical onset. *PLoS One* 6:e22031. doi: 10.1371/journal.pone.0022031

Vandenberghe, W., Ihle, E. C., Patneau, D. K., Robberecht, W., and Brorson, J. R. (2000). AMPA receptor current density, not desensitization, predicts selective motoneuron vulnerability. *J. Neurosci.* 20, 7158–7166. doi: 10.1523/jneurosci.20-19-07158.2000

Vandoorne, T., De Bock, K., and Van Den Bosch, L. (2018). Energy metabolism in ALS: an underappreciated opportunity? *Acta Neuropathol.* 135, 489–509. doi: 10.1007/s00401-018-1835-x

Vanselow, B. K., and Keller, B. U. (2000). Calcium dynamics and buffering in oculomotor neurones from mouse that are particularly resistant during amyotrophic lateral sclerosis (ALS)-related motoneurone disease. *J. Physiol.* 525, 433–445. doi: 10.1111/j.1469-7793.2000.t01-1-00433.x

Varadi, A., Johnson-Cadwell, L. I., Cirulli, V., Yoon, Y., Allan, V. J., and Rutter, G. A. (2004). Cytoplasmic dynein regulates the subcellular distribution of mitochondria by controlling the recruitment of the fission factor dynamin-related protein-1. *J. Cell. Sci.* 117, 4389–4400. doi: 10.1242/jcs.01299

Veldink, J. H. (2017). ALS genetic epidemiology "How simplex is the genetic epidemiology of ALS?". *J. Neurol. Neurosurg. Psychiatry* 88:537. doi: 10.1136/jnnp-2016-315469

Venkova, K., Christov, A., Kamaluddin, Z., Kobalka, P., Siddiqui, S., and Hensley, K. (2014). Semaphorin 3A signaling through neuropilin-1 is an early trigger for distal axonopathy in the SOD1G93A mouse model of amyotrophic lateral sclerosis. *J. Neuropathol. Exp. Neurol.* 73, 702–713. doi: 10.1097/NEN.0000000000000086

Venugopal, S., Hsiao, C.-F., Sonoda, T., Wiedau-Pazos, M., and Chandler, S. H. (2015). Homeostatic dysregulation in membrane properties of masticatory motoneurons compared with oculomotor neurons in a mouse model for amyotrophic lateral sclerosis. *J. Neurosci.* 35, 707–720. doi: 10.1523/JNEUROSCI.1682-14.2015

Vijg, J., and Suh, Y. (2013). Genome instability and aging. *Annu. Rev. Physiol.* 75, 645–668. doi: 10.1146/annurev-physiol-030212-183715

Vincent, A. M., and Feldman, E. L. (2002). Control of cell survival by IGF signaling pathways. *Growth Horm. IGF Res.* 12, 193–197. doi: 10.1016/s1096-6374(02)00017-5

Vinsant, S., Mansfield, C., Jimenez-Moreno, R., Del Gaizo Moore, V., Yoshikawa, M., Hampton, T. G., et al. (2013). Characterization of early pathogenesis in the SOD1(G93A) mouse model of ALS: part II, results and discussion. *Brain Behav.* 3, 431–457. doi: 10.1002/brb3.142

Volterra, A., and Meldolesi, J. (2005). Astrocytes, from brain glue to communication elements: the revolution continues. *Nat. Rev. Neurosci.* 6, 626–640. doi: 10.1038/nrn1722

Vucic, S., and Kiernan, M. C. (2010). Upregulation of persistent sodium conductances in familial ALS. *J. Neurol. Neurosurg. Psychiatry* 81, 222–227. doi: 10.1136/jnnp.2009.183079

Vucic, S., Nicholson, G. A., and Kiernan, M. C. (2008). Cortical hyperexcitability may precede the onset of familial amyotrophic lateral sclerosis. *Brain* 131, 1540–1550. doi: 10.1093/brain/awn071

Wainger, B. J., Kiskinis, E., Mellin, C., Wiskow, O., Han, S. S. W., Sandoe, J., et al. (2014). Intrinsic membrane hyperexcitability of amyotrophic lateral sclerosis patient-derived motor neurons. *Cell Rep.* 7, 1–11. doi: 10.1016/j.celrep.2014.03.019

Walhout, R., Verstraete, E., van den Heuvel, M. P., Veldink, J. H., and van den Berg, L. H. (2018). Patterns of symptom development in patients with motor neuron disease. *Amyotroph. Lateral. Scler. Frontotemporal Degener.* 19, 21–28. doi: 10.1080/21678421.2017.1386688

Walker, A. K., Farg, M. A., Bye, C. R., McLean, C. A., Horne, M. K., and Atkin, J. D. (2010). Protein disulphide isomerase protects against protein aggregation and is S-nitrosylated in amyotrophic lateral sclerosis. *Brain* 133, 105–116. doi: 10.1093/brain/awp267

Walker, A. K., Soo, K. Y., Sundaramoorthy, V., Parakh, S., Ma, Y., Farg, M. A., et al. (2013). ALS-associated TDP-43 induces endoplasmic reticulum stress, which drives cytoplasmic TDP-43 accumulation and stress granule formation. *PLoS One* 8:e81170. doi: 10.1371/journal.pone.0081170

Walker, A. K., Spiller, K. J., Ge, G., Zheng, A., Xu, Y., Zhou, M., et al. (2015). Functional recovery in new mouse models of ALS/FTLD after clearance of pathological cytoplasmic TDP-43. *Acta Neuropathol.* 130, 643–660. doi: 10.1007/s00401-015-1460-x

Walker, C., Herranz-Martin, S., Karyka, E., Liao, C., Lewis, K., Elsayed, W., et al. (2017). C9orf72 expansion disrupts ATM-mediated chromosomal break repair. *Nat. Neurosci.* 20, 1225–1235. doi: 10.1038/nn.4604

Walter, P., and Ron, D. (2011). The unfolded protein response: from stress pathway to homeostatic regulation. *Science* 334, 1081–1086. doi: 10.1126/science.1209038

Wang, I.-F., Wu, L.-S., Chang, H.-Y., and Shen, C.-K. J. (2008). TDP-43, the signature protein of FTLD-U, is a neuronal activity-responsive factor. *J. Neurochem.* 105, 797–806. doi: 10.1111/j.1471-4159.2007.05190.x

Wang, L., Gutmann, D. H., and Roos, R. P. (2011). Astrocyte loss of mutant SOD1 delays ALS disease onset and progression in G85R transgenic mice. *Hum. Mol. Genet.* 20, 286–293. doi: 10.1093/hmg/ddq463

Wang, L., Pytel, P., Feltri, M. L., Wrabetz, L., and Roos, R. P. (2012). Selective knockdown of mutant SOD1 in Schwann cells ameliorates disease in G85R mutant SOD1 transgenic mice. *Neurobiol. Dis.* 48, 52–57. doi: 10.1016/j.nbd.2012.05.014

Wang, L., Sharma, K., Grisotti, G., and Roos, R. P. (2009). The effect of mutant SOD1 dismutase activity on non-cell autonomous degeneration in familial amyotrophic lateral sclerosis. *Neurobiol. Dis.* 35, 234–240. doi: 10.1016/j.nbd.2009.05.002

Wang, X., Zaidi, A., Pal, R., Garrett, A. S., Braceras, R., Chen, X., et al. (2009). Genomic and biochemical approaches in the discovery of mechanisms for selective neuronal vulnerability to oxidative stress. *BMC Neurosci.* 10:12. doi: 10.1186/1471-2202-10-12

Wang, W., Li, L., Lin, W.-L., Dickson, D. W., Petrucelli, L., Zhang, T., et al. (2013). The ALS disease-associated mutant TDP-43 impairs mitochondrial dynamics and function in motor neurons. *Hum. Mol. Genet.* 22, 4706–4719. doi: 10.1093/hmg/ddt319

Wang, X., and Michaelis, E. K. (2010). Selective neuronal vulnerability to oxidative stress in the brain. *Front. Aging Neurosci.* 2:12. doi: 10.3389/fnagi.2010.00012

Wegorzewska, I., Bell, S., Cairns, N. J., Miller, T. M., and Baloh, R. H. (2009). TDP-43 mutant transgenic mice develop features of ALS and frontotemporal lobar degeneration. *Proc. Natl. Acad. Sci. U.S.A.* 106, 18809–18814. doi: 10.1073/pnas.0908767106

Wehner, A. B., Abdesselem, H., Dickendesher, T. L., Imai, F., Yoshida, Y., Giger, R. J., et al. (2016). Semaphorin 3A is a retrograde cell death signal in developing sympathetic neurons. *Development* 143, 1560–1570. doi: 10.1242/dev.134627

Westbury, D. R. (1982). A comparison of the structures of α- and γ-spinal motoneurones of the cat. *J. Physiol.* 325, 79–91. doi: 10.1113/jphysiol.1982.sp014137

Westergard, T., Jensen, B. K., Wen, X., Cai, J., Kropf, E., Iacovitti, L., et al. (2016). Cell-to-cell transmission of dipeptide repeat proteins linked to C9orf72-ALS/FTD. *Cell Rep.* 17, 645–652. doi: 10.1016/j.celrep.2016.09.032

Wheway, G., Schmidts, M., Mans, D. A., Szymanska, K., Nguyen, T.-M. T., Racher, H., et al. (2015). An siRNA-based functional genomics screen for the identification of regulators of ciliogenesis and ciliopathy genes. *Nat. Cell Biol.* 17, 1074–1087. doi: 10.1038/ncb3201

Wiedemann, F. R., Manfredi, G., Mawrin, C., Beal, M. F., and Schon, E. A. (2002). Mitochondrial DNA and respiratory chain function in spinal cords of ALS patients. *J. Neurochem.* 80, 616–625. doi: 10.1046/j.0022-3042.2001.00731.x

Williams, K. L., Topp, S., Yang, S., Smith, B., Fifita, J. A., Warraich, S. T., et al. (2016). CCNF mutations in amyotrophic lateral sclerosis and frontotemporal dementia. *Nat. Commun.* 7:11253. doi: 10.1038/ncomms11253

Williams, K. L., Warraich, S. T., Yang, S., Solski, J. A., Fernando, R., Rouleau, G. A., et al. (2012). UBQLN2/ubiquilin 2 mutation and pathology in familial amyotrophic lateral sclerosis. *Neurobiol. Aging* 33, 2527.e3–2527.e10. doi: 10.1016/j.neurobiolaging.2012.05.008

Williamson, T. L., and Cleveland, D. W. (1999). Slowing of axonal transport is a very early event in the toxicity of ALS-linked SOD1 mutants to motor neurons. *Nat. Neurosci.* 2, 50–56. doi: 10.1038/4553

Woehlbier, U., Colombo, A., Saaranen, M. J., Pérez, V., Ojeda, J., Bustos, F. J., et al. (2016). ALS-linked protein disulfide isomerase variants cause

motor dysfunction. *EMBO J.* 35, 845–865. doi: 10.15252/embj.201592224

Wong, P. C., Pardo, C. A., Borchelt, D. R., Lee, M. K., Copeland, N. G., Jenkins, N. A., et al. (1995). An adverse property of a familial ALS-linked SOD1 mutation causes motor neuron disease characterized by vacuolar degeneration of mitochondria. *Neuron* 14, 1105–1116. doi: 10.1016/0896-6273(95)90259-7

Woollacott, I. O. C., and Mead, S. (2014). The C9ORF72 expansion mutation: gene structure, phenotypic and diagnostic issues. *Acta Neuropathol.* 127, 319–332. doi: 10.1007/s00401-014-1253-7

Wu, C.-H., Fallini, C., Ticozzi, N., Keagle, P. J., Sapp, P. C., Piotrowska, K., et al. (2012). Mutations in the profilin 1 gene cause familial amyotrophic lateral sclerosis. *Nature* 488, 499–503. doi: 10.1038/nature11280

Wu, D., Yu, W., Kishikawa, H., Folkerth, R. D., Iafrate, A. J., Shen, Y., et al. (2007). Angiogenin loss-of-function mutations in amyotrophic lateral sclerosis. *Ann. Neurol.* 62, 609–617. doi: 10.1002/ana.21221

Xu, W., and Lipscombe, D. (2001). Neuronal Ca(V)1.3*alpha(*1) L-type channels activate at relatively hyperpolarized membrane potentials and are incompletely inhibited by dihydropyridines. *J. Neurosci.* 21, 5944–5951. doi: 10.1523/jneurosci.21-16-05944.2001

Xu, Y.-F., Gendron, T. F., Zhang, Y.-J., Lin, W.-L., D'Alton, S., Sheng, H., et al. (2010). Wild-type human TDP-43 expression causes TDP-43 phosphorylation, mitochondrial aggregation, motor deficits, and early mortality in transgenic mice. *J. Neurosci.* 30, 10851–10859. doi: 10.1523/JNEUROSCI.1630-10.2010

Yagi, K., Kitazato, K. T., Uno, M., Tada, Y., Kinouchi, T., Shimada, K., et al. (2009). Edaravone, a free radical scavenger, inhibits MMP-9-related brain hemorrhage in rats treated with tissue plasminogen activator. *Stroke* 40, 626–631. doi: 10.1161/STROKEAHA.108.520262

Yamamoto, Y., Mizuno, R., Nishimura, T., Ogawa, Y., Yoshikawa, H., Fujimura, H., et al. (1994). Cloning and expression of myelin-associated oligodendrocytic basic protein. A novel basic protein constituting the central nervous system myelin. *J. Biol. Chem.* 269, 31725–31730.

Yamanaka, K., Chun, S. J., Boillee, S., Fujimori-Tonou, N., Yamashita, H., Gutmann, D. H., et al. (2008). Astrocytes as determinants of disease progression in inherited ALS. *Nat. Neurosci.* 11, 251–253. doi: 10.1038/nn2047

Yamashita, T., Hideyama, T., Hachiga, K., Teramoto, S., Takano, J., Iwata, N., et al. (2012). A role for calpain-dependent cleavage of TDP-43 in amyotrophic lateral sclerosis pathology. *Nat. Commun.* 3:1307. doi: 10.1038/ncomms2303

Yanagi, K. S., Wu, Z., Amaya, J., Chapkis, N., Duffy, A. M., Hajdarovic, K. H., et al. (2019). Meta-analysis of genetic modifiers reveals candidate dysregulated pathways in amyotrophic lateral sclerosis. *Neuroscience* 396, A3–A20. doi: 10.1016/j.neuroscience.2018.10.033

Yoshino, H., and Kimura, A. (2006). Investigation of the therapeutic effects of edaravone, a free radical scavenger, on amyotrophic lateral sclerosis (Phase II study). *Amyotroph. Lateral. Scler.* 7, 241–245. doi: 10.1080/17482960600881870

Young, N. A., Collins, C. E., and Kaas, J. H. (2013). Cell and neuron densities in the primary motor cortex of primates. *Front. Neural Circ.* 7:30. doi: 10.3389/fncir.2013.00030

Yu, J., Anderson, C. T., Kiritani, T., Sheets, P. L., Wokosin, D. L., Wood, L., et al. (2008). Local-circuit phenotypes of layer 5 neurons in motor-frontal cortex of YFP-H mice. *Front. Neural Circ.* 2:6. doi: 10.3389/neuro.04.006.2008

Zajac, F. E., and Faden, J. S. (1985). Relationship among recruitment order, axonal conduction velocity, and muscle-unit properties of type-identified motor units in cat plantaris muscle. *J. Neurophysiol.* 53, 1303–1322. doi: 10.1152/jn.1985.53.5.1303

Zengel, J. E., Reid, S. A., Sypert, G. W., and Munson, J. B. (1985). Membrane electrical properties and prediction of motor-unit type of medial gastrocnemius motoneurons in the cat. *J. Neurophysiol.* 53, 1323–1344. doi: 10.1152/jn.1985.53.5.1323

Zhang, F., Ström, A.-L., Fukada, K., Lee, S., Hayward, L. J., and Zhu, H. (2007). Interaction between familial amyotrophic lateral sclerosis (ALS)-linked SOD1 mutants and the dynein complex. *J. Biol. Chem.* 282, 16691–16699. doi: 10.1074/jbc.M609743200

Zhang, H., Tan, C.-F., Mori, F., Tanji, K., Kakita, A., Takahashi, H., et al. (2008). TDP-43-immunoreactive neuronal and glial inclusions in the neostriatum in amyotrophic lateral sclerosis with and without dementia. *Acta Neuropathol.* 115, 115–122. doi: 10.1007/s00401-007-0285-7

Zhang, K., Donnelly, C. J., Haeusler, A. R., Grima, J. C., Machamer, J. B., Steinwald, P., et al. (2015). The C9orf72 repeat expansion disrupts nucleocytoplasmic transport. *Nature* 525, 56–61. doi: 10.1038/nature14973

Zhang, M., Xi, Z., Zinman, L., Bruni, A. C., Maletta, R. G., Curcio, S. A. M., et al. (2015). Mutation analysis of CHCHD10 in different neurodegenerative diseases. *Brain* 138:e380. doi: 10.1093/brain/awv082

Zhang, Y.-J., Gendron, T. F., Grima, J. C., Sasaguri, H., Jansen-West, K., Xu, Y.-F., et al. (2016). C9ORF72 poly(GA) aggregates sequester and impair HR23 and nucleocytoplasmic transport proteins. *Nat. Neurosci.* 19, 668–677. doi: 10.1038/nn.4272

Zhou, Y., Liu, D., and Kaminski, H. J. (2011). Pitx2 regulates myosin heavy chain isoform expression and multi-innervation in extraocular muscle. *J. Physiol.* 589, 4601–4614. doi: 10.1113/jphysiol.2011.207076

Zou, Z.-Y., Zhou, Z.-R., Che, C.-H., Liu, C.-Y., He, R.-L., and Huang, H.-P. (2017). Genetic epidemiology of amyotrophic lateral sclerosis: a systematic review and meta-analysis. *J. Neurol. Neurosurg. Psychiatry* 88, 540–549. doi: 10.1136/jnnp-2016-315018

Zwiegers, P., Lee, G., and Shaw, C. A. (2014). Reduction in hSOD1 copy number significantly impacts ALS phenotype presentation in G37R (line 29) mice: implications for the assessment of putative therapeutic agents. *J. Negat. Results Biomed.* 13:14. doi: 10.1186/1477-5751-13-14

Conflict of Interest Statement: The authors declare that the research was conducted in the absence of any commercial or financial relationships that could be construed as a potential conflict of interest.

frontiers in Neuroscience

METHODS
published: 03 July 2019
doi: 10.3389/fnins.2019.00682

Empiric Methods to Account for Pre-analytical Variability in Digital Histopathology in Frontotemporal Lobar Degeneration

Lucia A. A. Giannini[1,2,3], Sharon X. Xie[4†], Claire Peterson[1,2], Cecilia Zhou[1,2], Edward B. Lee[5,6], David A. Wolk[6], Murray Grossman[2], John Q. Trojanowski[6,7], Corey T. McMillan[2] and David J. Irwin[1,2*†]*

[1] Penn Digital Neuropathology Laboratory, Department of Neurology, Perelman School of Medicine, University of Pennsylvania, Philadelphia, PA, United States, [2] Penn Frontotemporal Degeneration Center, Department of Neurology, Perelman School of Medicine, University of Pennsylvania, Philadelphia, PA, United States, [3] Department of Neurology, University Medical Center Groningen – University of Groningen, Groningen, Netherlands, [4] Department of Biostatistics, Epidemiology and Informatics, Perelman School of Medicine, University of Pennsylvania, Philadelphia, PA, United States, [5] Translational Neuropathology Research Laboratory, Department of Pathology and Laboratory Medicine, Perelman School of Medicine, University of Pennsylvania, Philadelphia, PA, United States, [6] Alzheimer's Disease Center, Department of Neurology, Perelman School of Medicine, University of Pennsylvania, Philadelphia, PA, United States, [7] Center for Neurodegenerative Disease Research, Department of Pathology and Laboratory Medicine, Perelman School of Medicine, University of Pennsylvania, Philadelphia, PA, United States

OPEN ACCESS

Edited by:
Annakaisa Haapasalo, University of Eastern Finland, Finland

Reviewed by:
Tuomas Rauramaa, University of Eastern Finland, Finland
Daniel Pirici, University of Medicine and Pharmacy of Craiova, Romania

***Correspondence:**
Sharon X. Xie
sxie@pennmedicine.upenn.edu
David J. Irwin
dirwin@pennmedicine.upenn.edu
† These authors have contributed equally to this work

Specialty section:
This article was submitted to Neurodegeneration, a section of the journal Frontiers in Neuroscience

Received: *30 January 2019*
Accepted: *14 June 2019*
Published: *03 July 2019*

Citation:
Giannini LAA, Xie SX, Peterson C, Zhou C, Lee EB, Wolk DA, Grossman M, Trojanowski JQ, McMillan CT and Irwin DJ (2019) Empiric Methods to Account for Pre-analytical Variability in Digital Histopathology in Frontotemporal Lobar Degeneration. Front. Neurosci. 13:682. doi: 10.3389/fnins.2019.00682

Digital pathology is increasingly prominent in neurodegenerative disease research, but variability in immunohistochemical staining intensity between staining batches prevents large-scale comparative studies. Here we provide a statistically rigorous method to account for staining batch effects in a large sample of brain tissue with frontotemporal lobar degeneration with tau inclusions (FTLD-Tau, $N = 39$) or TDP-43 inclusions (FTLD-TDP, $N = 53$). We analyzed the relationship between duplicate measurements of digital pathology, i.e., percent area occupied by pathology (%AO) for grey matter (GM) and white matter (WM), from two distinct staining batches. We found a significant difference in duplicate measurements from distinct staining batches in FTLD-Tau (mean difference: GM = 1.13 ± 0.44, WM = 1.28 ± 0.56; $p < 0.001$) and FTLD-TDP (GM = 0.95 ± 0.66, WM = 0.90 ± 0.77; $p < 0.001$), and these measurements were linearly related (R-squared [Rsq]: FTLD-Tau GM = 0.92, WM = 0.92; FTLD-TDP GM = 0.75, WM = 0.78; $p < 0.001$ all). We therefore used linear regression to transform %AO from distinct staining batches into equivalent values. Using a train-test set design, we examined transformation prerequisites (i.e., Rsq) from linear-modeling in training sets, and we applied equivalence factors (i.e., beta, intercept) to independent testing sets to determine transformation outcomes (i.e., intraclass correlation coefficient [ICC]). First, random iterations (×100) of linear regression showed that smaller training sets ($N = 12$–24), feasible for prospective use, have acceptable transformation prerequisites (mean Rsq: FTLD-Tau ≥0.9; FTLD-TDP ≥0.7). When cross-validated on independent complementary testing sets, in FTLD-Tau, $N = 12$ training sets resulted in 100% of GM and WM transformations with optimal transformation outcomes (ICC ≥ 0.8), while in FTLD-TDP $N = 24$ training sets resulted in optimal ICC in testing sets (GM = 72%,

WM = 98%). We therefore propose training sets of $N = 12$ in FTLD-Tau and $N = 24$ in FTLD-TDP for prospective transformations. Finally, the transformation enabled us to significantly reduce batch-related difference in duplicate measurements in FTLD-Tau (GM/WM: $p < 0.001$ both) and FTLD-TDP (GM/WM: $p < 0.001$ both), and to decrease the necessary sample size estimated in a power analysis in FTLD-Tau (GM: −40%; WM: −34%) and FTLD-TDP (GM: −20%; WM: −30%). Finally, we tested generalizability of our approach using a second, open-source, image analysis platform and found similar results. We concluded that a small sample of tissue stained in duplicate can be used to account for pre-analytical variability such as staining batch effects, thereby improving methods for future studies.

Keywords: digital histopathology, frontotemporal lobar degeneration, pre-analytical variability, batch effects, linear transformation method, validation of a method

INTRODUCTION

Digital pathology is emerging as an important discipline in clinical pathology, biomedical research and medical education (Huisman, 2012; Hamilton et al., 2014; Griffin and Treanor, 2017). Digital methods of pathological analysis are also increasingly used in neurodegenerative disease research as they provide a high-throughput, objective measure of disease severity as compared with traditional ordinal ratings. Indeed, this quantitative approach to measuring pathological burden provides increased sensitivity to detect clinicopathological correlations (Neltner et al., 2012; Walker et al., 2015, 2017; Irwin et al., 2016b; Ferman et al., 2018), which are critical to improve the *antemortem* diagnosis of neurodegenerative diseases. This is especially important in less common, heterogeneous disorders such as frontotemporal lobar degeneration (FTLD) (Irwin et al., 2015).

Frontotemporal lobar degeneration comprises a heterogeneous group of neuropathologies, which present clinically as frontotemporal dementia syndromes (Irwin et al., 2015). The two most common FTLD neuropathologies are frontotemporal lobar degeneration with inclusions of the protein tau (FTLD-Tau) and frontotemporal lobar degeneration with inclusions of the transactive response DNA-binding protein of 43 kDa (FTLD-TDP) (Mackenzie et al., 2010; Irwin et al., 2015). FTLD-Tau can be classified into different neuropathological sub-entities with distinct morphological features, such as Pick's disease (PiD), corticobasal degeneration (CBD), and progressive supranuclear palsy (PSP) (Dickson et al., 2011; Kovacs, 2015). Genetically, mutations in the *MAPT* gene have been associated with FTLD-Tau (Sieben et al., 2012). FTLD-TDP is subdivided into type A-E based on the predominant type of inclusions (Mackenzie et al., 2011; Lee et al., 2017), and these have been variably associated with genetic mutations in a few different genes (e.g., *C9orf72, GRN*, *TARDBP*, *VCP*) (Sieben et al., 2012). Distinct FTLD proteinopathies cannot be differentiated during life, which poses a significant challenge for disease modifying therapies in development targeting tau and TDP-43 pathways of degeneration (Boxer et al., 2013). Thus, *postmortem* comparative studies of clinically similar FTLD-Tau and FTLD-TDP are urgently needed to improve *antemortem* diagnosis (Irwin et al., 2015).

With the increasing use of digital pathology, it is critical to develop rigorous empirically defined methods to account for the multiple pre-analytical factors that could influence these digital measurements. One major obstacle to large-scale comparative autopsy studies is the inability to simultaneously stain large amounts of tissue in a single staining batch. Yet, the use of multiple staining batches may be affected by staining batch effects, i.e., a potential important source of pre-analytical variability related to immunohistochemical (IHC) staining intensity that prevents valid inter-comparability of digital pathology measurements. It may be possible to account for this batch-related variability statistically, enabling to merge data from distinct staining batches without major issues of comparability, but we are not aware of any published methodologies used in neurodegenerative disease research.

It is advantageous for research centers to generate cumulative digital pathology data from prospective autopsies, and to build a library of digital pathology data by adding newly generated digital measurements to archived legacy data from prior autopsies. This strategy would preserve resources, and facilitate large-scale clinical, genetic and neuroimaging correlation studies urgently needed to improve the *antemortem* diagnosis of neurodegenerative diseases. While there is limited empirical evidence to guide methods for merging data obtained from tissue stained in different staining batches, this would be necessary to ameliorate comparability of digital measurements, and to prevent duplication of efforts of having to re-stain large amounts of tissue for prospective large-scale projects. Here we empirically test methodological steps to develop a working standard operating procedure (SOP) to transform digital pathology data from a new staining batch (i.e., staining batch 2 [SB2]) into equivalent values to a previous staining batch (i.e., staining batch 1 [SB1]), using a set of tissue samples stained in duplicate (i.e., in both SB1 and SB2). We test this approach in a large sample of FTLD with either tau inclusions (FTLD-Tau) or transactive response DNA binding protein 43 kDa (TDP-43) inclusions (FTLD-TDP). We focus on FTLD pathologies, since these are two distinct monoproteinopathies with varied histopathological morphologies in both grey matter (GM) and white matter (WM) (Irwin et al., 2015), and are thus ideal to test for variation due to staining batch effects as opposed to AD or LBD, which often

have mixed pathology (Montine et al., 2012; McKeith et al., 2017). These data provide an important methodological approach to guide future digital pathology analysis in brain bank programs for a spectrum of age-related neurodegenerative disorders.

MATERIALS AND METHODS

Patients

We selected a convenience sample of brain tissue from FTLD patients with high availability to use for comparative analysis of tissue samples stained in duplicate. Patients were evaluated clinically at the Penn Frontotemporal Degeneration Center or Alzheimer's Disease Center and met clinical criteria for an FTD spectrum diagnosis (Mesulam, 2001; Rascovsky et al., 2011). Patients were autopsied at the Penn Center for Neurodegenerative Disease Research with a primary neuropathological diagnosis of FTLD (n = 68) with either FTLD-Tau (n = 26) or FTLD-TDP (n = 42) (Mackenzie et al., 2010; Montine et al., 2012). We did not include less common neuropathologies associated with clinical FTD, including AD, or FUS proteinopathy (Irwin et al., 2015). This study was carried out in accordance with the recommendations of the Penn Institutional Review Board (IRB) on human subjects research protections guidelines. The protocol was approved by the Penn IRB. All subjects gave written informed consent prior to participation, in accordance with the Declaration of Helsinki.

Tissue Processing and Neuropathological Diagnosis

All tissue was processed in an identical manner as described (Toledo et al., 2014; Irwin et al., 2016b). Briefly, fresh tissue samples were fixed overnight in 10% neutral-buffered formalin, or 70% ethanol with 150 mM sodium chloride in a minority of cases (N = 4 in FTLD-Tau, N = 4 in FTLD-TDP), which has been previously validated using our digital method (Irwin et al., 2016b). Tissue samples were trimmed, placed into cassettes and processed through a series of alcohol, xylene and Surgipath EM-400 paraffin embedding media (Leica Microsystems; Buffalo Grove, IL, United States) with incubations overnight (70% ethanol × 2 h, 80% ethanol × 1 h, 95% ethanol × 1 h, 95% ethanol × 2 h, 100% ethanol × 2 h, twice, xylene × 30 min, xylene × 1 h, xylene × 1.5 h, and paraffin × 1 h, three times) in a Shandon tissue processor (Thermo Fisher Scientific; Waltham, MA, United States). All incubations were done under vacuum and at ambient temperature except paraffin (62°C). Tissue was embedded into paraffin blocks and 6-μm-thick sections were cut for analysis. For neuropathological diagnosis, tissue sections from standard brain regions were immunostained for tau, amyloid-beta, alpha-synuclein and TDP-43 using well-characterized antibodies and stained for neuritic plaques using thioflavin-S as described (Toledo et al., 2014). Neuropathological diagnoses were established by expert neuropathologists (EBL, JQT) using standard neuropathological criteria (Mackenzie et al., 2010; Montine et al., 2012; Lee et al., 2017).

For the current study, IHC was performed using well-characterized antibodies for phospho-tau (AT8; Millipore) (Mercken et al., 1992) in FTLD-Tau and TDP-43 (rat monoclonal TAR5P-1D3, p409/410; Ascenion) (Neumann et al., 2009) in FTLD-TDP. Each staining batch underwent identical processing using the same antigen retrieval methods and dilutions optimized in our lab, i.e., AT8 1:1K dilution with no antigen retrieval step; p409/410 1:500 dilution with Citrate Antigen Unmasking Solution (Vector Laboratories, Burgame, CA, United States, Catalog No: H-3300) as in previous work (Irwin et al., 2016b, 2018; Giannini et al., 2019). The same secondary antibodies were used in both staining batches of each pathology, i.e., Abcam (Cambridge, MA, United States, Goat Anti-Rat) for TDP-43 (Cat. No. ab97054) and Abcam Goat Anti-Mouse (for AT8) (Cat. No. ab97020). As a chromogen we used ImmPACT DAB kit (Vector Laboratories, Burgame, CA, United States, Cat. No. SK-4105) with VECTASTAIN ABC Kit (Vector Laboratories, Burgame, CA, United States, Cat. No. PK-4000) with identical incubation and developer times. Digital image acquisition of histology slides was performed at 20× magnification with transmitted light microscopy using Lamina (Perkin Elmer, Waltham, MA, United States) scanner, which has a slide scanning platform of 6.5 μm^2 (i.e., pixel resolution of 0.325 μm), and camera resolution of 2560 × 2160 with a bit depth of 16. Digital image acquisition was performed using an autocorrection step for even illumination, i.e., the scanner captures 10 empty fields of view to create a compensation image used to obtain evenly illuminated composite images. Digital images were analyzed using Halo digital image software v1.90 (Indica Labs, Albuquerque, NM, United States) as described (Irwin et al., 2016b, 2018). The digital measurement performed by the Halo software uses a color deconvolution process as described in our published methods (Irwin et al., 2016b). Briefly, we used the Area Quantification v1.0 Tool in Halo to calculate the % of positive pixels from the chromogen (i.e., %AO). This tool uses color deconvolution to first separate the chromogen signal from the haematoxylin counterstain, and then it applies a minimum optical density (OD) value threshold to exclude background and count the number of positive pixels for chromogen-labeled pathology in the total ROI. Detection algorithms for pathology stain and haematoxylin counterstain were developed empirically as described (Irwin et al., 2016b). Please see **Supplementary Table 1** for the specific parameters of our detection algorithms.

Validation Procedures

We included available tissue samples from two standard autopsy-sampled regions with high availability of tissue, i.e., an anterior region such as mid-frontal cortex (MFC) and a posterior region such as angular gyrus (ANG), in which we expected a broad range of pathological severity in our FTLD cohort. We studied the relationship between duplicate measurements of digital pathology in adjacent or near adjacent sections of the same tissue block, one of which was stained in the original staining batch (SB1), and the other one in a second staining batch (SB2). To specifically assess the impact of staining batch effects, duplicate measurements of digital pathology were obtained in a nearly identical manner except for being stained in two distinct staining batches. Tissue sections were obtained from the same cutting ribbon using adjacent or semi-adjacent tissue

(within ∼50 μm). By visual inspection we found no evident differences in the distribution and morphology of pathology between (semi-)adjacent slides, which were nearly identical. Using digital image analysis, we measured percent of area occupied by pathology (%AO) in regions of interest (ROIs) for both GM and WM on each section. GM ROIs were identified as the largest intact region of parallel-oriented cortex in a section of brain tissue using our previously validated sampling method (Irwin et al., 2016b). WM ROIs were sampled as the largest possible area of deep WM within a tissue section as described (Irwin et al., 2016b, 2018). To minimize sources of variation in our measurement other than staining batch effects, we used the image registration feature of the Halo software to map the ROI into equivalent regions of (semi-)adjacent tissue sections for comparable sampling between SB1 and SB2. When this was not possible, we pasted identical ROIs in a closely matched region using cellular landmarks (e.g., contours of gyri, blood vessels) to guide precision for placement.

Unusable or damaged tissue that precluded sampling in a comparable manner between adjacent sections was excluded from the analysis (N = 8 tissue samples in FTLD-Tau, N = 12 tissue samples in FTLD-TDP). Minor artifacts and vessels in brain tissue were sampled out of the area of analysis of digital images using the cropping tool in the Halo software. In total, available data from 92 tissue samples, including 39 samples from 26 patients with FTLD-Tau and 53 samples from 42 patients with FTLD-TDP, were used for this validation (see **Table 1**). Each tissue sample had two GM %AO measurements and two WM %AO measurements (i.e., duplicate measurements), corresponding to two nearly identical tissue sections, one stained in SB1 and the other one in SB2. Analyses were performed distinctly in FTLD-Tau and FTLD-TDP groups because these pathologies have distinct biology, morphological features and algorithms for digital image detection (Irwin et al., 2016b, 2018).

Statistics

All statistical analyses were performed using R Statistical Software 3.4.1. Since %AO measurements were not normally distributed, we applied natural log (ln) transformation and confirmed normal distribution graphically. We used ln-transformed data (i.e., ln %AO) in all our validation analyses. Digital pathology measurements were validated through comparison to gold-standard ordinal ratings (**Supplementary Figure 1**) as previously done (Irwin et al., 2016b, 2018). In this validation dataset (FTLD-Tau = 39, FTLD-TDP = 53; **Table 1**), all tissue samples were stained in duplicate in SB1 and SB2, which gave us the chance (1) to determine the impact of staining batch effects in a large sample of data, and (2) to assess our proposed transformation method using a planned train-test set design.

First, to determine the impact of staining batch effects, duplicate measurements of pathology in GM and WM ROIs from SB1 and SB2 were compared using the Bland-Altman (BA) statistics to test the mean difference between staining batches. We tested the null hypothesis that the mean difference between SB1 and SB2 measurements equaled zero using a one-sided t-test. Significant results were interpreted as providing evidence for a difference between these duplicate measurements (Bland and

TABLE 1 | Demographic and pathologic characterization of the cohort.

	FTLD-Tau (n = 26)	FTLD-TDP (n = 42)
Available tissue		
Total tissue samples (N)	39	53
ANG tissue samples (N)	20	38
MFC tissue samples (N)	19	15
Demographics		
Age at onset (y), mean ± SD	56.4 ± 12.9	59.5 ± 8.5
Age at death (y), mean ± SD	64.5 ± 13.5	65.7 ± 9.5
Disease duration (y), mean ± SD	8.6 ± 4.1	6.7 ± 4.1
Male sex, n (%)	17/26 (65.4)	21/42 (50.0)
Autopsy		
PMI (hr), mean ± SD	12.6 ± 6.8	12.9 ± 6.9
Brain weight (gr), mean ± SD	1089.2 ± 156.4	1106.2 ± 194.4
Primary NPD, n (%)		
TDP type A (incl. *GRN*)	–	17/42 (45.2)
TDP type B	–	13/42 (33.3)
TDP type C	–	7/42 (16.7)
TDP type E	–	5/42 (11.9)
CBD	5/26 (19.2)	–
PSP	4/26 (15.4)	–
PiD	9/26 (34.6)	–
Tau unclassifiable (incl. *MAPT*)	8/26 (30.8)	–
Secondary NPD, n (%)		
HiSc	1/26 (3.8)	5/42 (11.9)
LBD	2/26 (7.7)	1/42 (2.4)
AGD	0	2/42 (4.8)
Other[a]	0	2/42 (4.8)
Braak[b], n (%)		
0	12/26 (46.2)	15/42 (35.7)
1	8/26 (30.8)	19/42 (45.2)
2	1/26 (3.8)	6/42 (14.3)
3	5/26 (19.2)	2/42 (4.8)
CERAD, n (%)		
0	22/26 (84.6)	29/42 (69.0)
A	3/26 (11.5)	6/42 (14.3)
B	0	5/42 (11.9)
C	1/26 (3.8)	2/42 (4.8)
Genetic mutations, n (%)		
GRN	–	8/42 (19.0)
C9orf72	–	15/42 (35.7)
MAPT	6/26 (23.1)	–

AD, Alzheimer's disease; AGD, argyrophilic grain disease; ANG, angular gyrus; C9orf72, chromosome 9 open reading frame 72; CBD, corticobasal degeneration; FTLD-Tau, frontotemporal lobar degeneration with inclusions of the tau protein; FTLD-TDP, frontotemporal lobar degeneration with inclusions of the transactive response DNA-binding protein 43 kDa; gr, grams; GRN, progranulin gene; hr, hours; HiSc, hippocampal sclerosis; LBD, Lewy Body disease; MAPT, microtubule-associated protein tau gene; MFC, mid-frontal cortex; n, number of individuals; N, number of tissue samples; NPD, neuropathological diagnosis; PiD, Pick's disease; PMI, post-mortem interval; PSP, progressive supranuclear palsy; SD, standard deviation; TDP type A-E, FTLD-TDP subtypes (Mackenzie et al., 2011; Lee et al., 2017); y, years. [a]The two individuals with other secondary pathologies had minor amounts of cerebrovascular disease in one case, and tangle-predominant senile dementia in the other case. [b]For determination of Braak stages in FTLD-Tau patients, hippocampal sections were stained with an amyloid-binding dye, Thioflavin-S, to distinguish co-morbid age-related AD neurofibrillary tangle (NFT) pathology from primary FTLD-t autopathy as described (Irwin et al., 2017).

Altman, 1986). Subsequently, the relationship between duplicate measurements of pathology was explored using univariate linear regression. Linear modeling used SB1 measurements as dependent variable and SB2 measurements as independent variable. Based on the strong linear relationship in both FTLD-Tau and FTLD-TDP, we proposed to use the linear equivalence equation to transform SB2 data into values equivalent to SB1: *transformed SB2 (t-SB2) = beta * SB2 + intercept.*

Second, we used a planned train-test set design (see below for details) to validate our proposed transformation method, which relies upon the use of a small set of tissue stained in each prospective staining run to account for batch effects in digital measurements. We validated this method using a validation protocol involving different steps (**Figure 1**) to empirically determine the optimal conditions for a successful transformation of SB2 measurements into SB1-equivalent units (i.e., t-SB2). We first looked at transformation prerequisites (i.e., consistent and sufficiently high goodness of fit in linear models) in randomly assembled training sets using a relatively small sample size (i.e., N = 12–24) feasible for use in prospective staining runs (i.e., one-half to one full staining-rack in our lab) (Step 1). Thereafter, we applied regression-based equivalence factors (i.e., beta, intercept) to complementary independent testing sets. Next, we cross-validated transformation outcomes in these testing sets (Step 2) to verify the accuracy of transformation (i.e., whether t-SB2 values approximated SB1 values). We used Step 1 and Step 2 to determine whether a relatively small set of control tissue (N = 12–24) could be used in our SOP for prospective data addition to existing datasets. Finally, we looked at functional outcomes of this approach to facilitate and improve future studies, such as the reduction in batch-related difference in duplicate measurements and the increase in statistical power using transformed %AO values as opposed to untransformed values from tissue stained in different batches (Step 3).

Step 1: Examine Transformation Prerequisites in Feasible-Sized Training Sets

Our first analysis was to determine feasibility of using a small set of control tissue stained in each prospective staining run by testing whether small training sets (i.e., N = 12–24) could provide adequate transformation prerequisites for our transformation method. We performed linear regressions relating SB1 (dependent variable) to SB2 (independent variable) data in randomly subsampled training sets of N = 12 and N = 24 sample size. We performed 100 iterations per training-set sample size, and we obtained mean, standard deviation and a non-parametric quantile-based 95% confidence interval (CI) for Rsq, beta and intercept. Mean Rsq was our main outcome as a measure of the goodness of fit of linear modeling in these random iterations.

Step 2: Cross-Validate Transformation Outcomes in Independent Testing Sets

Next, we applied equivalence factors (i.e., beta, intercept) of the linear equivalence equation from iterated linear models (Step 1) to independent testing sets for cross-validation. Each N = 12 and N = 24 training set was retested on the respective complementary testing set (FTLD-Tau: train = 24/test = 15 or train = 12/test = 27; FTLD-TDP: train = 24/test = 29 or train = 12/test = 41).

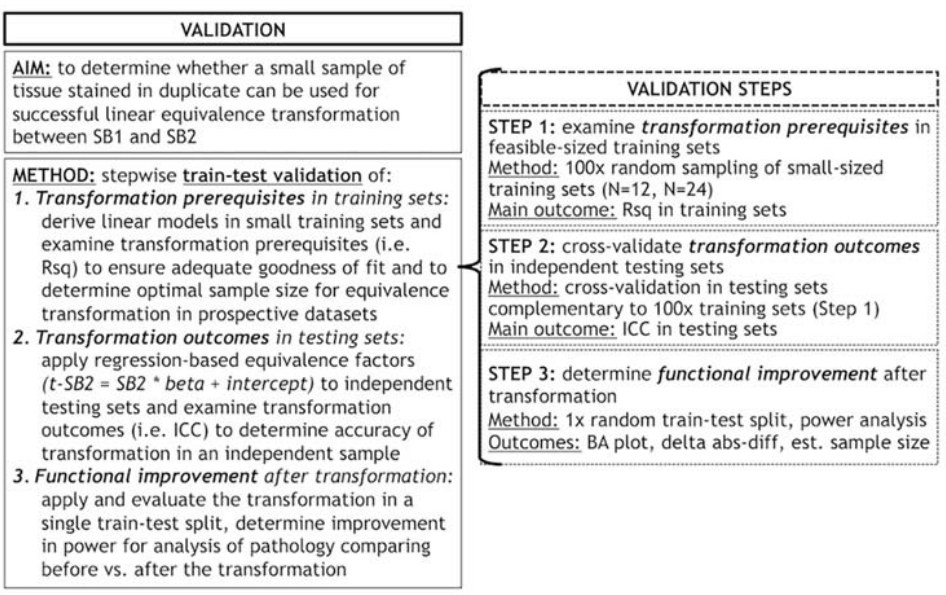

FIGURE 1 | Objectives and methods of this validation study and stepwise validation protocol. Panel outlines the aim and methods of our validation study to account for staining batch effects in digital pathology, including a stepwise protocol to assess relevant aspects of our proposed methodology. delta abs-diff, change in absolute difference; est. sample size, estimated required sample size in a power analysis; ICC, intraclass correlation coefficient; N, number of tissue samples; Rsq, R squared; SB1, staining batch 1 (original); SB2, staining batch 2 (new); t-SB2, transformed staining batch 2 (new).

Our main transformation outcome was intraclass correlation coefficient (ICC) to assess equivalence between transformed SB2 measurements (i.e., t-SB2) and original measurements from SB1. We defined an optimal transformation as ICC $\geq$ 0.8 and determined the frequency of optimal transformations out of 100 iterations per training-set sample size (100× N = 24 training sets, 100× N = 12 training sets) in GM and WM in both FTLD-Tau and FTLD-TDP.

Step 3: Determine Functional Improvement After Transformation

Finally, we were interested in determining whether the application of our transformation method resulted in improved functional outcomes for the performance of digital pathology analysis. To this end, we used a single random train-test split using a N = 12 training set in FTLD-Tau, and a N = 24 training set in FTLD-TDP, and we applied the transformation to independent testing sets including all remaining data in FTLD-Tau (N = 27) and FTLD-TDP (N = 29). Here, we assessed the impact of the transformation by testing whether there was a reduction in the difference between duplicate measurements from different staining batches. We estimated the mean difference between duplicate measurements, and visually compared Bland-Altman plots of test-retest agreement before and after the transformation (Bland and Altman, 1986). Additionally, we estimated the change in absolute difference in measurements (i.e., delta abs-diff) between after the transformation (i.e., absolute difference between t-SB2 and SB1) and before the transformation (i.e., absolute difference between SB2 and SB1). We tested whether delta abs-diff equaled zero using a one-sample t-test, where a significant finding ($p < 0.05$) indicated a significant reduction in batch-related difference in measurements after applying the transformation.

Finally, we performed a proof-of-concept power analysis to see how much increased power could be obtained using alternatively (1) data merged from a random selection of the original staining batch and the new staining batch without transformation (i.e., merged untransformed = SB1 + SB2), and (2) data merged from a random selection of the original staining batch and the new staining batch after transformation (i.e., merged transformed = SB1 + t-SB2). To this end, we used data from the MFC region to derive linear models in both FTLD-Tau (N = 19) and FTLD-TDP (N = 15). Next, we applied the transformation to independent testing sets with data exclusively from the ANG region (FTLD-Tau = 20; FTLD-TDP = 38). Merged untransformed (SB1 + SB2) and merged transformed (SB1 + t-SB2) variables were obtained in testing sets through random assignment with a 50:50 ration between SB1 and SB2/t-SB2. For our proof-of-concept power analysis, we calculated the standard deviation in these two sets of data (i.e., merged untransformed, merged transformed) and we used it as an approximation of the overall variance (ANG vs. any hypothetical region) for possible regional comparisons. We estimated the sample size necessary to detect varying differences between mean ANG and another hypothetical regional mean, i.e., 0.2, 0.5, and 0.8, corresponding to small, medium and large effect sizes (Cohen, 1988). The power analysis was performed with power of 0.8 and alpha of 0.05.

Analysis of Generalizability: Replication of Validation Outcomes Using an Open-Source Digital Platform

To test the generalizability of our approach, we replicated the main analyses of this validation using an open-source image analysis tool, i.e., QuPath (Bankhead et al., 2017). In QuPath, we quantified %AO by pathology importing the same RGB color deconvolution algorithms derived in Halo for tau and TDP-43 inclusions (**Supplementary Table 1**) in matched ROIs using the same cellular landmarks for precise ROI placement in QuPath as in Halo. First, we compared %AO measurements between SB1 and SB2 in comparable ROIs to assess whether similar staining batch effects were observable in another digital platform. Next, we applied the transformation method to verify the accuracy of transformation in data obtained from this open-source platform. Our main outcome measures were ICC, delta abs-diff and Bland-Altman statistics after transformation in a single random train-test split (Step 3).

Finally, we also tested an alternative approach to transformation of %AO values to correct for staining batch effects using the "Estimate stain vectors" tool in QuPath (Macenko et al., 2009), which enables to empirically and systematically develop a new color deconvolution algorithm for both haematoxylin counterstain and DAB chromogen in a subsequent staining batch. This QuPath function detects RGB color signal and plots individual pixel signal in each vector of RGB (stain vector plots), where the accuracy of color deconvolution is defined by the presence of pixels within the confines of the stain vector plots. To develop optimized algorithms using this tool, we used the same approach as the one we used to develop our original algorithms as published (Irwin et al., 2016b). Briefly, RGB and minimum OD values are estimated empirically in five random slides. Next, the final RGB and minimum OD parameters of the optimized algorithms are calculated as the average from these random slides. In this supplementary analysis, we derived optimized algorithms in SB2 to compare optimized SB2 measurements to original SB1 measurements analyzed in QuPath. We tested agreement between the original algorithm in SB1 and the optimized SB2 algorithm in the full dataset using Bland-Altman analysis for test-retest agreement.

RESULTS

Data Comparison Between Staining Batches

Patient demographics are summarized in **Table 1**. Consistent with our previous validation of specific algorithms for digital histopathological analysis, we found digital %AO measurements reflected gold-standard ordinal ratings of pathology (**Supplementary Figure 1**).

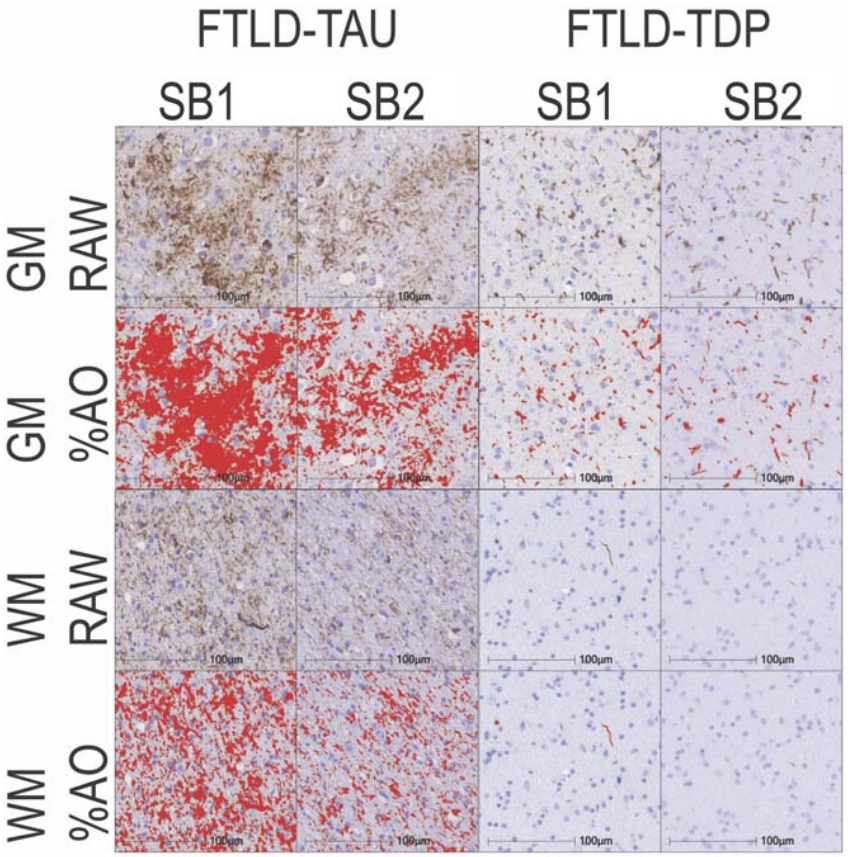

FIGURE 2 | Representative photomicrographs of staining batch variability in FTLD-Tau and FTLD-TDP. Photomicrographs depict a mid-frontal cortex section of FTLD-Tau (Corticobasal degeneration; left) and FTLD-TDP (TDP type A; right) with raw and digital %AO detection red overlay of pathology in gray matter (top) and white matter (bottom) in approximate matched areas in staining batch 1 (SB1) vs. staining batch 2 (SB2). There is slightly darker DAB chromogen signal and thus greater %AO in SB1 compared to SB2. Scale bar = 100 μm. FTLD-Tau, frontotemporal lobar degeneration with inclusions of the tau protein; FTLD-TDP, frontotemporal lobar degeneration with inclusions of the transactive response DNA-binding protein 43 kDa; GM, gray matter; SB1, staining batch 1 (original); SB2, staining run 2 (new); WM, white matter.

In our analysis of the impact of staining batch effects on digital measurements (see **Figure 2** for a visual representation of %AO by tau or TDP-43), we found that in FTLD-Tau the mean difference between SB1 and SB2 duplicate measurements was 1.13 ± 0.44 in GM and 1.28 ± 0.56 in WM. In FTLD-TDP, the mean difference between SB1 and SB2 duplicate measurements was 0.95 ± 0.66 in GM and 0.90 ± 0.77 in WM. Bland-Altman statistics showed that the mean difference between duplicate measurements significantly differed from zero (one-sided *t*-test, $p < 0.001$) in both GM and WM in FTLD-Tau and FTLD-TDP (**Figure 3**), suggesting that %AO measurements from different staining batches were not equivalent. The relationship between SB1 and SB2 was further explored using univariate linear regression, where SB1 data was employed as the dependent variable and SB2 as the independent variable. All models (i.e., GM and WM in FTLD-Tau and FTLD-TDP) were highly significant, indicating a linear relationship between duplicate measurements from our two staining batches (**Figure 4**). In FTLD-Tau, both GM and WM models had Rsq of 0.92; in FTLD-TDP, the Rsq was 0.75 in GM and 0.78 in WM. All summary statistics for SB1 and SB2 data are displayed in **Supplementary Table 2**.

Step 1: Examine Transformation Prerequisites in Feasible-Sized Training Sets

Since it is not practical to use a large number of duplicate tissue samples for each prospective staining batch in all future large-scale studies, we aimed to first determine whether a small set of tissue stained in duplicate could suffice to obtain an accurate transformation. We used samples of $N = 12$ and $N = 24$ as our training sets, i.e., half- or one-full rack in our staining batches. We performed iterations (100×) of linear modeling in training sets, looking at Rsq values as transformation prerequisites, and beta and intercept as equivalence factors (**Table 2**). In FTLD-Tau GM, the mean Rsq was 0.92 ± 0.03 in $N = 24$ sets and 0.91 ± 0.05 in $N = 12$ sets; the models were significant ($p < 0.05$) in 100% of $N = 24$ iterations and $N = 12$ iterations. In FTLD-Tau WM, the mean Rsq was 0.91 ± 0.02 in $N = 24$ sets and 0.90 ± 0.06

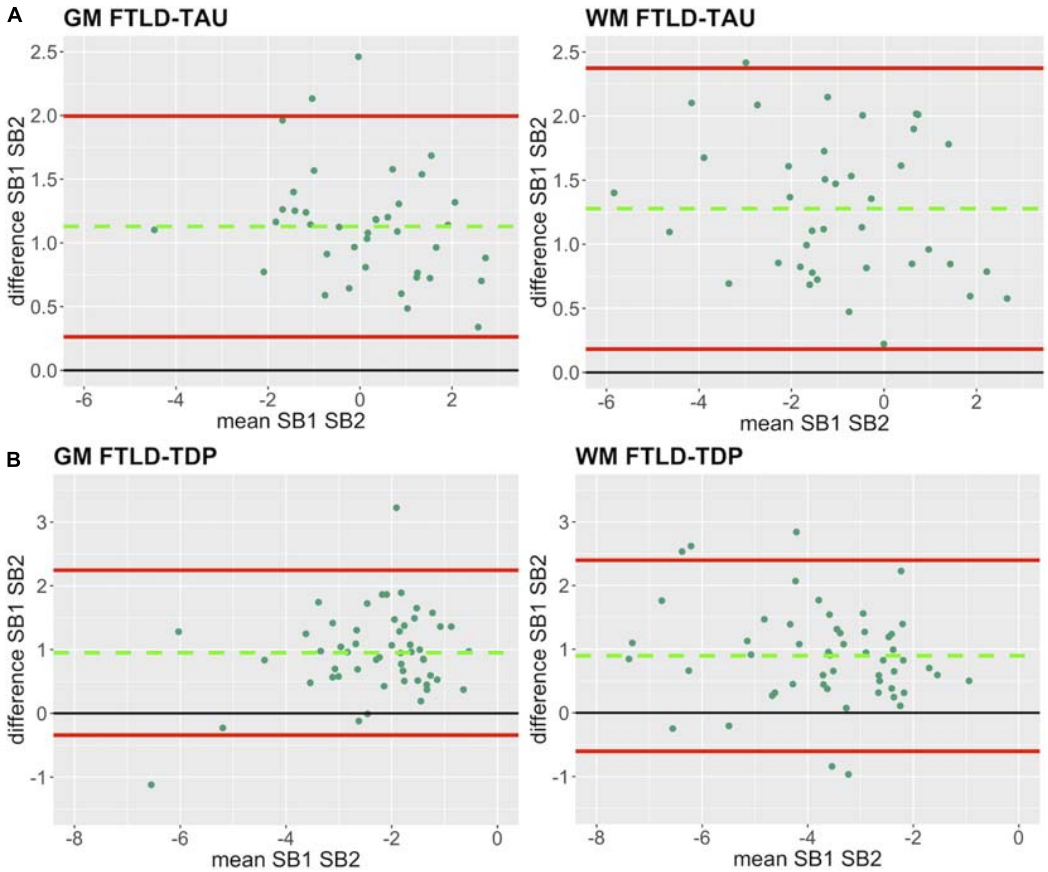

FIGURE 3 | Bland-Altman plots of test-retest agreement between duplicate measurements of pathology from two distinct staining batches. Bland-Altman plots show test-retest agreement between SB1 and SB2 measurements of digital pathology (i.e., ln %AO). The green dashed line indicates the mean difference between SB1 and SB2 measurements, while the red solid lines mark the 95% limits of agreement between the two measurements. We find that mean difference between SB1 and SB2 significantly differs from zero ($p < 0.001$) in FTLD-Tau **(A)** and FTLD-TDP **(B)** in both GM and WM. FTLD-Tau, frontotemporal lobar degeneration with inclusions of the tau protein; FTLD-TDP, frontotemporal lobar degeneration with inclusions of the transactive response DNA-binding protein 43 kDa; GM, gray matter; SB1, staining batch 1 (original); SB2, staining batch 2 (new); WM, white matter.

in $N = 12$ sets; the models were significant ($p < 0.05$) in 100% of $N = 24$ iterations and $N = 12$ iterations. In FTLD-TDP GM, the mean Rsq was 0.76 ± 0.10 in $N = 24$ sets and 0.72 ± 0.18 in $N = 12$ sets; the models were significant ($p < 0.05$) in 100% of $N = 24$ iterations and 97% of $N = 12$ iterations. In TDP WM, the mean Rsq was 0.78 ± 0.07 in $N = 24$ sets and 0.76 ± 0.12 in $N = 12$ sets; the models were significant ($p < 0.05$) in 100% of $N = 24$ iterations and 100% of $N = 12$ iterations. Overall we found a consistent strong linear association between %AO measurements from different staining batches equally in $N = 24$ and $N = 12$ training sets in FTLD-Tau, while FTLD-TDP had greatest reliability of this association in training sets of $N = 24$ sample size (**Table 2**).

Step 2: Cross-Validate Transformation Outcomes in Independent Testing Sets

Next, we cross-validated equivalence factors derived in Step 1 on independent testing sets including all remaining tissue samples not used in the training set (**Table 3**). We were interested in comparing transformation outcomes resulting from the application of equivalence factors from $N = 12$ as opposed to $N = 24$ training sets. We looked at the ICC as main transformation outcome and we set a value of ≥ 0.8 as our threshold for an optimal transformation. In FTLD-Tau GM, $N = 24$ training sets resulted in a mean ICC of 0.95 ± 0.02 in testing sets, while $N = 12$ training sets resulted in a mean ICC of 0.95 ± 0.01. Similarly, in FTLD-Tau WM, $N = 24$ training sets resulted in a mean ICC of 0.95 ± 0.02 in testing sets, while $N = 12$ training sets resulted in a mean ICC of 0.95 ± 0.01. We obtained optimal transformation outcomes in 100% of transformations in both GM and WM in FTLD-Tau (**Table 3**). In FTLD-TDP GM, $N = 24$ training sets resulted in a mean ICC of 0.82 ± 0.05 in testing sets, while $N = 12$ training sets resulted in a mean ICC of 0.81 ± 0.06. We found optimal transformation outcomes in 72% of transformations using $N = 24$ training sets and 70% using $N = 12$ training sets, while most remaining transformations (i.e., 25% using $N = 24$ training sets and 26% using $N = 12$ training sets) resulted in a moderate ICC between 0.7 and

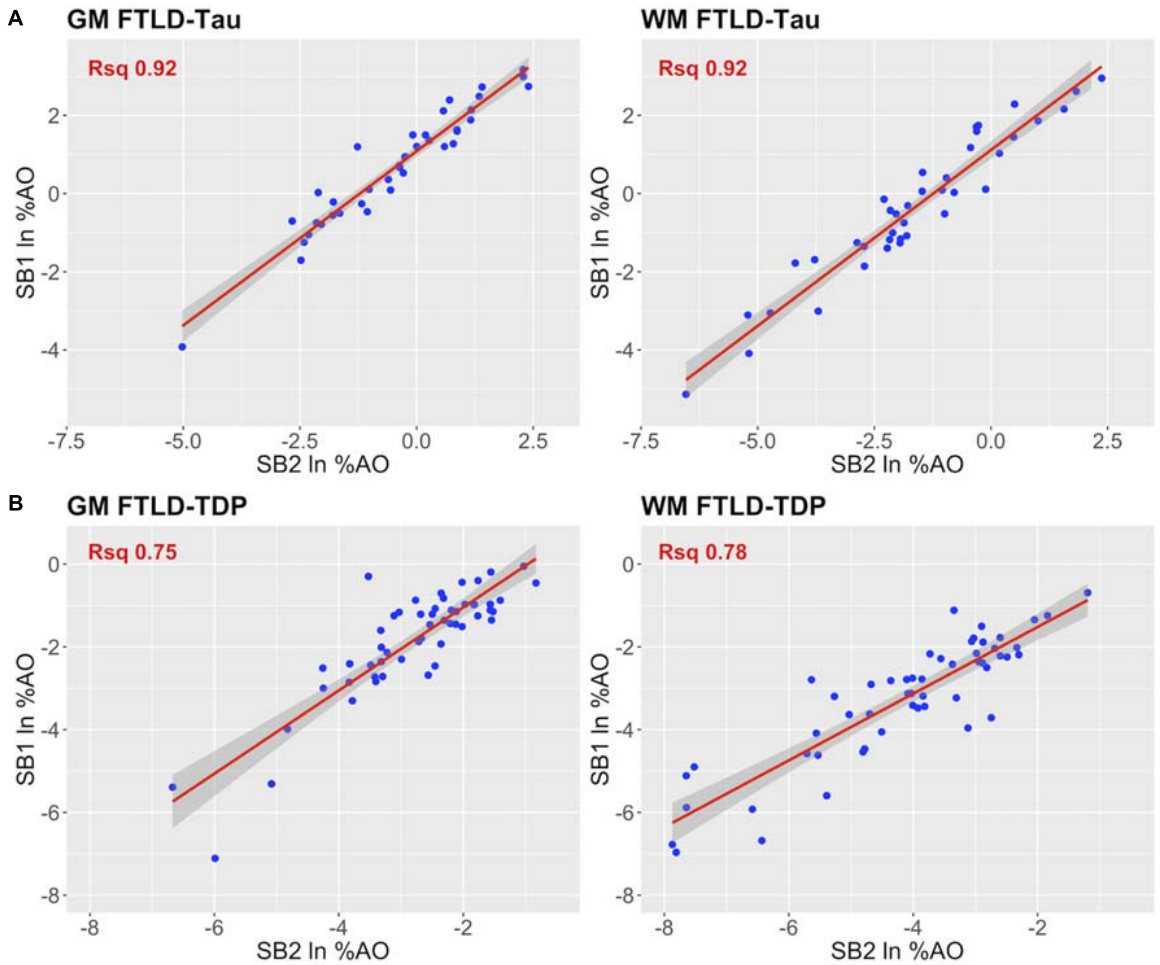

FIGURE 4 | Linear relationship between duplicate measurements of pathology from two distinct staining batches (SB1 *Y*-axis, SB2 *X*-axis). Scatterplots display the linear relationship between duplicate measurements of digital pathology (i.e., ln %AO) from SB1 (*y*-axis) and SB2 (*x*-axis) in FTLD-Tau **(A)** and FTLD-TDP **(B)**, for both GM and WM measurements. In FTLD-Tau GM, the model Rsq is 0.92 ($p < 0.001$); in FTLD-Tau WM, the model Rsq is 0.92 ($p < 0.001$). In FTLD-TDP GM, the model Rsq is 0.75 ($p < 0.001$); in FTLD-TDP WM, the model Rsq is 0.78 ($p < 0.001$). FTLD-Tau, frontotemporal lobar degeneration with inclusions of the tau protein; FTLD-TDP, frontotemporal lobar degeneration with inclusions of the transactive response DNA-binding protein 43 kDa; GM, gray matter; ln %AO, natural logarithmic transformation of percent area occupied by pathology; Rsq, R squared; SB1, staining batch 1 (original); SB2, staining batch 2 (new); WM, white matter.

0.8. In FTLD-WM, $N = 24$ training sets resulted in a mean ICC of 0.86 ± 0.03 in testing sets, while $N = 12$ training sets resulted in a mean ICC of 0.85 ± 0.03. We obtained optimal transformation outcomes in 98% of transformations using $N = 24$ training sets and 95% using $N = 12$ training sets (**Table 3**). Based on these frequencies, in prospective analyses we propose to use at least $N = 12$ training sets for FTLD-Tau and $N = 24$ training sets for FTLD-TDP, where we find the best compromise between feasibility of use and reliability of outcomes.

Step 3: Determine Functional Improvement After Transformation

Finally, we applied our cross-validated method to a single, randomly obtained train-test split to determine the improvement in functional outcomes, such as the reduction in batch-related difference between digital measurements. We checked the reliability of our transformation method as in the prior steps, by looking at transformation prerequisites in training sets (FTLD-Tau = 12, FTLD-TDP = 24) and transformation outcomes in testing sets (FTLD-Tau = 27, FTLD-TDP = 29) (**Table 4**). In FTLD-Tau, training sets had an Rsq of 0.92 in GM and 0.97 in WM. In complementary testing sets, ICC was 0.96 in GM and 0.95 in WM. Before transformation, Bland-Altman statistics showed highly significant mean difference between duplicate %AO measurements in both GM and WM. After transformation, we found a significant reduction in absolute difference (i.e., delta abs-diff) in both GM ($p < 0.001$) and WM ($p < 0.001$) %AO to a mean difference that approached zero, suggesting improved test-retest agreement (**Figure 5**). In FTLD-TDP, training

TABLE 2 | Transformation prerequisites and equivalence factors from iterated (×100) linear regression in feasible-sized training sets (Step 1).

	Size (N)	Iterations	Rsq mean	Rsq SD	Rsq 2.5Q–97.5Q		Beta mean	Beta SD	Beta 2.5Q–97.5Q		Itc mean	Itc SD	Itc 2.5Q–97.5Q	
FTLD-Tau GM	Tot	1	0.92	–	–	–	0.89	–	–	–	1.08	–	–	–
	24	100	0.92	0.03	0.87	0.96	0.89	0.04	0.80	0.96	1.08	0.04	0.99	1.16
	12	100	0.91	0.05	0.79	0.98	0.89	0.07	0.74	1.01	1.09	0.11	0.88	1.31
FTLD-Tau WM	Tot	1	0.92	–	–	–	0.90	–	–	–	1.11	–	–	–
	24	100	0.91	0.02	0.88	0.94	0.90	0.03	0.84	0.96	1.12	0.09	0.93	1.25
	12	100	0.90	0.06	0.77	0.97	0.90	0.08	0.75	1.05	1.12	0.19	0.79	1.49
FTLD-TDP GM	Tot	1	0.75	–	–	–	1.00	–	–	–	0.96	–	–	–
	24	100	0.76	0.10	0.44	0.87	1.00	0.14	0.74	1.25	0.95	0.35	0.37	1.67
	12	100	0.72	0.18	0.26	0.94	0.98	0.22	0.57	1.41	0.90	0.55	−0.12	1.98
FTLD-TDP WM	Tot	1	0.78	–	–	v	0.81	–	–	–	0.09	–	–	–
	24	100	0.78	0.07	0.64	0.87	0.81	0.07	0.65	0.93	0.10	0.29	−0.56	0.57
	12	100	0.76	0.12	0.47	0.92	0.81	0.13	0.61	1.10	0.14	0.53	−0.66	1.33

FTLD-Tau, frontotemporal lobar degeneration with inclusions of the tau protein; FTLD-TDP, frontotemporal lobar degeneration with inclusions of the transactive response DNA-binding protein 43 kDa; GM, gray matter; Itc, intercept; N, number of tissue samples; Q, quantile; Rsq, R squared; SD, standard deviation; Tot, total dataset; WM, white matter. Table shows transformation prerequisites (i.e., Rsq) and equivalence factors (i.e., beta, intercept) in randomly subsampled training sets of small sample size, corresponding to a half (N = 12) or one full rack (N = 24) in staining batches, feasible for use in prospective transformations. We performed 100 iterations of the linear regression, and we report mean, standard deviation and a non-parametric quantile-based confidence interval (2.5–97.5% of the distribution) for R squared, beta and intercept values of the linear models. For comparison, we also show these parameters from linear models obtained in the total datasets (i.e., FTLD-Tau GM/WM, FTLD-TDP GM/WM).

TABLE 3 | Transformation outcomes in independent complementary testing sets (Step 2).

	Training sets (Step 1)		Independent testing sets (Step 2)					
	Size (N)	Iterations	Size (N)	ICC mean	ICC SD	ICC 2.5Q–97.5Q		ICC ≥ 0.8 (%)
FTLD-Tau GM	24	100	15	0.95	0.02	0.90	0.98	100
	12	100	27	0.95	0.01	0.92	0.97	100
FTLD-Tau WM	24	100	15	0.95	0.02	0.91	0.98	100
	12	100	27	0.95	0.01	0.92	0.96	100
FTLD-TDP GM	24	100	29	0.82	0.05	0.69	0.91	72
	12	100	41	0.81	0.06	0.69	0.89	70
FTLD-TDP WM	24	100	29	0.86	0.03	0.80	0.91	98
	12	100	41	0.85	0.03	0.78	0.89	95

FTLD-Tau, frontotemporal lobar degeneration with inclusions of the tau protein; FTLD-TDP, frontotemporal lobar degeneration with inclusions of the transactive response DNA-binding protein 43 kDa; ICC, intraclass correlation coefficient; GM, gray matter; N, number of tissue samples; Q, quantile; SD, standard deviation; WM, white matter. We performed 100 iterations of linear regression in training sets of N = 12 and N = 24 sample size, and applied equivalence factors to independent testing sets including all remaining tissue samples in each iteration. Here, we report transformation outcomes (i.e., ICC) in these complementary testing sets. We report mean, standard deviation and a non-parametric quantile-based confidence interval (2.5–97.5% of the distribution) for the ICC. Additionally, we report the frequency of optimal transformations out of 100 iterations per group based on our threshold of ICC ≥ 0.8.

sets had an Rsq of 0.70 in GM and of 0.75 in WM. In complementary testing sets, ICC was 0.88 in both GM and WM. While before transformation, the mean difference between duplicate %AO measurements was highly significant using Bland-Altman statistics, after transformation there was a significant reduction in absolute difference (i.e., delta abs-diff) in both GM ($p < 0.001$) and WM ($p < 0.001$) %AO to a mean difference that approached zero, similarly suggesting improved test-retest agreement (**Figure 6**). These findings help us validate the functional implications of our SOP, where we propose to use a small sample of tissue stained in each prospective staining batch to transform newly acquired data into values equivalent to previously generated data, thereby accounting for staining batch effects (**Figure 7**).

Finally, we performed a proof-of-concept power analysis to determine the magnitude of improved statistical power after the application of our transformation method, compared to a standard approach using datasets of untransformed %AO obtained from two distinct staining batches. We compared the use of merged untransformed (SB1 + SB2) and merge transformed (SB1 + t-SB2) data in tissue from ANG (FTLD-Tau = 20, FTLD-TDP = 38), and we estimated the necessary sample size to detect a small, medium or large effect size when compared to another hypothetical brain region (power = 0.8, alpha = 0.05). We found that the application of our transformation method resulted in a reduction in estimated sample size required for analysis, i.e., −40% in FTLD-Tau GM, −34% in FTLD-Tau WM, −20% in FTLD-TDP GM, and −30% in FTLD-TDP WM (**Table 5**).

TABLE 4 | Application of transformation method in a single train-test split to determine reduction in batch-related difference in measurements (Step 3).

	Train (N)	Rsq	Beta	Itc	Test (N)	ICC	Mean diff before	BA before sig.	Mean diff after	BA after sig.	Delta abs- diff	Delta abs-diff sig.
1× train-test split FTLD-Tau												
GM	12	0.92	0.91	1.05	27	0.96	−1.16	5.04e-13	−0.05	0.513	−0.86	2.89e-11
WM	12	0.97	0.86	1.03	27	0.95	−1.32	2.08e-11	−0.03	0.808	−0.79	4.92e-07
1× train-test split FTLD-TDP												
GM	24	0.70	1.01	0.89	29	0.88	−1.02	1.48e-08	−0.16	0.226	−0.61	1.92e-08
WM	24	0.75	0.79	−0.08	29	0.88	−1.02	4.37e-08	−0.20	0.117	−0.50	1.31e-04

BA, Bland-Altman statistics; Delta abs-diff, change in absolute difference; diff, difference; FTLD-Tau, frontotemporal lobar degeneration with inclusions of the tau protein; FTLD-TDP, frontotemporal lobar degeneration with inclusions of the transactive response DNA-binding protein 43 kDa; ICC, intraclass correlation coefficient; Itc, intercept; GM, gray matter; N, number of tissue samples; Rsq, R squared; sig., significance; WM, white matter. Here, we display the results of the application of our cross-validated transformation method in a single randomly obtained train-test split. On the left side, table shows transformation prerequisites (i.e., Rsq) and equivalence factors (i.e., beta, intercept) in training sets (GM/WM in FTLD-Tau and FTLD-TDP). On the right side, we report corresponding transformation outcomes (i.e., ICC) in the complementary testing sets. Additionally, we look at measures of test-retest agreement, i.e., mean difference between SB1 and SB2 before and after the transformation, with Bland-Altman statistics ($p < 0.05$, significant mean difference between SB1 and SB2/t-SB2; $p > 0.05$, non-significant mean difference between SB1 and SB2/t-SB2), as well as the decrease in absolute difference tested with a one-sample t-test statistics ($p < 0.05$, significant reduction in difference between duplicate measurements after the transformation).

Exploratory Analysis: Application of Validated Method to Other Sources of Pre-analytical Variability

We tested whether this method could help account for other sources of pre-analytical variability. In our brain bank, tissue that is not sampled for IHC analysis is frozen at −80 degrees for use in biochemical studies (Toledo et al., 2014). It would be advantageous to harvest frozen tissue in key regions that are not routinely sampled by traditional protocols (Montine et al., 2012) for more extensive regional and bilateral analyses in FTD (Irwin et al., 2018; Giannini et al., 2019). To test this approach, we compared digital %AO measurements between standard fresh tissue fixed at autopsy and legacy frozen tissue samples. We obtained tissue samples from frozen cortical slabs adjacent to those sampled fresh at autopsy (N = 16 in FTLD-Tau, N = 12 in FTLD-TDP), and allowed the frozen samples to thaw prior to fixation overnight in 10% neutral buffered formalin. All subsequent processing was done in an identical manner to standard samples obtained fresh at autopsy (Toledo et al., 2014). Frozen-fixed and standard (i.e., fresh-fixed) tissue samples from adjacent cortical slabs in the MFC were stained in the same staining batch, and %AO was measured using our standard digital image approach (please see methods). We performed equivalence analyses and found a significant linear association between frozen-fixed and fresh-fixed duplicate measurements in both FTLD-Tau (Rsq = 0.77, $p < 0.001$) and FTLD-TDP (Rsq = 0.70, $p < 0.001$) in the MFC region (**Supplementary Figure 2**), suggesting that it may be possible to use a similar SOP approach to the one we propose for staining batch effects (**Figure 7**) to account for other pre-analytical factors, such as processing of frozen tissue for IHC analysis.

Analysis of Generalizability: Replication of Validation Outcomes Using an Open-Source Digital Platform

We examined whether our findings of staining batch variability and improved agreement after transformation were reproducible using another digital histopathology platform, i.e., QuPath (Bankhead et al., 2017), by importing our color deconvolution algorithm parameters (**Supplementary Table 1**) in this software and performing identical analyses. First, we found that %AO measurements obtained from identical images in Halo and QuPath platforms were highly correlated for both FTLD-Tau and FTLD-TDP (Rsq $\geq$ 0.84, $p < 0.001$; **Supplementary Figure 3**), suggesting a strong association of %AO measurements of pathology across platforms. Next, we compared duplicate measurements between staining batches in the total FTLD-Tau and FTLD-TDP datasets (**Supplementary Table 3**), and found a significant difference between SB1 and SB2 QuPath measurements ($p < 0.001$ all), which were linearly related ($p < 0.001$ all) similar to our analyses above (**Figures 3**, **4** and **Table 2**). Application of the transformation method to QuPath data enabled to account for this variability as in Step 3 (**Supplementary Table 4**); Bland-Altman analysis showed improved test-retest agreement after transformation in both FTLD-Tau and FTLD-TDP (**Supplementary Figures 4**, **5**) similar to our analyses using the Halo platform (**Table 4** and **Figures 5**, **6**).

Finally, we performed an exploratory analysis to test the ability of an empiric stain detection algorithm approach to account for staining batch effects of both haematoxylin and DAB in SB2. We used the "Estimate stain vectors" function in QuPath to define optimum RGB values for DAB and haematoxylin in SB2, resulting in optimized detection algorithms for SB2 (**Supplementary Table 5**). We thus compared the optimized SB2 measurements to original SB1 measurements in QuPath in the total dataset (see section "Materials and Methods"). Using this approach, we found good test-retest agreement between %AO values obtained using the original algorithm in SB1 and duplicate measurements in SB2 analyzed with the optimized algorithm (**Supplementary Figure 6**), similar to our results using the transformation approach in QuPath (**Supplementary Table 4** and **Supplementary Figures 4**, **5**) and in Halo (**Table 4** and **Figures 5**, **6**). These findings suggest that digitally accounting for both haematoxylin and DAB provides for a comparable effect as our validated statistical transformation method (**Figure 7**).

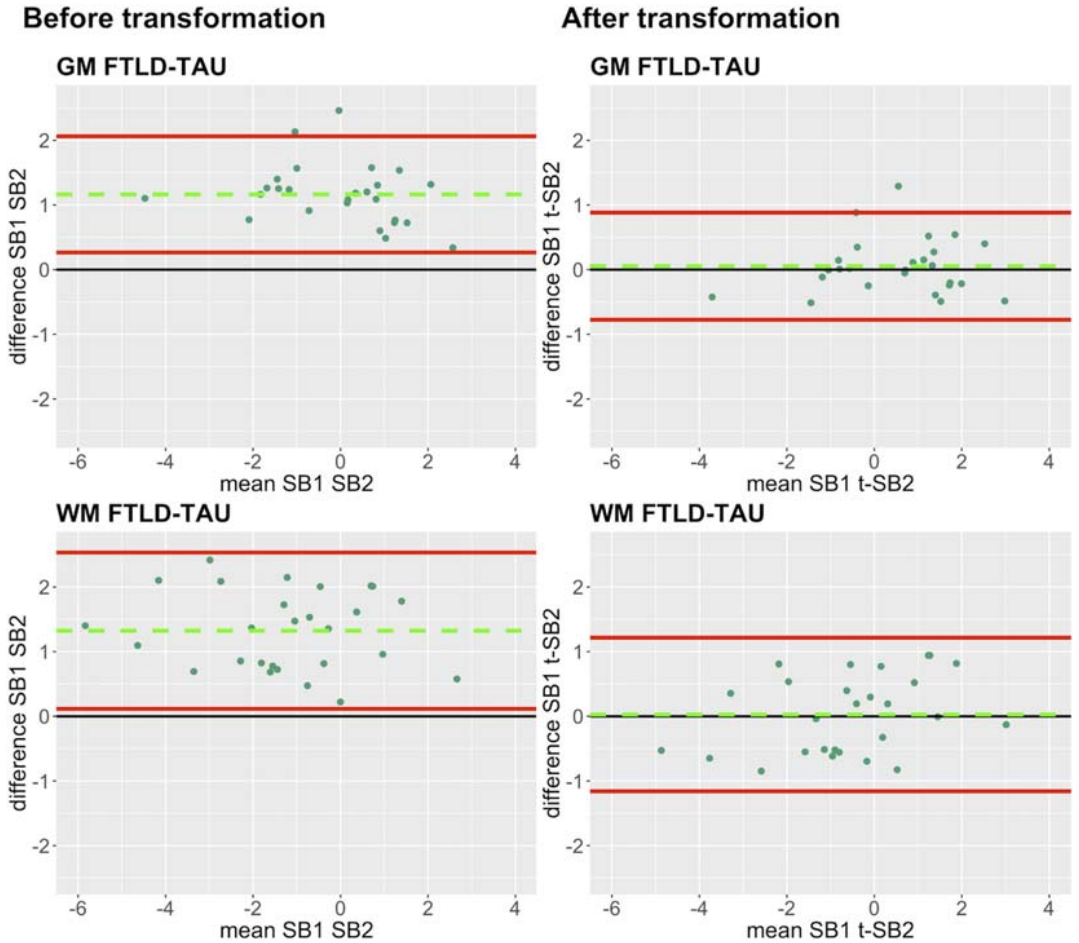

FIGURE 5 | Bland-Altman plots of test-retest agreement between duplicate measurements of pathology before vs. after transformation in FTLD-Tau. Plots portray test-retest agreement between duplicate measurements of digital pathology (i.e., ln %AO) in FTLD-Tau from SB1 and SB2 before and after transforming the data using our validated linear regression-based method. Here we illustrate the reduction in batch-related difference in digital measurements resulting from the application of our transformation method in a single train-test split in FTLD-Tau (Step 3). The green dashed line indicates the mean difference between SB1 and SB2 measurements, while the red solid lines mark the 95% limits of agreement between the two measurements. We find that mean difference between SB1 and SB2/t-SB2 is significantly different from zero before transformation ($p < 0.05$, one-sample *t*-test), whereas it is not significantly different from zero after transformation ($p > 0.05$) in both GM and WM. FTLD-Tau, frontotemporal lobar degeneration with inclusions of the tau protein; GM, gray matter; SB1, staining batch 1 (original); SB2, staining batch 2 (new); t-SB2, transformed staining batch 2 (new); WM, white matter.

DISCUSSION

Here we provide a statistically rigorous evaluation of pre-analytical variability in IHC staining intensity in FTLD (**Figure 1**), we develop an SOP for transformation of digital pathology measurements to account for this variability in both GM and WM (**Figure 7**), and we generalize our findings using a second, open-source, image analysis platform. First, Bland-Altman statistics suggests that variation in staining intensity is influential for measurements of digital pathology in both FTLD-Tau and FTLD-TDP in GM and WM (**Figure 3**), necessitating a method to transform values from different staining batches into equivalent values for more accurate analysis. Based on a highly correlated linear relationship between duplicate measurements of pathology from two different staining batches (**Figure 4**) in FTLD-Tau (GM: Rsq = 0.92, WM: Rsq = 0.92) and FTLD-TDP (GM: Rsq = 0.75, WM: Rsq = 0.78), we validate the use of a regression-based transformation method using a small set of tissue stained in duplicate to merge data obtained from different staining batches. First, we find that smaller datasets ($N = 12–24$) have adequate transformation prerequisites (i.e., Rsq), providing a consistently strong linear relationship (**Table 2**) to serve as training sets for our transformation protocol. Second, we find that training sets of $N = 12$ sample size in FTLD-Tau and $N = 24$ in FTLD-TDP result in optimal or near optimal transformation outcomes in complementary testing sets (**Table 3**). After applying our final transformation method, we observe a significant reduction in the difference between duplicate measurements from different staining batches in both FTLD-Tau ($p < 0.001$) and FTLD-TDP ($p < 0.001$) (**Figures 5**, **6**). Finally, we perform a proof-of-concept power analysis, which shows that the application of our transformation method improves statistical

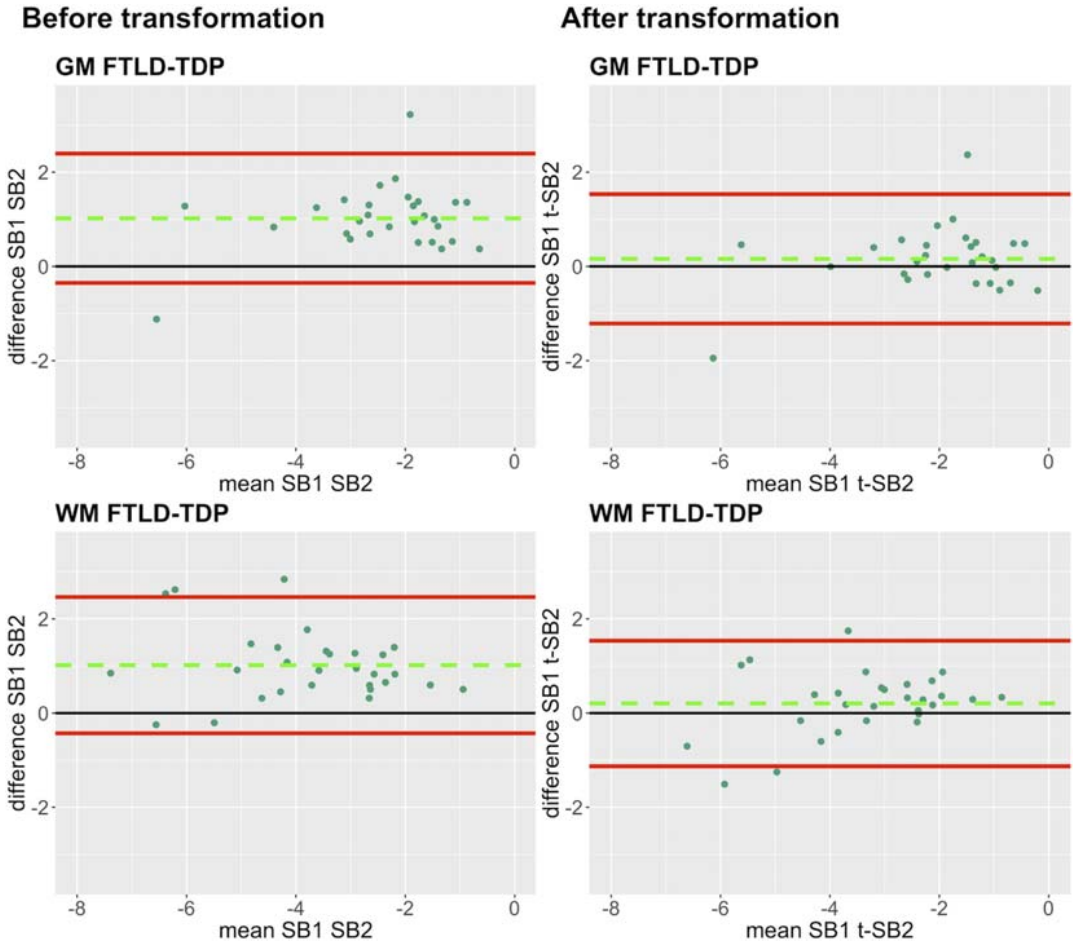

FIGURE 6 | Bland-Altman plots of test-retest agreement between duplicate measurements of pathology before vs. after transformation in FTLD-TDP. Plots portray test-retest agreement between duplicate measurements of digital pathology (i.e., ln %AO) in FTLD-TDP from SB1 and SB2 before and after transforming the data using our validated linear regression-based method. Here we illustrate the reduction in batch-related difference in digital measurements resulting from the application of our transformation method in a single train-test split in FTLD-TDP (Step 3). The green dashed line indicates the mean difference between SB1 and SB2 measurements, while the red solid lines mark the 95% limits of agreement between the two measurements. We find that mean difference between SB1 and SB2/t-SB2 is significantly different from zero before transformation ($p < 0.05$, one-sample *t*-test), whereas it is not significantly different from zero after transformation ($p > 0.05$) in both GM and WM. FTLD-TDP, frontotemporal lobar degeneration with inclusions of the transactive response DNA-binding protein 43; GM, gray matter; SB1, staining batch 1 (original); SB2, staining batch 2 (new); t-SB2, transformed staining batch 2 (new); WM, white matter.

power for analysis in both FTLD-Tau and FTLD-TDP, decreasing the required sample size by 20–40% (**Table 5**). Altogether, these results suggest that it is possible and advantageous to account for pre-analytical variability statistically, and this process can be performed using open-source platforms for greater rigor, reproducibility of digital measurements, and sharing of research methodologies. Therefore, these data have strong implications for digital pathology studies in neurodegenerative disease.

Digital measurements of pathology provide a novel and high-throughput means to obtain objective data of regional disease severity in the central nervous system of FTLD and related disorders. This approach allows for complex statistical modeling of quantitative pathology data for more fine-grained clinicopathological studies (Neltner et al., 2012; Hamilton et al., 2014; Walker et al., 2015; Coughlin et al., 2018; Ferman et al., 2018; Giannini et al., 2019). This is of importance as autopsy tissue remains the gold standard for diagnosis in neurodegenerative disease, and measurement of histopathological markers can inform biomarker discovery and validation. While clinicopathological studies have already been informative to improve the understanding of pathophysiological processes and guide clinical diagnostic criteria (Irwin et al., 2016a, 2017, 2018; Giannini et al., 2017), quantitative digital pathology has the potential to provide a more objective and detailed account of neuropathological burden, suitable for associations with biomarkers, imaging and other measures of disease (Irwin et al., 2018). Thus, a rigorous approach is needed to optimize digital pathology measurements for widespread use in the research community. We previously validated sampling methods and thresholding algorithms for FTLD (Irwin et al., 2016b), and successfully applied digital methods to relate *postmortem* FTLD histopathology to *antemortem* cerebrospinal

TABLE 5 | Outcomes of power analysis using merged SB1 and SB2/t-SB2 data to measure improvement before vs. after the transformation (Step 3).

	Merged untransformed (SB1 + SB2)			Merged transformed (SB1 + t-SB2)			Percent reduction
	ANG SD	Effect size	Est. sample	ANG SD	Effect size	Est. sample	Est. sample (%)
FTLD-Tau GM	1.96	0.8	95	1.52	0.8	58	−39
(*N* = 20)	1.96	0.5	242	1.52	0.5	146	−40
	1.96	0.2	1505	1.52	0.2	906	−40
FTLD-Tau WM	2.17	0.8	116	1.77	0.8	77	−33
(*N* = 20)	2.17	0.5	296	1.77	0.5	197	−34
	2.17	0.2	1845	1.77	0.2	1224	−34
FTLD-TDP GM	1.35	0.8	45	1.20	0.8	36	−20
(*N* = 38)	1.35	0.5	115	1.20	0.5	92	−20
	1.35	0.2	713	1.20	0.2	567	−20
FTLD-TDP WM	1.55	0.8	60	1.30	0.8	42	−29
(*N* = 38)	1.55	0.5	152	1.30	0.5	107	−30
	1.55	0.2	943	1.30	0.2	661	−30

ANG, angular gyrus; Est., estimated; FTLD-Tau, frontotemporal lobar degeneration with inclusions of the tau protein; FTLD-TDP, frontotemporal lobar degeneration with inclusions of the transactive response DNA-binding protein 43 kDa; GM, gray matter; N, number of tissue samples; SB1, original staining batch; SB2, new staining batch (untransformed); SD, standard deviation; t-SB2, new staining batch (transformed); WM, white matter. Here, we show a power analysis to estimate the sample size necessary for an independent samples t-test testing pathology burden (i.e., mean ln %AO) in ANG against any other hypothetical brain region. Our aim was to measure the improvement in power after transformation by comparing (1) data merged from the original staining batch and the new staining batch without transformation (i.e., merged untransformed = SB1 + SB2), and (2) data merged from the original staining batch and the new staining batch after transformation (i.e., merged transformed = SB1 + t-SB2). We calculated ANG SD in these two sets of data and used it as an approximation of the overall variance (ANG vs. hypothetical region). We used effect sizes of 0.2, 0.5, and 0.8, corresponding to small, medium, and large effect sizes (Cohen, 1988), to estimate the sample size necessary (i.e., Est. sample) to detect a difference between mean ANG and another hypothetical regional mean. Each power analysis used alpha 0.05 and power 0.8. We measured the change between merged untransformed and merged transformed data by means of a percent reduction in estimated sample size.

fluid (CSF) (Irwin et al., 2017) and quantitative MRI data (Irwin et al., 2018; Giannini et al., 2019). We have also used this approach in Alzheimer's disease (AD) and Lewy body disease (LBD) (Coughlin et al., 2018). Here, we validate a statistical methodology to account for an important pre-analytical factor in digital histopathology, similar to other approaches previously used for biofluid (Figurski et al., 2012) or neuroimaging (Cash et al., 2015) biomarkers, which helps us to account for staining batch effects in AO% measurements using a set of tissue stained in duplicate.

A unique aspect to digital pathology is the limited flexibility to stain large numbers of tissue samples in a single staining batch, which precludes the inclusion of large amounts of additional tissue as control sample for our transformation, as opposed to other biomarkers such as biofluid assays which often use multiple sets of >96 well plates. Therefore, our approach to determine a feasible number of tissue samples to use for this transformation method (i.e., ≤24, which is equivalent to a standard staining rack) is critical for implementation. We found relatively consistent goodness of fit (i.e., Rsq) in linear modeling derived from smaller trainings sets such as $N = 12$ or $N = 24$ in FTLD-Tau. FTLD-TDP showed relatively more heterogeneous transformation prerequisites (i.e., Rsq) in both GM and WM. We observed that lowering the number of samples in the training set increases the chance of a weaker linear relationship (**Table 2**). There may be several reasons for this observation. FTLD-Tau pathology has a wider magnitude and variance in overall %AO based on the morphology of tau inclusions, which in severe cases cover a large number of pixels (e.g., >70 %AO) (Irwin et al., 2017), compared to severe sections of FTLD-TDP, which cover a much smaller range of area (i.e., <5 %AO) (Irwin et al., 2018). The smaller variance in overall %AO in FTLD-TDP could potentially lead to an amplification of the effect of small changes in measurements between batches. Further, due to the small size of TDP-43 dystrophic neurites in GM and oligodendrocytic TDP-43 inclusions in WM (Neumann et al., 2009), biological variance in the amount of FTLD-TDP pathology in a given tissue sample may be influential even between adjacent sections. There may also be differences in antibody avidity or sensitivity to antigen retrieval, which could affect our outcomes focused on staining batch-related variability (Cummings et al., 2002). We used well-characterized antibodies (Goedert et al., 1995) with optimized staining parameters used in our lab and identical processing for both staining batches to reduce the influence of these factors.

It is well known that GM and WM have distinct densities and morphologies of disease in FTLD pathologies (Irwin et al., 2015). We therefore chose to analyze these two measures of disease separately in our validation analyses. In terms of transformation prerequisites and outcomes, we obtained relatively similar values between GM and WM within FTLD pathologies, indicating that these two measures of disease are affected by staining batch effects to a comparable extent. WM pathology in FTLD is important and understudied, especially using digital pathology methods. Indeed, in our most recent work we found greater overall burden of WM pathology in FTLD-Tau compared to FTLD-TDP (Irwin et al., 2018), which could help differentiate these pathologies during life (McMillan et al., 2013). While we now use a standardized sampling procedure (Irwin et al., 2017, 2018) of adjacent WM from cortical sections, future work will aim to explore sampling of

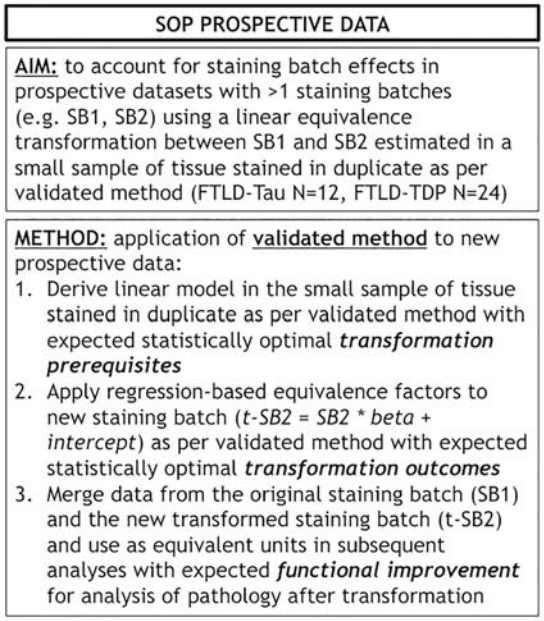

FIGURE 7 | Standard operating procedure for prospective use of our validated transformation method. Panel outlines a standard operating procedure (SOP) for prospective addition of new data to existing datasets where we use our validated transformation method to account for staining batch effects. FTLD-Tau, frontotemporal lobar degeneration with inclusions of the tau protein; FTLD-TDP, frontotemporal lobar degeneration with inclusions of the transactive response DNA-binding protein 43; LMN, number of tissue samples; SB1, staining batch 1 (original); SB2, staining batch 2 (new); SOP, standard operating procedure; t-SB2, transformed staining batch 2 (new).

specific deep WM tracks at the time of autopsy. Optimizing and validating pre-analytical methods for WM pathology analysis will be crucial to further the understanding of subcortical patterns of disease.

It is notable that the optimal size of training sets for an accurate transformation differed between FTLD-Tau and FTLD-TDP. These data suggest that transformation SOPs should be empirically determined for each disease (e.g., AD, LBD), and potentially for each antibody used in digital pathology studies. Here, we find optimal training-set sizes (i.e., $\geq$24) that are practical to use in prospective studies (i.e., requiring only half or one additional staining rack). It may be possible to further improve this transformation method using a larger number of training data by means of a tissue microarray slide with >100 pathology cores (Walker et al., 2017) in prospective staining runs, or tissue slides with standardized synthetic protein of interest for transformation (Sompuram et al., 2015). Our study provides important proof-of-concept findings for the use of linear regression to account for staining batch effects, thereby improving accuracy of digital histopathology, and new available tools may be used to facilitate and advance the implementation of this method.

Indeed, our method enabled us to correct for a large amount of variability due to staining batch effects (**Figures 4**, **5**). We were additionally interested in the implications of our method to improve clinicopathological correlations. Using a power analysis to compare the effects of our transformation on merged data from distinct staining batches, we found a positive improvement in both FTLD-Tau and FTLD-TDP after transformation (**Table 5**). This is of great importance for FTLD, which is a relatively rare neurodegenerative disease (Knopman and Roberts, 2011), and may also be beneficial in other more common disorders to preserve valuable autopsy tissue and improve statistical power.

Our study proposes and validates a method to account for staining batch effects in digital histopathology, but has some limitations. Relying on a statistical estimation, our proposed method does not help to escape other individual-sample sources of variability in digital measurements, such as artifacts or damaged tissue. For this reason we performed rigorous inspection of all tissue sections used in this study and we carefully excluded those that were not of sufficient quality for usage and comparison across staining batches. Therefore, in the selection of tissue samples to use in prospective transformations, it is crucial to ensure that anomalous sections with observable defects are not included. While (semi-)adjacent tissue sections compared across staining batches seemed near-identical by visual inspection, biological variation in pathology distribution as well as ROI sampling between (semi-)adjacent tissue sections may partly confound the linear relationship between different staining batches measured in this study. However, the highly consistent linear relationship between the two staining batches (**Figure 4**) suggests that these effects may be minimal. Additionally, there may be other pre-analytical factors that influence digital pathology measurements that have not been accounted for by our designed methodology. While the intensity of haematoxylin counterstain may be variable and introduce further noise in the digital measurements, the Halo quantification accounted for the counterstain in color deconvolution algorithms (**Supplementary Table 1**). Moreover, in our supplementary analysis using QuPath, we empirically derived an optimized RGB color deconvolution algorithm for both haematoxylin and DAB in SB2 (**Supplementary Table 5**) with similar favorable results for test-retest agreement (**Supplementary Figure 6**) as in our transformation approach (**Figure 7**). We used a transmitted light microscopy scanning system with identical image acquisition features and resolution. Further work is needed to validate image acquisition across different scanners at different labs as another pre-analytic factor that may be optimized to increase the rigor and reproducibility of digital histopathology for multicenter studies in neurodegenerative disease (Rojo et al., 2003). Further, the use of other available methods of digital histopathology such as multispectral analysis may improve quantification (Van Der Loos, 2008). In an exploratory analysis, we suggested a potential application of our methodology to equate data with alternative fixation methods (i.e., fresh-fixed vs. frozen-fixed tissue), based on an observed consistent linear relationship between duplicate measurements from these two approaches (**Supplementary Figure 2**). These findings suggest that the use of our SOP may be extended to other identifiable sources of pre-analytical variability, granted that the divergence between

digital measurements of pathology can be approximated to a linear relationship. Moreover, future targeted studies will be necessary to understand and address all potential sources of pre-analytical variability in digital histopathology systematically, and examine these variables carefully in large tissue samples with targeted study designs.

To conclude, we find that staining batch affects can significantly alter the accuracy of digital pathology measurements in neurodegenerative disease research. To account for this problem, we propose and validate a novel statistical approach using linear regression that enables to transform measurements from distinct staining batches into equivalent values, and to merge these data in a unique dataset without significant batch-related variability. Given the generalizability of our findings in an open-source digital pathology platform, we suggest that our method may provide a valid solution to researchers using different image analysis platforms. This approach will allow for more accurate and intercomparable measurements of digital pathology, and it will facilitate the creation of large-scale "libraries" of digital pathology data for future translational work.

ETHICS STATEMENT

This study was carried out in accordance with the recommendations of the Penn Institutional Review Board (IRB) on human subjects research protections guidelines. The protocol was approved by the Penn IRB. All subjects gave written informed consent prior to participation, in accordance with the Declaration of Helsinki.

AUTHOR CONTRIBUTIONS

LG, SX, CZ, CM, and DI contributed to the conception and design of the study. LG, CP, and CZ organized the database. LG conducted the statistical analysis. LG and DI wrote the first draft of the manuscript. All authors contributed to the data acquisition, data analysis, manuscript revision, and also read and approved the submitted version.

FUNDING

This study was supported by the NIH grants AG017586, AG038490, AG052943, AG054519, AG010124, AG043503, NS088341, AG10124, AG17586, and R01-NS102324, and the Penn Institute on Aging and the Wyncote Foundation.

ACKNOWLEDGMENTS

We thank our patients and their families who made this research possible. We thank Andrew Williams and Mendy Liang for their technical assistance. We also thank the Alzheimer Nederland for providing the student travel funding for LG.

SUPPLEMENTARY MATERIAL

The Supplementary Material for this article can be found online at: https://www.frontiersin.org/articles/10.3389/fnins.2019.00682/full#supplementary-material

REFERENCES

Bankhead, P., Loughrey, M. B., Fernández, J. A., Dombrowski, Y., McArt, D. G., Dunne, P. D., et al. (2017). QuPath: open source software for digital pathology image analysis. *Sci. Rep.* 7, 168–178. doi: 10.1038/s41598-017-17204-17205

Bland, M. J., and Altman, D. G. (1986). Statistical methods for assessing agreement between two methods of clinical measurement. *Lancet* 1, 307–310. doi: 10.1016/S0140-6736(86)90837-90838

Boxer, A. L., Gold, M., Huey, E., Hu, W. T., Rosen, H., Kramer, J., et al. (2013). The advantages of frontotemporal degeneration drug development (part 2 of frontotemporal degeneration: the next therapeutic frontier). *Alzheimer's Dement.* 9, 189–198. doi: 10.1016/j.jalz.2012.03.003

Cash, D. M., Frost, C., Iheme, L. O., Ünay, D., Kandemir, M., Fripp, J., et al. (2015). Assessing atrophy measurement techniques in dementia: results from the MIRIAD atrophy challenge. *Neuroimage* 123, 149–164. doi: 10.1016/j.neuroimage.2015.07.087

Cohen, J. (1988). *Statistical Power Anaylsis for the Behavioural Science*, 2nd Edn. Hillsdale, NJ: Lawrence Erlbaum.

Coughlin, D. G., Xie, S. X., Liang, M., Williams, A., Peterson, C., Weintraub, D., et al. (2018). Cognitive and pathological influences of tau pathology in lewy body disorders. *Ann. Neurol.* 85, 259–271. doi: 10.1002/ana.25392

Cummings, B. J., Mason, A. J. L., Kim, R. C., Sheu, P. C. Y., and Anderson, A. J. (2002). Optimization of techniques for the maximal detection and quantification of Alzheimer's-related neuropathology with digital imaging. *Neurobiol. Aging* 23, 161–170. doi: 10.1016/S0197-4580(01)00316-315

Dickson, D. W., Kouri, N., Murray, M. E., and Josephs, K. A. (2011). Neuropathology of frontotemporal lobar degeneration-Tau (FTLD-Tau). *J. Mol. Neurosci.* 45, 384–389. doi: 10.1007/s12031-011-9589-9580

Ferman, T. J., Aoki, N., Crook, J. E., Murray, M. E., Graff-Radford, N. R., van Gerpen, J. A., et al. (2018). The limbic and neocortical contribution of α-synuclein, tau, and amyloid β to disease duration in dementia with Lewy bodies. *Alzheimer's Dement.* 14, 330–339. doi: 10.1016/j.jalz.2017.09.014

Figurski, M. J., Waligórska, T., Toledo, J., Vanderstichele, H., Korecka, M., Lee, V. M. Y., et al. (2012). Improved protocol for measurement of plasma β-amyloid in longitudinal evaluation of Alzheimer's disease neuroimaging initiative study patients. *Alzheimers. Dement.* 8, 250–260. doi: 10.1016/j.jalz.2012.01.001

Giannini, L. A., Xie, S. X., McMillan, C. T., Liang, M., Williams, A., Jester, C., et al. (2019). Divergent patterns of TDP-43 and tau pathologies in primary progressive Aphasia. *Ann. Neurol.* 85, 630–643. doi: 10.1002/ana.25465

Giannini, L. A. A., Irwin, D. J., Mcmillan, C. T., Ash, S., Rascovsky, K., Wolk, D. A., et al. (2017). Clinical marker for Alzheimer disease pathology in logopenic primary progressive aphasia. *Neurology* 88, 2276–2284. doi: 10.1212/WNL.0000000000004034

Goedert, M., Jakes, R., and Vanmechelen, E. (1995). Monoclonal antibody AT8 recognises tau protein phosphorylated at both serine 202 and threonine 205. *Neurosci. Lett.* 189, 167–169. doi: 10.1016/0304-3940(95)11484-E

Griffin, J., and Treanor, D. (2017). Digital pathology in clinical use: where are we now and what is holding us back? *Histopathology* 70, 134–145. doi: 10.1111/his.12993

Hamilton, P. W., Bankhead, P., Wang, Y., Hutchinson, R., Kieran, D., McArt, D. G., et al. (2014). Digital pathology and image analysis in tissue biomarker research. *Methods* 70, 59–73. doi: 10.1016/j.ymeth.2014.06.015

Huisman, A. (2012). Digital pathology for education. *Stud. Health Technol. Inform.* 179, 68–71. doi: 10.3233/978-1-61499-086-4-68

Irwin, D. J., Brettschneider, J., McMillan, C. T., Cooper, F., Olm, C., Arnold, S. E., et al. (2016a). Deep clinical and neuropathological phenotyping of Pick disease. *Ann. Neurol.* 79, 272–287. doi: 10.1002/ana.24559

Irwin, D. J., Byrne, M. D., McMillan, C. T., Cooper, F., Arnold, S. E., Lee, E. B., et al. (2016b). Semi-automated digital image analysis of pick's disease and TDP-43 proteinopathy. *J. Histochem. Cytochem.* 64, 54–66. doi: 10.1369/0022155415614303

Irwin, D. J., Cairns, N. J., Grossman, M., McMillan, C. T., Lee, E. B., Van Deerlin, V. M., et al. (2015). Frontotemporal lobar degeneration: defining phenotypic diversity through personalized medicine. *Acta Neuropathol.* 129, 469–491. doi: 10.1007/s00401-014-1380-1381

Irwin, D. J., Lleó, A., Xie, S. X., McMillan, C. T., Wolk, D. A., Lee, E. B., et al. (2017). Ante mortem cerebrospinal fluid tau levels correlate with postmortem tau pathology in frontotemporal lobar degeneration. *Ann. Neurol.* 82, 247–258. doi: 10.1002/ana.24996

Irwin, D. J., McMillan, C. T., Xie, S. X., Rascovsky, K., Van Deerlin, V. M., Coslett, H. B., et al. (2018). Asymmetry of post-mortem neuropathology in behavioural-variant frontotemporal dementia. *Brain* 141, 288–301. doi: 10.1093/brain/awx319

Knopman, D. S., and Roberts, R. O. (2011). Estimating the number of persons with frontotemporal lobar degeneration in the US population. *J. Mol. Neurosci.* 45, 330–335. doi: 10.1007/s12031-011-9538-y

Kovacs, G. G. (2015). Invited review: neuropathology of tauopathies: principles and practice. *Neuropathol. Appl. Neurobiol.* 41, 3–23. doi: 10.1111/nan.12208

Lee, E. B., Porta, S., Michael Baer, G., Xu, Y., Suh, E. R., Kwong, L. K., et al. (2017). Expansion of the classification of FTLD-TDP: distinct pathology associated with rapidly progressive frontotemporal degeneration. *Acta Neuropathol.* 134, 65–78. doi: 10.1007/s00401-017-1679-1679

Macenko, M., Niethammer, M., Marron, J. S., Borland, D., Woosley, J. T., Guan, X., et al. (2009). A method for normalizing histology slides for quantitative analysis. *ISBI* 2009, 1107–1110. doi: 10.1109/ISBI.2009.5193250

Mackenzie, I. R., Neumann, M., Baborie, A., Sampathu, D. M., Du Plessis, D., Jaros, E., et al. (2011). A harmonized classification system for FTLD-TDP pathology. *Acta Neuropathol.* 122, 111–113. doi: 10.1007/s00401-011-0845-8

Mackenzie, I. R., Neumann, M., Bigio, E. H., Cairns, N. J., Alafuzoff, I., Kril, J., et al. (2010). Nomenclature and nosology for neuropathologic subtypes of frontotemporal lobar degeneration: an update. *Acta Neuropathol.* 119, 1–4. doi: 10.1007/s00401-009-0612-2

McKeith, I. G., Boeve, B. F., Dickson, D. W., Halliday, G., Taylor, J.-P., Weintraub, D., et al. (2017). Diagnosis and management of dementia with Lewy bodies: fourth consensus report of the dlb consortium. *Neurology* 89, 88–100. doi: 10.1212/WNL.0000000000004058

McMillan, C. T., Irwin, D. J., Avants, B. B., Powers, J., Cook, P. A., Toledo, J. B., et al. (2013). White matter imaging helps dissociate tau from TDP-43 in frontotemporal lobar degeneration. *J. Neurol. Neurosurg. Psychiatry* 84, 949–955. doi: 10.1136/jnnp-2012-304418

Mercken, M., Vandermeeren, M., Lübke, U., Six, J., Boons, J., Van de Voorde, A., et al. (1992). Monoclonal antibodies with selective specificity for Alzheimer Tau are directed against phosphatase-sensitive epitopes. *Acta Neuropathol.* 84, 265–272. doi: 10.1007/BF00227819

Mesulam, M. M. (2001). Primary progressive aphasia. *Ann. Neurol.* 49, 425–432. doi: 10.1002/ana.91

Montine, T. J., Phelps, C. H., Beach, T. G., Bigio, E. H., Cairns, N. J., Dickson, D. W., et al. (2012). National Institute on Aging-Alzheimer's Association guidelines for the neuropathologic assessment of Alzheimer's disease: a practical approach. *Acta Neuropathol.* 123, 1–11. doi: 10.1007/s00401-011-0910-913

Neltner, J. H., Abner, E. L., Schmitt, F. A., Denison, S. K., Anderson, S., Patel, E., et al. (2012). Digital pathology and image analysis for robust high-throughput quantitative assessment of Alzheimer disease neuropathologic changes. *J. Neuropathol. Exp. Neurol.* 71, 1075–1085. doi: 10.1097/NEN.0b013e3182768de4

Neumann, M., Kwong, L. K., Lee, E. B., Kremmer, E., Flatley, A., Xu, Y., et al. (2009). Phosphorylation of S409/410 of TDP-43 is a consistent feature in all sporadic and familial forms of TDP-43 proteinopathies. *Acta Neuropathol.* 117, 137–149. doi: 10.1007/s00401-008-0477-479

Rascovsky, K., Hodges, J. R., Knopman, D., Mendez, M. F., Kramer, J. H., Neuhaus, J., et al. (2011). Sensitivity of revised diagnostic criteria for the behavioural variant of frontotemporal dementia. *Brain* 134, 2456–2477. doi: 10.1093/brain/awr179

Rojo, M. G., García, G. B., and Vicente, M. C. (2003). Critical comparison of 31 commercially available. *Int J Surg Pathol.* 14, 285–305. doi: 10.1177/1066896906292274

Sieben, A., Van Langenhove, T., Engelborghs, S., Martin, J. J., Boon, P., Cras, P., et al. (2012). The genetics and neuropathology of frontotemporal lobar degeneration. *Acta Neuropathol.* 124, 353–372. doi: 10.1007/s00401-012-1029-x

Sompuram, S. R., Vani, K., Tracey, B., Kamstock, D. A., and Bogen, S. A. (2015). Standardizing Immunohistochemistry: a new reference control for detecting staining problems. *J. Histochem. Cytochem.* 63, 681–690. doi: 10.1369/0022155415588109

Toledo, J. B., Van Deerlin, V. M., Lee, E. B., Suh, E., Baek, Y., Robinson, J. L., et al. (2014). A platform for discovery: the university of pennsylvania integrated neurodegenerative disease biobank. *Alzheimers Dement* 10, 477.e–484.e. doi: 10.1016/j.jalz.2013.06.003

Van Der Loos, C. M. (2008). Multiple immunoenzyme staining: methods and visualizations for the observation with spectral imaging. *J. Histochem. Cytochem.* 56, 313–328. doi: 10.1369/jhc.2007.950170

Walker, L., McAleese, K. E., Johnson, M., Khundakar, A. A., Erskine, D., Thomas, A. J., et al. (2017). Quantitative neuropathology: an update on automated methodologies and implications for large scale cohorts. *J. Neural Transm.* 124, 671–683. doi: 10.1007/s00702-017-1702-1702

Walker, L., McAleese, K. E., Thomas, A. J., Johnson, M., Martin-Ruiz, C., Parker, C., et al. (2015). Neuropathologically mixed Alzheimer's and Lewy body disease: burden of pathological protein aggregates differs between clinical phenotypes. *Acta Neuropathol.* 129, 729–748. doi: 10.1007/s00401-015-1406-3

Conflict of Interest Statement: The authors declare that the research was conducted in the absence of any commercial or financial relationships that could be construed as a potential conflict of interest.

frontiers in Neuroscience

ORIGINAL RESEARCH
published: 06 August 2019
doi: 10.3389/fnins.2019.00757

The Use of Biomarkers and Genetic Screening to Diagnose Frontotemporal Dementia: Evidence and Clinical Implications

*Helena Gossye[1,2,3], Christine Van Broeckhoven[1,2] and Sebastiaan Engelborghs[2,3]**

[1] Neurodegenerative Brain Diseases Group, Center for Molecular Neurology, VIB, Antwerp, Belgium, [2] Institute Born – Bunge, University of Antwerp, Antwerp, Belgium, [3] Department of Neurology and Center for Neurosciences, UZ Brussel and Vrije Universiteit Brussel, Brussels, Belgium

Within the wide range of neurodegenerative brain diseases, the differential diagnosis of frontotemporal dementia (FTD) frequently poses a challenge. Often, signs and symptoms are not characteristic of the disease and may instead reflect atypical presentations. Consequently, the use of disease biomarkers is of importance to correctly identify the patients. Here, we describe how neuropsychological characteristics, neuroimaging and neurochemical biomarkers and screening for causal gene mutations can be used to differentiate FTD from other neurodegenerative diseases as well as to distinguish between FTD subtypes. Summarizing current evidence, we propose a stepwise approach in the diagnostic evaluation. Clinical consensus criteria that take into account a full neuropsychological examination have relatively good accuracy (sensitivity [se] 75–95%, specificity [sp] 82–95%) to diagnose FTD, although misdiagnosis (mostly AD) is common. Structural brain MRI (se 70–94%, sp 89–99%) and FDG PET (se 47–90%, sp 68–98%) or SPECT (se 36–100%, sp 41–100%) brain scans greatly increase diagnostic accuracy, showing greater involvement of frontal and anterior temporal lobes, with sparing of hippocampi and medial temporal lobes. If these results are inconclusive, we suggest detecting amyloid and tau cerebrospinal fluid (CSF) biomarkers that can indicate the presence of AD with good accuracy (se 74–100%, sp 82–97%). The use of P-tau$_{181}$ and the Aβ_{1-42}/Aβ_{1-40} ratio significantly increases the accuracy of correctly identifying FTD vs. AD. Alternatively, an amyloid brain PET scan can be performed to differentiate FTD from AD. When autosomal dominant inheritance is suspected, or in early onset dementia, mutation screening of causal genes is indicated and may also be offered to at-risk family members. We have summarized genotype–phenotype correlations for several genes that are known to cause familial frontotemporal lobar degeneration, which is the neuropathological substrate of FTD. The genes most commonly associated with this disease (*C9orf72, MAPT, GRN, TBK1*) are discussed, as well as some less frequent ones (*CHMP2B, VCP*). Several other techniques, such as diffusion tensor imaging, tau PET imaging and measuring serum neurofilament levels, show promise for future implementation as diagnostic biomarkers.

Keywords: dementia, frontotemporal dementia, Alzheimer, biomarker, genetics, cerebrospinal fluid, MRI

OPEN ACCESS

Edited by:
Alberto Lleo, Hospital de la Santa Creu i Sant Pau, Spain

Reviewed by:
Luisa Benussi, Centro San Giovanni di Dio Fatebenefratelli (IRCCS), Italy
Martin Ingelsson, Uppsala University, Sweden

***Correspondence:**
Sebastiaan Engelborghs
Sebastiaan.Engelborghs@uzbrussel.be;
Sebastiaan.Engelborghs@uantwerpen.be

Specialty section:
This article was submitted to Neurodegeneration, a section of the journal Frontiers in Neuroscience

Received: *10 February 2019*
Accepted: *08 July 2019*
Published: *06 August 2019*

Citation:
Gossye H, Van Broeckhoven C and Engelborghs S (2019) The Use of Biomarkers and Genetic Screening to Diagnose Frontotemporal Dementia: Evidence and Clinical Implications. Front. Neurosci. 13:757. doi: 10.3389/fnins.2019.00757

INTRODUCTION

Frontotemporal lobar degeneration (FTLD) represents a group of neurodegenerative brain diseases, characterized by relatively localized degeneration of the frontal and anterior temporal lobes. One of the clinical entities associated with FTLD is frontotemporal dementia (FTD), a neurodegenerative brain disorder with a diverse clinical presentation and multiple possible molecular pathways of disease. The prevalence of FTD is 1 to 461 per 100.000 individuals, accounting for approximately 2.7% of all dementias (Coyle-Gilchrist et al., 2016; Hogan et al., 2016). In patients under 65 years, FTD accounts for approximately 10.2% of all dementias, and is the second most common dementia subtype after Alzheimer's disease (AD) in this age group (Hogan et al., 2016).

Clinically, patients with FTLD display a progressive change in behavior, so-called behavioral variant FTD (bvFTD), and/or decline of language, or language variant presenting as primary progressive aphasias (PPA), such as semantic variant PPA (sv-PPA), non-fluent PPA (nfv-PPA), and logopenic PPA (lv-PPA) (Rascovsky et al., 2011). There may be a symptomatic overlap with atypical parkinsonian disorders or motor neuron disease (MND) (Chare et al., 2014).

Upon post-mortem examination of the affected brain, FTLD is characterized by protein inclusions in degenerating neurons. The composition of these inclusions varies across the disease spectrum. The majority of patients (85%) show cellular inclusion bodies that are comprised of either tau (FTLD-tau) or trans-active response DNA binding protein of 43 kDa (TDP-43) (FTLD-TDP). The latter can be subdivided into FTLD-TDP A to E (Mackenzie et al., 2010; Van Mossevelde et al., 2018). Another subgroup of cases present with inclusions of the fused in sarcoma (FUS) protein (FTLD-FUS). In the remaining cases, inclusions are comprised of (hitherto unidentified) proteins of the ubiquitin proteasome system (FTLD-UPS) or, infrequently, no protein inclusions are found (FTLD-ni) (Mackenzie et al., 2010; Sieben et al., 2012). The latter has also been described as dementia lacking distinct histopathology (DLDH), a term introduced by Knopman et al. (1990) in patients with degeneration of the brain without the presence of neuronal inclusions or senile plaques. Many of these cases have since been reclassified, as they were later found to have neuronal inclusions staining positive for ubiquitin (Mackenzie et al., 2006). The underlying disease mechanisms involved in this rare subtype are not yet fully understood.

In FTD, heritability plays a main role, with a positive family history in 39–50% of cases (Rosso et al., 2003; Rohrer et al., 2009; Sieben et al., 2012; Po et al., 2014). An autosomal dominant presentation is seen in 10–23% of patients (Goldman et al., 2005; Rohrer et al., 2009; Sieben et al., 2012). The most frequent mutated genes involved in FTD with a dominant inheritance pattern are the *C9orf72* (8.2%) (DeJesus-Hernandez et al., 2011; Renton et al., 2011; Gijselinck et al., 2012), the progranulin (*GRN*) (4.1%) (Baker et al., 2006; Cruts et al., 2006; Sieben et al., 2012) and the microtubule associated protein tau (*MAPT*) (5.6%) (Hutton et al., 1998). Less frequent disease genes are those coding for the protein fused in sarcoma (*FUS*) (Yan et al., 2010; Deng et al., 2014), chromatin-modifying protein 2b (*CHMP2B*) (van der Zee et al., 2008; Isaacs et al., 2011), TAR DNA-binding protein (*TARDBP*) (Lattante et al., 2013), TANK binding kinase 1 (*TBK1*) (Cirulli et al., 2015; Freischmidt et al., 2015; Gijselinck et al., 2015; Pottier et al., 2015), valosin containing protein (*VCP*) (Watts et al., 2004), sequestosome 1 (*SQSTM1*) (Fecto et al., 2011), and several others (Po et al., 2014; Woollacott and Rohrer, 2016; Che et al., 2018).

Amongst all of these heterogeneous subtypes in multiple domains, significant correlations can be found between causal gene, neuropathology and a certain set of clinical presentations. However, a one-to-one relationship is lacking (Sieben et al., 2012; Van Mossevelde et al., 2018).

The diagnosis of bvFTD and of the different language variants of FTD is most commonly based upon clinical diagnostic criteria (Gorno-Tempini et al., 2011; Rascovsky et al., 2011). These are based on the presenting core symptoms, complemented with results of (a combination of) brain magnetic resonance imaging (MRI), 18-fluorodeoxyglucose (FDG) positron emission tomography (PET) scan, perfusion single-photon emission tomography (SPECT) scan and DNA screening for causal mutations.

Several other techniques can aid in the differential diagnosis of FTD, especially when the clinical presentation is suggestive for other types of dementia as illustrated by our clinical vignette. To distinguish FTD from dementia caused by AD, cerebrospinal fluid (CSF) biomarkers demonstrating amyloid and tau pathology and amyloid tracer imaging techniques are widely used in clinical practice (Croisile et al., 2012; Dubois et al., 2014). Although these CSF biomarkers have a good diagnostic accuracy for AD, some cases display an atypical biochemical signature, as we will discuss below. Numerous other novel techniques are hitherto primarily carried out in a research setting.

Due to its heterogeneous nature, the diagnosis of FTD can be challenging. This review aims to summarize the state of the art in the current wide range of available diagnostic tools, covering neuropsychological evaluation, neurochemical and imaging biomarkers and genetic testing. More specifically, we will summarize the indications, evidence and added diagnostic and therapeutic value of these techniques within the framework of a clinical setting.

Clinical Vignette

A 65-year old patient consulted the neurologist with complaints of gradually progressive memory deficits.

Her previous medical history included arterial hypertension, surgical removal of an occipital meningioma and melanoma. Her medication intake was limited to a diuretic and a beta-blocker.

The presenting complaints were those of short term memory problems with insidious onset, progressively worsening over the course of 1 year. There was also occasional occurrence of diminished orientation in space.

The family history revealed that the maternal grandfather had late-onset dementia.

Clinical neurological examination was perfectly normal except for the presence of palmomental reflexes. No other frontal release signs, parkinsonism or any other pathological sign was found.

A diagnostic workup was performed:

- An extensive blood analysis showed no anomalies except for a slight macrocytic anemia. Thyroid function and blood vitamin levels were adequate.
- Neuropsychological testing revealed a single domain amnestic mild cognitive impairment.
- An MRI scan of the brain showed corticosubcortical atrophy, more than what would be expected for the patient's age (**Figure 1**).

Based upon initial anamnestic presentation, the suspicion for prodromal early onset AD was raised.
During the next encounter, the patient was accompanied by her husband who mentioned that 1 year prior to the onset of the memory complaints, he had begun to notice behavioral changes. There was slight disinhibition, with the tendency to laugh at socially inappropriate occasions. In addition, the patient had developed apathy, of which loss of initiative was the most prominent symptom. There were some dysexecutive symptoms, with difficulties managing her everyday tasks. These symptoms had implications on the course of the activities of daily living (ADL), with a lack of personal hygiene and self-care. Only later during the disease course did the memory complaints also become apparent.
Paraclinical re-evaluation of the patient was performed:

- An automated volumetric analysis of the brain MRI scan showed a more pronounced atrophy of the frontal lobes in comparison with age-matched controls. The hippocampal volume was normal for age (**Figure 2**).
- On an FDG PET scan of the brain, a significantly lower metabolism could be visualized anteromedially in the right frontal lobe and in the right temporal lobe. Minimal hypometabolism was found on the left side as well.
- CSF biomarker analysis revealed elevated T-tau (632 pg/ml; normal: <501 pg/ml) and P-tau (69.5 pg/ml; normal: <57 pg/ml) levels with normal values of $A\beta_{1-42}$ (1551 pg/ml; normal: >755 pg/ml) and $A\beta_{1-42}/A\beta_{1-40}$ ratio (0.196; normal: >0.106). This result indicated the presence of a neurodegenerative brain disease, but made the diagnosis of an underlying AD less likely.
- Genetic testing of known causal AD and FTD genes was performed and could not identify a causal mutation.

These biomarkers were incompatible with the diagnosis of prodromal AD. Furthermore, a striking localized atrophy in the frontal lobe on the automated volumetric analysis of the brain MRI scan (**Figure 2**) and a significantly lower metabolism in the right frontal and temporal lobes prompted the shift of focus to a possible FTD.
Based on the presenting clinical symptoms and the CSF and imaging biomarkers, the tentative diagnosis of behavioral variant FTD (bvFTD) was retained.
This case serves as an example of the importance of an extensive patient history as well as of specific biomarkers for the diagnosis of neurodegenerative brain disorders. Underneath an atypical clinical presentation, highly suggestive for prodromal AD, an underlying FTD could be unveiled.

CLINICAL DIAGNOSTIC CRITERIA FOR FTD: STRENGTHS AND LIMITATIONS

The most recently revised consensus criteria for the clinical diagnosis of bvFTD are those by Rascovsky et al. (2011). In this hierarchical framework, three levels of diagnostic certainty are distinguished. The first degree determines whether or not the term "possible" bvFTD is appropriate and is based upon presence of core symptoms (behavioral disinhibition, apathy/inertia, compulsive behavior, dietary changes and executive dysfunction with spared memory and visuospatial functions) alone. For "probable" and "definite" bvFTD, results of imaging and histopathology/DNA analysis, respectively, are taken into account. The consensus criteria for possible bvFTD have a sensitivity of 85–95% and a specificity of 82%, irrespective of the underlying proteinopathy (Rascovsky et al., 2011; Harris et al., 2013; Balasa et al., 2015). For probable bvFTD, sensitivity and specificity values are 75–85 and 95%, respectively (Rascovsky et al., 2011; Harris et al., 2013; Balasa et al., 2015). A higher sensitivity is reached in early onset dementia compared with late onset, as in younger age groups there is significantly more disinhibition, loss of empathy and compulsive behavior (Rascovsky et al., 2011; Balasa et al., 2015). False positive diagnoses are most common in patients with a later onset, an absence of family history for dementia and a more apathetic presentation. They mainly turn out to be AD upon neuropathological examination (Harris et al., 2013; Balasa et al., 2015).

Several other clinical tools exist to measure frontal lobe dysfunction and therefore differentiate between FTD and AD. Many assessment batteries of neurobehavioral symptoms, such as the Schedules for Clinical Assessment in Neuropsychiatry (Wing et al., 1990), the Scale for Emotional Blunting (Mendez et al., 2006), the Middelheim Frontality Score (De Deyn et al., 2005) and the Frontal Behavior Inventory (Kertesz et al., 2000) have a good discriminative ability (Milan et al., 2008; Mathias and Morphett, 2010).

Similar consensus criteria, with a stepwise approach to the level of evidence, exist for the language variants of FTD (Gorno-Tempini et al., 2011). The initial and most prominent symptoms should be deficits in language for the diagnosis of PPA to be considered. Subsequently, aphasia is characterized more specifically, distinguishing three separate entities: sv-PPA presenting with impaired comprehension but spared speech production, nfv-PPA with agrammatisms and speech apraxia, and lv-PPA with anomia and impaired single-word comprehension. The latter is only very rarely associated with FTLD; more commonly (77%) is it seen in patients with an underlying AD pathology (Chare et al., 2014; Leyton et al., 2015; Spinelli et al., 2017).

Both false-positive and false-negative diagnoses of FTD are most often confounded with AD (Harris et al., 2013). Analysis of a large neuropathological confirmed cohort brought to light that several clinical characteristics can discriminate FTD from AD with great accuracy (>86%); these were word finding difficulties, phonological errors, delusions and lack of object agnosia for AD, and relative lack of neuropsychiatric features, phonological errors and gait disturbance for FTD. Even then, about 36% of AD cases could not be differentiated from FTD based on clinical diagnostic criteria (Chare et al., 2014). 52% of AD patients with an atypical profile (commonly called "behavioral variant AD") meet the criteria for possible FTD, with apathy as the main overlapping feature (Ossenkoppele et al., 2015). The notion that deficits in episodic memory can reliably distinguish FTD from AD used to be considered a strong criterion (Neary et al., 1998). However, many FTD patients do initially present with complaints of memory loss and often meet AD consensus criteria

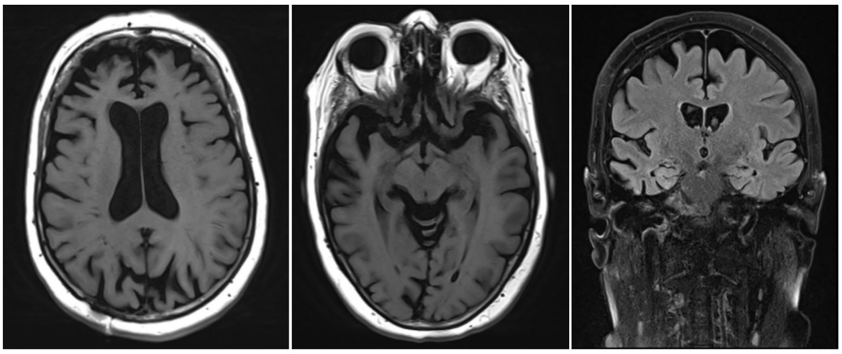

FIGURE 1 | Brain MRI of the patient described in the clinical vignette.

VISUAL RESULTS

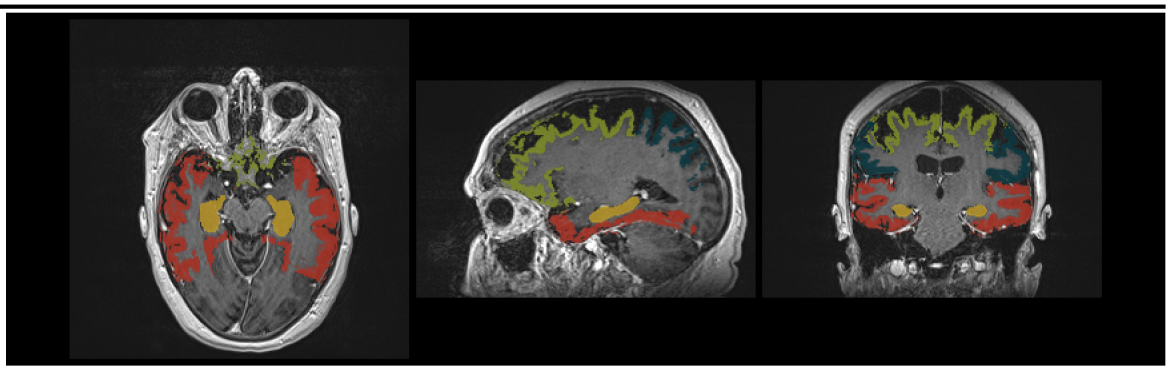

BRAIN VOLUMES

	Frontal cortex	Parietal cortex	Temporal cortex	Hippocampi
Volume	207 ml*	164 ml*	145 ml*	10.1 ml*
Normal range	209 - 269 ml*	125 - 166 ml*	136 - 171 ml*	9.0 - 13.1 ml*
Normative percentile	< 1	98.5	15.4	18.5

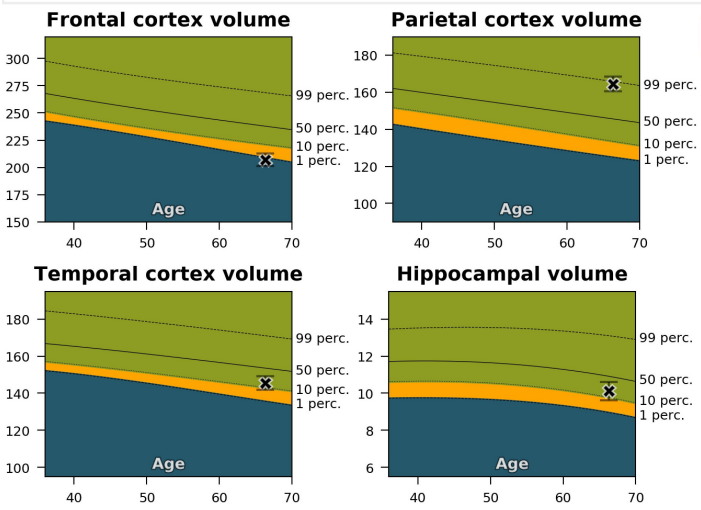

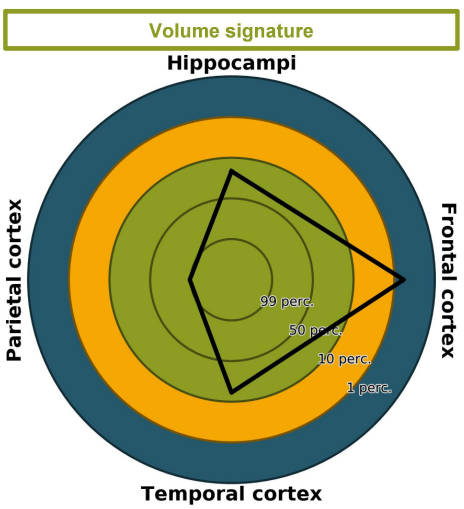

* Displayed brain volumes are normalized for head size. The normalization factor for this patient equals 0.78.

FIGURE 2 | Volumetric brain MRI of the patient described in the clinical vignette (report by Icometrix).

(Khachaturian, 2011; Fernandez-Matarrubia et al., 2017). Apart from AD, there is also substantial symptomatic overlap between FTD and MND, with co-occurrence of MND in 12.5–15% of FTD patients (Burrell et al., 2011; Saxon et al., 2017).

In many cases, some degree of parkinsonism is present upon initial presentation. When language and behavioral symptoms overlap, there is often a difficult differential diagnosis between so-called FTD with parkinsonism syndromes and atypical parkinsonian syndromes such as corticobasal degeneration (CBD) and progressive supranuclear palsy (PSP) (Espay and Litvan, 2011).

Another gray area exists along the borders of psychiatric disorders. An important limitation of the clinical diagnostic criteria is their relatively subjective and arbitrary nature. Symptoms like aberrant behavior are prone to observer bias, and are usually described by informants, making them inherently subjective and creating another layer of interaction in which nuances may be lost. Apathy, emotional withdrawal, hallucinations, delusions, psychosis, and compulsive behaviors can also easily be misdiagnosed as part of a psychiatric disorder such as depression, schizophrenia or bipolar disorder, especially with early onset dementia (Waldo et al., 2015).

In summary, these commonly used sets of clinical criteria offer a framework for the standardized classification of patients with FTD into subtypes. However, overlap between categories and with other disorders may exist as well as mixed presentations, as the disease progresses and new symptoms arise.

IMAGING TECHNIQUES TO DIAGNOSE FTD

Structural Brain MRI

A typical first step in obtaining an imaging-supported diagnosis of FTD is structural brain MRI. T1-weighted MRI images aid in evaluating (localized) brain atrophy, while flair images provide proof of possible vascular damage. In FTD, one typically expects a more pronounced loss of volume in the frontal lobes and the anterior temporal lobes (Varma et al., 2002; Boccardi et al., 2003; Kipps et al., 2007; Meyer et al., 2017; Che et al., 2018). Asymmetry is not uncommon, usually with a greater involvement of the dominant hemisphere, especially in language variants (Boccardi et al., 2003; Kipps et al., 2007; Che et al., 2018). The hippocampi and medial temporal lobes are typically relatively spared (Varma et al., 2002; Boccardi et al., 2003; Kipps et al., 2007; Meyer et al., 2017; Che et al., 2018).

The aforementioned clinical subtypes of FTD generally have a distinct MRI atrophy pattern, although overlap exists. bvFTD patients typically show atrophy in the dorsolateral, orbital and medial frontal cortices as well as other regions of the salience network (SN) (Che et al., 2018). sv-PPA patients show (often subtle) unilateral atrophy of the anterior temporal pole, with a characteristic "knife-edge" aspect in this area. Left-sided atrophy usually comes with a typical sv-PPA symptomatology, while patients with a predominantly right-sided atrophy tend to mimic bvFTD (Rabinovici and Miller, 2010). The former is most common, but involvement of the contralateral side tends to occur within 3 years (Rabinovici and Miller, 2010). nfv-PPA patients typically show volume loss in the left perisylvian region, more specifically the frontal operculum, premotor, and supplementary motor areas as well as the insula. Involvement of Broca's area explains the motor component of the aphasia (Pressman and Miller, 2014; Che et al., 2018). Comparable relatively specific patterns of atrophy exist within groups of carriers of the same causal mutation for FTD (Che et al., 2018; Van Mossevelde et al., 2018).

Sensitivity (se) and specificity (sp) of brain MRI for differentiating FTD from controls have been reported as 70–94 and 89–99%, respectively (Likeman et al., 2005; Harper et al., 2016; Vijverberg et al., 2016). Structural brain MRI is especially useful in distinguishing FTD from AD, with a sensitivity of 55–94% and a specificity of 81–97% by comparing patterns of atrophy (Boccardi et al., 2003; Likeman et al., 2005; Harper et al., 2016). FTD patients show significantly more frontal and (mostly anterior) temporal atrophy with relative sparing of the hippocampus, while AD patients typically show bilateral hippocampal and medial temporal lobe atrophy, with relative sparing of the frontal lobes. Asymmetrical involvement of the hemispheres is another feature that is common in FTD patients and rare in AD (Varma et al., 2002; Boccardi et al., 2003; Likeman et al., 2005). The left frontal and temporal regions are more often involved than the right in FTD (Boccardi et al., 2003). One study found that asymmetrical involvement of the brain differentiated FTD from non-FTD with a sensitivity of 38% and a specificity of 100% (Varma et al., 2002).

In the early stages of the disease, however, a brain MRI scan may not yet show abnormalities (Meeter et al., 2017). One study showed an incongruence between clinical subtypes: almost half of bvFTD patients had normal MRI scans, while all of the sv-PPA patients displayed a pathological scan. However, not all scans analyzed were made at initial presentation (Kipps et al., 2007). The presence of MRI abnormalities seems to be associated with more severe imitation behavior and disinhibition compared to those patients with normal MRI (Koedam et al., 2010). On the other hand, a large-scale trial examining presymptomatic carriers of a known causal mutation was able to find structural imaging changes 5–10 years before expected onset, based on the average onset within the family. The insular and temporal cortices were the earliest regions to show atrophy (Rohrer et al., 2015).

Comparing brain atrophy and abnormalities is classically done by visual evaluation with commonly used scales such as the rating scale for medial temporal lobe atrophy (MTA) (Scheltens et al., 1995), the global cortical atrophy (GCA) scale (Pasquier et al., 1996) and the Fazekas' scale (Fazekas et al., 1987). However, novel fully automated image quantification methods such as automated volumetry, voxel-based morphometry (VBM), tensor-based morphometry (TBM), manifold learning, region of interest (ROI)-based grading and automated measuring of vascular burden are increasingly used. One study (Koikkalainen et al., 2016) showed an accuracy rate of respectively 50, 65, 64, 50, 58, and 33% for these techniques in differentiating between normal controls, AD, FTD and Lewy body dementia (LBD). However, in combining different techniques, accuracy rates of 69% were reached. FTD patients were most often misclassified

as AD patients (21% of cases). Here, visual MRI ratings reached an accuracy of 52%, scoring significantly worse than combined automated quantification methods (Koikkalainen et al., 2016). A 2017 multi-centric MRI study found an accuracy rate of 85% for the diagnosis of bvFTD using automatic pattern recognition algorithms (Meyer et al., 2017).

A study by Munoz-Ruiz et al. (2012) compared hippocampal volumetry (HV) with VBM and TBM in differentiation between controls, FTD patients and AD patients. FTD patients were rather accurately distinguished from controls with all techniques (se and sp were 84 and 80% for HV, 80 and 71% for TBM, 87 and 81% with VBM). VBM was most suitable for the differential diagnosis of FTD versus AD, with a sensitivity of 72% and a specificity of 67% (Munoz-Ruiz et al., 2012). HV alone might be suitable to distinguish between FTD or AD and healthy controls, but in itself is not sufficient to differentiate between the two types of dementia (se and sp both 55%); here, a more extensive screening of the pattern of atrophy is needed (Munoz-Ruiz et al., 2012; de Souza et al., 2013).

These novel MRI techniques may aid in correctly identifying atypical presentations of neurodegenerative brain diseases. In AD patients with a predominantly behavioral or dysexecutive presentation, VBM shows marked atrophy in bilateral temporoparietal regions and only limited atrophy in the frontal cortex compared to controls, a pattern strikingly similar to AD patients with a typical presentation (Ossenkoppele et al., 2015).

Another relatively new tool is the automated measurement of cortical thickness, which shows a specific pattern of cortical thinning in FTD compared to AD. This technique has similar results in differentiating FTD from AD as the more classically measured cortical volume (Du et al., 2007). It is also useful to distinguish between clinical subtypes of FTD. One study showed distinct differences in cortical thinning between nfv-PPA and sv-PPA, resulting in an accurate diagnosis of 90% of cases (Agosta et al., 2015).

Brain FDG PET and Perfusion SPECT Scan to Diagnose FTD

Another part of the investigation of patients with suspected FTD is based on functional imaging of the brain (Rascovsky et al., 2011). A commonly used technique is the FDG PET scan, which visualizes the cerebral glucose metabolism. Another method for functional imaging is perfusion SPECT, which also requires the intravenous injection of a radiolabeled tracer molecule, but instead is a measure of cerebral blood flow (CBF). The radiotracers most commonly used are ^{99m}technetium-hexamethylpropylenamine oxime (^{99m}Tc-HMPAO) or ^{99m}technetium-ethyl-cysteinate dimer (^{99m}Tc-ECD) (Archer et al., 2015).

In FTD, hypometabolism and hypoperfusion are typically seen in the frontal and anterior temporal lobes, more specifically in bilateral medial, inferior and superior lateral frontal cortices, anterior cingulate, left temporal, and right parietal cortices and the caudate nuclei. Usually, the hypometabolism correlates with, but often precedes, the atrophy on MRI (Varma et al., 2002; Le Ber et al., 2006; Morbelli et al., 2016). Local hypometabolism is best observed in the frontal regions for bvFTD, temporal regions for sv-PPA and perisylvian regions for nfv-PPA (Che et al., 2018).

For FTD, the sensitivity of FDG PET scan ranges from 47 to 90%; the specificity from 68 to 98% (Foster et al., 2007; Kerklaan et al., 2014; Vijverberg et al., 2016). In subjects with late onset behavioral changes, bvFTD could be differentiated from other diagnoses with a sensitivity of 96% and a specificity of 73% when combined with structural MRI (Vijverberg et al., 2016). An increase of the abnormalities can be seen over time, indicating the potential usefulness of FDG PET as a biomarker of disease progression (Diehl-Schmid et al., 2007).

The sensitivity and specificity of SPECT for the differential diagnosis between FTD and AD were reported as 36–100 and 41–100%, respectively (Dougall et al., 2004; Yeo et al., 2013; Archer et al., 2015). A Belgian study comparing SPECT abnormalities between cohorts of FTD and AD patients showed that biparietal hypoperfusion was significantly more present in AD, while bifrontal hypometabolism was significantly associated with FTD. 74% of AD patients and 81% of FTD patients were correctly classified (Pickut et al., 1997). Another study showed that severely decreased frontal (se 76%, sp 60%) and temporal (se 71%, sp 55%) CBF and asymmetry between hemispheres (se 38%, sp 73%) were good markers to differentiate FTD from AD and vascular dementia (VaD) (Varma et al., 2002).

Thus, brain FDG PET or SPECT scans can significantly increase diagnostic accuracy and have the advantage of showing abnormalities fairly early in the disease process (Varma et al., 2002; Morbelli et al., 2016). A systematic review summarizing the evidence on the comparison of PET and SPECT for the diagnosis of neurodegenerative brain diseases showed that some studies find the techniques equally useful, while others describe better results with PET. However, there is a lack of methodologically good direct comparative studies. SPECT has the advantage of being more affordable whereas PET has a better spatial resolution (Davison and O'Brien, 2014).

NEUROCHEMICAL BIOMARKERS TO DIAGNOSE FTD

Core AD CSF Biomarkers: $A\beta_{1-42}$, $A\beta_{1-42}/A\beta_{1-40}$ Ratio, T-tau and P-tau

The currently most used panel to assess pathological markers of neurodegenerative brain disease is a combination of amyloid-β of 42 amino acids ($A\beta_{1-42}$), total tau protein (T-tau), and hyperphosphorylated tau (P-tau_{181}) in CSF (Engelborghs et al., 2008; Bjerke and Engelborghs, 2018; Niemantsverdriet et al., 2018). They are not, in fact, used for the diagnosis of FTD, but rather to make the diagnosis of AD less likely when doubt exists. A CSF biomarker profile characteristic for AD, with good diagnostic accuracy (>80%), shows decreased $A\beta_{1-42}$ values, in combination with increased T-tau and P-tau values (Engelborghs et al., 2008; Bjerke and Engelborghs, 2018). Some patients do not completely match this typical AD CSF profile. As amyloid pathology is measurable much earlier in the disease process than tau pathology, there may be an isolated decrease in $A\beta_{1-42}$ in

early disease stages (Blennow and Zetterberg, 2018). CSF tau markers are more strongly associated with cognitive decline and disease progression in AD than $A\beta_{1-42}$ (Niemantsverdriet et al., 2017b). The opposite may also be true, as between-individual variations in total Aβ production or secretion from neurons and variations in CSF dynamics may cause $A\beta_{1-42}$ to fall within a normal range, while underlying amyloid pathology is present (Blennow and Zetterberg, 2018).

In a large (n = 78) neuropathologically confirmed Belgian cohort of AD and non-AD dementia patients, the added diagnostic value for AD versus non-AD dementia (FTD amongst others) of the standard CSF biomarker panel to clinical consensus criteria was measured. In patients with an ambiguous (AD versus non-AD dementia) clinical diagnosis, the correct diagnosis would have been established in 67% of cases. As the diagnosis based on clinical consensus criteria was straightforward, no added diagnostic value could be measured. A misdiagnosis based on CSF biomarkers often occurs in patients with non-AD and AD co-pathology (Niemantsverdriet et al., 2017b, 2018). Apart from this, T-tau may also be significantly increased after stroke and in Creutzfeldt–Jakob's disease; whereas P-tau_{181} is a more specific CSF biomarker for AD. P-tau_{181} is indispensable for the differential diagnosis between AD and non-AD neurodegenerative brain disorders. Both $A\beta_{1-42}$ and T-tau may be abnormal at intermediate levels in DLB, FTD, VaD, and CJD (Niemantsverdriet et al., 2017b, 2018). Sensitivity and specificity to distinguish FTD from AD have been reported as 74–100 and 82–97%, respectively (Irwin et al., 2013).

To further improve diagnostic performance for AD, the use of the $A\beta_{1-42}/A\beta_{1-40}$ ratio has been proposed with good results (Janelidze et al., 2016; Leuzy et al., 2016; Niemantsverdriet et al., 2017a; Bjerke and Engelborghs, 2018), improving accuracy with 14–36% compared to $A\beta_{1-42}$ alone (Janelidze et al., 2016; Lewczuk et al., 2017). An isolated decrease in $A\beta_{1-42}$ is more specific to AD, while a global decrease in both Aβ isoforms may be correlated with subcortical damage in general or may even be due to interindividual variability (Janelidze et al., 2016; Lewczuk et al., 2017; Niemantsverdriet et al., 2017a).

Cerebrospinal fluid biomarker analysis of the aforementioned proteins is fairly cost-effective (Niemantsverdriet et al., 2017b). A disadvantage of all CSF biomarkers is the necessity to perform a lumbar puncture (LP). However, when performed correctly, LP has a low complication rate and a fairly good tolerability (Duits et al., 2016; Engelborghs et al., 2017). Overall, evidence shows a clear indication for the use of CSF biomarkers $A\beta_{1-42}$, $A\beta_{1-42}/A\beta_{1-40}$ ratio, T-tau and P-tau_{181} as an efficient measure to confirm or rule out AD when other biomarkers are inconclusive. FTLD cannot be diagnosed based on CSF biomarkers yet; non-specific, intermediate decreased $A\beta_{1-42}$ and increased T-tau CSF levels may or may not be present.

GENETIC SCREENING FOR KNOWN CAUSAL GENES FOR FTD

It has been suggested that the presence of a pathogenic mutation in an FTD gene in a patient with suspected FTD should be enough to confirm a diagnosis of "definite" FTD, putting genetic screening at the same level of diagnosis as autopsy brain histopathology analysis (Rascovsky et al., 2011). However, the absence of a mutation does not contribute to the diagnosis since FTD is frequently sporadic and FTD genes do not explain all families with FTD.

To elucidate further the value of genetic screening in clinical practice, we briefly outlined the known genotype–phenotype correlations of pathological mutations in the common FTD genes, including average age at onset and disease duration (overview in **Table 1**). We also mentioned the neuropathological correlation expected with each mutated gene, which is of particular interest when new disease-modifying therapies become available. The discovery of a mutation might mean a prognosis for the patient carrier and the presymptomatic family members.

TABLE 1 | Summary of genotype–phenotype correlations for gene defects most commonly associated with familial FTD.

Gene	Suggestive features
MAPT	- bvFTD, FTD with parkinsonism, (PPA)
	- No MND
	- AAO 48–55 years
	- Disease duration 9 years
GRN	- bvFTD (with apathy, social withdrawal), nfv-PPA
	- Presence of hallucinations, apraxia and amnestic syndrome
	- Presence of extrapyramidal symptoms; no MND
	- Asymmetric atrophy and fast rate of whole brain atrophy on MRI
	- Low serum progranulin
	- AAO 53–65 years
	- Disease duration 5–8 years
C9orf72	- bvFTD (nfv-PPA)
	- Presence of MND
	- Presence of psychiatric symptoms, bizarre behaviors, delusions, OCD-like behaviors
	- AAO 50–64 years
	- Disease duration 2.5–14 years, dependent on ALS comorbidity
	- Possible disease anticipation
TBK1	- bvFTD (with disinhibition, socially inappropriate behavior), (nfv-PPA, lv-PPA)
	- Presence of MND
	- Presence of extrapyramidal symptoms, early memory impairment, psychiatric symptoms
	- Asymmetric atrophy on MRI AAO 60–64 years
	- Disease duration 4–8 years
CHMP2B	- bvFTD with early personality change, disinhibition
	- Presence of parkinsonism, dystonia, pyramidal signs and myoclonus; no MND
	- AAO 58 years
VCP	- bvFTD (with apathy, emotional blunting, loss of initiative), SD
	- Presence of IBM, PDB
	- Presence of early psychosis, schizophrenia
	- AAO 48–65 years
	- Disease duration 6.5 years

It may also guide the clinician in coupling a presenting clinical phenotype to a specific FTD gene.

MAPT

Mutations in *MAPT*, located on chromosome 17, result in aberrant ratios of two of the six physiological isoforms of the tau protein. This disturbance in the equilibrium results in a disordered function of the cytoskeleton, affecting neuronal plasticity and axonal transport across the microtubules. It also leads to pathological tau aggregates, causing FTLD-tau. This association is not absolute, as *MAPT* mutations have been reported in the molecular pathogenetic pathways of PSP, CBD and, rarely, argyrophilic grain disease. The neuropathological correlations in these neurodegenerative brain disorders are distinct entities, with specific characteristics of the inclusion bodies as well as different localizations and distributions (Sieben et al., 2012).

FTLD-tau usually presents as bvFTD with mostly disinhibition, repetitive and stereotyped behaviors, or as FTD with parkinsonism, although PPA variants have been reported (Goldman et al., 2011; Seelaar et al., 2011; Sieben et al., 2012; Snowden et al., 2015; Che et al., 2018). Clinical heterogeneity is considerable, between and within families. Patients are frequently misdiagnosed with AD (Rademakers et al., 2004; Goldman et al., 2011). MND symptoms are uncommon. Symptoms develop at a particularly young age [average age 48–55 years (Seelaar et al., 2008, 2011; Goldman et al., 2011; Quaid, 2011; Sieben et al., 2012), and range 25–65 years (Goldman et al., 2011)]. Disease duration is 9 years on average (range: 5–20 years) (Seelaar et al., 2011; Sieben et al., 2012).

GRN

GRN, located on chromosome 17, neighboring *MAPT*, encodes for progranulin which is a multifunctional growth factor involved in cell proliferation, wound healing and inflammation regulation (Che et al., 2018). Loss-of-function (LOF) mutations in *GRN* lead to autosomal dominant FTD (Baker et al., 2006; Cruts et al., 2006; Sieben et al., 2012; Che et al., 2018), as they reduce progranulin levels by 50% resulting in *GRN* haploinsufficiency (Van Mossevelde et al., 2018). *GRN* carriers generally present at autopsy with FTLD-TDP type A (Beck et al., 2008; Sieben et al., 2012).

The clinical phenotype of *GRN* carriers is highly variable. Most commonly, patients present with bvFTD, frequently showing apathy and social withdrawal (Rademakers et al., 2007; Le Ber et al., 2008; Seelaar et al., 2011; Sieben et al., 2012; Irwin et al., 2015; Che et al., 2018; Van Mossevelde et al., 2018). Memory impairment is an early symptom (Rademakers et al., 2007; Goldman et al., 2011). Several *GRN* carriers present with nfv-PPA and, less often, with a syndrome resembling lv-PPA (Rademakers et al., 2007; Beck et al., 2008; Sieben et al., 2012; Irwin et al., 2015; Snowden et al., 2015; Van Mossevelde et al., 2018). One study reported a remarkably high proportion of PPA presentations, outnumbering bvFTD (Van Mossevelde et al., 2016). Parietal lobe dysfunction and atrophy are characteristic features of *GRN* carriers, as well as marked asymmetry and a fast rate of whole brain atrophy on MRI (Beck et al., 2008; Goldman et al., 2011; Rohrer and Warren, 2011; Whitwell et al., 2015). Extrapyramidal symptoms are common, while signs of MND are rare. Diagnosis of AD and parkinsonian disorders associated with *GRN* have been reported (Rademakers et al., 2007; Le Ber et al., 2008; Goldman et al., 2011; Seelaar et al., 2011; Sieben et al., 2012; Irwin et al., 2015; Che et al., 2018; Van Mossevelde et al., 2018). Hallucinations, apraxia and amnestic syndrome may be more specifically associated with *GRN* mutations (Le Ber et al., 2008; Seelaar et al., 2011).

The average onset age for *GRN* mutation-caused FTD is 53–65 years although highly variable (range: 35–89) (Rademakers et al., 2007; Beck et al., 2008; Seelaar et al., 2008, 2011; Goldman et al., 2011; Sieben et al., 2012; Van Mossevelde et al., 2018; Wauters et al., 2018). The disease duration is shorter in *GRN* carriers than in *MAPT* carriers (average: 5–8 years) (Beck et al., 2008; Seelaar et al., 2011; Sieben et al., 2012; Van Mossevelde et al., 2018).

C9orf72

The repeat expansion mutation in *C9orf72,* located on chromosome 9, is a major causal factor in the pathogenesis of both FTLD and ALS, forming a disease spectrum (Gijselinck et al., 2016). The hexanucleotide repeat of G_4C_2 is expanded in patients and is generally considered to be pathological when the expansion contains $\geq$ 2–24 repeat units (Renton et al., 2011; Gijselinck et al., 2012, 2018; Van Mossevelde et al., 2018). The exact mechanism of disease is unclear so far. Pathology may be due to haploinsufficiency or to gain-of-function, with toxic accumulation of the protein translated from the G_4C_2 repeat expansion as well as toxicity from the sense and antisense RNA foci transcribed from it (Gijselinck et al., 2012, 2016, 2018; Sieben et al., 2012; Van Mossevelde et al., 2018).

At the neuropathology level, *C9orf72* expansion carriers mostly have FTLD-TDP type A or B. Rarely, FTLD-UPS and FTLD-TDP type C were found (Sieben et al., 2012; Van Mossevelde et al., 2018). Clinically, *C9orf72* expansion carriers display a wide array of symptoms. Clinical heterogeneity of patient carriers is seen between and within families (Mahoney et al., 2012; Sieben et al., 2012; Van Mossevelde et al., 2018). FTD and ALS phenotypes frequently exist alone, while a combination of FTD and ALS symptoms has been reported in 17–30% of the *C9orf72* carriers (Sieben et al., 2012; Van Mossevelde et al., 2018). When FTD is present, it is mostly bvFTD (>65% of cases) with an early manifestation of executive dysfunction and some memory dysfunction, although PPA (most often nfv-PPA) has also been described (up to 30%) (Gijselinck et al., 2012; Mahoney et al., 2012; Sieben et al., 2012; Van Mossevelde et al., 2018). Symptoms of abnormal behavior are also frequently observed, like delusions, repetitive and typically complex behaviors that mimic obsessive-compulsive disorder (OCD) and irrational, bizarre behaviors. There is an absence of the increased sweet food preference as typically seen in bvFTD (Snowden et al., 2015; Van Mossevelde et al., 2018). There is an especially high occurrence of psychiatric symptoms (Mahoney et al., 2012; Devenney et al., 2014; Irwin et al., 2015;

Van Mossevelde et al., 2018) and associated parkinsonism is common (Devenney et al., 2014; Van Mossevelde et al., 2018). The *C9orf72* expansion has also been identified in patients clinically diagnosed with AD, PD or Huntington disease phenocopy and several other disorders (Van Mossevelde et al., 2018). This may partly be due to lack of typical neuroimaging features, which is not uncommon in carriers of the *C9orf72* expansion (Devenney et al., 2014).

The mean onset age of symptoms for FTD caused by *C9orf72* expansion ranges between 50 and 64 years, but may be anywhere between 27 and 83 years of age (Mahoney et al., 2012; Van Mossevelde et al., 2016, 2018). Disease anticipation with decreasing onset ages in younger generations through expansion of the repeat size has been reported (Sieben et al., 2012; Gijselinck et al., 2016; Van Mossevelde et al., 2017b, 2018). A significantly later onset age has been recorded in patients with a short (<80 units; mean 62 years) compared to a long (>80 units; mean 53 years) repeat size (Gijselinck et al., 2016). When analyzing parent-offspring pairs, an earlier onset (16 to 25 years) was reported in the younger generation. Evidence for intergenerational repeat amplification has also been found, with an increase in expansion size of about 1000 units between a parent to their offspring and an intergenerational increase in methylation level of the 5′ flanking CpG island (Gijselinck et al., 2016). One study analyzing onset ages in 36 families of *C9orf72* repeat expansion carriers showed significantly earlier mean onset ages across successive generations (Van Mossevelde et al., 2017b). Measuring of the exact repeat size has proved difficult because of its 100% GC content, its large size, somatic instability and the repetitive nature of its flanking sequences (Gijselinck et al., 2016; Van Mossevelde et al., 2017a). This generates technical difficulties in measuring repeat sizes, requiring large quantities of high molecular weight genomic DNA (Van Mossevelde et al., 2017a). Recent novel technologies have enabled an increased resolution of the *C9orf72* expansion including the use of long-read sequencing (Ebbert et al., 2018).

The disease duration in *C9orf72* repeat expansion carriers is strongly dependent on ALS comorbidity (Van Mossevelde et al., 2018). In pure FTD, progression is slow (Devenney et al., 2014), average disease duration of 14 years was reported, which is much higher than the 2.5–3.6 years in pure ALS, resulting in a wide range of possible disease duration (1.7–22 years) (Mahoney et al., 2012; Sieben et al., 2012; Van Mossevelde et al., 2018).

TBK1

TBK1, localized on chromosome 12, encodes the TBK1 protein, a serine-threonine kinase involved in autophagy, neuroinflammation, and phosporylation of a wide range of substrates. LOF mutations in *TBK1* lead to 50% reduction of TBK1, which is associated with clinical ALS and FTD, and inherited in families in an autosomal dominant pattern (Freischmidt et al., 2015; Gijselinck et al., 2015; Van Mossevelde et al., 2016, 2018; van der Zee et al., 2017). The associated underlying pathology is FTD-TDP (Freischmidt et al., 2015; Van Mossevelde et al., 2016).

Over 50% of *TBK1* carriers have a clinical presentation of MND. About 25% present with pure FTD, mostly bvFTD (>60%) but also nfv-PPA and lv-PPA (Gijselinck et al., 2015; Van Mossevelde et al., 2016, 2018). Disinhibition and socially inappropriate behavior are more frequent than apathy (Van Mossevelde et al., 2016). Extrapyramidal signs are common (Gijselinck et al., 2015; Van Mossevelde et al., 2016, 2018), as are early impairment of memory and psychiatric symptoms (Van Mossevelde et al., 2016). Structural MRI often shows marked asymmetry in atrophy (Van Mossevelde et al., 2016).

A mean age at onset of 60–64 years (range: 35–78 years) has been reported in TBK1 carriers and disease duration ranged from 1 to 16 years, with an average of 4–8 years (Freischmidt et al., 2015; Gijselinck et al., 2015; Van Mossevelde et al., 2016, 2018; van der Zee et al., 2017).

Less Common FTD Genes

CHMP2B

CHMP2B, located at chromosome 3p11.2, encodes a component of the heteromeric ESCRT-III complex with functions in the endosomal–lysosomal and the autophagic protein degradation pathway (van der Zee et al., 2008; Urwin et al., 2010). Rare mutations were identified that resulted in a premature stop codon and C-truncating of the protein (van der Zee et al., 2008; Isaacs et al., 2011). Neuropathologically, *CHMP2B* carriers are associated with FTLD-UPS proteinopathy (van der Zee et al., 2008; Urwin et al., 2010; Goldman et al., 2011; Sieben et al., 2012).

Clinically, *CHMP2B* carriers present commonly with bvFTD with early personality changes, frequently represented by less concern for others, an unkempt appearance, disinhibition, inappropriate emotional responses and restlessness which later can be accompanied by aggression. Apathy, hyperorality and motor symptoms such as parkinsonism, dystonia, pyramidal signs, and myoclonus occur later. MND is typically not present, although some cases have been reported (Goldman et al., 2011; Isaacs et al., 2011; Seelaar et al., 2011; Sieben et al., 2012). PPA syndromes have been described as well (Isaacs et al., 2011; Sieben et al., 2012). The average onset age is 58 years, ranging between 46 and 65 years (Sieben et al., 2012).

VCP

VCP, located on chromosome 9 at 9p13.3, is associated with impaired functioning of an ATPase with a wide range of cellular functions. This impairment is due to missense mutations, of which > 30 have been identified so far (van der Zee et al., 2009; Cruts et al., 2012; Meyer and Weihl, 2014). Pathogenesis may occur because of a disturbance in the ubiquitin–proteasome mediated protein degradation, autophagy, or both (van der Zee et al., 2009; Sieben et al., 2012). The associated neuropathological correlation is FTLD-TDP type D (Sieben et al., 2012; Irwin et al., 2015).

VCP carriers present with a specific clinical syndrome, combining FTD (present in 30% of cases) with inclusion body myopathy (IBM) (present in 90% of cases) and Paget's disease of the bone (PDB) (present in 50% of cases) in inclusion body myopathy with early onset Paget's disease and frontotemporal dementia (IBMPFD). Presentations may include any or all of these clinical entities, creating a disease spectrum. FTD symptoms usually fall within the category of bvFTD

(with apathy, emotional blunting and loss of initiative and spontaneity) and sv-PPA (Sieben et al., 2012; Van Mossevelde et al., 2018). Psychotic signs and schizophrenia are common early symptoms. Parkinsonism is not uncommon (Van Mossevelde et al., 2018). Other neurological diagnoses in *VCP* mutation carriers include PD, AD and, rarely, peripheral sensorimotor neuropathy, Charcot–Marie–Tooth disease type 2 and hereditary spastic paraplegia (Van Mossevelde et al., 2018).

Age at onset is 48–65 years (range: 39–73 years), with a disease duration of 6.5 years (Goldman et al., 2011; Sieben et al., 2012; Van Mossevelde et al., 2018). Onset age of FTD is considerably later than that of IBM and PDB (Van Mossevelde et al., 2018).

FUTURE BIOMARKERS FOR IMPROVED DIAGNOSIS OF FTD

Imaging Biomarkers in a Research Setting

Diffusion Tensor Imaging

Diffusion tensor imaging (DTI) is an MRI imaging technique visualizing the diffusion of water molecules throughout the brain. It is used as a technique for white matter tractography (Mahoney et al., 2014).

Studies have shown that white matter damage is an early marker for disease in FTD, and DTI may be used as a tool to screen for such abnormalities at the presymptomatic stage (Dopper et al., 2014; Mahoney et al., 2014; Jiskoot et al., 2019). Reduced integrity of the uncinate fasciculus and anterior corpus callosum is typical for FTD, and the degree of damage is correlated to age and disease severity (Dopper et al., 2014; Jiskoot et al., 2019). Even here, specific patterns can be recognized for different clinical subtypes, and for carriers of different causal mutations. These abnormalities are consistent with characteristic brain atrophy distributions (Dopper et al., 2014; Lam et al., 2014; Agosta et al., 2015; Jiskoot et al., 2019). The increase in white matter damage over time has been reported to be greater than that of gray matter atrophy, although only at the symptomatic stage, indicating the possible use of this technique as a marker for disease progression (Lam et al., 2014; Jiskoot et al., 2019).

Studies comparing FTD cohorts with AD patients and with normal controls found significantly more white matter pathology mostly in bilateral uncinate fasciculus, cingulum bundle, and corpus callosum in FTD compared to both other groups (Mahoney et al., 2014; Bang et al., 2015). More studies are needed to consolidate these findings and define the diagnostic accuracy for FTD of DTI, as well as its power to distinguish FTD from other types of neurodegenerative brain diseases.

Resting-State fMRI

In resting-state functional MRI (fMRI), regional connectivity is measured through fluctuations in blood-oxygen-level dependent (BOLD) signal. FTD patients, most often those with bvFTD, have decreased functional connectivity mostly in the SN, necessary for emotional processing, behavior and interpersonal experiences (Greicius, 2008; Zhou et al., 2010; Dopper et al., 2014). A distinction can be made between FTD and AD, as in the latter a different pattern of loss of functional connectivity is seen involving the default mode network (Greicius, 2008; Zhou et al., 2010). The changes on fMRI are thought to be measurable at the presymptomatic stage. However, more research is needed to allow for a large scale application of this technique (Dopper et al., 2014).

Arterial Spin Labeling

Arterial spin labeling (ASL) is an MRI technique which, like SPECT, measures cerebral blood flow. It does so by magnetically labeling water molecules and has the advantages of being a method of functional brain imaging that is non-invasive and cost-effective, as no tracer molecule is necessary and it can easily be added to a routine structural MRI scan (Grade et al., 2015).

One of its clinical applications is the identification of regional hypoperfusion in neurodegenerative disease (Du et al., 2006; Bron et al., 2014; Verfaillie et al., 2015; Steketee et al., 2016). Sensitivity and specificity to differentiate FTD from healthy controls have been reported as 78–79 and 76–92%, respectively. When distinguishing FTD from AD, these results were 69–83 and 68–93% (Steketee et al., 2016; Tosun et al., 2016). The accuracy in differentiating FTD from AD when ASL results are combined with structural MRI has been reported as 87% (Du et al., 2006). However, its added value compared to structural MRI alone might be limited (Bron et al., 2014). In direct comparison to FDG PET, ASL came out as comparable (Verfaillie et al., 2015; Tosun et al., 2016).

Tau PET Imaging

In recent years, amyloid PET scan measuring amyloid-β burden with tracers such as [C-11] Pittsburgh Compound B (PIB), flutemetamol, florbetapir (AV-45), florbetaben (AV-1), and AZD4694 has proven its value in quantifying underlying AD neuropathology. It is a well-established technique to confirm or rule out AD with great diagnostic accuracy. Abnormalities are present years before onset of symptoms, and this biomarker can be used as a measure for staging and monitoring of disease progression and distribution (Klunk et al., 2004; Dubois et al., 2007, 2014; Rowe et al., 2007; Jack et al., 2010).

No such imaging technique exists, yet, to confirm or rule out FTD. An extra hurdle here is the heterogeneity in underlying protein inclusions, as we mentioned earlier. For patients with an underlying FTLD-tau pathology, however, novel PET imaging techniques are being developed. The nature of the pathophysiology heightens the challenge in developing a useful ligand, as tau is a protein existing in six isoforms that undergo complex post-translational modifications. Moreover, the pathological tau aggregates [neurofibrillary tangles (NFTs)] are located intracellularly (Villemagne et al., 2017). Ligands such as [18F]THK523, [18F]THK5117, [18F]THK5105 and [18F]THK5351, [18F]AV1451(T807) and [11C]PBB3 have been proven to show the distribution of tau pathology *in vivo*. However, NFT are common in the pathophysiology of many other neurodegenerative brain diseases, such as AD, PSP, CBD, and chronic traumatic encephalopathy (Dani et al., 2016). Tau

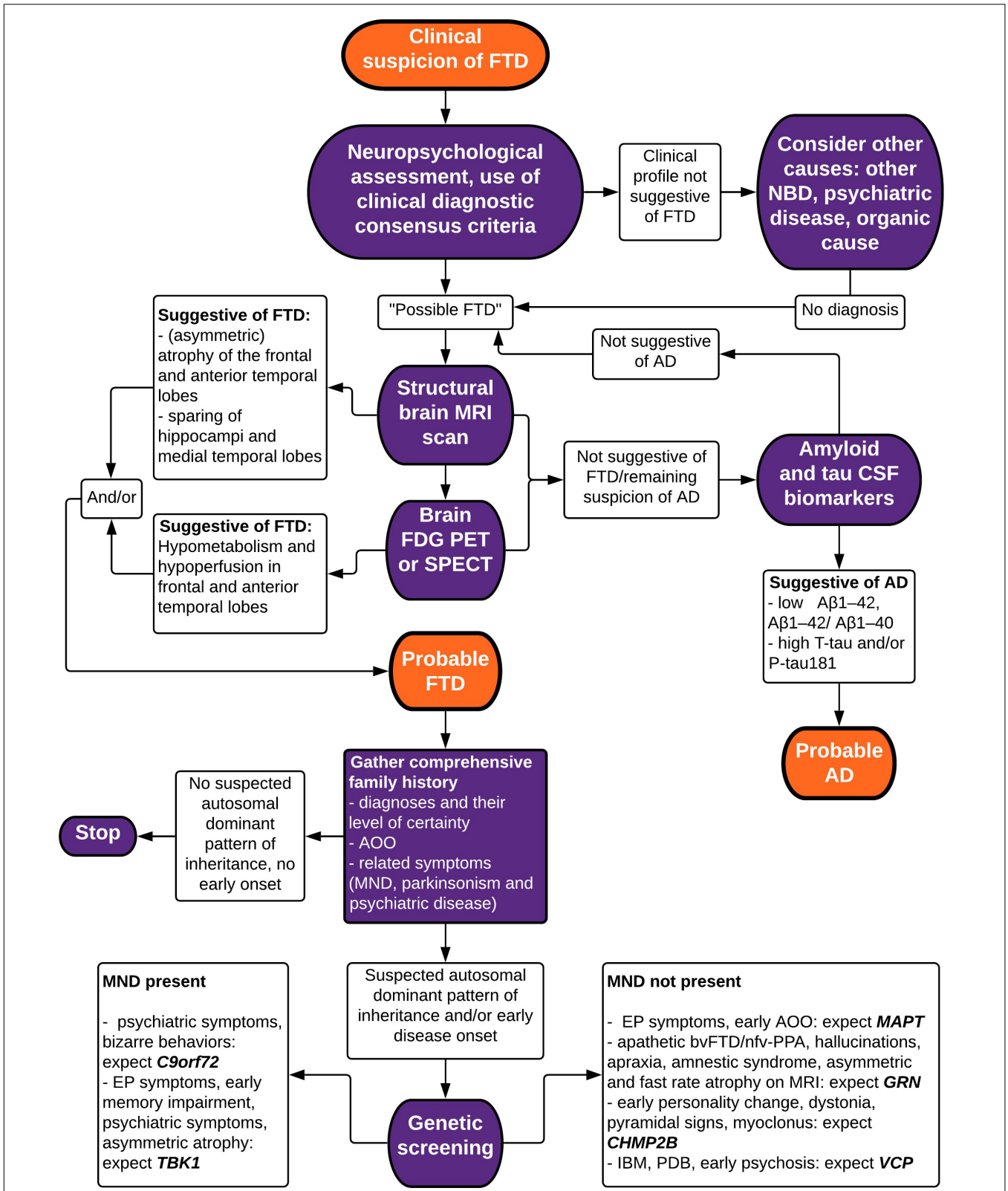

FIGURE 3 | Flowchart depicting a stepwise approach to the diagnosis of FTD. bv, behavioral variant; FTD, frontotemporal dementia; nfv-PPA, non-fluent variant primary progressive aphasia; AD, Alzheimer's disease; MND, motor neuron disease; NBD, neurodegenerative brain disease; PSP, progressive supranuclear palsy; IBM, inclusion body myopathy; PDB, Paget's disease of the bone; MRI, magnetic resonance imaging; FDG PET, fluorodeoxyglucose positron emission tomography; SPECT, single-photon emission computed tomography; CSF, cerebrospinal fluid; EP, extrapyramidal; AAO, age at onset.

TABLE 2 | Summary of potential future biomarkers to diagnose FTD.

Imaging biomarkers in a research setting	
DTI	- MRI technique, visualizes white matter damage
	- Damage in bilateral uncinate fasciculus, cingulum bundle, and corpus callosum are considered typical for FTD
	- Possibly also useful in presymptomatic stage
Resting state fMRI	- Measures regional connectivity through BOLD signal
	- Decreased connectivity in SN typical for FTD
	- Possibly also useful in presymptomatic stage
ASL	- Functional MRI technique, measures perfusion
	- Non-invasive, cost-effective (compared to FDG PET and perfusion SPECT)
	- Good diagnostic accuracy
Tau PET imaging	- Quantifies NFT burden
	- Search for optimal ligand still ongoing
	- Abnormalities expected to be present in all tauopathies, not specific to FTLD
	- Possibly also useful for staging and as marker for disease progression
EEG	- Not invasive, widely accessible
	- Good accuracy for differential diagnosis FTD-AD in moderate to severe dementia, more evidence required in early stage
TMS	- Measures cortical circuitry through external electromagnetic coil
	- Impairment of SICI-ICF typical for FTD
	- Possibly also useful in an early stage
Neurochemical biomarkers in a research setting	
NfL	- Marker suggestive of neurodegeneration
	- Measurable in both CSF and serum / plasma
	- Good diagnostic accuracy in research but clinical validation needed
	- Possibly also useful for staging and as marker for disease progression
TDP-43	- Marker of TDP-43 neuropathology
	- Specific to FTLD-TDP, although TDP co-pathology occurs in other neurodegenerative brain diseases
	- Search for optimal antibody still ongoing
Progranulin	- Marker for *GRN* LOF mutation
	- Measurable in both CSF and plasma
	- 100% sensitive and specific to *GRN* mutation carriers
	- Indicated for screening in (pre)symptomatic possible carriers of *GRN* defects

PET imaging also does not have the advantage of showing abnormalities at a presymptomatic stage, as there is a temporal relationship between tau-PET and symptoms. There is, however, a correlation between quantitative NFT burden and cognitive decline. Hence, through more research, tau PET imaging might be of use as a valuable marker for disease progression, staging and possibly therapeutic response (Dani et al., 2016; Villemagne et al., 2017).

Electroencephalography

Electroencephalography is a non-invasive, simple, widely accessible technique that can be used to measure the physiological functionality of the brain, and disruption thereof in neurodegenerative brain disease (Adamis et al., 2005; Goossens et al., 2017).

Through quantitative analysis of EEG aberrations as opposed to more commonly carried out visual assessment, a more robust diagnostic value of this biomarker can be achieved. Accuracy of differentiating FTD from AD in patients with moderate to severe dementia has been reported as 79–100%, with a significantly lower frequency of the dominant frequency peaks in AD than in FTD, amongst other findings (Garn et al., 2017; Goossens et al., 2017). Distinguishing FTD from healthy controls has proven more difficult, as EEG in FTD patients is usually relatively normal, especially in the early disease stages (Goossens et al., 2017).

Transcranial Magnetic Stimulation

Transcranial magnetic stimulation (TMS) is a painless, non-invasive procedure that assesses the cortical circuits and their function. An electromagnetic coil is placed on the scalp, where it generates a magnetic field. This induces a measurable electrical current in the brain, depolarizing the cells (Guerra et al., 2011).

This technique has shown some value in the differential diagnosis of FTD, although results differ, cohorts are small and methodologies are difficult to compare (Pierantozzi et al., 2004; Alberici et al., 2008; Issac et al., 2013; Benussi et al., 2016, 2017). The study with the largest scale so far is an Italian trial, where TMS differentiated FTD (n = 64) from AD (n = 79) with a sensitivity of 92% and a specificity of 89%, and FTD from healthy controls (n = 32) with a sensitivity of 90% and a specificity of 78% (Benussi et al., 2017). However, their setup was only partially blinded, as the operator knew whether the subject was a healthy control or a patient, but not what clinical diagnosis had been given. The major differences in both diseases were an impairment of the short interval intracortical inhibition/intracortical facilitation (SICI-ICF) in FTD and an impairment of the short-latency afferent inhibition in AD (Cantone et al., 2014; Benussi et al., 2017). The same group also published findings of a distinct difference between healthy controls and presymptomatic *GRN* mutation carriers (Benussi et al., 2016).

These results point to TMS as a possible early, non-invasive tool for diagnosis of FTD. More research is needed to consolidate this evidence.

Neurochemical Biomarkers in a Research Setting

Neurofilament Light Chain

Neurofilament light chain (NfL) is a new candidate CSF and serum biomarker for the diagnosis of FTD. Neurofilaments are structural axonal proteins, and their presence in CSF is a marker for neurodegeneration (Goossens et al., 2018).

Several studies have reported that CSF NfL levels are significantly increased in both FTD (se 78–84%, sp 82–100%) (Meeter et al., 2016, 2018; Abu-Rumeileh et al., 2018) and AD in comparison with controls (Goossens et al., 2018). However, NfL levels have been shown to be significantly higher in FTD than in AD, adding to the diagnostic accuracy achieved with a classic AD CSF biomarker panel alone

(Abu-Rumeileh et al., 2018; Goossens et al., 2018). Pathologically confirmed FTLD-TDP patients have been reported as having higher NfL levels than those with FTD-tau (se 80%, sp 81%) (Rohrer et al., 2016; Abu-Rumeileh et al., 2018), although other studies could not confirm these results (Goossens et al., 2018; Meeter et al., 2018).

Evidence for a good correlation between CSF and serum NfL levels exists, with a similar elevation in patients compared to healthy controls (Meeter et al., 2016; Rohrer et al., 2016) and presymptomatic causal mutation carriers (Meeter et al., 2016). NfL may also serve as a biomarker for disease severity and even rate of disease progression, and for conversion to the symptomatic stage in carriers of causal mutations (Meeter et al., 2016; Rohrer et al., 2016).

TDP-43

As mentioned earlier, one of the molecular pathways leading to FTLD neuropathology is the intraneuronal aggregation of TDP-43, accounting for approximately half of all FTLD cases (Goossens et al., 2015). The pathological protein has been proposed as a potential CSF biomarker specific to FTLD (Goossens et al., 2015). Some difficulties have arisen, however. Because of low absolute levels of TDP-43 in biofluids, a very sensitive immunoassay is required, preferably specific for pathological TDP-43. Many different assays have already been developed, but their sensitivity and specificity are not yet well-established (Goossens et al., 2015). Another obstacle is the occurrence of TDP-43 co-pathology in other neurodegenerative brain diseases, which may be present in 20–56% of patients with AD and other tauopathies, undermining the specificity of the biomarker (Arai et al., 2009; Goossens et al., 2015).

Progranulin

As we mentioned earlier, LOF mutations in *GRN* result in progranulin haploinsufficiency. Consequent decreased progranulin levels are detectable in plasma and CSF of carriers of such a causal mutation in *GRN*, both in patients with clinical FTD as in presymptomatic carriers, with a sensitivity and specificity of 100% (Ghidoni et al., 2008; Finch et al., 2009; Sleegers et al., 2009; Goossens et al., 2018).

Thus, dosage of plasma progranulin is a potential cheap and non-invasive tool for screening for carriers of genetic *GRN* defects. It is the only FTD-specific biomarker so far. However, given the small number of all FTD patients (both familial and sporadic) that carry a *GRN* mutation, its use may not be indicated for every patient in the initial diagnostic workup. The biomarker may be more useful in patients with a strong family history of FTD, although further genetic testing may then be required afterward, or to identify presymptomatic carriers amongst asymptomatic family members identified to have a causal *GRN* mutation. One must also take into account the region of origin of the patient, as *GRN* mutations represent a much larger share of all autosomal dominant FTD in certain regions (e.g., Belgium, Italy) than in others due to a founder effect (van der Zee et al., 2006; Rademakers et al., 2007; Benussi et al., 2013). This factor may provide an additional indication for measuring plasma progranulin.

CONCLUSION: RECOMMENDATIONS FOR DAILY CLINICAL PRACTICE

Making a correct and well-founded diagnosis of FTD is not an easy task, due to clinical heterogeneity and overlap with other neurodegenerative brain diseases. Atypical presentations are common, which is exemplified by our clinical vignette. A wide range of techniques exist to aid in the differential diagnosis, identifying characteristics of neuropsychology and biomarkers of neuroimaging, neurochemistry, and genetics. In this review paper, we have summarized current evidence for the diagnostic value of these techniques in differentiating FTD from other neurodegenerative diseases (mainly AD), and in differentiating between FTD subtypes. Taking this knowledge into account, we propose a stepwise approach in the diagnostic evaluation of a patient suspected to suffer from FTD (**Figure 3**).

Firstly, obtaining the patient history and a standardized neuropsychological testing are necessary to establish the presence of a typical neuropsychological profile suggestive of FTD. Clinical consensus criteria for bvFTD as well as for PPA variants of FTD have a reasonably good accuracy in differentiating FTD from other diagnoses, although misdiagnosis (especially misidentifying FTD as AD and vice versa) is common. They aid in guiding the clinician's view by standardizing and quantifying the presenting symptoms and play a major role in establishing the correct diagnosis.

A second step indicated in any patient with a presentation of possible neurodegenerative brain disease is the acquisition of neuroimaging biomarkers. Structural brain MRI is most commonly used and typically shows a more pronounced loss of volume in the frontal lobes and the anterior temporal lobes. Asymmetry and sparing of the hippocampi and medial temporal lobes are accurate markers to differentiate FTD from AD. Evidence also shows that specific patterns of brain atrophy are associated with different clinical, neuropathological, and genetic subtypes of FTD. An important advantage of brain MRI is the good resolution in visualizing the brain tissue, with a possibility to screen for other organic causes of symptoms, such as brain tumors and hydrocephalus, and to quantify vascular lesions, making this a great choice as a first screening diagnostic technique. In recent years, novel techniques such as automatic volumetry, VBM, TBM, manifold learning, ROI-based grading, automated measurement of vascular burden and of cortical thickness have been developed to add to the diagnostic accuracy of structural MRI.

Functional neuroimaging through brain FDG PET or perfusion SPECT scans can also be considered in the initial diagnostic workup, as studies have shown high sensitivity and specificity to diagnose FTD. Hypometabolism and relative hypoperfusion are typically seen in the frontal and anterior temporal lobes, usually correlating with atrophy on MRI but often preceding it. Some studies have shown a greater accuracy of FDG PET when compared to SPECT, but the evidence is not very robust. For the clinician, the local availability of the techniques as well as cost-effectiveness (with SPECT being more affordable) also need to be taken into account.

When these imaging biomarkers are not sufficient to establish a clear diagnosis, and certainly in case of differential diagnostic doubt with (atypical presentation of) AD, we suggest a further exploration through the analysis of CSF biomarkers $A\beta_{1-42}$, $A\beta_{1-42}/A\beta_{1-40}$ ratio, T-tau and P-tau_{181} that can indicate the presence of AD with good accuracy. FTD cannot be diagnosed based on CSF biomarkers, but non-specific, intermediate decreased $A\beta_{1-42}$ and increased T-tau levels may or may not be present. The use of P-tau_{181} and the $A\beta_{1-42}/A\beta_{1-40}$ ratio significantly increases the accuracy of correctly identifying FTD vs. AD.

Lastly, we have elaborated on the genetic basis of FTD. To ascertain the possible presence of a causal mutation for FTD, a comprehensive family history complete with diagnoses, their level of certainty, age at onset and possible other related symptoms such as MND, parkinsonism and psychiatric disease should be inquired. When an autosomal dominant pattern of inheritance is suspected upon pedigree analysis or when the patient presents with an early onset age, screening for causal mutations may be indicated in the affected patient. We have summarized genotype–phenotype correlations for the most commonly involved genes (*C9orf72*, *MAPT*, *GRN, TBK1*) and some less frequent ones (*CHMP2B*, *VCP*), including average age at onset and disease duration (**Table 1**). We also mentioned the neuropathological correlation expected with each gene defect, which may be of particular interest when new disease-modifying therapies become available.

More research into novel biomarkers for the diagnosis of FTD and other neurodegenerative brain diseases is needed. Above, we have summarized current evidence on some novel imaging biomarkers (DTI, resting state fMRI, ASL, tau pet imaging, EEG, TMS) as well as neurochemical biomarkers (NfL, TDP-43, progranulin) (**Table 2**). These promising techniques are currently still only used in an experimental setting, or are not yet routinely implemented for screening in patients with suspected FTD.

AUTHOR CONTRIBUTIONS

SE, HG, and CVB conceived of the presented idea. HG wrote the manuscript with support of and critical reading by SE and CVB.

FUNDING

This research of the authors has been funded in part by the Flemish Government initiated Flanders Impulse Program on Networks for Dementia Research and the Methusalem Excellence Program, the Research Foundation Flanders and the University of Antwerp Research Fund.

ACKNOWLEDGMENTS

The authors are grateful to the patient described in the clinical vignette and who has given written informed consent for the publication of this case report.

REFERENCES

Abu-Rumeileh, S., Mometto, N., Bartoletti-Stella, A., Polischi, B., Oppi, F., Poda, R., et al. (2018). Cerebrospinal fluid biomarkers in patients with frontotemporal dementia spectrum: a single-center study. *J. Alzheimers Dis.* 66, 551–563. doi: 10.3233/JAD-180409

Adamis, D., Sahu, S., and Treloar, A. (2005). The utility of EEG in dementia: a clinical perspective. *Int. J. Geriatr. Psychiatry* 20, 1038–1045. doi: 10.1002/gps.1393

Agosta, F., Ferraro, P. M., Canu, E., Copetti, M., Galantucci, S., Magnani, G., et al. (2015). Differentiation between subtypes of primary progressive aphasia by using cortical thickness and diffusion-tensor mr imaging measures. *Radiology* 276, 219–227. doi: 10.1148/radiol.15141869

Alberici, A., Bonato, C., Calabria, M., Agosti, C., Zanetti, O., Miniussi, C., et al. (2008). The contribution of TMS to frontotemporal dementia variants. *Acta Neurol. Scand.* 118, 275–280. doi: 10.1111/j.1600-0404.2008.01017.x

Arai, T., Mackenzie, I. R., Hasegawa, M., Nonoka, T., Niizato, K., Tsuchiya, K., et al. (2009). Phosphorylated TDP-43 in Alzheimer's disease and dementia with Lewy bodies. *Acta Neuropathol.* 117, 125–136. doi: 10.1007/s00401-008-0480-1

Archer, H. A., Smailagic, N., John, C., Holmes, R. B., Takwoingi, Y., Coulthard, E. J., et al. (2015). Regional cerebral blood flow single photon emission computed tomography for detection of frontotemporal dementia in people with suspected dementia*. *Cochrane Database Syst. Rev.* 6:CD010896. doi: 10.1002/14651858.CD010896.pub2

Baker, M., Mackenzie, I. R., Pickering-Brown, S. M., Gass, J., Rademakers, R., Lindholm, C., et al. (2006). Mutations in progranulin cause tau-negative frontotemporal dementia linked to chromosome 17. *Nature* 442, 916–919. doi: 10.1038/nature05016

Balasa, M., Gelpi, E., Martin, I., Antonell, A., Rey, M. J., Grau-Rivera, O., et al. (2015). Diagnostic accuracy of behavioral variant frontotemporal dementia consortium criteria (FTDC) in a clinicopathological cohort. *Neuropathol. Appl. Neurobiol.* 41, 882–892. doi: 10.1111/nan.12194

Bang, J., Spina, S., and Miller, B. L. (2015). Frontotemporal dementia. *Lancet* 386, 1672–1682. doi: 10.1016/S0140-6736(15)00461-4

Beck, J., Rohrer, J. D., Campbell, T., Isaacs, A., Morrison, K. E., Goodall, E. F., et al. (2008). A distinct clinical, neuropsychological and radiological phenotype is associated with progranulin gene mutations in a large UK series. *Brain* 131, 706–720. doi: 10.1093/brain/awm320

Benussi, A., Cosseddu, M., Filareto, I., Dell'era, V., Archetti, S., Sofia Cotelli, M., et al. (2016). Impaired long-term potentiation-like cortical plasticity in presymptomatic genetic frontotemporal dementia. *Ann. Neurol.* 80, 472–476. doi: 10.1002/ana.24731

Benussi, A., Di Lorenzo, F., Dell'era, V., Cosseddu, M., Alberici, A., Caratozzolo, S., et al. (2017). Transcranial magnetic stimulation distinguishes Alzheimer disease from frontotemporal dementia. *Neurology* 89, 665–672. doi: 10.1212/WNL.0000000000004232

Benussi, L., Rademakers, R., Rutherford, N. J., Wojtas, A., Glionna, M., Paterlini, A., et al. (2013). Estimating the age of the most common Italian GRN mutation: walking back to Canossa times. *J. Alzheimers Dis.* 33, 69–76. doi: 10.3233/JAD-2012-121306

Bjerke, M., and Engelborghs, S. (2018). Cerebrospinal fluid biomarkers for early and differential Alzheimer's Disease Diagnosis. *J. Alzheimers Dis.* 62, 1199–1209. doi: 10.3233/JAD-170680

Blennow, K., and Zetterberg, H. (2018). Biomarkers for Alzheimer's disease: current status and prospects for the future. *J. Int. Med.* 284, 643–663. doi: 10.1111/joim.12816

Boccardi, M., Laakso, M. P., Bresciani, L., Galluzzi, S., Geroldi, C., Beltramello, A., et al. (2003). The MRI pattern of frontal and temporal brain atrophy in fronto-temporal dementia. *Neurobiol. Aging* 24, 95–103. doi: 10.1016/s0197-4580(02)00045-3

Bron, E. E., Steketee, R. M., Houston, G. C., Oliver, R. A., Achterberg, H. C., Loog, M., et al. (2014). Diagnostic classification of arterial spin labeling and structural MRI in presenile early stage dementia. *Hum. Brain Mapp.* 35, 4916–4931. doi: 10.1002/hbm.22522

Burrell, J. R., Kiernan, M. C., Vucic, S., and Hodges, J. R. (2011). Motor neuron dysfunction in frontotemporal dementia. *Brain* 134, 2582–2594. doi: 10.1093/brain/awr195

Cantone, M., Di Pino, G., Capone, F., Piombo, M., Chiarello, D., Cheeran, B., et al. (2014). The contribution of transcranial magnetic stimulation in the diagnosis and in the management of dementia. *Clin. Neurophysiol.* 125, 1509–1532. doi: 10.1016/j.clinph.2014.04.010

Chare, L., Hodges, J. R., Leyton, C. E., Mcginley, C., Tan, R. H., Kril, J. J., et al. (2014). New criteria for frontotemporal dementia syndromes: clinical and pathological diagnostic implications. *J. Neurol. Neurosurg. Psychiatry* 85, 866–871.

Che, X. Q., Song, N., Gao, Y., Ren, R. J., and Wang, G. (2018). Precision medicine of frontotemporal dementia: from genotype to phenotype. *Front. Biosci.* 23, 1144–1165. doi: 10.2741/4637

Cirulli, E. T., Lasseigne, B. N., Petrovski, S., Sapp, P. C., Dion, P. A., Leblond, C. S., et al. (2015). Exome sequencing in amyotrophic lateral sclerosis identifies risk genes and pathways. *Science* 347, 1436–1441. doi: 10.1126/science.aaa3650

Coyle-Gilchrist, I. T. S., Dick, K. M., Patterson, K., Rodriquez, P. V., Wehmann, E., Wilcox, A., et al. (2016). Prevalence, characteristics, and survival of frontotemporal lobar degeneration syndromes. *Neurology* 86, 1736–1743. doi: 10.1212/WNL.0000000000002638

Croisile, B., Auriacombe, S., Etcharry-Bouyx, F., and Vercelletto, M. (2012). [The new 2011 recommendations of the National Institute on Aging and the Alzheimer's association on diagnostic guidelines for Alzheimer's disease: preclinal stages, mild cognitive impairment, and dementia]. *Rev. Neurol.* 168, 471–482.

Cruts, M., Gijselinck, I., Van Der Zee, J., Engelborghs, S., Wils, H., Pirici, D., et al. (2006). Null mutations in progranulin cause ubiquitin-positive frontotemporal dementia linked to chromosome 17q21. *Nature* 442, 920–924. doi: 10.1038/nature05017

Cruts, M., Theuns, J., and Van Broeckhoven, C. (2012). Locus-specific mutation databases for neurodegenerative brain diseases. *Hum. Mutat.* 33, 1340–1344. doi: 10.1002/humu.22117

Dani, M., Brooks, D. J., and Edison, P. (2016). Tau imaging in neurodegenerative diseases. *Eur. J. Nucl. Med. Mol. Imaging* 43, 1139–1150. doi: 10.1007/s00259-015-3231-2

Davison, C. M., and O'Brien, J. T. (2014). A comparison of FDG-PET and blood flow SPECT in the diagnosis of neurodegenerative dementias: a systematic review. *Int. J. Geriatr. Psychiatry* 29, 551–561. doi: 10.1002/gps.4036

De Deyn, P. P., Engelborghs, S., Saerens, J., Goeman, J., Marien, P., Maertens, K., et al. (2005). The middelheim frontality score: a behavioural assessment scale that discriminates frontotemporal dementia from Alzheimer's disease. *Int. J. Geriatr. Psychiatry* 20, 70–79. doi: 10.1002/gps.1249

de Souza, L. C., Chupin, M., Bertoux, M., Lehericy, S., Dubois, B., Lamari, F., et al. (2013). Is Hippocampal volume a good marker to differentiate Alzheimer's Disease from Frontotemporal Dementia? *J. Alzheimers Dis.* 36, 57–66. doi: 10.3233/JAD-122293

DeJesus-Hernandez, M., Mackenzie, I. R., Boeve, B. F., Boxer, A. L., Baker, M., Rutherford, N. J., et al. (2011). Expanded ggggcc hexanucleotide repeat in noncoding region of C9orf72 causes chromosome 9p-linked FTD and ALS. *Neuron* 72, 245–256. doi: 10.1016/j.neuron.2011.09.011

Deng, H., Gao, K., and Jankovic, J. (2014). The role of FUS gene variants in neurodegenerative diseases. *Nat. Rev. Neurol.* 10, 337–348. doi: 10.1038/nrneurol.2014.78

Devenney, E., Hornberger, M., Irish, M., Mioshi, E., Burrell, J., Tan, R., et al. (2014). Frontotemporal dementia associated With the C9orf72 mutation a unique clinical profile. *Jama Neurol.* 71, 331–339. doi: 10.1001/jamaneurol.2013.6002

Diehl-Schmid, J., Grimmer, T., Drzezga, A., Bornschein, S., Riemenschneider, M., Forstl, H., et al. (2007). Decline of cerebral glucose metabolism in frontotemporal dementia: a longitudinal 18F-Fdg-Pet-study. *Neurobiol. Aging* 28, 42–50. doi: 10.1016/j.neurobiolaging.2005.11.002

Dopper, E. G. P., Rombouts, S., Jiskoot, L. C., Den Heijer, T., De Graaf, J. R. A., De Koning, I., et al. (2014). Structural and functional brain connectivity in presymptomatic familial frontotemporal dementia. *Neurology* 83, E19–E26. doi: 10.1212/WNL.0000000000000583

Dougall, N. J., Bruggink, S., and Ebmeier, K. P. (2004). Systematic review of the diagnostic accuracy of Tc-99m-HWAO-SPECT in dementia. *Am. J. Geriatr. Psychiatry* 12, 554–570. doi: 10.1097/00019442-200411000-00002

Du, A. T., Jahng, G. H., Hayasaka, S., Kramer, J. H., Rosen, H. J., Gorno-Tempini, M. L., et al. (2006). Hypoperfusion in frontotemporal dementia and Alzheimer disease by arterial spin labeling MRI. *Neurology* 67, 1215–1220. doi: 10.1212/01.wnl.0000238163.71349.78

Du, A. T., Schuff, N., Kramer, J. H., Rosen, H. J., Gorno-Tempini, M. L., Rankin, K., et al. (2007). Different regional patterns of cortical thinning in Alzheimer's disease and frontotemporal dementia. *Brain* 130, 1159–1166. doi: 10.1093/brain/awm016

Dubois, B., Feldman, H. H., Jacova, C., Dekosky, S. T., Barberger-Gateau, P., Cummings, J., et al. (2007). Research criteria for the diagnosis of Alzheimer's disease: revising the NINCDS-ADRDA criteria. *Lancet Neurol.* 6, 734–746. doi: 10.1016/s1474-4422(07)70178-3

Dubois, B., Feldman, H. H., Jacova, C., Hampel, H., Molinuevo, J. L., Blennow, K., et al. (2014). Advancing research diagnostic criteria for Alzheimer's disease: the IWG-2 criteria. *Lancet Neurol.* 13, 614–629.

Duits, F. H., Martinez-Lage, P., Paquet, C., Engelborghs, S., Lleo, A., Hausner, L., et al. (2016). Performance and complications of lumbar puncture in memory clinics: results of the multicenter lumbar puncture feasibility study. *Alzheimers Dement.* 12, 154–163. doi: 10.1016/j.jalz.2015.08.003

Ebbert, M. T. W., Farrugia, S. L., Sens, J. P., Jansen-West, K., Gendron, T. F., Prudencio, M., et al. (2018). Long-read sequencing across the C9orf72 'GGGGCC' repeat expansion: implications for clinical use and genetic discovery efforts in human disease. *Mol. Neurodegener.* 13:46. doi: 10.1186/s13024-018-0274-4

Engelborghs, S., De Vreese, K., Van De Casteele, T., Vanderstichele, H., Van Everbroeck, B., Cras, P., et al. (2008). Diagnostic performance of a CSF-biomarker panel in autopsy-confirmed dementia. *Neurobiol. Aging* 29, 1143–1159. doi: 10.1016/j.neurobiolaging.2007.02.016

Engelborghs, S., Niemantsverdriet, E., Struyfs, H., Blennow, K., Brouns, R., Comabella, M., et al. (2017). Consensus guidelines for lumbar puncture in patients with neurological diseases. *Alzheimers Dement* 8, 111–126.

Espay, A. J., and Litvan, I. (2011). Parkinsonism and frontotemporal dementia: the clinical overlap. *J. Mol. Neurosci.* 45, 343–349. doi: 10.1007/s12031-011-9632-1

Fazekas, F., Chawluk, J. B., Alavi, A., Hurtig, H. I., and Zimmerman, R. A. (1987). MR signal abnormalities at 1.5 T in Alzheimer's dementia and normal aging. *AJR Am. J. Roentgenol.* 149, 351–356. doi: 10.2214/ajr.149.2.351

Fecto, F., Yan, J., Vemula, S. P., Liu, E., Yang, Y., Chen, W., et al. (2011). SQSTM1 mutations in familial and sporadic amyotrophic lateral sclerosis. *Arch. Neurol.* 68, 1440–1446. doi: 10.1001/archneurol.2011.250

Fernandez-Matarrubia, M., Matias-Guiu, J. A., Cabrera-Martin, M. N., Moreno-Ramos, T., Valles-Salgado, M., Carreras, J. L., et al. (2017). Episodic memory dysfunction in behavioral variant frontotemporal dementia: a clinical and FDG-PET study. *J. Alzheimers Dis.* 57, 1251–1264. doi: 10.3233/JAD-160874

Finch, N., Baker, M., Crook, R., Swanson, K., Kuntz, K., Surtees, R., et al. (2009). Plasma progranulin levels predict progranulin mutation status in frontotemporal dementia patients and asymptomatic family members. *Brain* 132, 583–591. doi: 10.1093/brain/awn352

Foster, N. L., Heidebrink, J. L., Clark, C. M., Jagust, W. J., Arnold, S. E., Barbas, N. R., et al. (2007). FDG-PET improves accuracy in distinguishing frontotemporal dementia and Alzheimer's disease. *Brain* 130, 2616–2635. doi: 10.1093/brain/awm177

Freischmidt, A., Wieland, T., Richter, B., Ruf, W., Schaeffer, V., Muller, K., et al. (2015). Haploinsufficiency of TBK1 causes familial ALS and fronto-temporal dementia. *Nat. Neurosci.* 18, 631–636. doi: 10.1038/nn.4000

Garn, H., Coronel, C., Waser, M., Caravias, G., and Ransmayr, G. (2017). Differential diagnosis between patients with probable Alzheimer's disease, Parkinson's disease dementia, or dementia with lewy bodies and frontotemporal dementia, behavioral variant, using quantitative electroencephalographic features. *J. Neural. Transm.* 124, 569–581. doi: 10.1007/s00702-017-1699-6

Ghidoni, R., Benussi, L., Glionna, M., Franzoni, M., and Binetti, G. (2008). Low plasma progranulin levels predict progranulin mutations in frontotemporal lobar degeneration. *Neurology* 71, 1235–1239. doi: 10.1212/01.wnl.0000325058.10218.fc

Gijselinck, I., Cruts, M., and Van Broeckhoven, C. (2018). The Genetics of C9orf72 Expansions. *Cold Spring Harb. Perspect. Med.* 8:a026757. doi: 10.1101/cshperspect.a026757

Gijselinck, I., Van Langenhove, T., Van Der Zee, J., Sleegers, K., Philtjens, S., Kleinberger, G., et al. (2012). A C9orf72 promoter repeat expansion in a flanders-belgian cohort with disorders of the frontotemporal lobar degeneration-amyotrophic lateral sclerosis spectrum: a gene identification study. *Lancet Neurol.* 11, 54–65. doi: 10.1016/S1474-4422(11)70261-7

Gijselinck, I., Van Mossevelde, S., Van Der Zee, J., Sieben, A., Engelborghs, S., De Bleecker, J., et al. (2016). The C9orf72 repeat size correlates with onset age of disease, DNA methylation and transcriptional downregulation of the promoter. *Mol. Psychiatr.* 21, 1112–1124. doi: 10.1038/mp.2015.159

Gijselinck, I., Van Mossevelde, S., Van Der Zee, J., Sieben, A., Philtjens, S., Heeman, B., et al. (2015). Loss of TBK1 is a frequent cause of frontotemporal dementia in a Belgian cohort. *Neurology* 85, 2116–2125. doi: 10.1212/WNL.0000000000002220

Goldman, J. S., Farmer, J. M., Wood, E. M., Johnson, J. K., Boxer, A., Neuhaus, J., et al. (2005). Comparison of family histories in FTLD subtypes and related tauopathies. *Neurology* 65, 1817–1819. doi: 10.1212/01.wnl.0000187068.92184.63

Goldman, J. S., Rademakers, R., Huey, E. D., Boxer, A. L., Mayeux, R., Miller, B. L., et al. (2011). An algorithm for genetic testing of frontotemporal lobar degeneration. *Neurology* 76, 475–483. doi: 10.1212/WNL.0b013e31820a0d13

Goossens, J., Bjerke, M., Van Mossevelde, S., Van Den Bossche, T., Goeman, J., De Vil, B., et al. (2018). Diagnostic value of cerebrospinal fluid tau, neurofilament, and progranulin in definite frontotemporal lobar degeneration. *Alzheimers Res. Ther.* 10:31. doi: 10.1186/s13195-018-0364-0

Goossens, J., Laton, J., Van Schependom, J., Gielen, J., Struyfs, H., Van Mossevelde, S., et al. (2017). EEG dominant frequency peak differentiates between alzheimer's disease and frontotemporal lobar degeneration. *J. Alzheimers Dis.* 55, 53–58. doi: 10.3233/jad-160188

Goossens, J., Vanmechelen, E., Trojanowski, J. Q., Lee, V. M., Van Broeckhoven, C., Van Der Zee, J., et al. (2015). TDP-43 as a possible biomarker for frontotemporal lobar degeneration: a systematic review of existing antibodies. *Acta Neuropathol. Commun.* 3:15. doi: 10.1186/s40478-015-0195-1

Gorno-Tempini, M. L., Hillis, A. E., Weintraub, S., Kertesz, A., Mendez, M., Cappa, S. F., et al. (2011). Classification of primary progressive aphasia and its variants. *Neurology* 76, 1006–1014. doi: 10.1212/WNL.0b013e31821103e6

Grade, M., Tamames, J. A. H., Pizzini, F. B., Achten, E., Golay, X., and Smits, M. (2015). A neuroradiologist's guide to arterial spin labeling MRI in clinical practice. *Neuroradiology* 57, 1181–1202. doi: 10.1007/s00234-015-1571-z

Greicius, M. (2008). Resting-state functional connectivity in neuropsychiatric disorders. *Curr. Opin. Neurol.* 21, 424–430. doi: 10.1097/WCO.0b013e328306f2c5

Guerra, A., Assenza, F., Bressi, F., Scrascia, F., Del Duca, M., Ursini, F., et al. (2011). Transcranial magnetic stimulation studies in Alzheimer's disease. *Int. J. Alzheimers Dis.* 2011:263817. doi: 10.4061/2011/263817

Harper, L., Fumagalli, G. G., Barkhof, F., Scheltens, P., O'brien, J. T., Bouwman, F., et al. (2016). MRI visual rating scales in the diagnosis of dementia: evaluation in 184 post-mortem confirmed cases. *Brain* 139, 1211–1225. doi: 10.1093/brain/aww005

Harris, J. M., Gall, C., Thompson, J. C., Richardson, A. M., Neary, D., Du Plessis, D., et al. (2013). Sensitivity and specificity of FTDC criteria for behavioral variant frontotemporal dementia. *Neurology* 80, 1881–1887. doi: 10.1212/WNL.0b013e318292a342

Hogan, D. B., Jette, N., Fiest, K. M., Roberts, J. I., Pearson, D., Smith, E. E., et al. (2016). The Prevalence and Incidence of Frontotemporal Dementia: a Systematic Review. *Can. J. Neurol. Sci.* 43(Suppl. 1), S96–S109. doi: 10.1017/cjn.2016.25

Hutton, M., Lendon, C. L., Rizzu, P., Baker, M., Froelich, S., Houlden, H., et al. (1998). Association of missense and 5'-splice-site mutations in tau with the inherited dementia FTDP-17. *Nature* 393, 702–705.

Irwin, D. J., Cairns, N. J., Grossman, M., Mcmillan, C. T., Lee, E. B., Van Deerlin, V. M., et al. (2015). Frontotemporal lobar degeneration: defining phenotypic diversity through personalized medicine. *Acta Neuropathol.* 129, 469–491. doi: 10.1007/s00401-014-1380-1

Irwin, D. J., Trojanowski, J. Q., and Grossman, M. (2013). Cerebrospinal fluid biomarkers for differentiation of frontotemporal lobar degeneration from Alzheimer's disease. *Front. Aging Neurosci.* 5:6. doi: 10.3389/fnagi.2013.00006

Isaacs, A. M., Johannsen, P., Holm, I., and Nielsen, J. E. (2011). Frontotemporal dementia caused by chmp2B mutations. *Curr. Alzheimer Res.* 8, 246–251. doi: 10.2174/156720511795563764

Issac, T. G., Chandra, S. R., and Nagaraju, B. C. (2013). Transcranial magnetic stimulation in patients with early cortical dementia: a pilot study. *Ann. Indian Acad Neurol.* 16, 619–622.

Jack, C. R., Knopman, D. S., Jagust, W. J., Shaw, L. M., Aisen, P. S., Weiner, M. W., et al. (2010). Hypothetical model of dynamic biomarkers of the Alzheimer's pathological cascade. *Lancet Neurol.* 9, 119–128. doi: 10.1016/s1474-4422(09)70299-6

Janelidze, S., Zetterberg, H., Mattsson, N., Palmqvist, S., Vanderstichele, H., Lindberg, O., et al. (2016). CSF Aβ42/Aβ40 and Aβ42/Aβ38 ratios: better diagnostic markers of Alzheimer disease. *Ann. Clin. Transl. Neurol.* 3, 154–165.

Jiskoot, L. C., Panman, J. L., Meeter, L. H., Dopper, E. G. P., Donker Kaat, L., Franzen, S., et al. (2019). Longitudinal multimodal MRI as prognostic and diagnostic biomarker in presymptomatic familial frontotemporal dementia. *Brain* 142, 193–208. doi: 10.1093/brain/awy288

Kerklaan, B. J., Van Berckel, B. N. M., Herholz, K., Dols, A., Van Der Flier, W. M., Scheltens, P., et al. (2014). The added value of 18-fluorodeoxyglucose-positron emission tomography in the diagnosis of the behavioral variant of frontotemporal dementia. *Am. J. Alzheimers Dis. Other Dement.* 29, 607–613. doi: 10.1177/1533317514524811

Kertesz, A., Nadkarni, N., Davidson, W., and Thomas, A. W. (2000). The frontal behavioral Inventory in the differential diagnosis of frontotemporal dementia. *J. Int. Neuropsychol. Soc.* 6, 460–468.

Khachaturian, Z. S. (2011). Revised criteria for diagnosis of alzheimer's disease: national institute on aging-alzheimer's association diagnostic guidelines for alzheimer's disease. *Alzheimers Dement* 7, 253–256. doi: 10.1016/j.jalz.2011.04.003

Kipps, C. M., Davies, R. R., Mitchell, J., Kril, J. J., Halliday, G. M., and Hodges, J. R. (2007). Clinical significance of lobar atrophy in frontotemporal dementia: application of an MRI visual rating scale. *Dement. Geriatr. Cogn. Disord.* 23, 334–342. doi: 10.1159/000100973

Klunk, W. E., Engler, H., Nordberg, A., Wang, Y. M., Blomqvist, G., Holt, D. P., et al. (2004). Imaging brain amyloid in Alzheimer's disease with Pittsburgh Compound-B. *Ann. Neurol.* 55, 306–319.

Knopman, D. S., Mastri, A. R., Frey, W. H. II, Sung, J. H., and Rustan, T. (1990). Dementia lacking distinctive histologic features: a common non-Alzheimer degenerative dementia. *Neurology* 40, 251–256.

Koedam, E., Van Der Flier, W. M., Barkhof, F., Koene, T., Scheltens, P., and Pijnenburg, Y. A. L. (2010). Clinical characteristics of patients with frontotemporal dementia with and without lobar atrophy on MRI. *Alzheimer Dis. Assoc. Disord.* 24, 242–247.

Koikkalainen, J., Rhodius-Meester, H., Tolonen, A., Barkhof, F., Tijms, B., Lemstra, A. W., et al. (2016). Differential diagnosis of neurodegenerative diseases using structural MRI data. *Neuroimage Clin.* 11, 435–449. doi: 10.1016/j.nicl.2016.02.019

Lam, B. Y., Halliday, G. M., Irish, M., Hodges, J. R., and Piguet, O. (2014). Longitudinal white matter changes in frontotemporal dementia subtypes. *Hum. Brain Mapp.* 35, 3547–3557. doi: 10.1002/hbm.22420

Lattante, S., Rouleau, G. A., and Kabashi, E. (2013). TARDBP and FUS mutations associated with amyotrophic lateral sclerosis: summary and update. *Hum. Mutat.* 34, 812–826. doi: 10.1002/humu.22319

Le Ber, I., Camuzat, A., Hannequin, D., Pasquier, F., Guedj, E., Rovelet-Lecrux, A., et al. (2008). Phenotype variability in progranulin mutation carriers: a clinical, neuropsychological, imaging and genetic study. *Brain* 131, 732–746. doi: 10.1093/brain/awn012

Le Ber, I., Guedj, E., Gabelle, A., Verpillat, P., Volteau, M., Thomas-Anterion, C., et al. (2006). Demographic, neurological and behavioural characteristics and brain perfusion SPECT in frontal variant of frontotemporal dementia. *Brain* 129, 3051–3065. doi: 10.1093/brain/awl288

Leuzy, A., Chiotis, K., Hasselbalch, S. G., Rinne, J. O., De Mendonca, A., Otto, M., et al. (2016). Pittsburgh compound B imaging and cerebrospinal fluid amyloid-beta in a multicentre European memory clinic study. *Brain* 139, 2540–2553. doi: 10.1093/brain/aww160

Lewczuk, P., Matzen, A., Blennow, K., Parnetti, L., Molinuevo, J. L., Eusebi, P., et al. (2017). Cerebrospinal fluid abeta42/40 Corresponds Better than Abeta42

to Amyloid PET in Alzheimer's Disease. *J. Alzheimers Dis.* 55, 813–822. doi: 10.3233/jad-160722

Leyton, C. E., Hodges, J. R., Mclean, C. A., Kril, J. J., Piguet, O., and Ballard, K. J. (2015). Is the logopenic-variant of primary progressive aphasia a unitary disorder? *Cortex* 67, 122–133. doi: 10.1016/j.cortex.2015.03.011

Likeman, M., Anderson, V. M., Stevens, J. M., Waldman, A. D., Godbolt, A. K., Frost, C., et al. (2005). Visual assessment of atrophy on magnetic resonance imaging in the diagnosis of pathologically confirmed young-onset dementias. *Arch. Neurol.* 62, 1410–1415.

Mackenzie, I. R., Neumann, M., Bigio, E. H., Cairns, N. J., Alafuzoff, I., Kril, J., et al. (2010). Nomenclature and nosology for neuropathologic subtypes of frontotemporal lobar degeneration: an update. *Acta Neuropathol.* 119, 1–4. doi: 10.1007/s00401-009-0612-2

Mackenzie, I. R., Shi, J., Shaw, C. L., Duplessis, D., Neary, D., Snowden, J. S., et al. (2006). Dementia lacking distinctive histology (DLDH) revisited. *Acta Neuropathol.* 112, 551–559. doi: 10.1007/s00401-006-0123-3

Mahoney, C. J., Beck, J., Rohrer, J. D., Lashley, T., Mok, K., Shakespeare, T., et al. (2012). Frontotemporal dementia with the C9ORF72 hexanucleotide repeat expansion: clinical, neuroanatomical and neuropathological features. *Brain* 135, 736–750. doi: 10.1093/brain/awr361

Mahoney, C. J., Ridgway, G. R., Malone, I. B., Downey, L. E., Beck, J., Kinnunen, K. M., et al. (2014). Profiles of white matter tract pathology in frontotemporal dementia. *Hum. Brain Mapp.* 35, 4163–4179. doi: 10.1002/hbm.22468

Mathias, J. L., and Morphett, K. (2010). Neurobehavioral differences between Alzheimer's disease and frontotemporal dementia: a meta-analysis. *J. Clin. Experiment. Neuropsychol.* 32, 682–698. doi: 10.1080/13803390903427414

Meeter, L. H., Dopper, E. G., Jiskoot, L. C., Sanchez-Valle, R., Graff, C., Benussi, L., et al. (2016). Neurofilament light chain: a biomarker for genetic frontotemporal dementia. *Ann. Clin. Transl. Neurol.* 3, 623–636. doi: 10.1002/acn3.325

Meeter, L. H., Kaat, L. D., Rohrer, J. D., and Van Swieten, J. C. (2017). Imaging and fluid biomarkers in frontotemporal dementia. *Nat. Rev. Neurol.* 13, 406–419. doi: 10.1038/nrneurol.2017.75

Meeter, L. H. H., Vijverberg, E. G., Del Campo, M., Rozemuller, A. J. M., Kaat, L. D., De Jong, F. J., et al. (2018). Clinical value of neurofilament and phospho-tau/tau ratio in the frontotemporal dementia spectrum. *Neurology* 90, e1231–e1239. doi: 10.1212/WNL.0000000000005261

Mendez, M. F., Mcmurtray, A., Licht, E., Shapira, J. S., Saul, R. E., and Miller, B. L. (2006). The scale for emotional blunting in patients with frontotemporal dementia. *Neurocase* 12, 242–246. doi: 10.1080/13554790600910375

Meyer, H., and Weihl, C. C. (2014). The VCP/p97 system at a glance: connecting cellular function to disease pathogenesis. *J. Cell Sci.* 127, 3877–3883. doi: 10.1242/jcs.093831

Meyer, S., Mueller, K., Stuke, K., Bisenius, S., Diehl-Schmid, J., Jessen, F., et al. (2017). Predicting behavioral variant frontotemporal dementia with pattern classification in multi-center structural MRI data. *Neuroimage Clin.* 14, 656–662. doi: 10.1016/j.nicl.2017.02.001

Milan, G., Lamenza, F., Iavarone, A., Galeone, F., Lore, E., De Falco, C., et al. (2008). Frontal Behavioural Inventory in the differential diagnosis of dementia. *Acta Neurol. Scand.* 117, 260–265. doi: 10.1111/j.1600-0404.2007.00934.x

Morbelli, S., Ferrara, M., Fiz, F., Dessi, B., Arnaldi, D., Picco, A., et al. (2016). Mapping brain morphological and functional conversion patterns in predementia late-onset BVFTD. *Eur. J. Nucl. Med. Mol. Imaging* 43, 1337–1347. doi: 10.1007/s00259-016-3335-3

Munoz-Ruiz, M. A., Hartikainen, P., Koikkalainen, J., Wolz, R., Julkunen, V., Niskanen, E., et al. (2012). Structural mri in frontotemporal dementia: comparisons between hippocampal volumetry, tensor-based morphometry and voxel-based morphometry. *Plos One* 7:12.

Neary, D., Snowden, J. S., Gustafson, L., Passant, U., Stuss, D., Black, S., et al. (1998). Frontotemporal lobar degeneration: a consensus on clinical diagnostic criteria. *Neurology* 51, 1546–1554. doi: 10.1212/wnl.51.6.1546

Niemantsverdriet, E., Feyen, B. F. E., Le Bastard, N., Martin, J. J., Goeman, J., De Deyn, P. P., et al. (2018). Added diagnostic value of cerebrospinal fluid biomarkers for differential dementia diagnosis in an autopsy-confirmed cohort. *J. Alzheimers Dis.* 63, 373–381. doi: 10.3233/JAD-170927

Niemantsverdriet, E., Ottoy, J., Somers, C., De Roeck, E., Struyfs, H., Soetewey, F., et al. (2017a). The cerebrospinal fluid abeta1-42/Abeta1-40 ratio improves concordance with amyloid-pet for diagnosing alzheimer's disease in a clinical setting. *J. Alzheimers Dis.* 60, 561–576. doi: 10.3233/JAD-170327

Niemantsverdriet, E., Valckx, S., Bjerke, M., and Engelborghs, S. (2017b). Alzheimer's disease CSF biomarkers: clinical indications and rational use. *Acta Neurol. Belg.* 117, 591–602. doi: 10.1007/s13760-017-0816-5

Ossenkoppele, R., Pijnenburg, Y. A. L., Perry, D. C., Cohn-Sheehy, B. I., Scheltens, N. M. E., Vogel, J. W., et al. (2015). The behavioural/dysexecutive variant of Alzheimer's disease: clinical, neuroimaging and pathological features. *Brain* 138, 2732–2749. doi: 10.1093/brain/awv191

Pasquier, F., Leys, D., Weerts, J. G., Mounier-Vehier, F., Barkhof, F., and Scheltens, P. (1996). Inter- and intraobserver reproducibility of cerebral atrophy assessment on MRI scans with hemispheric infarcts. *Eur. Neurol.* 36, 268–272. doi: 10.1159/000117270

Pickut, B. A., Saerens, J., Mariën, P., Borggreve, F., Goeman, J., Vandevivere, J., et al. (1997). Discriminative use of SPECT in frontal lobe-type dementia versus (senile) dementia of the Alzheimer's type. *J. Nucl. Med.* 38, 929–934.

Pierantozzi, M., Panella, M., Palmieri, M. G., Koch, G., Giordano, A., Marciani, M. G., et al. (2004). Different TMS patterns of intracortical inhibition in early onset Alzheimer dementia and frontotemporal dementia. *Clin. Neurophysiol.* 115, 2410–2418. doi: 10.1016/j.clinph.2004.04.022

Po, K., Leslie, F. V., Gracia, N., Bartley, L., Kwok, J. B., Halliday, G. M., et al. (2014). Heritability in frontotemporal dementia: more missing pieces? *J. Neurol.* 261, 2170–2177. doi: 10.1007/s00415-014-7474-9

Pottier, C., Bieniek, K. F., Finch, N., Van De Vorst, M., Baker, M., Perkersen, R., et al. (2015). Whole-genome sequencing reveals important role for TBK1 and OPTN mutations in frontotemporal lobar degeneration without motor neuron disease. *Acta Neuropathol.* 130, 77–92. doi: 10.1007/s00401-015-1436-x

Pressman, P. S., and Miller, B. L. (2014). Diagnosis and management of behavioral variant frontotemporal dementia. *Biol. Psychiatry* 75, 574–581. doi: 10.1016/j.biopsych.2013.11.006

Quaid, K. A. (2011). Genetic counseling for frontotemporal dementias. *J. Mol. Neurosci.* 45, 706–709. doi: 10.1007/s12031-011-9557-8

Rabinovici, G. D., and Miller, B. L. (2010). Frontotemporal lobar degeneration: epidemiology, pathophysiology, diagnosis and management. *CNS Drugs* 24, 375–398. doi: 10.2165/11533100-000000000-00000

Rademakers, R., Baker, M., Gass, J., Adamson, J., Huey, E. D., Momeni, P., et al. (2007). Phenotypic variability associated with progranulin haploinsufficiency in patients with the common 1477C– > T (Arg493X) mutation: an international initiative. *Lancet Neurol.* 6, 857–868. doi: 10.1016/s1474-4422(07)70221-1

Rademakers, R., Cruts, M., and Van Broeckhoven, C. (2004). The role of tau (MAPT) in frontotemporal dementia and related tauopathies. *Hum. Mutat.* 24, 277–295. doi: 10.1002/humu.20086

Rascovsky, K., Hodges, J. R., Knopman, D., Mendez, M. F., Kramer, J. H., Neuhaus, J., et al. (2011). Sensitivity of revised diagnostic criteria for the behavioural variant of frontotemporal dementia. *Brain* 134, 2456–2477. doi: 10.1093/brain/awr179

Renton, A. E., Majounie, E., Waite, A., Simon-Sanchez, J., Rollinson, S., Gibbs, J. R., et al. (2011). A hexanucleotide repeat expansion in C9ORF72 is the cause of chromosome 9p21-linked ALS-FTD. *Neuron* 72, 257–268. doi: 10.1016/j.neuron.2011.09.010

Rohrer, J. D., Guerreiro, R., Vandrovcova, J., Uphill, J., Reiman, D., Beck, J., et al. (2009). The heritability and genetics of frontotemporal lobar degeneration. *Neurology* 73, 1451–1456. doi: 10.1212/WNL.0b013e3181bf997a

Rohrer, J. D., Nicholas, J. M., Cash, D. M., Van Swieten, J., Dopper, E., Jiskoot, L., et al. (2015). Presymptomatic cognitive and neuroanatomical changes in genetic frontotemporal dementia in the Genetic Frontotemporal dementia Initiative (GENFI) study: a cross-sectional analysis. *Lancet Neurol.* 14, 253–262. doi: 10.1016/S1474-4422(14)70324-2

Rohrer, J. D., and Warren, J. D. (2011). Phenotypic signatures of genetic frontotemporal dementia. *Curr.Opin. Neurol.* 24, 542–549. doi: 10.1097/WCO.0b013e32834cd442

Rohrer, J. D., Woollacott, I. O. C., Dick, K. M., Brotherhood, E., Gordon, E., Fellows, A., et al. (2016). Serum neurofilament light chain protein is a measure of disease intensity in frontotemporal dementia. *Neurology* 87, 1329–1336. doi: 10.1212/WNL.0000000000003154

Rosso, S. M., Donker Kaat, L., Baks, T., Joosse, M., De Koning, I., Pijnenburg, Y., et al. (2003). Frontotemporal dementia in the Netherlands: patient characteristics and prevalence estimates from a population-based study. *Brain* 126, 2016–2022. doi: 10.1093/brain/awg204

Rowe, C. C., Ng, S., Ackermann, U., Gong, S. J., Pike, K., Savage, G., et al. (2007). Imaging beta-amyloid burden in aging and dementia. *Neurology* 68, 1718–1725.

Saxon, J. A., Thompson, J. C., Jones, M., Harris, J. M., Richardson, A. M., Langheinrich, T., et al. (2017). Examining the language and behavioural profile in FTD and ALS-FTD. *J. Neurol. Neurosurg. Psychiatry* 88, 675–680. doi: 10.1136/jnnp-2017-315667

Scheltens, P., Launer, L. J., Barkhof, F., Weinstein, H. C., and Van Gool, W. A. (1995). Visual assessment of medial temporal lobe atrophy on magnetic resonance imaging: interobserver reliability. *J. Neurol.* 242, 557–560. doi: 10.1007/bf00868807

Seelaar, H., Kamphorst, W., Rosso, S. M., Azmani, A., Masdjedi, R., De Koning, I., et al. (2008). Distinct genetic forms of frontotemporal dementia. *Neurology* 71, 1220–1226. doi: 10.1212/01.wnl.0000319702.37497.72

Seelaar, H., Rohrer, J. D., Pijnenburg, Y. A. L., Fox, N. C., and Van Swieten, J. C. (2011). Clinical, genetic and pathological heterogeneity of frontotemporal dementia: a review. *J. Neurol. Neurosurg. Psychiatry* 82, 476–486. doi: 10.1136/jnnp.2010.212225

Sieben, A., Van Langenhove, T., Engelborghs, S., Martin, J. J., Boon, P., Cras, P., et al. (2012). The genetics and neuropathology of frontotemporal lobar degeneration. *Acta Neuropathol.* 124, 353–372. doi: 10.1007/s00401-012-1029-x

Sleegers, K., Brouwers, N., Van Damme, P., Engelborghs, S., Gijselinck, I., Van Der Zee, J., et al. (2009). Serum biomarker for progranulin-associated frontotemporal lobar degeneration. *Ann. Neurol.* 65, 603–609. doi: 10.1002/ana.21621

Snowden, J. S., Adams, J., Harris, J., Thompson, J. C., Rollinson, S., Richardson, A., et al. (2015). Distinct clinical and pathological phenotypes in frontotemporal dementia associated with MAPT, PGRN and C9orf72 mutations. *Amyotroph. Lateral Scler. Frontotemporal Degener.* 16, 497–505. doi: 10.3109/21678421.2015.1074700

Spinelli, E. G., Mandelli, M. L., Miller, Z. A., Santos-Santos, M. A., Wilson, S. M., Agosta, F., et al. (2017). Typical and atypical pathology in primary progressive aphasia variants. *Ann. Neurol.* 81, 430–443. doi: 10.1002/ana.24885

Steketee, R. M. E., Bron, E. E., Meijboom, R., Houston, G. C., Klein, S., Mutsaerts, H. J., et al. (2016). Early-stage differentiation between presenile Alzheimer's disease and frontotemporal dementia using arterial spin labeling MRI. *Eur. Radiol.* 26, 244–253. doi: 10.1007/s00330-015-3789-x

Tosun, D., Schuff, N., Rabinovici, G. D., Ayakta, N., Miller, B. L., Jagust, W., et al. (2016). Diagnostic utility of ASL-MRI and FDG-PET in the behavioral variant of FTD and AD. *Ann. Clin. Transl. Neurol.* 3, 740–751. doi: 10.1002/acn3.330

Urwin, H., Authier, A., Nielsen, J. E., Metcalf, D., Powell, C., Froud, K., et al. (2010). Disruption of endocytic trafficking in frontotemporal dementia with CHMP2B mutations. *Hum. Mol. Genet.* 19, 2228–2238. doi: 10.1093/hmg/ddq100

van der Zee, J., Gijselinck, I., Van Mossevelde, S., Perrone, F., Dillen, L., Heeman, B., et al. (2017). TBK1 mutation spectrum in an extended european patient cohort with frontotemporal dementia and amyotrophic lateral sclerosis. *Hum. Mutat.* 38, 297–309. doi: 10.1002/humu.23161

van der Zee, J., Pirici, D., Van Langenhove, T., Engelborghs, S., Vandenberghe, R., Hoffmann, M., et al. (2009). Clinical heterogeneity in 3 unrelated families linked to VCP p.Arg159His. *Neurology* 73, 626–632. doi: 10.1212/WNL.0b013e3181b389d9

van der Zee, J., Rademakers, R., Engelborghs, S., Gijselinck, I., Bogaerts, V., Vandenberghe, R., et al. (2006). A Belgian ancestral haplotype harbours a highly prevalent mutation for 17q21-linked tau-negative FTLD. *Brain* 129, 841–852. doi: 10.1093/brain/awl029

van der Zee, J., Urwin, H., Engelborghs, S., Bruyland, M., Vandenberghe, R., Dermaut, B., et al. (2008). CHMP2B C-truncating mutations in frontotemporal lobar degeneration are associated with an aberrant endosomal phenotype in vitro. *Hum. Mol. Genet.* 17, 313–322. doi: 10.1093/hmg/ddm309

Van Mossevelde, S., Engelborghs, S., Van Der Zee, J., and Van Broeckhoven, C. (2018). Genotype-phenotype links in frontotemporal lobar degeneration. *Nat. Rev. Neurol.* 14, 363–378. doi: 10.1038/s41582-018-0009-8

Van Mossevelde, S., Van Der Zee, J., Cruts, M., and Van Broeckhoven, C. (2017a). Relationship between C9orf72 repeat size and clinical phenotype. *Curr. Opin. Genet. Dev.* 44, 117–124. doi: 10.1016/j.gde.2017.02.008

Van Mossevelde, S., Van Der Zee, J., Gijselinck, I., Sleegers, K., De Bleecker, J., Sieben, A., et al. (2017b). Clinical evidence of disease anticipation in families segregating a C9orf72 repeat expansion. *Jama Neurol.* 74, 445–452. doi: 10.1001/jamaneurol.2016.4847

Van Mossevelde, S., Van Der Zee, J., Gijselinck, I., Engelborghs, S., Sieben, A., Van Langenhove, T., et al. (2016). Clinical features of TBK1 carriers compared with C9orf72, GRN and non-mutation carriers in a Belgian cohort. *Brain* 139, 452–467. doi: 10.1093/brain/awv358

Varma, A. R., Adams, W., Lloyd, J. J., Carson, K. J., Snowden, J. S., Testa, H. J., et al. (2002). Diagnostic patterns of regional atrophy on MRI and regional cerebral blood flow change on SPECT in young onset patients with Alzheimer's disease, frontotemporal dementia and vascular dementia. *Acta Neurol. Scand.* 105, 261–269. doi: 10.1034/j.1600-0404.2002.1o148.x

Verfaillie, S. C., Adriaanse, S. M., Binnewijzend, M. A., Benedictus, M. R., Ossenkoppele, R., Wattjes, M. P., et al. (2015). Cerebral perfusion and glucose metabolism in Alzheimer's disease and frontotemporal dementia: two sides of the same coin? *Eur. Radiol.* 25, 3050–3059. doi: 10.1007/s00330-015-3696-1

Vijverberg, E. G. B., Wattjes, M. P., Dols, A., Krudop, W. A., Moller, C., Peters, A., et al. (2016). Diagnostic accuracy of MRI and additional F-18 FDG-PET for behavioral variant frontotemporal dementia in patients with late onset behavioral changes. *J. Alzheimers Dis.* 53, 1287–1297. doi: 10.3233/jad-160285

Villemagne, V. L., Dore, V., Bourgeat, P., Burnham, S. C., Laws, S., Salvado, O., et al. (2017). A beta-amyloid and tau imaging in dementia. *Semin. Nucl. Med.* 47, 75–88. doi: 10.1053/j.semnuclmed.2016.09.006

Waldo, M. L., Gustafson, L., Passant, U., and Englund, E. (2015). Psychotic symptoms in frontotemporal dementia: a diagnostic dilemma? *Int. Psychogeriatr.* 27, 531–539. doi: 10.1017/S1041610214002580

Watts, G. D., Wymer, J., Kovach, M. J., Mehta, S. G., Mumm, S., Darvish, D., et al. (2004). Inclusion body myopathy associated with Paget disease of bone and frontotemporal dementia is caused by mutant valosin-containing protein. *Nat. Genet.* 36, 377–381. doi: 10.1038/ng1332

Wauters, E., Van Mossevelde, S., Sleegers, K., Van Der Zee, J., Engelborghs, S., Sieben, A., et al. (2018). Clinical variability and onset age modifiers in an extended Belgian GRN founder family. *Neurobiol. Aging* 67, 84–94. doi: 10.1016/j.neurobiolaging.2018.03.007

Whitwell, J. L., Boeve, B. F., Weigand, S. D., Senjem, M. L., Gunter, J. L., Baker, M. C., et al. (2015). Brain atrophy over time in genetic and sporadic frontotemporal dementia: a study of 198 serial magnetic resonance images. *Eur. J. Neurol.* 22, 745–752. doi: 10.1111/ene.12675

Wing, J. K., Babor, T., Brugha, T., Burke, J., Cooper, J. E., Giel, R., et al. (1990). SCAN. schedules for clinical assessment in neuropsychiatry. *Arch. Gen. Psychiatry* 47, 589–593.

Woollacott, I. O. C., and Rohrer, J. D. (2016). The clinical spectrum of sporadic and familial forms of frontotemporal dementia. *J. Neurochem.* 138, 6–31. doi: 10.1111/jnc.13654

Yan, J., Deng, H. X., Siddique, N., Fecto, F., Chen, W., Yang, Y., et al. (2010). Frameshift and novel mutations in FUS in familial amyotrophic lateral sclerosis and ALS/dementia. *Neurology* 75, 807–814. doi: 10.1212/WNL.0b013e3181f07e0c

Yeo, J. M., Lim, X., Khan, Z., and Pal, S. (2013). Systematic review of the diagnostic utility of SPECT imaging in dementia. *Eur. Arch. Psychiatry Clin. Neurosci.* 263, 539–552. doi: 10.1007/s00406-013-0426-z

Zhou, J., Greicius, M. D., Gennatas, E. D., Growdon, M. E., Jang, J. Y., Rabinovici, G. D., et al. (2010). Divergent network connectivity changes in behavioural variant frontotemporal dementia and Alzheimer's disease. *Brain* 133, 1352–1367. doi: 10.1093/brain/awq075

Conflict of Interest Statement: The authors declare that the research was conducted in the absence of any commercial or financial relationships that could be construed as a potential conflict of interest.

The reviewer LB declared a past co-authorship with two of the authors CVB and SE to the handling Editor.

frontiers in Genetics

CASE REPORT
published: 08 November 2019
doi: 10.3389/fgene.2019.01109

Haplotype Analysis of the First A4V-*SOD1* Spanish Family: Two Separate Founders or a Single Common Founder?

Cecilia Garcia[1,2,3†], *Jose Manuel Vidal-Taboada*[1,2,3†], *Enrique Syriani*[2,3], *Maria Salvado*[1,2,3,4], *Miguel Morales*[2,3] *and Josep Gamez*[1,2,3,4*]

[1] ALS Unit, Neurology Department, Vall d'Hebron University Hospital, Barcelona, Spain, [2] Vall d'Hebron Research Institute (VHIR), Barcelona, Spain, [3] European Reference Network on Rare Neuromuscular Diseases (ERN EURO-NMD), Barcelona, Spain, [4] Department of Medicine, Universitat Autònoma de Barcelona (UAB), Barcelona, Spain

Despite the genetic heterogeneity reported in familial amyotrophic lateral sclerosis (ALS) (fALS), Cu/Zn superoxide-dismutase (SOD1) gene mutations are the second most common cause of the disease, accounting for around 20% of all families (ALS1) and isolated sporadic cases (sALS). At least 186 different mutations in the SOD1 gene have been reported to date. The possibility of a single founder and separate founders have been investigated for D90A (p.D91A) and A4V (p.A5V), the most common mutations worldwide. High-throughput single nucleotide polymorphism genotyping studies have suggested two founders for A4V (one for the Amerindian population and another for the European population) although the possibility that the two populations are descended from a single ancient founder cannot be ruled out. We used 15 genetic variants spanning the human chromosome 21 from the SOD1 gene to the *SCAF4* gene, comparing them with the population reference panels, to demonstrate that the first A4V Spanish pedigree shared the genetic background reported in the European population.

Keywords: SOD1, A4V, p.A5V, amyotrophic lateral sclerosis, familial amyotrophic lateral sclerosis, ALS1, founder effect

OPEN ACCESS

Edited by:
Anne Marja Remes,
University of Oulu, Finland

Reviewed by:
Fan Jin,
Zhejiang University, China
Adriano Chio,
University of Turin, Italy

***Correspondence:**
Josep Gamez
josepgamez.bcn@gmail.com

†These authors have contributed equally to this work

Specialty section:
This article was submitted to Genetic Disorders, a section of the journal Frontiers in Genetics

Received: *04 March 2019*
Accepted: *16 October 2019*
Published: *08 November 2019*

Citation:
Garcia C, Vidal-Taboada JM, Syriani E, Salvado M, Morales M and Gamez J (2019) Haplotype Analysis of the First A4V-SOD1 Spanish Family: Two Separate Founders or a Single Common Founder?. Front. Genet. 10:1109. doi: 10.3389/fgene.2019.01109

INTRODUCTION

About 10% of amyotrophic lateral sclerosis (ALS) cases are familial (fALS), and genetics is the discipline that has made the greatest contribution to understanding the complexity of the disease's pathogenesis, with a major impact on clinical practice, especially in the field of genetic counseling. Since the discovery of mutations in the SOD1 gene linked to ALS in 1993, an increasing number of genes have been reported as associated with the disease, justifying the term "genetic heterogeneity of ALS". At least 31 major genes and 2 different genetic loci with dominant, recessive, and X-linked patterns of inheritance have been identified for fALS, and an increasing number of susceptibility or modifying gene loci have been suggested for fALS and several sporadic ALS (sALS) cases. The ALSoD database currently lists genetic variants in 126 genes as associated to ALS. Gene–gene and gene–environment interactions have also been suggested as playing a major role in the disease's appearance and phenotype (Andersen and Al-Chalabi, 2011; van Blitterswijk et al., 2012; Abel et al., 2013; Al-Chalabi et al., 2013; Leblond et al., 2014; Renton et al., 2014; Jones et al., 2015; Al-Chalabi et al., 2017; Brown and Al-Chalabi, 2017; Hardiman et al., 2017; van Es et al., 2017; Chia et al., 2018).

Mutations in the gene encoding Cu/Zn superoxide dismutase (SOD1) are the second most common cause of fALS cases worldwide, accounting for approximately 20% of all families. ALS1 is the designation for fALS linked to the SOD1 gene (MIM 105400). At least 186 different mutations in the SOD1 gene have been described, of which over 90% are missense, confirming its allelic heterogeneity (ALSoD[1]). The SOD1 mutations reported in ALS1 pedigrees are primarily associated with a dominant inheritance pattern and high penetrance, despite occasionally being found in apparently sporadic or recessive cases. Clinical heterogeneity, including gender predominance, age at symptom onset, site of onset, penetrance, and progression of the disease, has also been reported in many ALS1 families. The type of mutation and the resulting phenotype are strongly correlated in some cases (Andersen et al., 2003a; Andersen, 2003b; Andersen, 2006). However, information about the clinical–genetic correlations for most of these mutations is scarce. As a result, clinical and genetic data from families with ALS1 from around the world are being compiled in the constantly updated ALS database (ALSoD[1]). This database provides clinicians with information on research into the genetic characterization of ALS1 and other forms of familial ALS, as well as new candidate genes.

Epidemiological studies report that D90A is the most common mutation worldwide, although the most frequent mutation in North America is A4V (formally designated p.A5V, rs121912442), which accounts for 50% of North American ALS1 families (ALSoD[1], Watanabe et al., 2000; Andersen, 2003b; Andersen, 2006). The most striking features of the p.A5V mutation are rapid progression, with a mean survival time of less than 2 years from clinical onset, predominant lower motor neuron symptoms, and its rarity in the European population. The possibility of two founder haplotypes—one Native American and another European—has recently been suggested (Rosen, 2004; Broom et al., 2008; Armon, 2009; Saeed et al., 2009; Tang et al., 2018). The p.A5V-*SOD1* mutation has been described in a very small number of families in Europe, and never in the Spanish population.

Here we report the clinical characterization and high-throughput single nucleotide polymorphism (SNP) genotyping of the first p.A5V (A4V) Spanish ALS kindred with high penetrance, predominant lower motor neuron involvement, fast progression, short survival times, and no cognitive impairment.

MATERIAL AND METHODS

Subjects

This study was carried out following the protocol approved by the Hospital Universitari Vall d'Hebron Institutional Review Board with written informed consent from all subjects in accordance with the Declaration of Helsinki.

Our pedigree originated in north-western Spain. The simplified pedigree of the family is shown in **Figure 1**. We examined two ALS patients and two healthy individuals in the pedigree after obtaining informed consent. There were no skipped generations. The affected individuals were clinically characterized according to gender, age at onset, initial topography, signs of dementia, and survival time (**Supplementary Table S1**).

The proband, a 53-year-old male (II:1), noticed weakness in his left leg beginning 7 months previously, which he attributed to a traumatism he had experienced when working in construction. An initial electromyographic study showed denervation in all four extremities. Transcranial magnetic stimulation and brain and spinal MRI were normal. Cerebrospinal fluid, hemogram, biochemical screening, and serological tests for neurotropic infectious diseases all presented normal values, except for *creatine kinase*, which was 735 U/l (normal values < 135). The patient subsequently experienced pain, with frequent falls in the months after his first examination, when muscle strength in his upper limbs and right lower limb was completely normal. His Amyotrophic Lateral Sclerosis Functional Rating (ALSFRS-R) score was 44. In the next visit, 3 months later, we observed weakness and amyotrophy in the left upper limb, particularly in the proximal muscles. We observed generalized fasciculations, which were more marked in the muscles on the left side of the body, where it was difficult to elicit deep tendon reflexes. Eight months after the initial visit, the patient was admitted to the emergency ward complaining of dyspnea and orthopnea, and non-invasive mechanical ventilation was fitted. The patient was offered a gastrostomy, but declined. The patient died 19 months after symptom onset.

Two years later, the proband's 47-year-old brother (II:5) came to our clinic due to presenting clumsiness and difficulties climbing stairs, running and walking. He had experienced recurring episodes of cramp in both calves in the 2 months before his visit. We observed weakness and amyotrophy in the proximal muscles of the right lower limb and a minimal loss of muscle mass in the first interosseous of the right hand. Deep tendon reflexes were normal, except for the patellar and Achilles reflexes. Fasciculation was observed in the musculature of the four extremities. His ALSFRS-R rating at this point was 39. Like his brother, neurophysiological studies showed signs of denervation in three regions and an absence of upper motor neuron signs. The patient declined any follow-up, life support, ventilation or nutritional measures. He died 17 months after clinical onset.

In their family, their two sisters requested genetic screening for familial forms of ALS, as they remembered that their father had died at 57 years of age due to respiratory insufficiency after 2 years of weakness in the upper limbs. To the best of our knowledge, this pedigree contains no other cases of neurodegenerative disorders, including frontotemporal dementia and Parkinson's disease.

Genetic Studies

Selection of Single Nucleotide Polymorphisms for Analysis of the *SOD1* Haplotype

In order to saturate the *SOD1* region with genetic markers, we performed a scientific literature search of haplotypes previously described in the *SOD1* gene. We consulted various databases (1K Genomes, dbSNP, and Ensembl Web sites) for SNPs in the *SOD1* region of the IBerian populations in Spain (IBS) population, and analyzed 14 SNPs and 1 repeat. Thirteen SNPs were selected from

[1]http://alsod.iop.kcl.ac.uk/mutations/mutationsFoundGeneOnly.aspx?gene_id=SOD1. Web site access on Oct 8th 2019.

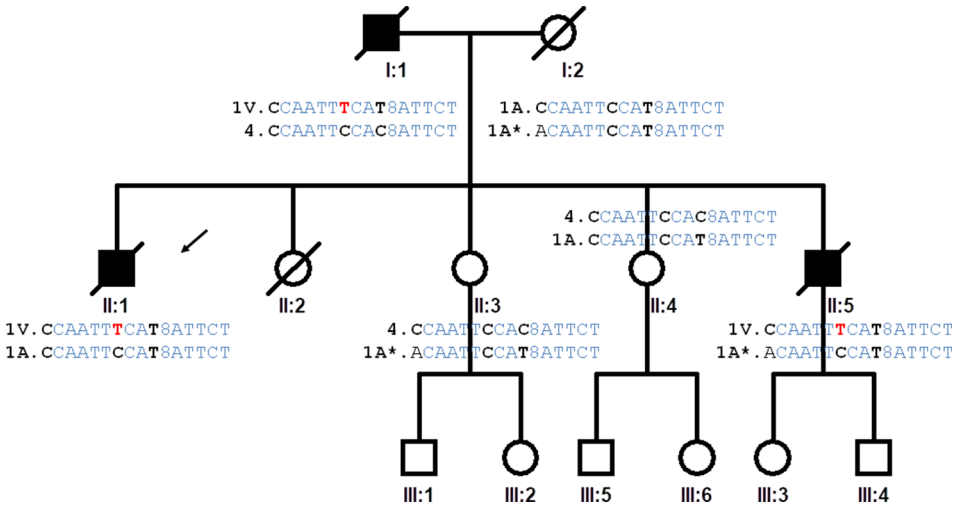

FIGURE 1 | Pedigree of the family studied. The proband is indicated by an arrow (II:1). The haplotypes of the progenitors are inferred from the haplotypes of the offspring. Highlighted in red the genetic variation causing A5V mutation, in bold the single nucleotide polymorphisms that determine the differences between haplotypes of the IBS population. Haplotype (variation order): rs4817415, rs2070422, rs1008270, rs9974610, rs2173962, rs202445, rs121912442, rs4816405, Rs2070424, rs1041740, CA_repeat, rs2833475, rs16988427, rs2833481, rs2070423, rs2833483.

the results of 79 A4V families (Broom et al., 2008) (rs4817415, rs2070422, rs1008270, rs9974610, rs2173962, rs4816405, rs2070424, rs1041740, rs2833475, rs16988427, rs2833481, rs2070423, rs2833483); and 1 additional SNP (rs202445) and a CA repeat from a study of 54 patients (Saeed et al., 2009) and genetic data from an isolated Chinese case (Tang et al., 2018). The locations of all markers and their previous designations are shown in **Supplementary Table S2**.

Genotyping of Normal and Mutant p.A5V Alleles in SOD1

The SNP rs121912442 (*SOD1* p.A5V) region was amplified by PCR and the allele detected by Sanger sequencing. DreamTaq Master Mix was used under standard conditions according to the manufacturer's instructions. Primer sequences and PCR cycling conditions are shown in **Supplementary Table S3**. PCR products were purified with ExoSAP-IT™ (Thermo Fisher Scientific Inc.) prior to automated Sanger sequencing using a BigDye® v3.1 terminator Cycle Sequencing Kit in an ABI3730XL® (Thermo Fisher Scientific Inc., USA). DNA sequences were analyzed using the Finch TV 1.5.0 software.

Genotyping of Single Nucleotide Polymorphisms and Microsatellite

PCR Amplification of CA-repeat region was performed, and the products were analyzed by Sanger sequencing. The results were validated by Fragment Size Analysis using an ABI3730XL® system and GeneMapper 4.0 Software (Applied Biosystems). Most SNPs were genotyped by PCR amplification and Sanger sequencing as indicated above. In other cases, SNPs were detected by allele-specific PCR using standard conditions and an internal PCR control. Their primers and annealing temperature are shown in **Supplementary Table S3**. PCR primers were designed using Primer3 version 4.0. (Untergasser et al., 2012).

The entire coding regions of SOD1, FUS, TARDBP, and PFN1 genes and the *C9orf72* expansion were screened using Sanger sequencing.

Analysis of Data

LDhap software (Machiela and Chanock, 2015) was used with a 1K Genomes dataset to identify inferred haplotype blocks in the Iberian (IBS) population. Linkage disequilibrium between SNPs was calculated using LDMatrix software (LDLink). The *SOD1* p.A5V haplotypes detected in our Spanish patients were compared with the haplotypes associated in American, Swedish, and Chinese populations (Broom et al., 2008; Tang et al., 2018). The genetic data for the comparisons with the African (ACB, ASW, ESN, GWC, LWK, MSL, YRI), Asian (CHB, CHS, CDX, JPT, KHV), European (CEU, FIN, GBR, IBS, TSI), and Mixed American (CLM, MXL, PEL, PUR) populations were obtained from all the available subjects (n = 2,312 individuals from 19 populations, including 102 IBS subjects) of the 1K Genomes Project (phase 3, version 5) (The 1000 Genomes Project Consortium, 2015). Haplotype assembly was carried out by manual phasing of the alleles from the different variants analyzed.

RESULTS

Clinical Characteristics of the p.A5V-*SOD1* Pedigree

The clinical phenotype in the affected members in our family—a mean age of onset of 51.7 years, spinal onset, predominant lower motor neuron signs, and a survival time of 20 months—is consistent with the phenotype in the American, Italian, and Swedish families. No cognitive impairment in either brother was detected in the neuropsychological test (**Supplementary Table S1**).

Genetic Results

Mutation analysis of the *SOD1* gene by direct PCR sequencing revealed a C-to-T transition at nucleotide position 14 (c.14C > T, **Supplementary Figure S1**) leading to a p.A5V (rs121912442, A4V in the old nomenclature) sequence change at protein level in the two affected ALS patients: the proband (individual II:1) and his brother (individual II:5) (**Table 1**). This exon 1 mutation was not found in the two healthy members of the family (individuals II:3 and II:4) who requested details of their genetic situation (**Supplementary Figure S1**).

No mutations were detected in the *FUS*, *TARDBP*, and *PFN1* genes, and no *C9orf72* expansions were identified in the two ALS patients.

Haplotype Analysis

We analyzed the 15 genetic variants spanning the human chromosome 21 from the *SOD1* gene to the *SCAF4* gene (**Supplementary Table S2**). The genetic markers around the *SOD1* gene were genotyped to infer the *SOD1* haplotypes of the ALS patients and the family members. Based on the genotypes of the four siblings, it was possible to identify four different inferred haplotypes present in the family and propose the haplotypes of the affected father and the mother (**Figure 1**).

Fourteen of the 16 SNPs analyzed in the *SOD1* gene were detected in subjects of the IBS population from the 1K Genomes Project. Eight phased haplotypes of the *SOD1* region were inferred in the IBS population with different frequencies

TABLE 1 | SOD1 p.A5V mutation founder haplotype in IBS population compared to other populations.

RS number	SOD1 A5V founder haplotype				Patients genotype	
	USA*	SWE*	CHN**	IBS	II:1	II:5
rs4817415	C	C	–	C	C/C	C/A
rs2070422	T	C	C	C	C/C	C/C
rs1008270	A	A	–	A	A/A	A/A
rs9974610	A	A	–	A	A/A	A/A
rs2173962	T	T	–	T	T/T	T/T
rs202445	-	-	–	T	T/T	T/T
rs121912442	T	T	T	T	T/C	T/C
rs4816405	G	C	C/G	C	C/C	C/C
rs2070424	G	A	A	A	A/A	A/A
rs1041740	C	T	C/T	T	T/T	T/T
rs2833475	G	A	A	A	A/A	A/A
rs16988427	C	T	T/C	T	T/T	T/T
rs2833481	C	T	T	T	T/T	T/T
rs2070423	T	C	C/T	C	C/C	C/C
rs2833483	C	T	T/C	T	T/T	T/T

**Data from Broom et al., 2008. **Data from Tang et al., 2018. (-) Not available.*

Variant	Position (GRCh38)	Allele Frequencies	SOD1 Haplotypes								
rs4817415	Chr21:g.31619348	C=0.77, A=0.23	C	C	C	A	C	A	C	C	A
rs2070422	Chr21:g.31628043	C=0.89, T=0.11	C	C	C	C	C	C	T	T	T
rs1008270	Chr21:g.31629832	A=0.85, C=0.15	A	A	A	C	A	A	A	A	A
rs9974610	Chr21:g.31646056	A=0.83, G=0.17	A	A	G	A	A	A	A	A	A
rs2173962	Chr21:g.31649707	T=0.95, C=0.05	T	T	T	T	T	T	T	C	C
rs202445	Chr21:g.31653354	T=0.85, C=0.15	T	T	T	C	T	T	T	T	T
rs121912442	Chr21:g.31659782	C=1.00, T=0.00*	T	C	C	C	C	C	C	C	C
rs4816405	Chr21:g.31660688	C=0.93, G=0.07	C	C	C	C	C	C	G	C	C
rs2070424	Chr21:g.31667007	A=0.93, G=0.07	A	A	A	A	A	A	G	A	A
rs1041740	Chr21:g.31667849	C=0.64, T=0.36	T	T	C	C	C	C	C	C	C
rs2833475	Chr21:g.31672507	A=0.93, G=0.07	A	A	A	A	A	A	G	A	A
rs16988427	Chr21:g.31678472	T=0.93, C=0.07	T	T	T	T	T	T	C	T	T
rs2833481	Chr21:g.31690038	T=0.88, C=0.12	T	T	T	T	T	T	C	C	C
rs2070423	Chr21:g.31691041	C=0.94, T=0.06	C	C	C	C	C	C	T	C	C
rs2833483	Chr21:g.31703091	T=0.93, C=0.07	T	T	T	T	T	T	C	T	T
	IBS Haplotype Count		*	76	35	31	30	11	11	8	3
	IBS Haplotype Frequency		*	0.3551	0.1636	0.1449	0.1402	0.0514	0.0514	0.0374	0.014
	IBS haplotype_ID		**1V**	**1A**	2	3	**4**	**5**	6	7	8

FIGURE 2 | Haplotypes inferred in the IBS population (1K Genomes Project). The IBS haplotype_ID codification is based on the frequency of the haplotype in the IBS population, and in the case of the most frequent (IBS haplotype_ID = 1) the presence of the *SOD1* p.A5V protein mutation (1V). (*) The haplotype 1V and allele rs121912442T are only present in the Spanish ALS patients with the *SOD1* p.A5V mutation.

(**Figure 2**). The haplotypes were named (1 to 8) according to their frequency in the population, ranging from higher to lower frequency (**Figure 2**). The mutation p.A5V-*SOD1* detected in the ALS patients is only compatible with haplotype 1 (haplo1V), which is the most common in the IBS population (haplo1A) (**Figure 2** and **Table 1**). According to the nomenclature proposed, the family has the IBS haplotypes 1A, 1V, 4, and 1A* (**Figure 1**).

The linkage disequilibrium of these 14 SNPs was calculated for the IBS population (**Supplementary Figure S2**). A conserved haplotype block, in high linkage disequilibrium, was detected between the start of intron 1 and the end of *SOD1*, and including the *SCAF4* gene. The *SOD1* exon 1, including the c.14C > T (p.A5V) mutation, is located outside this conserved haplotype in the IBS population (**Supplementary Figure S2**). Using data for all the populations deposited in the 1K Genomes Project, the analysis of linkage disequilibrium showed the same results for the conservation of this *SOD1* haplotype block (data not shown).

The founder p.A5V-*SOD1* haplotype in our patients is the same as the one found in the Swedish population, and differs from the founder haplotype observed in patients from North America (Table 1).

We determined all the inferred *SOD1* haplotypes for these 14 SNPs in the IBS, European, Asian, African, and Mixed American populations, using all the available subjects from the 1K Genomes Project as a control group (**Figure 3**). A total of 21 phased inferred haplotypes were detected in all the populations. The European haplotype (p.A5V-EUR) was the most common in all the populations. The American haplotype (p.A5V-USA) was the second most common worldwide. However, both haplotypes appear with similar frequencies in the Asian population (0.386 for p.A5V-EUR, 0.385 for p.A5V-USA) (**Figure 3**).

DISCUSSION

Redefining the p.A5V-SOD1 Phenotype. Reasons for the Disease's Aggressive Course

Over 186 *SOD1* mutations have been reported in amyotrophic lateral sclerosis (ALSoD). Previous epidemiological studies suggest that p.D91V is the most common worldwide, followed by p.I113T and p.A5V. The latter is the most commonly reported in the United States, accounting for 41% of the mutations identified in that population. It is one of the most aggressive mutations, as the mean survival time is under 2 years. The mutation has rarely been described among European populations. This is the first time that the p.A5V-*SOD1* has been reported in the Spanish population.

With the rare exception of a 73-year-old male presenting facial diplegia and unilateral vocal cord paralysis as the initial symptoms of ALS (Salameh et al., 2009), the phenotype associated with p.A5V in the American population is characterized by rapid progression and short survival. Patients present predominantly lower motor neuron signs, with limb weakness in 51% of patients, and bulbar symptoms in less than 11% of cases (Cudkowicz et al., 1997; Juneja et al., 1997; Andersen, 2003b; Andersen, 2006; Broom et al., 2008; Saeed et al., 2009). In a recent review of 57 p.A5V-*SOD1* cases, the mean survival time was 1.4 years, with clinical onset at a mean age of 50.0 years, and a male-female ratio of 1.3:1. Other characteristics associated with this *SOD1* mutation include fast progression, predominantly spinal onset, high penetrance, involvement of primarily lower motor neuron signs, and an absence of dementia (Bali et al., 2017).

However, the cases reported in European families differ slightly from those in America. For example, Andersen reported the clinical characteristics of a Swedish family (Andersen et al.,

A

RS Number	Allele Frequencies	SOD1 Haplotypes																						
rs4817415	C=0.719, A=0.281	C	C	A	C	A	C	C	C	A	C	C	C	C	A	C	C	A	A	C	C	A
rs2070422	C=0.733, T=0.267	C	T	C	C	C	C	C	T	T	C	T	T	T	T	C	T	C	T	T	C	C
rs1008270	A=0.899, C=0.101	A	A	A	C	A	A	A	A	A	A	A	A	A	A	C	A	A	A	A	A	A
rs9974610	A=0.914, G=0.086	A	A	A	A	A	G	A	A	A	A	A	A	A	A	A	A	A	A	A	A	G
rs2173962	T=0.943, C=0.057	T	T	T	T	T	T	T	C	T	T	C	T	T	C	T	T	T	T	T	T	T
rs202445	T=0.9, C=0.1	T	T	T	T	C	T	T	T	T	T	T	T	T	T	C	T	T	T	T	T	T
rs4816405	C=0.773, G=0.227	C	G	C	C	C	C	G	C	G	C	C	C	C	C	C	G	C	C	C	G	C
rs2070424	A=0.752, G=0.248	A	G	A	A	A	A	G	A	G	A	A	G	A	A	A	G	A	G	A	G	A
rs1041740	C=0.757, T=0.243	T	C	C	C	C	C	C	C	C	C	C	C	C	C	C	C	C	C	C	C	C
rs2833475	A=0.751, G=0.249	A	G	A	A	A	A	G	A	G	A	A	G	A	A	A	G	A	G	A	G	A
rs16988427	T=0.774, C=0.226	T	C	T	T	T	T	C	T	C	T	T	T	T	T	T	C	T	T	T	T	T
rs2833481	T=0.662, C=0.338	T	C	T	T	T	T	C	C	C	C	C	C	C	T	T	C	C	C	C	C	T
rs2070423	C=0.757, T=0.243	C	T	C	C	C	C	T	C	T	C	C	T	C	C	C	T	C	T	C	C	C
rs2833483	T=0.703, C=0.297	T	C	T	T	T	T	C	C	C	T	T	C	C	T	T	C	T	C	T	C	T
		EUR	USA																			

B

ALL	Haplotype Count	1175	724	636	447	423	392	246	119	116	95	68	68	61	54								
	Haplotype Frequency	0.2346	0.1446	0.127	0.0893	0.0845	0.0783	0.0491	0.0238	0.0232	0.019	0.0136	0.0136	0.0122	0.0108								
African	Haplotype Count	59	49	357	69	59	52		114	107	93		66	58	52			27	23	20			
	Haplotype Frequency	0.0446	0.0371	0.27	0.0522	0.0446	0.0393		0.0862	0.0809	0.0703		0.0499	0.0439	0.0393			0.0204	0.0174	0.0151			
European	Haplotype Count	300	62	90	129	165	167					45											
	Haplotype Frequency	0.2982	0.0616	0.0895	0.1282	0.164	0.166					0.0447											
East Asian	Haplotype Count	308	388	53	95		15	106													12		
	Haplotype Frequency	0.3056	0.3849	0.0526	0.0942		0.0149	0.1052													0.0119		
South Asian	Haplotype Count	294	191	76	107	93	98	26								36							
	Haplotype Frequency	0.3006	0.1953	0.0777	0.1094	0.0951	0.1002	0.0266								0.0368							
Mixed American	Haplotype Count	214	107	60		99	60				47	13					34						7
	Haplotype Frequency	0.3084	0.1542	0.0865		0.1427	0.0865				0.0677	0.0187					0.049						0.0101

FIGURE 3 | Inferred haplotypes around the *SOD1* gene detected in all populations from the 1K Genomes Project. **(A)** 21 inferred haplotypes. **(B)** Haplotype frequencies and counts are shown for each subpopulations: African (ACB, ASW, ESN, GWC, LWK, MSL, YRI); European (CEU, FIN, GBR, IBS, TSI); East Asian (CHB, CHS, CDX, JPT, KHV); South Asian (GIH, PJL, BEB, STU, ITU); Mixed American (CLM, MXL, PEL, PUR); all (African + European + East Asian + South Asian + Mixed Americans). EUR, haplotype base for *p.A5V*-EU. USA, haplotype base for *p.A5V*-USA.

1997; Andersen, 2007). One case had leg onset, another had hand onset, another had shoulder onset, and a further case had bulbar onset. These individuals were aged between 56 and 68 years old, and survival ranged from 8 months to 2 years. In the members of the two Italian families reported in 2001, information was available for two probands. One had shoulder onset at 55 years old, and died 8 months later. The other proband presented hand onset at 57 years old. No information about this individual's survival time is available, although the course was rapidly progressive (Gellera et al., 2001). Our family's phenotype—a mean age of onset of 51.7 years, spinal onset, predominant lower motor neuron signs, no cognitive alteration, and a survival time of 20 months—is consistent with the phenotype in these European families. Interestingly, none of the women inherited the mutation. Whether this was due to chance or a protective factor is unknown.

The reasons why p.A5V-*SOD1* predicts fast progression and short survival are unknown. *In vitro* studies have pointed to this mutation leading to a decline in dimerization capacity, a loss of metalation (a 30-fold decrease in zinc-binding affinity), and aberrant oligomerization, leading to misfolding and aggregation in the form of insoluble toxic inclusions within motor system cells, a key pathological hallmark of ALS. There is some variability in the propensity of *SOD1* mutants to aggregate, which could be related to the duration of the disease. High-aggregation propensities have been described for p.A5V, which could be the factor responsible for the disease's short duration (Prudencio et al., 2009; Zhao et al., 2014; Farrawell et al., 2018; Maurel et al., 2018; Srinivasan and Rajasekaran, 2018).

Another alternative and complementary hypothesis to explain the aggressive nature of p.A5V is its position in the tertiary structure of the protein. Interestingly, of the 30 mutations reported in exon 1, most of those in residue A5 (A4 in the previous nomenclature) predispose to a rapid progression and survival of under 24 months (Syriani et al., 2009). According to the tertiary structure of *SOD1*, residue A5 is located in the first β-strand that forms part of the dimer interface. A5 mutations affect *SOD1* dimerization and/or destabilize the Greek key β-barrel because A5 packs into the *SOD1* monomer's hydrophobic core (Getzoff et al., 1990; Deng et al., 1993; Cardoso et al., 2002; Galaleldeen et al., 2009; Schmidlin et al., 2009; Schmidlin et al., 2013; Kumar et al., 2018).

Founder Effect

Two earlier studies investigated a possible founder effect in the cases of North American and European origin. Following these haplotype studies, there is evidence to suggest at least two different origins: one European (probably a Scandinavian founder effect) and one Amerindian (Native Americans). The latter presents in 82% of North American families with the p.A5V-*SOD1* mutation. In European populations, p.A5V-*SOD1* has been reported in Scandinavia (three cases) and Italy (six cases). An isolated case has recently been reported in China, which shares most of the European haplotype. These findings could be interpreted in terms of the existence of various founders for p.A5V patients worldwide, rather than one founder, as previously assumed (Broom et al., 2008; Saeed et al., 2009). Some authors suggest that the European founder effect is older than the Amerindian, hypothesizing that the American families were in fact descendants of the European founder. Other authors argue that the European origin is different from the American one (Rosen, 2004; Armon, 2009).

After analyzing the *SOD1* haplotypes in different populations (European, Asian, African, and all the populations analyzed in the 1K Genomes Project), we found that the *SOD1* haplotype in which the p.A5V mutation is located in European fALS patients (p.A5V-EU) is the most common in the population worldwide, and the haplotype for American p.A5V-*SOD1* patients (p.A5V-USA) is the second most common. These variants appear to be linked to the most common haplotypes, and not linked to rare haplotypes. The haplotype p.A5V-USA is the most common (0.385) in the East Asian population and the p.A5V-EU haplotype is the second most common (0.306), with little difference between their allelic frequencies. However, in the European population, the haplotype p.A5V-EU is the most common haplotype (0.298), far below the frequency of the haplotype p.A5V-USA (0.062). The haplotypes p.A5V-EU (0.037) and p.A5V-USA (0.045) are rare in the African populations (as shown in **Figure 3**).

Based on these data, we propose two possible hypotheses for the origin of this mutation in two different haplotypes:

A Single Origin for All p.A5V-*SOD1* Families Worldwide

Information from previous linkage analyses suggests an origin for p.A5V around 13,000 years ago, probably in Asia. The p.A5V mutation appears in the p.A5V-EU haplotype and would have disseminated in Europe and Asia. A homologous recombination could have occurred in an ALS American family, leading to the linkage of the p.A5V mutation to the p.A5V-USA haplotype. A founder effect in North America could explain the p.A5V mutation associated to the p.A5V-USA haplotype in most (82%) cases in the American families (Rosen et al., 1994; Rosen, 2004; Broom et al., 2008; Armon, 2009; Saeed et al., 2009) and to the p.A5V-EU in only 18% of the other fALS cases. Only the p.A5V mutation linked to the haplotype p.A5V-EU is detected in Asia and Europe. Interestingly, linkage analysis of the haplotype of *SOD1* SNPs, a highly conserved haplotypic block (with a strong correlation) is observed after exon 1, but does not contain exon 1.

Several Origins (One for Asians, One for Americans, and Perhaps One or More for Europeans)

Previous studies investigating the haplotypic region around *SOD1* have suggested different mutational events to explain the mutation in USA and European ALS patients (Rosen, 2004; Broom et al., 2008, Eisen et al., 2008; Saeed et al., 2009). It is possible that the mutation in A5 was generated in the haplotypes p.A5V-USA and p.A5V-EU independently, since the two haplotypes are the most frequent in the population worldwide, and the locus at codon 5 of *SOD1* would be prone to mutations (a hotspot) since four additional mutations (p.A5T, p.A5S, p.A5F,

and p.A5P) have been described in this codon (Syriani et al., 2009; Pratt, 2014).

From the molecular point of view, the most parsimonious hypothesis would be a single origin for the A5V mutation. Our hypothesis of a common founder for p.A5V is supported by research investigating who first colonized America and when they did so. These genetic studies showed that the first inhabitants of the Americas came from a single Siberian population, who used the Bering Land Bridge to migrate from Beringia to the Americas sometime after 16,500 years ago (Bonatto and Salzano, 1997; Goebel et al., 2008). We propose a Eurasian origin for the A5V mutation in the haplotype p.A5V-EU. A Eurasian individual could have introduced the A5V mutation of the haplotype p.A5V-EU in America, and the mutation could have recombined in their descendants to obtain the p.A5V-USA haplotype linked to the p.A5V mutation. A genetic drift in America could therefore explain the founder effect of p.A5V in the haplotype p.A5V-USA being the most frequent ALS1 mutation in USA. A similar genetic phenomenon was described for the D90A mutation. Initial studies proposed two different founder effects (one for heterozygous cases and one for homozygous cases) (Al-Chalabi et al., 1998). After increasing the sample set and the markers, they concluded that there was a single founder for all cases. These studies for this mutation showed that the D90A mutation arose in Eurasia approximately 20,000 years ago (Parton et al., 2002).

Asian or Amerindian origins have been proposed for the A5V mutation based on their high frequency in USA and the haplotype p.A5V-USA being the most frequent haplotype in Asian populations (Rosen 2004; Broom et al., 2008; Saeed et al., 2009). The hypothesis of these two origins (Amerindian and Asian) is contradicted by the failure to detect the A5V mutation in the p.A5V-USA haplotype in ALS cases from Africa, Europe, Asia, and among Native Americans. Current data, including our results, indicate that the A5V mutation cases have been associated to the p.A5V-EU haplotype in different populations from Europe, USA, and Asia.

The *SOD1* haplotypes inferred from the IBS population enabled us to identify the haplotypes of the four members of a Spanish ALS family of Caucasian origin with two affected brothers with the p.A5V-*SOD1* mutation. The *SOD1* haplotype associated to the A5V mutation in our Spanish cases is the most frequent in the IBS and European populations. To our knowledge, our Spanish family is unrelated to the other p.A5V reported cases from Sweden (three subjects from one family) or Italy (six subjects from two families). A more detailed haplotype analysis of the European fALS cases with this mutation will be necessary to investigate whether there is a common origin for the p.A5V-*SOD1* mutation in the European ALS cases, or if it is a consequence of different mutational events. This research could be carried out through an international collaborative consortium to enroll and analyze these ALS families, as in the study suggested by an Italian group (Gellera et al., 2001).

In conclusion, this is the first report on the p.A5V-*SOD1* mutation in the Spanish population. The age at onset, site of onset, and survival were similar to those reported mainly in North American kindreds, in a few European families and in one Asian individual. SNP and haplotype analyses identify 21 haplotypes worldwide for the *SOD1* genomic region. Our family shares the haplotype reported in the founder European effect rather than the more frequent Amerindian haplotype.

DATA AVAILABILITY STATEMENT

Publicly available datasets were analyzed in this study. This data can be found here: http://www.internationalgenome.org/data.

ETHICS STATEMENT

This study was carried out in accordance with the recommendations of the Hospital Universitari Vall d'Hebron Institutional Review Board (VdHIRB) with written informed consent from all subjects. All subjects gave written informed consent in accordance with the Declaration of Helsinki. The protocol was approved by the VdHIRB.

AUTHOR CONTRIBUTIONS

JG and JV-T conceived the study. JG and MS collected the clinical information. CG, JV-T, ES, MM, and JG analyzed the data. JV-T and CG conducted the bioinformatics analysis. CG, JV-T, and JG drafted the manuscript. CG and JV-T contributed equally to this work. All the authors approved the final version of manuscript.

FUNDING

This study has been supported by Instituto de Salud Carlos III (grant numbers PIS-FEDER PI16/01673 and PI19/00593). JG and JV-T are the recipients of grant 2017SGR00939 from Agència de Gestió d'Ajuts Universitaris i de Recerca (AGAUR) of the Generalitat de Catalunya.

ACKNOWLEDGMENTS

The authors are indebted to the patients and their relatives for their cooperation. We thank the multidisciplinary ALS Unit Team from Vall d'Hebron University Hospital.

SUPPLEMENTARY MATERIAL

The Supplementary Material for this article can be found online at: https://www.frontiersin.org/articles/10.3389/fgene.2019.01109/full#supplementary-material

REFERENCES

Abel, O., Powell, J. F., Andersen, P. M., and Al-Chalabi, A. (2013). Credibility analysis of putative disease-causing genes using bioinformatics. *PloS One* 8, e64899. doi: 10.1371/journal.pone.0064899

Al-Chalabi, A., Andersen, P. M., Chioza, B., Shaw, C., Sham, P. C., Robberecht, W., et al. (1998). Recessive amyotrophic lateral sclerosis families with the D90A SOD1 mutation share a common founder: evidence for a linked protective factor. *Hum. Mol. Genet.* 7, 2045–2050. doi: 10.1093/hmg/7.13.2045

Al-Chalabi, A., Kwak, S., Mehler, M., Rouleau, G., Siddique, T., Strong, M., et al. (2013). Genetic and epigenetic studies of amyotrophic lateral sclerosis. *Amyotroph. Lateral. Scler. Frontotemporal Degener.* 14 (Suppl 1), 44–52. doi: 10.3109/21678421.2013.778571

Al-Chalabi, A., van den Berg, L. H., and Veldink, J. (2017). Gene discovery in amyotrophic lateral sclerosis: implications for clinical management. *Nat. Rev. Neurol.* 13, 96–104. doi: 10.1038/nrneurol.2016.182

Andersen, P. M., Nilsson, P., Keränen, M. L., Forsgren, L., Hägglund, J., Karlsborg, M., et al. (1997). Phenotypic heterogeneity in motor neuron disease patients with CuZn-superoxide dismutase mutations in Scandinavia. *Brain* 120, 1723–1737. doi: 10.1093/brain/120.10.1723

Andersen, P. M., Sims, K. B., Xin, W. W., Kiely, R., O'Neill, G., Ravits, J., et al. (2003a). Sixteen novel mutations in the Cu/Zn superoxide dismutase gene in amyotrophic lateral sclerosis: a decade of discoveries, defects and disputes. *Amyotroph. Lateral. Scler. Motor. Neuron. Disord.* 4, 62–73.

Andersen, P. M. (2003b). "Genetic aspects of amyotrophic lateral sclerosis/motor neuron disease," in *Motor neuron disorders*. Eds. Shaw, P. J., and Strong, M. J. (Philadelphia: Butterworth Heinemann).

Andersen, P. M. (2006). Amyotrophic lateral sclerosis associated with mutations in the CuZn superoxide dismutase gene. *Curr. Neurol. Neurosci. Rep.* 6, 37–46.

Andersen, P. (2007). The genetics of ALS/MND and the role of modifier genes: a clinical perspective. *Amyotroph. Lateral. Scler.* 8 (Suppl 1), 7–8. Abstract retrieved from 18th International Symposium on ALS/MND. doi: 10.1080/14660820701660642.

Andersen, P. M., and Al-Chalabi, A. (2011). Clinical genetics of amyotrophic lateral sclerosis: what do we really know? *Nat. Rev. Neurol.* 7, 603–615. doi: 10.1038/nrneurol.2011.150

Armon, C. (2009). SOD1 A4V familial ALS in North America: can understanding the past lead to a better future? *Neurology.* 72, 1628–1629. doi: 10.1212/01.wnl.0000344651.66120.ea

Bali, T., Self, W., Liu, J., Siddique, T., Wang, L. H., Bird, T. D., et al. (2017). Defining SOD1 ALS natural history to guide therapeutic clinical trial design. *J. Neurol. Neurosurg. Psychiatry* 88, 99–105. doi: 10.1136/jnnp-2016-313521

Bonatto, S. L., and Salzano, F. M. (1997). A single and early migration for the peopling of the Americas supported by mitochondrial DNA sequence data. *Proc. Natl. Acad. Sci. U.S.A.* 94, 1866–1871. doi: 10.1073/pnas.94.5.1866

Broom, W. J., Johnson, D. V., Auwarter, K. E., Iafrate, A. J., Russ, C., Al-Chalabi, A., et al. (2008). SOD1A4V-mediated ALS: absence of a closely linked modifier gene and origination in Asia. *Neurosci. Lett.* 430, 241–245. doi: 10.1016/j.neulet.2007.11.004

Brown, R. H., and Al-Chalabi, A. (2017). Amyotrophic Lateral Sclerosis. *N. Engl. J. Med.* 377, 162–172. doi: 10.1056/NEJMra1603471

Cardoso, R. M., Thayer, M. M., DiDonato, M., Lo, T. P., Bruns, C. K., Getzoff, E. D., et al. (2002). Insights into Lou Gehrig's disease from the structure and instability of the A4V mutant of human Cu, Zn superoxide dismutase. *J. Mol. Biol.* 324, 247–256. doi: 10.1016/s0022-2836(02)01090-2

Chia, R., Chiò, A., and Traynor, B. J. (2018). Novel genes associated with amyotrophic lateral sclerosis: diagnostic and clinical implications. *Lancet Neurol.* 17, 94–102. doi: 10.1016/S1474-4422(17)30401-5

Cudkowicz, M. E., McKenna-Yasek, D., Sapp, P. E., Chin, W., Geller, B., Hayden, D. L., et al. (1997). Epidemiology of mutations in superoxide dismutase in amyotrophic lateral sclerosis. *Ann. Neurol.* 41, 210–221. doi: 10.1002/ana.410410212

Deng, H. X., Hentati, A., Tainer, J. A., Iqbal, Z., Cayabyab, A., Hung, W. Y., et al. (1993). Amyotrophic lateral sclerosis and structural defects in Cu,Zn superoxide dismutase. *Science* 261, 1047–1051. doi: 10.1126/science.8351519

Eisen, A., Mezei, M. M., Stewart, H. G., Fabros, M., Gibson, G., and Andersen, P. M. (2008). SOD1 gene mutations in ALS patients from British Columbia, Canada: clinical features, neurophysiology and ethical issues in management. *Amyotroph. Lateral Scler.* 9, 108–119. doi: 10.1080/17482960801900073

Farrawell, N. E., Lambert-Smith, I., Mitchell, K., McKenna, J., McAlary, L., Ciryam, P., et al. (2018). SOD1A4V aggregation alters ubiquitin homeostasis in a cell model of ALS. *J. Cell Sci.* 131, jcs209122. doi: 10.1242/jcs.209122

Galaleldeen, A., Strange, R. W., Whitson, L. J., Antonyuk, S. V., Narayana, N., Taylor, A. B., et al. (2009). Structural and biophysical properties of metal-free pathogenic SOD1 mutants A4V and G93A. *Arch. Biochem. Biophys.* 492, 40–47. doi: 10.1016/j.abb.2009.09.020

Gellera, C., Castellotti, B., Riggio, M. C., Silani, V., Morandi, L., Testa, D., et al. (2001). Superoxide dismutase gene mutations in Italian patients with familial and sporadic amyotrophic lateral sclerosis: identification of three novel missense mutations. *Neuromuscul. Disord.* 11, 404–410. doi: 10.1016/S0960-8966(00)00215-7

Getzoff, E. D., Tainer, J. A., Stempien, M. M., Bell, G. I., and Hallewell, R. A. (1990). Evolution of CuZn superoxide dismutase and the Greek key beta-barrel structural motif. *Proteins.* 5, 322–336 Erratum in: Proteins 8,398–399. doi: 10.1002/prot.340050408

Goebel, T., Waters, M. R., and O'Rourke, D. H. (2008). The late Pleistocene dispersal of modern humans in the Americas. *Science.* 319, 1497–1502. doi: 10.1126/science.1153569

Hardiman, O., Al-Chalabi, A., Chio, A., Corr, E. M., Logroscino, G., Robberecht, W., et al. (2017). Amyotrophic. lateral sclerosis. *Nat. Rev. Dis. Primers.* 3, 17071. doi: 10.1038/nrdp.2017.71

Jones, A. R., Troakes, C., King, A., Sahni, V., De Jong, S., Bossers, K., et al. (2015). Stratified gene expression analysis identifies major amyotrophic lateral sclerosis genes. *Neurobiol. Aging.* 36, 2006.e1–9. doi: 10.1016/j.neurobiolaging.2015.02.017

Juneja, T., Pericak-Vance, A., Laing, N. G., Dave, S., and Siddique, T. (1997). Prognosis in familial lateral sclerosis: progression and survival in patients with glu100gly and ala4val mutations in Cu,Zn superoxide dismutase. *Neurology* 48, 55–57. doi: 10.1212/wnl.48.1.55

Kumar, V., Prakash, A., and Lynn, A. M. (2018). Alterations in local stability and dynamics of A4V SOD1 in the presence of trifluoroethanol. *Biopolymers.* 109, e23102. doi: 10.1002/bip.23102

Leblond, C. S., Kaneb, H. M., Dion, P. A., and Rouleau, G. A. (2014). Dissection of genetic factors associated with amyotrophic lateral sclerosis. *Exp. Neurol.* 262, 91–101. doi: 10.1016/j.expneurol.2014.04.013

Machiela, M. J., and Chanock, S. J. (2015). LDlink: a web-based application for exploring population-specific haplotype structure and linking correlated alleles of possible functional variants. *Bioinformatics* 31, 3555–3557. doi: 10.1093/bioinformatics/btv402

Maurel, C., Dangoumau, A., Marouillat, S., Brulard, C., and Chami, A. (2018). Causative genes in amyotrophic lateral sclerosis and protein degradation pathways: a link to neurodegeneration. *Mol. Neurobiol.* 55, 6480–6499. doi: 10.1007/s12035-017-0856-0

Parton, M. J., Broom, W., Andersen, P. M., Al-Chalabi, A., Nigel Leigh, P., et al. (2002). D90A SOD1 ALS Consortium. D90A-SOD1 mediated amyotrophic lateral sclerosis: a single founder for all cases with evidence for a Cis-acting disease modifier in the recessive haplotype. *Hum. Mutat.* 20, 473. doi: 10.1002/humu.9081

Pratt, A. J. (2014). Aggregation propensities of superoxide dismutase G93 hotspot mutants mirror ALS clinical phenotypes Proc. *Natl. Acad. Sci. U.S.A.* 111, E4568–E4576. doi: 10.1073/pnas.1308531111

Prudencio, M., Hart, P. J., Borchelt, D. R., and Andersen, P. M. (2009). Variation in aggregation propensities among ALS-associated variants of SOD1: correlation to human disease. *Hum. Mol. Genet.* 18, 3217–3226. doi: 10.1093/hmg/ddp260

Renton, A. E., Chiò, A., and Traynor, B. J. (2014). State of play in amyotrophic lateral sclerosis genetics. *Nat. Neurosci.* 17, 17–23. doi: 10.1038/nn.3584

Rosen, D. R., Bowling, A. C., Patterson, D., Usdin, T. B., Sapp, P., Mezey, E., et al. (1994). A frequent ala 4 to val superoxide dismutase-1 mutation is associated with a rapidly progressive familial amyotrophic lateral sclerosis. *Hum. Mol. Genet.* 3, 981–987. doi: 10.1093/hmg/3.6.981

Rosen, D. R. (2004). A shared chromosome-21 haplotype among amyotrophic lateral sclerosis families with the A4V SOD1 mutation. *Clin. Genet.* 66, 247–250. doi: 10.1111/j.1399-0004.2004.00298.x

Saeed, M., Yang, Y., Deng, H. X., Hung, W. Y., Siddique, N., Dellefave, L., et al. (2009). Age and founder effect of SOD1 A4V mutation causing ALS. *Neurology* 72, 1634–1639. doi: 10.1212/01.wnl.0000343509.76828.2a

Salameh, J. S., Atassi, N., and David, W. S. (2009). SOD1 (A4V)-mediated ALS presenting with lower motor neuron facial diplegia and unilateral vocal cord paralysis. *Muscle Nerve.* 40, 880–882. doi: 10.1002/mus.21321

Schmidlin, T., Kennedy, B. K., and Daggett, V. (2009). Structural changes to monomeric CuZn superoxide dismutase caused by the familial amyotrophic lateral sclerosis-associated mutation A4V. *Biophys. J.* 97, 1709–1718. doi: 10.1016/j.bpj.2009.06.043

Schmidlin, T., Ploeger, K., Jonsson, A. L., and Daggett, V. (2013). Early steps in thermal unfolding of superoxide dismutase 1 are similar to the conformational changes associated with the ALS-associated A4V mutation. *Protein Eng. Des. Sel.* 26, 503–513. doi: 10.1093/protein/gzt030

Srinivasan, E., and Rajasekaran, R. (2018). Cysteine to Serine Conversion at 111th Position Renders the Disaggregation and Retains the Stabilization of Detrimental SOD1 A4V Mutant Against Amyotrophic Lateral Sclerosis in Human-A Discrete Molecular Dynamics Study. *Cell Biochem. Biophys.* 76, 231–241. doi: 10.1007/s12013-017-0830-5

Syriani, E., Morales, M., and Gamez, J. (2009). The p.E22G mutation in the Cu/Zn superoxide-dismutase gene predicts a long survival time: clinical and genetic characterization of a seven-generation ALS1 Spanish pedigree. *J. Neurol. Sci.* 285, 46–53. doi: 10.1016/j.jns.2009.05.011

Tang, L., Ma, Y., Liu, X., Chen, L., and Fan, D. (2018). Identification of an A4V SOD1 mutation in a Chinese patient with amyotrophic lateral sclerosis without the A4V founder effect common in North America. *Amyotroph. Lateral Scler. Frontotemporal Degener.* 19, 466–468. doi: 10.1080/21678421.2018.1451895

The 1000 Genomes Project Consortium (2015). A global reference for human genetic variation. *Nature* 526, 68–74. doi: 10.1038/nature15393

Untergasser, A., Cutcutache, I., Koressaar, T., Ye, J., Faircloth, B. C., et al. (2012). Primer3-new capabilities and interfaces. *Nucleic Acids Res.* 40, e115. doi: 10.1093/nar/gks596

van Es, M. A., Hardiman, O., Chio, A., Al-Chalabi, A., Pasterkamp, R. J., Veldink, J. H., et al. (2017). Amyotrophic lateral sclerosis. *Lancet* 390, 2084–2098. doi: 10.1016/S0140-6736(17)31287-4

van Blitterswijk, M., van Es, M. A., Hennekam, E. A., Dooijes, D., van Rheenen, W., Medic, J., et al. (2012). Evidence for an oligogenic basis of amyotrophic lateral sclerosis. *Hum. Mol. Genet.* 21, 3776–3784. doi: 10.1093/hmg/dds199

Watanabe, Y., Kato, S., Adachi, Y., and Nakashima, K. (2000). Frameshift, nonsense and nonamino acid altering mutations in SOD1 in familial ALS: report of a Japanese pedigree and literature review. *Amyotroph. Lateral Scler. Other Mot. Neuron. Disord.* 1, 251–258. doi: 10.1080/14660820050515070

Zhao, D., Zhang, S., Meng, Y., Xiongwei, D., Zhang, D., Liang, Y., et al. (2014). Polyanion binding accelerates the formation of stable and low-toxic aggregates of ALS-linked SOD1 mutant A4V. *Proteins.* 82, 3356–3372. doi: 10.1002/prot.24691

Conflict of Interest: The authors declare that the research was conducted in the absence of any commercial or financial relationships that could be construed as a potential conflict of interest.

Advantages of publishing in Frontiers

OPEN ACCESS
Articles are free to read for greatest visibility and readership

FAST PUBLICATION
Around 90 days from submission to decision

HIGH QUALITY PEER-REVIEW
Rigorous, collaborative, and constructive peer-review

TRANSPARENT PEER-REVIEW
Editors and reviewers acknowledged by name on published articles

Frontiers
Avenue du Tribunal-Fédéral 34
1005 Lausanne | Switzerland

Visit us: www.frontiersin.org
Contact us: frontiersin.org/about/contact

REPRODUCIBILITY OF RESEARCH
Support open data and methods to enhance research reproducibility

DIGITAL PUBLISHING
Articles designed for optimal readership across devices

FOLLOW US
@frontiersin

IMPACT METRICS
Advanced article metrics track visibility across digital media

EXTENSIVE PROMOTION
Marketing and promotion of impactful research

LOOP RESEARCH NETWORK
Our network increases your article's readership